Publicaciones Geológicas Especiales

SERVICIO GEOLÓGICO COLOMBIANO

El futuro es de todos — Minenergía

ISBN: 978-958-52959-2-6

The Geology of Colombia book provides an updated background of the geological knowledge of Colombia by integrating the most up–to–date research covering paleontology, biostratigraphy, sedimentary basin analysis, sedimentology, sequence stratigraphy, stratigraphy, geophysics, geochronology, geochemistry, thermochronology, tectonics, structure, volcanology, petrology, environmental science, climate change, and space geodesy.

Each chapter has a complete framework of a major branch of geology providing an invaluable resource for geologists interested in the geological history of Colombia.

The first volume presents a comprehensive, ten chapter overview covering the physiographic and geological setting in Colombia, geophysical data of eastern Colombia, continental tectonostratigraphic terranes in Colombia, evolution of the Proterozoic basement of the West Guyana Shield, the Putumayo Orogen of Amazonia, the Ediacaran and Paleozoic in the Llanos Basin and Colombian Andes, and the Permian arc on the western margin of the Neoproterozoic basement of Colombia.

Other volumes in *The Geology of Colombia* book
Volume 2: Mesozoic
Volume 3: Paleogene – Neogene
Volume 4: Quaternary

Jorge GÓMEZ TAPIAS
Daniela MATEUS–ZABALA
Editors

THE GEOLOGY OF COLOMBIA
VOLUME 1 • PROTEROZOIC – PALEOZOIC

35

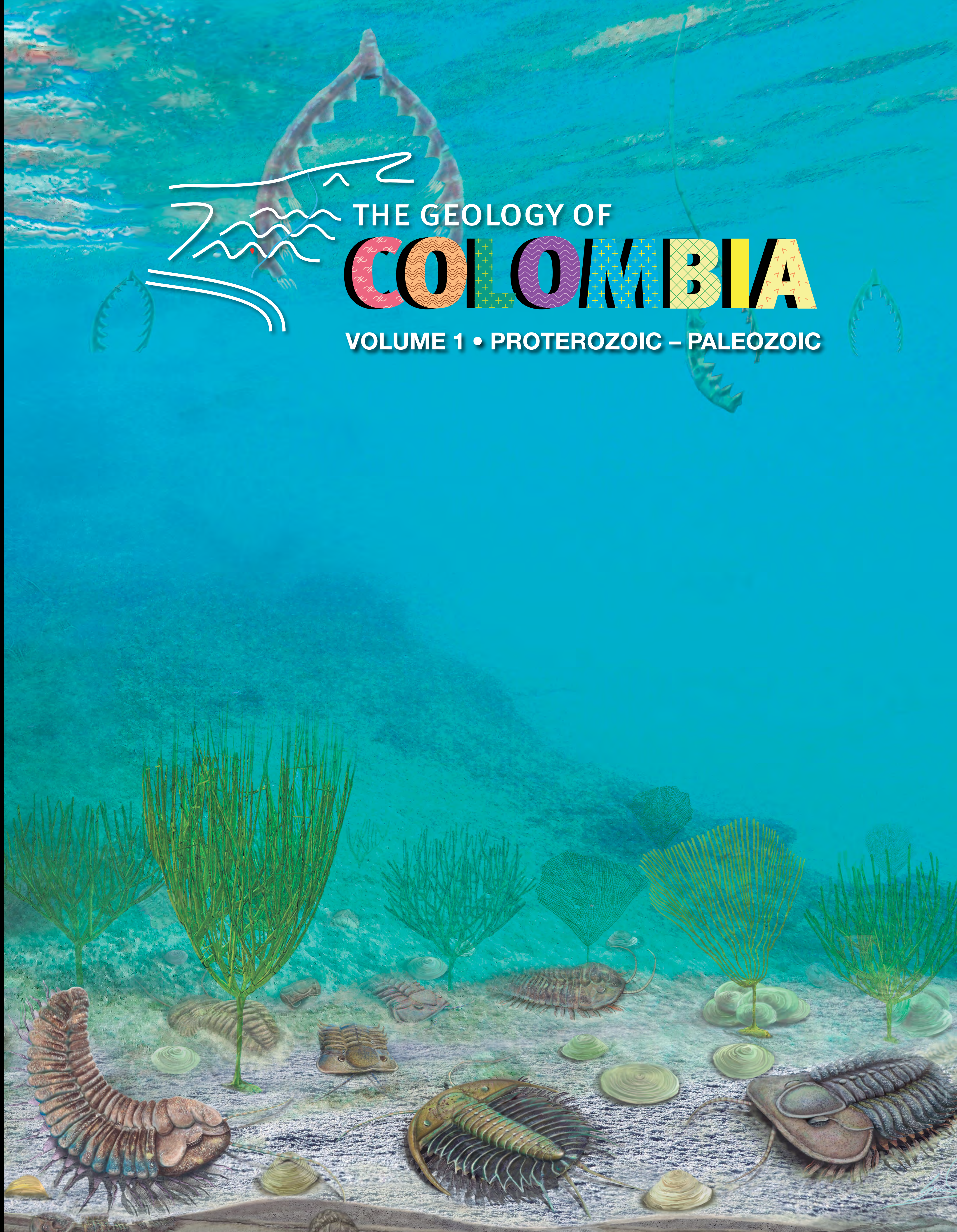

THE GEOLOGY OF COLOMBIA

VOLUME 1 • PROTEROZOIC – PALEOZOIC

Publicaciones Geológicas Especiales

THE GEOLOGY OF COLOMBIA

Jorge GÓMEZ TAPIAS and Daniela MATEUS–ZABALA
Servicio Geológico Colombiano
Editors

SERVICIO GEOLÓGICO COLOMBIANO

El futuro es de todos

Minenergía

ISBN impreso obra completa: 978-958-52959-1-9
ISBN digital obra completa: 978-958-52959-6-4

ISBN impreso Vol. 1: 978-958-52959-2-6
ISBN digital Vol. 1: 978-958-52959-7-1

Jorge GÓMEZ TAPIAS
Daniela MATEUS–ZABALA
Ana PINILLA–PACHON
Editores

Miguel Gerardo RAMÍREZ–LEAL
Diseñador

Imprenta Nacional de Colombia
Impresión

Bogotá D. C., Colombia
2020

Cover

Illustration showing typical fauna of the sea basin in Llanos Orientales Basin during Ordovician. There are crinoids; brachiopods (*Acotetra* sp); trilobites (*Jujuyaspis* spp., *Helieranella negritoensis* and *Triarthus* sp.); and graptolites (*Janagraptus* sp., *Didymograptus extensus* and *Dyctionema* spp.). See chapter 7, *Paleontology of the Paleozoic Rocks of the Llanos Orientales Basin, Colombia*, for getting further information.

Scientific illustration made by Marie Joëlle GIRAUD, a geologist. The fossil record was found at La Heliera–1 and Negritos–1 wells, drilled in the Llanos Orientales Basin, Colombia.

Suggested citation for Volume 1

Gómez, J. & Mateus–Zabala, D., editors. 2020. The Geology of Colombia, Volume 1 Proterozoic – Paleozoic. Servicio Geológico Colombiano, Publicaciones Geológicas Especiales 35, 239 p. Bogotá. https://doi.org/10.32685/pub.esp.35.2019

INTERNATIONAL CHRONOSTRATIGRAPHIC CHART

www.stratigraphy.org — **International Commission on Stratigraphy** — **v 2020/03**

IUGS

Numerical age (Ma) given for each unit is the age of its lower boundary.

Eonothem / Eon	Erathem / Era	System / Period	Series / Epoch	Stage / Age	GSSP	numerical age (Ma)
						present
Phanerozoic	Cenozoic	Quaternary	Holocene (U/L)	Meghalayan	✓	0.0042
			Holocene (M)	Northgrippian	✓	0.0082
			Holocene (L/E)	Greenlandian	✓	0.0117
			Pleistocene (U/L)	*Upper*		0.129
			Pleistocene (M)	Chibanian	✓	0.774
			Pleistocene (L/E)	Calabrian	✓	1.80
				Gelasian	✓	2.58
		Neogene	Pliocene	Piacenzian	✓	3.600
				Zanclean	✓	5.333
			Miocene	Messinian	✓	7.246
				Tortonian	✓	11.63
				Serravallian	✓	13.82
				Langhian		15.97
				Burdigalian		20.44
				Aquitanian	✓	23.03
		Paleogene	Oligocene	Chattian	✓	27.82
				Rupelian	✓	33.9
			Eocene	Priabonian	✓	37.71
				Bartonian		41.2
				Lutetian	✓	47.8
				Ypresian	✓	56.0
			Paleocene	Thanetian	✓	59.2
				Selandian	✓	61.6
				Danian	✓	66.0
	Mesozoic	Cretaceous	Upper	Maastrichtian	✓	72.1 ±0.2
				Campanian		83.6 ±0.2
				Santonian	✓	86.3 ±0.5
				Coniacian		89.8 ±0.3
				Turonian	✓	93.9
				Cenomanian	✓	100.5
			Lower	Albian	✓	~ 113.0
				Aptian		~ 125.0
				Barremian		~ 129.4
				Hauterivian	✓	~ 132.6
				Valanginian		~ 139.8
				Berriasian		~ 145.0

Eonothem / Eon	Erathem / Era	System / Period	Series / Epoch	Stage / Age	GSSP	numerical age (Ma)
						~ 145.0
Phanerozoic	Mesozoic	Jurassic	Upper	Tithonian		152.1 ±0.9
				Kimmeridgian		157.3 ±1.0
				Oxfordian		163.5 ±1.0
			Middle	Callovian		166.1 ±1.2
				Bathonian	✓	168.3 ±1.3
				Bajocian	✓	170.3 ±1.4
				Aalenian	✓	174.1 ±1.0
			Lower	Toarcian	✓	182.7 ±0.7
				Pliensbachian	✓	190.8 ±1.0
				Sinemurian	✓	199.3 ±0.3
				Hettangian	✓	201.3 ±0.2
		Triassic	Upper	Rhaetian		~ 208.5
				Norian		~ 227
				Carnian	✓	~ 237
			Middle	Ladinian	✓	~ 242
				Anisian		247.2
			Lower	Olenekian		251.2
				Induan	✓	251.902 ±0.024
	Paleozoic	Permian	Lopingian	Changhsingian	✓	254.14 ±0.07
				Wuchiapingian	✓	259.1 ±0.5
			Guadalupian	Capitanian	✓	265.1 ±0.4
				Wordian	✓	268.8 ±0.5
				Roadian	✓	272.95 ±0.11
			Cisuralian	Kungurian		283.5 ±0.6
				Artinskian		290.1 ±0.26
				Sakmarian	✓	293.52 ±0.17
				Asselian	✓	298.9 ±0.15
		Carboniferous (Pennsylvanian)	Upper	Gzhelian		303.7 ±0.1
				Kasimovian		307.0 ±0.1
			Middle	Moscovian		315.2 ±0.2
			Lower	Bashkirian	✓	323.2 ±0.4
		Carboniferous (Mississippian)	Upper	Serpukhovian		330.9 ±0.2
			Middle	Visean	✓	346.7 ±0.4
			Lower	Tournaisian	✓	358.9 ±0.4

Eonothem / Eon	Erathem / Era	System / Period	Series / Epoch	Stage / Age	GSSP	numerical age (Ma)
						358.9 ±0.4
Phanerozoic	Paleozoic	Devonian	Upper	Famennian	✓	372.2 ±1.6
				Frasnian	✓	382.7 ±1.6
			Middle	Givetian	✓	387.7 ±0.8
				Eifelian	✓	393.3 ±1.2
			Lower	Emsian	✓	407.6 ±2.6
				Pragian	✓	410.8 ±2.8
				Lochkovian	✓	419.2 ±3.2
		Silurian	Pridoli		✓	423.0 ±2.3
			Ludlow	Ludfordian	✓	425.6 ±0.9
				Gorstian	✓	427.4 ±0.5
			Wenlock	Homerian	✓	430.5 ±0.7
				Sheinwoodian	✓	433.4 ±0.8
			Llandovery	Telychian	✓	438.5 ±1.1
				Aeronian	✓	440.8 ±1.2
				Rhuddanian	✓	443.8 ±1.5
		Ordovician	Upper	Hirnantian	✓	445.2 ±1.4
				Katian	✓	453.0 ±0.7
				Sandbian	✓	458.4 ±0.9
			Middle	Darriwilian	✓	467.3 ±1.1
				Dapingian	✓	470.0 ±1.4
			Lower	Floian	✓	477.7 ±1.4
				Tremadocian	✓	485.4 ±1.9
		Cambrian	Furongian	*Stage 10*		~ 489.5
				Jiangshanian	✓	~ 494
				Paibian	✓	~ 497
			Miaolingian	Guzhangian	✓	~ 500.5
				Drumian	✓	~ 504.5
				Wuliuan	✓	~ 509
			Series 2	*Stage 4*		~ 514
				Stage 3		~ 521
			Terreneuvian	*Stage 2*		~ 529
				Fortunian	✓	541.0 ±1.0

	Eonothem / Eon	Erathem / Era	System / Period	GSSP / GSSA	numerical age (Ma)
					541.0 ±1.0
Precambrian	Proterozoic	Neoproterozoic	Ediacaran	GSSP	~ 635
			Cryogenian		~ 720
			Tonian	GSSA	1000
		Mesoproterozoic	Stenian	GSSA	1200
			Ectasian	GSSA	1400
			Calymmian	GSSA	1600
		Paleoproterozoic	Statherian	GSSA	1800
			Orosirian	GSSA	2050
			Rhyacian	GSSA	2300
			Siderian	GSSA	2500
	Archean	Neoarchean		GSSA	2800
		Mesoarchean		GSSA	3200
		Paleoarchean		GSSA	3600
		Eoarchean		GSSA	4000
	Hadean				~ 4600

Units of all ranks are in the process of being defined by Global Boundary Stratotype Section and Points (GSSP) for their lower boundaries, including those of the Archean and Proterozoic, long defined by Global Standard Stratigraphic Ages (GSSA). Italic fonts indicate informal units and placeholders for unnamed units. Versioned charts and detailed information on ratified GSSPs are available at the website http://www.stratigraphy.org. The URL to this chart is found below.

Numerical ages are subject to revision and do not define units in the Phanerozoic and the Ediacaran; only GSSPs do. For boundaries in the Phanerozoic without ratified GSSPs or without constrained numerical ages, an approximate numerical age (~) is provided.

Ratified Subseries/Subepochs are abbreviated as U/L (Upper/Late), M (Middle) and L/E (Lower/Early). Numerical ages for all systems except Quaternary, upper Paleogene, Cretaceous, Triassic, Permian and Precambrian are taken from 'A Geologic Time Scale 2012' by Gradstein et al. (2012), those for the Quaternary, upper Paleogene, Cretaceous, Triassic, Permian and Precambrian were provided by the relevant ICS subcommissions.

Colouring follows the Commission for the Geological Map of the World (www.ccgm.org)

CCGM CGMW

Chart drafted by K.M. Cohen, D.A.T. Harper, P.L. Gibbard, J.-X. Fan

To cite: Cohen, K.M., Finney, S.C., Gibbard, P.L. & Fan, J.-X. (2013; updated) The ICS International Chronostratigraphic Chart. Episodes 36: 199-204.

URL: http://www.stratigraphy.org/ICSchart/ChronostratChart2020-03.pdf

TABLA CRONOESTRATIGRÁFICA INTERNACIONAL

IUGS

www.stratigraphy.org — **Comisión Internacional de Estratigrafía** — **v 2020/03**

Eonotema / Eón	Eratema / Era	Sistema / Período	Serie / Época	Piso / Edad	Edad (Ma)
					actualidad
Fanerozoico	Cenozoico	Cuaternario	Holoceno	S Megalayano	0.0042
				M Norgripiano	0.0082
				I Groenlandiano	0.0117
			Pleistoceno	S *Superior*	0.129
				M Chibaniano	0.774
				I Calabriano	1.80
				I Gelasiano	2.58
		Neógeno	Plioceno	Piacenziano	3.600
				Zancliano	5.333
			Mioceno	Mesiniano	7.246
				Tortoniano	11.63
				Serravaliano	13.82
				Langhiano	15.97
				Burdigaliano	20.44
				Aquitaniano	23.03
		Paleógeno	Oligoceno	Chattiano	27.82
				Rupeliano	33.9
			Eoceno	Priaboniano	37.71
				Bartoniano	41.2
				Lutetiano	47.8
				Ypresiano	56.0
			Paleoceno	Thanetiano	59.2
				Selandiano	61.6
				Daniano	66.0
	Mesozoico	Cretácico	Superior	Maastrichtiano	72.1 ±0.2
				Campaniano	83.6 ±0.2
				Santoniano	86.3 ±0.5
				Coniaciano	89.8 ±0.3
				Turoniano	93.9
				Cenomaniano	100.5
			Inferior	Albiano	~ 113.0
				Aptiano	~ 125.0
				Barremiano	~ 129.4
				Hauteriviano	~ 132.6
				Valanginiano	~ 139.8
				Berriasiano	~ 145.0

Eonotema / Eón	Eratema / Era	Sistema / Período	Serie / Época	Piso / Edad	Edad (Ma)
					~ 145.0
Fanerozoico	Mesozoico	Jurásico	Superior	Titoniano	152.1 ±0.9
				Kimmeridgiano	157.3 ±1.0
				Oxfordiano	163.5 ±1.0
			Medio	Calloviano	166.1 ±1.2
				Bathoniano	168.3 ±1.3
				Bajociano	170.3 ±1.4
				Aaleniano	174.1 ±1.0
			Inferior	Toarciano	182.7 ±0.7
				Pliensbachiano	190.8 ±1.0
				Sinemuriano	199.3 ±0.3
				Hettangiano	201.3 ±0.2
		Triásico	Superior	Rhaetiano	~ 208.5
				Noriano	~ 227
				Carniano	~ 237
			Medio	Ladiniano	~ 242
				Anisiano	247.2
			Inferior	Olenekiano	251.2
				Induano	251.902 ±0.024
	Paleozoico	Pérmico	Lopingiano	Changhsingiano	254.14 ±0.07
				Wuchiapingiano	259.1 ±0.5
			Guadalupiano	Capitaniano	265.1 ±0.4
				Wordiano	268.8 ±0.5
				Roadiano	272.95 ±0.11
			Cisuraliano	Kunguriano	283.5 ±0.6
				Artinskiano	290.1 ±0.26
				Sakmariano	293.52 ±0.17
				Asseliano	298.9 ±0.15
		Carbonífero	Pennsylvaniano Superior	Gzheliano	303.7 ±0.1
				Kasimoviano	307.0 ±0.1
			Pennsylvaniano Medio	Moscoviano	315.2 ±0.2
			Pennsylvaniano Inferior	Bashkiriano	323.2 ±0.4
			Mississippiano Superior	Serpukhoviano	330.9 ±0.2
			Mississippiano Medio	Viseano	346.7 ±0.4
			Mississippiano Inferior	Tournaisiano	358.9 ±0.4

Eonotema / Eón	Eratema / Era	Sistema / Período	Serie / Época	Piso / Edad	Edad (Ma)
					358.9 ±0.4
Fanerozoico	Paleozoico	Devónico	Superior	Famenniano	372.2 ±1.6
				Frasniano	382.7 ±1.6
			Medio	Givetiano	387.7 ±0.8
				Eifeliano	393.3 ±1.2
			Inferior	Emsiano	407.6 ±2.6
				Pragiano	410.8 ±2.8
				Lochkoviano	419.2 ±3.2
		Silúrico	Pridoliano		423.0 ±2.3
			Ludloviano	Ludfordiano	425.6 ±0.9
				Gorstiano	427.4 ±0.5
			Wenlockiano	Homeriano	430.5 ±0.7
				Sheinwoodiano	433.4 ±0.8
			Llandoveriano	Telychiano	438.5 ±1.1
				Aeroniano	440.8 ±1.2
				Rhuddaniano	443.8 ±1.5
		Ordovícico	Superior	Hirnantiano	445.2 ±1.4
				Katiano	453.0 ±0.7
				Sandbiano	458.4 ±0.9
			Medio	Darriwiliano	467.3 ±1.1
				Dapingiano	470.0 ±1.4
			Inferior	Floiano	477.7 ±1.4
				Tremadociano	485.4 ±1.9
		Cámbrico	Furongiano	*Piso 10*	~ 489.5
				Jiangshaniano	~ 494
				Paibiano	~ 497
			Miaolingiano	Guzhangiano	~ 500.5
				Drumiano	~ 504.5
				Wuliuano	~ 509
			Serie 2	*Piso 4*	~ 514
				Piso 3	~ 521
			Terreneuviano	*Piso2*	~ 529
				Fortuniano	541.0 ±1.0

Eonotema / Eón	Eratema / Era	Sistema / Período	Edad (Ma)
			541.0 ±1.0
Precámbrico — Proterozoico	Neoproterozoico	Ediacariano	~ 635
		Criogeniano	~ 720
		Toniano	1000
	Mesoproterozoico	Steniano	1200
		Ectasiano	1400
		Calymmiano	1600
	Paleoproterozoico	Statheriano	1800
		Orosiriano	2050
		Rhyaciano	2300
		Sideriano	2500
Arqueano	Neoarqueano		2800
	Mesoarqueano		3200
	Paleoarqueano		3600
	Eoarqueano		4000
Hadeano			~ 4600

La definición del Estratotipo Global de Límite (GSSP–Global Boundary Stratotype Section and Point) para la base de las unidades de los diversos rangos es un proceso que aún no ha sido completado. Tampoco para los estratotipos de límite de las unidades del Arqueano y Proterozoico, cuya división se fundamentó por mucho tiempo en una convención de edades absolutas (GSSA–Global Standard Stratigraphic Ages). Las fuentes en cursiva indican unidades informales y marcadores de posición para unidades innominadas. Las diferentes versiones de la Tabla y los detalles de los GSSP están disponibles en el sitio web http://www.stratigraphy.org. La URL de esta versión de la Tabla se encuentra más adelante.

Las edades numéricas están sujetas a revisión y no definen unidades en el Fanerozoico ni en el Ediacariano; solo los GSSP lo hacen. Para los límites en el Fanerozoico que no tienen un GSSP formal o edades numéricas restringidas, se proporciona una edad numérica aproximada (~).

Las Subseries/Subepocas ratificadas se abrevian como S (Superior), M (Medio) e I (Inferior). Las edades numéricas para todos los sistemas, excepto para el Cuaternario, Paleógeno superior, Cretácico, Triásico, Pérmico y Precámbrico se tomaron de *A Geologic Time Scale 2012* de Gradstein et al. (2012), las del Cuaternario, Paleógeno superior, Cretácico, Triásico, Pérmico y Precámbrico fueron proporcionadas por las subcomisiones respectivas de la ICS.

La norma de colores se rige por la de la Comisión del Mapa Geológico del Mundo (CCGM-IUGS) – www.ccgm.org

Esta tabla cronoestratigráfica es una adaptación al español de América y una edición del Servicio Geológico Colombiano (SGC). La coordinación estuvo a cargo de Juan Carlos Gutiérrez–Marco de la Universidad Complutense de Madrid y Jorge Gómez Tapias del SGC, quienes recibieron contribuciones de diversas subcomisiones estratigráficas, servicios geológicos y profesionales radicados en México, Argentina, Chile, Perú, Ecuador y Uruguay. En Venezuela, la terminología cronoestratigráfica sigue las pautas del castellano de España.

SERVICIO GEOLÓGICO COLOMBIANO

Tabla diseñada por K.M. Cohen, D.A.T. Harper, P.L. Gibbard, J.-X. Fan

Citar como: Cohen, K.M., Finney, S.C., Gibbard, P.L. y Fan, J.-X. (2013; actualizado) The ICS International Chronostratigraphic Chart. Episodes 36: 199-204.

URL: http://www.stratigraphy.org/ICSchart/ChronostratChart2020-03SpanishAmer.pdf

Proterozoic Cambrian Ordovician Silurian Devonian Carboniferous Permian Triassic Jurassic Cretaceous Paleogene Neogene Quaternary

Content

Volume 1

Foreword
Oscar PAREDES ZAPATA xiii

Prefacio del director general del Servicio Geológico Colombiano
Oscar PAREDES ZAPATA xv

Preface
Jorge GÓMEZ TAPIAS and Daniela MATEUS–ZABALA xvii

Prefacio de los editores
Jorge GÓMEZ TAPIAS and Daniela MATEUS–ZABALA xix

Prologue
Victor A. RAMOS xxi

Prólogo
Victor A. RAMOS xxv

Presentation of *The Geology of Colombia*
Jorge GÓMEZ TAPIAS , Daniela MATEUS–ZABALA, Ana Oliva PINILLA–PACHON, Alberto NÚÑEZ–TELLO, Rubby Melissa LASSO–MUÑOZ, Fernando Alirio ALCÁRCEL–GUTIÉRREZ, Eliana MARÍN–RINCÓN, María Paula MARROQUÍN–GÓMEZ, Lisbeth FOG–CORRADINE, Alejandra CARDONA–MAYORGA , and Miguel Gerardo RAMÍREZ–LEAL xxix

Chapter 1 Physiographic and geological setting of the Colombian territory
Jorge GÓMEZ TAPIAS, Alberto NÚÑEZ–TELLO, Daniela MATEUS–ZABALA, Fernando Alirio ALCÁRCEL–GUTIÉRREZ, Rubby Melissa LASSO–MUÑOZ, Eliana MARÍN–RINCÓN, and María Paula MARROQUÍN–GÓMEZ 1

Chapter 2 Contribution of new airborne geophysical information to the geological knowledge of eastern Colombia
Ismael Enrique MOYANO–NIETO, Renato CORDANI, Lorena Paola CÁRDENAS–ESPINOSA, Norma Marcela LARA–MARTÍNEZ, Oscar Eduardo ROJAS–SARMIENTO, Manuel Fernando PUENTES–TORRES, Diana Lorena OSPINA–MONTES, Andrés Felipe SALAMANCA–SAAVEDRA, and Gloria PRIETO–RINCÓN 17

Chapter 3 Tectonostratigraphic terranes in Colombia: An update. First part: Continental terranes
Jorge Julián RESTREPO and Jean–François TOUSSAINT 37

Chapter 4 Zircon U–Pb geochronology and Hf–Nd–O isotope geochemistry of the Paleo– to Mesoproterozoic basement in the westernmost Guiana Shield
Mauricio IBAÑEZ–MEJIA and Umberto G. CORDANI 65

Chapter 5 Neoproterozoic records of the Llanos Orientales Basin, Colombia
Hernando DUEÑAS–JIMÉNEZ and Jorge MONTALVO–JÓNSSON 91

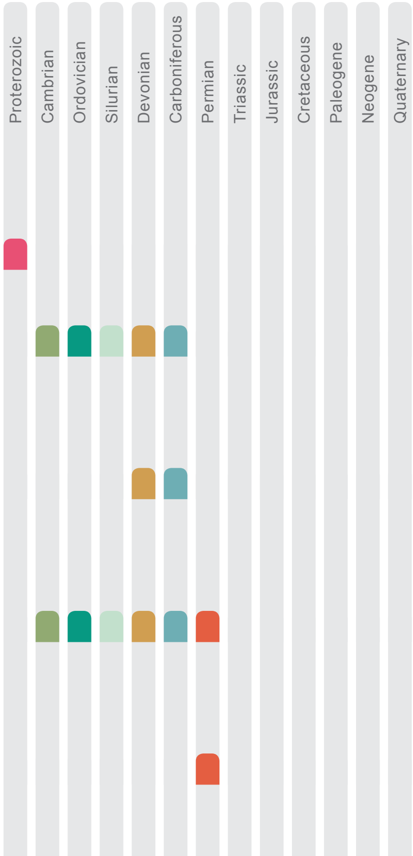

Chapter 6 The Putumayo Orogen of Amazonia: A synthesis
Mauricio IBAÑEZ–MEJIA 101

Chapter 7 Paleontology of the Paleozoic rocks of the Llanos Orientales Basin, Colombia
Hernando DUEÑAS–JIMÉNEZ, Victoria Elena CORREDOR–BOHÓRQUEZ, and Jorge MONTALVO–JÓNSSON 133

Chapter 8 The Anacona Terrane: A small early Paleozoic peri–Gondwanan terrane in the Cauca–Romeral Fault System
Jorge Julián RESTREPO, Uwe MARTENS, and Wilmer E. GIRALDO–RAMÍREZ 149

Chapter 9 Paleozoic of Colombian Andes: New paleontological data and regional stratigraphic review
Mario MORENO–SÁNCHEZ, Arley GÓMEZ–CRUZ, and José BUITRAGO–HINCAPIÉ 167

Chapter 10 Fragments of a Permian arc on the western margin of the Neoproterozoic basement of Colombia
Gabriel RODRÍGUEZ–GARCÍA, Ana María CORREA–MARTÍNEZ, Juan Pablo ZAPATA–VILLADA, and Gloria OBANDO–ERAZO 205

Contributing authors

Fernando Alirio ALCÁRCEL–GUTIÉRREZ
José BUITRAGO–HINCAPIÉ
Lorena Paola CARDENAS–ESPINOSA
Alejandra CARDONA–MAYORGA
Renato CORDANI
Umberto G. CORDANI
Ana María CORREA–MARTÍNEZ
Victoria Elena CORREDOR–BOHÓRQUEZ
Hernando DUEÑAS–JIMÉNEZ
Lisbeth FOG–CORRADINE
Wilmer E. GIRALDO–RAMÍREZ
Jorge GÓMEZ TAPIAS
Arley GÓMEZ–CRUZ
Mauricio IBAÑEZ–MEJIA
Norma Marcela LARA–MARTÍNEZ
Rubby Melissa LASSO–MUÑOZ
Eliana MARÍN–RINCÓN
María Paula MARROQUÍN–GÓMEZ
Uwe MARTENS
Daniela MATEUS–ZABALA
Jorge MONTALVO–JÓNSSON
Mario MORENO–SÁNCHEZ
Ismael Enrique MOYANO–NIETO
Alberto NÚÑEZ–TELLO
Gloria OBANDO–ERAZO
Diana Lorena OSPINA–MONTES
Ana Oliva PINILLA–PACHON
Gloria PRIETO–RINCÓN
Manuel Fernando PUENTES–TORRES
Miguel Gerardo RAMÍREZ–LEAL
Victor A. RAMOS
Jorge Julián RESTREPO
Gabriel RODRÍGUEZ–GARCÍA
Oscar Eduardo ROJAS–SARMIENTO
Andrés Felipe SALAMANCA–SAAVEDRA
Jean–François TOUSSAINT
Juan Pablo ZAPATA–VILLADA

Peer reviewers

María Beatriz AGUIRRE URRETA
Universidad de Buenos Aires

I. Yucel AKKUTLU
Texas A&M University

Marcelo Esteves ALMEIDA
Serviço Geológico do Brasil

Uwe ALTENBERGER
Universität Potsdam

Guillermo E. ALVARADO INDUNI
Universidad de Costa Rica

Sergio AMAYA–FERREIRA
Servicio Geológico Colombiano

Franck A. AUDEMARD M.
Fundación Venezolana de Investigaciones Sismológicas (Funvisis)

Claudio BARTOLINI
Repsol USA

Germán BAYONA
Corporación Geológica ARES

Hermann Darío BERMÚDEZ
Grupo de Investigación Paleoexplorer

Matthias BERNET
Université Grenoble Alpes

Idael Francisco BLANCO–QUINTERO
Universidad de Alicante

David M. BUCHS
Cardiff University

Grant M. BYBEE
University of the Witwatersrand

Agustín CARDONA
Universidad Nacional de Colombia Sede Medellín

Andrew CARTER
Birkbeck University of London

Octavian CATUNEANU
University of Alberta

John Franklin CERÓN ABRIL
Asociación Colombiana de Geólogos y Geofísicos del Petróleo

David M. CHEW
Trinity College Dublin

Umberto G. CORDANI
Universidade de São Paulo

Alexander CORREA METRIO
Universidad Nacional Autónoma de México

Carlos H. COSTA
Universidad Nacional de San Luis

Fabio Marco DALLA VECCHIA DALLA VIA
Institut Català de Paleontologia Miquel Crusafont (ICP)

Stanley C. FINNEY
California State University at Long Beach

Lêda Maria Barreto FRAGA
Serviço Geológico do Brasil

Julián GARCÍA MAYORDOMO
Instituto Geológico y Minero de España (IGME)

Carlos Alberto GUZMÁN LÓPEZ
Universidad de Caldas

Luis Felipe HINOJOSA OPAZO
Universidad de Chile

Gerardo HIRIART LE BERT
GeoKeri

Brian K. HORTON
University of Texas at Austin

Étienne JAILLARD
Institut des Sciences de la Terre (ISTerre)

James N. KELLOGG
University of South Carolina

Barry Paul KOHN
University of Melbourne

Salomon KROONENBERG
Delf University of Technology

Felipe LAMUS OCHOA
Universidad del Norte

Alberto LOBO–GUERRERO
LOGEMIN S.A.

Federico LUCCHI
Università di Bologna

Paul MANN
University of Houston

Luis C. MANTILLA FIGUEROA
Universidad Industrial de Santander (UIS)

María Isabel MARÍN CERÓN
Universidad Eafit

Foreword

Published online 24 November 2020

Over the last decades, geoscientific research in Colombia has grown exponentially as a result of modern geological, geochemical, geophysical, and geochronological research techniques; the establishment and access to national and international laboratories; the training and updating of professionals at the master's and doctorate levels in national and foreign institutions, together with the exchange between advanced institutions and researchers. The consequence of these positive developments has brought about an advance in the understanding of our national geology and the recognition of an urgent need to make known the geological knowledge of the country. It is also worth noting that, at present, there is no book that compiles what is known about the geology of Colombia, while other South American countries, Argentina for example, already have more than a dozen books dedicated to their national geology.

Faced with this situation, and true to its vision, the Servicio Geológico Colombiano (SGC), a government entity with more than 100 years serving the country and a leader in research and generation of geoscientific knowledge and nuclear applications, makes available to the scientific and citizenship of the world *The Geology of Colombia*. This editorial work contains updated geological knowledge of the Colombian territory and raises questions that must be resolved in the future about the geology of Colombia and about the setting of the northwestern South American subcontinent and the geological processes that transformed it from the Proterozoic to the Quaternary.

The contributions within this publication come from the results and conclusions of research projects completed or in development, and from activities of the SGC. These projects have been led by national and foreign researchers, together with their work groups, affiliated to public and private research and education institutions, as well as from different branches of industry, totaling 179 authors. This knowledge has an impact on the progress of Colombia and will thus be recognized nationally and internationally. It is necessary to highlight that with the publication of this work, studies that until now were unknown or difficult to access, mainly for the international academic community, are now made available.

With the future in mind, *The Geology of Colombia* should be seen as a strategic guide for scientific work, not only for the SGC, but for all institutions that have to do with research in the Earth sciences. The contents of this multivolume book will help to identify information gaps to guide projects that allow progress in the geoscientific knowledge of the nation's surface and subsurface, as well as the geological events that shape the territory and can affect the life of the communities settled upon it.

I invite readers to take advantage of this work that brings together, for the first time, the research of scientists who for years have dedicated their professional practice to the study of Colombian geology across different areas of work. This is a freely available work with quality content that was endorsed by the professional team that wrote, evaluated, and edited the chapters. I also invite you to enjoy the graphic quality of the work, the detail and care in the preparation of the graphic material, the detail of each illustration, and the beauty of the photographs included in the chapters, that are a faithful reflection of the magnificence of Colombian landscapes. For this reason, even though the work is a specialized technical text, it will be enjoyed by the Colombian who marvels at the country's natural wealth, as well as the global reader. The specialized reader of *The Geology of Colombia* will find in the work a starting point to discover not only the current state of knowledge, but also find the first works that allowed the study of events and features of Colombian geology, which are cited in the pages of this editorial work. The publication materialized from years of intellectual growth and effort and economic investment for the acquisition of geoscientific data.

I have no doubt that, with the delivery of this valuable work, the SGC will contribute to the economic activation and social progress of the country for the benefit of all Colombians and the global community. The contents of this work will help recognize areas with potential mineral, energy, geothermal, hydrocarbon, and groundwater resources, besides the planning and organization of the territory, the management of risks of geological origin, and the guidance of environmental management policies. This means the SGC will continue to promote knowledge that is transformed into action, action that is useful for the Colombian population, the main recipient of the services of this government entity.

Oscar PAREDES ZAPATA
Bogotá, 23 October 2020

Prefacio del director general del Servicio Geológico Colombiano

Published online 24 November 2020

En las últimas décadas, las investigaciones geocientíficas en Colombia han tenido un crecimiento exponencial como resultado de técnicas modernas de investigación geológica, geoquímica, geofísica y geocronológica; el establecimiento y acceso a laboratorios nacionales e internacionales; la formación y actualización de profesionales a nivel de maestría y doctorado en instituciones nacionales y extranjeras, así como el intercambio con instituciones e investigadores de avanzada. Este conjunto de aspectos positivos trajo como consecuencia un avance en el entendimiento de nuestra geología nacional y una apremiante necesidad de dar a conocer el conocimiento geológico del país. Vale la pena destacar además que, en la actualidad, no hay un libro que compile lo que se sabe sobre la geología de Colombia, mientras otros países suramericanos, Argentina por ejemplo, ya cuentan con más de una decena de libros dedicados a su geología nacional.

Frente a esta situación y fiel a su visión, el Servicio Geológico Colombiano (SGC), entidad pública con más de 100 años al servicio del país y líder en investigación y generación de conocimiento geocientífico y aplicaciones nucleares, pone a disposición de la comunidad científica y la ciudadanía *The Geology of Colombia*. Esta obra editorial contiene conocimiento geológico actualizado del territorio colombiano y plantea interrogantes que deberán ser resueltos en el futuro sobre la geología de Colombia y sobre la configuración del noroccidente del subcontinente suramericano y los procesos geológicos que lo transformaron desde el Proterozoico hasta el Cuaternario.

Las contribuciones de esta publicación provienen de los resultados y conclusiones de proyectos de investigación finalizados o en desarrollo y de actividades propias del SGC. Estos proyectos han sido liderados por investigadores nacionales y extranjeros, junto con sus grupos de trabajo, adscritos a instituciones públicas y privadas de investigación y educación, así como de diferentes ramas de la industria, que en total suman 179 autores. Este conocimiento tiene un impacto en el progreso de Colombia y así será reconocido a nivel nacional e internacional. Es necesario resaltar que con la publicación de esta obra se dan a conocer estudios que hasta el momento eran desconocidos o de difícil acceso principalmente para la comunidad académica internacional.

Pensando en el futuro, *The Geology of Colombia* debe ser vista como una guía estratégica del quehacer científico, no solo del SGC, sino de todas las instituciones que tienen que ver con investigación en ciencias de la Tierra. Los contenidos de la obra ayudarán a identificar vacíos de información para orientar los proyectos que permitan progresar en el conocimiento geocientífico del suelo y subsuelo de la nación, así como sobre los eventos geológicos que modelan el territorio y pueden afectar la vida de las comunidades asentadas en él.

Invito a los lectores a aprovechar esta obra que reúne por primera vez las investigaciones de científicos que por años han dedicado su ejercicio profesional al estudio de la geología colombiana desde diferentes áreas de trabajo. Esta es una obra multivolumen gratuita con contenidos de calidad que fueron avalados por el equipo profesional que escribió, evaluó y editó los capítulos. También, los invito a disfrutar la calidad gráfica de la publicación, el detalle y esmero en la preparación de cada gráfico e ilustración y la belleza de las fotografías contenidas en los capítulos, que son fiel reflejo de la magnificencia de los paisajes colombianos. Por esta razón, aun cuando la obra es un texto técnico especializado, será del disfrute del colombiano que se maravilla con las riquezas naturales del país, así como del lector internacional. El público especializado que lea *The Geology of Colombia* encontrará en la obra el punto de partida para descubrir no solo el estado de conocimiento actual, sino también los trabajos pioneros que permitieron emprender el estudio de los eventos y rasgos de la geología colombiana y que están citados en las páginas de la obra editorial. La publicación es la materialización de años de crecimiento intelectual y esfuerzo e inversión económica para la adquisición de información geocientífica.

No dudo que, con la entrega de este valioso documento, el SGC contribuirá a la activación económica y progreso social del país en beneficio de todos los colombianos y la comunidad internacional. Los contenidos de la obra ayudarán a identificar áreas con potencial de recursos minerales, energéticos, geotérmicos, hidrocarburos y aguas subterráneas, así como a la planeación y ordenación del territorio, la gestión de riesgos de origen geológico y la orientación de políticas de gestión ambiental. Quiere esto decir que el SGC seguirá promoviendo que el conocimiento se transforme en acción y que está acción sea de utilidad para la población colombiana, principal receptora de los servicios de esta entidad gubernamental.

Oscar PAREDES ZAPATA

Bogotá, 23 de octubre de 2020

Preface

Published online 24 November 2020

The Grupo Mapa Geológico de Colombia (GMGC) was formally created in 2004 and affiliated with the Dirección de Geociencias Básicas to produce periodic editions to the national geological map at different scales. Two map editions have since been produced, in 2007 and 2015. Accordingly, the GMGC has been gained an integral knowledge on Colombia geology and compiled the available scientific publications from indexed journals, conferences, and reports of the Servicio Geológico Colombiano (SGC). Therefore, the GMGC has one of the best databases on the geology of Colombia.

In 2015, the GMGC published the book *Compilando la geología de Colombia: Una visión a 2015*, together with the Geological Map of Colombia 2015. The book included an article entitled *Catálogo de dataciones radiométricas de Colombia en ArcGIS y Google Earth* that integrated radiometric ages —4427 ages— obtained up to 31 October 2014, throughout the country. The catalog served as a reference for the map and was made available to the geological community to further research and publications. The large number of isotopic datings in Colombia has mainly resulted from an increase in the number of master's and doctoral theses.

The GMGC's work was recognized in February 2010 by the appointment of the group coordinator, Jorge GÓMEZ TAPIAS, as the deputy secretary general for South America of the Comission for the Geological Map of the World. He immediately began codirecting the Geological Map of South America at a scale of 1:5 M that was published on 26 November 2019. The Commission's work forged relationships among prestigious researchers worldwide, many of whom served as reviewers for *The Geology of Colombia*. At the national level, beneficial relationships among Colombian and foreign researchers working in Colombia resulted from the organization of geological conventions, such as the XIV Congreso Latinoamericano de Geología and the XIII Congreso Colombiano de Geología in 2011 and the Simposio Servicio Geológico Colombiano: 100 años de producción científica al servicio de los colombianos in 2016.

In preparation of the Geological Map of South America, the Tectonic Evolution of the Andes Workshop was conducted by Professor Victor A. RAMOS from the Universidad de Buenos Aires, from 5 to 9 December 2016. During the workshop, Professor RAMOS received a copy of *Compilando la Geología de Colombia: Una visión a 2015* and straight away he expressed admiration for the numerous geological ages acquired for Colombia and the need for the country to have a Colombian geology book that would show the world the advanced state of knowledge and include the new data. This comment motivated the editorial initiative that the Grupo Mapa Geológico de Colombia led by Jorge GÓMEZ TAPIAS had been contemplating for years. The production of *The Geology of Colombia* was supported from its inception by Dr. Oscar PAREDES ZAPATA, the director general of the SGC.

At the beginning of January 2017, the GMGC was entrusted with the task of creating a book on the geology of Colombia. To carry out this titanic work, a multidisciplinary team of 11 young, enthusiastic professionals with high technical qualifications and agreeable personalities was formed who worked passionately and with dedication to bring the work to fruition.

The team became an editorial committee per se. It was established from the beginning that *The Geology of Colombia* would be published in English, be freely distributed, and contain contributions from several experts on specific topics and periods of geological time. In addition, the editorial project would include a social outreach component for the dissemination of scientific knowledge, which has been both an interest and a strength of the GMGC.

After four years of hard work, we delivered *The Geology of Colombia* in November 2020 to the national and international scientific community as 58 chapters distributed over four volumes, surpassing the initial goal of producing a single book with approximately 20 chapters. The book will be formally presented at Simposio *The Geology of Colombia*: La historia geológica del territorio colombiano, a free virtual event that will be held from 24 to 27 November 2020. Over four days of conferences, the authors will present the book chapters, and the Grupo Mapa Geológico de Colombia members will discuss their editorial contributions to *The Geology of Colombia*.

We are confident that this book will become a national geological reference because current Colombian geoscientific knowledge has been compiled following standard evaluation processes and international guidelines for graphic and textual editing. We hope that students who read the publication will be inspired to begin or continue studies to become outstanding professionals and lovers of national geology. We invite geoscientists to use this book as a starting point for developing new research, to fill in information gaps and to expand current discussions on the geological evolution of both the Colombian territory and its geotectonic framework. Beyond being a scientific work, *The Geology of Colombia* is produced by the SGC to further Colombians' knowledge and enjoyment of the territory.

Jorge GÓMEZ TAPIAS and Daniela MATEUS–ZABALA
Bogotá, 27 October 2020

Prefacio de los editores

Published online 24 November 2020

En 2004 se creó formalmente el Grupo Mapa Geológico de Colombia adscrito a la Dirección de Geociencias Básicas con el objetivo de realizar versiones periódicas y a diferentes escalas del mapa geológico nacional. Dos ediciones se han producido desde entonces, la primera en 2007 y la segunda en 2015. Esta labor le ha permitido al Grupo tener un conocimiento integral de la geología de Colombia y compilar los trabajos científicos publicados en revistas indexadas, congresos e informes del Servicio Geológico Colombiano (SGC). Es así como cuenta con una de las mejores bases de datos acerca de la geología de Colombia.

En 2015, junto con el Mapa Geológico de Colombia 2015, el Grupo publicó el libro *Compilando la geología de Colombia: Una visión a 2015* que incluía el artículo del "Catálogo de dataciones radiométricas de Colombia en ArcGIS y Google Earth". En este catálogo se integraron las edades radiométricas obtenidas hasta el 31 de octubre de 2014 a lo largo del territorio nacional, 4427 dataciones. El catálogo sirvió de soporte al mapa y se puso a disposición de la comunidad geológica como base para nuevas investigaciones y publicaciones. El crecimiento en el número de dataciones realizadas en el país se ha dado principalmente por el aumento en la cantidad de tesis a nivel de maestría y doctorado.

Como un reconocimiento a la labor del Grupo Mapa Geológico de Colombia, en febrero de 2010, Jorge GÓMEZ TAPIAS, coordinador del equipo, fue nombrado como secretario general adjunto para Suramérica de la Comisión del Mapa Geológico del Mundo y de inmediato empezó a codirigir el Mapa Geológico de Suramérica a escala 1:5 000 000 que se publicó el 26 de noviembre de 2019. El trabajo en la comisión ha permitido establecer relaciones con investigadores extranjeros reconocidos a nivel mundial, muchos de los cuales se desempeñaron como revisores de la obra *The Geology of Colombia*. También, a nivel nacional se han establecido buenas relaciones con los investigadores colombianos y extranjeros que trabajan particularmente en Colombia, gracias a la organización de eventos geológicos como el XIV Congreso Latinoamericano de Geología y el XIII Congreso Colombiano de Geología en 2011 y el Simposio Servicio Geológico Colombiano: 100 años de producción científica al servicio de los colombianos en 2016.

Para la realización del Mapa Geológico de Suramérica, del 5 al 9 de diciembre de 2016, se realizó el Taller evolución tectónica de los Andes con el profesor Victor A. RAMOS de la Universidad de Buenos Aires. Durante este evento, el profesor RAMOS recibió copia del libro *Compilando la Geología de Colombia: Una visión a 2015* y de inmediato manifestó su admiración por la cantidad de edades que se habían adquirido en Colombia y la necesidad de que el país contara con un libro de geología colombiana que le mostrara al mundo el estado avanzado de conocimiento y que incluyera los nuevos datos. Fue así como se gestó la iniciativa editorial que el Grupo Mapa Geológico de Colombia bajo la coordinación de Jorge GÓMEZ TAPIAS había tenido en mente desde años atrás. La producción de *The Geology of Colombia* fue apoyada desde el inicio por el doctor Oscar PAREDES ZAPATA, director general del SGC.

A comienzos de enero de 2017 le fue encomendada la tarea de realizar el libro de geología de Colombia al Grupo Mapa Geológico de Colombia. Para llevar a cabo esta titánica labor se conformó un equipo multidisciplinario, joven y entusiasta de 11 profesionales con altas calidades técnicas y humanas que trabajaron con pasión y esmero para sacar la obra a flote.

El equipo se convirtió en un comité editorial *per se*. Desde el inicio se estableció que la obra *The Geology of Colombia* sería en inglés, de distribución gratuita y escrita a varias manos por expertos en temas y períodos del tiempo geológico específicos. Además, se definió que el proyecto editorial llevaría una componente de apropiación social del conocimiento científico, que ha sido uno de los intereses y fortalezas del Grupo Mapa Geológico de Colombia.

En noviembre de 2020, después de cuatro años de ardua labor entregamos la obra *The Geology of Colombia* a la comunidad científica nacional e internacional con 58 capítulos distribuidos en 4 volúmenes, superando la meta inicial de producir un solo libro con alrededor de 20 capítulos. La entrega formal de la publicación se realizará a través del *Simposio The Geology of Colombia: La historia geológica del territorio colombiano*, un evento virtual gratuito a realizarse del 24 al 27 de noviembre de 2020. En cuatro días de conferencias, los autores presentarán los capítulos de la obra y los miembros del Grupo Mapa Geológico de Colombia el trabajo editorial detrás de *The Geology of Colombia*.

Estamos seguros que esta obra se convertirá en un referente de la geología nacional, porque además de reunir el estado del conocimiento geocientífico colombiano, se realizó siguiendo procesos estándar de evaluación y pautas internacionales de edición gráfica y textual. Deseamos que los estudiantes que lean la publicación encuentren en ella la motivación para iniciar o continuar los estudios que les permitirán a futuro desempeñarse como profesionales destacados y amantes de la geología nacional. A los profesionales invitarlos a que esta publicación sea el punto de partida para el desarrollo de nuevas investigaciones, para determinar los vacíos de información y para ampliar las discusiones actuales sobre la evolución geológica no solo del territorio colombiano, sino también de su marco geotectónico. Más allá de ser una obra científica, *The Geology of Colombia* es una publicación producida por el SGC para el conocimiento del territorio y disfrute de los colombianos.

Jorge GÓMEZ TAPIAS y Daniela MATEUS–ZABALA

Bogotá, 27 de octubre de 2020

Prologue

https://doi.org/10.32685/pub.esp.35.2019.Prologue
Published online 12 November 2020

This work marks a fundamental milestone in the geological knowledge of Colombia. This work is the result of four years of intense work by the editors Jorge GÓMEZ TAPIAS and Daniela MATEUS ZABALA and a small group of collaborators who, through the Servicio Geológico Colombiano, present the work ***The Geology of Colombia***. These four volumes would not have been completed without the firm support of Dr. Oscar PAREDES ZAPATA, who, as director of the Servicio Geológico Colombiano, provided the material and human resources that made this work a success.

Previous attempts to compile the vast knowledge of fascinating Colombian geology have been incomplete. The *Evolución geológica de Colombia* carried out by Jean–François TOUSSAINT between 1993 and 1999 was a great and highly commendable effort by a single author. The partial syntheses made by Fabio CEDIEL and collaborators in 2003 and the most recent version edited by CEDIEL and SHAW (2019) *Geology and Tectonics of Northwestern South America* were outstanding efforts. The 2006 publication *Tectonic Evolution of the Colombian Andes* in a special issue of the *Journal of South American Earth Sciences,* which we edited with Manuel MORENO, was another important intent written almost entirely by Colombian geologists.

This work is more significant compared to previous geologic summaries. The present legion of geologists and geophysicists contributed their regional expertise and specialties to thoroughly represent the current geological knowledge of the country. Participation from academia and industry shows that Colombian geology is vigorous and active.

The editorial treatment of the chapters and their peer evaluation, the professional presentation of figures and maps, the style corrections, and the final layout of each chapter further enhance the already important scientific value of all the contributions.

At times like these, we should remember the observations and work of those who laid the foundations of our present knowledge. As a scholar and observer of the Andes who is located more than 6000 km away, I consider myself privileged to have been able to follow the evolution of that knowledge through the decades. First, I would like to remember Paul GANSSER (1910–2012), who after his successful investigations in the Himalayas, landed in Colombia and performed fundamental studies during the 1930s and 1940s, leaving us his *Facts and Theories on the Andes* of 1973. In this work, he first divided the Andes based on plate tectonics, a division that is still used by Andean geologists. In the following decade, we participated in a nearly month–long field trip to Antarctica, where we and Paul GANSSER discussed his explanations of the complex structure of the Colombian Andes. These talks were in correct Spanish and full of incredible stories and anecdotes. I also would like to recall the works of Jacques BOURGOIS and collaborators, who unraveled the complex structure of ophiolites in a sector of the Western Cordillera. We shared discussions during several Andean symposia with François MÉGARD, another great promoter of Colombian tectonic evolution with his models of the Mesozoic – Cenozoic island arc accretion by reverse subduction and collision. Another person who introduced me to this fascinating geology was Professor Manuel JULIVERT, who in his visits to Buenos Aires, described the structural geology of the Eastern Cordillera fold belts. His experience was obtained through several years of teaching and research at the Universidad Industrial de Santander and the Universidad Nacional Sede Bogotá between 1957 and 1963. His work on *Cover and Basement Tectonics in the Cordillera Oriental of Colombia, South America, and a Comparison with Some Other Folded Chains* pre–dated by several years the acceptance of tectonic inversion as a structural style. This group of colleagues, and others, introduced me to exciting Colombian geology.

However, the person most responsible for me being here today is Dr. Umberto CORDANI, a great promoter of the geochronology of Colombia and editor of the *Tectonic Evolution of South America*, on the occasion of the International Geological Congress held in Rio de Janeiro in 2000. CORDANI telephoned me to tell me that he had to send this book to the printer but the Northern Andes chapter was missing; the invited authors had not provided their work. We met with my colleague and friend Antenor ALEMÁN in Houston, and in a few days, we prepared the chapter that awakened my curiosity about the geology of the Colombian Andes.

I learned from the pioneering studies of Darío BARRERO to recognize oceanic rocks in the Western Cordillera and about their accretion in the Late Cretaceous. From Alberto FORERO SUÁREZ I learned about the North American affinities of the Eastern Cordilleran basement terrane and the Laurentian influence of the associated Paleozoic basins. While sharing a room at a symposium in Medellín, Hermann DUQUE CARO and I had long conversations about the collision of the Chocó terrane and the determination of its age through precise micropaleontological analyses. Jorge RESTREPO and Jean–François TOUSSAINT taught me the complex accretion history of Colombia during the Magmatic Evolution of the Andes (IGCP–Unesco) symposia, and on a visit to Arizona, I learned about the isotopic interactions between Colombia and southern México blocks from Joaquín RUIZ.

These initial encounters showed me the complex problems of Colombian geology, and our new work *The Geology of Colombia* shows how much our knowledge has increased.

Numerous novelties are presented as reviews or original works in different chapters. One example is the precise geochronological determinations of the Putumayo Orogen, which changed our vision of the ancient Orinoquensis Orogeny by showing different ages and orogenic belts on the western margin of the Guiana Shield. Another example is the new ages of the Andean Proterozoic basement, which suggest a complex paleogeographic history.

The analysis of Paleozoic terranes and their paleogeographic distribution reaffirms the previously defined limits of these allochthonous blocks. However, new geochronological data allow us to re–evaluate Famatinian tectogenesis. Successive chapters show the dynamics of the Eopaleozoic accretion of Chibcha in the Late Ordovician and its influence on the distribution of Devonian and Neopaleozoic faunas with clear Laurentic affinities.

The increasing identification of a Permian magmatic arc in the Central Cordillera deserves to be mentioned since its obliteration by deformation and superimposed metamorphism makes it hard to identify. This destruction prevents an assessment of the vergence of deformation or metamorphism that could associate the magmatic arc with the Alleghanides Orogeny.

Later anathectic processes culminated in a Triassic extension, which is widely distributed along the Paleozoic continental proto–margin, with a strong presence in the Central Cordillera.

Jurassic evolution shows a complex paleogeography driven by the interaction between different Caribbean and Pacific Plates. The combination of paleomagnetic data, detrital zircon provenance studies, structural analysis, and the evolution of the Jurassic and Early Cretaceous magmatic arcs show different episodes controlled by the subduction kinematics along the Pacific margin.

Special mention should be made of the analyses showing the transition from an early Mesozoic extensional subduction regime to a compressive regime. For the first time, this important change is associated with the dynamics of the continental margin. Provenance studies in developed basins, the characteristics of their magmatic arcs, and the associated deformation allow us to explain the distribution of their deposits.

New dates, petrological analysis, and geochemical characterization of the accreted ocean terranes on the Pacific margin, highlight the processes that constructed the new margin. The characterization of areas with significant high–pressure metamorphism sheds light on their common characteristics and differences.

Studies on the source and provenance of the synorogenic deposits in the Eastern Cordillera and interpretation of their uplift history through fission track analysis allow different chapters to reconstruct the tectonic evolution of this Andean region.

Analysis of Pacific margin basins and Caribbean margin Cenozoic belts shows interaction mechanics in the accretionary prisms of the Farallón and Nazca Plates as well as the deformation from the passage of the Caribbean Plate through northern South America. The interaction of the Isthmus of Panamá and the South American continent deserves special attention because it shows connections prior to the collision of the Chocó Block and before the great faunal exchange.

Sedimentological studies and assessment of oleogenetic potential of the sedimentary sequences provide essential information to enhance the hydrocarbon value of these basins.

Analyses of the Cenozoic volcanic arc and presentation of the active Western and Central Cordilleran volcanic centers show the recent evolution of knowledge and the influence of Caldas Tear on the development. Geophysical and geothermal studies in the northern region of Eastern Cordillera show the hydrothermal processes associated with acidic volcanism and the remnants of the foreland migrated late Cenozoic arc.

Analyses of Quaternary sedimentation, neotectonic structures, and the evolution of the tropical biome are presented in an interrelated way, allowing them to be linked to global events that affected the entire continent.

A detailed reading of this work demonstrates the rapid advance of geological knowledge in recent years, the dynamic evolution of concepts with the application of new technologies and the degree of specialization obtained in different disciplines. The different presentations through successive chapters show us that old problems and questions have been solved, while the information provided illuminates new unknowns and opens up new challenges.

I would like to again congratulate the editors, editorial group, and numerous authors for their effort, which will undoubtedly be a difficult milestone to surpass in the advancement Colombian geologic knowledge.

Victor A. RAMOS
Buenos Aires, 3 November 2020

Prólogo

https://doi.org/10.32685/pub.esp.35.2019.Prologue
Published online 12 November 2020

La presente obra marca un hito fundamental en el conocimiento geológico de Colombia. Es el resultado de cuatro años de intenso trabajo de los editores Jorge GÓMEZ TAPIAS y Daniela MATEUS ZABALA y un reducido grupo de colaboradores, a través del Servicio Geológico Colombiano, que permite hoy presentar ***The Geology of Colombia***. Los esfuerzos realizados no hubieran cristalizado en estos cuatro completos volúmenes sin el firme apoyo del dr. Oscar PAREDES ZAPATA, quien como director del Servicio Geológico Colombiano procuró los medios materiales y humanos para el éxito de esta obra.

Si bien ha habido algunos intentos previos de reunir el vasto conocimiento que se tenía de la fascinante geología colombiana, estos han sido parciales o incompletos. La *Evolución geológica de Colombia* realizada por Jean–François TOUSSAINT entre 1993 y 1999 fue un gran esfuerzo de único autor, lo cual es muy loable. La síntesis realizada por Fabio CEDIEL y colaboradores en 2003 y la más reciente editada por CEDIEL y SHAW (2019) *Geology and Tectonics of Northwestern South America* fueron esfuerzos parciales destacados. La publicación de *Tectonic Evolution of the Colombian Andes*, editado por Manuel MORENO y quien subscribe en 2006, como número especial del *Journal of South American Earth Sciences* fue otra importante contribución escrita casi en su totalidad por geólogos colombianos.

Cuando se comparan estos intentos de resumir la geología de Colombia se realza aún más el valor de la presente obra. Toda una legión de geólogos y geofísicos contribuyó con su experticia regional y especialidad a la comprehensión cabal del conocimiento geológico actual del país. Participaron autores de diferentes instituciones, tanto académicas como de la industria, lo que nos muestra en conjunto lo pujante y activa que está la geología colombiana.

El tratamiento editorial de los capítulos y su evaluación por pares, la presentación profesional de las figuras y mapas, las correcciones de estilo y la compaginación final y acabada de cada capítulo valorizan aún más el ya importante valor científico de las distintas contribuciones.

En momentos como estos es necesario también recordar a quienes han contribuido en el pasado cercano, con sus observaciones y trabajos a través de los años, a sentar las bases del presente conocimiento. Como estudioso y observador de los Andes, ubicado a más de 6000 km de distancia, me considero un espectador privilegiado que a través de décadas ha podido seguir la evolución de ese conocimiento. En primer lugar, me gustaría recordar a Paul GANSSER (1910–2012) que después de sus exitosas investigaciones en los Himalayas recaló en Colombia e hizo estudios fundamentales durante las décadas del 30 y el 40 dejándonos como legado su *Facts and Theories on the Andes* de 1973. En esta obra hace la primera división de los Andes basada en la tectónica de placas, división que aún se usa por geólogos andinos. En la década siguiente participamos en un *fieldtrip* a la Antártida de casi un mes de duración donde compartíamos con Paul GANSSER, todas las noches, sus explicaciones de la compleja estructura de los Andes colombianos. Estas charlas fueron en un correcto español y llenas de historias y anécdotas increíbles. Deseo recordar los trabajos de Jacques BOURGOIS y colaboradores, quienes desentrañaron la compleja estructura de las ofiolitas de un sector de la cordillera Occidental. Compartimos discusiones durante varios simposios andinos con François MÉGARD, otro gran divulgador de la evolución tectónica de Colombia con sus modelos de acreción por subducción reversa de los arcos de islas mesozoicos–cenozoicos y sus colisiones. La otra persona que me fue introduciendo a esta fascinante geología fue el profesor Manuel JULIVERT, quien en sus visitas a Buenos Aires nos describía la geología estructural de los cinturones de plegamiento de la cordillera Oriental. Obtuvo su experiencia a través de varios años de docencia e investigación en la Universidad Industrial de Santander y la Universidad Nacional de Colombia Sede Bogotá entre 1957 y 1963. Su trabajo sobre *Cover and Basement Tectonics in the Cordillera Oriental of Colombia, South America, and a Comparison with Some Other Folded Chains* se anticipó varios años a la aceptación de la inversión tectónica como estilo estructural. Este grupo de colegas, entre otros, me introdujeron a la apasionante geología colombiana.

Sin embargo, el responsable de que yo esté hoy acá es el dr. Umberto CORDANI. Él es un gran propulsor de la geocronología de Colombia y editor de una magna obra: *Tectonic Evolution of South America,* en ocasión del Congreso Geológico Internacional realizado en Río de Janeiro en el año 2000. CORDANI me llamó por teléfono para decirme que tenía que mandar el libro a la imprenta y le faltaba el capítulo *"Northern Andes",* dado que los autores invitados no habían cumplido. Nos reunimos con mi colega y amigo Antenor ALEMÁN en Houston y en unos pocos días preparamos ese capítulo que terminó de despertar mi curiosidad por la geología de los Andes colombianos.

Aprendí de los pioneros estudios de Darío BARRERO el reconocimiento de las rocas oceánicas en la cordillera Occidental y su acreción en el Cretácico Tardío; de Alberto FORERO SUÁREZ, las afinidades norteamericanas del basamento de la cordillera Oriental y la influencia lauréntica de las cuencas paleozoicas asociadas; de Hermann DUQUE CARO, en largas conversaciones en un simposio en Medellín, la colisión del terreno de Chocó y sus edades a través de sus precisos análisis micropaleontológicos; de Jorge RESTREPO y Jean–François TOUSSAINT, la compleja historia de acreción de Colombia a través de los simposios de *Magmatic Evolution of the Andes* (IGCP–Unesco), y de Joaquín RUIZ, en una visita a Arizona, las conexiones isotópicas e interacciones entre Colombia y los diferentes bloques del sur de México.

Estos encuentros iniciales me mostraron la compleja geología colombiana y los numerosos problemas pendientes que al ser contrastados con los resultados de *The Geology of Colombia* nos dejan con una fuerte admiración por el salto conceptual en el nivel de conocimiento puesto en esta obra.

En ella numerosas novedades son presentadas como revisiones o trabajos originales a través de los diferentes capítulos. Por ejemplo, las precisas determinaciones geocronológicas del Orógeno Putumayo, que han cambiado nuestra visión de esa antigua Orogenia Orinoquensis al mostrar diferentes edades y cinturones orogénicos en el margen occidental del Escudo de Guayana. Otro ejemplo corresponde a las nuevas edades del basamento proterozoico de los Andes, que sugieren una compleja historia paleogeográfica.

El análisis de los terrenos paleozoicos y su distribución paleogeográfica reafirma las pioneras identificaciones de los límites de estos bloques alóctonos. Sin embargo, los nuevos datos geocronológicos permiten revalorizar la tectogénesis famatiniana. Sucesivos capítulos muestran la dinámica de la acreción eopaleozoica de Chibcha en el Ordovícico Tardío y su control en la distribución de las faunas devónicas y neopaleozoicas posteriores de netas afinidades laurénticas.

Una mención destacada merece la identificación de un arco magmático de edad pérmica que, obliterado por deformaciones y metamorfismos sobrepuestos, va incrementando su representación en la cordillera Central. Los relictos de este arco impiden aún una valoración de la vergencia de la deformación o metamorfismo para asociarlos a la Orogenia de los Alleghánides.

Los procesos anatécticos posteriores que culminaron con la extensión triásica están ampliamente distribuidos a lo largo del antiguo margen continental paleozoico con fuertes evidencias en la cordillera Central.

La evolución jurásica muestra una compleja paleogeografía dada por la interacción entre diferentes placas de las regiones caribeña y pacífica. La combinación de datos paleomagnéticos, estudios de procedencia a través de circones detríticos, análisis de las estructuras y la evolución de los arcos magmáticos del Jurásico y Cretácico Temprano permitieron reconocer diferentes episodios controlados por la cinemática de la subducción a lo largo del margen pacífico.

Una mención especial merecen los análisis presentados de la transición de un régimen de subducción extensional del Mesozoico temprano a un régimen compresivo. Por primera vez se asocia este importante cambio a la dinámica del margen continental. Los estudios de procedencia en las cuencas desarrolladas, las características de sus arcos magmáticos y la deformación asociada permiten explicar la distribución de sus depósitos.

La acreción de los terrenos oceánicos sobre el margen pacífico y la caracterización petrológica y geoquímica de estas rocas, junto a nuevas dataciones, ponen en valor los procesos que llevaron a la construcción del nuevo margen. La caracterización de las distintas zonas con importante metamorfismo de alta presión arroja luz en sus características comunes y diferencias.

Los estudios sobre la fuente y procedencia de los depósitos sinorogénicos en la cordillera Oriental y la interpretación de su historia de levantamiento mediante análisis de trazas de fisión permiten en diferentes capítulos reconstruir la evolución tectónica de los Andes a estas latitudes.

El análisis de las cuencas del margen pacífico y de los cinturones cenozoicos del margen caribeño muestra la mecánica de interacción de las placas de Farallón y de Nazca en los prismas de acreción, así como la deformación asociada al pasaje de la placa caribeña por el norte de Suramérica. Una atención especial merece la interacción del Istmo de Panamá con el continente sudamericano porque muestra conexiones previas a la colisión del Bloque Chocó y al gran intercambio faunístico.

Los estudios sedimentológicos y la evaluación del potencial oleogenético de las secuencias sedimentarias brindan información esencial para la puesta en valor de los hidrocarburos en las cuencas analizadas.

El análisis del arco volcánico cenozoico y la presentación de los centros volcánicos activos ubicados tanto en la cordillera Occidental como en la cordillera Central muestran la evolución del conocimiento obtenido en estos últimos años y la influencia del Caldas Tear en su desarrollo. Los estudios geofísicos y geotérmicos realizados en el sector norte de la cordillera Oriental iluminan los procesos hidrotermales asociados al volcanismo ácido remanente del arco cenozoico tardío migrado al antepaís.

El análisis de la sedimentación cuaternaria, las estructuras neotectónicas y la evolución del bioma tropical son presentados en forma interrelacionada, lo que permite vincularlos con los acontecimientos globales que afectan a todo el continente.

Una lectura detallada de esta obra demuestra el rápido avance del conocimiento geológico en los últimos años, la dinámica evolución de los conceptos ante la aplicación de nuevas tecnologías y el grado de especialización obtenido en las diferentes disciplinas. Las distintas presentaciones a través de sucesivos capítulos nos muestran que se han solucionado viejos problemas e interrogantes, a la vez que la información brindada ilumina nuevas incógnitas y abre nuevos desafíos para el conocimiento.

Solo queda felicitar una vez más a los editores y grupo editorial y a los numerosos autores por el esfuerzo desarrollado, que sin lugar a dudas será un hito difícil de superar en el avance del conocimiento de la geología colombiana.

Victor A. RAMOS
Buenos Aires, 3 de noviembre de 2020

Presentation of *The Geology of Colombia*

https://doi.org/10.32685/pub.esp.35.2019.Presentation

Published online 24 November 2020

Jorge GÓMEZ TAPIAS[1*], Daniela MATEUS–ZABALA[2], Ana Oliva PINILLA–PACHON[3], Alberto NÚÑEZ–TELLO[4], Rubby Melissa LASSO–MUÑOZ[5], Fernando Alirio ALCÁRCEL–GUTIÉRREZ[6], Eliana MARÍN–RINCÓN[7], María Paula MARROQUÍN–GÓMEZ[8], Lisbeth FOG–CORRADINE[9], Alejandra CARDONA–MAYORGA[10], and Miguel Gerardo RAMÍREZ–LEAL[11]

Abstract The number of research papers and brand new geoscientific data of the Colombian territory has increased progressively in recent years. This has generated the rise of new hypotheses to explain the origin of what is now Colombia, but also the updating of pioneering ideas. This fact, added to the need to gather the increasing amount of information produced by different areas of the Earth sciences, encouraged the Servicio Geológico Colombiano to edit the first scientific book about The Geology of Colombia. The aim of this chapter is to describe The Geology of Colombia in terms of how the editorial process was outlined, the main issues considered to improve texts and figures, and the content the reader will find in each chapter. It also presents the scientific outreach strategy designed paralleled to the editorial process which includes two audiences mainly: one created for scientists based on topical sessions related to the geology of Colombia and oral presentations in scientific conferences, and secondly a strategy aimed at the general public which consisted in writing stories that were published in national and local newspapers, and producing multimedia content for social media and the web page. As a result, the editorial work presented in four volumes includes 58 chapters, almost three times the initial projection, written by 179 researchers and edited according to the international quality standards. On the other hand, the number of readers of the articles published in the newspapers as well as the engagement of the social media content by diverse audiences reflects the multidisciplinary and well–oriented work during the process.

Keywords: *Colombian geology, editorial process, editing figures, scientific outreach.*

Resumen El número de investigaciones y nuevos datos geocientíficos del territorio colombiano ha aumentado progresivamente en los últimos años. Esto ha generado el surgimiento de recientes hipótesis para explicar la formación de lo que hoy es Colombia, pero también la actualización de las ideas pioneras. Este hecho sumado a la necesidad de reunir el volumen creciente de información que se produce desde diferentes áreas de las ciencias de la Tierra llevó al Servicio Geológico Colombiano a producir la primera obra editada sobre la geología nacional: *The Geology of Colombia*. El objetivo con este capítulo es presentar qué es *The Geology of Colombia*, cómo fue

Citation: Gómez, J., Mateus–Zabala, D., Pinilla–Pachon, A.O., Núñez–Tello, A., Lasso–Muñoz, R.M., Alcárcel–Gutiérrez, F.A., Marín–Rincón, E., Marroquín–Gómez, M.P., Fog–Corradine, L., Cardona, A. & Ramírez, M.G. 2020. Presentation of The Geology of Colombia. In: Gómez, J. & Mateus–Zabala, D. (editors), The Geology of Colombia, Volume 1 Proterozoic – Paleozoic. Servicio Geológico Colombiano, Publicaciones Geológicas Especiales 35, p. xxix–lxxii. Bogotá. https://doi.org/10.32685/pub.esp.35.2019.Presentation

1 mapageo@sgc.gov.co
Servicio Geológico Colombiano
Dirección de Geociencias Básicas
Grupo Mapa Geológico de Colombia
Diagonal 53 n.° 34–53
Bogotá, Colombia

2 dmateus@sgc.gov.co
Servicio Geológico Colombiano
Dirección de Geociencias Básicas
Grupo Mapa Geológico de Colombia
Diagonal 53 n.° 34–53
Bogotá, Colombia

3 aopinillap@unal.edu.co
Servicio Geológico Colombiano
Dirección de Geociencias Básicas
Grupo Mapa Geológico de Colombia
Diagonal 53 n.° 34–53
Bogotá, Colombia

4 anunez@sgc.gov.co
Servicio Geológico Colombiano
Dirección de Geociencias Básicas
Grupo Mapa Geológico de Colombia
Diagonal 53 n.° 34–53
Bogotá, Colombia

5 mlasso@sgc.gov.co
Servicio Geológico Colombiano
Dirección de Geociencias Básicas
Grupo Mapa Geológico de Colombia
Diagonal 53 n.° 34–53
Bogotá, Colombia

6 falcarcel@sgc.gov.co
Servicio Geológico Colombiano
Dirección de Geociencias Básicas
Grupo Mapa Geológico de Colombia
Diagonal 53 n.° 34–53
Bogotá, Colombia

7 emarinr@sgc.gov.co
Servicio Geológico Colombiano
Dirección de Geociencias Básicas
Grupo Mapa Geológico de Colombia
Diagonal 53 n.° 34–53
Bogotá, Colombia

8 mpmarroquin@sgc.gov.co
Servicio Geológico Colombiano
Dirección de Geociencias Básicas
Grupo Mapa Geológico de Colombia
Diagonal 53 n.° 34–53
Bogotá, Colombia

9 lisfog@yahoo.com
Servicio Geológico Colombiano
Dirección de Geociencias Básicas
Grupo Mapa Geológico de Colombia
Diagonal 53 n.° 34–53
Bogotá, Colombia

10 acardona@sgc.gov.co
Servicio Geológico Colombiano
Dirección de Geociencias Básicas
Grupo Mapa Geológico de Colombia
Diagonal 53 n.° 34–53
Bogotá, Colombia

11 mramirezl@sgc.gov.co
Servicio Geológico Colombiano
Dirección de Geociencias Básicas
Grupo Mapa Geológico de Colombia
Diagonal 53 n.° 34–53

* Corresponding author

Supplementary Information:

S1: https://www2.sgc.gov.co/LibroGeologiaColombia/tgc/sgcpubesp352019Presentations1.pdf

S2: https://www2.sgc.gov.co/LibroGeologiaColombia/tgc/sgcpubesp352019Presentations2.pdf

S3: https://www2.sgc.gov.co/LibroGeologiaColombia/tgc/sgcpubesp352019Presentations3.pdf

S4: https://www2.sgc.gov.co/LibroGeologiaColombia/tgc/sgcpubesp352019Presentations4.ens

S5: https://www2.sgc.gov.co/LibroGeologiaColombia/tgc/sgcpubesp352019Presentations5.pdf

el proceso editorial para su producción, cuáles son los principales aspectos que se consideraron para la mejora de textos y figuras y qué se puede encontrar en cada capítulo. Adicionalmente, se presenta la estrategia de divulgación científica que se realizó junto con el proceso editorial. La estrategia se dirigió a público especializado a través de la organización de sesiones técnicas sobre geología de Colombia y la presentación de conferencias en encuentros científicos y a público lego con la creación de contenidos de texto y multimedia que se publicaron en periódicos de circulación nacional, revistas, radio y en redes sociales y página web. El resultado de este trabajo editorial y de divulgación se ve reflejado en la producción de 58 capítulos, cerca del triple de capítulos proyectados durante la fase inicial del proyecto, que fueron escritos por 179 geocientíficos y editados siguiendo estándares internacionales de calidad. También, se refleja en los resultados positivos de la estrategia de divulgación para público lego: número de lectores de artículos periodísticos, alcance de las publicaciones en redes sociales, entre otros, que fueron posibles gracias al trabajo multidisciplinar y orientado durante la elaboración y publicación del contenido.

Palabras claves: *geología colombiana, proceso editorial, edición de figuras, divulgación científica.*

1. Introduction

Since its creation in 1916, the Servicio Geológico Colombiano (SGC) has been in charge of the research and publication of official geological information to support the development of state policies. With this aim, the SGC generates and makes available to the community scientific information related to the processes that occur inside the Earth and the external processes that shape the landscape of the Colombian territory. This information is useful for the planning and progress of the country, constituting one of the essential pillars for the balanced and sustainable development of Colombia, as expressed in the "Plan estratégico del conocimiento geológico del territorio colombiano 2014–2023" presented by the SGC.

With this approach and in light of the recent increase in the production of geoscientific information due to technological advances and accessibility of various analytical methods, the SGC considered it timely to compile the work *The Geology of Colombia*. This multivolume book includes the geological history of Colombia from the Proterozoic to the Quaternary and aligns with SGC's goal of generating and providing high–quality and sufficient knowledge. *The Geology of Colombia* reports updates on the main paradigms of regional geology and unpublished research and data that have not been released to the international geoscientific community. These factors account for the progress in the knowledge of the geology of the country and the development and implementation of new tools and technologies for Earth science research applied to the national territory.

The Geology of Colombia presents information on the regional geology of the country, local geological events of international interest, and contributions and results of some of the projects carried out by the SGC. This knowledge is fundamental to the management and planning of the territory and to compliance with the mining–energy and water demands, among others, for economic revival. The work also highlights the development and level of geoscientific research in Colombia. Through this publication, numerous research proposals and possibilities for establishing agreements and collaborations that strengthen geological research processes and encourage the training of Colombian geoscientists will emerge. Due to the type of information presented in the publication, will become a reference for those interested in Colombian regional geology as well as for those who study the geological evolution of the northern Andes.

Fifty–eight chapters distributed in four volumes make up *The Geology of Colombia*. Volume 1 brings together research on the events that occurred during the Proterozoic – Paleozoic; volume 2 deals with the Mesozoic geological history of the Colombian territory; volume 3 compiles Paleogene to Neogene events and record; and volume 4 groups research on the most recent processes (those that occurred during the Quaternary) and modern analytical techniques and national territory data acquired by the SGC in recent years. *The Geology of Colombia* is an edited, peer–reviewed editorial work written in English, the communication channel of the international scientific community. The chapters are presented in the same format in which research papers are delivered for discussion and debate: scientific articles.

The authors of *The Geology of Colombia* are geoscientists specializing in the study of processes, events, and geological features of the Colombian territory. Because the current level of knowledge in geology makes it impossible for books to be written by a single author, the SGC brought together renowned researchers who have worked in different areas of the country to produce a book written from various areas of geoscientific knowledge. In total, 179 researchers participated as authors representing 12 countries: Colombia, Argentina, Brasil, España, Switzerland, Germany, the United States of America, Sweden, the United Kingdom, France, Japan, and the Netherlands. They also represent 55 national and international institutions, including research institutes, universities, academies, public institutions, and private and mixed companies. Fifteen of the twenty researchers with the highest h–index who publish on Colombian geology, according to Scopus, are authors of *The Geology of Colombia*. The h–index is understood as a numerical value that scores both the number of publications of a researcher and the impact or number of citations of their work.

The editorial group consisted of eight geoscientists, a graphic designer, an audiovisual producer, and a scientific journalist from the Grupo Mapa Geológico de Colombia of the SGC. This group led the two editions of the Geological Map of Colombia at a scale of 1:1 M, versions 2007 (Gómez et al., 2007) and 2015 (Gómez et al., 2015); the Geological Map of South America at a scale of 1:5 M published in 2019 (Gómez et al., 2019), and the production and editing of several scientific publications and scientific outreach, including the book *Compilando la geología de Colombia: Una visión a 2015* (Gómez & Almanza, 2015). It is worth mentioning that the main function of the Grupo Mapa Geológico de Colombia is to periodically update the Geological Map of Colombia. This entails the compilation and review of publications regarding Colombia in national and international indexed journals. This background was valuable since it allowed us to know who were the most suitable researchers, based on their trajectory, to write the different chapters, in addition to knowing what unpublished information of the SGC was relevant to be published in *The Geology of Colombia*.

The work of the editorial group focused on improving the quality of texts and images and developing an outreach strategy to disseminate the research published in the work. The editorial and scientific outreach activities were led by the coordinator of the working group and editor–in–chief of the work. To ensure that the publication met the highest technical specifications and indexing criteria, the editorial group had the support and counsel of the Observatorio Colombiano de Ciencia y Tecnología and the Asociación Colombiana para el Avance de la Ciencia. The Spanish–English translation and proofreading services in English were performed with American Journal Experts, an American publishing services company that works with world–class publishers such as Springer, Nature, AGU, Cambridge University Press, and Elsevier. The English translations and style corrections were carried out by scientists with postgraduate degrees in various branches of geoscience and whose native language is English. The editorial team also had the support of four globally recognized geoscientists with experience in the editorial field. These individuals formed the Scientific Committee of the publication:

Victor A. RAMOS: Senior researcher of the Consejo Nacional de Investigaciones Científicas y Técnicas (Conicet), professor emeritus at the Universidad de Buenos Aires, Argentina, and president of the Academia Nacional de Ciencias Exactas, Físicas y Naturales of Argentina. He has dedicated more than 50 years to the understanding of the tectonic evolution of the Andes. His contributions have helped establish the tectonic processes responsible for the Andean orogeny, from Tierra del Fuego in the south to the Colombian Andes in the north. He was recognized by the World Academy of Sciences in 2017 for his outstanding contributions in the field of geology. In addition to encouraging the production of the editorial work and actively participating in the planning of the project, Professor RAMOS supported the editorial committee through the review of the chapters on tectonics and advice on specific aspects of the editorial process. He was also the author of the Prologue of *The Geology of Colombia* (Ramos, 2020).

Cees PASSCHIER: Professor of structural geology and tectonophysics in the Department of Earth Sciences of the Johannes Gutenberg–Universität Mainz in Germany. He has been president of the Commission on Tectonics and Structural Geology of the International Union of Geological Sciences (IUGS) and editor–in–chief of the *Journal of Structural Geology* since 2008. His research focuses on the quantitative analysis of the kinematics of deformed rocks through microtectonic studies and numerical and laboratory procedures. Professor PASSCHIER helped with the review of the chapters on structural geology.

David BUCHS: Professor at the School of Earth and Ocean Sciences of Cardiff University in the United Kingdom. Professor BUCHS works on the formation and accretion of seamounts, as well as on the magmatic and tectonic evolution of the Isthmus of Panamá. He is the coordinator of the Erasmus+ exchange program, an editor for PLOS ONE and a consulting geologist for the Panamá Canal Authority. Professor BUCHS helped review the geochemistry content.

Agustín CARDONA: Professor at the Universidad Nacional de Colombia Sede Medellín. His research includes topics such as the geological evolution of the Andes and the Caribbean, the analysis of convergent margins, and the geochemistry and geochronology of igneous, sedimentary, and metamorphic rocks. Professor CARDONA helped review of the content regarding the geochronology and geology of Colombia.

As academic reviewers of the chapters, 81 researchers from different countries participated. They were selected by the editorial group based on their experience, scientific production, and knowledge on the subject of the chapter to be evaluated. The quality of the group of reviewers is demonstrated by the publication index scores (h–index) of the researchers that compose it. Peer–reviewed work was essential for ensuring the quality of the research included in the editorial work. The comments and criteria arising from the reviews of the peer reviewers allowed us to correct and enrich the first versions of the manuscripts and supporting material.

With this background, *The Geology of Colombia* is destined to become a classic of Colombian geology, both for the amount

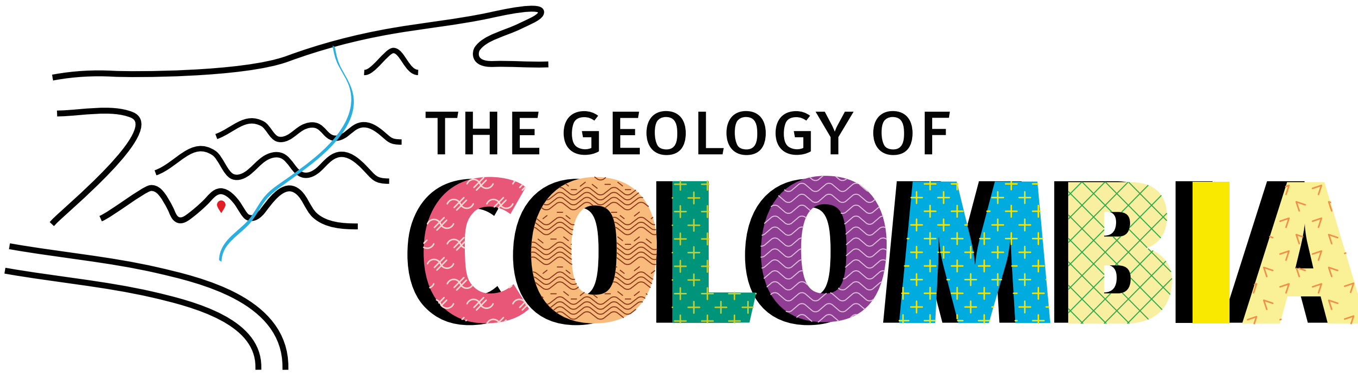

Figure 1. Image of *The Geology of Colombia*.

of new data and for the interpretations and novel ideas about the geological evolution of the Colombian territory and, in general, about the northwest South American subcontinent. The work was funded by the SGC, contains, 917 color figures, 190 tables, and 5873 bibliographic references and can be downloaded free of charge from the SGC website:

- Volume 1: https://doi.org/10.32685/pub.esp.35.2019
- Volume 2: https://doi.org/10.32685/pub.esp.36.2019
- Volume 3: https://doi.org/10.32685/pub.esp.37.2019
- Volume 4: https://doi.org/10.32685/pub.esp.38.2019

2. The logo of *The Geology of Colombia*

The logo of *The Geology of Colombia* (Figure 1) was inspired by major physiographic features of the Colombian territory and geological conditions and major geologic events that are shown in the Geological Map of Colombia 2015 (Gómez et al., 2015). The sinking Nazca Plate of the subduction zone, the three cordilleras, the Sierra Nevada de Santa Marta, the positioning of the actual magmatic chamber located in the Central Cordillera, and the Magdalena River, the most important river in Colombia in terms of its economy, culture, and history, are depicted.

Colors and patterns were used to fill in the word **COLOMBIA**. The colors were taken from the International Chronostratigraphic Chart (Cohen et al., 2013; updated v2020/01) and represent chronostratigraphic units of the Geological Map of Colombia 2015 (Gómez et al., 2015). The letter **C** is shaded in pink to represent the medium–grade gneisses of the Mitú Migmatitic Complex cropping out from the eastern region of Colombia in the Amazonas Craton from the Paleoproterozoic. The letter **O** is filled with a pattern that represents Mesoproterozoic and Neoproterozoic gneisses of the Putumayo Orogen (Ibañez–Mejia, 2020) that crop out from the Llanos Foothills, the Eastern Cordillera, Sierra Nevada de Santa Marta, and La Guajira. The letter **L** is shaded in green to represent Ordovician plutonic rocks of the Santander Massif representing the Famatinian Orogeny of Ramos (2018). The Triassic schists of the Central Cordillera, which are related to the assembly of Pangea, are represented in the letter **O**. The letter **M** is shaded in Jurassic blue to represent the numerous igneous rocks found in the Jurassic magmatic arc. The Upper Cretaceous strata deposited in the Cretaceous epicontinental basin of Colombia, which serve as a source of oil, are represented in the letter **B**. The Miocene sedimentary continental rocks of the Andean Orogeny compose the letter **I**. Finally, the letter **A** is shaded with a pattern that represents the active volcanic arc of the Central Cordillera of Colombia.

Thus, the colors and patterns used in the word *Colombia* symbolize major geological events that have occurred in Colombia, whose geological history is described in *The Geology of Colombia*.

3. The Editorial Process

The editorial production of *The Geology of Colombia* was carried out following a series of steps that are presented as a flow diagram (Figure 2). The editorial team developed this step by step process to ensure the quality of the publication, the standardization of the processes, and the accurate dissemination of the work among the geoscientific community. The process was created based on the international standards of the production and editing of scientific publications of research articles, the editorial experience of the working group in the preparation and editing of previous scientific publications, and the advice of the Observatorio Colombiano de Ciencia y Tecnología. The activities indicated in the diagram were carried out by the editorial team, the authors, the reviewers and, in some cases, involved the work of more than one of these contributors at the same time. Far from being a static working guide proposed at the beginning of the project, this editorial process was adapted and improved throughout the revision, adjustment, and publication of the chapters.

Although the diagram contains the stages typical of the editorial process of a publication such as *The Geology of Co-*

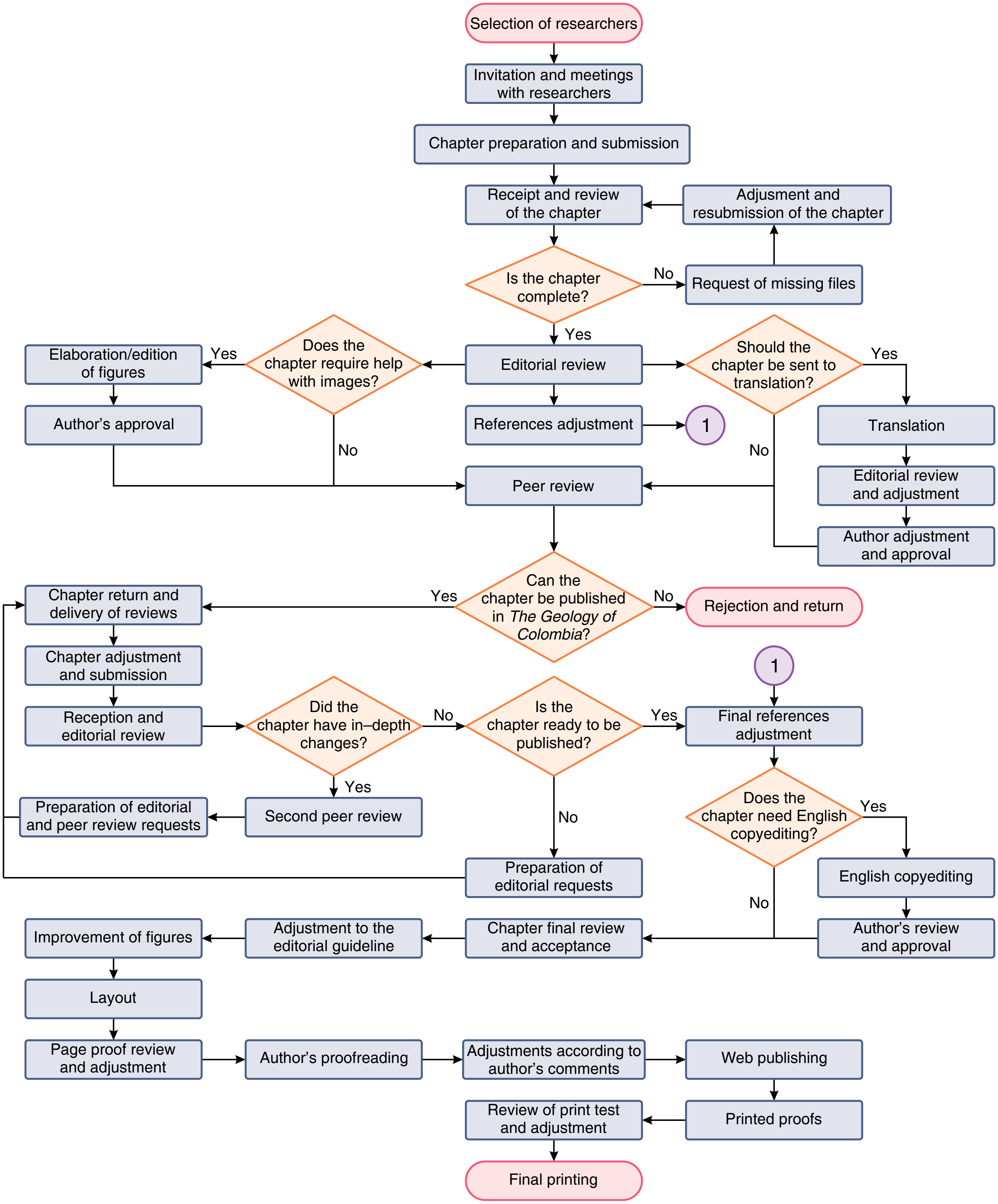

Figure 2. Editorial process of *The Geology of Colombia*.

Figure 3. Presentation of the editorial project in the offices of Ecopetrol. On the right, Jorge GÓMEZ TAPIAS, editor of *The Geology of Colombia*, and on the left, Andrés MORA, geologist and author and coauthor of seven chapters of the work.

lombia, it presents several characteristics that are detailed throughout this section. Note the support that the editorial team offered to the authors during the preparation of the chapters and before sending the manuscripts for peer review. In these stages, the support provided by the team focused on developing the figures, searching and consulting for information to complement the manuscript, and translation of content. The bibliographic references were created and adjusted following a citation style adapted to the publications generated in the country, the figures were developed and reworked based on concepts and hierarchies used by the Grupo Mapa Geológico de Colombia for several years, and editorial guidelines were created based on scientific and international style guides and manuals.

3.1. Call for and Submission of Chapters

The production of *The Geology of Colombia* began in 2017. After planning the project in the first months of the year, the editorial group selected and invited authors to contribute. In total, 74 geoscientists recognized for their expertise in specific topics of national geology and the number and impact of their publications in geological cartography, volcanology, seismology, geochemistry, stratigraphy, and other branches of geosciences were convened. These scientists were invited to participate in the work together with their research groups. In the selection of authors, the coverage of the main geological events of the national territory was also considered. This allowed the work to cover the vast majority of events and outstanding geological features of national geology.

The editorial team made visits to universities, companies, and research centers to present the editorial project and convince the authors to participate, highlighting the relevance of their contributions. There were 57 presentations on the project and several meetings and teleconferences with the invited authors during April, May, and June 2017 (Figures 3, 4). This convening work resulted in the production and submission for publication of more than 50 chapters, even though based on similar editorial experiences in other countries, a maximum of 20 submitted chapters were expected.

During the chapter development phase, the editorial team prepared the necessary editorial guidelines for the generation of texts and figures (Authors' recommendations, Template, Checklist, and Reference Citation Style; see Supplementary Information 1, 2, 3, and 4, respectively), organized the editorial work scheme, and prepared everything from the image to the outreach pieces and the promotion of the editorial project. The material for the preparation of the chapters was sent to the authors through periodic newsletters that included videos and promotional pieces of the work to motivate them. During this phase and with the support of the Observatorio Colombiano de Ciencia y Tecnología, peer evaluation forms, certificates for reviewers, confidentiality agreements, and other documentation required in later phases of the editorial process were prepared.

Figure 4. Virtual meeting with Mauricio PARRA, professor at the Universidade de São Paulo, Brasil.

Additionally, a photographic record was compiled that accompanies the biographical notes of the publication and several field trips were made to collect high–quality photographic material. This material was used to replace low–quality photographs in some chapters, to develop the covers and back covers of the work, and to prepare the graphic pieces that were used for the chapter outreach campaign on the website (https://www2.sgc.gov.co/LibroGeologiaColombia/Paginas/Inicio.aspx) and the SGC social networks. Approximately 1500 photographs were obtained.

In this phase, the editorial team supported, in addition, the development of 70 chapter figures and the editing of more than 20 at the request of the authors, and the preparation of bibliographic references for 10 chapters (about 12 000 references). The team began the preparation of three chapters for publication in *The Geology of Colombia*: (1) *Presentation of The Geology of Colombia* , (2) *Physiographic and Geological Setting of the Colombian Territory*, and (3) *Rear–Arc Small–Volume Basaltic Volcanism in Colombia: Monogenetic Volcanic Fields*.

During the manuscript preparation stage, four workshops were organized for authors affiliated with the SGC to improve the technical level of the chapters. The workshops were on geochemistry, tectonics, geochronology, and structural geology with emphasis on the interpretation of geological outcropping structures and a cross–cutting theme that was addressed in all the workshops: recommendations for the writing, editing, and publication of high–impact scientific texts. The workshops were guided by the Scientific Committee of the publication: Victor A. RAMOS, Cees PASSCHIER (Figure 5), David BUCHS (Figure 6), and Agustín CARDONA. In these workshops, the authors had the opportunity to present their progress and resolve specific concerns about their research and writing process. The workshops were very useful since some of the authors had never presented their research in a scientific article format for indexed publication written in English.

Between October 2017 and 2018 the chapters that make up *The Geology of Colombia* were received. Once submitted, the chapters went through an editorial review in which an editorial concept or document was generated with the findings of the review and some comments or suggestions for the author. This review allowed to know the contents of the chapters to select possible reviewers and whether the chapter required improvement of the figures or translation into English before academic peer review.

The adjustment of the references was one of the main works carried out by the editorial team. This phase began in the early stages of the editorial process. It consisted of completing and adjusting the list of references according to the style proposed for the publication, as well as ensuring the citation of all the references in the text, figures, and tables.

3.2. Bibliographic Reference Style

The style of references adopted in the work *The Geology of Colombia* is the product of a historical work carried out by the Grupo Mapa Geológico de Colombia. This group has authored the different versions of the Geological Map of Colombia 1M,

Figure 5. Workshop on structural geology and publication of scientific articles offered by Professor Cees PASSCHIER. As part of this event, a field trip was conducted to determine the deformation of the Pericos and Ibagué Faults in the surroundings of Ibagué.

a work that is broadly based on compiling and synthesizing the geoscientific information of different national and international publications that have been generated by the SGC, universities, and other institutions. This resulted in an extensive and varied bibliography that had to be standardized for use and publication. The references were standardized considering the types of documents found and from the review of high–impact journals, from which the best reference criteria were obtained. Although this work began with the development of the first versions of the geological maps of Colombia, it has been perfected to give the reader, in the clearest and most accurate way, the information necessary to consult the supporting references.

The style of the references of *The Geology of Colombia* was initially based on the style of *Tectonophysics* and elements of other journals, such as the use of '&' instead of 'and' in the citations of references implemented in the publications of the Geological Society of London. This style had already been used in the book *Compilando la geología de Colombia: Una visión a 2015* (Gómez & Almanza, 2015). However, taking into account some particularities and the variety of information compiled on *The Geology of Colombia*, it was necessary to include additional information or to create different categories; thus, models for more than 10 types of scientific documents were obtained. Among these are the explanatory reports of the maps and unpublished reports, for which the SGC uses the Geoscientific Information Integration Engine (Motor de Integración de Información Geocientífica, MIIG), which allows access to a large portion of the documents that are widely cited in *The Geology of Colombia*. This search engine can be found on the web page https://miig.sgc.gov.co/Paginas/advanced.aspx.

Next, the references used for each type of document are described, a template and an example for each one are presented:

Geological Maps

In this type of document, it is important to specify whether the authors are compilers of the information contained in the maps, as is the case of the Geological Map of Colombia, so the word "compilers" is included. If this is not the case and the maps were created by the authors, this word is omitted, but all the available information provided is organized in the following model:

Last names of the authors, First and middle name initials. & Last names of the authors, First and middle name initials, compilers. Year. Name of the map. Scale. Publisher, number of pages (in case it has more than one). City of publication. DOI

Example:

Gómez, J., Montes, N.E., Nivia, Á. & Diederix, H., compilers. 2015. Geological Map of Colombia 2015. Scale 1:1 000 000. Servicio Geológico Colombiano, 2 sheets. Bogotá. https://doi.org/10.32685/10.143.2015.936

Figure 6. Geochemistry workshop offered by Professor David BUCHS.

Scientific Journals

Due to the large number of publications in scientific journals, it is important to provide all the information available to help the reader locate the reference. In addition to the name of the journal, volume, issue number, and range of pages must be included. Finally, the digital object identifier (DOI) is indicated, if available, which is the easiest way to access the article information.

Last names of the authors, First and middle name initials. & Last names of the authors, First and middle name initials. Year. Title of the article. Journal, Volume(Issue): Range of pages. DOI

Example:

Gómez, J., Montes, N.E., Almanza, M.F., Alcárcel, F.A., Madrid, C.A. & Diederix, H. 2017. Geological Map of Colombia 2015. Episodes, 40(3): 201–212. https://doi.org/10.18814/epiiugs/2017/v40i3/017023

Edited Books

One of the most common errors when citing this type of publication is the omission of the editors, so the proposed model ensures that this information is included correctly.

Last names of the authors, First and middle name initials. & Last names of the authors, First and middle name initials. Year. Title of the article. **In:** Last names of the editors, First and middle name initials. **(editors)**, Title of the book, Editor or publisher, Name of the edition Number, Range of pages. DOI

Example:

Moreno–Sánchez, M., Gómez–Cruz, A. & Buitrago–Hincapié, J. 2020. Paleozoic of Colombian Andes: New paleontological data and regional stratigraphic review. In: Gómez, J. & Mateus–Zabala, D. (editors), The Geology of Colombia, Volume 1 Proterozoic – Paleozoic. Servicio Geológico Colombiano, Publicaciones Geológicas Especiales 35, p. 167–203. Bogotá. https://doi.org/10.32685/pub.esp.35.2019.09

A variation occurs when only the book editors are mentioned:

Gómez, J. & Almanza, M.F., **editors**. 2015. Compilando la geología de Colombia: Una visión a 2015. Servicio Geológico Colombiano, Publicaciones Geológicas Especiales 33, 401 p. Bogotá.

Books and Booklets

The following model contains the information necessary for referencing this type of document:

Last names of the authors, First and middle name initials. & Last names of the authors, First and middle name initials. Year. Title of the book, Editor or publisher, Number of pages. City of publication, Country. DOI

Example:

McGavin, G.C. 2001. Essential entomology: An order–by–order introduction. Oxford University Press, 328 p. Oxford, UK.

Proceedings from a Congress, Symposium, or Conference

For the documents obtained from different scientific outreach events, the type of format in which the information is found must be specified; this can include memoirs, abstracts, and summaries on CD–ROM, among others.

Last names of the authors, First and middle name initials. & Last names of authors, First and middle name initials. Year of the event. Title of the presentation. Name and version of the event. Document format, number of pages or page. City of the event. DOI

Example:

Bermúdez, H.D., Stinnesbeck, W., Bolívar, L., Rodríguez, J.V., García, J. & Vega, F.J. 2015. Paleosismitas asociadas al límite K–Pg en la isla de Gorgonilla, Pacífico colombiano. XV Congreso Colombiano de Geología. Abstracts CD Rom, p. 1080. Bucaramanga.

In some congresses, the PDFs of the abstracts are given a code; in these cases, it is recommended to use the code of the abstract instead of the pages.

Theses

In most university repositories, there is an option for filtering theses by the degree obtained with their presentation; therefore, in the reference for this type of document, whether it is an undergraduate, master's, or doctoral thesis must be specified.

Last names of the authors, First and middle name initials. & Last names of authors, First and middle name initials. Year. Title of the thesis. Degree of thesis. University, number of pages. City of presentation.

Example:

Leal–Mejía, H. 2011. Phanerozoic gold metallogeny in the Colombian Andes: A tectono–magmatic approach. Doctorade thesis, Universitat de Barcelona, 989 p. Barcelona.

Map Memoirs

These explanatory reports are documents that accompany the geological maps of the SGC. To differentiate a reference to this type of document from a reference to a map, "Explanatory memoir" is included before the name of the map to which it corresponds, as shown in the following model:

Last names of the authors, First and middle name initials. & Last names of authors, First and middle name initials. Year. Explanatory memoir: Name of the map. Scale. Publisher, number of pages. City of publication.

Example:

Rodríguez, G., Zapata, G., Velasquez, M.E., Cossio, U. & Londoño, A.C. 2003. Memoria explicativa: Geología de las planchas 367 Gigante, 368 San Vicente del Caguán, 389 Timaná, 390 Puerto Rico, 391 Lusitania (parte noroccidental) y 414 El Doncello. Scale 1:100 000. Ingeominas, 166 p. Bogotá.

Unpublished Reports

Unpublished reports refer to the products of projects developed by professionals of the SGC or other national entities. These can be found on the MIIG page mentioned above and are referenced as follows:

Last names of the authors, First and middle name initials. & Last names of authors, First and middle name initials. Year. Name of the report. Publisher, unpublished report, number of pages. City of publication.

Example:

Celada, C.M., Garzón, M., Gómez, E., Khurama, S., López, J.A., Mora, M., Navas, O., Pérez, R., Vargas, O. & Westerhof, A.B. 2006. Potencial de recursos minerales en el oriente colombiano: Compilación y análisis de la información geológica disponible (fase 0). Servicio Geológico Colombiano, unpublished report, 165 p. Bogotá.

For internal reports of the SGC that are consecutive, it is recommended to indicate the number and use the expression 'Internal report'.

Hubach, E. & Alvarado, B. 1932. Estudios geológicos en la ruta Popayán–Bogotá. Servicio Geológico Nacional, Internal report 213, 132 p. Bogotá.

Web Links

When the information contained in web pages is referenced, it is important to specify the year and month in which it was accessed, since the information can be modified. If a program obtained from the web is referenced, the version used must be included.

Last names of the authors, First and middle name initials. & Last names of authors, First and middle name initials. Year. Name of the document: link (accessed on month year).

Example:

Dyment, J., Lesur, V., Hamoudi, M., Choi, Y., Thebault, E. & Catalan, M. 2015. World digital magnetic anomaly map version 2.0: http://www.wdmam.org (accessed on October 2017).

Others

There are a number of references that fall outside of the previous categories. For these, the suggestions usually given are to cite them as closely as possible to the style described above.

Cohen, K.M., Finney, S.C., Gibbard, P.L. & Fan, J.X. 2013 (updated v2020/01). The ICS International Chronostratigraphic Chart. Episodes, 36(3): 199–204. https://doi.org/10.18814/epiiugs/2013/v36i3/002

FGDC (prepared for the Federal Geographic Data Committee by the U.S. Geological Survey). 2006. Federal Geographic Data Committee Digital cartographic standard for geologic map symbolization. Federal Geographic Data Committee Document Number FGDC–STD–013–2006, 290 p. Reston, USA.

International Commission on Zoological Nomenclature (ICZN). 1999. International code of zoological nomenclature. The International Trust for Zoological Nomenclature, 401 p. London, UK.

Newell, D.B. & Tiesinga, E., editors. 2019. The International System of Units (SI). National Institute of Standards and Technology. NIST Special Publication 330, 122 p. https://doi.org/10.6028/NIST.SP.330-2019

USGS. 2004. Shuttle Radar Topography Mission, 1 Arc Second–República de Colombia, Unfilled Unfinished 2.0, Global Land Cover Facility. University of Maryland, February 2000. Maryland, USA.

3.2.1. Organization of the list of references

In addition to the standardization of the references, the order of the references had to be agreed upon to allow the reader to find the reference that corresponds to the citations within the chapters. The organization of this list mainly followed two guidelines:

1. The references were arranged alphabetically based on the surname of the first author.
2. The references with the same principal author were organized as follows: First, the references with a single author were chronologically ordered from oldest to most recent. Then, the references with a coauthor were organized alphabetically by the surname of the second author. Finally, references with two or more coauthors were sorted by year of publication.

Example:

Jaramillo, C. 2002. Response of tropical vegetation to Paleogene warming. Paleobiology, 28(2): 222–243. https://doi.org/10.1666/0094-8373(2002)028<0222:ROTVTP>2.0.CO;2

Jaramillo, C. 2018. Evolution of the Isthmus of Panama: Biological, paleoceanographic, and paleoclimatological implications. In: Hoorn, C., Perrigo, A. & Antonelli, A. (editors), Mountains, climate and biodiversity. Wiley–Blackwell, p. 323–338. Chichester, UK.

Jaramillo, C. & Cárdenas, A. 2013. Global warming and Neotropical rainforests: A historical perspective. Annual Review of Earth and Planetary Sciences, 41: 741–766. https://doi.org/10.1146/annurev-earth-042711-105403

Jaramillo, C. & Dilcher, D.L. 2000. Microfloral diversity patterns of the late Paleocene – Eocene interval in Colombia, northern South America. Geology, 28(9): 815–818. https://doi.org/10.1130/0091-7613(2000)28<815:MDPOTL>2.0.CO;2

Jaramillo, C. & Dilcher, D.L. 2001. Middle Paleogene palynology of central Colombia, South America: A study of pollen and spores from tropical latitudes. Palaeontographica Abteilung B, 258(4–6): 87–213.

Jaramillo, C., Rueda, M. & Mora, G. 2006. Cenozoic plant diversity in the Neotropics. Science, 311(5769): 1893–1896. https://doi.org/10.1126/science.1121380

Jaramillo, C.A., Moreno, F., Hendy, F., Sánchez–Villagra, M. & Marty, D. 2015. Preface: La Guajira, Colombia: A new window into the Cenozoic neotropical biodiversity and the Great American Biotic Interchange. Swiss Journal of Palaeontology, 134: 1–4. https://doi.org/10.1007/s13358-015-0075-0

Supplementary Information 4 includes the EndNote style of *The Geology of Colombia* for the different categories.

3.3. Complementing and Improving the Chapters Prior to Their Academic Peer Review

To achieve excellent quality chapters before peer review, the editorial team helped in the translation of more than 15 chapters and the reworking and editing of figures. In both stages, the author validated the adjustments before continuing with the following steps of the editorial process. The translation was carried out by scientific professionals at American Journal Experts. The profile of the translator was selected according to the area or areas of knowledge covered in the chapter (stratigraphy, geochemistry, etc.). The figure editing was led by the professionals of the editorial team in charge of the graphic arts. Although the editing and reworking of figures began in this initial phase of the editorial process, it was carried out continuously until the chapters were reviewed before their web publication, at which time it was still necessary to perfect the graphic material.

3.3.1. Developing and Editing Figures

The reworking and editing of the figures of the work *The Geology of Colombia* was performed using the software CorelDRAW® 2018 and Corel PHOTO–PAINT 2018, graphic design programs that facilitate the creation and editing of vector figures and photographs. Adjustments were made to improve the graphic quality of the figures, to standardize them according to the editorial guidelines created for texts, and to standardize the use of terms in the text and figures. This allowed for clearer and more readable figures. The editing was based on visual hierarchy, which is a technique of graphic design for highlighting certain characteristics through line thickness, color, contrast, size, and alignment of the elements of the figure: points, lines, polygons, and texts. To ensure that the figures had the appropriate quality, both in printed and digital format, they were all obtained in vector format, since these types of images can be scaled to different sizes without losing resolution, in contrast to bitmap images. In cases where the original figures did not have this format, they were digitized using vectorization to ensure proper graphic output.

The figure size was important to the layout of the different chapters of the work. Three sizes were used: (1) Full page with 180.9 mm width in a vertical orientation. This format was rotated 90° to horizontally adjust the image. (2) Column and a half with 122 mm width. (3) Column with 88 mm width. For the three sizes, the maximum length in the vertical figures was 236.5 mm. The color profile used was CMYK (cyan, magenta, yellow, black). This profile is recommended for printing and digital versions in PDF format.

The typeface used for the text in the figures was Helvetica, with a variation between normal and narrow, except for the bodies of water, where the Book Antiqua font was used. The text sizes varied between 6 and 11 points, where 8 most often appropriate. Full uppercase text was not used to avoid visual distraction when reading the figures. For the highlights, the color, contrast, size, and alignment were considered.

The text was positioned horizontally except for names of oriented structures such as faults, folds, drainages, and indicative arrows. For structures with NE to SW inclinations, the direction of labeling is in the south–north direction, and for those inclined NW to SE, the direction of labeling is north–south. The text is straight or curved according to the shape of the structure. For the texts indicating an exact point, the text is positioned to the right of the point, preferably above rather than below. When one of these two positions is not possible, placements to the left are recommended, preferably above rather than below. The last option is to place the text directly above or below the point.

According to the editorial guidelines of texts for *The Geology of Colombia*, the coordinates were expressed geographically (latitude and longitude in degrees, minutes, and seconds) to facilitate and ensure that readers, especially those who do not know Colombian geography, can more easily locate them.

Additionally, shaded relief base maps were developed to visually improve several of the figures, for which the digital elevation model (DEM) with 30 m resolution of the Shuttle Radar Topography Mission (SRTM) of the National Aeronautics and Space Administration (NASA) and distributed by the United States Geological Survey (USGS) EROS Data Center (U.S. Geological Survey, 2004) was used. The methodology used to obtain the images was based on the *Hillshade* tool of the ArcMap software through image processing. Initially, two images were produced with a solar altitude angle of 45°, differentiated by the azimuth: The first with the shadow generated by a solar azimuth angle of 315° and the second by a solar azimuth angle of 45°. This second image is assigned transparency of 50% and overlaps the first generated image; thus, a shaded relief image with well–defined geomorphological features is obtained (Figure 7).

Figures 8a and 9a show two examples of the editing of an initial figure submitted for one of the chapters. By using a shaded relief image and digitizing the vector elements of the figure, following the visual hierarchy technique and the editorial guidelines, a figure with greater quality and legibility is obtained (Figures 8b, 9b).

For the 58 chapters of *The Geology of Colombia*, 942 figures were edited.

3.3.2. Peer Review and Chapter Adjustments

Once the submitted chapters were reviewed by the editorial team and some of them were translated and/or improved in terms of the quality of the figures and the style and consistency of the citations and bibliographic references, the editorial team sent the chapters for peer review. This process was supported by the Observatorio Colombiano de Ciencia y Tecnología and the Asociación Colombiana para el Avance de la Ciencia. Each chapter was reviewed by at least two reviewers. When peer evaluation concepts were dissimilar, an additional opinion was requested to support the acceptance or rejection of the chapter. The peer evaluation format included open questions with which the reviewer could express opinions on the content and presentation of the manuscript, as well as a numerical rating section that allowed quantification of the quality of the chapter and thereby the reviewer's decision to accept the revised chapter, to accept it with minimal changes, to accept it with significant changes, or to definitively reject it (see Format Review Editorial Board in Supplementary Information 5). The decision to accept or reject a chapter was made considering only the outcome of the peer review.

The chapters rejected for publication in *The Geology of Colombia* were returned to the author, along with a letter from the editorial committee. In the case of accepted chapters, the results of the peer review and the editorial concept containing the editorial criteria arising from the initial review were sent to the authors. Once the chapter was corrected by the author and resubmitted to continue the editorial process, the editorial group reviewed the new version and compared it with the initial

Figure 7. Shaded relief image of the northwestern corner of South America.

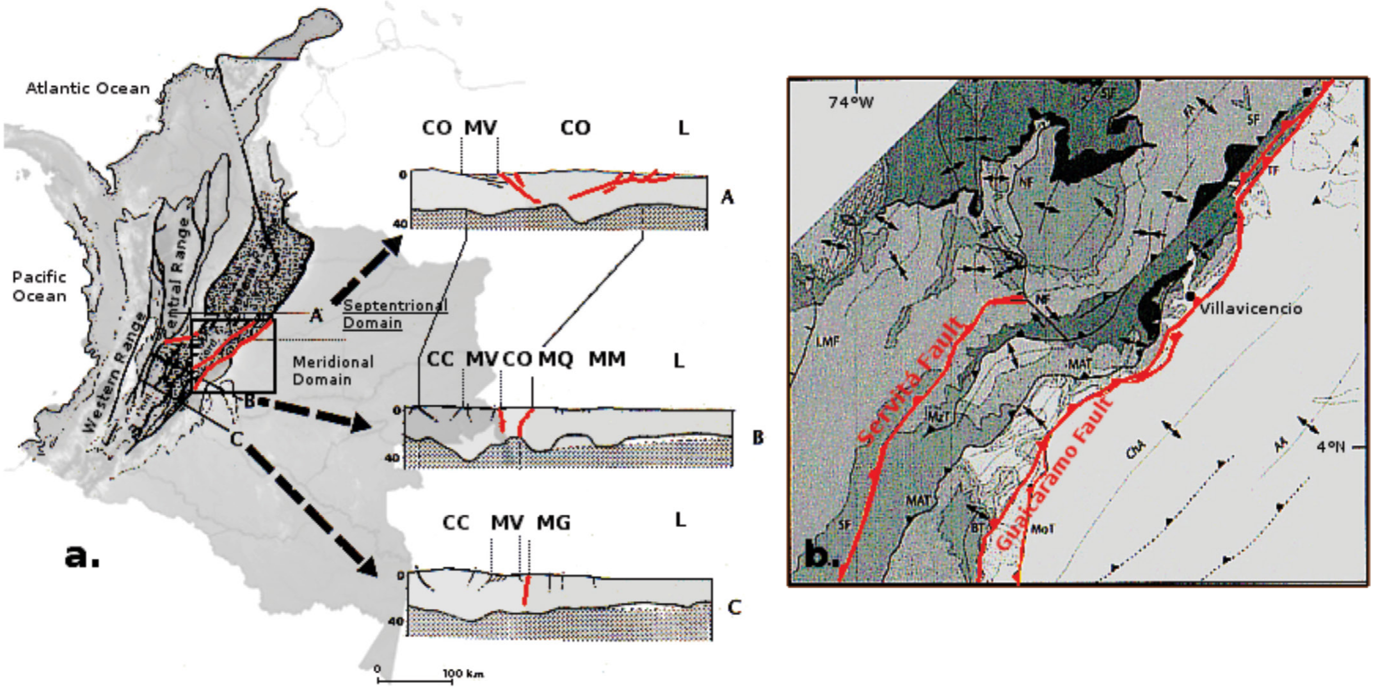

Figure 8a. Initial figure, first example.

version, reviewing the reviewer's comments and the author's responses one by one. When the chapter included considerable changes in content or the arbitrator requested to revise the chapter to verify that the modifications and additions were made, the chapter was sent to a second reviewer. Otherwise, the review of the editorial team was sufficient to verify whether the chapter was ready for publication.

From the review of most of the resubmitted chapters, editorial board's remarks emerged that were sent to the authors for review and response. In some cases, this process was carried out several times to ensure that the chapter met the editorial criteria before continuing to the next phase of the editorial process. The editorial group helped the authors to respond to the criteria, especially in terms of bibliographic references and figures. The correction of the bibliographic references was a process that was carried out in all stages of the editorial process; however, with the chapter ready for publication (in terms of content), a final review and update of the list of adjusted references was performed.

In the final version of the chapter, style correction was made in English for the chapters that, according to the comments of the peer review or the request of the author, required this action. With the correction of the style, the clarity, precision, and coherence of the language were improved. At this stage, grammatical, punctuation, and spelling errors were corrected. American Journal Experts supported this stage of the process once the team selected the style corrector profile. The style correction was validated by the author. In this phase, answers were provided to some questions or clarifications that the corrector, in general, had indicated in the edited document. With the approved version of the style correction, a final revision of the chapter was carried out before proceeding with the formal acceptance and moving to the stage of adjustment of the chapters to the editorial guidelines.

3.3.3. Adjustment of the Chapters to the Editorial Guidelines

After the English style correction, the chapters went through a stage of adjustment to the editorial guidelines to review the macrostructure and homogenize the style of the entire work. This stage was fundamental considering that the chapters were written by more than 100 different authors. For each chapter, the process of adjustment to the guidelines began with the review and final adjustment of the citations and bibliographic references, an ongoing activity that had already advanced since the initial submission of chapters. With the references ready, a cross–check that consisted of comparing all the citations in the chapter with their respective references and checking that the surnames of the authors and the year of publication in citations and references were the same was performed. Additionally, the DOI indicated in the references was tested to ensure that it linked to the corresponding document. Generally, in this activity, missing references or those that newly appeared in the final list of references without being cited in the chapter were detected.

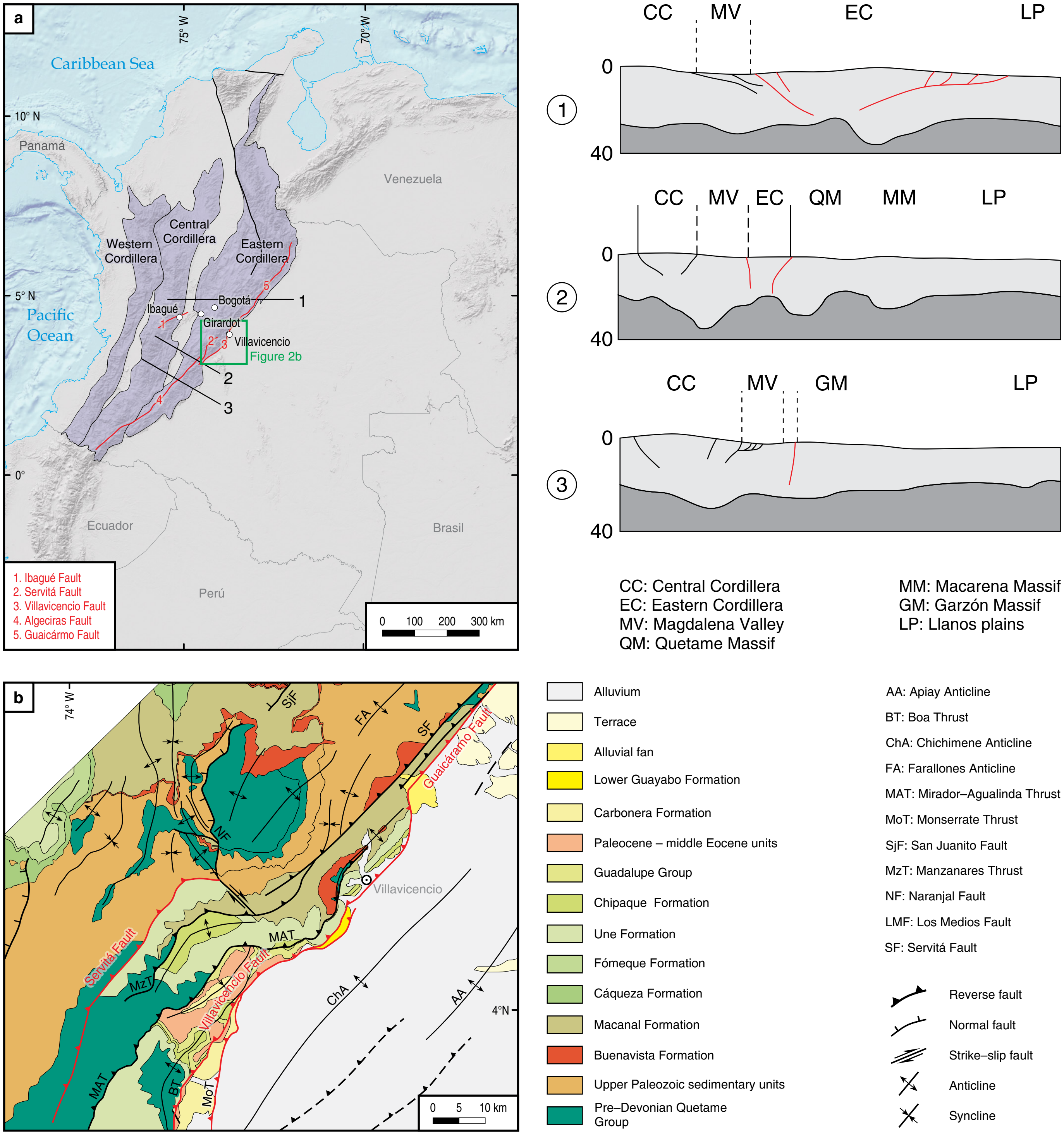

Figure 8b. Figure edited according to the image editing and reworking guidelines of *The Geology of Colombia*, where a shaded relief image is used that improves the visualization of the structural elements and the vector elements are digitized. First example.

The next step was to read the entire manuscript to review its macrostructure. This activity was carried out to detect inconsistencies and possible errors in context or wording that could result in ambiguities or erroneous interpretations. The objective in this step was to identify the problems causing ambiguity and then communicate these problems to the author. Also, in this reading, the abbreviations, acronyms, and symbols used throughout the chapter were identified and compiled in a list at the end of each chapter.

In parallel, a review of the figures, tables, and supplementary information was performed. In the case of the figures, the versions that had been edited following the guide for editing and reworking the figures were reviewed. These were compared with their description, and the changes that had to be made for

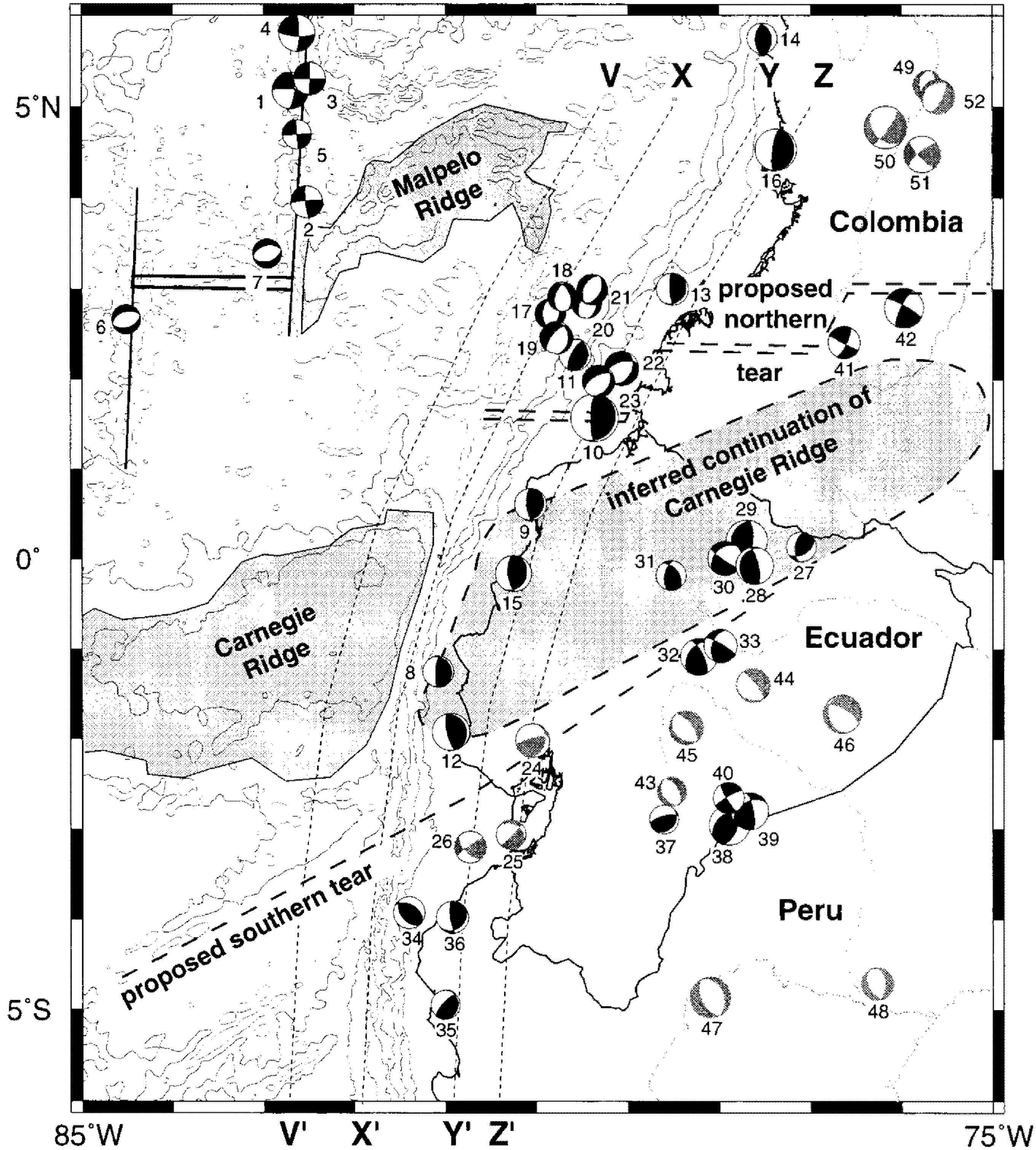

Figure 9a. Initial figure, second example.

consistency with the manuscript, the editorial guidelines, and the original figures submitted by the author in terms of content were identified. These modifications were left as comments and were sent to the person in charge of the adjustment. In this

Figure 9b. Figure edited according to the image editing and reworking guidelines of *The Geology of Colombia*, where a shaded relief image is used that improves the visualization of the structural elements and the vector elements are digitized. Second example.

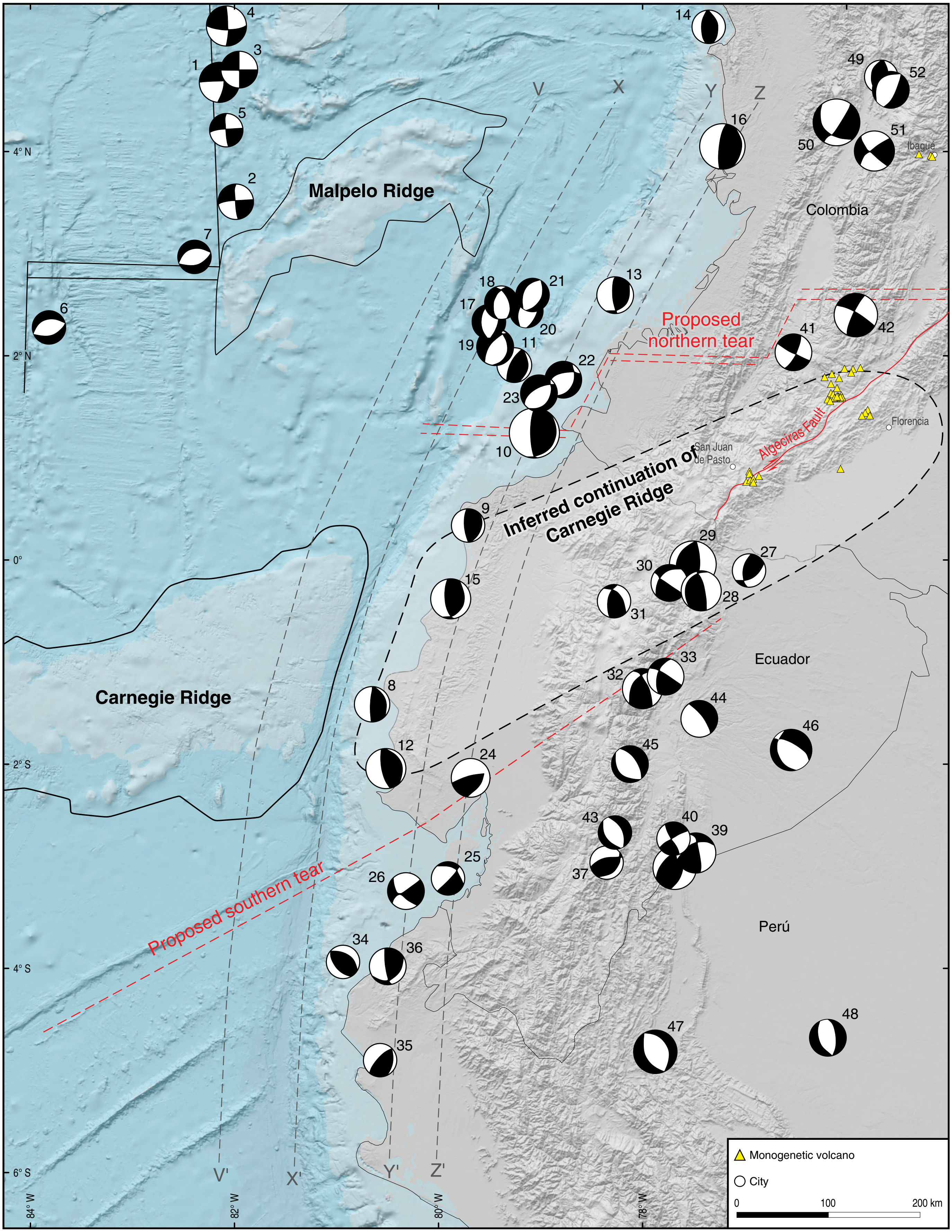

Malpelo Ridge
Carnegie Ridge
Colombia
Ecuador
Perú
Proposed northern tear
Proposed southern tear
Inferred continuation of Carnegie Ridge
Algeciras Fault
San Juan de Pasto
Florencia
Ibagué
V
X
Y
Z
V'
X'
Y'
Z'
4° N
2° N
0°
2° S
4° S
6° S
84° W
82° W
80° W
78° W
Monogenetic volcano
City
0
100
200 km

step, it was essential to verify that the information projected by the figure was the same as that presented in the manuscript, since discrepancies and inconsistencies were frequently found between the figures and the text. In the same way, when the chapter included tables, these were reviewed and adjusted by comparing the information with that provided in both the manuscript and the figures. The most common modifications made to the tables included changing the coordinate system (the entire work was conducted in geographic coordinates), adjusting the footnotes, and converting punctuation between thousands and decimals.

Then, the chapter was standardized to the editorial guidelines. This pattern of text presentation was created by the editorial group as they advanced in the editorial process and is mainly based on *The Chicago Manual of Style, 16th Edition* (University of Chicago Press Staff, 2010), a detailed guide on the editorial process and writing standards in English. *The Chicago Guide to Grammar, Usage, and Punctuation* (Garner, 2016) and the Merriam–Webster online dictionary were used to resolve English grammar and spelling issues (https://www.merriam-webster.com/).

For the creation of the guidelines, the best manuals, guides, and articles for standards in geology were also used, such as *Suggestions to Authors of the Reports of the United States Geological Survey* (Hansen, 1991), *International Stratigraphic Guide* (Salvador, 1994), *North American Stratigraphic Code* (North American Commission on Stratigraphic Nomenclature, 2005), *Metamorphic Rocks: A Classification and Glossary of Terms* (Fettes & Desmos, 2007), *Igneous Rocks: A Classification and Glossary of Terms* (Le Maitre, 2002), *How to Use Stratigraphic Terminology in Papers, Illustrations, and Talks* (Owen, 2009), and *International Code of Zoological Nomenclature* (International Commission on Zoological Nomenclature, 1999).

Standards widely used by the international scientific community, such as *The International System of Units* (Newell & Tiesinga, 2019) and *The ACS Style Guide: Effective Communication of Scientific Information* (Coghill & Garson, 2006), were also taken into account. According to the manuals, guides, articles, and standards, the style of the terms used was established not only in the manuscript but also in all the components of the chapter: Figures, tables, and supplementary information. During the process of creating the guidelines, the writing style of some terms was established based on a thorough search of their use in high–impact international journals. In other cases, a consensus was reached among the editorial group to define the form of use.

In the adjustment of the chapters to the editorial guidelines, editorial board's remarks usually arose that were drafted and sent to the author. The author's responses were reviewed, and the necessary changes were made so that the chapter could move to the layout stage.

3.3.4. From the Layout to the Publication

At the end of the adjustment to the guidelines phase, the Spanish style correction of the abstract and the chapter keywords was performed. These were reviewed and corrected considering the writing guidelines used by the Grupo Mapa Geológico de Colombia in its publications in Spanish and recent updates to the orthographic and grammatical rules of the Real Academia Española (Real Academia Española, 2010). For the names of the geographic sites, the Geographical Dictionary of Colombia website of the Instituto Geográfico Agustín Codazzi was used: http://ssiglwps.igac.gov.co/digeo/app/index.html. Since they are proper names, they were used in the same way in texts written in Spanish and English.

With the chapters now complete (texts, figures, tables, and in some cases supplementary information), the next step was the layout. A quick review was performed on the layout version to ensure that all content had been included. If required, adjustments were made before sending the chapter layout to the author for proofreading. In this stage, the author, in addition to verifying the layout of the chapter, reviewed the contact information and biographical notes, the citation of figures, tables, and supplementary material throughout the chapter, and the acronyms and abbreviations, among others. However, note that at this stage, no changes in the content of the accepted chapter were allowed.

With the comments and requests of the author, two members of the editorial team who had not previously read or reviewed the chapters performed a detailed reading and review to identify errors that had been overlooked in previous phases of the process. In this review, some writing errors and even small content inconsistencies were found; however, most errors were related to the omission of relevant information in the final list of references, spelling errors, incorrect use of confusing geological terms (sediments for sedimentites, late for upper, early for lower, etc.), lack of consistency in some words and geological terms, and distribution of figures and texts throughout the document regarding readability and visual cleanliness. All these adjustments were indicated as comments in the PDF version of the chapter layout, and together with the authors' criteria, they were sent to the layout designer for adjustment. Finally, a new version was revised for adjustment verification. Once this stage was completed, the chapters were published on the website (https://www2.sgc.gov.co/LibroGeologiaColombia/Paginas/Inicio.aspx).

On the website, the chapters, supplementary materials, and citations suggested in EndNote were released for consultation and free download. The chapters were released one by one on the web to highlight each of the investigations of the editorial work. Once the chapter was published on the web, a promotional campaign was carried out through mass mailings, and posts were published on the social networks of the SGC with graphics developed from material in each chapter accompanied by text that summarizes the content. The last stages of the editorial process correspond to printing, reviewing, and proofreading before the final printing.

4. Contents of *The Geology of Colombia*

4.1. Volume 1 Proterozoic – Paleozoic

Volume 1 Proterozoic – Paleozoic of *The Geology of Colombia* includes 10 chapters (Gómez & Mateus–Zabala, 2020a). The cover of this volume is a scientific illustration by the geologist Marie Joëlle GIRAUD that shows the Colombian sea during the Ordovician based on the fossil record collected from La Heliera–1 well in the Llanos Orientales Basin.

Chapter 1, written by Gómez et al. (2020), summarizes the physiographic, geographic, and geological context of the national territory and generalizes the Colombian sedimentary basins. This chapter serves as a basis for better understanding the chapters of the work. This chapter is useful, especially for foreign readers who are not familiar with the geography and physiography of the country.

The magnetometric and gamma spectrometric information (more than 400 000 linear km of information) generated by the SGC on the Colombian Amazon is presented in chapter 2. With these data, Moyano–Nieto et al. (2020) differentiated igneous and metamorphic rocks of Proterozoic age and structural trends of the Guiana Shield. The region is partially covered by sedimentary rocks from the Miocene and some Quaternary deposits, in addition to dense vegetation cover, so the authors propose a methodology for processing geophysical information that facilitates geological mapping in this region of the country.

In chapter 3, Restrepo & Toussaint (2020), who were the first to introduce the concept of geological terranes in Colombia, present a new vision on the mosaic of continental terranes that constitute the Colombian territory.

In chapter 4, using isotopic data (U–Pb, Sm–Nd, Lu–Hf, and δ18O), Ibañez–Mejia & Cordani (2020) show that the western part of the Guiana Shield, which includes the Proterozoic basement of eastern Colombia, has crystallization ages ranging from ca. 1.99 to ca. 1.38 Ga. This period corresponds to four periods of magmatic activity: two in the middle to late Paleoproterozoic, one in the early Mesoproterozoic, and another in the middle Mesoproterozoic.

Chapter 5 contains the first and to this day only report on the presence of acritarchs in the Ediacaran – Cryogenian in Colombia. The fossils reported by Dueñas–Jiménez & Montalvo–Jónsson (2020) come from well cores drilled in the Llanos Orientales Basin.

In chapter 6, Ibañez–Mejia (2020) describes the Putumayo Orogen, identified below the sedimentary wedge of the Putumayo Basin. The author exposes the evolution of this orogenic cycle, with an emphasis on its reconstruction, based on the interaction between Laurentia, Amazonia, and Baltica in the Proterozoic and the accretion of the supercontinent Rodinia. This discovery is an important contribution to the reconstruction of the geological history of the Colombian territory because directly correlates the basement blocks exposed in the Colombian Andes and the western margin of the Guiana Shield.

Chapter 7 presents the Paleozoic sedimentary record, over 6000 m thick, in the subsoil of the Llanos Orientales Basin. Dueñas–Jiménez et al. (2020) document the associations between acritarchs, chitinozoans, and trilobites, which allowed them to differentiate sequences from the Cambrian, the Lower and Middle Ordovician, the Devonian, and the Carboniferous.

Chapter 8 presents the lithological units, boundaries, and U–Pb data in the detrital zircons of the Anacona Terrane, considered by Restrepo et al. (2020) as a peri–Gondwanan terrane. In addition, its relationship with the Acatlán Complex in southern México and Marañón Complex in Perú is presented.

Chapter 9 contains a review of the stratigraphy, biostratigraphy, and geochronology of the Paleozoic rocks of Colombia. Moreno–Sánchez et al. (2020) proposed a relationship between the Paleozoic units and the underlying basement and reconstructed the geological history and paleogeography of the Colombian territory during the Paleozoic.

The magmatic activity of the late Carboniferous and the Permian is documented by Rodríguez–García et al. (2019) in chapter 10. With recent data from petrography, geochemistry, and geochronology, the authors identified this fragmented magmatic arc on the eastern flank of the Central Cordillera, the serranía de San Lucas, and the Sierra Nevada de Santa Marta. They indicate that it is made up of emplaced plutons on the western margin of the basement and that its origin may be related to a subduction zone located on the western margin of Gondwana.

4.2. Volume 2 Mesozoic

Volume 2 includes 14 chapters on the Mesozoic (Gómez & Pinilla–Pachon, 2020a). The scientific illustration on the cover, drawn by Marie Joëlle GIRAUD, recreates what Colombia would have looked like 110 million years ago in a Google Earth image and the crustal and mantle configuration that would produce this geography.

Chapter 1 is dedicated to the Permian and Triassic magmatic rocks of Colombia and Ecuador. Spikings & Paul (2019) present a review of outcrops and geochronological, geochemical, isotopic, and thermochronological data of these rocks and propose an evolutionary model for northwest South America during the formation and separation of Pangea. Additionally, the authors provide a large–scale reconstruction of western Pangea.

In chapter 2, Garcia–Casco et al. (2020) report the primary mantle mineralogical composition of the Medellín Dunite and confirm its harzburgite composition and subsequent metamorphism. The authors suggest that the unit may be the result of the cooling and hydration of the oceanic mantle in a back–arc basin, events prior to the tectonic processes that led to the emplacement of the metaharzburgite in the western margin of Pangea.

With the analysis of geochemical and geochronological data of the volcanic and plutonic rocks that make up the magmatic belt from the Late Triassic to the Jurassic, in chapter 3, López–Isaza & Zuluaga (2020) conclude that these rocks are the result of the interaction between the partial fusion of the crust and fluids derived from the mantle on a continental margin. This margin progressively changed from a post–collisional extension in the Late Triassic to a volcanic arc developed in a suprasubduction regime in the Late Jurassic.

The magmatic activity of the Mesozoic, recorded in several blocks of the Colombian Andes, is documented by Rodríguez–García et al. (2020) in chapter 4. The authors indicate that magmatism began in the Late Triassic and ended in the Early Cretaceous. They add that magmatism developed in at least three different magmatic arcs, the Santander Massif, the Upper Magdalena Valley, and the northern sector of the Ibagué Batholith, in clearly defined time intervals and on basements of different lithological characteristics.

In chapter 5, Bayona et al. (2020) synthesize knowledge about the metamorphic, plutonic, volcanic, and calcareous and clastic sedimentary rocks of the Jurassic exposed from northern Perú to Venezuela. From this synthesis, the authors evaluate three tectonic models proposed for the evolution of the northwestern corner of Gondwana and conclude that the presence of an orthogonal margin with a complex configuration such as the extreme northwest of Gondwana cannot be explained by the development of a single geodynamic process. To clarify this situation, they identified a need to improve the knowledge based on the gathering of information in the field and various analyses of each of the metamorphic, magmatic, and sedimentary sequences recognized.

The study of the origin and development of neotropical biomes is essential to understand existing ecosystems and making predictions about their future. With this in mind, Jaramillo (2019) states in chapter 6 that in the Colombian territory, during the Cretaceous, the biomass of tropical forests was dominated by gymnosperms and ferns and that the current tropical forests developed at the beginning of the Cenozoic as a result of the mass extinction that occurred in the Cretaceous – Paleocene boundary. The author illustrates that several existing biomes, including the páramos, the cloud forest, the savannas, and the dry forest, have increased significantly during the late Neogene at the expense of the tropical forest.

In chapter 7, Toussaint & Restrepo (2020) state that to the west of the San Jerónimo Fault, considered the boundary of continental terranes, there are several allochthonous oceanic terranes. The authors state that these were formed in the Pacific Ocean and migrated north to their current positions between the Late Cretaceous and the Miocene and that at least two of these terranes are part of the Caribbean Plateau.

Based on mineralogical, geochemical, thermochronological, and U–Pb dating of Cretaceous and Cenozoic sedimentary rocks of the Cordillera Oriental, Guerrero et al. (2020a) confirm the existence of a basin whose main depositional axis was in the current core of the aforementioned mountain range in chapter 8. The authors document two source areas, one in the magmatic/metamorphic arc of the Central Cordillera and another in the Guiana Shield. They add that the sediments deposited in the basin began their exhumation during the Late Miocene episode of the Andean Orogeny.

In chapter 9, Guerrero et al. (2020b) analyze and evaluate the potential of unconventional hydrocarbons in the Cretaceous back–arc basin of Colombia in terms of the total organic content (TOC), gas, vitrinite reflectance, porosity, permeability, pyrolysis, and organic geochemistry. They conclude that the best properties correspond to the limestone of La Luna Formation and laterally equivalent units deposited in a transgressive interval and relatively high sea level.

In chapter 10, Cardona et al. (2020) document that a change in the tectonic style is evident in the entire western continental margin of South America, going from the Mariana subduction to Andean subduction style. This change is associated with regional kinematic plate reorganizations that mark the onset of the construction of the Andean chain. The authors identify this change in the Cretaceous sedimentary and magmatic rocks of the Central Cordillera.

In Colombia, dinosaur remains are rare; therefore, the report by Noè et al. (2020) in chapter 11 on the discovery of six dinosaur tracks in rocks of the Batá Formation of the late Valanginian – early Hauterivian is important. The authors report that four of the tracks form a track left by a single dinosaur, interpreted as a subadult ornithopod of the ichnogenus *Iguanodontipus*. These findings suggest the existence of terrestrial communication during the Early Cretaceous, between Europe and North Africa today, that would have allowed migration along the northern coast of Gondwana to what is now South America.

In chapter 12, Patarroyo (2020) describes the marine sedimentary deposits of the Barremian in Colombia represented by different lithostratigraphic units that are found from the central zone to the north of the country, which are rarely studied except for the Paja Formation. The author indicates that the biostratigraphy of ammonites is the main tool for identifying chronostratigraphic levels because it facilitates more accurate relative dates than can be obtained by fossils of other animal and plant organisms. The author also explains that the fauna of Tethys allows correlation of the successions of the Barremian of Colombia with the standard biozones of the Mediterranean area and supports that the sedimentary and ecological variations are a consequence of the environmental factors, the paleoecology, and the differentiation of the sub–basins that were subject to variations in the ocean floor.

In chapter 13, Noè & Gómez–Pérez (2020) propose that the Paja Formation, exposed in the alto Ricaurte region (Villa de Leyva, Sáchica, and Sutamarchán), is a unique *Lagerstätte* of marine vertebrates of the Lower Cretaceous worldwide. In this formation, very well–preserved marine fossils of plesiosaurs, ichthyosaurs, fish, turtles, and ammonites are found.

Based on the interpretation of the most recent data on total rock geochemistry and Ar–Ar and Lu–Hf ages, Bustamante & Bustamante (2019) conclude in chapter 14 that the three manifestations of high P/T metamorphism documented in the Central Cordillera of Colombia correspond to two different uncorrelated subduction events. The oldest (ca. 130–120 Ma) produced the high–pressure rocks of Pijao and Barragán, and the most recent (ca. 70–60 Ma) is represented by the blue schists of Jambaló.

4.3. Volume 3 Paleogene – Neogene

Volume 3 covers the events that occurred during the Paleogene – Neogene and includes 17 chapters (Gómez & Mateus–Zabala, 2020b). The image on the cover shows the Cretaceous – Paleogene boundary deposits of Gorgonilla Island in a photograph provided by the geologist Hermann BERMÚDEZ.

Chapter 1 of this volume, written by Bermúdez et al. (2019), presents the first record from Gorgonilla Island of the Chicxulub impact occurred at the K/Pg boundary in the Yucatán Peninsula. The tektite and microtektite stratum, approximately 20 mm thick, left by the impact constitutes one of the best–preserved accumulations in the world, and its age is confirmed with $^{40}Ar/^{39}Ar$ dating and micropaleontological analysis.

The origin, structure, age of the basement, and tectono–stratigraphy from the Late Cretaceous to the Holocene of the Lower Magdalena Valley Basin and the folded belt of San Jacinto are described by Mora–Bohórquez et al. (2020) in chapter 2. The authors explain that the subsidence controlled by faults between the late Oligocene and the early Miocene facilitated the initial filling of the lower valley, while contemporaneous uplift pulses in Andean terranes made the connection of the Lower and Middle Magdalena and the formation of the largest drainage system in Colombia (Magdalena River) possible. In addition, they highlight the relationship between the changes in the kinematics of the plate tectonics, the structures inherited from the basement, and the contribution of sediments in the evolution of forearc basins.

The sedimentary record of the northern Andes contains important evidence on the geological history of the Eastern Cordillera, which separates the hinterland basin of the Magdalena Valley from the Llanos Foreland Basin. This Mesozoic – Cenozoic marine and continental sedimentation, as revealed by Horton et al. (2020) in chapter 3, took place during contrasting and well–differentiated tectonic regimes.

In chapter 4, Mora et al. (2020a) provide a summary of the evolution of the uplift of the northern Andes. With a combination of the cooling histories and analysis of the provenance, they offer a critical view of the most recent paleogeographic interpretations. The authors draw attention to the use of limited data to provide paleogeographic interpretations that are often presented as definitive and unequivocal.

In chapter 5, Mora et al. (2020b) outline the structural geometry and the evolution of the eastern foothills of the Eastern Cordillera, comparing the shortening records of thick– and thin–skinned deformational styles of the Caguán–Putumayo and Llanos Foothills along the Andean deformation front. According to the proposals, the main factor in the thick–skinned deformation style is the basement composition, which is crystalline in the Caguán–Putumayo region and metasedimentary in the Piedemonte Llanero (Llanos Foothills). They note that the evolution of the foothills of the Colombian Andes began in the Oligocene with similar structural styles and that divergence occurred in the accelerated shortening that took place between the Miocene and the recent, when a rapid sedimentation of thick fluvial sequences allowed the source rocks of the foothills to enter the oil generation window and to assist with the formation of efficient detachment horizons for the thin–skinned deformation.

The tectonic of the Eastern Cordillera is described by Kammer et al. (2020) in chapter 6, in which the authors seek to clarify the relationships between the inherited pre–Cretaceous crustal structures and those formed by a more superficial folding during the Neogene. For this, they differentiate three structural domains: a meridional domain that presents shortening in its lower structural levels and folding in the upper; an intermediate domain, north of the first, characterized by large–scale antiforms involving a basement in the core; and a northern domain that includes an antiformal lobe with considerable topographic relief, which corresponds to the Cocuy Syntaxis. The authors also propose the existence of a forebulge during the Cretaceous from an impinging mantle plume.

In chapter 7, Parra et al. (2020) reconstruct the history of the uplift of the Sierra Nevada de Santa Marta and the erosive processes that acted on its relief, based on the results of bedrock and detrital thermochronology, new contributions from fission tracks and (U–Th)/He in apatites of active sediments, and the stratigraphic study of adjacent marginal basins of the Miocene – Pliocene. With this information, the authors posit that the uplift was an episodic and asymmetric process that began with a rapid uplift during the late Eocene – early Miocene and that the southwestern sector experienced a faster uplift than the north. They also showed that the uplift of the Sierra Nevada de Santa Marta is a very recent phenomenon, less than 2 million years old.

The Tumaco Forearc Basin is described by Pardo–Trujillo et al. (2020) in chapter 8 as a symmetric basin whose depocenter accumulated more than 8000 m of sediments, containing information on the geological evolution of southwestern Colombia, where the subduction of the Farallón and Nazca Plates under the South American Plate controlled the subsidence and magmatic activity between the Oligocene and the Holocene. Volcanoclastic fans, as well as fluvial and coastal sediments associated with the Patía and Mira Rivers, partially cover the Miocene – Pliocene deposits.

In chapter 9, Silva–Tamayo et al. (2020a) describe the successions of Cenozoic marine carbonates from different sedimentary basins in Colombia; the authors analyze the biological associations and relate them to the deposition conditions and the movements of continental and marine blocks.

In the basins of the Middle Magdalena Valley and south of the Llanos, the outcrops, the core and well records, and the existing sedimentological and palynological investigations allow Caballero et al. (2020), in chapter 10, to study shallow and continental marine sedimentary records in the context of sequence stratigraphy and to obtain information on the evolution of reservoirs and their properties.

The Amagá Formation, a carbon–rich unit, of the late Oligocene – middle Miocene is described in chapter 11. This formation constitutes, according to Silva–Tamayo et al. (2020b), one of the most complete tropical siliciclastic sedimentary sequences deposited in an intramontane basin in the northern sector of the Colombian Andes. The integration of the available information and new sedimentological, biostratigraphic, geochronological, and thermochronological data allow the authors to evaluate the mechanisms that controlled the sedimentological evolution along Andean–type convergent margins.

The Combia Formation, exposed in the northwest of the Colombian Andes, is a unique occurrence of tholeiitic magmatism formed in an extensional basin and associated with calc–alkaline magmatic rocks. The review of geochemical and geochronological information by Weber et al. (2020) described in chapter 12 indicates that the two magmas coexisted. The tholeiites were formed from a primitive mantle, with a limited supply of sedimentary or continental contaminants, and the calc–alkaline magmas, mainly adakitic, were formed from the fractionation of garnet and amphibole at high pressures from a hydrated melt from an enriched source.

Chapter 13 describes the Morales Formation of the Patía Sub–basin, defined by Gallego–Ríos et al. (2020) as a sequence consisting of mudrocks interbedded with thin beds of sandstones. The authors interpret this sequence as deposited in an environment of lakes and swamps with adjacent fluvial channels. The sudden increase in volcanic material in the sequence is explained by the authors as the onset of volcanic activity of the Central Cordillera, which continues until the present.

In chapter 14, Zapata–García & Rodríguez–García (2020) summarize the state of knowledge of the Chocó–Panamá Arc, presenting the petrographic, lithogeochemical, and geochronological characteristics of the vulcanites and plutons that constitute it and, for the first time, a segment to the south formed by the Timbiquí Formation and Napi Tonalite. This synthesis allows the authors to define, with greater precision, this geological block exposed on the western flank of the Western Cordillera between the border with Panamá and the Nariño Department.

Montes & Hoyos (2020) present, in chapter 15, a review of the geology of the basement of the Isthmus of Panamá. They indicate that tectonic deformation is the main factor controlling the sites and modes of Cenozoic sedimentation and the geological evolution of the isthmus. They also propose an evolutionary geological process.

In chapter 16, Urueña–Suárez et al. (2020) describe how the determination of crystallization and the cooling ages of detrital zircons in ancient sedimentary rocks or modern river sediments can be used to identify the sediments provenance and the exhumation of orogenic belts. To support these considerations, they present the results of U–Pb dating and fission tracks in the zircons of sedimentary units of the Eastern Cordillera and sediments of modern rivers that drain both flanks of this mountain range and the eastern flank of the Central Cordillera. The authors highlight the advantages and limitations of using U–Pb dating and fission tracks for provenance studies, including the identification of original source areas, the recycling of sediments, and the difficulty in detecting amagmatic orogens in the detrital zircon record.

With fission tracks data in apatites and zircons from crystalline rocks and thermal history modeling Amaya–Ferreira et al. (2020) present, in chapter 17, a thermal history in four stages for the Santander Massif in the Eastern Cordillera of Colombia. At 60 million years, a burial heating from the Late Jurassic to the Late Cretaceous was followed by three cooling phases that began at approximately 65–60 Ma, related to regional tectonic events.

4.4. Volume 4 Quaternary

Volume 4 presents the chapters on the Quaternary and was written mainly by researchers from the SGC (Gómez & Pinilla–Pachon, 2020b). On the cover is the Alsacia Volcano, a monogenetic volcanic center that is reported for the first time in *The Geology of Colombia*.

The tectonic history of the intermountain basin of the Cauca River valley, described in chapter 1 by López & Toro–Toro (2020), exhibits alternating compressional and extensional phases in the Miocene – Quaternary interval. These phases are reflected in the Miocene – Pliocene La Paila Formation deposited during an extensional phase influenced by arc volcanism, and the Pleistocene Zarzal Formation and Quaternary deposits that record compressive tectonic activity that initiated after the accretion of the Isthmus of Panamá.

In chapter 2, Hooghiemstra & Flantua (2019) summarize sixty years of palynological research in the Colombian territory. The authors present an overview of Quaternary history through the identification of environmental and climate changes characterized by a set of glacial–interglacial cycles very well–documented in the Quaternary sedimentary record of Colombia.

Following the review of existing information, Monsalve–Bustamante (2020) describes, in chapter 3, the most relevant characteristics of Colombia's active volcanic front, the identified volcanic centers, the tectonic context, and the historical and recent activity. The author states that the systematic study of active volcanoes and continuous monitoring by the SGC has made it possible to advance knowledge about the most superficial processes, stratigraphy, and eruptive history of the volcanic front. The author proposes topics for future research on volcanism in Colombia.

In chapter 4, the Paipa geothermal system is classified as unusual by Alfaro–Valero et al. (2020) due to its location in the Cretaceous sedimentary environment of the Eastern Cordillera, associated with rhyolitic to trachydacite volcanic activity of the Neogene – Quaternary. This chapter proposes a conceptual model of this system based on geological, geophysical, and geochemical studies conducted by the Grupo de Exploración de Recursos Geotérmicos of the SGC.

Pulgarín–Alzate et al. (2020), in chapter 5, present the constitution and origin of the Paramillo de Santa Rosa Volcanic Complex, located in the Central Cordillera. The authors interpret it as the result of a succession of events related to a subduction zone in an active continental margin between the early Pleistocene and the Holocene. This knowledge contributes to the assessment of the volcanic hazard in this region of the Colombian territory.

In chapter 6, written by Correa–Tamayo et al. (2020), the Nevado del Huila Volcanic Complex located in the Central Cordillera is studied. The authors divide the eruptive activity of this volcano into three stages: Pre–Huila, Old Huila, and Recent Huila, that began in the early Pleistocene and produced two main volcanic edifices (Pre–Huila and Huila).

Recent research, integrated with previous studies and geochronological, petrographic, and geochemical data, helped Ceballos–Hernández et al. (2020) define, in chapter 7, the Nevado del Ruiz Volcanic Complex, located in the Northern Volcanic Segment of the active volcanism of Colombia, and expose the geological evolution that produced it. The authors identified four major eruptive periods characterized by the construction and destruction of volcanic edifices: The Pre–Ruiz eruptive period, the First eruptive period Ruiz, the Intermediate eruptive period Ruiz, and the Second eruptive period Ruiz. On 13 November 1985, an eruption of the Nevado del Ruiz resulted in the disappearance of the city of Armero and the death of 23 000 people.

The Cerro Machín Volcano, located on the eastern flank of the Central Cordillera, is an active volcano that generated explosive eruptions over the last 10 000 years that, according to Cortés–Jiménez (2020) in chapter 8, originated thick deposits of pyroclastic material. The pyroclasts were mixed with water of diverse origin, forming torrential flows (lahars) that were mobilized to areas more than 100 km away from the volcano to the Magdalena River Valley. The lahars constitute one of the greatest threats of this volcano.

The origin of the Quindío–Risaralda Quaternary deposit described in chapter 9 occurred, according to Espinosa–Baquero (2020), in two major phases: A constructive phase associated with the strong volcanic activity of the Paramillo de Santa Rosa and the Nevado del Quindío, which corresponds to the accumulation of proximal fans, and another destructive phase controlled by the final uplift of the Central Cordillera along large fault systems, which produced intermediate and distal fans. Over this deposit were built Armenia and numerous towns of the Quindío and Risaralda Departments.

Monsalve–Bustamante et al. (2020), in chapter 10, locate and describe 36 monogenetic volcanoes, 22 of which are reported for the first time in *The Geology of Colombia*. This chapter is considered to be informative and a call to investigate the presence and mechanisms that produced these volcanic manifestations concentrated in certain regions of the national territory, with very particular geological conditions, where there are populated centers and expansive agricultural development.

In chapter 11, Vargas (2020) explains how, from seismological, geodetic, and geophysical information, he estimated tomograms of anomalies of seismic velocity, the depth of the Curie point, and the stress field along the western margin of South America to explain the geometry and the subduction process of the Caribbean and Nazca Plates under the South American Plate.

The Algeciras Fault System is presented in chapter 12. This tectonic system is considered by Diederix et al. (2020a) to be the largest active fault system in Colombia. The authors state that their study is essential for understanding the geodynamics of the northern Andes. The great seismic activity of the past and present suggest to the authors that the Algeciras Fault System is the most dangerous in Colombia and is capable of generating large–scale earthquakes in the future.

The recent results of neotectonics, paleoseismology, and paleomagnetism allowed Diederix et al. (2020b), in chapter 13, to quantitatively corroborate the quaternary activity of the Bucaramanga Fault. The authors report that recent activity is not reflected in instrumental seismicity, while geomorphological expression suggests high displacement rates during the Pleistocene. They confirm that the analysis of eight seismic events during the Holocene yields a displacement rate of 2.5 mm/y and that the paleomagnetism in sediments of the Bucaramanga alluvial fan indicates a similar movement rate.

Chapter 14 describes the geodetic satellite measurements obtained by the GeoRED project of the SGC. Mora–Páez et al. (2020a) explain how this project contributes to the understanding of regional tectonics in the northern Andes and the southwest of the Caribbean, including the seismic hazards in the Colombian trench, the Caribbean margin, the fault system of the eastern foothills of the Eastern Cordillera, and the collision zone of Panamá in northwestern Colombia, as well as the deformation of Colombian volcanoes.

Based on data obtained by GeoRED, Sagiya & Mora–Páez (2020) report, in chapter 15, how is the coupling between tectonic plates in the Nazca subduction zone, along the Pacific coast of Colombia and Ecuador, where earthquakes of great magnitude frequently occur, to evaluate the future seismic potential of the region. The results of the analyses show 4 main locked patches. Based on the seismic moment accumulation rate, researchers estimate that the recurrence interval for the 1979 earthquake is approximately 124 years.

In chapter 16, Mora–Páez et al. (2020b) analyze land subsidence in the urban area of Bogotá, where more than 7 million inhabitants live. With the analyses performed, using radar images, subsidence values were obtained in the central area of the city on the order of 3.3 cm/y.

Based on the analysis of focal mechanisms and GPS measurements, Arcila & Muñoz–Martín (2020) describe, in chapter 17, the stress regime in Colombia and formulate a seismotectonic model for the NW corner of South America, characterized by the displacement towards the SE of the Caribbean Plate, the convergence of the Andean, Coiba, and Panamá Blocks in NW Colombia, and the W–E convergence of the Nazca and South American Plates.

5. Outreach Strategy of the Work *The Geology of Colombia* for the Specialized Public

With the aim of presenting the state of knowledge on the geological evolution of Colombia and the surrounding regions to the international geoscientific community, the editorial team of *The Geology of Colombia* organized three sessions in annual meetings that include a considerable number of geoscientists from various parts of the world. The sessions promoted interdisciplinary exchanges and debates on Colombian geology in the framework of the geology of the northwestern corner of South America and provided new research approaches and opportunities for research collaborations.

5.1. Participation in the GSA Annual Meeting 2018

From 4 to 7 November 2018, the GSA Meeting 2018 was held in Indianapolis, Indiana, USA, an event with 5628 attendees. The editorial team of *The Geology of Colombia* chose this annual meeting and the exhibition of the Geological Society of America for conducting the first special session on the geology of Colombia: Session "T183. The Geology of Colombia" (Figure 10).

The session had 12 oral conferences and 6 posters that were presented mostly by researchers linked to the editorial work as authors (https://bit.ly/2zJNdL4). In addition to leading the session, the editorial team presented two oral presentations: "The Geology of Colombia Book: A journey through the geological history of Colombia" and "The social appropriation of geological knowledge from the Colombian Geological Survey: The successful case of The Geology of Colombia Book" to present the content of the 4 volumes of the editorial work and the outreach strategy that was designed in the project. The team also presented a poster on the volcanism of the Combia Formation, the main theme of one of the chapters.

5.2. Participation in the AGU Fall Meeting 2019

From 9 to 13 December 2019, the AGU Fall Meeting 2019 of the American Geophysical Union was held in San Francisco, California, USA, an event that was attended by more than 30 000 scientists and decision–makers from all over the world. In this, the biggest international meeting of Earth sciences in the world, the editorial team led two sessions on Colombian geology (Figure 11).

The first session, "T13B. New Advances on the Geologic and Tectonic Framework of Colombia and Its Surrounding Regions I", included oral presentations. In total, seven talks were presented about the tectonic setting of the northwestern corner of South America based on relocated seismic events and new ideas on the construction of the Eastern Cordillera from the sedimentary record.

Likewise, the Cenozoic tectonic evolution of the Sierra Nevada de Santa Marta, the magmatic record in Colombia of the collision of the Panamá Arc and the subduction of the Nazca Plate, the geometry of subduction in Colombia, and the late Silurian exhumation of the proto–Andean margin and the uplift of the northern Andes were discussed.

The second session, "T21E. New Advances on the Geologic and Tectonic Framework of Colombia and Its Surrounding Regions II", included poster presentations. The seismicity along the subduction zone in Colombia, the geochemical evolution of arc magmatism across Panamá and Colombia, and the axis rotations associated with inverted

Figure 10. Official photograph of session "T183. The Geology of Colombia".

Figure 11. Attendees at the session "T13B. New Advances on the Geologic and Tectonic Framework of Colombia and Its Surrounding Regions I" of the AGU Fall Meeting 2019.

faults in the Colombian Eastern Cordillera were some of the 11 topics developed by the researchers in this session (https://bit.ly/2QE0mOU). In addition, in this space, the editorial team presented the contributions of the SGC to the state of knowledge of Colombian geology, including the work *The Geology of Colombia* (Figure 12).

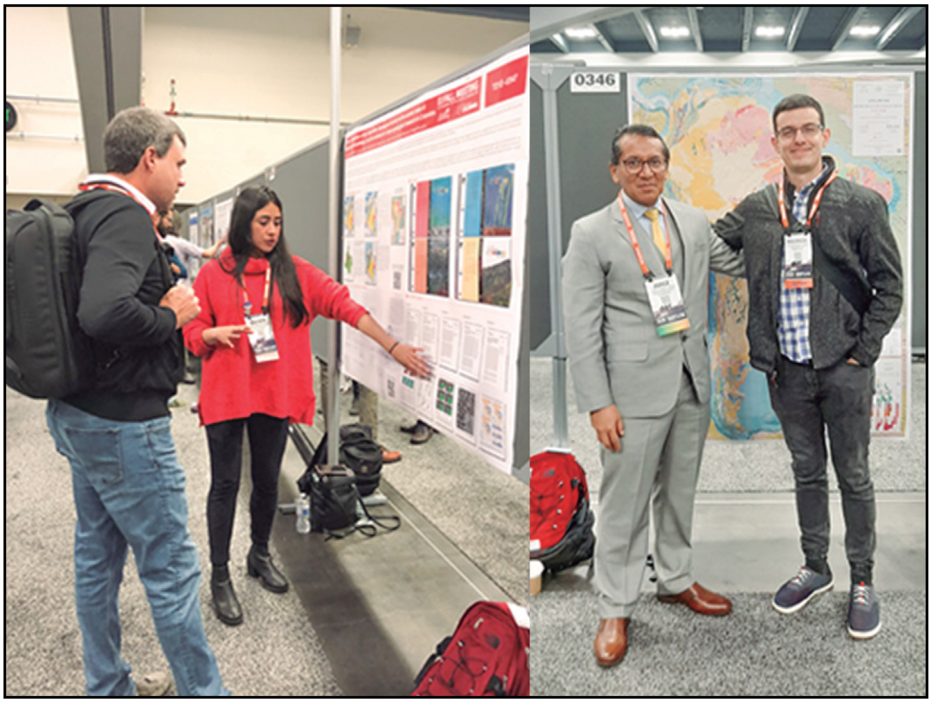

Figure 12. Participation of the editorial team in the session "T21E. New Advances on the Geologic and Tectonic Framework of Colombia and Its Surrounding Regions II".

6. Outreach Strategy of the Work *The Geology of Colombia* for the Lay Public

Because *The Geology of Colombia* brings together current knowledge on the formation and evolution of the national territory, its mineral resources, and its geological hazards, information that is relevant to the social and economic development of the country, it was important that the research, findings, and interpretations presented in the publication be comprehensible to people not specialized in geosciences.

Aware of this situation, the members of the editorial group of the work and the executives of the SGC considered it essential to create an outreach strategy for disseminating geoscientific knowledge aimed at the lay public. The planning for this strategy started in 2017, and the outreach was launched in 2018. The design and implementation were carried out by a multidisciplinary team consisting of a scientific journalist, a geologist, an audiovisual producer, and a graphic designer. This group was led by the senior geologist and principal editor of *The Geology of Colombia*.

The strategy consisted of generating text and multimedia content from the chapters of the editorial work with the most media impact or with the highest impact on society in terms of risk and environmental management, tourism, economy, or with new contributions to scientific knowledge. These were published in national newspapers, magazines, and radio and on social networks and websites so that they became familiar to government entities for their decision making and the community for taking ownership of their environment and expanding their knowledge about the geology of Colombia.

Publications emerging from this strategy included newspaper articles, videos, photo galleries, photo publications, and specific messages on social networks (Facebook, Twitter, Instagram, and YouTube) and comics with geological cartoons. The stages for the generation of informative products are described below:

1. Selection of the chapters of the work *The Geology of Colombia* with novel, timely issues and, importantly, with social relevance. The selection was made considering that not all the topics investigated by geoscientists are relevant to the lay public.
2. An invitation to the authors of the selected chapters to participate in a field trip with a journalistic focus. In cases where the author was unable to attend, an interview was conducted, and the supporting photographs and videos, which were usually acquired in the field, were provided by the author. With the confirmation of the author, the journalist began reading the chapter and reference documentation. As part of the journalistic investigation, she contacted the author and relied on the geologist of the group for explanations of the topic. The chapter was carefully broken down, and the central theme of the outreach strategy was defined. Then, a dialogue was established from the journalistic and geological approaches to specify the terminol-

Figure 13. Field trip to Aguadas, Caldas with professor Agustín CARDONA in the serpentinites of Pácora. Topic: Evolution of the Central Cordillera of Colombia.

ogy and establish a script for the entire team involved in the execution of the communicative pieces.

3. Field trip to the area where the investigation of the selected chapter was carried out. Before the videos were recorded and the images were captured, a pre–production stage was carried out in which the researcher prepared a simple explanatory discourse about their research (different from that usually used in the scientific world) and instructions to record the video (Figure 13). In this stage, it was borne in mind that what is interesting to a geologist may not be equally interesting when translated into journalistic content. The author was the protagonist of the story, and as such, his or her active participation was required.

   The field trips were also opportunities to exchange knowledge with the inhabitants of the area. In addition to talking with the community, the team went to the local media (Figure 14), visited government authorities, schools (Figure 15), and the national police to involve them in the activities, to tell them what is being studied in the area, and to listen to their knowledge of the territory, positions, and concerns.

   The team that accompanied the researcher on the field trip was composed of a scientific journalist, one or more geologists, and an audiovisual producer. With their different areas of expertise, these professionals collected material presented by the researcher, recorded audio and video, and took photographs in the field. The journalist asked the researcher questions that were previously discussed and aimed at content production. A friendly professional work environment was created to encourage the researcher to express the results of their studies in a pleasant storytelling style (Figure 16).

   During the field trips, interviews and high–quality videos and photographs were obtained using professional photographic equipment, filters, and specialized lenses for landscape photography, as well as for capturing video and documentary photography. The variety of optics and the technical capacity of the teams generated rich visual narratives, resulting in aesthetically pleasing images to entice the viewer.

4. Writing of the newspaper article. In this phase, the scientific journalist wrote the first version of the article; then, the researchers and some of the geologists of the editorial group reviewed the article, clarified concepts, and added or removed information without changing the journalistic style. Thus, a final version was produced. This way of working brought excellent results. Past experience of researchers working with journalists has not been ideal because press releases and articles do not usually include a final review by the scientist, which has resulted in publications lacking technical rigor. The fact that the researcher could validate the accuracy of the data and concepts before publication yielded good results.

Figure 14. The volcanologist Gloria Patricia CORTÉS with the journalist Lisbeth FOG and journalists from El Nuevo Día newspaper in the city of Ibagué, talking about the Cerro Machín Volcano.

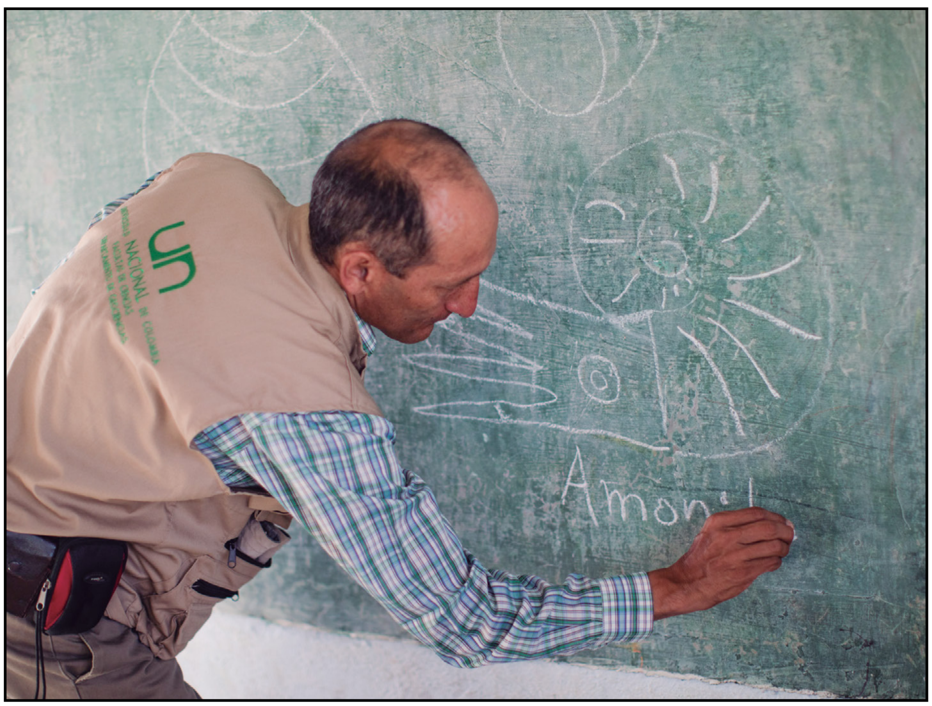

Figure 15. Professor Pedro PATARROYO, in a rural school in La Guajira, explains to students the extinct Cretaceous marine fauna and its importance in the study of the evolution of species and climate changes.

5. Production of a video lasting from three to seven minutes to expand upon the explanation of the topic addressed in the newspaper article. For this, a video script was generated, and the approach was determined. The videographer began the production of the video, framed within a specific editorial line for each topic and that provided an identity for the product. In addition to the video footage in the field, maps, graphics, and animations designed by

Figure 16. Geologist Alberto NÚÑEZ TELLO in the Huila Department explaining what monogenetic volcanoes are. Most monogenetic volcanoes are tourist destinations, but more often than not neither the inhabitants nor the tourists know that these mountains are volcanoes.

the geologist of the group were used to help exemplify the topics covered in the videos. The videos were published on the YouTube channel of the SGC. These highlighted the question that the researchers are solving with their studies, the geological importance of the places visited in the field trip, and the human side of the researchers.

6. Generation of photo reports. For each of the social networks, a set of ten photographs of the field trip was chosen that could tell a story, in the same line of the newspaper article and the video of the selected chapter. Additionally, simple texts were written with a clear message to accompany each photograph. The texts helped to spin the story, just as the images were adapted according to the social network. By way of the photo reports, the public was guided through different emotional and scientific moments of the subject to be shared. The photo reports were posted on the Facebook, Instagram, and Twitter accounts of the SGC (Figure 17).
7. Creation of geological cartoons. In parallel with the production of the mentioned products, the Familia Piedrahita was created, a Colombian family of rocks, minerals, and fossils (Figure 18). For its creation, representative samples of Colombian geology were selected, most of them from the Museo Geológico José Royo y Gómez of the SGC. Then, they were photographed and digitally manipulated. Finally, the different personalities of each character were generated. With these characters, comics were constructed, and graphics and stickers were designed to address concepts about the geology of Colombia and the project *The Geology of Colombia.*

   The comics used humor and everyday events to generate empathy for geology on the part of the lay public. For its production, the social dissemination of the knowledge team as a whole conceptually analyzed the idea that the story would tell, the characters that were going to appear were chosen, and dialogues were created to finally assemble the story (Figure 19). The comics or images with the characters of the Familia Piedrahita were published on the social networks of the SGC. The first comics explained the origin of each character from the geological point of view. Then, geological concepts or topics previously published in press articles were explained. Additionally, a geological glossary was generated with the Familia Piedrahita.

Figure 20 summarizes the stages for generating the dissemination products in the outreach strategy.

6.1. The results

The results and impact of this outreach strategy for disseminating knowledge to lay audiences were quantitatively evaluated through the analytics of the SGC social networks and the reach of readers of national newspapers. Additionally, the results and impact were qualitatively evaluated based on how each type of

Figure 17. Instagram posts about monogenetic volcanoes.

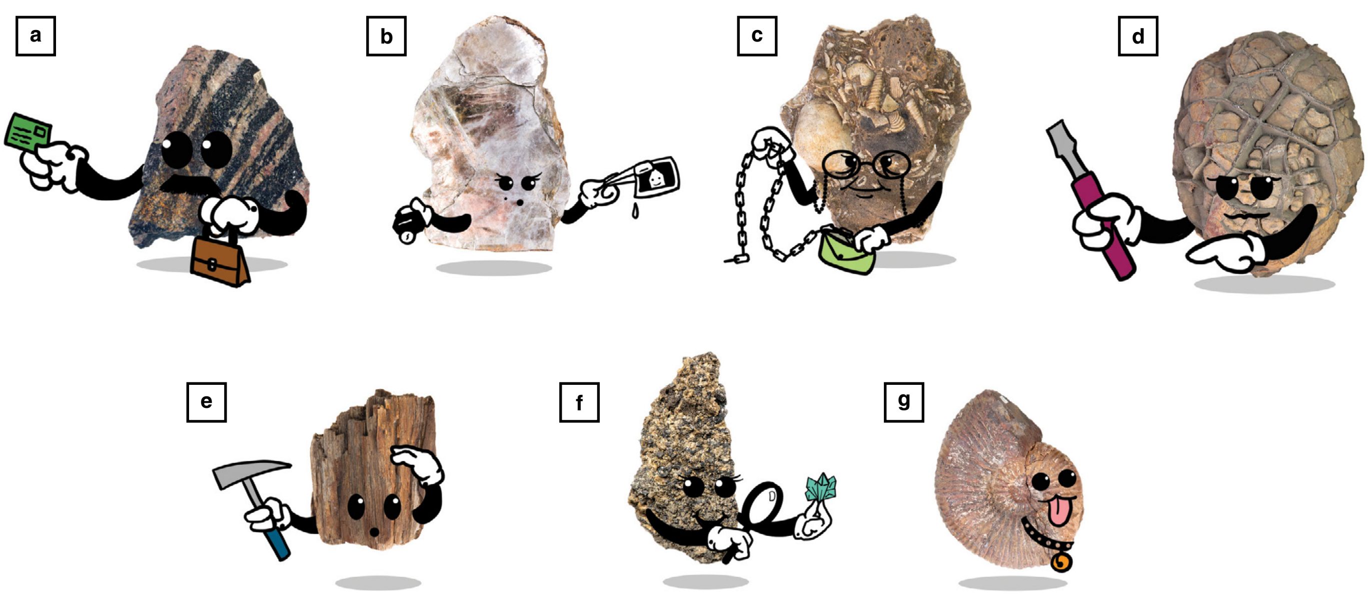

Figure 18. Members of the Familia Piedrahita. **(a)** Father Gneiss Piedrahita, **(b)** mother Flo Piedrahita, **(c)** grandmother Concha Piedrahita, **(d)** aunt Calca Piedrahita, **(e)** son Xilo Piedrahita, **(f)** daughter Pili Piedrahita, and **(g)** the pet Amón Piedrahita.

content was received, which was reflected in the comments left by users on each published content. The results by product with a January 2020 cutoff are as follows:

Twelve articles in national media: Eight in the newspaper *El Tiempo* (print and web), two in the magazine *Semana* (web), and two in the newspaper *El Espectador* (print and web), where one was covered in the print edition of Sunday 10 June 2018 (Figure 21). Each article had an average of 200 000 readers in print and more than 13 000 readers in the digital publication. The web pages for consulting the articles are presented in Table 1.

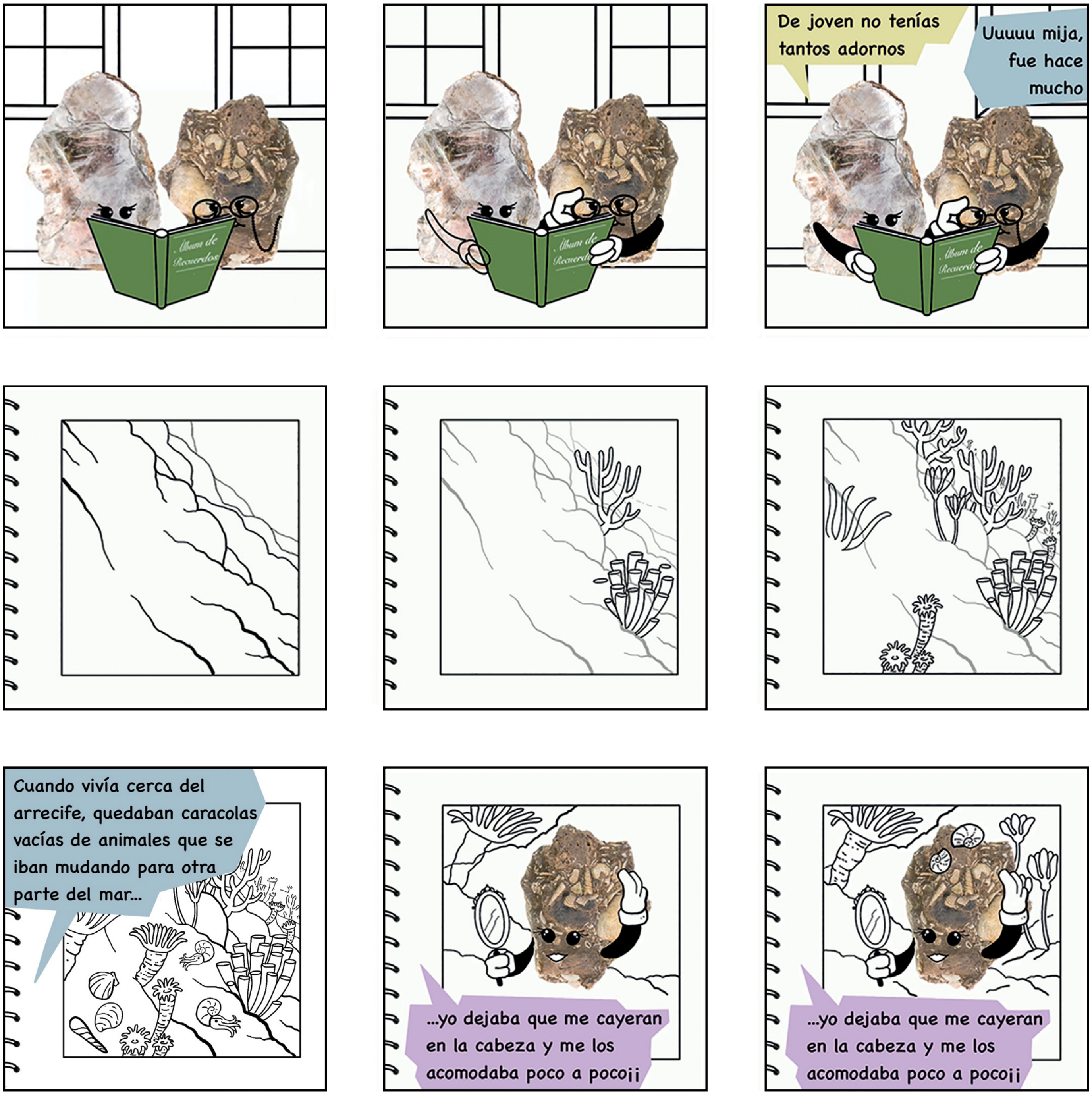

Figure 19. Creation process of the Familia Piedrahita comics.

A total of 114 posts were published on Facebook, 121 on Instagram, and 135 on Twitter, with an average reach of between 10 000 and 13 000 views for each publication. The publications of the campaign can be filtered on the SGC social networks using the hashtag #SGCGeologiaDeColombia. Some examples can also be accessed at https://www2.sgc.gov.co/LibroGeologiaColombia/Paginas/Social_Media.aspx. The creative content, with good graphic and textual quality, had a positive impact on the number of followers of the SGC social media accounts, especially on Instagram, and inspired other groups of the SGC to begin sharing the results of their research in this format.

A total of ten videos were published on YouTube averaging 2200 views for each video (Table 2).

Ten comics of the Familia Piedrahita were published (Figure 22) as well as 31 stickers that can be downloaded free of charge at https://www2.sgc.gov.co/LibroGeologiaColombia/Paginas/historias-de-geologia.aspx

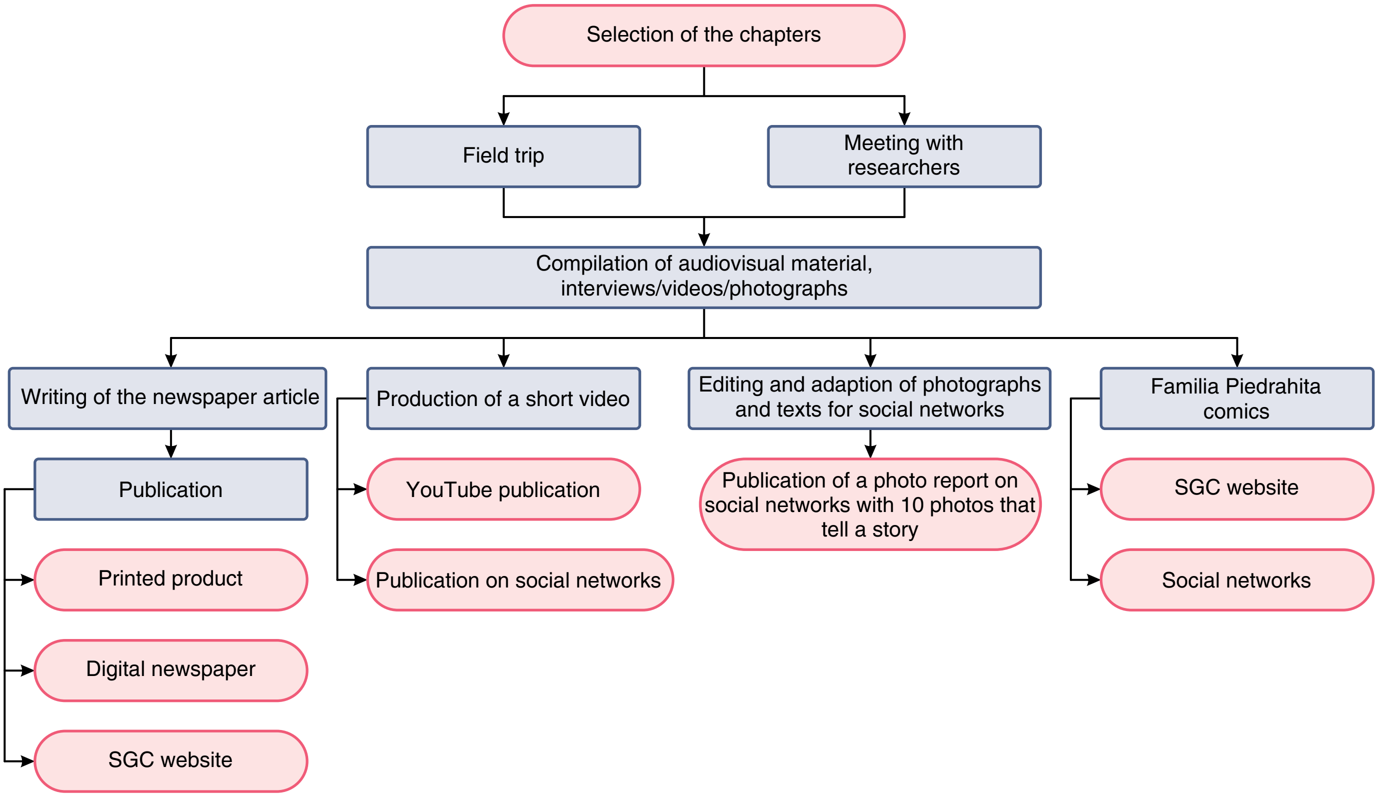

Figure 20. Flow chart of the stages of the outreach strategy for disseminating geoscientific knowledge from the work *The Geology of Colombia.*

Finally, to measure whether there was an audience that watched posts on social media and wanted to learn more about the work *The Geology of Colombia,* the number of website visits was used. From 1 June 2018 to 16 September 2019, the page reached 26 651 visits.

Although the strategy for disseminating the work *The Geology of Colombia* to the lay public is framed within the institutional policy of Social Appropriation of Geoscientific Knowledge (Apropiación Social de Conocimiento Geocientífico) that the SGC has been developing for several years, it is a pioneering strategy. In addition to being an organized and intentional process that involved the participation of different actors, among other scientists, local communities, and communicators, the strategy included several innovative components that resulted in quality products and impact.

Among the distinctive factors of this strategy, the constitution of a multidisciplinary team to design and develop the process stands out; this team conducted field trips that facilitated the presentation of the activities that geoscientists perform daily to the public, facilitated efficient and respectful communication between the geoscientific world and journalism, planned and prepared content with specific objectives, and produced high–quality graphic and textual pieces.

Social networks and the website played a key role within the strategy because they allowed for greater reach, mapping the audiences that consulted each social network, which provided knowledge with their interests and facilitated refinement of the material that was published. For each platform, the type of photographic content that had the greatest impact or interactions was studied.

The strategy was presented at the following national and international scientific events: XIII Technical Week of Geology, Geological Engineering and Geosciences in Manizales, Colombia; GSA Annual Meeting 2018 in Indianapolis, Indiana, USA; International Congress of Science and Technology Governance in Bogotá, Colombia; ^{5th}YES Congress 2019 "Rocking Earth's Future" in Berlin, Germany; AGU Fall Meeting 2019 in San Francisco, USA. In the presentations, the feedback was received from geoscientists, communicators, and scientists from other disciplines, in addition to inspiring professionals interested in the dissemination of science.

Additionally, with the strategy, some limitations of communication of science through digital media could be identified, the future path or activities recommended for measuring the continuity and loyalty of the audience could be determined, and the knowledge that has penetrated the users could be calculated. It is expected that *The Geology of Colombia*'s public outreach strategy will be a model and a motivation for more researchers to disseminate their knowledge.

In conclusion, all the efforts made in the dissemination of science are satisfactory and help achieve a more equitable so-

EL ESPECTADOR

BOGOTÁ COLOMBIA **FUNDADO EN 1887** N° 37.935 **10 DE JUNIO DE 2018** 64 PÁGINAS **www.elespectador.com** ISSN 01222856 **$3.700**

D Domingo

ESTE EJEMPLAR FUE IMPRESO CON TINTAS ECOLÓGICAS

AN ENVIRONMENTALLY FRIENDLY INK SYSTEM AGRI-WEB A trademark of Flint Group

El volcán que nadie ve

A propósito de la tragedia en Guatemala por el volcán de Fuego, expertos del Servicio Geológico Colombiano nos explicaron por qué el volcán Machín, en el departamento del Tolima, lleva miles de años anunciando un peligro similar sin que sus habitantes le presten suficiente atención. / Vivir p. 18

Un niño en el cráter del volcán Machín. Parece un potrero cualquiera, pero guarda una fuerza natural cuyas avalanchas han dejado huella sobre el río Coello. / Alejandra Cardona, Servicio Geológico Colombiano

Protagonistas de novela de la mafia en Argentina

Un excapo perseguido hace 20 años por EE. UU., reputados empresarios, un exfutbolista y familiares de Pablo Escobar forman parte del reparto. **p. 4**

¿Quiénes aconsejan a los candidatos presidenciales?

Les mostramos el organigrama de las campañas de Iván Duque y Gustavo Petro. Estos asesores serán personajes influyentes del próximo gobierno. **p. 6**

¿Criptomonedas de papas criollas colombianas?

La misma tecnología del bitcoin permite representar este y prácticamente cualquier activo, innovación que brindará al país nuevas oportunidades de financiamiento. **p. 12**

Trump-Kim Jong-un: el esperado encuentro

Análisis de la trascendencia de la reunión entre los presidentes de Estados Unidos y de Corea del Norte, prevista para mañana en Singapur. **p. 15**

Todos en modo Mundial de Fútbol

Un abrebocas a Rusia 2018 con los retos que enfrentan Messi, Cristiano Ronaldo, Neymar y James Rodríguez, y la presentación de los enviados especiales y analistas de **El Espectador**. **p. 58**

Figure 21. Journal articles of the outreach strategy of *The Geology of Colombia* published in national newspapers and magazines.

ciety. Scientific research does not end with the publication of a paper but when the information is known and applied by both the scientific community and the lay public.

7. Conclusions

- *The Geology of Colombia* is the result of collaborative work between authors with different specialties and experience in the study of processes, specific periods of the geological time, and particular regions of Colombia, and a multidisciplinary editorial team supported by the executives of the SGC. The support offered to authors since the first stages of the project to improve the graphic and textual quality of the chapters (training, adjustment and elaboration of figures, translations, etc.) became a novel factor in editorial processes of this type and allowed having a number of chapters (58) submitted that tripled the initial expectations.

Table 1. Articles and web pages published as of January 2020 that can be viewed as part of the strategy for the dissemination of the work *The Geology of Colombia*.

nº	Title	Newspaper/ magazine	Date of publication	Consultation link
1	How the plesiosaur of Villa de Leyva found its head (De cómo el plesiosaurio de Villa de Leyva encontró su cabeza)	*Semana*	6 April 2018	https://www.semana.com/educacion/articulo/servicio-geologico-colombiano-recupero-el-plesiosaurio-encontrado-en-villa-de-leyva/562660
2	La Guajira and the Mediterranean were connected (La Guajira y el Mediterráneo estuvieron conectados)	*El Tiempo*	24 April 2018	https://www.eltiempo.com/vida/ciencia/la-guajira-y-el-mediterraneo-estuvieron-conectados-hace-125-millones-de-anos-208694
3	The evolution of planet Earth as seen through plants (La evolución del planeta Tierra vista a través de las plantas)	*Semana*	17 May 2018	https://www.semana.com/cultura/articulo/la-evolucion-del-planeta-tierra-vista-a-traves-de-las-plantas/567419
4	Gorgonilla rocks speak of what happened 66 million years ago (Rocas de Gorgonilla hablan de lo que sucedió hace 66 millones de años)	*El Tiempo*	31 May 2018	https://www.eltiempo.com/vida/ciencia/rocas-de-gorgonilla-hablan-de-lo-que-sucedio-hace-66-millones-de-anos-225102
5	The warnings of the Machín Volcano (Los avisos del Volcán Machín)	*El Espectador*	9 June 2018	https://www.elespectador.com/noticias/ciencia/los-avisos-del-volcan-machin/
6	The marine fauna of Boyacá from 125 million years ago (La fauna marina boyacense de hace 125 millones de años)	*El Tiempo*	26 July 2018	https://www.eltiempo.com/vida/ciencia/fauna-marina-boyacense-de-hace-millones-de-anos-247522
7	Small volcanoes that blend into the landscape (Pequeños volcanes que se mimetizan en el paisaje)	*El Tiempo*	9 September 2018	https://www.eltiempo.com/vida/ciencia/que-son-los-volcanes-monogeneticos-y-donde-se-localizan-265608
8	The Central Cordillera emerged from an ocean full of volcanoes (La cordillera Central surgió de un océano plagado de volcanes)	*El Tiempo*	31 October 2018	https://www.eltiempo.com/vida/ciencia/formacion-de-la-cordillera-central-de-los-andes-288224
9	The Colombian Andes sail northeast (Los Andes colombianos navegan hacia el noreste)	*El Tiempo*	27 November 2018	https://www.eltiempo.com/vida/ciencia/estudio-sobre-los-movimientos-de-colombia-298616
10	The enigmatic heat source of the Paipa hot springs (Boyacá) (La enigmática fuente de calor de los termales de Paipa (Boyacá))	*El Espectador*	12 March 2019	https://www.elespectador.com/noticias/medio-ambiente/la-enigmatica-fuente-de-calor-de-los-termales-de-paipa-boyaca/
11	The adolescent Cordillera Oriental continues to grow (La adolescente cordillera Oriental sigue creciendo)	*El Tiempo*	12 August 2019	https://www.eltiempo.com/vida/ciencia/estudio-revela-crecimiento-de-la-cordillera-oriental-en-colombia-399748
12	Ancient pollen hints at the evolution of the planet's climate (El polen antiguo da pistas sobre la evolución del clima del planeta)	*El Tiempo*	1 January 2020	https://www.eltiempo.com/vida/ciencia/el-polen-antiguo-da-pistas-sobre-la-evolucion-del-clima-del-planeta-448046?fbclid=IwAR2FemxgWcFN5BoW5KBJvHr7IBMa4ad9DYCC5qDJJpSItHs5lGs09solmHI

- One of the factors that allowed for a successful convening and development of a targeted editorial process was that the editorial team had knowledge of the geology of Colombia and fulfilled its work of collaborating with the authors during the different stages of the editorial process. The advice offered by the Scientific Committee, geoscientists with experience in the editorial field, and two Colombian associations for research and scientific and technological development of the country, allowed to build an organized editorial process that was evaluated and improved during the advance of the project.

- *The Geology of Colombia* brings together the knowledge that has been built up over years. So, the inclusion, presentation, and verification of bibliographical references and citations were one of the details that the editorial team cared. The citation style used for the work is an adaptation that responds to the particularities of the type of publications generated in the country (conferences summaries, explanatory reports, internal reports). The standardization of bibliographic references was carried out based on 10 different categories of scientific documents; for each one was established a standard format.

Table 2. Videos published on YouTube of *The Geology of Colombia* outreach strategy.

nº	Name	Description	Consultation link
1	Pedro PATARROYO/Cerro Yuruma in La Guajira (Cerro Yuruma en La Guajira)	In La Guajira Department, the geologist Pedro PATARROYO of the Universidad Nacional de Colombia climbed Cerro Yuruma step–by–step, finding in each layer key information confirming the evidence of the Barremian era in our territory.	https://youtu.be/7RyviRyhipQ
2	Marcela GÓMEZ/Environment of Villa de Leyva (Ambiente de Villa de Leyva)	What was the landscape like in Villa de Leyva, Sutamarchán, and Sáchica 125 million years ago? It was a warm sea, approximately one hundred meters deep with abundant and diverse fauna, including giant reptiles, according to paleontologist Marcela GÓMEZ.	https://youtu.be/rOTHHnTgnrw
3	Leslie NOÈ/Pliosaurs (Pliosaurios)	The marine reptiles that lived in the sea of what is now Villa de Leyva shared the landscape with dinosaurs 125 million years ago. Among them are giant tortoises, plesiosaurs, and pliosaurs. What were the latter like?	https://youtu.be/bZ1W8c3gDEo
4	Carlos JARAMILLO/Plant evolution (Evolución plantas)	Although plants already existed, the first fossil record of a flower is from 140 million years ago. When a meteorite hits the Yucatán Peninsula and the extinction of many species occurs –65 million years ago– flowering plants start taking over the landscape.	https://youtu.be/LYvr_JP1D_o
5	Gloria Patricia CORTÉS/Machín lahars (Lahares Machín)	In the Coello River (Tolima, Colombia), geologists have found the tracks left by the eruptions of the Cerro Machín Volcano, one of the most dangerous in the country in the last ten thousand years: Devastating avalanches that have even reached the Magdalena River in Cundinamarca.	https://youtu.be/rij3bhiSwAM
6	The geological secrets of Gorgonilla Island (Los secretos geológicos de la isla Gorgonilla)	How can one imagine that 66 million years ago, the island of Gorgonilla was submerged two kilometers below sea level and that fragments of glass arrived in these depths produced by the meteorite that collided with what is now the Yucatán Peninsula?	https://youtu.be/qWhtbp77fXw
7	The origin of the Central Cordillera (El origen de la cordillera Central)	The planet Earth is transformed by the action of earthquakes, tsunamis, volcanoes… In the more than 70 million years that the Cretaceous lasted, changes occurred. From being submerged in an ocean, our Colombia began to form its mountains.	https://youtu.be/d_Zgz8LaQAE
8	Héctor MORA/GeoRED	More than 120 geodetic stations measure the motion of tectonic plates found under Colombian territory. From Bogotá, a group of scientists and technicians of GeoRED track the incoming data from each of them second–by–second.	https://youtu.be/lxo-zv7FvaI
9	Monogenetic volcanoes (Volcanes monogenéticos)	South of the Colombian Andes, geologists have discovered more than 20 monogenetic volcanoes (which means that they erupt only once); after eruption, these volcanoes blend into the mountainous landscape, making it difficult to identify them.	https://youtu.be/hLDZefUNMRY
10	The origin of the Paipa hot springs (El origen de las aguas termales de Paipa)	The remnants of a volcano that last erupted a million years ago are found in the depths of the Paipa soil, in Boyacá. Researchers from the Servicio Geológico Colombiano study this source that heats the relaxing Paipa hot springs.	https://youtu.be/xUdgGzDmjoE

- In a publication, the figures synthesize and group much of the information and the ideas of the text. They are a means to facilitate the transmission of the message that the author wants to deliver. For this reason, *The Geology of Colombia*'s chapters had no restriction on the number of figures. These were made in full color and edited based on concepts and visual hierarchies that the Grupo Mapa Geológico de Colombia of the SGC has been working on for several years to guarantee legibility and clarity.
- The editorial guidelines for *The Geology of Colombia* were based on the best articles, guides, and manuals of style for international use, like the suite of Chicago Guides to Writing, Editing and Publishing; this allowed us to take right, logical, and defensible decisions. The adjustment of the chapters to the editorial guideline was a careful work that involved training and dedication. The most important part of this task was to convert 58 publications from different authors into a single work by ensuring a consistent style throughout the whole multivolume book.
- During the development of the editorial process to produce *The Geology of Colombia,* the work team participated in national and international scientific events. These conferences and the organization of topical sessions about Colombian geology allow to promoting the research presented in the editorial work and encouraged interdisciplinary exchanges and debates on Colombian geology in a local and regional context. These spaces also served to elucidate new research approaches and opportunities for research collaborations.
- Communicating science makes it materialize in daily life. The outreach strategy of the geoscience knowledge for a lay public derive from *The Geology of Colombia* estab-

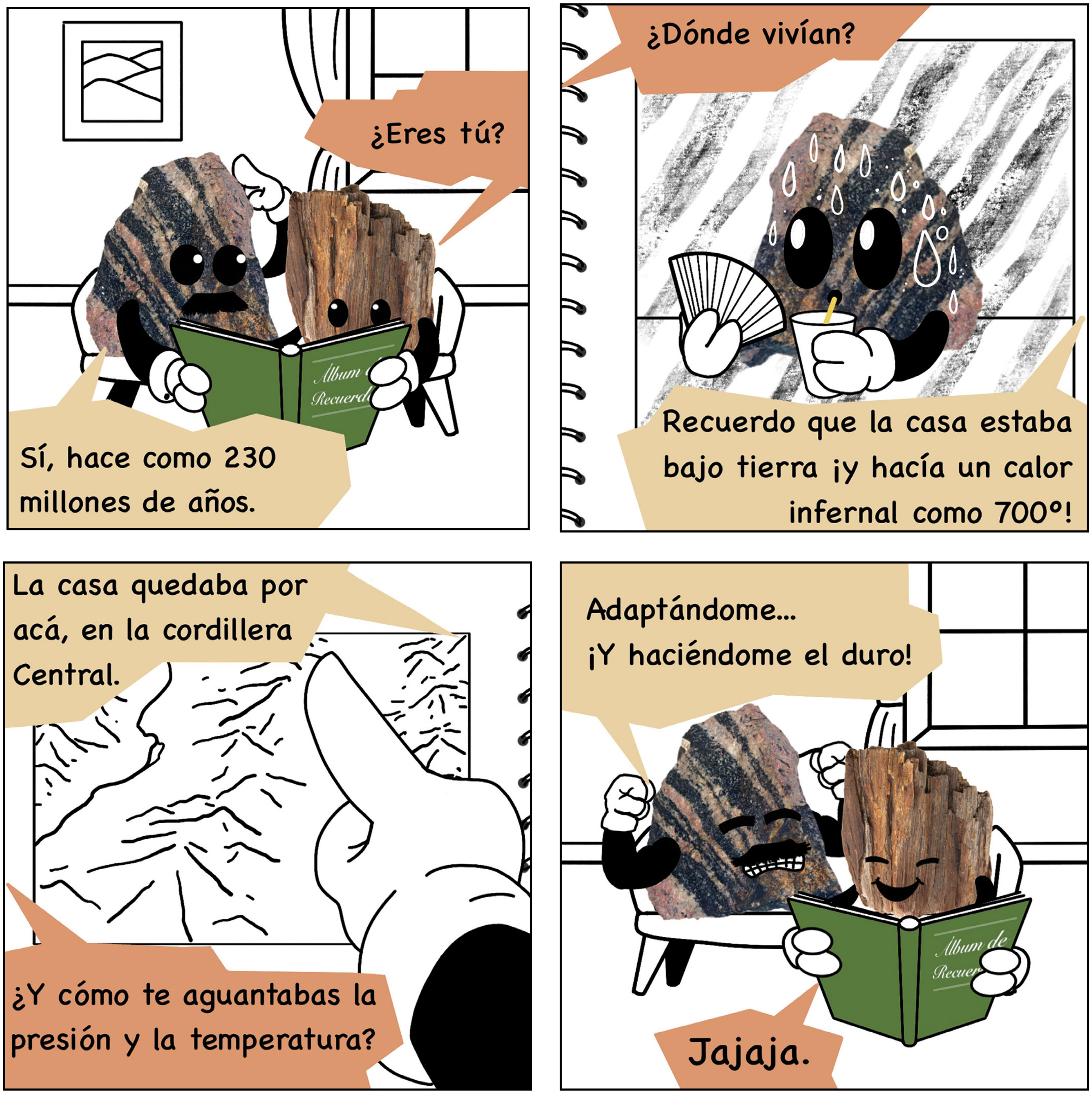

Figure 22. Example of the comics with characters from the Familia Piedrahita.

lished the need and importance of taking science out of the laboratories and into sensory experiences that involve a broad and diverse public.

- As the geological processes occur in the subsoil or happened millions of years ago, it is difficult for lay audiences to imagine those events. It becomes even more challenging to succeed in strategies aimed to look for the appropriation of geological knowledge by them. However, many topics can become attractive, we must be creative and explore other worlds of communication, keeping in mind that to communicate science it is necessary to use clear and pleasant graphic content, and a language easy to understand that capture the curiosity of the audiences.
- Social media is an effective channel to communicate science to both lay public and researchers because it allows us to create collaborative networks on a topic of common interest. We must know the function and the public of each

social media channel to focus our contents and design them accordingly.

- The editorial work, the scientific outreach strategy, the guidelines, and lessons learned from the whole process shared in this chapter can serve as a reference not only for producing other technical or scientific works but also for the reader who is writing an academic article or who is contemplating scientific popularization activities in his or her project.
- Considering that the members of the Grupo Mapa Geológico de Colombia of the SGC have a great knowledge of the Colombian geology, the team will continue to produce publications on the geological origin and evolution of the national territory. These editorial production processes will have an adequate dissemination strategy that will allow bringing geoscientific research to all Colombians.

Acknowledgments

We would like to thank the authors of the chapters for believing in an ambitious editorial project that is necessary for the country. They provided the data and results of their research, as well as their ideas, conclusions, and projections. We acknowledge the four scientists who were part of the Scientific Committee of the publication, Victor RAMOS, Cess PASSCHIER, Agustín CARDONA, and David BUCHS, for their recommendations and training spaces that helped improve the process of developing the chapters. We would like to thank the group of academic reviewers because with their evaluations, they not only allowed us to strengthen the initial chapters but also motivated the authors in the work they do every day to understand the national geology. Special thanks go to Alberto OCHOA YARZA, director of the Dirección de Geociencias Básicas of the Servicio Geológico Colombiano from 2013 to 2018 for supporting the project in its initial stage. We acknowledge the Observatorio Colombiano de Ciencia y Tecnología for advice during the planning and development of the editorial process. We would like to thank Clara Natalia LEÓN MONTENEGRO, geologist of the Grupo Mapa Geológico de Colombia in 2018, for her proactive work during the planning and initial development of the outreach strategy for the lay public. We also would like to thank Nohora MONTES RAMÍREZ, Astrid SIACHOQUE VELANDIA, Ana María PATIÑO ACEVEDO, and Carolina MORALES FERNÁNDEZ, geologists of the Grupo Mapa Geológico de Colombia nowadays, for their support in the final stage of the work. Finally, we thank Dr. Oscar PAREDES ZAPATA, director general of the Servicio Geológico Colombiano, who gave the directive to do the work *The Geology of Colombia*, for his trust, unconditional support, and motivation throughout the development of the project and for recognizing the value of a publication such as *The Geology of Colombia* for the socio–economic development of the country.

References

Alfaro–Valero, C.M., Rueda–Gutiérrez, J.B., Matiz–León, J.C., Beltrán–Luque, M.A., Rodríguez–Rodríguez, G.F., Rodríguez–Ospina, G.Z., González–Idárraga, C.E. & Malo–Lázaro, J.E. 2020. Paipa geothermal system, Boyacá: Review of exploration studies and conceptual model. In: Gómez, J. & Pinilla–Pachon, A.O. (editors), The Geology of Colombia, Volume 4 Quaternary. Servicio Geológico Colombiano, Publicaciones Geológicas Especiales 38, p. 161–196. Bogotá. https://doi.org/10.32685/pub.esp.38.2019.04

Amaya–Ferreira, S., Zuluaga, C.A. & Bernet, M. 2020. Different levels of exhumation across the Bucaramanga Fault in the Cepitá area of the southwestern Santander Massif, Colombia: Implications for the tectonic evolution of the northern Andes in northwestern South America. In: Gómez, J. & Mateus–Zabala, D. (editors), The Geology of Colombia, Volume 3 Paleogene – Neogene. Servicio Geológico Colombiano, Publicaciones Geológicas Especiales 37, p. 491–507. Bogotá. https://doi.org/10.32685/pub.esp.37.2019.17

Arcila, M. & Muñoz–Martín, A. 2020. Integrated perspective of the present–day stress and strain regime in Colombia from analysis of earthquake focal mechanisms and geodetic data. In: Gómez, J. & Pinilla–Pachon, A.O. (editors), The Geology of Colombia, Volume 4 Quaternary. Servicio Geológico Colombiano, Publicaciones Geológicas Especiales 38, p. 549–569. Bogotá. https://doi.org/10.32685/pub.esp.38.2019.17

Bayona, G., Bustamante, C., Nova, G. & Salazar–Franco, A.M. 2020. Jurassic evolution of the northwestern corner of Gondwana: Present knowledge and future challenges in studying Colombian Jurassic rocks. In: Gómez, J. & Pinilla–Pachon, A.O. (editors), The Geology of Colombia, Volume 2 Mesozoic. Servicio Geológico Colombiano, Publicaciones Geológicas Especiales 36, p. 171–207. Bogotá. https://doi.org/10.32685/pub.esp.36.2019.05

Bermúdez, H.D., Arenillas, I., Arz, J.A., Vajda, V., Renne, P.R., Gilabert, V. & Rodríguez, J.V. 2019. The Cretaceous/Paleogene boundary deposits on Gorgonilla Island. In: Gómez, J. & Mateus–Zabala, D. (editors), The Geology of Colombia, Volume 3 Paleogene – Neogene. Servicio Geológico Colombiano, Publicaciones Geológicas Especiales 37, p. 1–19. Bogotá. https://doi.org/10.32685/pub.esp.37.2019.01

Bustamante, C. & Bustamante, A. 2019. Two Cretaceous subduction events in the Central Cordillera: Insights from the high P–low T metamorphism. In: Gómez, J. & Pinilla–Pachon, A.O. (editors), The Geology of Colombia, Volume 2 Mesozoic. Servicio Geológico Colombiano, Publicaciones Geológicas Especiales 36, p. 485–498. Bogotá. https://doi.org/10.32685/pub.esp.36.2019.14

Caballero, V.M., Rodríguez, G., Naranjo, J.F., Mora, A. & De La Parra, F. 2020. From facies analysis, stratigraphic surfaces, and depositional sequences to stratigraphic traps in the Eocene – Oligocene record of the southern Llanos Basin and northern Magdalena

Basin. In: Gómez, J. & Mateus–Zabala, D. (editors), The Geology of Colombia, Volume 3 Paleogene – Neogene. Servicio Geológico Colombiano, Publicaciones Geológicas Especiales 37, p. 283–330. Bogotá. https://doi.org/10.32685/pub.esp.37.2019.10

Cardona, A., León, S., Jaramillo, J.S., Valencia, V., Zapata, S., Pardo–Trujillo, A., Schmitt, A.K., Mejía, D. & Arenas, J.C. 2020. Cretaceous record from a Mariana– to an Andean–type margin in the Central Cordillera of the Colombian Andes. In: Gómez, J. & Pinilla–Pachon, A.O. (editors), The Geology of Colombia, Volume 2 Mesozoic. Servicio Geológico Colombiano, Publicaciones Geológicas Especiales 36, p. 335–373. Bogotá. https://doi.org/10.32685/pub.esp.36.2019.10

Ceballos–Hernández, J.A., Martínez–Tabares, L.M., Valencia–Ramírez, L.G., Pulgarín–Alzate, B.A., Correa–Tamayo, A.M. & Narváez–Marulanda, B.L. 2020. Geological evolution of the Nevado del Ruiz Volcanic Complex. In: Gómez, J. & Pinilla–Pachon, A.O. (editors), The Geology of Colombia, Volume 4 Quaternary. Servicio Geológico Colombiano, Publicaciones Geológicas Especiales 38, p. 267–296. Bogotá. https://doi.org/10.32685/pub.esp.38.2019.07

Coghill, A.M. & Garson, L.R., editors. 2006. The ACS style guide: Effective communication of scientific information, 3rd edition. American Chemical Society and Oxford University Press, 430 p. Washington, USA; Oxford, UK. https://doi.org/10.1021/bk-2006-STYG

Cohen, K.M., Finney, S.C., Gibbard, P.L. & Fan, J.X. 2013 (updated v2020/01). The ICS International Chronostratigraphic Chart. Episodes, 36(3): 199–204. https://doi.org/10.18814/epiiugs/2013/v36i3/002

Correa–Tamayo, A.M., Pulgarín–Alzate, B.A. & Ancochea–Soto, E. 2020. The Nevado del Huila Volcanic Complex. In: Gómez, J. & Pinilla–Pachon, A.O. (editors), The Geology of Colombia, Volume 4 Quaternary. Servicio Geológico Colombiano, Publicaciones Geológicas Especiales 38, p. 227–265. Bogotá. https://doi.org/10.32685/pub.esp.38.2019.06

Cortés–Jiménez, G.P. 2020. Holocene lahar deposits associated with the eruptive activity of Cerro Machín Volcano, Colombia: Impact on landscape and associated potential hazard. In: Gómez, J. & Pinilla–Pachon, A.O. (editors), The Geology of Colombia, Volume 4 Quaternary. Servicio Geológico Colombiano, Publicaciones Geológicas Especiales 38, p. 297–331. Bogotá. https://doi.org/10.32685/pub.esp.38.2019.08

Diederix, H., Bohórquez, O.P., Mora–Páez, H., Peláez, J.R., Cardona, L., Corchuelo, Y., Ramírez, J. & Díaz–Mila, F. 2020a. The Algeciras Fault System of the Upper Magdalena Valley, Huila Department. In: Gómez, J. & Pinilla–Pachon, A.O. (editors), The Geology of Colombia, Volume 4 Quaternary. Servicio Geológico Colombiano, Publicaciones Geológicas Especiales 38, p. 423–452. Bogotá. https://doi.org/10.32685/pub.esp.38.2019.12

Diederix, H., Bohórquez, O.P., Mora–Páez, H., Peláez, J.R., Cardona, L., Corchuelo, Y., Ramírez, J. & Díaz–Mila, F. 2020b. Quaternary activity of the Bucaramanga Fault in the Departments of Santander and Cesar. In: Gómez, J. & Pinilla–Pachon, A.O. (editors), The Geology of Colombia, Volume 4 Quaternary. Servicio Geológico Colombiano, Publicaciones Geológicas Especiales 38, p. 453–477. Bogotá. https://doi.org/10.32685/pub.esp.38.2019.13

Dueñas–Jiménez, H. & Montalvo–Jónsson, J. 2020. Neoproterozoic records of the Llanos Orientales Basin, Colombia. In: Gómez, J. & Mateus–Zabala, D. (editors), The Geology of Colombia, Volume 1 Proterozoic – Paleozoic. Servicio Geológico Colombiano, Publicaciones Geológicas Especiales 35, p. 91–99. Bogotá. https://doi.org/10.32685/pub.esp.35.2019.05

Dueñas–Jiménez, H., Corredor–Bohórquez, V.E. & Montalvo–Jónsson, J. 2020. Paleontology of the Paleozoic rocks of the Llanos Orientales Basin, Colombia. In: Gómez, J. & Mateus–Zabala, D. (editors), The Geology of Colombia, Volume 1 Proterozoic – Paleozoic. Servicio Geológico Colombiano, Publicaciones Geológicas Especiales 35, p. 133–148. Bogotá. https://doi.org/10.32685/pub.esp.35.2019.07

Espinosa–Baquero, A. 2020. A model of the Quindío and Risaralda Quaternary deposits. In: Gómez, J. & Pinilla–Pachon, A.O. (editors), The Geology of Colombia, Volume 4 Quaternary. Servicio Geológico Colombiano, Publicaciones Geológicas Especiales 38, p. 333–352. Bogotá. https://doi.org/10.32685/pub.esp.38.2019.09

Fettes, D. & Desmons, J., editors. 2007. Metamorphic Rocks: A Classification and Glossary of Terms. Recommendations of the International Union of Geological Sciences Subcommission on the Systematics of Metamorphic Rocks. Cambridge University Press, 244 p. Cambridge, UK.

Gallego–Ríos, A.F., Pardo–Trujillo, A., López–Plazas, G.A. & Echeverri, S. 2020. The Morales Formation (new unit): Record of fluvial–lacustrine environments and the beginning of the Miocene explosive volcanism in the Patía Sub–basin (SW Colombia). In: Gómez, J. & Mateus–Zabala, D. (editors), The Geology of Colombia, Volume 3 Paleogene – Neogene. Servicio Geológico Colombiano, Publicaciones Geológicas Especiales 37, p. 395–415. Bogotá. https://doi.org/10.32685/pub.esp.37.2019.13

Garcia–Casco, A., Restrepo, J.J., Correa–Martínez, A.M., Blanco–Quintero, I.F., Proenza, J.A., Weber, M. & Butjosa, L. 2020. The petrologic nature of the "Medellín Dunite" revisited: An algebraic approach and proposal of a new definition of the geological body. In: Gómez, J. & Pinilla–Pachon, A.O. (editors), The Geology of Colombia, Volume 2 Mesozoic. Servicio Geológico Colombiano, Publicaciones Geológicas Especiales 36, p. 45–75 Bogotá. https://doi.org/10.32685/pub.esp.36.2019.02

Garner, B.A. 2016. The Chicago Guide to Grammar, Usage, and Punctuation (Chicago Guides to Writing, Editing, and Publishing). University of Chicago Press, 552 p. Chicago, USA.

Gómez, J. & Almanza, M.F., editors. 2015. Compilando la geología de Colombia: Una visión a 2015. Servicio Geológico Colombiano, Publicaciones Geológicas Especiales 33, 401 p. Bogotá.

Gómez, J., Nivia, Á., Montes, N.E., Tejada, M.L., Jiménez, D.M., Sepúlveda, M.J., Osorio, J.A., Gaona, T., Diederix, H., Uribe, H. & Mora, M., compilers. 2007. Geological Map of Colombia. Scale 1:1 000 000. Ingeominas. Bogotá.

Gómez, J., Montes, N.E., Nivia, Á. & Diederix, H., compilers. 2015. Geological Map of Colombia 2015. Scale 1:1 000 000. Servicio Geológico Colombiano, 2 sheets. Bogotá. https://doi.org/10.32685/10.143.2015.936

Gómez, J., Schobbenhaus, C. & Montes, N.E., compilers. 2019. Geological Map of South America 2019. Scale 1:5 000 000. Commission for the Geological Map of the World (CGMW), Colombian Geological Survey and Geological Survey of Brazil. Paris. https://doi.org/10.32685/10.143.2019.929

Gómez, J. & Mateus–Zabala, D., editors. 2020a. The Geology of Colombia, Volume 1 Proterozoic – Paleozoic. Servicio Geológico Colombiano, Publicaciones Geológicas Especiales 35, 239 p. Bogotá. https://doi.org/10.32685/pub.esp.35.2019

Gómez, J. & Mateus–Zabala, D., editors. 2020b. The Geology of Colombia, Volume 3 Paleogene – Neogene. Servicio Geológico Colombiano, Publicaciones Geológicas Especiales 37, 507 p. Bogotá. https://doi.org/10.32685/pub.esp.37.2019

Gómez, J. & Pinilla–Pachon, A.O., editors. 2020a. The Geology of Colombia, Volume 2 Mesozoic. Servicio Geológico Colombiano, Publicaciones Geológicas Especiales 36, 498 p. Bogotá. https://doi.org/10.32685/pub.esp.36.2019

Gómez, J. & Pinilla–Pachon, A.O., editors. 2020b. The Geology of Colombia, Volume 4 Quaternary. Servicio Geológico Colombiano, Publicaciones Geológicas Especiales 38, 569 p. Bogotá. https://doi.org/10.32685/pub.esp.38.2019

Gómez, J., Núñez–Tello. A., Mateus–Zabala, D., Alcárcel–Gutiérrez, F.A., Lasso–Muñoz, R.M., Marín–Rincón, E. & Marroquín–Gómez, M.P. 2020. Physiographic and geological setting of the Colombian territory. In: Gómez, J. & Mateus–Zabala, D. (editors), The Geology of Colombia, Volume 1 Proterozoic – Paleozoic. Servicio Geológico Colombiano, Publicaciones Geológicas Especiales 35, p. 1–16. Bogotá. https://doi.org/10.32685/pub.esp.35.2019.01

Guerrero, J., Mejía–Molina, A. & Osorno, J. 2020a. Detrital U–Pb provenance, mineralogy, and geochemistry of the Cretaceous Colombian back–arc basin. In: Gómez, J. & Pinilla–Pachon, A.O. (editors), The Geology of Colombia, Volume 2 Mesozoic. Servicio Geológico Colombiano, Publicaciones Geológicas Especiales 36, p. 261–297. Bogotá. https://doi.org/10.32685/pub.esp.36.2019.08

Guerrero, J., Mejía–Molina, A. & Osorno, J. 2020b. Biomicrite, marlstone, and shale properties: Exploration of nonconventional hydrocarbons in the Cretaceous Colombian back–arc basin. In: Gómez, J. & Pinilla–Pachon, A.O. (editors), The Geology of Colombia, Volume 2 Mesozoic. Servicio Geológico Colombiano, Publicaciones Geológicas Especiales 36, p. 299–333. Bogotá. https://doi.org/10.32685/pub.esp.36.2019.09

Hansen, W.R., editor. 1991. Suggestions to authors of the reports of the United States Geological Survey, 7th edition. U.S. Geological Survey Unnumbered Series, 289 p. https://doi.org/10.3133/7000088

Hooghiemstra, H. & Flantua, S.G.A. 2019. Colombia in the Quaternary: An overview of environmental and climatic change. In: Gómez, J. & Pinilla–Pachon, A.O. (editors), The Geology of Colombia, Volume 4 Quaternary. Servicio Geológico Colombiano, Publicaciones Geológicas Especiales 38, p. 43–95. Bogotá. https://doi.org/10.32685/pub.esp.38.2019.02

Horton, B.K., Parra, M. & Mora, A. 2020. Construction of the Eastern Cordillera of Colombia: Insights from the sedimentary record. In: Gómez, J. & Mateus–Zabala, D. (editors), The Geology of Colombia, Volume 3 Paleogene – Neogene. Servicio Geológico Colombiano, Publicaciones Geológicas Especiales 37, p. 67–88. Bogotá. https://doi.org/10.32685/pub.esp.37.2019.03

Ibañez–Mejia, M. 2020. The Putumayo Orogen of Amazonia: A synthesis. In: Gómez, J. & Mateus–Zabala, D. (editors), The Geology of Colombia, Volume 1 Proterozoic – Paleozoic. Servicio Geológico Colombiano, Publicaciones Geológicas Especiales 35, p. 101–131. Bogotá. https://doi.org/10.32685/pub.esp.35.2019.06

Ibañez–Mejia, M. & Cordani, U.G. 2020. Zircon U–Pb geochronology and Hf–Nd–O isotope geochemistry of the Paleo– to Mesoproterozoic basement in the westernmost Guiana Shield. In: Gómez, J. & Mateus–Zabala, D. (editors), The Geology of Colombia, Volume 1 Proterozoic – Paleozoic. Servicio Geológico Colombiano, Publicaciones Geológicas Especiales 35, p. 65–90. Bogotá. https://doi.org/10.32685/pub.esp.35.2019.04

International Commission on Zoological Nomenclature (ICZN). 1999. International code of zoological nomenclature, 4th edition. The International Trust for Zoological Nomenclature, 401 p. London, UK.

Jaramillo, C. 2019. 140 million years of tropical biome evolution. In: Gómez, J. & Pinilla–Pachon, A.O. (editors), The Geology of Colombia, Volume 2 Mesozoic. Servicio Geológico Colombiano, Publicaciones Geológicas Especiales 36, p. 209–236. Bogotá. https://doi.org/10.32685/pub.esp.36.2019.06

Kammer, A., Piraquive, A., Gómez, C., Mora, A., & Velásquez, A. 2020. Structural styles of the Eastern Cordillera of Colombia. In: Gómez, J. & Mateus–Zabala, D. (editors), The Geology of Colombia, Volume 3 Paleogene – Neogene. Servicio Geológico Colombiano, Publicaciones Geológicas Especiales 37, p. 143–183. Bogotá. https://doi.org/10.32685/pub.esp.37.2019.06

Le Maitre, R.W., Streckeisen, A., Zanettin, B., Le Bas, M.J., Bonin, B., Bateman, P., Bellieni, G., Dudek, A., Efremova, S., Keller, J., Lameyre, J., Sabine, P.A., Schmid, R., Sørensen, H. & Woolley, A.R., editors. 2002. Igneous rocks: A classification and glossary of terms. Recommendations of the International Union of Geological Sciences Subcommission on the systematics of igneous rocks. Cambridge University Press, 236 p. Cambridge, UK. https://doi.org/10.1017/CBO9780511535581

López, M.C. & Toro–Toro, L.M. 2020. Stratigraphy and tectonics of the Neogene and Quaternary of the Cauca Basin of Colombia. In: Gómez, J. & Pinilla–Pachon, A.O. (editors), The Geology of Colombia, Volume 4 Quaternary. Servicio Geológico Colombiano, Publicaciones Geológicas Especiales 38, p. 1–41. Bogotá. https://doi.org/10.32685/pub.esp.38.2019.01

López–Isaza, J.A. & Zuluaga, C.A. 2020. Late Triassic to Jurassic magmatism in Colombia: Implications for the evolution of the northern margin of South America. In: Gómez, J. & Pinilla–Pachon, A.O. (editors), The Geology of Colombia, Volume 2 Mesozoic. Servicio Geológico Colombiano, Publicaciones Geológicas Especiales 36, p. 77–116. Bogotá. https://doi.org/10.32685/pub.esp.36.2019.03

Monsalve–Bustamante, M.L. 2020. The volcanic front in Colombia: Segmentation and recent and historical activity. In: Gómez, J. & Pinilla–Pachon, A.O. (editors), The Geology of Colombia, Volume 4 Quaternary. Servicio Geológico Colombiano, Publicaciones Geológicas Especiales 38, p. 97–159. Bogotá. https://doi.org/10.32685/pub.esp.38.2019.03

Monsalve–Bustamante, M.L., Gómez, J. & Núñez–Tello, A. 2020. Rear–arc small–volume basaltic volcanism in Colombia: Monogenetic volcanic fields. In: Gómez, J. & Pinilla–Pachon, A.O. (editors), The Geology of Colombia, Volume 4 Quaternary. Servicio Geológico Colombiano, Publicaciones Geológicas Especiales 38, p. 353–396 Bogotá. https://doi.org/10.32685/pub.esp.38.2019.10

Montes, C. & Hoyos, N. 2020. Isthmian bedrock geology: Tilted, bent, and broken. In: Gómez, J. & Mateus–Zabala, D. (editors), The Geology of Colombia, Volume 3 Paleogene – Neogene. Servicio Geológico Colombiano, Publicaciones Geológicas Especiales 37, p. 451–467. Bogotá. https://doi.org/10.32685/pub.esp.37.2019.15

Mora, A., Villagómez, D., Parra, M., Caballero, V.M., Spikings, R., Horton, B.K., Mora–Bohórquez, J.A., Ketcham, R.A. & Arias–Martínez, J.P. 2020a. Late Cretaceous to Cenozoic uplift of the northern Andes: Paleogeographic implications. In: Gómez, J. & Mateus–Zabala, D. (editors), The Geology of Colombia, Volume 3 Paleogene – Neogene. Servicio Geológico Colombiano, Publicaciones Geológicas Especiales 37, p. 89–121. Bogotá. https://doi.org/10.32685/pub.esp.37.2019.04

Mora, A., Tesón, E., Martínez, J., Parra, M., Lasso, Á., Horton, B.K., Ketcham, R.A., Velásquez, A. & Arias–Martínez, J.P. 2020b. The Eastern Foothills of Colombia. In: Gómez, J. & Mateus–Zabala, D. (editors), The Geology of Colombia, Volume 3 Paleogene – Neogene. Servicio Geológico Colombiano, Publicaciones Geológicas Especiales 37, p. 123–142. Bogotá. https://doi.org/10.32685/pub.esp.37.2019.05

Mora–Bohórquez, J.A., Oncken, O., Le Breton, E., Ibañez–Mejia, M., Veloza, G., Mora, A., Vélez, V. & De Freitas, M. 2020. Formation and evolution of the Lower Magdalena Valley Basin and San Jacinto fold belt of northwestern Colombia: Insights from Upper Cretaceous to recent tectono–stratigraphy. In: Gómez, J. & Mateus–Zabala, D. (editors), The Geology of Colombia, Volume 3 Paleogene – Neogene. Servicio Geológico Colombiano, Publicaciones Geológicas Especiales 37, p. 21–66. Bogotá. https://doi.org/10.32685/pub.esp.37.2019.02

Mora–Páez, H., Díaz–Mila, F. & Cardona, L. 2020b. Mapping land subsidence in Bogotá, Colombia, using the interferometric synthetic aperture radar (InSAR) technique with TerraSAR–X images. In: Gómez, J. & Pinilla–Pachon, A.O. (editors), The Geology of Colombia, Volume 4 Quaternary. Servicio Geológico Colombiano, Publicaciones Geológicas Especiales 38, p. 515–548. Bogotá. https://doi.org/10.32685/pub.esp.38.2019.16

Mora–Páez, H., Kellogg, J.N. & Freymueller, J.T. 2020a. Contributions of space geodesy for geodynamic studies in Colombia: 1988 to 2017. In: Gómez, J. & Pinilla–Pachon, A.O. (editors), The Geology of Colombia, Volume 4 Quaternary. Servicio Geológico Colombiano, Publicaciones Geológicas Especiales 38, p. 479–498. Bogotá. https://doi.org/10.32685/pub.esp.38.2019.14

Moreno–Sánchez, M., Gómez–Cruz, A. & Buitrago–Hincapié, J. 2020. Paleozoic of Colombian Andes: New paleontological data and regional stratigraphic review. In: Gómez, J. & Mateus–Zabala, D. (editors), The Geology of Colombia, Volume 1 Proterozoic – Paleozoic. Servicio Geológico Colombiano, Publicaciones Geológicas Especiales 35, p. 167–203. Bogotá. https://doi.org/10.32685/pub.esp.35.2019.09

Moyano–Nieto, I.E., Cordani, R., Cárdenas–Espinosa, L.P., Lara–Martínez, N.M., Rojas–Sarmiento, O.E., Puentes–Torres, M.F., Ospina–Montes, D.L., Salamanca–Saavedra, A.F. & Prieto–Rincón, G. 2020. Contribution of new airborne geophysical information to the geological knowledge of eastern Colombia. In: Gómez, J. & Mateus–Zabala, D. (editors), The Geology of Colombia, Volume 1 Proterozoic – Paleozoic. Servicio Geológico Colombiano, Publicaciones Geológicas Especiales 35, p. 17–36. Bogotá. https://doi.org/10.32685/pub.esp.35.2019.02

Newell, D.B. & Tiesinga, E., editors. 2019. The International System of Units (SI). National Institute of Standards and Technology. NIST Special Publication 330, 122 p. https://doi.org/10.6028/NIST.SP.330-2019

Noè, L.F. & Gómez–Pérez, M. 2020. Plesiosaurs, palaeoenvironments, and the Paja Formation Lagerstätte of central Colombia: An overview. In: Gómez, J. & Pinilla–Pachon, A.O. (editors), The Geology of Colombia, Volume 2 Mesozoic. Servicio Geológico Colombiano, Publicaciones Geológicas Especiales 36, p. 441–483. Bogotá. https://doi.org/10.32685/pub.esp.36.2019.13

Noè, L.F., Gómez–Pérez, M., Rodríguez, J.V., Corrales–García, A. & Caranton–Mateus, W.G. 2020. Dinosaur footprints from the Lower Cretaceous, Batá Formation, Colombia (South America), and the possible interchange of large ornithopods between southern Laurasia and northern Gondwana. In: Gómez, J. & Pinilla–Pachon, A.O. (editors), The Geology of Colombia, Volume 2 Mesozoic. Servicio Geológico Colombiano, Publicaciones Geológicas Especiales 36, p. 375–401. Bogotá. https://doi.org/10.32685/pub.esp.36.2019.11

North American Commission on Stratigraphic Nomenclature (NACSN). 2005. North American Stratigraphic Code. American Association of Petroleum Geologists Bulletin, 89(11): 1547–1591. https://doi.org/10.1306/07050504129

Owen, D.E. 2009. How to use stratigraphic terminology in papers, illustrations, and talks. Stratigraphy, 6(2): 106–116.

Pardo–Trujillo, A., Echeverri, S., Borrero, C., Arenas, A., Vallejo, F., Trejos, R., Plata, Á., Flores, J.A., Cardona, A., Restrepo, S., Barbosa, Á., Murcia, H., Giraldo, C., Celis, S. & López, S.A. 2020. Cenozoic geologic evolution of the southern Tumaco Forearc Basin (SW Colombian Pacific). In: Gómez, J. & Mateus–Zabala, D. (editors), The Geology of Colombia, Volume 3 Paleogene – Neogene. Servicio Geológico Colombiano, Publicaciones Geológicas Especiales 37, p. 215–247. Bogotá. https://doi.org/10.32685/pub.esp.37.2019.08

Parra, M., Echeverri, S., Patiño, A.M., Ramírez, J.C., Mora, A., Sobel, E.R., Almendral, A. & Pardo–Trujillo, A. 2020. Cenozoic evolution of the Sierra Nevada de Santa Marta, Colombia. In: Gómez, J. & Mateus–Zabala, D. (editors), The Geology of Colombia, Volume 3 Paleogene – Neogene. Servicio Geológico Colombiano, Publicaciones Geológicas Especiales 37, p. 185–213. Bogotá. https://doi.org/10.32685/pub.esp.37.2019.07

Patarroyo, P. 2020. Barremian deposits of Colombia: A special emphasis on marine successions. In: Gómez, J. & Pinilla–Pachon, A.O. (editors), The Geology of Colombia, Volume 2 Mesozoic. Servicio Geológico Colombiano, Publicaciones Geológicas Especiales 36, p. 403–439. Bogotá. https://doi.org/10.32685/pub.esp.36.2019.12

Pulgarín–Alzate, B.A., Tamayo–Alzate, M., Correa–Tamayo, A.M., Ceballos–Hernández, J.A., Cruz–Toro, Y.P. & Méndez–Fajury, R. 2020. Stratigraphy and geological evolution of the Paramillo de Santa Rosa Volcanic Complex and its Pleistocene to Holocene eruptive history. In: Gómez, J. & Pinilla–Pachon, A.O. (editors), The Geology of Colombia, Volume 4 Quaternary. Servicio Geológico Colombiano, Publicaciones Geológicas Especiales 38, p. 197–226. Bogotá. https://doi.org/10.32685/pub.esp.38.2019.05

Ramos, V.A. 2018. The Famatinian Orogen along the protomargin of western Gondwana: Evidence for a nearly continuous Ordovician magmatic arc between Venezuela and Argentina. In: Folguera, A., Contreras–Reyes, E., Heredia, N., Encinas, A., Iannelli, S.B., Oliveros, V., Dávila, F.M., Collo, G., Giambiagi, L., Maksymowicz, A., Iglesia–Llanos, M.P., Turienzo, M., Naipauer, M., Orts, D., Litvak, V.D.,Alvarez, O. & Arriagada, C. (editors), The Evolution of the Chilean–Argentinean Andes. Springer Earth System Sciences. Springer, p. 133–161. https://doi.org/10.1007/978-3-319-67774-3_6

Ramos, V.A. 2020. Prologue. In: Gómez, J. & Mateus–Zabala, D. (editors), The Geology of Colombia, Volume 1 Proterozoic – Paleozoic. Servicio Geológico Colombiano, Publicaciones Geológicas Especiales 35, p. xxi–xxiii. *Bogotá.* https://doi.org/10.32685/pub.esp.35.2019.Prologue

Real Academia Española (RAE). 2010. Nueva gramática de la lengua española: Manual. Asociación de Academias de la Lengua Española. Espasa Libros, 993 p. Madrid, Spain.

Restrepo, J.J. & Toussaint, J.F. 2020. Tectonostratigraphic terranes in Colombia: An update. First part: Continental terranes. In: Gómez, J. & Mateus–Zabala, D. (editors), The Geology of Colombia, Volume 1 Proterozoic – Paleozoic. Servicio Geológico Colombiano, Publicaciones Geológicas Especiales 35, p. 37–63. Bogotá. https://doi.org/10.32685/pub.esp.35.2019.03

Restrepo, J.J., Martens, U. & Giraldo–Ramírez, W.E. 2020. The Anacona Terrane: A small early Paleozoic peri–Gondwanan terrane in the Cauca–Romeral Fault System. In: Gómez, J. & Mateus–Zabala, D. (editors), The Geology of Colombia, Volume 1 Proterozoic – Paleozoic. Servicio Geológico Colombiano, Publicaciones Geológicas Especiales 35, p. 149–165. Bogotá. https://doi.org/10.32685/pub.esp.35.2019.08

Rodríguez–García, G., Correa–Martínez, A.M., Zapata–Villada, J.P. & Obando–Erazo, G. 2019. Fragments of a Permian arc on the western margin of the Neoproterozoic basement of Colombia. In: Gómez, J. & Mateus–Zabala, D. (editors), The Geology of Colombia, Volume 1 Proterozoic – Paleozoic. Servicio Geológico Colombiano, Publicaciones Geológicas Especiales 35, p. 205–239. Bogotá. https://doi.org/10.32685/pub.esp.35.2019.10

Rodríguez–García, G., Correa–Martínez, A.M., Zapata–García, G., Arango–Mejía, M.I., Obando–Erazo, G., Zapata–Villada, J.P. & Bermúdez, J.G. 2020. Diverse Jurassic magmatic arcs of the Colombian Andes: Constraints from petrography, geochronology, and geochemistry. In: Gómez, J. & Pinilla–Pachon, A.O. (editors), The Geology of Colombia, Volume 2 Mesozoic. Servicio Geológico Colombiano, Publicaciones Geológicas Especiales 36, p. 117–170. Bogotá. https://doi.org/10.32685/pub.esp.36.2019.04

Sagiya, T. & Mora–Páez, H. 2020. Interplate coupling along the Nazca subduction zone on the Pacific coast of Colombia deduced from GeoRED GPS observation data. In: Gómez, J. & Pinilla–Pachon, A.O. (editors), The Geology of Colombia, Volume 4 Quaternary. Servicio Geológico Colombiano, Publicaciones Geológicas Especiales 38, p. 499–513. Bogotá. https://doi.org/10.32685/pub.esp.38.2019.15

Salvador, A. 1994. International stratigraphic guide: A guide to stratigraphic classification, terminology, and procedure, 2nd edition. International Union of Geological Sciences and Geological Society of America, 214 p. Trondheim, Norway; Boulder, USA. https://doi.org/10.1130/9780813774022

Silva–Tamayo, J.C., Rincón–Martínez, D., Barrios, L.M., Torres–Lasso, J.C. & Osorio–Arango, C. 2020a. Cenozoic marine carbonate systems of Colombia. In: Gómez, J. & Mateus–Zabala, D. (editors), The Geology of Colombia, Volume 3 Paleogene – Neogene. Servicio Geológico Colombiano, Publicaciones Geológicas Especiales 37, p. 249–282. Bogotá. https://doi.org/10.32685/pub.esp.37.2019.09

Silva–Tamayo, J.C., Lara, M. & Salazar–Franco, A.M. 2020b. Oligocene – Miocene coal–bearing successions of the Amagá Formation, Antioquia, Colombia: Sedimentary environments, stratigraphy, and tectonic implications. In: Gómez, J. & Mateus–Zabala, D. (editors), The Geology of Colombia, Volume 3 Paleogene – Neogene. Servicio Geológico Colombiano, Publicaciones Geológicas Especiales 37, p. 331–353. Bogotá. https://doi.org/10.32685/pub.esp.37.2019.11

Spikings, R. & Paul, A. 2019. The Permian – Triassic history of magmatic rocks of the northern Andes (Colombia and Ecuador): Supercontinent assembly and disassembly. In: Gómez, J. & Pinilla–Pachon, A.O. (editors), The Geology of Colombia, Volume 2 Mesozoic. Servicio Geológico Colombiano, Publicaciones Geológicas Especiales 36, p. 1–43. Bogotá. https://doi.org/10.32685/pub.esp.36.2019.01

Toussaint, J.F. & Restrepo, J.J. 2020. Tectonostratigraphic terranes in Colombia: An update. Second part: Oceanic terranes. In: Gómez, J. & Pinilla–Pachon, A.O. (editors), The Geology of Colombia, Volume 2 Mesozoic. Servicio Geológico Colombiano, Publicaciones Geológicas Especiales 36, p. 237–260. Bogotá. https://doi.org/10.32685/pub.esp.36.2019.07

University of Chicago Press Staff. 2010. The Chicago Manual of Style, 16th Edition. The University of Chicago Press, 1026 p. Chicago, USA.

Urueña–Suárez, C.L., Peña–Urueña, M.L., Muñoz–Rocha, J.A., Rayo–Rocha, L.P., Villamizar–Escalante, N., Amaya–Ferreira, S., Ibañez–Mejia, M. & Bernet, M. 2020. Zircon U–Pb and fission–track dating applied to resolving sediment provenance in modern rivers draining the Eastern and Central Cordilleras, Colombia. In: Gómez, J. & Mateus–Zabala, D. (editors), The Geology of Colombia, Volume 3 Paleogene – Neogene. Servicio Geológico Colombiano, Publicaciones Geológicas Especiales 37, p. 469–490. Bogotá. https://doi.org/10.32685/pub.esp.37.2019.16

U.S. Geological Survey. 2004. Shuttle Radar Topography Mission, 1 Arc Second–Republic of Colombia, Unfilled Unfinished 2.0, Global Land Cover Facility. University of Maryland, February 2000. Maryland, USA.

Vargas, C.A. 2020. Subduction geometries in northwestern South America. In: Gómez, J. & Pinilla–Pachon, A.O. (editors), The Geology of Colombia, Volume 4 Quaternary. Servicio Geológico Colombiano, Publicaciones Geológicas Especiales 38, p. 397–422. Bogotá. https://doi.org/10.32685/pub.esp.38.2019.11

Weber, M., Duque, J.F., Hoyos, S., Cárdenas–Rozo, A.L., Gómez, J. & Wilson, R. 2020. The Combia Volcanic Province: Miocene post–collisional magmatism in the northern Andes. In: Gómez, J. & Mateus–Zabala, D. (editors), The Geology of Colombia, Volume 3 Paleogene – Neogene. Servicio Geológico Colombiano, Publicaciones Geológicas Especiales 37, p. 355–394. Bogotá. https://doi.org/10.32685/pub.esp.37.2019.12

Zapata–García, G. & Rodríguez–García, G. 2020. New contributions to the knowledge about the Chocó–Panamá Arc in Colombia, including a new segment south of Colombia. In: Gómez, J. & Mateus–Zabala, D. (editors), The Geology of Colombia, Volume 3 Paleogene – Neogene. Servicio Geológico Colombiano, Publicaciones Geológicas Especiales 37, p. 417–450. Bogotá. https://doi.org/10.32685/pub.esp.37.2019.14

Explanation of Acronyms, Abbreviations, and Symbols:

SGC Servicio Geológico Colombiano

Authors' Biographical Notes

Jorge GÓMEZ TAPIAS is a geologist and has worked as a cartographer at the Servicio Geológico Colombiano for 20 years, during which time, he has authored approximately 70 geological maps. He is the coordinator of the Grupo Mapa Geológico Colombiano of the Dirección de Geociencias Básicas, which was recognized by Colciencias as a research group in 2017. GÓMEZ is the first author of the Geological Map of Colombia at a scale of 1:1 M —editions 2007 and 2015— and of the 26 map sheets of the Geological Atlas of Colombia at a scale of 1:500 K and is the co–editor of the book *Compilando la geología de Colombia: Una visión a 2015*. Since February 2018, he has served as vice president for South America on the Commission for the Geological Map of the World. He was a co–coordinator and the first author of the Geological Map of South America at a scale of 1:5 M 2019. Since October 2020, he was elected as a member of the International Union of Geological Sciences (IUGS) Nominating Committee for the term 2020–2024. Currently, he is the editor–in–chief of *The Geology of Colombia*. GÓMEZ is in charge of coordinating all the activities related to the project and the editorial process.

Daniela MATEUS–ZABALA is a geologist who graduated from the Universidad Nacional de Colombia Sede Bogotá in 2016 and is a copyeditor of scientific and science outreach texts. She has participated in geological and geomorphological mapping projects, petrographic and geochemical characterization of rocks, and geochemical evaluation of soils. Since 2017, she has been part of the Grupo Mapa Geológico de Colombia and is a deputy editor of *The Geology of Colombia*. In this editorial project, she supported the coordination of the editorial process stages and coordinated the advisory work for the project provided by the Observatorio Colombiano de Ciencia y Tecnología and the Asociación Colombiana para el Avance de la Ciencia; she was also in charge of the writing and proofreading of texts written in Spanish and English and conducted the editorial review of the chapters.

Ana Oliva PINILLA–PACHON is a geologist who graduated from the Universidad Nacional de Colombia in 2018. PINILLA is the deputy editor of the book series *The Geology of Colombia*, and is in charge of establishing the book series' editorial guidelines based on the *Chicago Manual of Style*. Thereby, she ensures consistency throughout the entire work, fosters the correct use of grammar and bibliographic citations, and establishes a stringent hierarchization of the content.

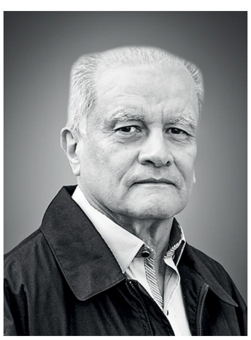

Alberto NÚÑEZ–TELLO is a geologist who graduated from the Universidad Nacional de Colombia and is a specialist in environmental management and disaster prevention for the Universidad del Tolima. He has worked for 32 years at the Servicio Geológico Colombiano in different positions, including that of technical director. His main interest is in regional geological mapping and geological risk management.

Rubby Melissa LASSO–MUÑOZ is a geological engineer who graduated from the Universidad Nacional de Colombia Sede Medellín in 2016. LASSO has worked in the petroleum industry and conducted science outreach with communities. Since 2019, she has worked on the Grupo Mapa Geológico de Colombia in the Servicio Geológico Colombiano and has been in charge of coordinating the project promotion and the science outreach activities. She is also responsible for updating *The Geology of Colombia* website and producing text, graphics, and audiovisual content for it.

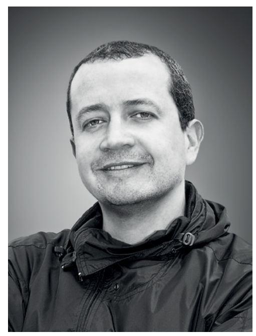

Fernando Alirio ALCÁRCEL–GUTIÉRREZ is a geologist who graduated from the Universidad Nacional de Colombia and is a specialist in geomatics graduated from the Universidad Militar Nueva Granada. He has been part of the Grupo Mapa Geológico de Colombia since 2012. He has co–authored several publications from the group, including the *Catálogo de dataciones radiométricas de Colombia en ArcGIS y Google Earth*, and he is also the first author of the informative Geological Map of Colombia 2019 at a scale of 1:2 M. ALCÁRCEL has extensive experience in the vectorization and digitization of graphic material for scientific publications, which is why he is the main graphic artist for *The Geology of Colombia* and is in charge of elaborating and improving the figures and maps.

Eliana MARÍN–RINCÓN is a geologist who graduated from the Universidad de Caldas in 2017. In the editorial process of *The Geology of Colombia*, she is in charge of preparing and adjusting the chapters' figures. MARÍN also supports the science outreach events through general logistics management and maintains the correspondence with and databases of participants.

María Paula MARROQUÍN–GÓMEZ is a geoscientist who graduated from the Universidad de los Andes in 2019, where she completed her studies with the financial support of *Bachilleres por Colombia Ecopetrol* scholarship. She has been part of the Grupo Mapa Geológico de Colombia since 2019, supporting the editorial and thematic reviews for *The Geology of Colombia* by ensuring the clarity and consistency of the chapters.

Lisbeth FOG–CORRADINE is a social communicator and journalist from the Universidad Jorge Tadeo Lozano who earned a Master of Science degree in science journalism from Boston University, United States, as a Fulbright scholar. In *The Geology of Colombia* project, she leads activities related to the social engagement of knowledge. FOG produces news articles in plain language based on the content of the chapters. These stories are then published in the Colombian media.

Alejandra CARDONA–MAYORGA is a graphic designer and specialist in photography from the Universidad Nacional de Colombia. CARDONA handles all visual aspects of the project, such as visual communications in printed and digital media. In addition, she is in charge of carrying out photographic and video documentation of all the activities related to the project, including taking photographs of the authors and establishing photographic records of the field trips, as well as developing the project's storytelling through audiovisual material.

Miguel Gerardo RAMÍREZ–LEAL is a graphic designer from the Universidad Nacional de Colombia with 14 years of experience in the fields of graphic design and illustration. In *The Geology of Colombia*, he is in charge of the layout, design, and printing of the book. In addition, he supports the layout of graphic pieces and is in charge of the illustration of the comic strips *Familia Piedrahita* as part of the project's science outreach strategy.

Volume 1

Chapter 1

https://doi.org/10.32685/pub.esp.35.2019.01
Published online 24 November 2020

Physiographic and Geological Setting of the Colombian Territory

Jorge GÓMEZ TAPIAS[1*], Alberto NÚÑEZ–TELLO[2], Daniela MATEUS–ZABALA[3], Fernando Alirio ALCÁRCEL–GUTIÉRREZ[4], Rubby Melissa LASSO–MUÑOZ[5], Eliana MARÍN–RINCÓN[6], and María Paula MARROQUÍN–GÓMEZ[7]

Abstract The territory of the Republic of Colombia is in the northwestern corner of South America, a region influenced by the Caribbean and Nazca oceanic plates, and the South American continental plate. In Colombia, six natural regions are distinguished: Andean, Caribbean, Pacific, Orinoquia, Amazonian, and Insular. The Andean region corresponds to the great mountain belt of the Andes, which in Colombia is divided into the Western, Central, and Eastern Cordilleras, separated by the inter–Andean valleys of the Cauca and Magdalena Rivers. The Caribbean region is to the north and include the coastal areas of the Caribbean Sea. It is a region of flat to undulating relief, with some high topography, among which the Sierra Nevada de Santa Marta stands out. The Pacific region, in the west of Colombia, has flat to undulating morphology and host the serranía de Baudó. To the east, the territory consists of the Orinoquia and Amazonian regions, with their flat and undulating surface, the first corresponds to plains and savannas, while the second corresponds to the Amazonian jungle, where are some isolated ranges as the serranía de Chiribiquete. The Caribbean Insular region groups the San Andrés, Providencia, and Santa Catalina Islands, besides of islets, atolls, and reef banks; whilst the Pacific Island region encompass the Gorgona and Gorgonilla Islands, and the Malpelo Islet. Caribe, Magdalena–Cauca, Orinoco, Amazonas, and Pacífico are the main hydrographic watersheds of the country. The geological setting of Colombia is diverse, with rocks of multiple types and ages, spanning the Paleoproterozoic to Holocene, as well as geological structures of diverse type and origin, reflecting a complex and diverse geological history. This geological framework has led to the identification of 23 marine and continental sedimentary basins.

Keywords: *Colombian geography, natural regions, hydrographic watersheds, sedimentary basins.*

Resumen El territorio de la República de Colombia está ubicado en la esquina noroccidental de Suramérica, región influenciada por las placas oceánicas del Caribe y de Nazca y la placa continental de Suramérica. Seis regiones naturales han sido identificadas: Andina, Caribe, Pacífica, Orinoquia, Amazonia e Insular. La zona andina es la prolongación de la gran cordillera de los Andes, que en Colombia se divide en las cordilleras Occidental, Central y Oriental separadas por los valles interandinos de los ríos Cauca

1 mapageo@sgc.gov.co
Servicio Geológico Colombiano
Dirección de Geociencias Básicas
Grupo Mapa Geológico de Colombia
Diagonal 53 n.° 34–53
Bogotá, Colombia

2 anunez@sgc.gov.co
Servicio Geológico Colombiano
Dirección de Geociencias Básicas
Grupo Mapa Geológico de Colombia
Diagonal 53 n.° 34–53
Bogotá, Colombia

3 dmateus@sgc.gov.co
Servicio Geológico Colombiano
Dirección de Geociencias Básicas
Grupo Mapa Geológico de Colombia
Diagonal 53 n.° 34–53
Bogotá, Colombia

4 falcarcel@sgc.gov.co
Servicio Geológico Colombiano
Dirección de Geociencias Básicas
Grupo Mapa Geológico de Colombia
Diagonal 53 n.° 34–53
Bogotá, Colombia

5 mlasso@sgc.gov.co
Servicio Geológico Colombiano
Dirección de Geociencias Básicas
Grupo Mapa Geológico de Colombia
Diagonal 53 n.° 34–53
Bogotá, Colombia

6 emarinr@sgc.gov.co
Servicio Geológico Colombiano
Dirección de Geociencias Básicas
Grupo Mapa Geológico de Colombia
Diagonal 53 n.° 34–53
Bogotá, Colombia

7 mpmarroquin@sgc.gov.co
Servicio Geológico Colombiano
Dirección de Geociencias Básicas
Grupo Mapa Geológico de Colombia
Diagonal 53 n.° 34–53
Bogotá, Colombia

* Corresponding author

Supplementary Information:
S: https://www2.sgc.gov.co/LibroGeologiaColombia/tgc/sgcpubesp35201901s.kmz

Citation: Gómez, J., Núñez–Tello, A., Mateus–Zabala, D., Alcárcel–Gutiérrez, F.A., Lasso–Muñoz, R.M., Marín–Rincón, E. & Marroquín–Gómez, M.P. 2020. Physiographic and geological setting of the Colombian territory. In: Gómez, J. & Mateus–Zabala, D. (editors), The Geology of Colombia, Volume 1 Proterozoic – Paleozoic. Servicio Geológico Colombiano, Publicaciones Geológicas Especiales 35, p. 1–16. Bogotá. https://doi.org/10.32685/pub.esp.35.2019.01

y Magdalena. La región Caribe se localiza al norte y corresponde a las zonas costeras del mar Caribe. Es un área de relieve plano a ondulado con algunas elevaciones, entre las que se destaca la Sierra Nevada de Santa Marta. La región Pacífica, ubicada al occidente colombiano, es de morfología plana a ondulada. Allí se encuentra la serranía de Baudó. Las regiones Orinoquia y Amazonia, de superficie ondulada y plana, ocupan el oriente del territorio; la primera corresponde a llanuras y sabanas, mientras que la segunda es selvática, con algunas zonas montañosas aisladas como la serranía de Chiribiquete. La región Insular del Caribe está conformada por las islas de San Andrés, Providencia y Santa Catalina, con islotes, atolones y bancos de arrecifes; las islas de Gorgona y Gorgonilla y el islote de Malpelo hacen parte de la zona Insular del océano Pacífico. Hidrográficamente se identifican cinco cuencas: Caribe, Magdalena–Cauca, Orinoco, Amazonas y Pacífico. La constitución geológica del territorio de Colombia es muy variada, con rocas de diferentes tipos y edades entre el Paleoproterozoico y el Holoceno, así como estructuras geológicas de diverso tipo y origen, que reflejan una historia geológica compleja. Esta armazón geológica ha dado lugar a la identificación de 23 cuencas sedimentarias, algunas marinas y otras continentales.

Palabras claves: *geografía colombiana, regiones naturales, cuencas hidrográficas, cuencas sedimentarias.*

1. Introduction

Geographically, the 2 070 408 km^2 that make up the continental (55.15%) and marine (44.85%) territory of the Republic of Colombia are located in the northwestern corner of South America. Politically, this area is divided into 32 departments and a capital district, Bogotá (Figure 1). The second political–administrative division is by municipalities. In total, Colombia has 1101 that grouped make up the departments (see the 1101 municipalities of Colombia in Google Earth, Supplementary Information). These political–administrative divisions must be borne in mind when reading The Geology of Colombia, since in several chapters they are indicated and used as reference points.. In addition, in the national territory, six large natural regions are distinguished: Andean, Caribbean, Pacific, Orinoquia, Amazonian, and Insular (Figure 2).

It is believed that the current Colombia geological setting results of the accretion of different continental and oceanic affinity geological terranes that allowed the growth of the national territory from the Proterozoic basement located to the east of the country (Gómez et al., 2015a, 2015b). Mountain uplift and the formation of the inter–Andean valleys, as a consequence of the Andean Orogeny, shaped the Colombian landscape. The main physiographic features, such as cordilleras and ranges, and some localities that due to their geological relevance deserve to be highlighted, including massifs and valleys, are present in Figure 3. Figure 4 shows the main rivers of Colombia and the five major hydrographic watersheds that group the Colombian drainage systems: Caribe, Magdalena–Cauca, Orinoco, Amazonas, and Pacífico.

The tectonic framework of Colombia is influenced by the interaction between the Caribbean and Nazca oceanic plates, and the South American continental plate, with ocean ridges, oceanic trenches, subduction zones, accretionary prisms, deformation belts, transform faults, and several other structural elements, as defined by Gómez et al. (2015a, 2015b) based on the findings of numerous researchers (Figure 5).

The geological processes that contributed to the formation of the national territory yield different types of rocks (Figure 6) and controlled the formation of folds and faults (Figure 7), some of which mark the boundaries between geological terranes and sedimentary basins, where converged the processes that allowed the formation and accumulation of hydrocarbons. Based on geological criteria and multiple aspects that Pardo et al. (2007a) considered for oil and gas exploration, the Agencia Nacional de Hidrocarburos (ANH) delimited 23 marine and continental sedimentary basins (Figure 8).

2. Andean Region

The Andean region corresponds to the great mountain belt of the Andes, which in Colombia is divided into three branches: the Western, Central, and Eastern Cordilleras. The Western and Central Cordilleras are forked north of the border of Colombia and Ecuador, in the so–called Nudo de Los Pastos; they run N–S, relatively parallel to the coast of the Pacific Ocean, and are separated by the inter–Andean valley of the Cauca River, a tributary of the Magdalena River. The Eastern Cordillera is the longest, oriented NE, and is detached from the Central Cordillera in the Macizo Colombiano, and on the border with Venezuela forks into the serranía de Perijá, N–S oriented, marking the binational limit. The Central and Eastern Cordilleras are separated by the Magdalena River Valley, which discharges into the Caribbean Sea. Each of the three mountain ranges has a different geological composition and geotectonic environment.

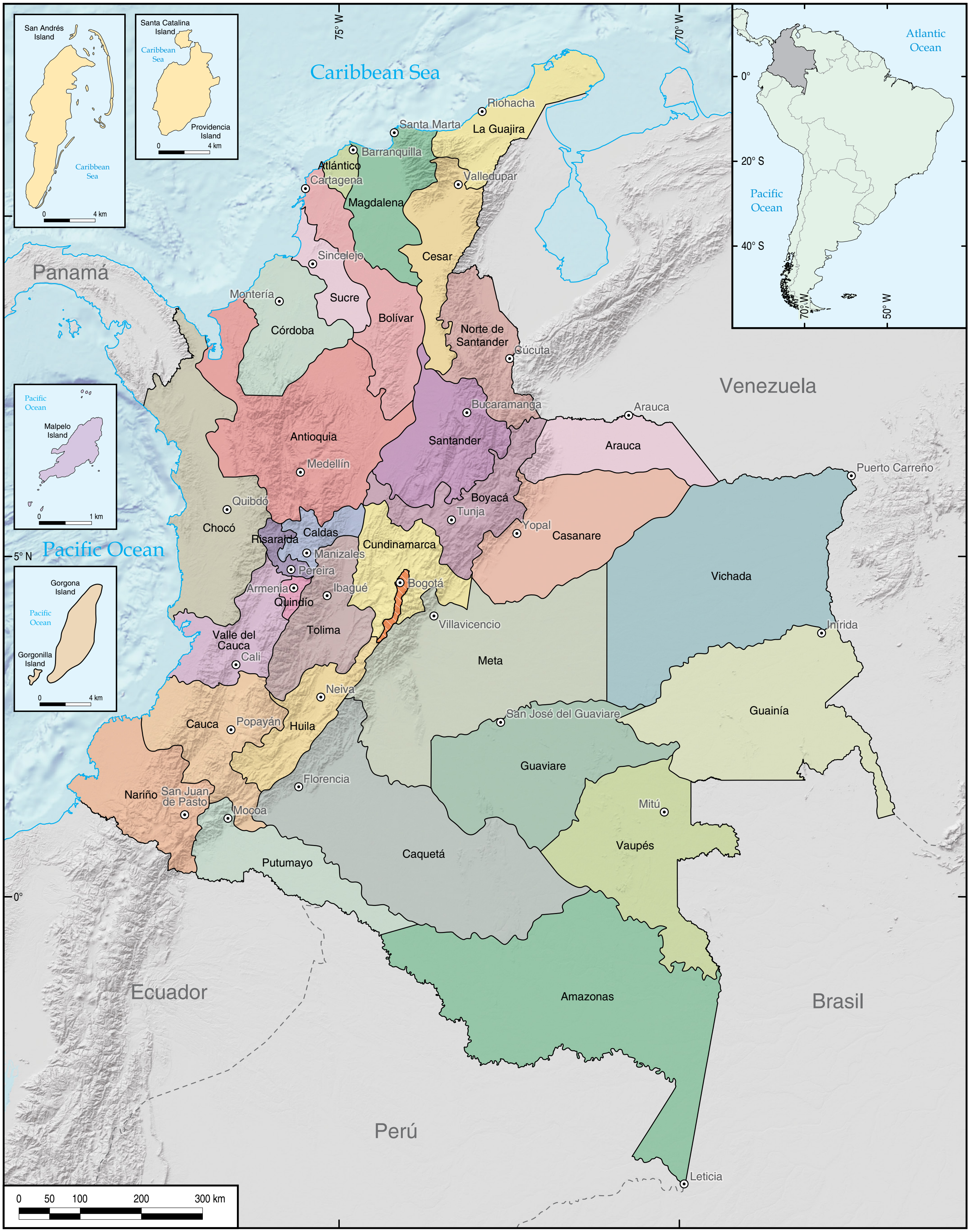

Figure 1. Political–administrative division of Colombia into departments. The figure also shows the capitals of the 32 departments. Modified from Instituto Geográfico Agustín Codazi (1999).

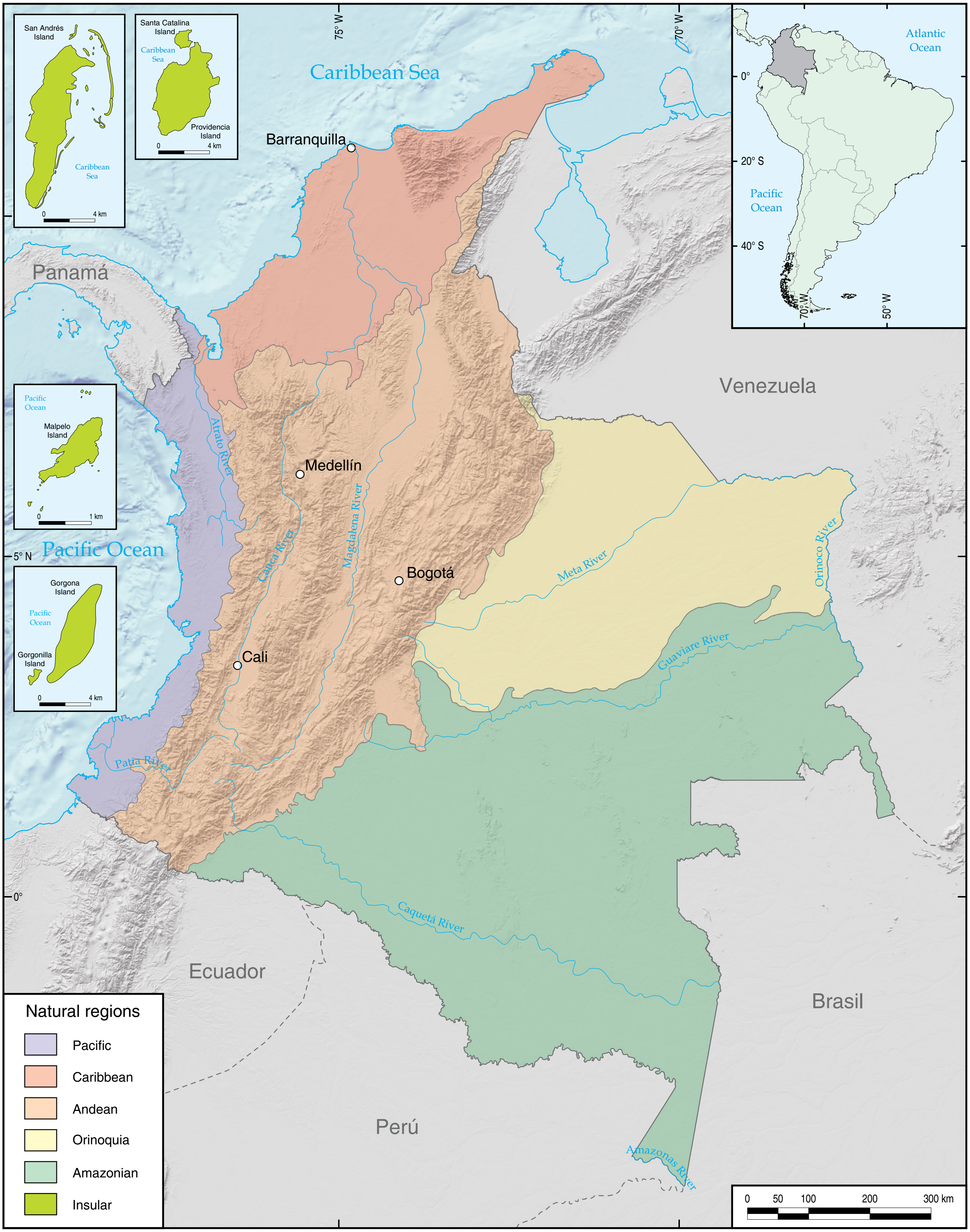

Figure 2. Natural regions and main cities of Colombia.

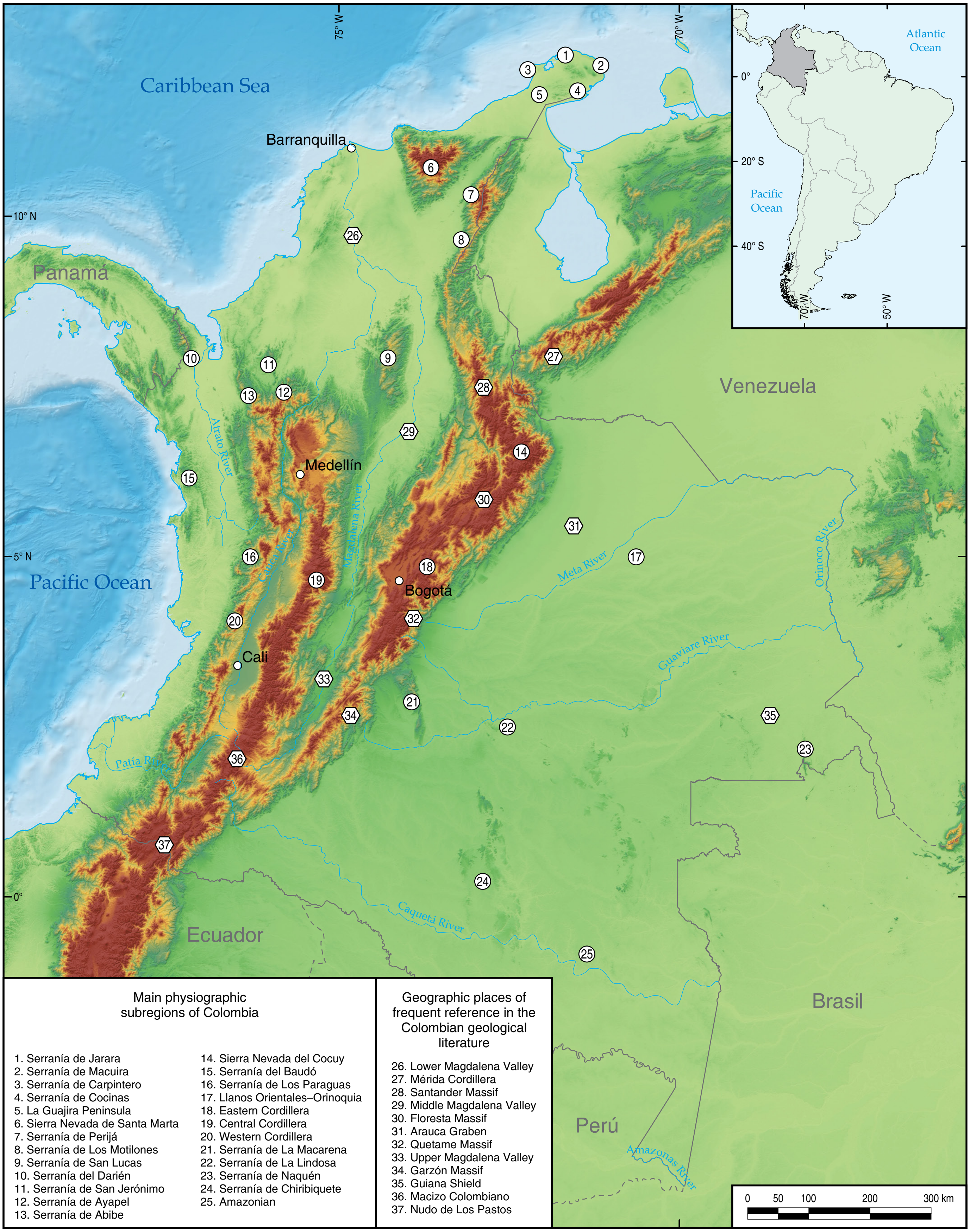

Figure 3. Main physiographic features of the Colombian territory and geographic places of frequent reference in the literature on Colombian geology.

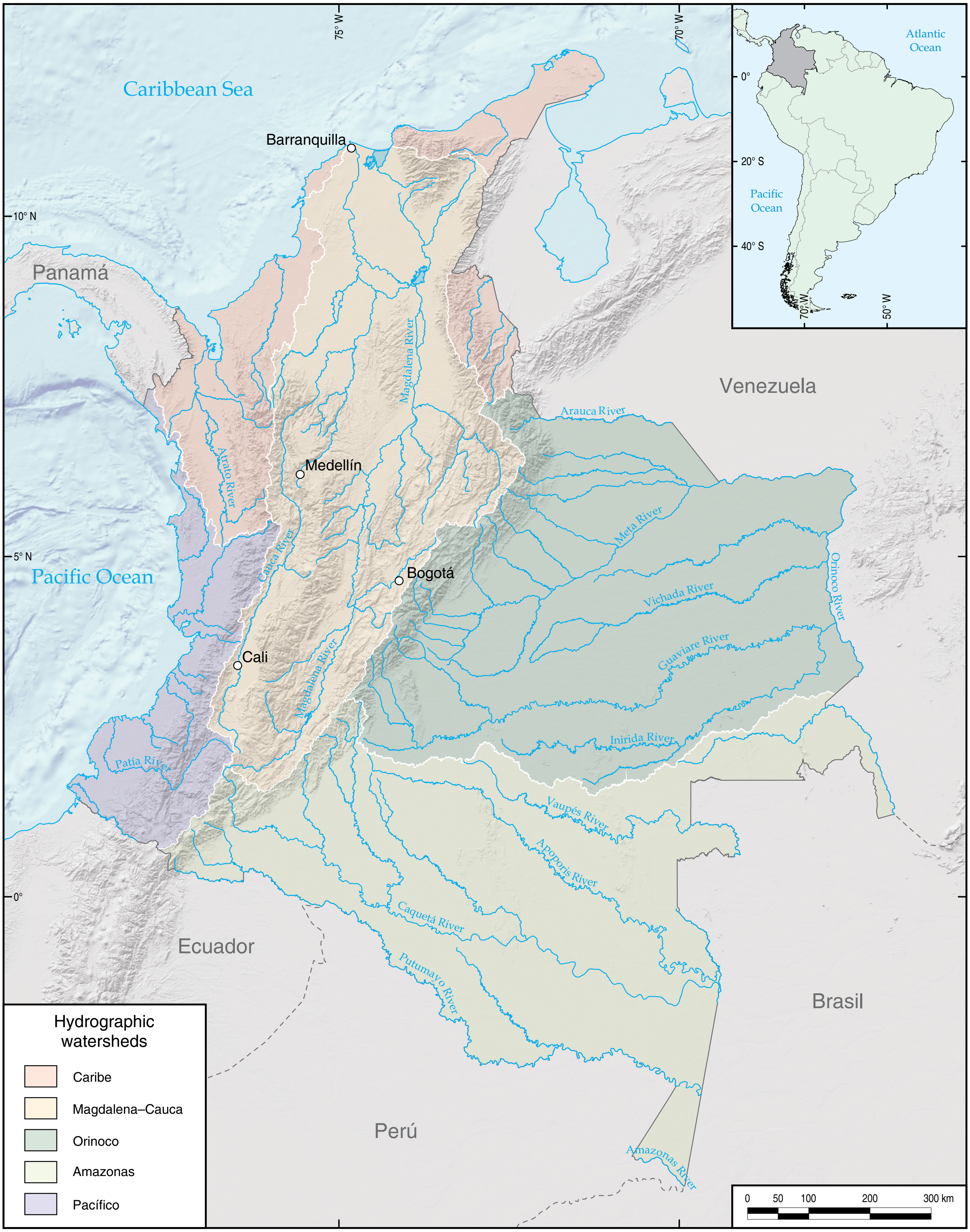

Figure 4. Main rivers of the country and hydrographic watersheds. Modified from Instituto de Hidrología, Meteorología y Estudios Ambientales (2013).

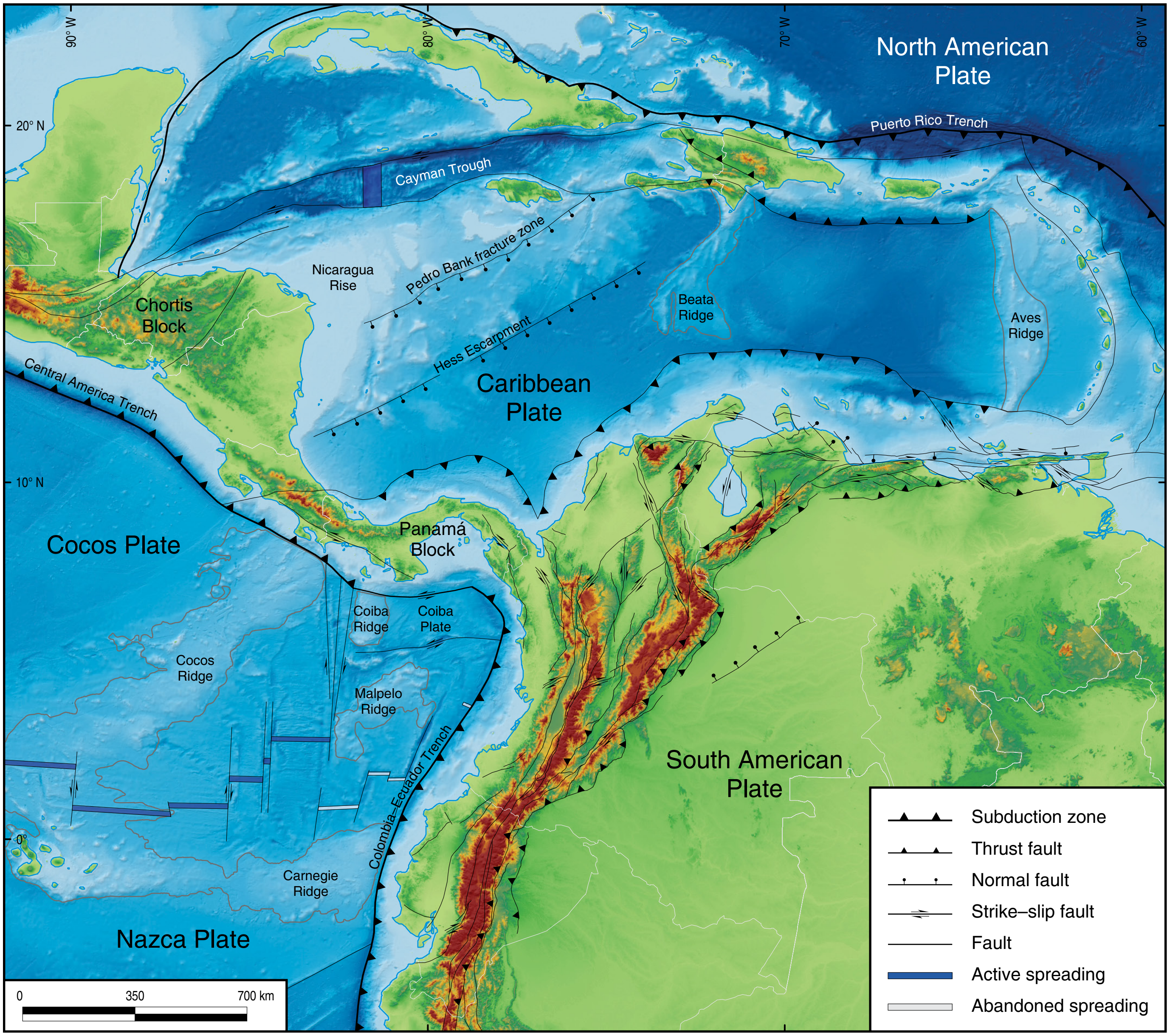

Figure 5. Tectonic scheme of northern South America and the Caribbean (Gómez et al., 2015a, 2015b).

The Western Cordillera is essentially constituted by Cretaceous sedimentary, gabbroic, and basaltic rocks of the Caribbean–Colombian oceanic plateau, accreted to the western margin of Colombia during the Late Cretaceous to Paleogene. In the southern sector, there are Paleogene plutonic and volcanoclastic rocks, while in the northern part, there are Miocene basalts and Pliocene volcanoclastic rocks, as well as small Neogene intrusions. At the southern end of the mountain range are deposits of Neogene and Quaternary volcanic eruptions, and some of the volcanoes in this area are active and are part of the Southern Volcanic Segment of Colombia (Monsalve–Bustamante, 2020).

The Central Cordillera has a low–grade polymetamorphic Triassic basement, with the last event recorded in the Jurassic. This basement is intruded by Permian, Mesozoic, and some Cenozoic plutons generated by the subduction of the Nazca Plate under the South American Plate. In the eastern flank, the Mesozoic intrusions are linked to Jurassic volcaniclastic sequences. Also, Mesoproterozoic – Neoproterozoic high–grade metamorphic rocks incorporated during the different orogenies recorded in Colombia are exposed. In the western flank, are found volcanoclastic and low–grade metamorphic rocks of the Cretaceous. Locally, Cretaceous marine sedimentary sequences are presented both the western and eastern flanks of the cordillera. The Neogene – Quaternary volcanoes, some of which are active, of the central and northern segments of Colombia (Monsalve–Bustamante, 2020) are located towards the summit of this mountain range. The Miocene molasse deposits of the Magdalena River Valley and volcanoclastic fans overlies the eastern foothills of

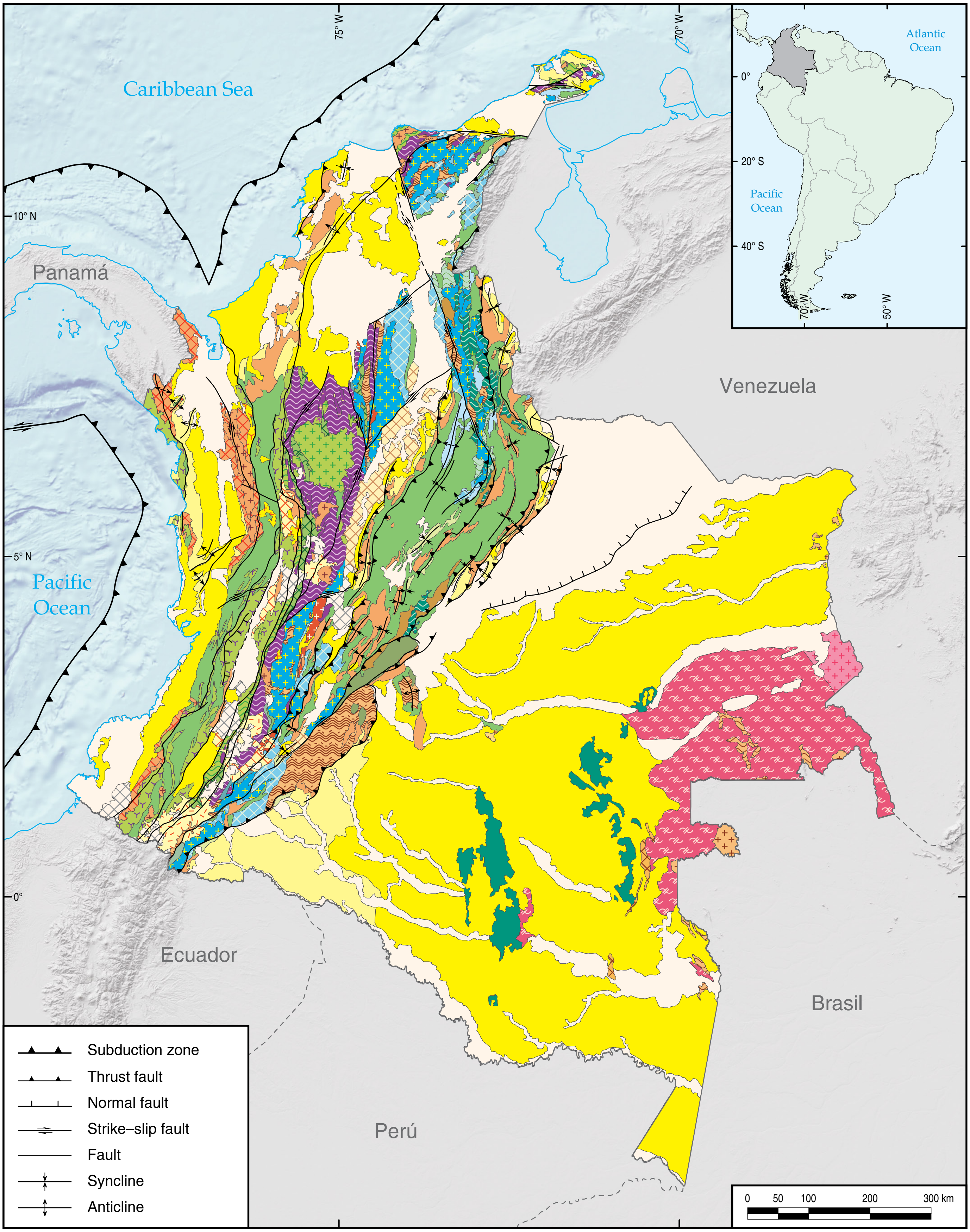

Figure 6. Geological map of Colombia. After Gómez et al. (2019).

Legend

- Quaternary basaltic rocks
- Quaternary volcanic rocks
- Quaternary volcaniclastic rocks
- Quaternary sedimentary rocks
- Pliocene – Pleistocene volcaniclastic rocks
- Pliocene volcanic rocks
- Pliocene volcaniclastic rocks
- Miocene basaltic rocks
- Neogene sedimentary rocks
- Neogene plutonic rocks
- Paleogene – Neogene sedimentary rocks
- Paleogene sedimentary rocks
- Paleogene plutonic rocks
- Paleogene volcaniclastic rocks
- Cretaceous – Paleogene sedimentary rocks
- Cretaceous sedimentary rocks
- Cretaceous volcanic rocks
- Cretaceous medium grade metamorphic rocks
- Cretaceous plutonic ultramafic rocks
- Cretaceous basaltic rocks
- Cretaceous volcaniclastic rocks
- Cretaceous low grade metamorphic rocks
- Cretaceous plutonic rocks
- Jurassic sedimentary rocks
- Jurassic volcaniclastic rocks
- Jurassic volcanic rocks
- Jurassic plutonic rocks
- Triassic sedimentary rocks
- Triassic volcaniclastic rocks
- Triassic plutonic ultramafic rocks
- Triassic plutonic rocks
- Triassic low grade metamorphic rocks
- Paleozoic sedimentary rocks
- Permian plutonic rocks
- Carboniferous plutonic rocks
- Carboniferous sedimentary rocks
- Devonian sedimentary rocks
- Silurian – Devonian low grade metamorphic rocks
- Ordovician plutonic rocks
- Ordovician low grade metamorphic rocks
- Ordovician sedimentary rocks
- Cambrian – Ordovician sedimentary rocks
- Neoproterozoic plutonic rocks
- Neoproterozoic volcaniclastic rocks
- Meso–Neoproterozoic high grade metamorphic rocks
- Mesoproterozoic plutonic rocks
- Mesoproterozoic low grade metamorphic rocks
- Paleoproterozoic plutonic rocks
- Paleoproterozoic medium grade metamorphic rocks

this mountain range. The Cauca–Almaguer and Silvia–Pijao Faults, exposed in the western foothills, are the tectonic limits of the Colombian continental terranes.

The Eastern Cordillera has a basement of Mesoproterozoic – Neoproterozoic high–grade metamorphic rocks exposed in the Garzón and Santander Massifs and the serranía de La Macarena. In this mountain range are also found Ordovician low–grade metamorphic rocks, especially in the Santander Massif; Paleozoic (Cambrian – Ordovician and Devonian) sedimentary sequences, some of them fossiliferous; and a thick succession of Cretaceous marine and Cenozoic continental sedimentary rocks that were deformed during the Andean Orogeny. In the Santander Massif and the western flank of the serranía de Perijá, the Jurassic record consist of sedimentary rocks, intrusions, and volcaniclastic sequences. Jurassic plutons are also present in the extreme south of the cordillera. South of the eastern flank, the Borde Amazónico Fault System and the Algeciras Fault mark the boundary with the Caguán–Putumayo Basin. To the north, the Borde Llanero Fault System serves as a boundary with the Llanos Orientales

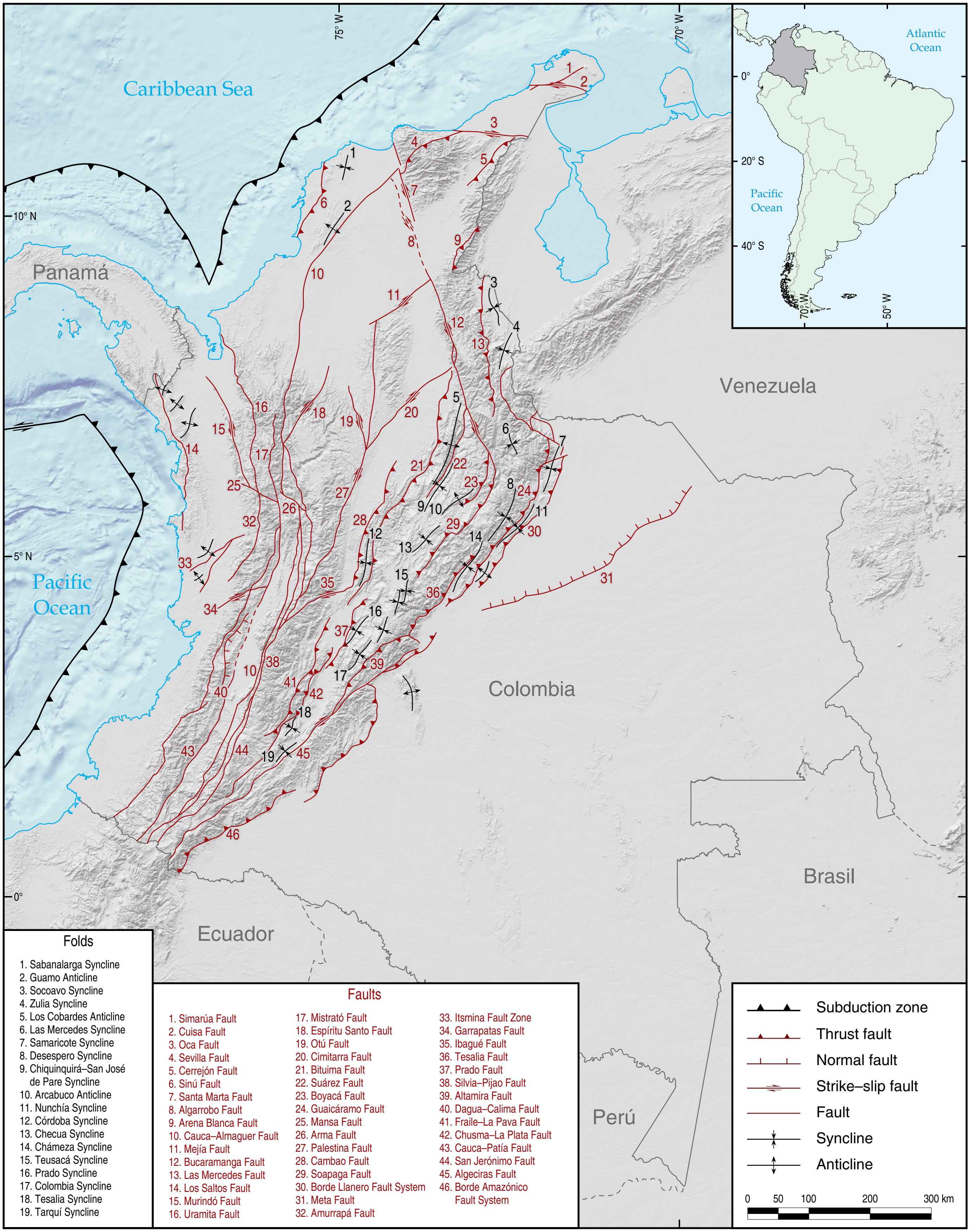

Figure 7. Main geological structures of Colombia. After Gómez et al. (2019).

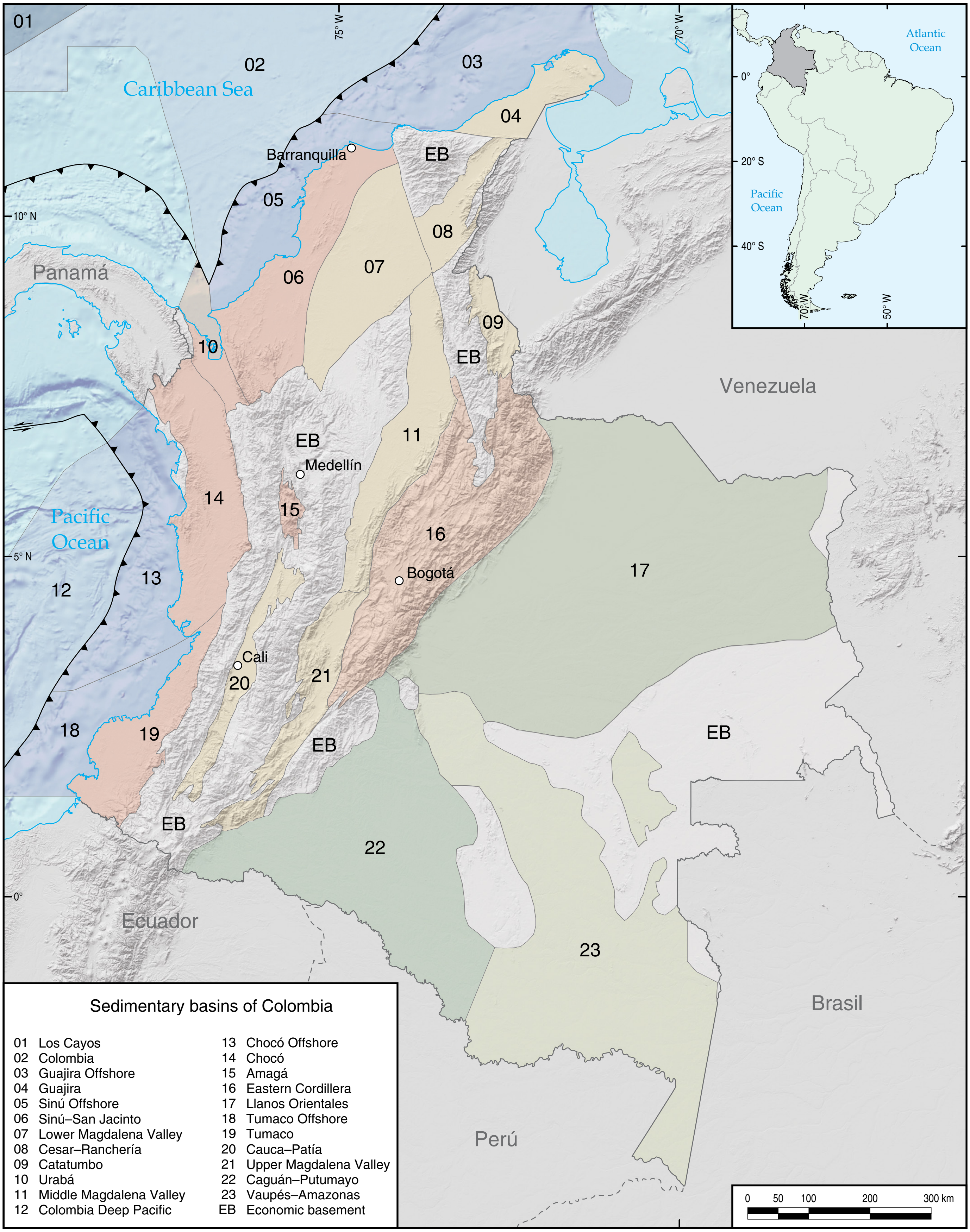

Figure 8. Sedimentary basins of Colombia. Modified from Pardo et al. (2007b).

Basin. These geological structures mark the limit of the Andean zone over eastern Colombia.

3. Caribbean Region

The Caribbean Region is between the Caribbean Sea and the northern foothills of the Andes. This region has 85% flat to undulating relief and some low–elevation hills, associated with lowland coasts, and include coastal plains, alluvial plains, salt flats and floodplains, mangrove plains, coastal lagoons, beaches and sandbanks, dune fields, platforms and reef bars, among other geomorphological features (Molina et al., 1998). The other 15% of the littoral corresponds to cliffs, where stands out the Sierra Nevada de Santa Marta (SNSM), with the Cristóbal Colón and Simón Bolívar Peaks over 5700 masl, the serranías de Jarara, Macuira, Carpintero, and Cocinas in La Guajira Peninsula; and the serranías de Abibe, Ayapel, Darién, and San Jerónimo in the southwestern sector. Mud diapirism and the alluvial delta of the Magdalena River are important geological features of this region.

The serranías de Jarara, Macuira, Carpintero and Cocinas, located in the Alta Guajira, are composed by Triassic and Cretaceous low–grade metamorphic assemblages. In some areas, Jurassic intrusives are exposed, as well as Triassic and Cretaceous marine and Jurassic continental sedimentary rocks.

The SNSM is a triangular block bounded to the north by the Oca Fault and to the west by the Santa Marta Fault. The Sevilla Fault cross the range in SW–NE direction. To the east, along the boundary with the Cesar–Ranchería Basin, are mainly found Cretaceous marine and Cenozoic continental sedimentary rocks. This basin separates it from the serranía de Perijá, the north extension of the Eastern Cordillera. The oldest rocks exposed are Mesoproterozoic high–grade metamorphic rocks, while Jurassic plutons conform most of the SNSM. To the northwestern corner, Triassic and Cretaceous medium to low–grade metamorphic rocks are intruded by a Paleogene granitoid, and to the eastern flank are found mainly Triassic and Jurassic sedimentary and volcaniclastic rocks.

The serranías de Abibe, Ayapel, Darién, and San Jerónimo are formed by Paleogene sedimentary rocks surrounded by Neogene sedimentary formations and Quaternary alluvial deposits.

4. Pacific Region

The coastal plains of western Colombia and some mountain ranges, such as the serranía del Baudó, make up the Pacific region. This region is a narrow fringe that extends between the Pacific Ocean and the foothills of the Western Cordillera. Morphologically, the northern sector has high coasts with cliffs, beaches, and floodplains in the interior of large bays (González et al., 1998). The central and southern parts are dominated by low alluvial and flooded coasts interrupted by short cliffs (González et al., 1998).

In the serranía del Baudó, Cretaceous basalts and Paleogene volcaniclastic sequences are found, derived from an island arc accreted to the continental margin. In the other areas of the Pacific region, there are Paleogene and Neogene sedimentary units, and alluvial and coastal deposits of the Quaternary.

5. Orinoquia and Amazonian Regions

The plains of the northern sector of eastern Colombia form Orinoquia, while the Amazonian constitutes the jungle region of southeastern Colombia, where the serranía de Chiribiquete stands out. These two regions are the largest in the country, the least inhabited and the least developed. Both regions are bounded to the west by the foothills of the Eastern Cordillera, while to the east, they extend until the borders of Brasil and Venezuela. Geographically, the boundary between the Orinoquia and the Amazonian regions is defined along the Guaviare River.

In Orinoquia and Amazonian, the basement is formed by Paleoproterozoic and Mesoproterozoic medium– and low–grade metamorphic rocks, respectively, with Paleoproterozoic and Mesoproterozoic granitic intrusions and Neoproterozoic volcaniclastic rocks. This igneous–metamorphic assemblage is part of the western sector of the Guiana Shield and is covered by Neoproterozoic (Ediacaran and Cryogenian), Cambrian – Ordovician, and Ordovician marine sedimentary rocks with fossiliferous levels, exposed in mountainous areas such as serranías de Chiribiquete and La Lindosa or reported in borehole cores (Dueñas–Jiménez & Montalvo–Jónsson, 2020; Dueñas–Jiménez et al., 2020). Cretaceous marine and Cenozoic continental sedimentary rocks cover, in most of these regions, the oldest rocks. Ibañez–Mejia et al. (2011) indicate that in wells located in the southwestern part of the Putumayo Basin, they found Proterozoic metamorphic rocks under the sedimentary cover, confirming that the Proterozoic basement extends to the Eastern Cordillera.

6. Insular Region

The insular region in the Caribbean Sea comprises the archipelago of San Andrés and Providencia and several cays, while in the Pacific Ocean comprise the Gorgona, Gorgonilla, and Malpelo Islands.

The insular region of the Colombian Caribbean includes three main islands: San Andrés, Providencia, and Santa Catalina, and other smaller islands, atolls, and coral reefs (Ortiz–Royero, 2012). Geologically, this zone is located in the Lower Nicaragua Rise between the Pedro fracture zone and the Hess Escarpment (Rogers et al., 2007).

According to Geister & Díaz (2007), the archipelago consists of a platform of carbonates and reefs that cover deep volcanic cones. The authors state that according to the available information, the atolls, islands, and coral banks to the south of the archipelago were formed around volcanoes in the early Cenozoic, and that subsidence and settlement of carbonates over shallow areas and in the summits of the volcanoes during the Cenozoic and the Quaternary facilitated their formation. Additionally, these features are oriented NNE, possibly following geological structures with the same orientation (Geister & Díaz, 2007). The island of San Andrés comprises mainly limestone deposits of the Pleistocene, while Providencia and Santa Catalina are part of the same composite volcanic cone; they are essentially alkaline and calc–alkaline volcanic rocks of middle Miocene and Pliocene age, respectively (Álvarez–Gutiérrez et al., 2014). To the south of Providencia, some intercalations of Miocene reef limestone between volcanic series and Quaternary marine sedimentary deposits are located (Geister & Díaz, 2007).

The Colombian insular region in the Pacific Ocean is made up of the Gorgona and Gorgonilla Islands, the Malpelo Islet, and El Viudo and El Horno rocky promontories (Díaz et al., 2001). More than 80% of the surface of the two main islands is constituted by igneous rocks, including basal peridotites and gabbros covered by basaltic lavas with komatiite flows (Díaz et al., 2001; Echeverría, 1982; Gansser et al., 1979; Parada & Tchegliakova, 1990). The remaining 15% corresponds to upper Eocene to upper Miocene sedimentary rocks and Quaternary sedimentary deposits that conform beaches, small deltas of surface currents, and some terraces. Reef zones surround the southern part of the main island (Díaz et al., 2001). Malpelo is a cliff formed entirely by basic volcanic rocks and in Gorgonilla, Bermúdez et al. (2016, 2019) report the boundary of the Cretaceous – Paleogene with the presence of tektites from the Chicxulub impact.

7. Conclusions

The marine and continental territory of the Republic of Colombia is in the northwest of South America, where interact the Caribbean and Nazca oceanic plates and the South American continental plate. Between the Proterozoic and the Holocene multiple geological events originated the current physiography setting that comprises six natural regions, five major drainage basins, 23 sedimentary basins, and diverse lithologies.

Acknowledgements

Authors recognize the support provided by the management of the Servicio Geológico Colombiano, especially by the director general Dr. Oscar PAREDES ZAPATA, for the writing of this chapter. The geologist Ana María PATIÑO ACEVEDO supported the style review.

References

Álvarez–Gutiérrez, Y., Amaya–López, C., Barbosa–Mejía, L.N., Builes–Carvajal, J.B., Henao–Casas, J.D., Montoya–Cañola, S.M., Pacheco–Sintura, P.A., Ramírez–Hoyos, L.F., Urrego–Osorio, S., Zapata–Montoya, A.M., Ordóñez–Carmona, O., Restrepo–Álvarez, J.J. 2014. Descripción e interpretación geológica de las Islas de Providencia y Santa Catalina. Boletín Ciencias de la Tierra, (35): 67– 81.

Bermúdez, H.D., García, J., Stinnesbeck, W., Keller, G., Rodríguez, J.V., Hanel, M., Hopp, J., Schwarz, W.H., Trieloff, M., Bolívar, L. & Vega, F.J. 2016. The Cretaceous – Paleogene boundary at Gorgonilla Island, Colombia, South America. Terra Nova, 28(1): 83–90. https://doi.org/10.1111/ter.12196

Bermúdez, H.D., Arenillas, I., Arz, J.A., Vajda, V., Renne, P.R., Gilabert, V. & Rodríguez, J.V. 2019. The Cretaceous/Paleogene boundary deposits on Gorgonilla Island. In: Gómez, J. & Mateus–Zabala, D. (editors), The Geology of Colombia, Volume 3 Paleogene – Neogene. Servicio Geológico Colombiano, Publicaciones Geológicas Especiales 37, p. 1–19. Bogotá. https://doi.org/10.32685/pub.esp.37.2019.01

Díaz, J.M., Pinzón, J.H., Perdomo, A.M, Barrios, L.M. & López–Victoria, M. 2001. Generalidades. In: Barrios, L.M. & López–Victoria, M. (editors), Gorgona marina: contribución al conocimiento de una isla única. Instituto de Investigaciones Marinas y Costeras José Benito Vives De Andreis, Publicaciones Especiales, 7: 17–26.

Dueñas–Jiménez, H. & Montalvo–Jónsson, J. 2020. Neoproterozoic records of the Llanos Orientales Basin, Colombia. In: Gómez, J. & Mateus–Zabala, D. (editors), The Geology of Colombia, Volume 1 Proterozoic – Paleozoic. Servicio Geológico Colombiano, Publicaciones Geológicas Especiales 35, p. 91–99. Bogotá. https://doi.org/10.32685/pub.esp.35.2019.05

Dueñas–Jiménez, H., Corredor–Bohórquez, V.E. & Montalvo–Jónsson, J. 2020. Paleontology of the Paleozoic rocks of the Llanos Orientales Basin, Colombia. In: Gómez, J. & Mateus–Zabala, D. (editors), The Geology of Colombia, Volume 1 Proterozoic – Paleozoic. Servicio Geológico Colombiano, Publicaciones Geológicas Especiales 35, p. 133–148. Bogotá. https://doi.org/10.32685/pub.esp.35.2019.07

Echeverría, L.M. 1982. Komatiites from Gorgona Island, Colombia. In: Arndt, N.T. & Nisbet, E.G. (editors), Komatiites. George Allen & Unwin, p. 199–209. London, UK.

Gansser, A., Dietrich, V.J. & Cameron, W.E. 1979. Palaeogene komatiites from Gorgona Island. Nature, 278: 545–546. https://doi.org/10.1038/278545a0

Geister, J. & Díaz, J.M. 2007. Ambientes arrecifales y geología de un archipiélago oceánico: San Andrés, Providencia y Santa Catalina, Mar Caribe, Colombia; con guía de campo. Ingeominas, 114 p. Bogotá.

Gómez, J., Montes, N.E., Nivia, Á. & Diederix, H., compilers. 2015. Geological Map of Colombia 2015. Scale 1:1 000 000. Servicio Geológico Colombiano, 2 sheets. Bogotá. https://doi.org/10.32685/10.143.2015.936

Gómez, J., Nivia, Á., Montes, N.E., Diederix, H., Almanza, M.F., Alcárcel, F.A. & Madrid, C.A. 2015b. Explanatory notes: Geological Map of Colombia. In: Gómez, J. & Almanza, M.F. (editors), Compilando la geología de Colombia: Una visión a 2015. Servicio Geológico Colombiano, Publicaciones Geológicas Especiales 33, p. 35–60. Bogotá.

Gómez, J., Schobbenhaus, C. & Montes, N.E., compilers. 2019. Geological Map of South America 2019. Scale 1:5 000 000. Commission for the Geological Map of the World (CGMW), Colombian Geological Survey and Geological Survey of Brazil. Paris. https://doi.org/10.32685/10.143.2019.929

González, J.L., Marín, L., Martínez, J.O. & Carvajal, J.H. 1998. Geomorfología y aspectos erosivos del Litoral Pacífico colombiano. Publicaciones Geológicas Especiales del Ingeominas, (21): 75–111. Bogotá.

Ibañez–Mejia, M., Ruiz, J., Valencia, V.A., Cardona, A., Gehrels, G.E. & Mora, A.R. 2011. The Putumayo Orogen of Amazonia and its implications for Rodinia reconstructions: New U–Pb geochronological insights into the Proterozoic tectonic evolution of northwestern South America. Precambrian Research, 191(1–2): 58–77. https://doi.org/10.1016/j.precamres.2011.09.005

Instituto de Hidrología, Meteorología y Estudios Ambientales (IDEAM). 2013. Zonificación y codificación de unidades hidrográficas e hidrogeológicas de Colombia. Comité de Comunicaciones y Publicaciones del IDEAM, 47 p. Bogotá

Instituto Geográfico Agustín Codazzi (IGAC). 1999. Mapa oficial político–administrativo de Colombia. Bogotá.

Molina, L.E., Pérez, F., Martínez, J.O., Franco, J.V., Marín, L., González, J.L. & Carvajal, J.H. 1998. Geomorfología y aspectos erosivos del Litoral Caribe colombiano. Publicaciones Geológicas Especiales del Ingeominas, (21): 1–73. Bogotá.

Monsalve–Bustamante, M.L. 2020. The volcanic front in Colombia: Segmentation and recent and historical activity. In: Gómez, J. & Pinilla–Pachon, A.O. (editors), The Geology of Colombia, Volume 4 Quaternary. Servicio Geológico Colombiano, Publicaciones Geológicas Especiales 38, p. 97–159. Bogotá. https://doi.org/10.32685/pub.esp.38.2019.03

Ortiz–Royero, J.C. 2012. Exposure of the Colombian Caribbean coast, including San Andrés Island, to tropical storms and hurricanes, 1900–2010. Natural Hazards, 61(2):815–827. https://doi.org/10.1007/s11069-011-0069-1

Parada, C. & Tchegliakova, N.N. 1990. Foraminíferos y sedimentos de Playa Blanca, Isla Gorgona. Geología Colombiana, (17): 227–237.

Pardo, A., Barrero, D., Vargas, C.A. & Martínez, J.F. 2007a. Sedimentary basins of Colombia: Geological framework. In: Barrero, D., Pardo, A., Vargas, C.A. & Martínez, J.F. (editors), Colombian Sedimentary Basins: Nomenclature, boundaries and petroleum geology, a new proposal. ANH and B&M Exploration Ltda., p. 14–20. Bogotá.

Pardo, A., Vargas, C.A., Barrero, D. & Martínez, J.F. 2007b. Review of nomenclature and boundaries of Colombian basins. In: Barrero, D., Pardo, A., Vargas, C.A. & Martínez, J.F. (editors), Colombian Sedimentary Basins: Nomenclature, boundaries and petroleum geology, a new proposal. ANH and B&M Exploration Ltda., p. 22–52. Bogotá.

Rogers, R.D., Mann, P. & Emmet, P.A. 2007. Tectonic terranes of the Chortis Block based on integration of regional aeromagnetic and geologic data. In: Mann, P. (editor), Geologic and tectonic development of the Caribbean Plate in northern Central America. Geological Society of America, Special Paper 428, p. 65–88. https://doi.org/10.1130/2007.2428(04)

Explanation of Acronyms, Abbreviations, and Symbols:

SNSM	Sierra Nevada de Santa Marta

Authors' Biographical Notes

Jorge GÓMEZ TAPIAS is a geologist and has worked as a cartographer at the Servicio Geológico Colombiano for 20 years, during which time, he has authored approximately 70 geological maps. He is the coordinator of the Grupo Mapa Geológico Colombiano of the Dirección de Geociencias Básicas, which was recognized by Colciencias as a research group in 2017. GÓMEZ is the first author of the Geological Map of Colombia at a scale of 1:1 M –editions 2007 and 2015– and of the 26 map sheets of the Geological Atlas of Colombia at a scale of 1:500 K and is the co–editor of the book *Compilando la geología de Colombia: Una visión a 2015*. Since February 2018, he has served as vice president for South America on the Commission for the Geological Map of the World. He was a co–coordinator and the first author of the Geological Map of South America at a scale of 1:5 M 2019. Since October 2020, he was elected as a member of the International Union of Geological Sciences (IUGS) Nominating Committee for the term 2020–2024. Currently, he is the editor–in–chief of *The Geology of Colombia*. GÓMEZ is in charge of coordinating all the activities related to the project and the editorial process.

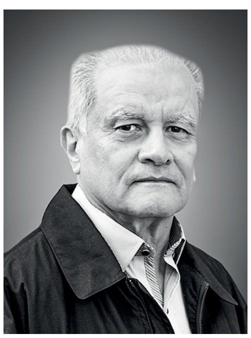

Alberto NÚÑEZ–TELLO is a geologist who graduated from the Universidad Nacional de Colombia and is a specialist in environmental management and disaster prevention for the Universidad del Tolima. He has worked for 32 years at the Servicio Geológico Colombiano in different positions, including that of technical director. His main interest is in regional geological mapping and geological risk management.

Daniela MATEUS–ZABALA is a geologist who graduated from the Universidad Nacional de Colombia Sede Bogotá in 2016 and is a copyeditor of scientific and science outreach texts. She has participated in geological and geomorphological mapping projects, petrographic and geochemical characterization of rocks, and geochemical evaluation of soils. Since 2017, she has been part of the Grupo Mapa Geológico de Colombia and is a deputy editor of *The Geology of Colombia*. In this editorial project, she supported the coordination of the editorial process stages and coordinated the advisory work for the project provided by the Observatorio Colombiano de Ciencia y Tecnología and the Asociación Colombiana para el Avance de la Ciencia; she was also in charge of the writing and proofreading of texts written in Spanish and English and conducted the editorial review of the chapters.

Fernando Alirio ALCÁRCEL–GUTIÉRREZ is a geologist who graduated from the Universidad Nacional de Colombia and a is specialist in geomatics graduated from the Universidad Militar Nueva Granada. He has been part of the Grupo Mapa Geológico de Colombia since 2012. He has co–authored several publications from the group, including the *Catálogo de dataciones radiométricas de Colombia en ArcGIS y Google Earth*, and he is also the first author of the informative Geological Map of Colombia 2019 at a scale of 1:2 M. ALCÁRCEL has extensive experience in the vectorization and digitization of graphic material for scientific publications, which is why he is the main graphic artist for *The Geology of Colombia* and is in charge of elaborating and improving the figures and maps.

Rubby Melissa LASSO–MUÑOZ is a geological engineer who graduated from the Universidad Nacional de Colombia Sede Medellín in 2016. LASSO has worked in the petroleum industry and conducted science outreach with communities. Since 2019, she has worked on the Grupo Mapa Geológico de Colombia in the Servicio Geológico Colombiano and has been in charge of coordinating the project promotion and the science outreach activities. She is also responsible for updating *The Geology of Colombia* website and producing text, graphics, and audiovisual content for it.

Eliana MARÍN–RINCÓN is a geologist who graduated from the Universidad de Caldas in 2017. In the editorial process of *The Geology of Colombia*, she is in charge of preparing and adjusting the chapters' figures. MARÍN also supports the science outreach events through general logistics management and maintains the correspondence with and databases of participants.

María Paula MARROQUÍN–GÓMEZ is a geoscientist who graduated from the Universidad de los Andes in 2019, where she completed her studies with the financial support of *Bachilleres por Colombia Ecopetrol* scholarship. She has been part of the Grupo Mapa Geológico de Colombia since 2019, supporting the editorial and thematic reviews for *The Geology of Colombia* by ensuring the clarity and consistency of the chapters.

Volume 1

Chapter 2

https://doi.org/10.32685/pub.esp.35.2019.02
Published online 17 April 2020

Contribution of New Airborne Geophysical Information to the Geological Knowledge of Eastern Colombia

Ismael Enrique MOYANO–NIETO[1]*, Renato CORDANI[2], Lorena Paola CÁRDENAS–ESPINOSA[3], Norma Marcela LARA–MARTÍNEZ[4], Oscar Eduardo ROJAS–SARMIENTO[5], Manuel Fernando PUENTES–TORRES[6], Diana Lorena OSPINA–MONTES[7], Andrés Felipe SALAMANCA–SAAVEDRA[8], and Gloria PRIETO–RINCÓN[9]

1 imoyano@sgc.gov.co
Servicio Geológico Colombiano
Dirección de Recursos Minerales
Diagonal 53 n.° 34–53
Bogotá, Colombia

2 rcordani@reconsult.com.br
RECONSULT Geofisica
Cerqueira César, Rua Augusta, 2690–loja 322,
CEP 01412–100
São Paulo–SP, Brasil

3 lopaca7@gmail.com
Carrera 8 n.° 58–67
Cali, Colombia

4 nlara@sgc.gov.co
Servicio Geológico Colombiano
Dirección de Recursos Minerales
Diagonal 53 n.° 34–53
Bogotá, Colombia

5 orojas@sgc.gov.co
Servicio Geológico Colombiano
Dirección de Recursos Minerales
Diagonal 53 n.° 34–53
Bogotá, Colombia

6 mpuentes@sgc.gov.co
Servicio Geológico Colombiano
Dirección de Recursos Minerales
Diagonal 53 n.° 34–53
Bogotá, Colombia

7 dcospina@sgc.gov.co
Servicio Geológico Colombiano
Dirección de Recursos Minerales
Diagonal 53 n.° 34–53
Bogotá, Colombia

8 asalamanca@gidco.com
Gidco SAS
Carrera 20 n.° 70ª–21
Bogotá, Colombia

9 gprieto@sgc.gov.co
Servicio Geológico Colombiano
Dirección de Recursos Minerales
Diagonal 53 n.° 34–53
Bogotá, Colombia

* Corresponding author

Abstract Airborne geophysics is an easy way to increase and complement the geological knowledge of large areas, especially very remote areas like the Colombian Amazonia. For this objective and to identify areas of interest for mineral resources, the Colombian government has made extensive efforts to fly the Andean and eastern parts of the country, collecting more than 400 000 linear km of magnetic and gamma spectrometric information over the Colombian Amazonia. This document focuses on describing the potential of these data to increase the geological knowledge of the Amazonian region. It presents a methodology to interpret the geophysical data and its application over a specific area in the eastern Guainía Department. It was possible to identify Paleoproterozoic to Mesoproterozoic igneous and metamorphic rocks of the Guiana Shield (Mitú Complex, Parguaza Granite) and several lineaments and structural trends that have not been previously reported. These crystalline basement rocks are partially covered by Miocene sedimentary rocks, recent alluvial deposits, and dense rainforest coverage, which make geological mapping very difficult. The results increase the relevance of this type of geophysical interpretation to the geoscientific knowledge about Colombia. This paper also highlights the training of Colombian geoscientists in modern geophysical interpretation techniques.

Keywords: *geophysical interpretation, magnetics, gamma spectrometry, Colombian Amazonia.*

Resumen Usar la geofísica aerotransportada es una forma sencilla de aumentar y complementar el conocimiento geológico de grandes áreas, especialmente si son muy remotas como la Amazonia colombiana. Para lograr este objetivo y además identificar áreas de interés para recursos minerales, el Gobierno colombiano realizó esfuerzos para sobrevolar las zonas andina y oriental del país y adquirió más de 400 000 km lineales de información magnetométrica y gamma espectrométrica sobre la Amazonia colombiana. Este documento se centra en describir el potencial de estos datos geofísicos para aumentar el conocimiento geológico sobre la región Amazónica. Presenta la metodología que se utilizó para la interpretación de los datos geofísicos adquiridos y

Citation: Moyano–Nieto, I.E., Cordani, R., Cárdenas–Espinosa, L.P., Lara–Martínez, N.M., Rojas–Sarmiento, O.E., Puentes–Torres, M.F., Ospina–Montes, D.L., Salamanca–Saavedra, A.F. & Prieto–Rincón, G. 2020. Contribution of new airborne geophysical information to the geological knowledge of eastern Colombia. In: Gómez, J. & Mateus–Zabala, D. (editors), The Geology of Colombia, Volume 1 Proterozoic – Paleozoic. Servicio Geológico Colombiano, Publicaciones Geológicas Especiales 35, p. 17–36. Bogotá. https://doi.org/10.32685/pub.esp.35.2019.02

su aplicación en un área específica ubicada al oriente del departamento de Guainía, donde la interpretación geofísica permitió diferenciar las rocas ígneas y metamórficas paleoproterozoicas a mesoproterozoicas del Escudo de Guayana (Complejo Mitú y Granito de Parguaza) y varios lineamientos y tendencias estructurales que no han sido reportados anteriormente. Estas rocas cristalinas del basamento se encuentran parcialmente cubiertas por rocas sedimentarias del Mioceno, algunos depósitos aluviales recientes y una densa cobertura vegetal, la cual hace muy difícil el mapeo geológico. Los resultados aumentan la relevancia de este tipo de interpretaciones geofísicas para el conocimiento geocientífico de Colombia. Adicionalmente, en este trabajo se resalta el entrenamiento de geocientíficos colombianos en las técnicas modernas de interpretación geofísica.

Palabras clave: *interpretación geofísica, magnetometría, gamma espectrometría, Amazonia colombiana.*

1. Introduction

Modern geophysical techniques are commonly used by geological surveys, academia, and industry around the world to aid in geological mapping, provide basic information about mining prospects, and strategic information to geological surveys even in areas where mining is restricted or prohibited (Dods et al., 1989; Geological Survey of Ireland, 2017; Nakamura, 2015; Oliveira, 2014a; Oliveira, 2014b; Silva, 2014).

For these objectives, the easiest and most inexpensive way to cover large areas with geophysical data at regional to semi–detailed resolutions is the use of fixed wing aircraft equipped with specific geophysical sensors suitable for the purposes of the survey (Table 1; Dentith & Mudge, 2014; Reeves, 2005), such as magnetic and gravimetric sensors over sedimentary basins and offshore regions for hydrocarbon exploration (Graterol & Vargas, 2010a, 2010b) and magnetic and gamma spectrometric sensors for mineral resource and geological mapping (Oliveira, 2014a; Oliveira, 2014b; Silva, 2014).

Table 1. Geophysical methods commonly used in the exploration of several important types of mineral deposits.

Deposit type	Gravimetry	Magnetometry	Resistivity	Radioactivity
Iron formation	M D	M D	D	M
Coal		M D		
IOCG	M D	M D	D	D
Magmatic	M D	M D	D	
Primary diamonds	M	M		
Uranium	M	M	M	D
Porphyry Cu, Mo	M	M D	D	D
SEDEX Pb–Zn	M	M	D	
Placer deposits	M		M	
Skarns	M	M D		
Groundwater			M D	
Petroleum	M	M	M	

Source: Data modified from Dentith & Mudge (2014).

Note: M—geological mapping of prospective terrains; D—detection/delineation of the mineral environment.

To increase the geological knowledge of the country and identify areas of interest for mineral resources, the Servicio Geológico Colombiano, in collaboration with external experts of the World Bank, selected areas of the country where geological, geochemical, and metallogenical information could be integrated with geophysical data to evaluate the mineral resource potential of these areas (Andean region) and other ones where the lack of geoscientific information could be complemented with the same geophysical information, such as the Orinoquia and Amazonian regions of eastern Colombia (Moyano et al., 2016).

Airborne magnetometry and gamma spectrometry data acquisition surveys were designed for selected areas. The surveys were distributed in parallel lines at 500 to 1000 meter spacings to attain a good resolution for the areal coverage (Reeves, 2005) and to acquire multi–purpose geophysical data (Oliveira, 2014a; Oliveira, 2014b; Silva, 2014). This survey design represents more than 1 million line kilometers of geophysical information, of which nearly 400 000 line kilometers are in the Amazonian region (Figure 1).

Regionally, the geological basement in eastern Colombia (Orinoquia and Amazonian regions; Figure 2) is composed of rocks of the Amazonian Craton (Tassinari & Macambira, 1999) and within Colombia corresponds to the Mitú Migmatitic Complex (PP–Mmg1 sensu Gómez et al., 2015) or the Mitú Complex (Celada et al., 2006; López & Cramer, 2012; López et al., 2007; Rodríguez et al., 2011). These rocks include gneisses and amphibolites with migmatites, granitoids of different compositions and alkaline and calc–alkaline affinities, and doleritic dikes (Bruneton et al., 1982; Celada et al., 2006; Galvis et al., 1979; López & Cramer, 2012; Rodríguez et al., 2011). The rocks of this complex outcrop in the Guainía, Vaupés, and Caquetá Departments. The U–Pb SHRIMP and Sm–Nd ages for

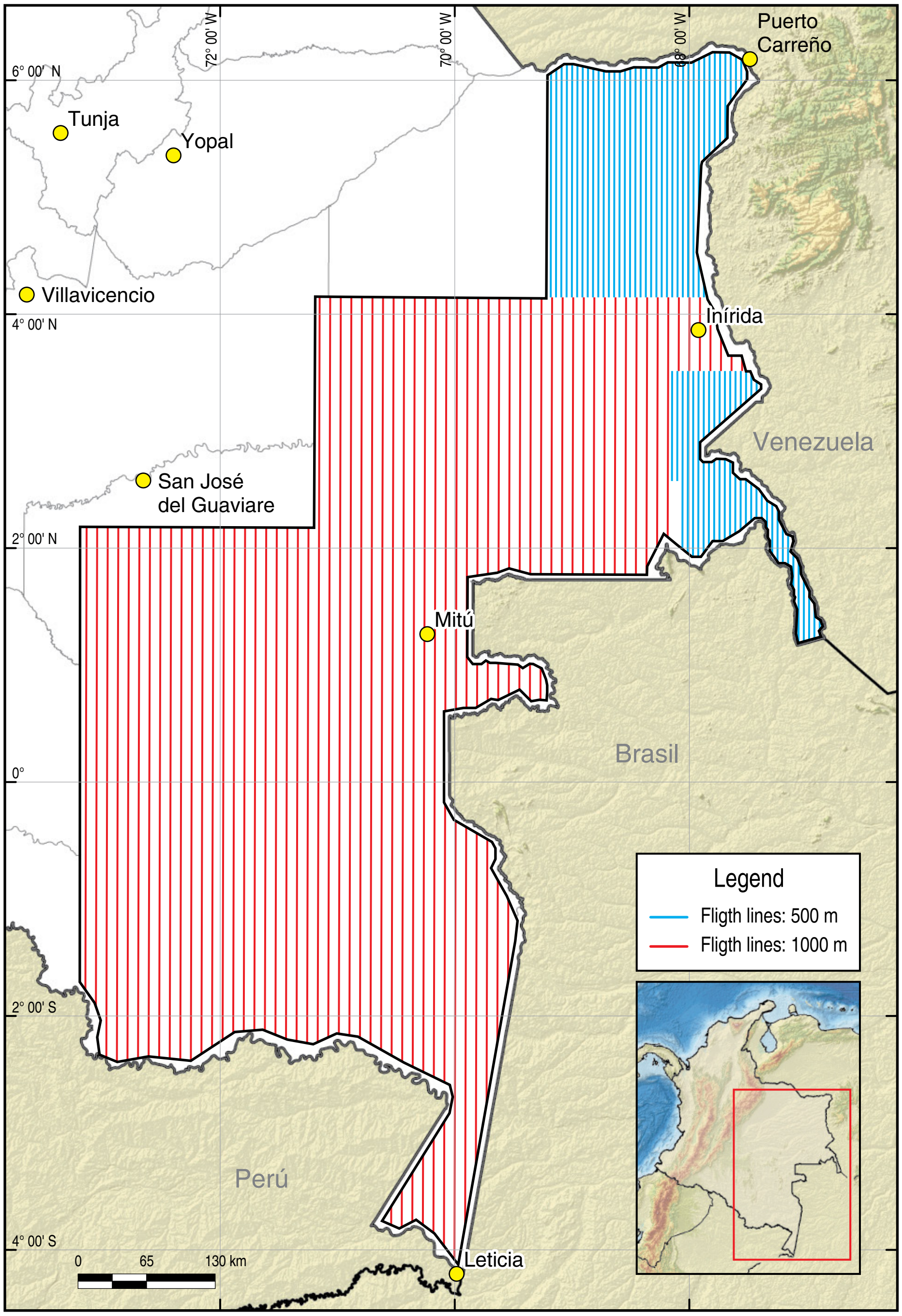

Figure 1. Location and line spacing of the airborne geophysical surveys.

the rocks of the Mitú Complex range from 2.2 Ga to 1520 Ma (Cordani et al., 2016; Tassinari et al., 1996).

The Roraima and Pedrera Formations (MP–Mvlg1 sensu Gómez et al., 2015), which were introduced by Gansser (1954), are a sequence of oligomictic conglomerates with alternating shales and ferruginous conglomerate sandstones that unconformably overlies the Mitú Complex. It has been identified in the Naquén and Caracanoa mountain ranges (Santos et al., 2003) and along the Vaupés and Guaviare Rivers (Julivert, 1968). Galvis et al. (1979) identified outcrops in the central and southeastern areas of the Guainía Department (Ingeominas, 1988). Acid subvolcanic dikes in the Roraima Formation metasedimentites have a 1496 ± 30 Ma Rb–Sr whole–rock age and an age of 1045 ± 19 Ma – 1293 ± 18 Ma K–Ar for several muscovite schists (Pinheiro et al., 1976). A maximum age of 1895 ± 15 Ma was derived from U–Pb SHRIMP dating (Santos et al., 2000).

The Parguaza Granite (MP–Pf1) is characterized as a granite with alkaline affinity (González & Pinto, 1990) that outcrops as isolated bodies in the plains in the eastern parts of the Vichada and Guainía Departments (Celada et al., 2006) and along the western margin of the Orinoco River. Numerous dikes with

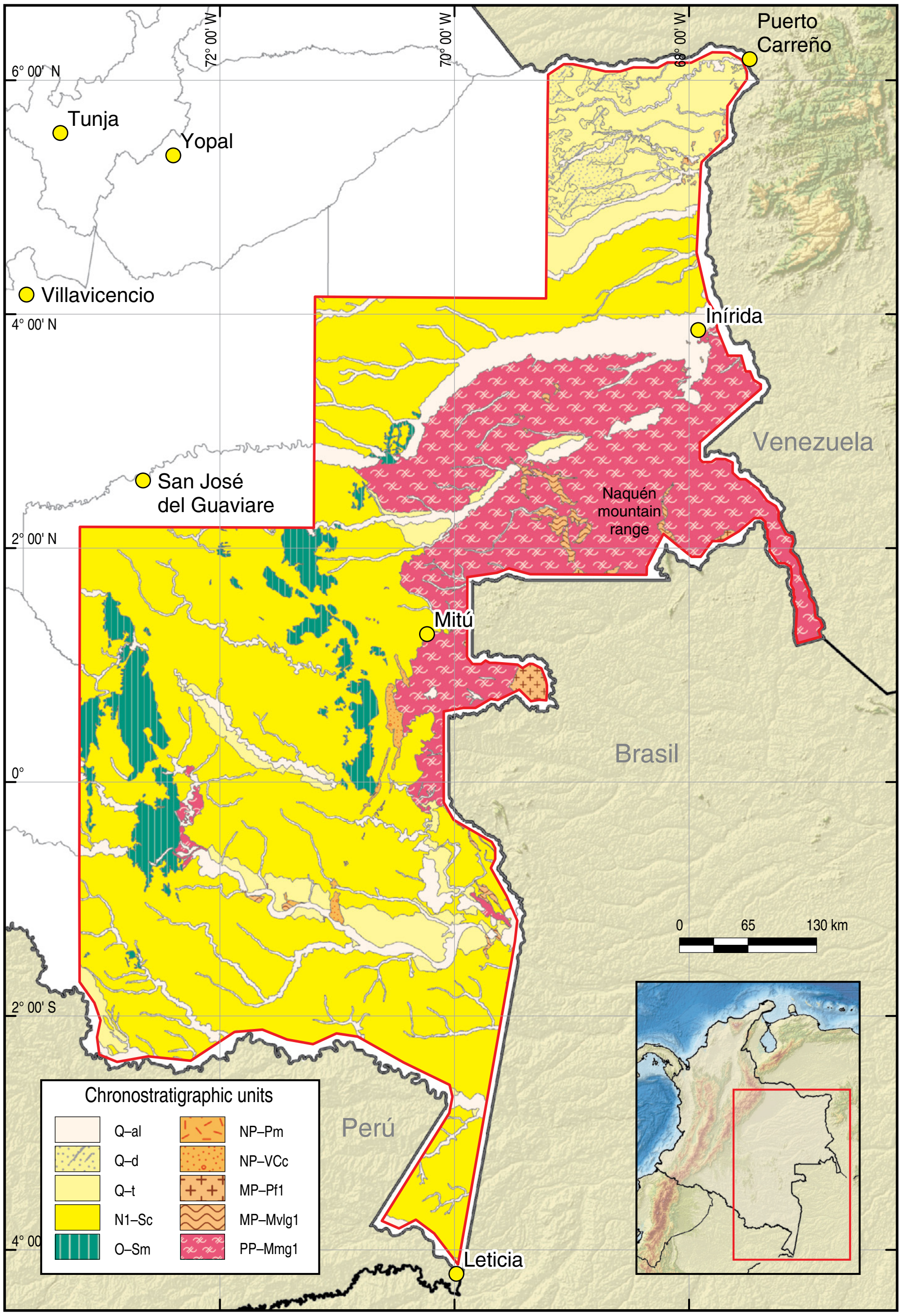

Figure 2. Geological framework of eastern Colombia (simplified from Gómez et al., 2015).

lenticular and tabular shapes, irregular bodies of microgranites, quartz and K–feldspar pegmatites, and quartz dikes intrude the Parguaza Granite (Celada et al., 2006). The geochronological data of Priem et al. (1982) suggest an age of 1575–1450 Ma for the emplacement of the Parguaza Granite (López & Cramer, 2012), whereas U–Pb ages of zircons by LA–ICP–MS give an age of 1401 ± 2 Ma (Bonilla–Pérez et al., 2013).

The Piraparaná Formation (NP–VCc) is composed of rhyodacitic lava flows toward the base with pyroclastic deposits mixed with polymictic conglomerates and arkosic sandstones that grade into quartz sandstones toward the top (Celada et al., 2006). It is represented by a folded sedimentary to metasedimentary sequence that outcrops at Yaca–Yaca on the Vaupés River and on the Piraparaná River to the south (Galvis et al., 1979). Preliminary Rb/Sr whole–rock isotopic dating results give the Piraparaná Formation an age of 1200 Ma (Priem et al., 1982).

The sedimentary rocks (O–Sm) form non–continuous plateaus that trend north–south and include a sequence of marine siltstones, shales, limonites, metasiltstones, feldspar metasandstones, and fine–grained metasandstones with marble lenses.

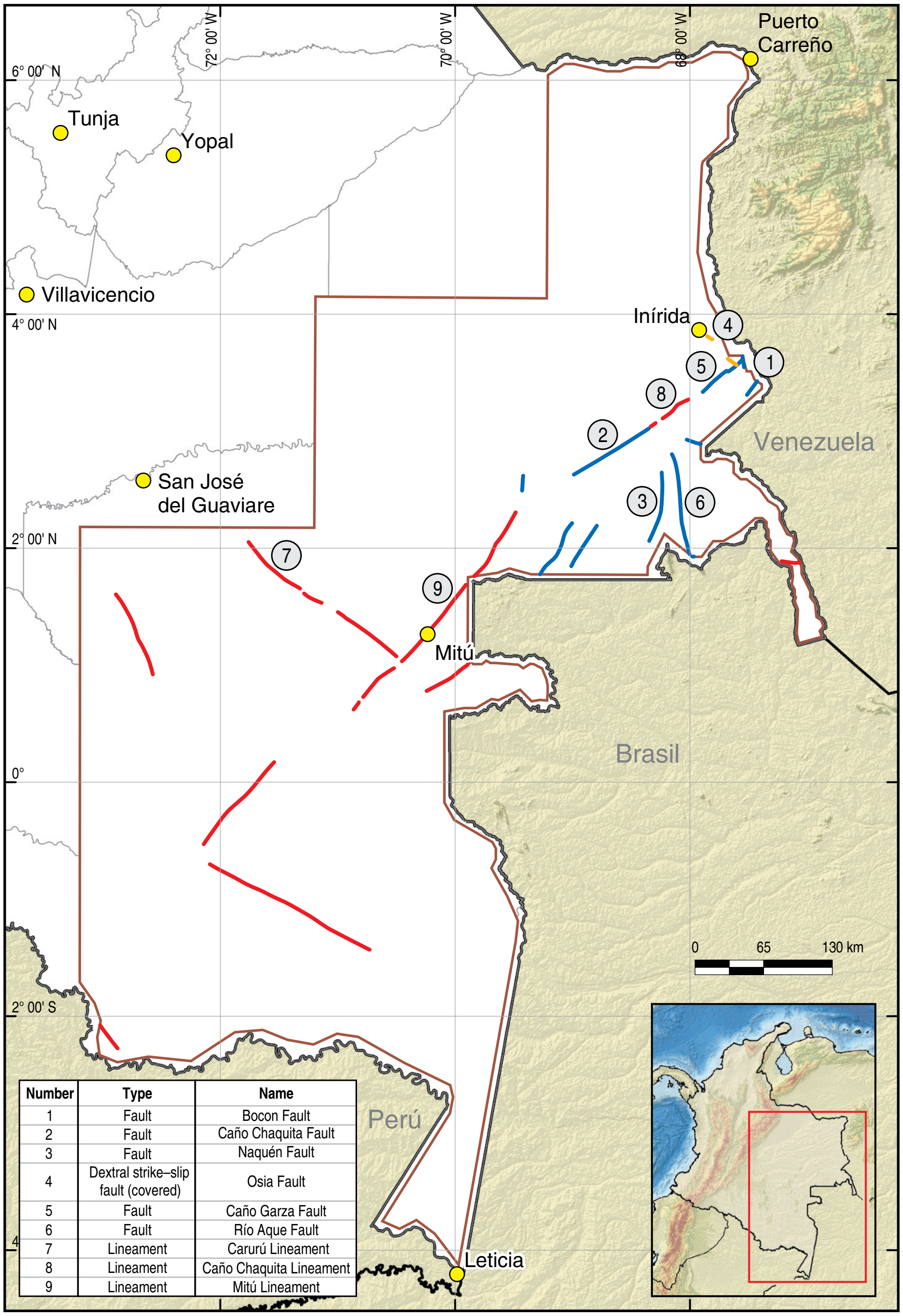

Figure 3. Structural features of the study area (simplified from Gómez et al., 2015).

Thery (1982) and Bogotá (1982) proposed an Ordovician age for this unit. Finally, several Cenozoic and Quaternary deposits (N1–Sc, Q–t, Q–d, Q–al) composed of eolian sandstones, lateritic terraces, and recent alluvial sediments cover the area.

The Quaternary deposits and dense vegetation coverage of the area make it difficult to identify structural features, but regional lineaments that affect the sedimentary cover and control the drainage can be identified in the area (Figure 3). The faults in the Naquén mountain range affect the Mitú Complex and can be related to regional structural features (Ingeominas, 1989). The Carurú Lineament (Gómez et al., 2015) strikes approximately N30°W and was described by De Boorder (1980) as a lineament drawn from scarps in the Roraima and Pedrera Formations that also controls the channels of the Inírida and Vaupés Rivers in some areas (Celada et al., 2006). To the south of this area, other lineaments that strike approximately N30°W control the upper portions of the Caquetá and Apaporis Rivers. Furthermore, a lineament that strikes N40°E between the Caquetá and Apaporis Rivers also controls portions of their channels.

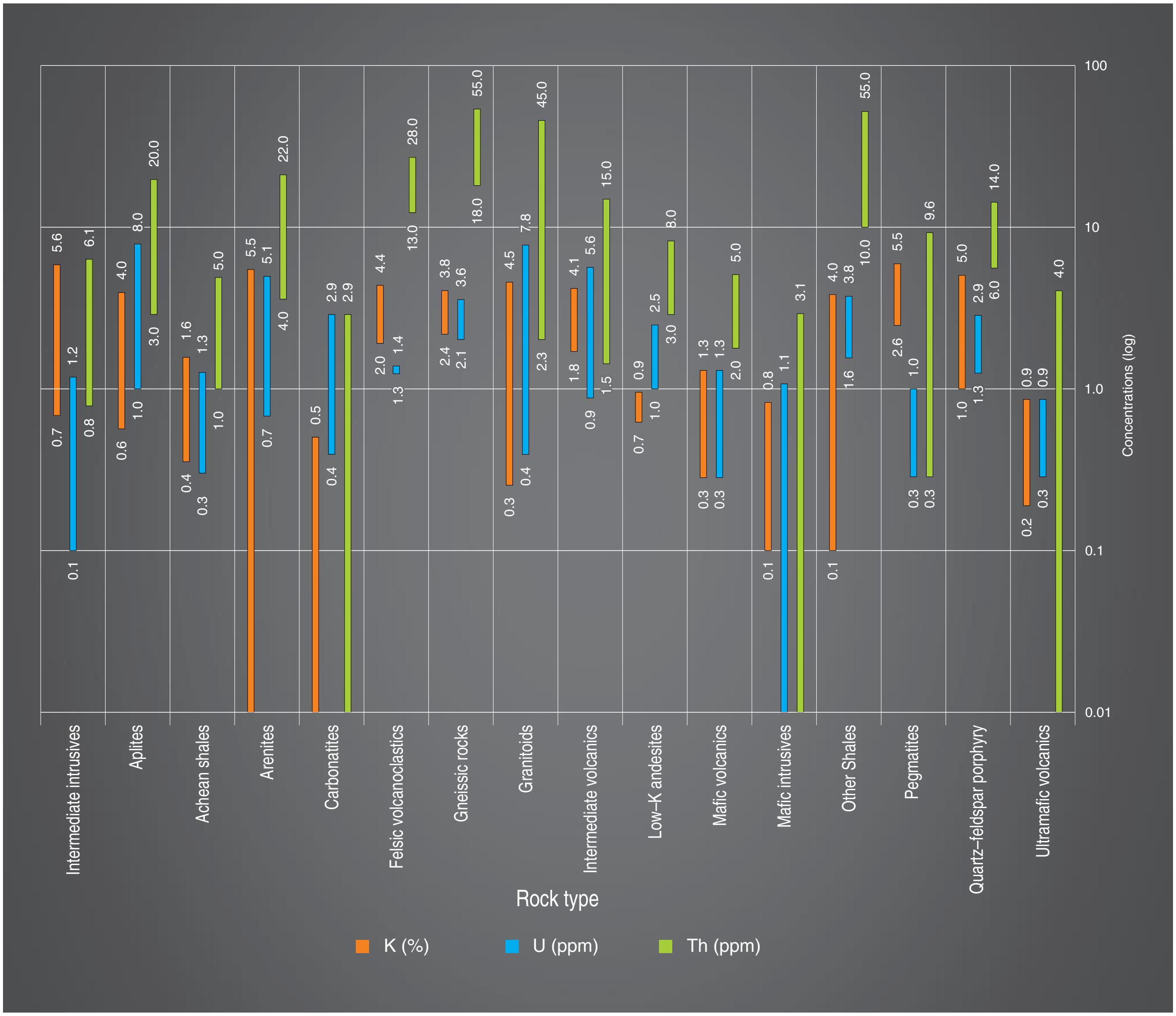

Figure 4. K, U, and Th isotope concentrations in different types of rocks (modified from Dickson & Scott, 1997).

The Mitú Fault is described by Galvis et al. (1979) as part of a fault system that strikes N40°E to N60°E (Celada et al., 2006) and was identified as a lineament by Gómez et al. (2015). Another fault of this system that affects the Mitú Complex is the Caño Chaquita Fault, which extends to the SW and may be a continuation of the Mitú Fault (Celada et al., 2006). The Naquén Fault is described by De Boorder (1980) as a fault with a dip–slip component where the rocks associated with the Roraima and Pedrera Formations are in contact with the Mitú Complex. This fault was later called the "Maimachi Fault System" by Ingeominas (1989) (Celada et al., 2006). The Río Aque Fault is located on the eastern side of the Naquén mountain range and is considered to be a fault with a dip–slip component that was reactivated from the Precambrian to the Cenozoic (Ingeominas, 1989). The Río Aque and Naquén Faults define the wedge that is composed of the Naquén mountain range (Galvis et al., 1979).

2. Geophysical Methods Used

2.1. Gamma Ray Spectrometry

Gamma ray spectrometry is a geophysical method used to measure the energy spectrum and intensity of the radiation emitted from the materials at the earth's surface. Radioactive isotopes of the elements potassium (^{40}K), uranium (^{231}U, ^{238}U, and their daughters), and thorium (^{232}Th and its daughter) are the only ones that produce sufficient intensities to be used in radiometric mapping (International Atomic Energy Agency, 1991).

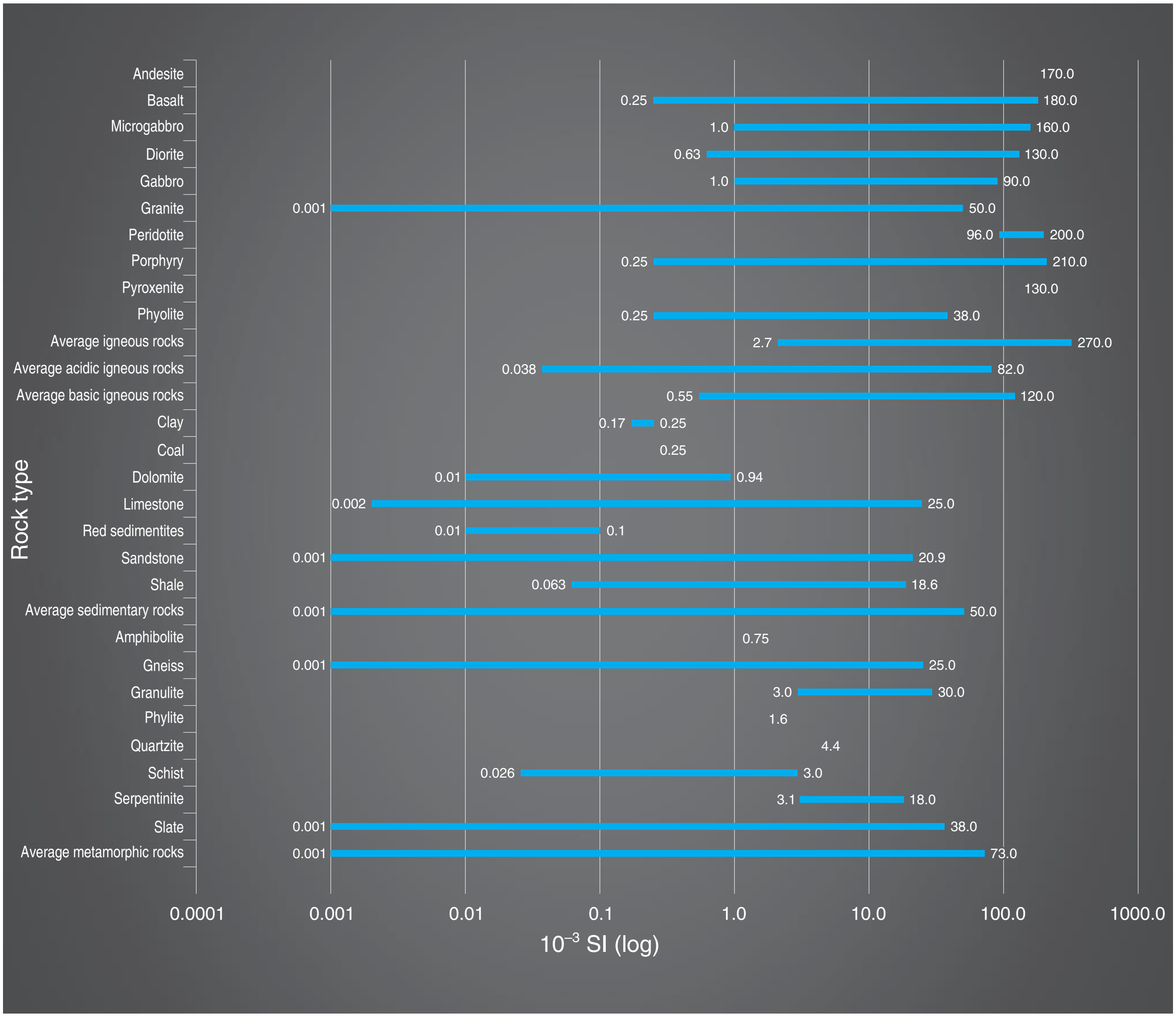

Figure 5. Magnetic susceptibilities of common rock types (modified from Hunt et al., 1995).

Gamma ray spectrometry is a passive method, which means that no external signal is necessary to generate a response from the source. Its applications include geological mapping (Nakamura, 2015; Oliveira, 2014a; Oliveira, 2014b; Silva, 2014), taking into account the variation on the concentrations of K, U, and Th isotopes according to the type of rock (Figure 4), detection of zones with hydrothermal alteration (Fueg, 2010), particularly in the identification of potassic alteration related to porphyry–type, silver and hydrothermal gold deposits and in volcanic massive sulfides (Shives et al., 1997).

The acquisition equipment includes a gamma ray spectrometer, which is composed of crystal detectors of NaI (thallium activated) that are sensitive to gamma radiation and generate pulses that pass through a photomultiplier that convert them into an electrical signal that can be counted, discriminated, and compiled into an energy spectrum (California State University, 2014). This energy corresponds to isotopes from many sources, so it is necessary to perform pre–processing to remove noise from the raw data. The reduction process involves several parameters and coefficients that must be calculated in a calibration range (International Atomic Energy Agency, 1991) using calibration pads of known K, U, Th and background concentrations and also by test lines performed before and after every data acquisition flight.

From the raw database of the counts per unit time of each element (whose energy levels are known), several corrections must be applied, including the dead time (small gaps of time when the equipment registers the number of counts and does not measure data), aircraft and cosmic radiation background removal, radon removal, Compton scattering (influence of de-

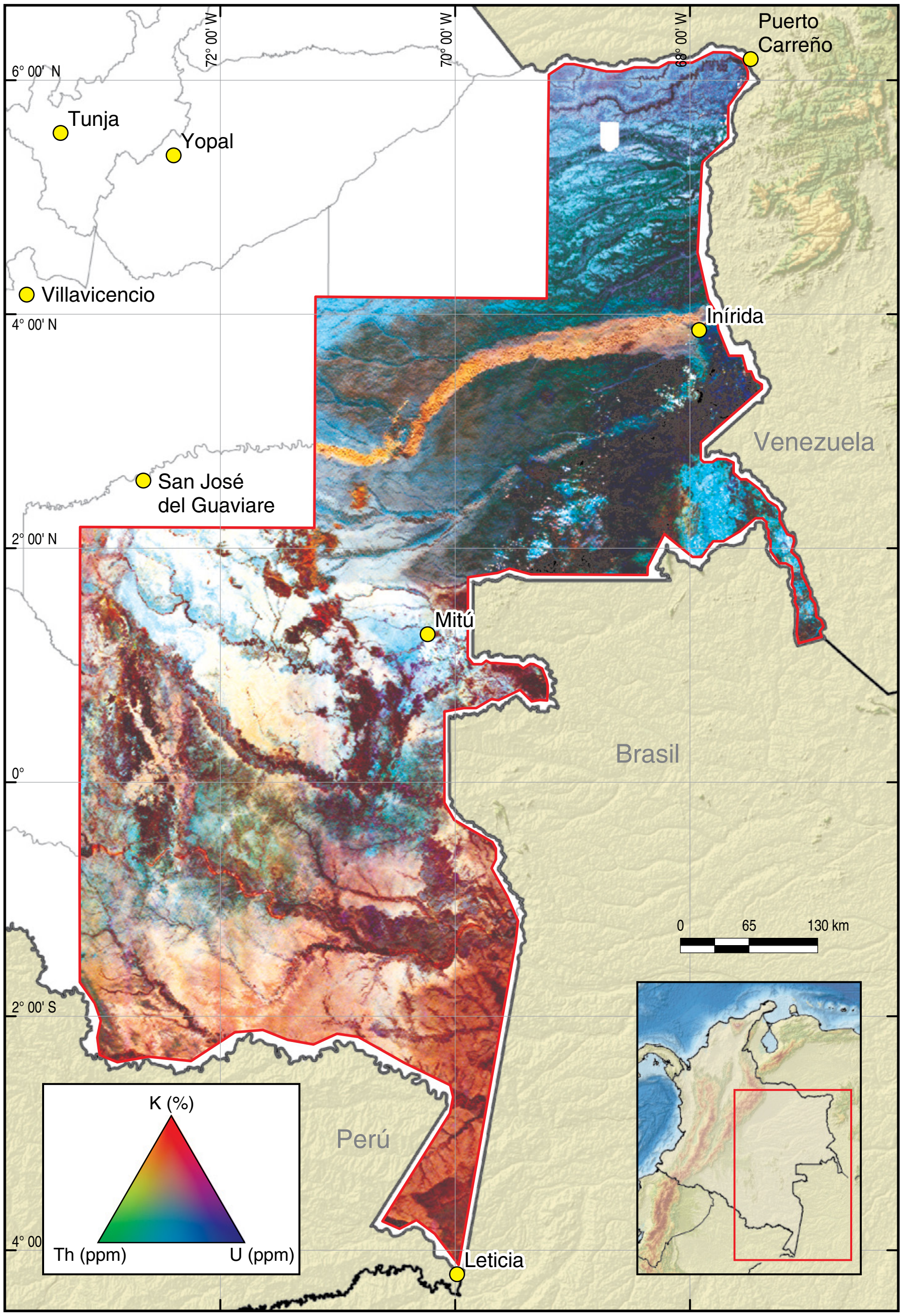

Figure 6. Radiometric ternary image (U, Th, K) of eastern Colombia (modified from Moyano et al., 2016).

caying isotopes from higher energy isotopes into lower energy isotopes), and atmospheric attenuation related to the flight height above the ground. Finally, these corrected counts per unit time are transformed into grids of the relative concentrations of K (%), U (ppm), and Th (ppm) (International Atomic Energy Agency, 2003).

2.2. Magnetometry

Magnetometry is a potential field method (Telford et al., 1990) that measures the variations of the Earth's magnetic field. The variations from the International Geomagnetic Reference Field (IGRF) (National Oceanic & Atmospheric Administration, 2018) are considered "anomalies" that are responses to changes in the magnetic properties (magnetic susceptibility) of the rocks (Figure 5) and materials of the Earth's crust. This total magnetic field anomaly (TFA) map is the basis of the processing and interpretation of magnetometry data.

The acquisition equipment for aeromagnetic surveys consists of a magnetometer that measures the intensity of the magnetic field along each flight line. Before calculating the TFA, the raw data must be compensated for and reduced from noise

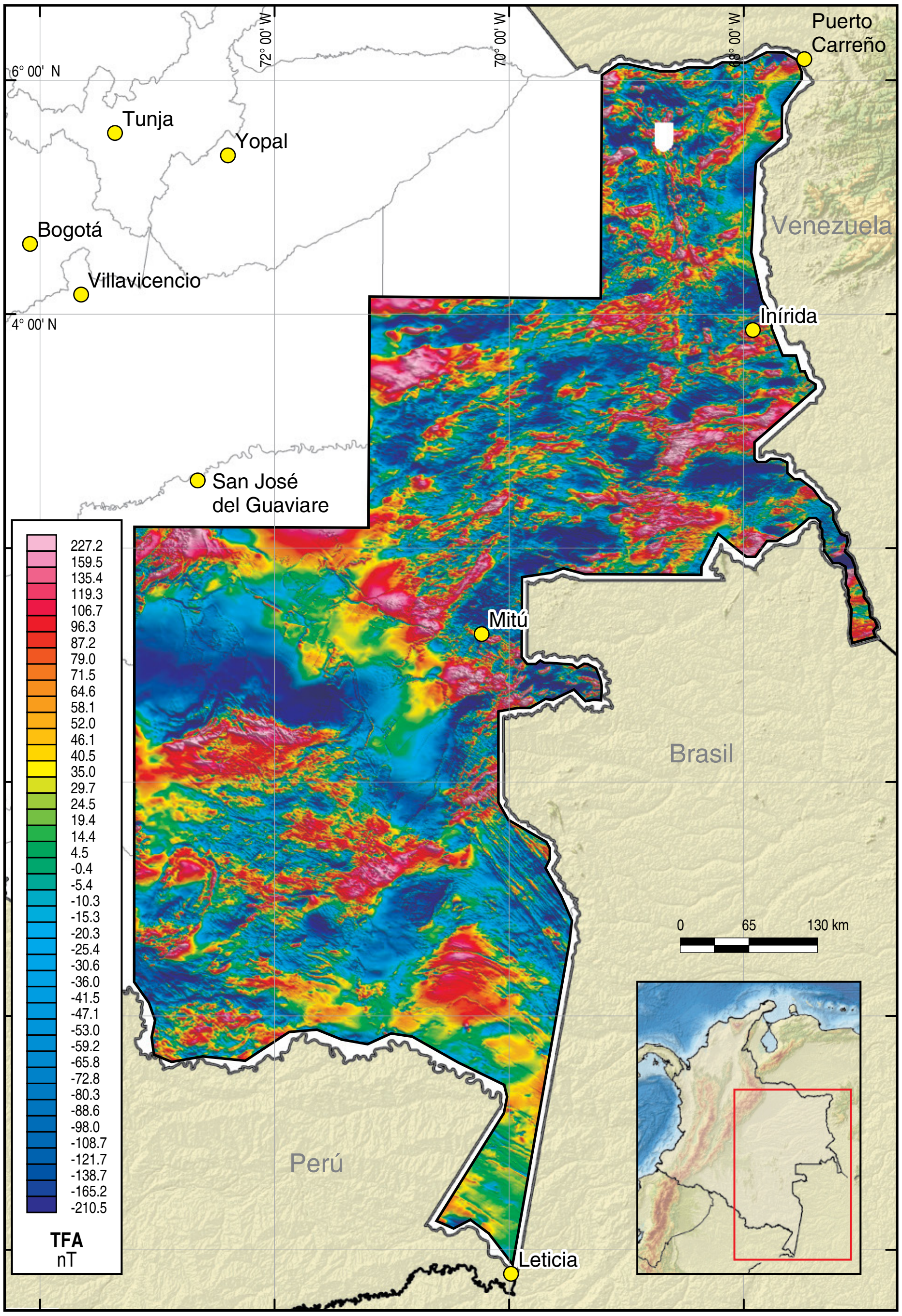

Figure 7. TFA map of eastern Colombia (modified from Moyano et al., 2016).

and variations related to the acquisition itself, including lag correction, heading, diurnal variations, levelling, and micro–levelling (Reeves, 2005). After these corrections are performed, the resulting measured magnetic field grid is subtracted from the IGRF to obtain the TFA.

Aeromagnetic surveys provide magnetic anomaly maps (Corrêa et al., 2017; Dentith & Mudge, 2014; De Sousa–Moro et al., 2018). Large areas can be mapped quickly, without interpretation bias, irrespective of surface cover and with minimal terrain restrictions (Reeves, 2005). Most importantly, the geologic and structural information that can be gleaned from aeromagnetic data (Dentith & Mudge, 2014; Reeves, 2005) make magnetometry a unique tool for earth scientists.

The main applications of magnetometry are (Table 1) geological mapping (Oliveira, 2014a; Oliveira, 2014b; Silva, 2014), delineation of geological structures (De Sousa–Moro et al., 2018; Ramos et al., 2014), studies of porphyry copper/gold deposits and related hydrothermal alteration/mineralization (Heithersay & Walshe, 1995; Jhon et al., 2010), direct searches for iron oxide copper–gold (IOCG) systems, alkaline bodies containing diamonds and iron deposits (Nannini et al., 2017), and studies on continental–scale geotectonic trends (Kronenberg & Reeves, 2011).

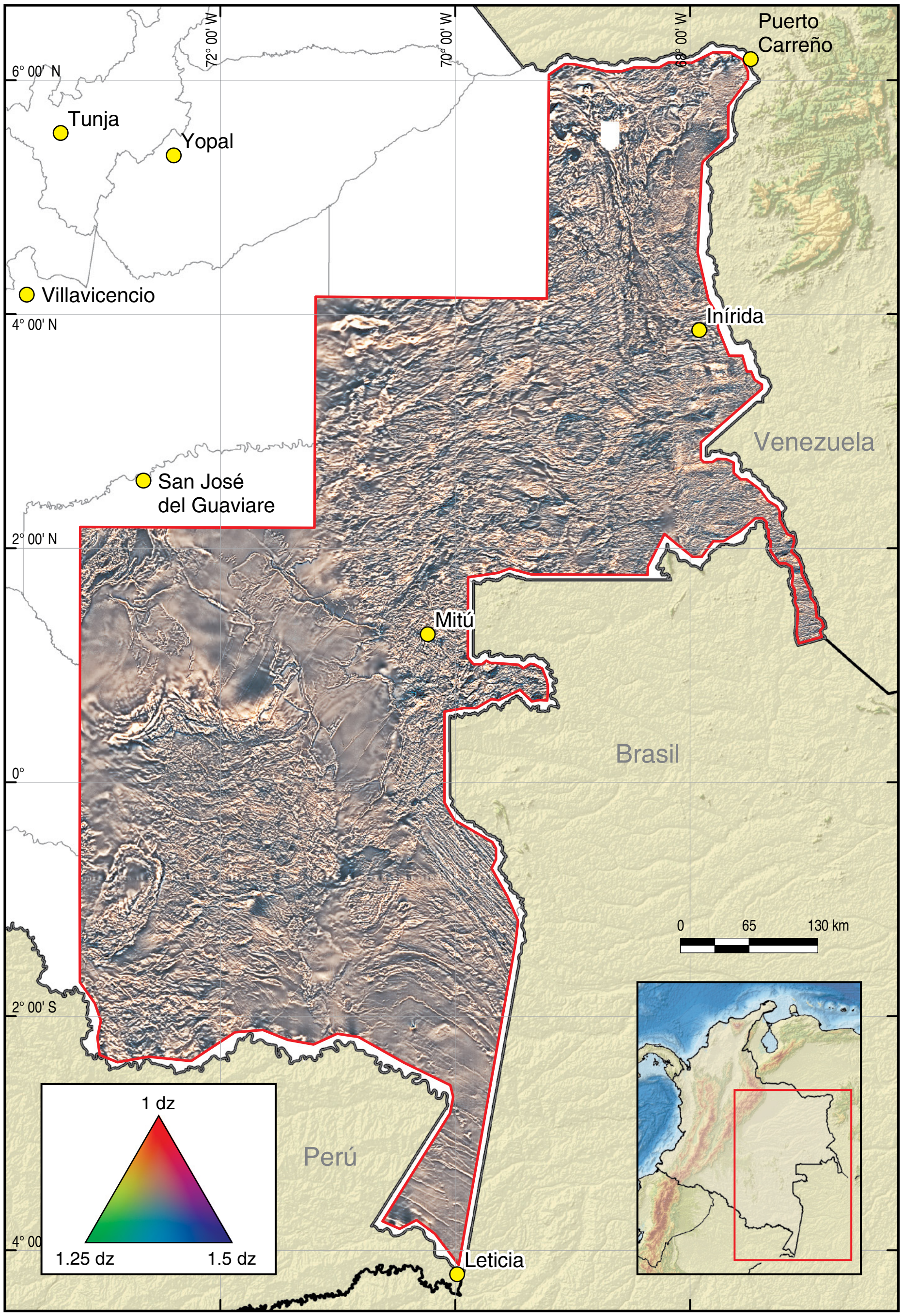

Figure 8. Ternary image of partial derivatives (1 dz, 1.25 dz, 1.5 dz) of the TFA for eastern Colombia.

3. Processing the Geophysical Datasets

The principal objective of these airborne surveys was to evaluate the potential for mineral resources in Colombia using high–resolution geophysical data processing for target selection and characterization over selected areas of the country. In addition, the acquisition of this type of broad coverage geophysical information for the first time in the history of the country provides data with a resolution that was not previously available (Graterol & Vargas, 2010a, 2010b; Kronenberg & Reeves, 2011). The data provide a tool to enhance the geological knowledge about areas of limited accessibility and dense vegetation and soil coverage, like the Amazonian region.

This gamma spectrometric and magnetometric information (Figures 6, 7) provides the Colombian government with high quality geophysical data suitable for surface geological mapping and mineral resource exploration and also for the research of the geology and evolution of the Amazonian Craton because the magnetometry method is more sensitive to the higher magnetic susceptibilities of the metamorphic and igneous rocks of

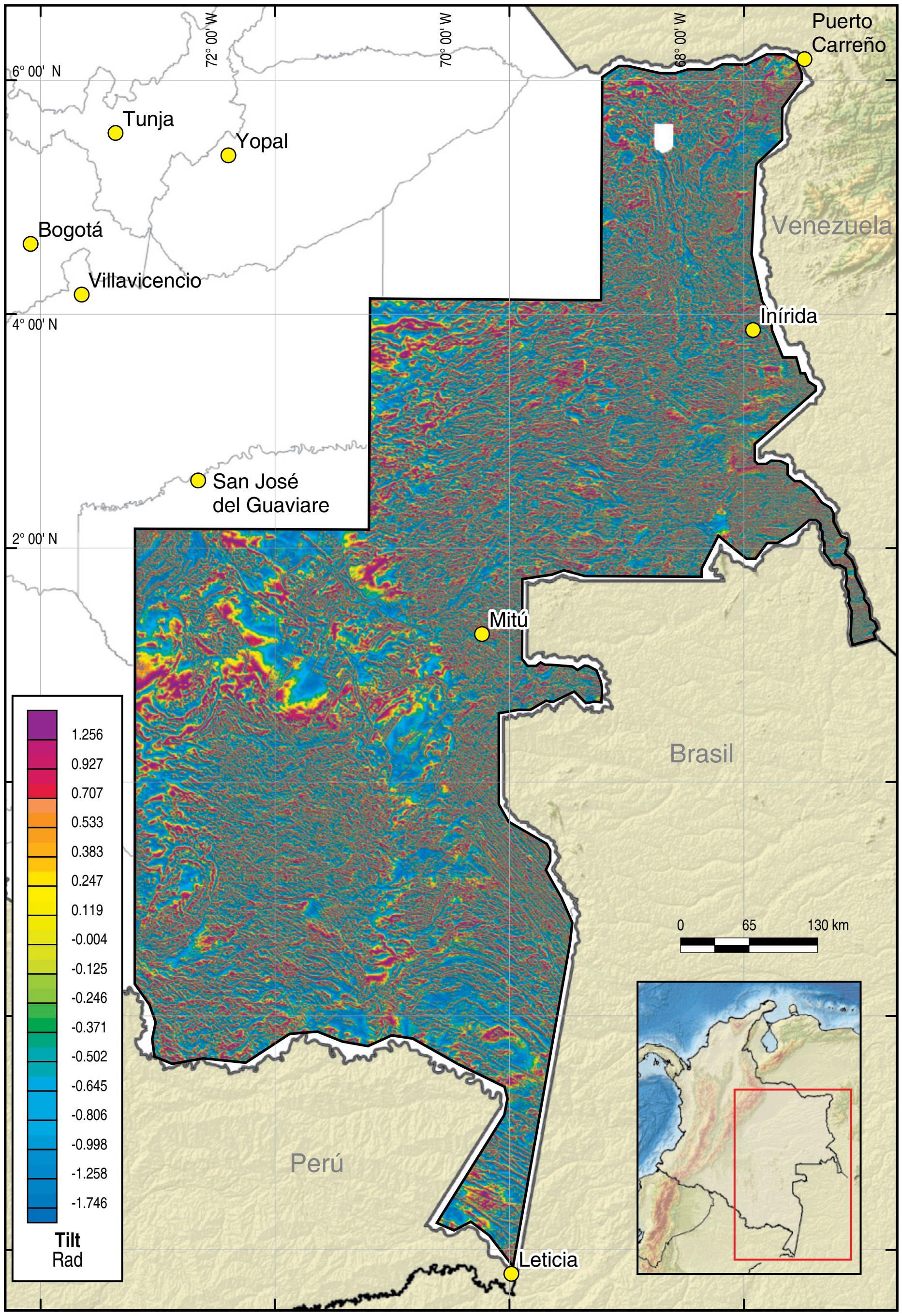

Figure 9. Tilt derivatives of the RTP (TFA) for eastern Colombia.

the basement than to the low–magnetic susceptibility of the sedimentary rocks and soil in the study area (Graterol, 2006, 2009; Graterol & Vargas 2007).

A procedure was developed to process the airborne geophysical data to generate information that will help geoscientists increase the geological knowledge and to select areas of interest for mineral resource exploration over remote areas. The steps of this procedure are:

- Construct a ternary image (International Atomic Energy Agency, 2003) that represents the surface distribution of radioactive isotopes over the survey area as a combination of the relative concentrations of K (red), Th (green), and U (blue). Qualitative regional to semi–detailed litho–geophysical maps can be constructed that show different radiometric domains based on the variability on the proportions of the three isotopes, which provide information to improve the geological cartography (Dentith & Mudge, 2014; Ford et al., 2008; International Atomic Energy Agency, 2003; Martelet et al., 2006; Minty, 1997; Oliveira, 2014a; Oliveira 2014b; Ramos et al., 2014) as shown in Figure 6.

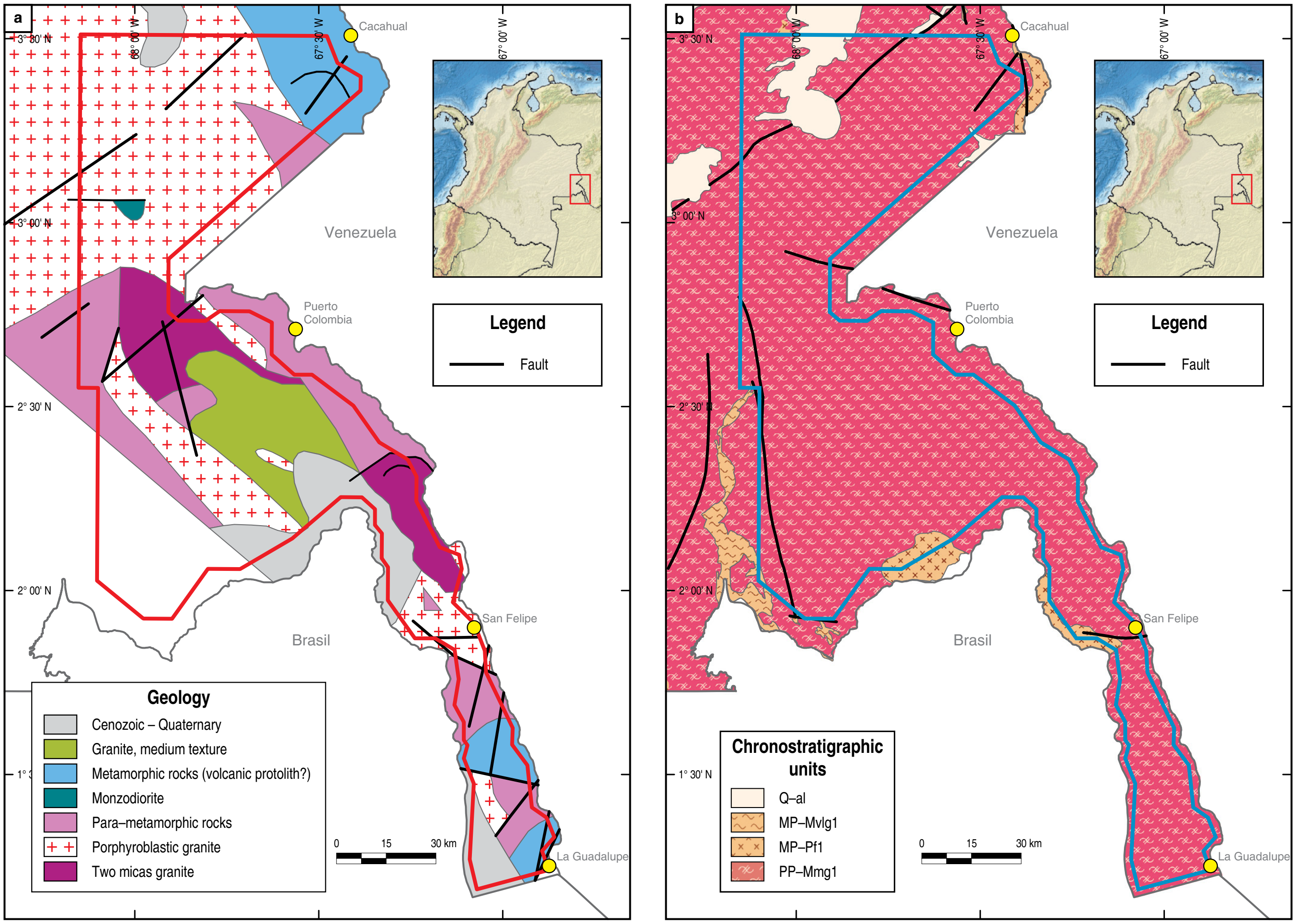

Figure 10. Regional geology of the study area. **(a)** Modified from Bruneton et al. (1982). **(b)** Simplified from Gómez et al. (2015).

- Calculate the vertical derivatives (1 dz, 1.25 dz, and 1.50 dz) of the TFA (Dentith & Mudge, 2014) and display it on a ternary image (Figure 8). This representation provides a coverage suitable for delineating magnetic domains (Dentith & Mudge, 2014) because it enhances the high frequency attributes of the magnetometric data and their lateral variations, which allows the interpreter to separate different textures that could be related to variations in the magnetic susceptibility of the basement rocks and hence to possibly discriminate different lithologies.
- Calculate the tilt angle derivative (Salem et al., 2015) and display it on a grid (Figure 9). The tilt image results from the arctangent of the vertical derivative divided by the total horizontal derivatives (x, y) of the reduction to magnetic pole (RTP) (Baranov & Naudy, 1964) of the TFA. Tilt derivative calculation provides an image that enhances the borders and linear features of magnetic data that are useful for identifying magnetic lineaments of geological interest, such as fractures, faults, and dikes (Curto et al., 2013; Fairhead et al., 2004).

4. Results

To illustrate the potential of the geophysical data and the interpretation procedure for geological interpretation, an area of the Guainía Department near the Venezuela and Brasil border was selected due to the regional geology (Bruneton et al., 1982, Celada et al., 2006; López et al., 2007; López & Cramer, 2012; Gómez et al., 2015), which can be correlated with the geophysical features to extend the geological/geophysical interpretation (Figure 10).

Figure 11 shows the ternary image of the gamma spectrometric data for the east Guainía area. The northern part of this area contains low values of the relative concentrations of radioactive elements (domain 3; see Figure 11b), which are reflected by the darker colors on the ternary image (Figure 11a). In the central and southern parts of the area, the relative concentrations of the radioactive elements increase (light colors; see Figure 11a). From these gamma spectrometric domains, it is possible to differentiate a group of domains with relatively high counts of radioactive isotopes (e.g., 1, 4, 6, 7, 10; see Figure 11b) and others with lower radioactive element contents (e.g., 3, 8, 9;

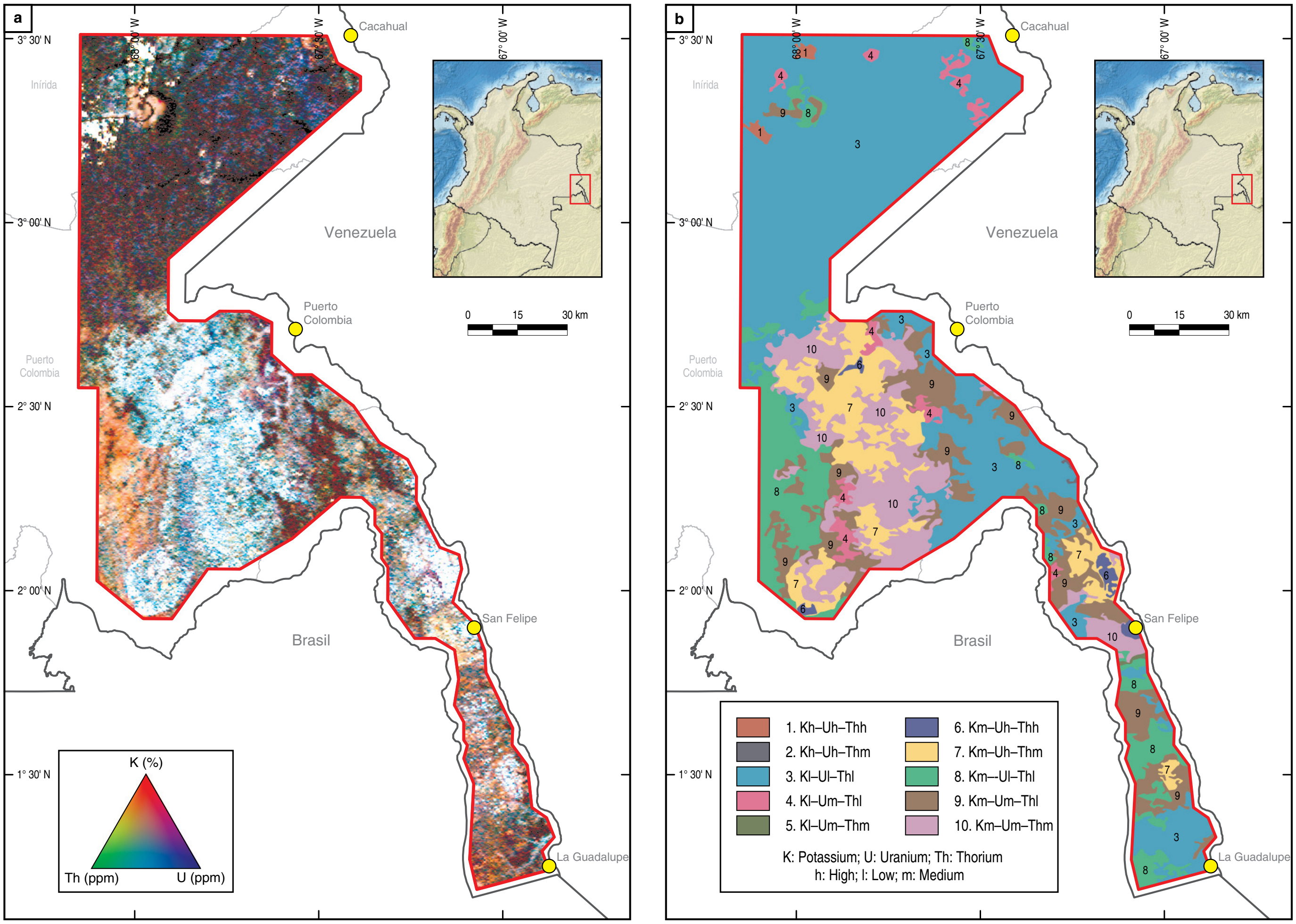

Figure 11. (a) Ternary gamma spectrometric image of the Guainía area. **(b)** Delineated radiometric domains of the Guainía area.

see Figure 11b). A comparison with the geological information (Figure 10a; Bruneton et al., 1982) shows a correlation between the groups with high radioisotope contents and areas with more igneous rocks and between the groups with lower radioisotopes contents and areas with more metamorphic lithologies.

Figure 12 shows the ternary image for the magnetometry data. The qualitative contrasts in the texture and intensity of the magnetic responses over the area indicate several magnetic domains (Figure 12b) that can be grouped into high magnetic responses (e.g., 1, 2; see Figure 12b) and low magnetic responses (e.g., 3, 4; see Figure12b). Based on the average magnetic susceptibilities of common rock types (Figure 5), the magnetic response of igneous rocks will be higher than that of metamorphic rocks. Furthermore, a comparison of the magnetic domains with the available geological information (Bruneton et al., 1982) shows an association between high to medium magnetic domains and igneous lithologies and between low to medium magnetic domains and metamorphic lithologies.

The magnetic lineaments extracted from the tilt derivative image (Figure 13b) show three different patterns. The first includes N50°E to N60°E lineaments that affect the structure at a large scale and are parallel to the Caño Chaquita Lineament to the north of the study area and that were also identified in Brasil to the south (Almeida et al., 2004). The N50°E lineaments are closely related to another group of major lineaments that strike N40°W to form a nearly orthogonal family that is present over the entire area. Several dike– or pegmatite–like lineaments along the southeastern border of the Guainía Department are similar to the N40°W trends (Figure 13). Finally, an incipient pattern with trends of N10°E to N15°E was delineated from the magnetic and radiometric images (Figure 14).

5. Discussion

Based on the available geological data, in the eastern part of the Guainía region, approximately 80% of the total area corresponds to granitoids (Bruneton et al., 1982). The area also contains metamorphic rocks of high amphibolite facies, such as orthogneisses and paragneisses with high potassium contents due to metasomatism (Bruneton et al., 1982; Galvis et al., 1979). However, the absence of outcrops in the region did not allow the boundaries between the granitoids and the metamorphic rocks to be estab-

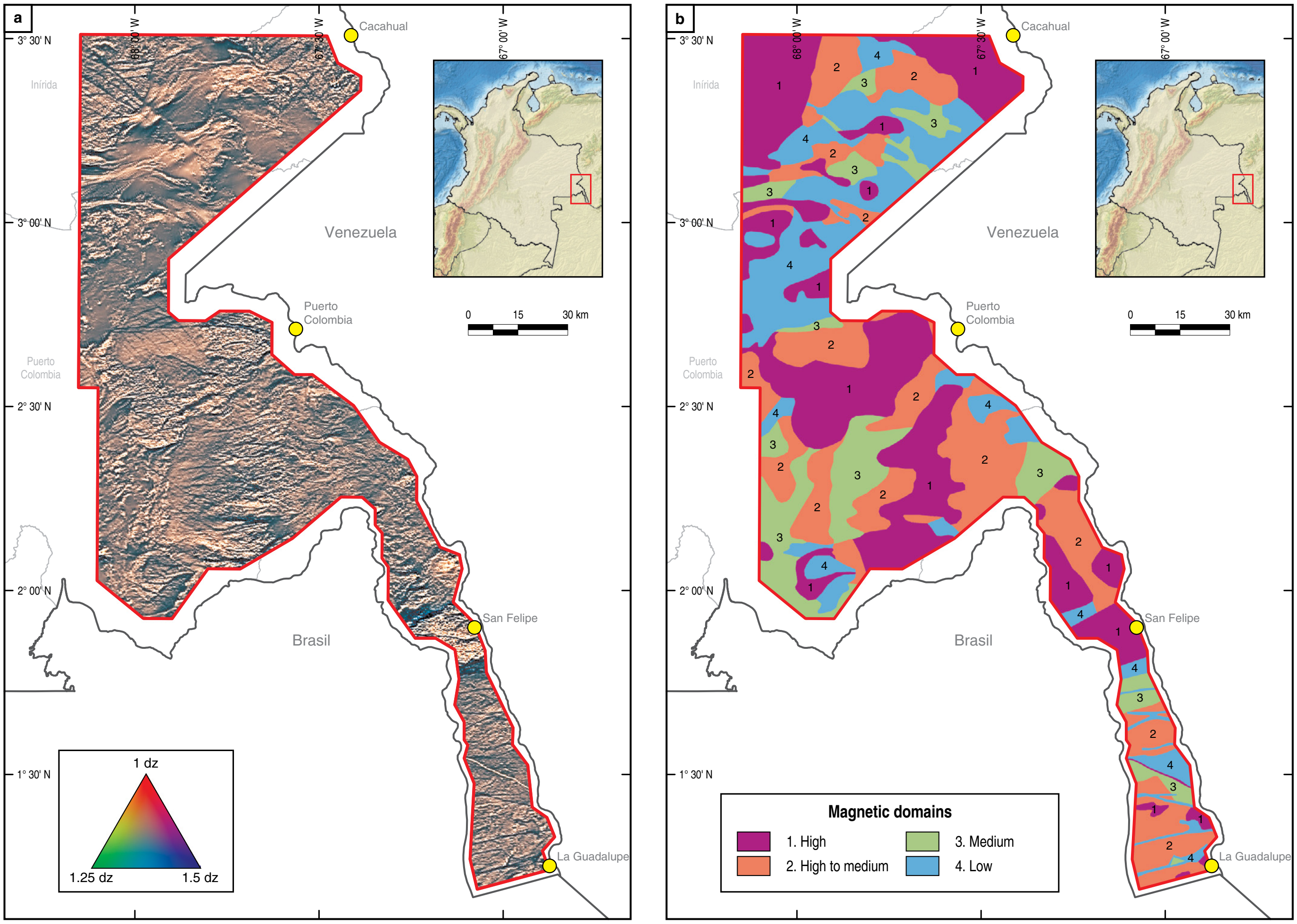

Figure 12. (a) Ternary image of the magnetic derivatives for the Guainía area. **(b)** Delineated magnetometric domains for the Guainía area.

lished accurately. For this reason, the geological mapping can be improved by the use of the geophysical domains and lineaments obtained in this study, which were interpreted as variations in the physical properties of the different types of rocks identified in the area. Using the new geophysical data, the magnetic and radiometric domains, and magnetic lineaments defined here are linked with some of the lithologies of the Mitú Complex, Parguaza Granite, and other igneous rocks (Figure 14).

The geophysical signatures of the localities in which Parguaza–type granitoids have been described include polygonal areas with low magnetism and sharp magnetic borders. In addition, relatively high K, Th, and U contents (Figure 4) are commonly related to this type of granitoid. Consequently, low magnetic and high gamma spectrometric domains with these polygonal shapes were mapped in the southwestern Guainía area as Parguaza–type granitoids (Figure 14).

The San Felipe–type porphyroblast granite and the biotite granite, mapped by Bruneton et al. (1982) as porphyroblastic granite and two micas granite, respectively (Figure 10a), are correlated with high magnetic responses (Figure 12a), medium K contents and medium to high Th–U contents (Figure 11a). For that reason, the geophysical domains with the same characteristics were mapped as San Felipe–type and biotite granites. For example, in the northern part of the study area, several highly magnetic bodies are associated with biotite granites, although they do not have the same gamma signature. Also in the north, an intrusive body was mapped based on its circular shape, high K content, and high magnetic response.

Several low magnetic responses with low to medium K–U contents and low Th contents are correlated with metamorphic rocks mapped by Bruneton et al. (1982). These metamorphic rocks continue into Brasil as the "Complexo Cumati, Fácies Tonu" (Almeida et al., 2004) as a sequence of locally migmatitic biotite orthogneisses. These rock types also contain magnetic lineaments (Figure 13) with prevalent E–W and N70°E–N80°E strikes, which could be related to foliations and/or fractures that also bend in some locations.

6. Conclusions

The Servicio Geológico Colombiano, in collaboration with external experts from the World Bank, designed an airborne

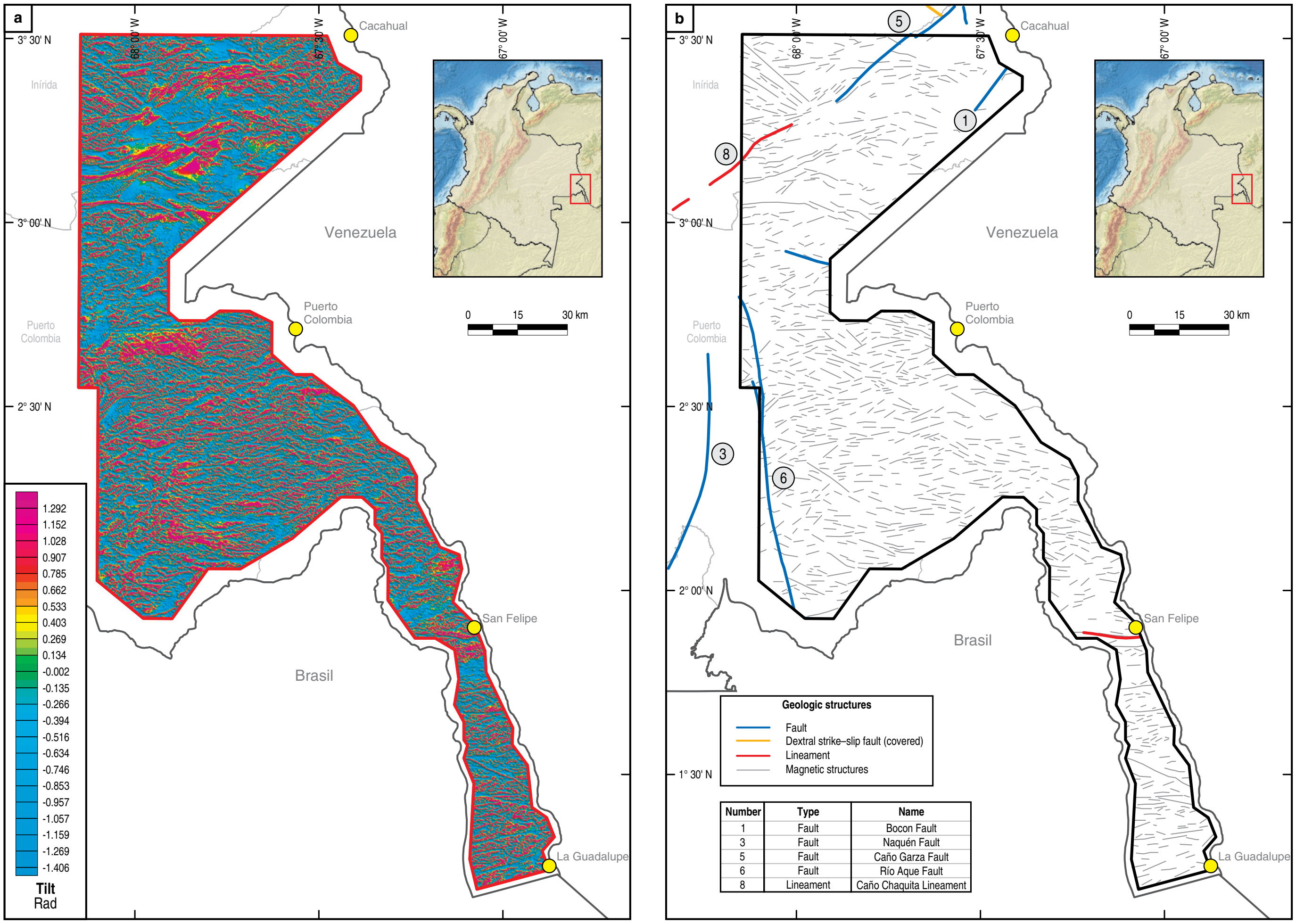

Figure 13. (a) Tilt derivatives of the RTP of the TFA. **(b)** Delineated magnetic lineaments and geological structures.

magnetometry and gamma spectrometry data acquisition survey to collect multi–purpose geophysical data to evaluate the mineral resource potential of the country and to increase the geoscientific knowledge of remote areas like the Amazonian region. For this purpose, a methodology for processing geophysical information to generate datasets and images with an emphasis on geological mapping was presented.

To illustrate the applicability of the methodology, the procedure was applied to an area in the Guainía Department. The geophysical domains and lineaments were compared and integrated with the available geological information, which allowed these domains to be classified into geological units and also allowed new units with similar geophysical signatures to be delineated. All of these data were incorporated into a litho–geophysical map of the study area (Figure 14).

The lineaments and faults identified on the available geological maps were also identified in the magnetic images. For example, the Caño Chaquita Lineament and the lineament near the town of San Felipe are clearly identifiable in the tilt derivative image and the ternary diagram of the derivatives. The Río Aque Fault is also easily recognizable to the southwest of the study area. In addition, several other linear features share the same orientation with lineaments mapped in Brasil.

This example demonstrates that this methodology of interpreting gamma spectrometric and magnetometric data is a good complement for early stage geological mapping in remote areas like the Amazonian region, where the collection of regional scale cartography will require several decades. Using the data collected in this survey, costs and time can be optimized by distinguishing prominent control localities to identify and map geological contacts and structural elements, which will have a significant effect on further mapping.

Acknowledgments

The authors would like to thank the Servicio Geológico Colombiano for allowing the use of the geophysical data from ongoing contracts and for the time to write this paper.

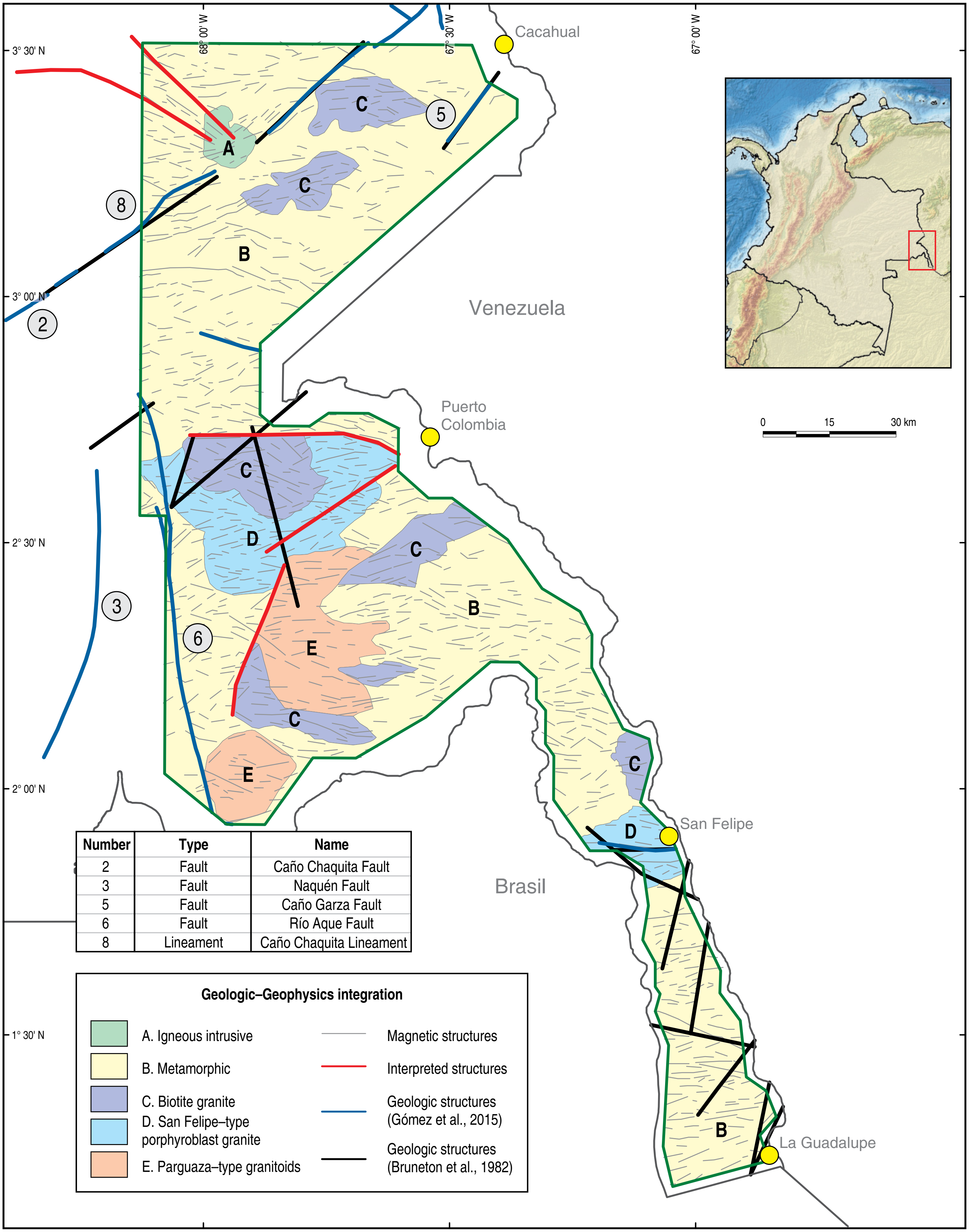

Figure 14. Map showing the integration of geophysical and geological information of the Guainía area.

References

Almeida, M.E., Luzardo, R., Pinheiro, S.S. & Oliveira, M.A. 2004. Folha NA.19–Pico da Neblina. Scale 1:1 000 000. In: Schobbenhaus, C., Gonçalves, J.H., Santos, J.O.S., Abram, M.B., Leão–Neto, R., Matos, G.M.M., Vidotti, R.M., Ramos, M.A.B. & De Jesus, J.D.A. (editors), Carta geológica do Brasil ao milionésimo, Sistemas de Informações Geográficas–SIG. Programa Geologia do Brasil, Companhia de Pesquisa de Recursos Minerais–Serviço Geológico do Brasil. Brasília.

Baranov, V. & Naudy, H. 1964. Numerical calculation of the formula of reduction to the magnetic pole. Geophysics, 29(1): 67–79.

Bogotá, J. 1982. Estratigrafía del Paleozoico inferior en el área amazónica de Colombia. Geología Norandina, (6): 29–38.

Bonilla–Pérez, A., Frantz, J.C., Charão–Marques, J., Cramer, T., Franco–Victoria, J.A., Mulocher, E. & Amaya–Perea, Z. 2013. Petrografía, geoquímica y geocronología del Granito de Parguaza en Colombia. Boletín de Geología, 35(2): 83–104.

Bruneton, P., Pallard, B., Duselier, D., Varney, E., Bogotá, J., Rodríguez, C. & Martín, E. 1982. Contribución a la geología del oriente de las comisarías del Vichada y del Guainía (Colombia). Geología Norandina, (6): 3–12.

California State University. 2014. Gamma ray spectroscopy using a NaI (Ti). Scintillation Counter, 3 p. Stanislaus, USA.

Celada, C.M., Garzón, M., Gómez, E., Khurama, S., López, J.A., Mora, M., Navas, O., Pérez, R., Vargas, O. & Westerhof, A.B. 2006. Potencial de recursos minerales en el oriente colombiano: Compilación y análisis de la información geológica disponible (fase 0). Servicio Geológico Colombiano, unpublished report, 165 p. Bogotá.

Cordani, U.G., Sato, K., Sproessner, W. & Santos–Fernandes, F. 2016. U–Pb zircon ages of rocks from the Amazonas territory of Colombia and their bearing on the tectonic history of the NW sector of the Amazonian Craton. Brazilian Journal of Geology, 46(1): 5–35. https://doi.org/10.1590/2317-4889201620150012

Corrêa, J.W., Corrêa, J.W. & Bokelmann, G. 2017. Lateral variation of crustal properties from aerogeophysical data in northern Brazil. Geophysics, 82(5): J39–J60. https://doi.org/10.1190/geo2016-0206.1

Curto, J.B., Vidotti, R.M., Fuck, R.A., Blakely, R.J., Alvarenga, C.J. & Dantas, E.L. 2013. Unveiling the Transbrasiliano Fault System in northern Paraná Basin using airborne magnetic data. 13th International Congress of the Brazilian Geophysical Society and EXPOGEF. Proceedings, p. 452–456. Rio de Janeiro, Brazil. https://doi.org/10.1190/sbgf2013-095

De Boorder, H. 1980. Contribución preliminar al estudio de la estructura geológica de la Amazonia colombiana. Revista CIAF, 5(1): 49–96.

Dentith, M. & Mudge, S. 2014. Geophysics for the mineral exploration geoscientist. Cambridge University Press, 454 p. New York.

De Sousa–Moro, P., Vidoti, R.M. & Dantas, E.L. 2018. Structural framework from gravity and magnetic data in the Paleo/Mesoproterozoic Araí rift–sag Basin, central Brazil. Geophysics, 83(4): B195–B207. https://doi.org/10.1190/geo2017-0627.1

Dickson, B.L. & Scott, K.M. 1997. Interpretation of aerial gamma–ray surveys–adding the geochemical factors. AGSO Journal of Australian Geology & Geophysics, 17(2): 187–200.

Dods, S.D., Teskey, D.J. & Hood, P.J. 1989. Magnetic anomaly map of Canada. Canadian geophysical atlas, map 11. Scale 1:10 000 000. Geological Survey of Canada. Ottawa.

Fairhead, J.D., Mackenzie, C., Green, C.M & Verduzco, B. 2004. A new set of magnetic field derivatives for mapping mineral prospects. 17th Geophysical Conference and Exhibition. Australian Society of Exploration Geophysicists Extended Abstracts, 2004(1), p.1–4. https://doi.org/10.1071/ASEG2004ab042

Ford, K., Harris, J.R, Shives, R., Carson, J. & Buckle, J. 2008. Remote predictive mapping 2. Gamma–ray spectrometry: A tool for mapping Canada's north. Geoscience Canada, 35(3–4): 109–126.

Fueg, J. 2010. The airborne geophysical survey of the Greens Creek area. In: Taylor, C.D. & Johnson, C.A. (editors), Geology, geochemistry, and genesis of the Greens Creek massive sulfide deposit, Admiralty Island, Southeastern Alaska. U.S. Geological Survey, Professional Paper 1763, p. 109–121. Reston, USA.

Galvis, J., Huguett, A. & Ruge, P. 1979. Geología de la Amazonia colombiana. Boletín Geológico, 22(3): 3–86.

Gansser, A. 1954. The Guiana Shield (South America): Geological observations. Ecologae Geologicae Helvetiae, 47(1): 77–112.

Geological Survey of Ireland. 2017. Tellus A3 & A4 airborne. Geological Survey of Ireland, geophysical technical report, 89 p.

Gómez, J., Montes, N.E., Nivia, Á. & Diederix, H., compilers. 2015. Geological Map of Colombia 2015. Scale 1:1 000 000. Servicio Geológico Colombiano, 2 sheets. Bogotá. https://doi.org/10.32685/10.143.2015.936

González, C.F. & Pinto, H. 1990. Petrografía del Granito de Parguaza y otras rocas precámbricas en el oriente de Colombia. Geología Colombiana, 17: 107–121.

Graterol, V. 2006. Programa aerogravimétrico y aeromagnético de la Cuenca del Yarí–Caguán, Colombia. Contrato No. 2052332. Agencia Nacional de Hidrocarburos, informe final de interpretación, 50 p. Bogotá.

Graterol, V. 2009. Levantamiento aerogravimétrico y aeromagnético de los sectores norte y oriental de la Cuenca de los Llanos Orientales, Colombia: Contrato n.° 034. Agencia Nacional de Hidrocarburos, informe final de interpretación, 51 p. Bogotá.

Graterol, V. & Vargas, A. 2007. Levantamiento aerogravimétrico y aeromagnético de la Cuenca de los Llanos Orientales, Colombia: Contrato n.° 036–2007. Agencia Nacional de Hidrocarburos, informe final de interpretación, 48 p. Bogotá.

Graterol, V. & Vargas, A. 2010a. Mapa de anomalía de intensidad magnética total (IMT) de la República de Colombia. Scale 1:2 500 000. Agencia Nacional de Hidrocarburos. Bogotá.

Graterol, V. & Vargas, A. 2010b. Mapa de anomalía de intensidad magnética total reducida al polo (IMTRP) de la República de Colombia. Scale 1:2 500 000. Agencia Nacional de Hidrocarburos. Bogotá.

Heithersay, P. & Walshe, J. 1995. Endeavour 26 north: A porphyry copper–gold deposit in the Late Ordovician, Shoshonitic Goonumbla Volcanic Complex, New South Wales, Australia. Economic Geology, 90(6): 1506–1532. http://dx.doi.org/10.2113/gsecongeo.90.6.1506

Hunt, C.P., Moskowitz, B.M. & Banerjee, S.K. 1995. Magnetic properties of rocks and minerals. In: Ahrens, T.J. (editor), Rock physics and phase relations: A handbook of physical constants, AGU reference shelf series 3. American Geophysical Union, p. 189–204. Washington D.C.

Ingeominas. 1988. Memoria explicativa: Mapa geológico de Colombia. Scale 1:1 500 000, p. 1–71. Bogotá.

Ingeominas. 1989. Exploración geológica preliminar de la serranía de Naquén, comisaria del Guainía. Ingeominas, unpublished report, 112 p. Bogotá.

International Atomic Energy Agency. 1991. Airborne gamma ray spectrometer surveying. Technical report series N° 323, 116 p. Vienna, Austria.

International Atomic Energy Agency. 2003. Guidelines for radioelement mapping using gamma ray spectrometry data. Technical report series N° 1363, 179 p. Vienna, Austria.

Jhon, D.A., Ayuso, R.A., Barton, M.D., Blakely, R.J., Bodnar, R.J., Dilles, J.H., Gray, F., Graybeal, F.T., Mars, J.C., McPhee, D.K., Seal, R.R., Taylor, R.D. & Vikre, P.G. 2010. Porphyry copper deposit model. Scientific Investigations Report 2010–5070–B. U.S. Geological Survey, 186 p. Reston, USA.

Julivert, M. 1968. Lexique Stratigraphique Internacional, Amérique Latine. Colombie (première partie), Précambrien, Paléozoïque, Mésozoïque, et intrusions d'âge mésozoïque–tertiaire. Centre National de la Recherche Scientifique 5, fascicule 4 a, 651 p. Paris.

Kronenberg, S. & Reeves, C.V. 2011. Vaupés and Amazonas Basins. In: Cediel, F. (editor), Petroleum geology of Colombia: Geology and hydrocarbon potential, 15. Agencia Nacional de Hidrocarburos and Universidad Eafit, 103 p. Medellín.

López, J.A. & Cramer, T. 2012. Ambiente geológico del Complejo Mitú y perspectivas de ocurrencias minerales de niobio y tantalio en el territorio colombiano. Geología Colombiana, 37: 75–93.

López, J.A., Khurama, S., Bernal, L.E. & Cuéllar, M.A. 2007. El Complejo Mitú: Una nueva perspectiva. XI Congreso Colombiano de Geología. Memoirs CD ROM, p 16. Bucaramanga, Santander.

Martelet, G., Truffert, C., Tourlière, B., Ledru, P. & Perrin, J. 2006. Classifying airborne radiometry data with agglomerative hierarchical clustering: A tool for geological mapping in context of rainforest (French Guiana). International Journal of Applied Earth Observation and Geoinformation, 8(3): 208–223. https://doi.org/10.1016/j.jag.2005.09.003

Minty, B.R.S. 1997. Fundamentals of airborne gamma–ray spectrometry. AGSO Journal of Australian Geology & Geophysics, 17(2): 39–50.

Moyano, I.E., Lara, N.M., Puentes, M.F., Rojas, O.E. & Cárdenas L.P. 2016. Mapa de anomalías geofísicas de Colombia para recursos minerales: Anomalía magnética de campo total (nT); Distribución ternaria de la concentración de K, U y Th; Señal analítica de la anomalía magnética de campo total (nT/m). Scale 1:1 500 000. Servicio Geológico Colombiano, 3 sheets. Bogotá.

Nakamura, A. 2015. Radiometric map of Australia (3rd edition). Scale 1:15 000 000. Geoscience Australia. Canberra.

Nannini, F., Cabral–Neto, I., Silveira, F.V., Cunha, L.M., Oliveira, R.G. & Weska, R.K. 2017. Informe de recursos minerais: Programa geologia do Brasil: Áreas kimberlíticas e diamantíferas do estado do Mato Grosso. Série Pedras Preciosas N° 12. Programa Geologia do Brasil, Companhia de Pesquisa de Recursos Minerais–Serviço Geológico do Brasil, 46 p. Brasilia.

National Oceanic & Atmospheric Administration. 2018. Magnetic Field Calculators. https://www.ngdc.noaa.gov/geomag-web/#igrfwmm (consulted in August 2018).

Oliveira, A.C. 2014a. Carta interpretativa geofísica–geológica folha NA.20–Z–B Caracaraí. Scale 1:250 000. Companhia de Pesquisa de Recursos Minerais–Serviço Geológico do Brasil, 1 sheet. Manaus, Brazil.

Oliveira, V. 2014b. Carta interpretativa geofísica–geológica folha NA.20–X–D Boa Vista. Scale 1:250 000. Companhia de Pesquisa de Recursos Minerais–Serviço Geológico do Brasil, 1 sheet. Manaus, Brazil.

Pinheiro, S.S., Fernandes, P.E.C.A., Pereira, E.R., Vasconcelos, E.G., Pinto, A.C., de Montalvão, R.M.G., Issler, R.S., Dall'Agnol, R., Teixeira, W. & Fernandes, C.A.C. 1976. Geologia. In: Divisão de Publicação. (editor), Projeto RADAMBRASIL. Levantamento de recursos naturais: Folha NA. 19 Pico da Neblina, 11, p. 19–137. Rio de Janeiro.

Priem, H.N.A, Andriessen, P.A.M., Boelrijk, N.A.I.M., De Booder, H., Hebeda, E.H., Huguett, A., Verdumen, E.A.T. & Verschure, R.H. 1982. Geochronology of the Precambrian in the Amazonas region of southeastern Colombia (western Guiana Shield). Geologie en Mijnbouw, 61(3): 229–242.

Ramos, L., Pires, A. & Benfica, C. 2014. Airborne gamma–ray spectrometric and magnetic signatures of Fazenda Nova region, east portion of Arenópolis magmatic arc, Goiás. Revista Brasileira de Geofísica, 32(1): 123–140. https://doi.org/10.22564/rbgf.v32i1.401

Reeves, C. 2005. Aeromagnetic surveys: Principles, practice & interpretation. GEOSOFT, 155 p. Delft, the Netherlands.

Rodríguez, G., Sepúlveda, J., Ramírez, C., Ortiz, F.H., Ramos, K., Bermúdez, J.G. & Sierra, M.I. 2011. Unidades, petrografía y composición química del Complejo Migmatítico de Mitú en los alrededores de Mitú. Boletín de Geología, 33(1): 27–42.

Salem, A., Williams, S., Fairhead, D., Smith, R. & Ravat, D. 2008. Interpretation of magnetic data using tilt–angle derivatives. Geophysics, 73(1): L1–L10. https://doi.org/10.1190/1.2799992

Santos, J.O.S., Hartman, L.A., Gaudette, H.E., Groves, D.I., McNaughton, N.J. & Fletcher, I.R. 2000. A new understanding of the provinces of the Amazon Craton based on integration field mapping and U–Pb and Sm–Nd geochronology. Gondwana Research, 3(4): 453–488. https://doi.org/10.1016/S1342-937X(05)70755-3

Santos, J.O.S., Potter, P.E., Reis, N.J., Hartmann, L.A., Fletcher, I.R. & McNaughton, N.J. 2003. Age, source, and regional stratigraphy of the Roraima Supergroup and Roraima–like outliers in northern South America based on U–Pb geochronology. Geological Society of America Bulletin, 115(3): 331–348. https://doi.org/10.1130/0016-7606(2003)115<0331:ASARSO>2.0.CO;2

Shives, R.B.K., Charbonneau, B.W. & Ford, K.L. 1997. The detection of potassic alteration by gamma–ray spectrometry–recognition of alteration related to mineralization. Geophysics and Geochemistry at the Millenium, Exploration 97, p. 1–17.

Silva, M. 2014. Carta interpretativa geofísica–geológica folha NA.20–Z–C Rio Demini. Scale 1:250 000. Companhia de Pesquisa de Recursos Minerais–Serviço Geológico do Brasil, 1 sheet. Manaus, Brazil.

Tassinari, C.C.G. & Macambira, M.J.B. 1999. Geochronological provinces of the Amazonian Craton. Episodes, 22(3): 174–182.

Tassinari, C.C.G., Cordani, U.G., Nutman, A.P., van Schmus, W.R., Bettencourt, J.S. & Taylor, P.N. 1996. Geochronological systematics on basement rocks from the Río Negro–Juruena province (Amazonian Craton) and tectonic implications. International Geology Review, 38(2): 161–175. https://doi.org/10.1080/00206819709465329

Telford, W.M., Geldart, L.P. & Sheriff, R.E. 1990. Applied geophysics, 2nd edition. Cambridge University Press, 770 p. Cambridge, UK.

Thery, J.M. 1982. Constitution du Nord–Ouest du continente Sud Américain avant les tectoniques Andines. Doctoral thesis, Université Bourdeaux II, 3 volumes, 221 p. Burdeous, France.

Explanation of Acronyms, Abbreviations, and Symbols:

dz	Vertical derivative
IGRF	International Geomagnetic Reference Field
IOCG	Iron oxide copper–gold
LA–ICP–MS	Laser ablation multi–collector inductively coupled plasma mass spectrometry
MP–Mvlg1	Pedrera and Roraima Formations
MP–Pf1	Parguaza Granite
NaI	Sodium iodide
NP–Pm	Neoproterozoic alkaline gabbros
NP–VCc	Piraparaná Formation
N1–Sc	Miocene sedimentary rocks
O–Sm	Ordovician sedimentary rocks
PP–Mmg1	Migmatitic Complex of Mitú
Q–al	Alluvial and alluvial plains deposits
Q–d	Aeolian deposits
Q–t	Alluvial terraces
RTP	Reduction to magnetic pole
SHRIMP	Sensitive high–resolution ion microprobe
TFA	Total magnetic field anomaly

Authors' Biographical Notes

Ismael Enrique MOYANO–NIETO graduated in geology in 2002, earned a MS in geophysics (2015) and currently is a PhD student at the Universidad Nacional de Colombia. He works as a geologist–geophysicist for the research group in applied geochemistry and geophysics at the Dirección de Recursos Minerales of the Servicio Geológico Colombiano (2009–present).

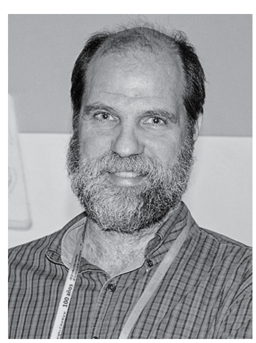

Renato CORDANI graduated in geophysics in 1994 and earned an MS (1997) and a PhD (2008) at the Institute of Astronomy and Geophysics of the Universidade de São Paulo (IAG/USP). Renato has contributed to finding several mineral deposits around the globe and has published several technical papers related to mineral exploration and airborne surveys. He collaborates as a reviewer for the *RBGf* (*Brazilian Jour-*

nal of Geophysics) and *RBG* (*Brazilian Journal of Geology*). Renato is a member of the council of the Brazilian Geophysical Society (SBGf) (2009–present).

Lorena Paola CÁRDENAS–ESPINOSA graduated in physics in 2011 and earned a MS in geophysics at the Universidad Nacional de Colombia. She worked at the Dirección de Recursos Minerales of the Servicio Geológico Colombiano (2013–2018) and teached geophysics at Universidad de Ciencias Aplicadas y Ambientales (environmental engineering) (2016–2018).

Norma Marcela LARA–MARTÍNEZ graduated in cadastral engineering and geodesy at the Universidad Distrital Francisco José de Caldas (2005) and earned a specialization degree in geomatics at the Universidad Militar Nueva Granada (2018). She has 10 years of experience in geomatics topics and has worked at the Dirección de Recursos Minerales of the Servicio Geológico Colombiano in the area of geophysical exploration since 2013.

Oscar Eduardo ROJAS–SARMIENTO graduated in mining engineering in 2006 from the Universidad Nacional de Colombia (Medellín) and earned an MS in geophysics at the Universidad Nacional de Colombia (Bogotá) in 2012. Oscar has contributed to geophysical exploration for geothermal energy, geological characterization using resistivity methods, and mineral exploration using airborne magnetometry and gamma spectrometry.

Manuel Fernando PUENTES–TORRES graduated in physics from Universidad Distrital Francisco José de Caldas of Bogotá in 2014. Since 2011, he has worked in the Servicio Geológico Colombiano in the Dirección de Recursos Minerales in the field of geophysics for mineral resources. Since 2014, he has contributed to the processing and interpretation of airborne magnetometric and gamma spectrometric data.

Diana Lorena OSPINA–MONTES graduated in geology from Universidad de Caldas (2007) and earned a MS in geophysics at the Universidad Nacional de Colombia (Bogotá). She works in the geophysics section of the Dirección de Recursos Minerales of the Servicio Geológico Colombiano (2017–present).

Andrés Felipe SALAMANCA–SAAVEDRA graduated in geology from the Universidad Nacional de Colombia (2013) and geophysics (MS) from the Universidad Nacional de Colombia, Bogotá. Andrés has worked on seismic processing and signal analysis. He worked on the interpretation and processing of radiometric and magnetometric anomalies at the Dirección de Recursos Minerales of the Servicio Geológico Colombiano until December 2019.

Gloria PRIETO–RINCÓN is the current technical director of the Dirección de Recursos Minerales of the Servicio Geológico Colombiano. She studied chemistry at the Universidad Nacional de Colombia and earned DSc in geochemistry and petrology. She has completed training courses in environmental management, mineral resource processing, and prospecting, exploration and management of mineral resources. She has developed research and directed projects in geochemical characterization, multipurpose geochemical mapping, medical and environmental geochemistry, and mineral prospection and exploration. Gloria has published reports and scientific papers in national and international journals. She is member of the Editorial Committee of the journal *Geochemistry: Exploration, Environment, Analysis* (*GEEA*) and a representative for South America in the IUGS/IAGC Task Group on Global Geochemical Baselines. She is also a member of the Scientific Committee and part of the Governing Council of the UNESCO International Centre on Global–Scale Geochemistry.

Volume 1

Chapter 3

https://doi.org/10.32685/pub.esp.35.2019.03
Published online 14 April 2020

Tectonostratigraphic Terranes in Colombia: An Update First Part: Continental Terranes

Jorge Julián RESTREPO[1]* and Jean–François TOUSSAINT[2]

1 jjrestrepoa@gmail.com
Universidad Nacional de Colombia
Sede Medellín
GEMMA Research Group
Medellín, Colombia

2 jftoussaint@hotmail.com
Universidad Nacional de Colombia
Medellín, Colombia

* Corresponding author

Abstract The quite abundant geological information that has been produced in recent years in Colombia, especially in geochronological and geological mapping, necessitates updating the mosaic of geological terranes that comprise the Colombian territory. Several modifications to these characteristics and boundaries are proposed for terranes such as Chibcha, Tahamí, and Calima. Some small terranes that have been defined recently, including Anacona, Ebéjico (Quebradagrande), and Pozo (Arquía), are placed within the context of the larger terranes. In addition, some new terranes, including Yalcón, Bocaná, Aburrá, Kogi, and Tairona, are defined and their characteristics are described. With these new geochronological data, we propose that the metamorphic Cajamarca Complex be replaced by two new lithodemical units: the Antioquia Complex, which covers mostly rocks that formed during Permian and Triassic metamorphism, and the Coello Complex, which comprises metamorphic rocks that formed during Jurassic metamorphism. Future lines of investigation are proposed to solve remaining problems, especially the boundaries of some of the newly defined terranes.
Keywords: *continental terranes, accretions, displaced terranes, Colombia, Andes.*

Resumen La abundante cantidad de información geológica que se ha generado en los últimos años en Colombia, en particular geocronológica y cartográfica, implica la necesidad de actualizar el mosaico de terrenos geológicos que constituyen el territorio colombiano. En este capítulo se proponen modificaciones relacionadas con las características y las fronteras de varios terrenos incluidos el Chibcha, el Tahamí y el Calima. Algunos pequeños terrenos que han sido propuestos recientemente, entre ellos el Anacona, el Ebéjico (Quebradagrande) y el Pozo (Arquía), se localizan dentro del contexto de los grandes terrenos. También, se definen y describen nuevos terrenos, incluidos el Yalcón, el Bocaná, el Aburrá, el Kogi y el Tairona. Con los datos geocronológicos recientes disponibles se propone que el Complejo Cajamarca sea remplazado por dos nuevas unidades litodémicas: el Complejo Antioquia que agrupe rocas formadas durante un evento metamórfico pérmico–triásico y el Complejo Coello que agrupe rocas formadas por metamorfismo jurásico. Además, se sugieren futuras líneas de investigación para resolver las incógnitas que quedan por solucionar, en particular en relación con las fronteras de algunos de los nuevos terrenos.
Palabras clave: *terrenos continentales, acreciones, terrenos desplazados, Colombia, Andes.*

Citation: Restrepo, J.J. & Toussaint, J.F. 2020. Tectonostratigraphic terranes in Colombia: An update. First part: Continental terranes. In: Gómez, J. & Mateus–Zabala, D. (editors), The Geology of Colombia, Volume 1 Proterozoic – Paleozoic. Servicio Geológico Colombiano, Publicaciones Geológicas Especiales 35, p. 37–63. Bogotá. https://doi.org/10.32685/pub.esp.35.2019.03

1. Introduction

The concept of terranes, which emerged in the 1970s in western North America (Berg et al., 1978; Coney et al., 1980; and others), has been used in Colombia since 1983, particularly in two regional studies that suggested that the northwestern corner of South America consists of a mosaic of terranes, which would have been accreted into the Amazonian Craton during several geological periods. A recompilation that was conducted by the Servicio Geológico Colombiano (SGC) and coordinated by Etayo–Serna et al. (1983) proposed 34 terranes or geological provinces primarily based on the lithostratigraphy of each terrane or province. Restrepo & Toussaint (1988) focused on comparing and contrasting the lithostratigraphic and tectonic characteristics of each of the five proposed megaterranes. Toussaint & Restrepo (1989) named each terrane after a pre–Columbian ethnic group to avoid confusion with the names of formations, groups, or geological provinces and proposed a new map. In addition to the cratonic region, the Terranes Andaquí, Chibcha, and Tahamí, which have continental basements, and the Terranes Calima and Cuna, which have oceanic basements, were proposed from east to west. Subsequently, other authors (e.g., Restrepo–Pace et al., 1997; Cediel et al., 2003; Moreno–Sánchez & Pardo–Trujillo, 2003; and others) conducted regional studies by using the concept of terranes. New terranes were identified in the area between the Tahamí and Calima Terranes, that is, between the continental and oceanic domains, namely, the Panzenú, Anacona, Pozo (Arquía), Ebéjico (Quebradagrande), and Amagá–Sinifaná Terranes, among others, which divide megaterranes into smaller terranes (e.g., Ordóñez–Carmona & Pimentel, 2002; Restrepo et al., 2009; Martens et al., 2014). Some terrane names, which are indicated in parentheses previously, were also changed to indigenous names. The use of U–Pb zircon in situ dating with laser ablation multi–collector inductively coupled plasma mass spectrometry (LA–MC–ICP–MS) reassessed the ages of several metamorphic units that were previously determined based on K–Ar and Rb–Sr dating, which changed the characteristics of the terranes. Moreover, several research studies sought to locate the terranes of Colombia within the geodynamic framework of the relationships among the Amazonian Craton, Laurentia, Pangea, proto–Caribbean, Caribbean, and other terranes in the region (i.e., Kennan & Pindell, 2009).

Based on the above topics, an updated overview of the terranes of Colombia is performed (see Figure 1). The continental terranes are treated in this chapter, whereas the oceanic terranes are examined in another chapter in this multivolume book (Toussaint & Restrepo, 2020). Furthermore, new questions are raised for future research studies because one can no longer understand the geological relationships among neighboring areas that belong to different terranes and the geological evolution of Colombian territory while disregarding the theory of tectono–stratigraphic terranes, especially in an area bordering the Pacific Ocean. This task would be similar to trying to understand the relationships between living beings while disregarding the concept of biological evolution.

However, some recent articles presented autochthonistic models based on abundant geochemical and geochronological data (i.e., Cochrane et al., 2014a), but some critical field relationships were not discussed in depth. In addition, well–known important geological facts that imply the terrane concept to be explained were not mentioned. Although new instrumental measures are very important in geology, good field work is irreplaceable.

2. Amazonian Craton in Colombia

2.1. Introduction

In Colombia, the geological units that are considered to be autochthonous in relation to the Amazonian Craton are located between the foothills of the Garzón Massif and Eastern Cordillera and the borders with Venezuela, Brasil, and Perú.

The Amazonian Craton in Colombia mainly consists of a metamorphic basement called the Mitú Migmatitic Complex, which is Paleoproterozoic in age and is affected by syn– and post–tectonic plutonism, some of which is anorogenic, of intermediate to acidic composition and Mesoproterozoic in age. Local sedimentary rocks, which were sometimes affected by low–grade Neoproterozoic metamorphism, cover the high–grade metamorphic basement. These rocks include the Tunuí Group, La Pedrera Formation, and the Piraparaná Formation. Paleozoic, Cretaceous, and Cenozoic sedimentary rocks cover a great portion of the Precambrian basement.

2.2. Characteristics of the Autochthonous Region

In the eastern region of Colombia along the borders with Brasil and Venezuela, high–grade metamorphic rocks were described by Galvis et al. (1979), who named these rocks the Mitú Migmatitic Complex. This unit was renamed the Mitú Complex to include magmatic rocks (López et al., 2007), but this terminology has not been widely accepted (i.e., Rodríguez et al., 2011). Because of the diversity of rocks in the area, Ibañez–Mejia & Cordani (2020) recommend discontinuing the use of this name. The rocks are mostly migmatites, granitic gneisses, amphibolites, and granitoids. According to Cordani et al. (2016), two different belts are present in the area: the Atabapo belt, which was named after the Atabapo River along the border between Colombia and Venezuela, and the Vaupés belt. In the Atabapo belt, the rocks range in age from 1800 to 1740 Ma (U–Pb zircon ages for all the dates in this paragraph), while the rocks in the Vaupés belt range from 1580 to 1520 Ma. In the younger Vaupés belt, older rocks from 1780 to 1740 Ma are considered “basement inliers”. A

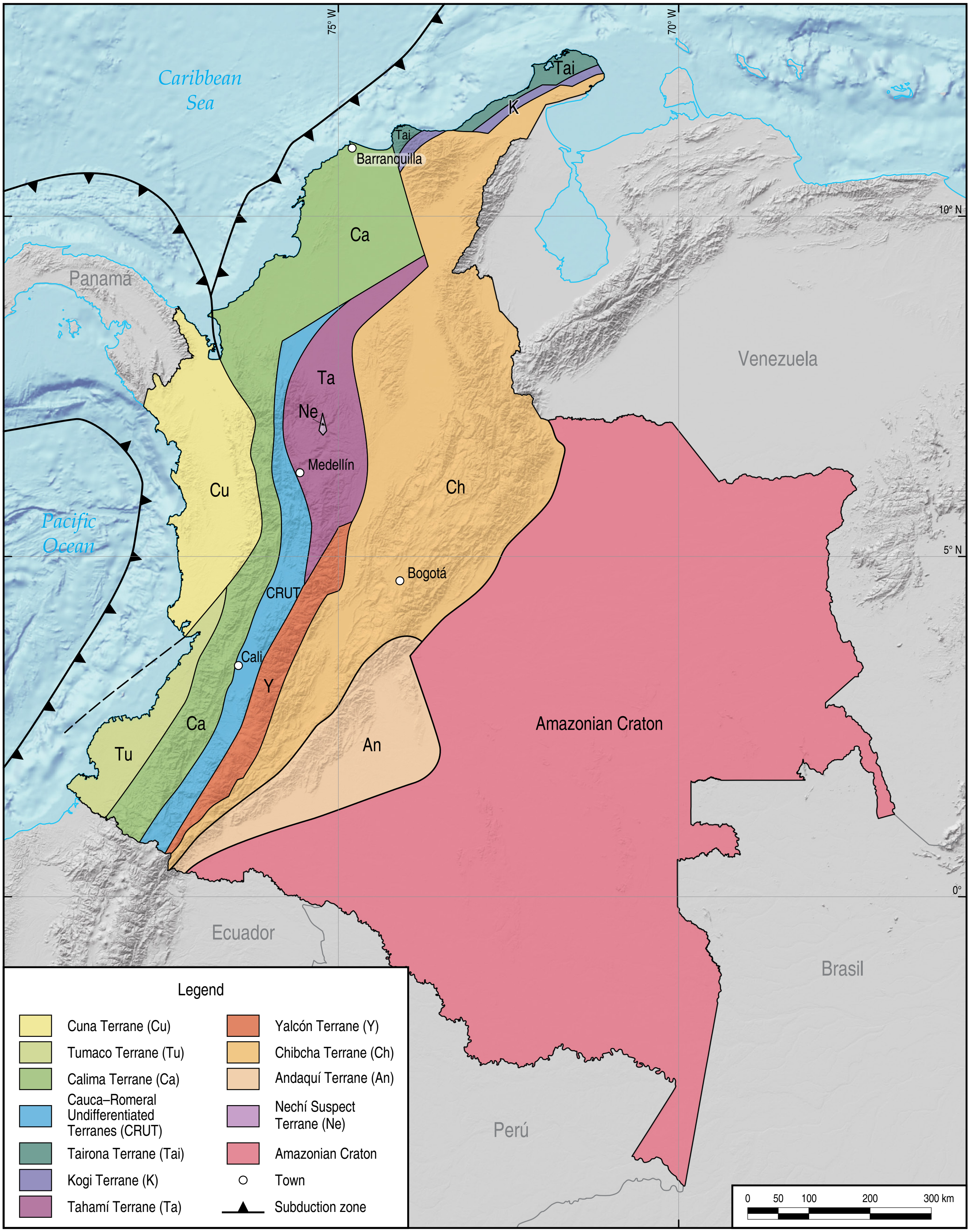

Figure 1. Schematic map of the proposed geologic terranes in Colombia: (An) Andaquí Terrane; (Ch) Chibcha Terrane; (Y) Yalcón Terrane; (Ta) Tahamí Terrane; (K) Kogi Terrane; (Ca) Calima Terrane; (Tu) Tumaco Terrane; (Tai) Tairona Terrane; (Cu) Cuna Terrane; (Ne) Nechí Suspect Terrane; (CRUT) Cauca–Romeral Undifferentiated Terranes: strips formed by smaller continental and oceanic terranes, such as the Pozo (Arquía), Ebéjico (Quebradagrande), and Amagá–Sinifaná Terranes, among others.

similar situation occurs within the Araracuara basement, which was dated between 1725 and 1756 Ma (Ibañez–Mejia et al., 2011; Cordani et al., 2016), but datings in the nearby Apaporis River yielded ages between 1593 and 1530 Ma, with the older ages interpreted by the latter authors as basement inliers. These units belong to the so–called Río Negro–Juruena Province of the Amazonian Craton (Cordani et al., 2000).

The Mitú Migmatitic Complex is intruded by several plutons and particularly by the Parguaza Batholith, whose western edge crops out in Colombia between Puerto Carreño and Inírida and spans over 30 000 km^2 in Venezuela. Generally, these rocks are monzogranites with Rapakivi–type orbicular texture such as the Mitú Monzogranite or the Matraca Granite, syenogranites such as the Parguaza Syenite, and potassium granites with riebeckite. The Parguaza Granite is an A–type granite that corresponds to intraplate anorogenic intrusions. In the Venezuelan portion of the granite, only a conventional U–Pb age of 1.54 Ga and Rb–Sr isochron ages of 1531 and 1545 Ma were obtained (Gaudette et al., 1978); in the western portion in Colombia, eight Ar–Ar datings in biotite and hornblende yielded ages from 1237 to 1383 Ma (Ochoa et al., 2012), while two ages of 1401 ± 2 and 1392 ± 5 Ma were obtained by U–Pb LA–ICP–MS in zircons (Bonilla–Pérez et al., 2013). Although these later authors argued that the Colombian portion of the granite was younger, another possibility is that the conventional method that was used for the Venezuelan sample did not date the intrusion's age. The small Matraca Granite, which is another anorogenic granite near Inírida, was dated at 1343 ± 8 Ma (Bonilla et al., 2016).

In Guainía, the Mitú Migmatitic Complex is unconformably covered by sedimentary or metasedimentary sequences. Gold–bearing metasedimentary rocks in Guainía and Vaupés yielded detritic zircon ages that indicated a maximum deposition age of 1776 Ma (Amaya et al., 2017), enabling these researchers to correlate these rocks with the Tunuí Group in serranía de Naquén, which consists of a basal metaconglomerate, metamudstone, quartzite, and phyllites that were metamorphosed in the greenschist facies (Renzoni, 1989; González, 1989). The general sedimentation environment was fluvial and deltaic with tidal flat deposits and meandering rivers. In the Amazon Region, the cover is represented by La Pedrera and Piraparaná Formations (Galvis et al., 1979). La Pedrera Formation consists of very low–grade metamorphic rocks, mainly metaconglomerates and metasandstones, while schistose quartzites are covered by the Piraparaná Formation, which consists of a volcanic material that includes rhyolitic and rhyodacitic lavas, pyroclasts, agglomerates, doleritic dikes and sills, and gabbros such as the Tijereto Gabbro (Galvis et al., 1979). Arkose sandstones and ferruginous sedimentites are associated with this volcanic sequence. Priem et al. (1982, 1989) obtained an Rb–Sr age of 1200 Ma and several K–Ar ages from 920 Ma to 732 Ma for the volcanic rocks in the Piraparaná Formation, which may suggest a late Neoproterozoic event.

The origin of the granitic rocks in the Mitú Complex has been subjected to different interpretations. The Parguaza and Matraca Granites are generally agreed to be anorogenic granites (Gaudette et al., 1978; Bonilla et al., 2016). Based on chemical analyses of the granitic orthogneisses in the Mitú area, Rodríguez et al. (2011) showed that these rocks plotted entirely within the field of A–type granites, while Cordani et al. (2016) considered that these rocks formed during orogenic cycles. Defining the true nature of these granites is important to understand the evolution of the craton.

In the Guayana Shield, a very low– to low–grade metamorphism event, which is reflected in some K–Ar datings for the Mitú Complex at that age, is called the Nickerie event (1400–1200 Ma). This regional intraplate thermal event affected the entire crust (Cordani et al., 2016). The event was followed by the development of major faults, which are mainly oriented in the NW direction and are associated with intense mylonitization. Notwithstanding, as noted by Kroonenberg (1982a), the characteristics of the Nickerie event in the Guayana Shield in general and the Orinoquia and Amazonia regions in particular seem very different from those in the Precambrian region of the Garzón Massif in the Andaquí Terrane. Intraplate magmatism occurred locally in the region of San José de Guaviare with the intrusion of peralkaline nepheline syenites. Priem et al. (1982) reported Rb–Sr and K–Ar ages from 445 to 495 Ma, and Rodríguez et al. (2011) determined U–Pb zircon and Ar–Ar biotite ages from 577 to 494 Ma. The oldest age was interpreted as the intrusion age during the Pan–African Orogeny that affected Gondwana, while the Ordovician age was interpreted as the cooling event.

Because of the anorogenic origin of many of the granites in this area, including the Parguaza Granite, the extensive formation of anorogenic granitoid rocks from 1400 Ma to around 600 Ma was an important continental–crust builder in the area of the NW Amazonian Craton as contrasted with subduction–related magmatic rocks.

The younger units, particularly those with lower Paleozoic, Mesozoic, and Cenozoic sedimentites, are components of the Amazonian Craton–Andaquí Supraterrane and will be discussed below, as well as the position of the boundary between the Amazonian Craton and the terranes to the west.

3. Andaquí Suspect Terrane

3.1. Introduction

Located between the eastern edge of the Eastern Cordillera and the Llanos Orientales, the Andaquí Terrane crops out between latitudes 1° N and 3° 30' N. This terrane is elongated in the N–NE direction and essentially consists of the Garzón Massif and the serranía de La Macarena, which are basement blocks that were uplifted at the end of the Cenozoic.

A review of the Colombian terranes by Etayo–Serna et al. (1983) considered the existence of both the serranía de La Macarena Terrane and Garzón Terrane. Toussaint & Restrepo (1989) defined the Andaquí Terrane as including both terranes, whereas Gómez et al. (2015a) posited that these rocks belonged to the Chibcha Terrane.

The Andaquí Terrane is characterized by a continental basement that experienced high–grade metamorphism in the Stenian – Tonian period during the Grenvillian Orogeny.

3.2. Andaquí Terrane's Characteristics

The Garzón Group (Álvarez, 1981; Kroonenberg, 1982b), which mainly consists of a banded sequence of granulites and the Guapotón and Mancagua augen gneisses, is the basement of the Andaquí Terrane that crops out in the Garzón Massif and serranía de La Macarena. This group consists of banded granulites, felsic charnockitic granulites, granitic orthogneisses, amphibolites, paragneisses, quartzites and marbles. Based on several U–Pb, Pb–Pb, Ar–Ar, and Sm–Nd datings, Cordani et al. (2005) specified a Grenvillian age for the Guapotón–Moncagua Gneisses, El Vergel Granulites, and Las Margaritas Gneisses, which comprise the basement of the Garzón Massif. The datings by Ibañez–Mejia et al. (2011, 2015), who used the U–Pb zircon LA–MC–ICP–MS method, indicated that the genesis of the igneous protoliths occurred between 1.47 and 1.15 Ga. Some oil wells in the Putumayo Basin reached the basement. Thus, a migmatitic gneiss was dated at 986 Ma in the Payara–1 well, a migmatitic paragneiss in the Solita–1 well was dated at 1046 Ma, an amphibolite in the Mandur–2 well was dated at 1019 Ma, and a leuco–monzonite in the Caimán–3 well was dated at 952 Ma (Ibañez–Mejia et al., 2011). These results confirmed the Grenvillian age for the metamorphism of the Andaquí Terrane during the Putumayo Orogeny (Ibañez–Mejia et al., 2015). However, for these authors, the Putumayense Orogeny occurred because of the collision of NW Amazonia (present coordinates) with Baltica, while the Grenville Orogeny occurred because of the collision of western Amazonia with Laurentia, both occurring during the assembly of Rodinia.

The high–grade metamorphic rocks in the serranía de La Macarena are covered by marine sedimentites from the Güejar Group (Trumpy, 1943; Bridger, 1982), which were dated as Cambrian – Ordovician by numerous fossils, including trilobites, brachiopods, and graptolites (Harrington & Kay, 1951).

3.3. Andaquí Terrane's Boundaries with the Autochthonous Region and Accretion Age

A westward–dipping reverse–fault system, such as the Caguán and El Paujil Faults, overthrusts the Garzón Massif and serranía de La Macarena on the Llanos Orientales Basin (Figure 2). Notwithstanding, this complex network, which consists of faults that experienced important Cenozoic and particularly Miocene – Pliocene movements, is not the original suture, which is located below the thick sedimentary sequence of the basin's borders; therefore, the original area of the Andaquí Terrane would be considerably larger than the exposed section, which is shown in Figure 1. This suture would be located between the Mandur–2 well, which was amphibolite U–Pb zircon dated at 1019 Ma (Ibañez–Mejia et al., 2011), that is, Grenvillian in age, and belongs to the Andaquí Terrane, and a syenogranitic gneiss that was dated at 1756 Ma by U–Pb zircons (Cordani et al., 2016) and belongs to the Amazonian Craton near Araracuara at the confluence of the Yarí and Caquetá Rivers. NE of serranía de La Macarena, the boundary is also covered by Cenozoic sedimentites. The accretion would have occurred by the late Neoproterozoic. Additionally, many faults that currently delimit various Colombian terranes experienced important Cenozoic and particularly Miocene – Pliocene movements, implying that the characteristics of the original sutures are barely known. Based on the above, most of the current cartographic limits between terranes should not be considered to have been the original sutures or boundaries.

The Putumayo Orogeny (Grenvillian) in the Andaquí Terrane, which experienced high–grade metamorphism and intense tectonism, has the characteristics of a continental–collision orogeny. This orogeny occurred during the assemblage of the Rodinia supercontinent by the collision of Laurentia with western Amazonia and southern Baltica with NW Amazonia (Cawood & Pisarevsky, 2017; Ibañez–Mejia et al., 2011). One of the characteristics of this type of mountain chain is the overthrusting of the deepest metamorphic units of the roots, which then became allochthonous (Figure 3). Thus, the Garzón Group may have assimilated the roots of the mountain chain that were thrusted east over the Amazonian Craton or autochthonous block. In this hypothesis, the accretion of the Andaquí Terrane would have occurred at the end of the Putumayan Orogeny. Ibañez–Mejia et al. (2015) considered that a large portion of the Putumayo Orogeny formed during "the accretion of fringing arc terranes against the [Amazonia] continental margin". However, this concept cannot be discarded at the end of the Neoproterozoic during the assemblage of the Pannotia supercontinent. In any case, the accretion occurred before the sedimentation of the lower Paleozoic rocks because lower Paleozoic sedimentites such as those of the Güejar Group, Negritos Formation, and Araracuara Formation are found on both sides of the boundary (Restrepo & Toussaint, 1988).

The lack of paleomagnetic and microtectonic data from the area and the thick sedimentary cover of the boundary prevents us from defining the original position of the terrane, although the collisional nature of the chain does not suggest that this area formed as a completely autochthonous block.

However, the hypothesis that the Andaquí and Chibcha Terranes are allochthonous with respect to the Amazonian Craton does not imply that they were generated at considerable distances from Amazonia. Even though both the Andaquí and Chibcha Ter-

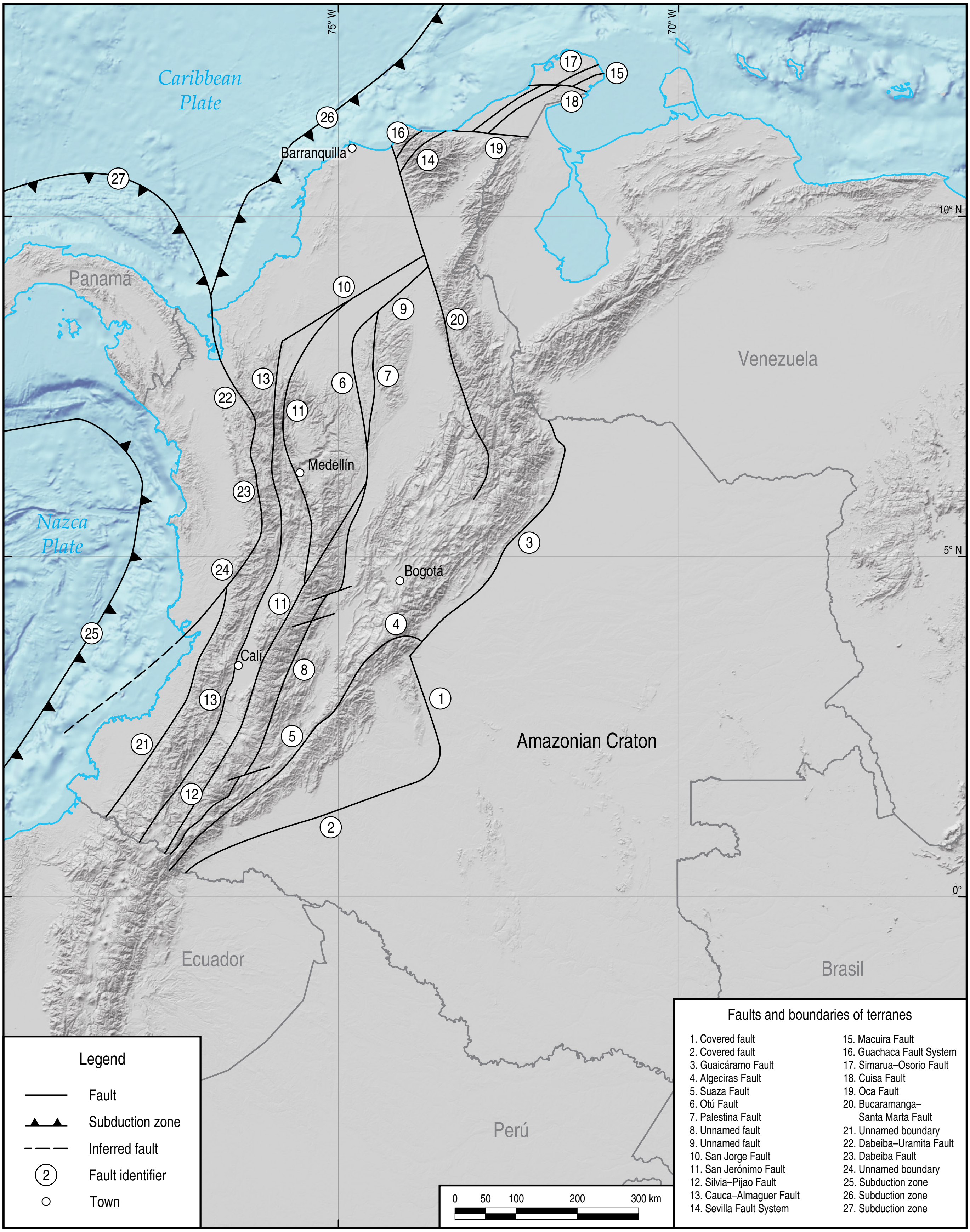

Figure 2. Map that shows the main faults in Colombia.

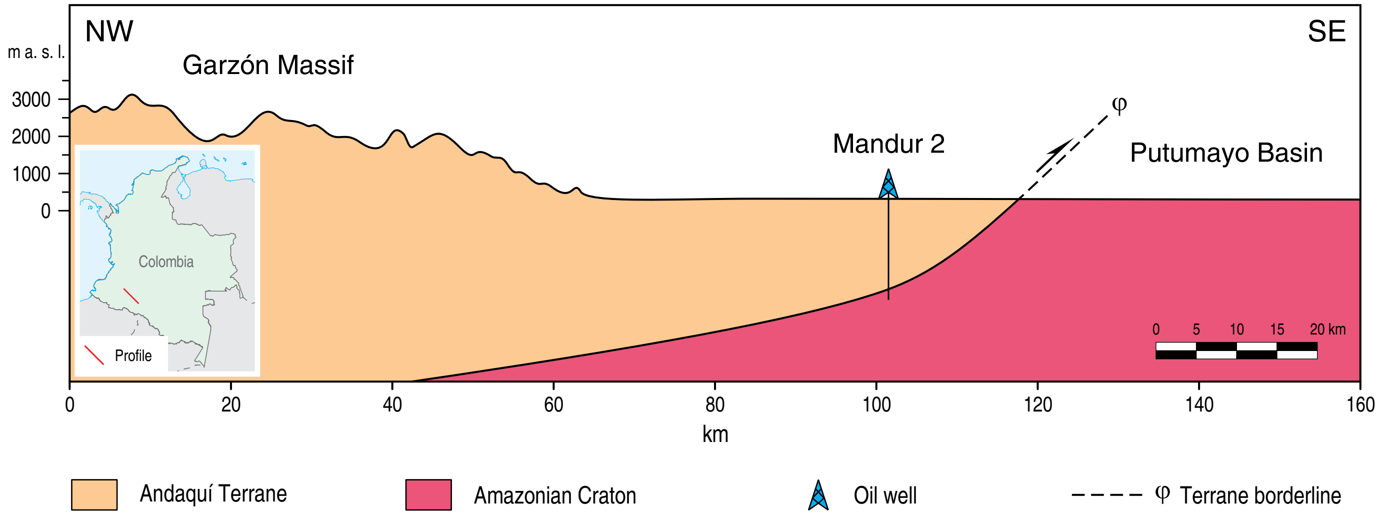

Figure 3. Overthrusting of the present Andaquí Terrane on the Amazonian Craton during the Putumayo Orogeny.

ranes have basements that formed during the Putumayan Orogeny as part of a larger Grenvillian event, this fact does not by itself imply that these rocks are components of the same terrane.

The Andaquí Terrane's western boundary with the Chibcha Terrane is quite complex, mostly because of important post–accretion movements. The current western boundary is represented, from north to south in the vicinity of the town of San Luis de Cubarral, by an east–west reverse fault that overthrusts the Andaquí Terrane on the Chibcha Terrane. Farther south, the limit is represented by the Altamira reverse fault, a short portion of the Algeciras dextral fault, and the Suaza reverse fault, which overthrusts the Andaquí Terrane on the Chibcha Terrane.

The late Paleozoic age of the Chibcha Terrane's accretion into the assemblage that comprises the Amazonian Craton and Andaquí Terrane will be discussed below.

3.4. Amazonian Craton–Andaquí Terrane Supraterrane

In the Macarena and Garzón Massifs, the unmetamorphosed Güejar Group, which was dated by abundant Cambrian – Ordovician fossils, is well known. The basal unit of the Güejar Group is represented by the Calizas de Ariari, which was detected during hydrocarbon explorations in the Amazonian Craton. The Güejar Group (Trumpy, 1943) is correlated with several sedimentary units that cover the craton, such as the Huitoto and Macaya (Bogotá, 1982), Araracuara (Herrera & Velásquez, 1978), and Negritos Formations, which were dated as Ordovician (Ulloa et al., 1982). The upper Paleozoic is largely absent from the Amazonian Craton region and Andaquí Terrane, although some thin layers that were found during hydrocarbon explorations in the Llanos Orientales may be upper Paleozoic (Agencia Nacional de Hidrocarburos, 2012). This characteristic of the Autochthonous Region–Andaquí Terrane strongly differentiates this assemblage from the processes that occurred to the west in the Chibcha Terrane, where the Cambrian and Ordovician are metamorphosed and the upper Paleozoic forms a thick sequence that will be discussed below.

4. Chibcha Terrane

4.1. Introduction

The Chibcha Terrane is located in the Eastern Cordillera, Santander Massif, serranía de Perijá, Magdalena River Valley, and eastern flank of the Central Cordillera. In this study, the SE regions of Sierra Nevada de Santa Marta (SNSM) and La Guajira Peninsula are also included in the Chibcha Terrane.

The review of Colombia terranes by Etayo–Serna et al. (1983) considered that this region consists of seven terranes and/or geological provinces. Restrepo & Toussaint (1988) defined the characteristics of an Eastern Andean Terrane, and Toussaint & Restrepo (1989) named this terrane the Chibcha Terrane. According to Gómez et al. (2015a), the Andaquí Terrane would be included in the Chibcha Terrane.

The Chibcha Terrane mainly consists of a Grenville metamorphic basement, primarily Stenian – Tonian, and a low– to medium–grade Famatinian (Caledonian) metamorphic event. Magmatism of intermediate to acidic composition prior to the Devonian mainly affected the Santander Massif, followed by an important late Paleozoic marine sedimentation that occurred throughout the Chibcha Terrane. Its accretion into the Amazonian Craton and Andaquí Terrane may have been late Paleozoic in age.

4.2. Characteristics of the Chibcha Terrane

The basement of the Chibcha Terrane is characterized by high–grade metamorphic rocks that formed during the Grenville tectogenesis. These rocks are primarily granitic gneisses, migmatites, amphibolites, paragneisses, marbles, and schists.

In the Santander Massif, the basement is identified as Bucaramanga Gneiss, in SNSM as Los Mangos Granulite, and in the eastern flank of the Central Cordillera as the San Lucas, El Vapor, and Guamocó Gneisses. The southernmost region of the terrane includes small outcrops such as the Davis Gneiss, Icarco Complex, and El Pital and Zancudo Migmatites.

The presence of a Precambrian basement in the Chibcha Terrane is corroborated by multiple radiometric data that indicate Grenville and late Neoproterozoic events. The Bucaramanga Gneiss, which mainly consists of quartz–feldspathic gneisses, granulites, orthogneisses, amphibolites, quartzites, and marbles, has been dated by K–Ar, Rb–Sr, and Ar–Ar between 945 Ma and 574 Ma (Goldsmith et al., 1971; Ward et al., 1973; Restrepo–Pace et al., 1997). Cordani et al. (2005) obtained a SHRIMP U–Pb zircon age of 864 Ma, which is interpreted as a metamorphic event.

Grenvillian ages were found for the section of the Chibcha Terrane in the eastern flank of the Central Cordillera; in particular in El Vapor Gneiss, El Hígado Amphibolite, El Pital Migmatite, and Zancudos Migmatite; and in the serranía de San Lucas. In fact, metamorphism ages between 1180 and 930 Ma were obtained by U–Pb LA–ICP–MS in zircons from a granulite in the San Lucas Gneiss, while the igneous age was defined as 1527 Ma (Cuadros et al., 2014); the Guamocó Gneiss was dated at 1048 Ma by U–Pb LA–ICP–MS (Leal–Mejía, 2011); both rocks are components of the serranía de San Lucas.

El Vapor Gneiss at latitude 6° 30’ N was dated at 894 ± 36 Ma by Rb–Sr WR isochrons (Ordóñez–Carmona et al., 1999); in this case, the age may correspond to a period of mylonitization. El Hígado Amphibolite to the west of the Garzón Massif was dated by Ar–Ar at 911 Ma (Restrepo–Pace et al., 1997). El Pital and Zancudo Migmatites (latitude 2° N) were dated between 1005 Ma and 972 Ma by U–Pb LA–MC–ICP–MS by Ibañez–Mejia et al. (2011).

The problems that are posed by Mesozoic dating in the Migmatitic Complex of La Cocha–Río Téllez, the metamorphic Complex of Aleluya, and the Tierradentro Gneisses and Amphibolites will be analyzed below.

Perhaps the most distinguishing feature of the Chibcha Terrane is the widespread metamorphism that affected Cambrian – Ordovician and Silurian sedimentary rocks. These metamorphic rocks are covered in several locations by unmetamorphosed Devonian sedimentary rocks, which indicate a Famatinian Orogeny. Neither the sedimentary rocks that cover the Andaquí Terrane nor the craton were affected by this metamorphism.

The early Paleozoic region of the Chibcha Terrane is represented by several assemblages, which include metasedimentary sequences that were affected by very low– to medium–grade metamorphism. The age of the protoliths is recognized, in some cases, by the presence of a few relatively well–preserved Ordovician fossils, and the age of the tectometamorphic event has been detected by both geochronological methods and the stratigraphic position of the overlying Devonian sedimentary formations. This Famatinian tectogenesis is well marked in the Quetame Massif by low–grade metamorphic rocks from the Quetame Group, which are covered by the Devonian Gutiérrez Sandstones (De La Espriella & Cortés, 1989); the Floresta Massif with the Busbanzá Phyllites and Schists, which was intruded by the Chuscales Pluton at 471 ± 22 Ma (Manosalva et al., 2017); the Santander Massif with Silgará Schists and Chicamocha Schists, whose metamorphism was defined as Famatinian (or Quetame–Caparonensis) by detrital zircons (Mantilla–Figueroa et al., 2016); the Perijá Andes with the Perijá Formation (Forero, 1970); the eastern flank of the Central Cordillera with La Cristalina Formation, which contains Ordovician graptolites and a low–grade metamorphic event up to a biotite isograd that unconformably cover high–grade metamorphic rocks from El Vapor Gneiss; and the southern portion of the Chibcha Terrane by the Amoyá and El Hígado Formations (Núñez et al., 1984; Mojica et al., 1988). Some of these pre–Devonian low–grade metamorphic rocks were deposited over high–grade Precambrian metamorphic rocks and have Ordovician fossils. The lithology of these units mainly consists of chloritic and muscovitic schists, phyllites, slates with some quartzite levels, and metaconglomerates with scarce marble. Ordovician fossils are found in La Cristalina, El Hígado, and Río Nevado Formations. The position of the Pompeya Metamorphites, Mazamorras Schists, Vitonco Metasedimentites, and Chingual Formation in southern Colombia suggests that these rocks could be correlated with formations that were affected by low–grade metamorphism during the early Paleozoic, although some of these rocks would have been affected by Jurassic metamorphism, which will be discussed below. Low– to medium–grade metamorphic units of Famatinian age are unconformably covered by well–dated sedimentary sequences of Devonian age, which is the case for sedimentary sequences such as the Devonian sedimentites of the Rovira, El Imán Formation, and Jagua and Granadillo Mudstones and Limestones, as dated by fossils.

In the Santander Massif, a key magmatic event occurred at the end of the Famatinian tectogenesis and before the deposition of Devonian sedimentites. These rocks are hornblendic metadiorites, syntectonic gneissic granites, granodiorites, and gabbros that were dated between 471 and 413 Ma (Boinet et al., 1985). In the Floresta Massif, the Chuscales granitic stock was Rb–Sr dated at 471 ± 22 Ma (Ulloa & Rodríguez, 1982). In the Quetame Massif, several small plutons intruded the metamorphic rocks of the Quetame Group and are unconformably covered by Devonian sedimentites (Renzoni, 1968).

After the erosional period that followed the Famatinian tectogenesis and emplacement of pre–Devonian plutons, which is marked by the absence or scarcity of Silurian sedimentites throughout the Colombian territory, the sea transgressed on a relatively well–leveled erosion surface. The main outcrops of Devonian sedimentites in Colombia are located in the serranía de Perijá, the Santander Massif through Las Mercedes Formation, La Floresta Massif through the Tíbet and La Floresta Formations, the Quetame Massif through the Gutiérrez Sandstones and Portachuelo Lutites, and Rovira near Ibagué along the eastern flank of the Central Cordillera. The ages of these formations were proven by the presence of numerous fossils.

In Colombia, non–metamorphosed, thick sequences of sedimentites of Carboniferous and Permian age are only found in the Chibcha Terrane, in which important epicontinental marine sequences were deposited; in the Llanos Basin, only thin upper Paleozoic sequences have been found (Agencia Nacional de Hidrocarburos, 2012). The Carboniferous is mainly represented by compact quartz sandstones that are frequently red, associated with gray–to–red limestones that are sometimes oolitic, and dark lutites with numerous fossils, particularly brachiopods, bryozoans, and crinoids, which show that the base of the Mississippian is generally absent and indicate the beginning of the transgression at the end of this period or the beginning of the Pennsylvanian. The Permian primarily consists of massive gray limestones, dark lutites, and few sandstones. These rocks were only clearly detected in the Santander Massif and serranía de Perijá and show fossiliferous levels with fusulinids and algae. During the Carboniferous and Permian, sedimentation was characterized by both clastic and calcareous deposits, indicating a shallow–marine platform environment. In several regions, these sedimentites are layered in angular unconformities over Devonian sedimentary sequences or Cambrian – Ordovician and Precambrian metamorphic complexes, although concordance between Devonian and Carboniferous layers is observed in other areas.

4.3. Chibcha Terrane's Accretion into the Andaquí Terrane–Amazonian Craton Assemblage

At the end of the Paleozoic, the Chibcha Terrane accreted into the assemblage that had consisted of the Andaquí Terrane and Amazonian Craton since the end of the Precambrian or earlier. Large differences between the geologic processes that occurred on both sides of the boundary are noted during the Paleozoic.

The differences are well marked during the early Paleozoic, when the important Famatinian tectogenesis occurred in the Chibcha Terrane, including the Quetame Massif now being adjacent to the craton, whereas calm marine sedimentation occurred on the other side of the boundary. Differences are also noted in the development of pre–Devonian, intermediate to acidic magmatism in the Chibcha Terrane, whereas no magmatism was detected in the Amazonian Craton. The differences continued during the late Paleozoic with important marine sequences in the Chibcha Terrane, whereas these rocks are very thin or absent from the Amazonian Craton (Agencia Nacional de Hidrocarburos, 2012). Thus, Devonian sequences with thicknesses that exceed 2400 m occur in the Quetame Massif, and Carboniferous sequences with thicknesses that exceed 2000 m occur in the Labateca and Río Batá areas; however, no evidence of this thick deposition is found east of the boundary.

Regarding the type of movement of the boundary, only a dextral movement can be assumed at that time because of the dextral movement of North America in relation to the Amazonian Craton during the Paleozoic and the faunal similarity of the later Devonian, Carboniferous, and Permian rocks in Colombia with those of the SW region of North America (see, in particular, Forero, 1984; Dalziel, 1997). Thus, the Chibcha Terrane most likely was derived from the vicinity of this region, and accretion probably occurred during the complex movements between Gondwana and Laurentia, which ultimately facilitated the formation of Pangea. In contrast, early Mesozoic units, such as the Saldaña Formation (Upper Triassic) and Motema Formation (Jurassic), are located on both sides of the eastern boundary of the Chibcha Terrane. Thus, an assemblage called "Colombian East" formed at the end of the Paleozoic or beginning of the Mesozoic, which brought together the autochthonous Amazonian Craton, the Andaquí Terrane, and the Chibcha Terrane.

4.4. Chibcha Terrane's Boundaries

A section of the Chibcha Terrane's boundary with the Amazonian Craton is found to the north of Villavicencio. This boundary is currently represented by the Guaicáramo Fault System, which has reverse characteristics at the latitude of Nevado del Cocuy and dextral movement farther south. This network of faults experienced an important Cenozoic movement and is therefore not the original boundary. The Chibcha Terrane's boundary with the assemblage that consisted of the autochthonous regions and the Andaquí Terrane during the Neoproterozoic has been previously treated.

The data that have been collected thus far indicate that the Chibcha and Tahamí Terranes have quite different histories. The extensive Jurassic plutonism that occurred in the Chibcha Terrane had no effect on the Tahamí Terrane, whereas the Permian – Triassic metamorphism and intense Late Cretaceous magmatism of the Tahamí Terrane had no effect on the western boundary of the Colombian East, as confirmed by the presence of non–metamorphosed, Paleozoic sedimentary rocks in the Chibcha Terrane. The compressional tectonic events that affected the Tahamí Terrane during the Cretaceous also clearly contrast with the environment of calm distension that occurred during that time in the Chibcha Terrane. The boundary between these terranes is represented by the Otú Fault, which was intersected during the Paleocene by the Palestina Fault. The large differences on both sides of the Otú Fault had already been detected by Feininger (1970). The northern boundary in the Plato depression is covered by a thick sequence of Cenozoic sedimentites. In this study, the basement of this area is assumed to be oceanic, as proposed by Mora–Bohórquez et al. (2017) based on seismic profiles.

4.5. Post–accretion Events in the Colombian East Supraterrane

After the formation of the Colombian East, the supraterrane that comprised the Amazonian Craton, the Andaquí Terrane, and the Chibcha Terrane was characterized by an important Triassic and Jurassic magmatism event that affected the western region of the Colombian East and a very thick sequence of Cretaceous marine sedimentites that deposited in a calm subsidence environment without interruptions by any compressional tectonic movement. This situation shows a strong contrast between the processes that occurred during the Mesozoic in the Colombian East with those in the westernmost regions of the country, particularly in the Tahamí Terrane and terranes with oceanic basements, which experienced important metamorphic and magmatic events and intense tectonism.

Since the Late Triassic, an environment of regional distension permitted the formation of grabens that were limited by normal faults, and important clastic sedimentary sequences, most of which were continental, were deposited, including the Girón Group, the Quinta Formation in serranía de Perijá, and the Luisa Formation. Some small marine incursions were detected, including the Payandé Formation, the Morrocoyal Formation in serranía de San Lucas, and the Batá Formation north of the Quetame Massif. Volcanism of quite varied composition, such as the Saldaña Formation, occurred during the Early Jurassic; this formation consists of banks of limestones, siltstones, and conglomerates that were intercalated with rhyolitic, dacitic, andesitic, and basaltic lavas. The fauna indicates a Late Triassic to Early Jurassic age (Mojica, 1980; Mojica & Macía, 1981).

An important Jurassic magmatism event affected the western boundary of the Chibcha Terrane and its eastern boundary in the Santander Massif. It includes several important batholiths in the SNSM that will be discussed below, the Rionegro Batholith, which was dated between 196 and 172 Ma in the Santander Massif; the Norosí and Guamocó Batholiths in Serranía de San Lucas; the Norosí and Guamocó Batholiths in serranía de San Lucas, which were dated between 187 and 174 Ma (Leal–Mejía, 2011); and the Segovia and Ibagué Batholiths along the eastern flank of the Central Cordillera, which were dated at approximately 189 and 166 Ma by U–Pb dating, respectively (Leal–Mejía, 2011; Bustamante et al., 2010, 2017). In the southern portion of the terrane, several intrusives were dated at 187–170 Ma (Jaramillo et al., 1980; Arango et al., 2015; Zapata et al., 2015). The Mocoa Monzogranite was dated between 181 and 170 Ma, and the Algeciras and Altamira monzogranites and Teruel Latite were dated between 172 and 169 Ma. Some of metamorphic rocks associated to these igneous bodies were attributed to La Cocha–Río Téllez Migmatitic Complex (Zapata et al., 2017).

A recent study by Rodríguez et al. (2017) showed that the so–called Ibagué Batholith actually consists of two bodies: one that was subjected to metamorphism and another that is exclusively igneous. A similar situation likely occurs in the southernmost region. The metamorphic rocks in the Tierradentro Gneisses and Amphibolites and La Cocha–Río Téllez Migmatitic Complex also likely belong to various units, albeit undifferentiated (see the discussion of the Yalcón Terrane below).

The massive volume of magma that intruded during the Jurassic stands out, being the most important magmatic event of the Colombian Andes.

During the Cretaceous, the Colombian East was affected by tectonic distension phenomena and strong subsidence, which enabled epicontinental marine sedimentation in a calm environment, reaching a thickness of 10 000 m in the Cundinamarca Basin. No unconformities have been detected in this sedimentary sequence; the magmatism is reduced to some small gabbro stocks, whereas metamorphism is totally absent. Thus, the characteristics of the Colombian East during the Mesozoic were very different from those of the terranes to the west.

4.6. Chibcha Terrane of the SNSM and La Guajira Peninsula (LGP)

The SNSM was divided into three different terranes in the overview by Etayo–Serna et al. (1983). From SE to NW, these terranes are the Sierra Nevada, Sevilla, and Santa Marta Terranes. In the LGP, the Baja Guajira, Cosinas, and Ruma Terranes have been proposed. Restrepo & Toussaint (1988) considered that the Sierra Nevada Terrane and sections of the Baja Guajira and Cosinas Terranes could be correlated with the Chibcha Terrane and that the Sevilla Terrane is quite similar to the Tahamí Terrane. According to Gómez et al. (2015a), the Sierra Nevada Terrane could be correlated with the Chibcha Terrane, whereas the Cosinas Terrane and the SE region of the Baja Guajira Terrane could be correlated with the Tahamí Terrane. According to these authors, the Santa Marta and Ruma terranes are included in the Caribbean Megaterrane.

As shown, the terminology that is used for the SNSM and LGP terranes is confusing. Indeed, a terrane such as Baja Guajira, as defined by Etayo–Serna et al. (1983), likely encompasses three different Terranes; similarly, the correlations with the Tahamí and Calima terranes that were proposed by Restrepo & Toussaint (1989) are not fully proven. Based on the above, the Sierra Nevada Terrane and SE section of the Baja Guajira Terrane are included in the Chibcha Terrane. The term "Kogi Terrane" ("Kogui" in Spanish) is proposed to name the assemblage that comprises the Sevilla Terrane and the metamorphic rocks in the midsection of the Baja Guajira and Cosinas Terranes. We also propose grouping the Santa Marta and Ruma Terranes into a single terrane, which could be called "Tairona" (Figure 1).

New geochronological studies and the increased mapping accuracy of some of these regions will help us improve the knowledge base regarding the SNSM and LGP Terranes, although much remains to be investigated.

The Chibcha Terrane in the SNSM is characterized by a Precambrian continental basement, typified by Los Mangos Granulites, which was U–Pb zircon dated at 971 Ma, the age of metamorphism (Ordóñez–Carmona et al., 2002); the Dibulla Gneiss, which was dated between 1184 Ma by isochron Rb–Sr dating (Cardona, 2003) and 1145 Ma by U–Pb zircon dating (Cordani et al., 2005); and several anorthosites, such as those of Niyala, Río Frío, Orihueca, and the Río Sevilla. Los Mangos Granulites and Dibulla Gneiss are assemblages of migmatites, granulites, amphibolites, orthogneisses, quartzites, and marbles. In the LGP, the SE region of the Baja Guajira Terrane is similar to the Chibcha Terrane in the SNSM, with the Jojoncito Gneiss U–Pb dated at 916 ± 19 Ma (Cordani et al., 2005).

The Chundua Formation, which consists of Carboniferous dark lutites, limestones, and sandstones, crops out in the Chibcha Terrane in the SNSM and is the only occurrence of Paleozoic sedimentites at this location. Indeed, the SNSM apparently lacks the typical Cambrian – Ordovician units that were affected by low–grade metamorphism and Devonian sedimentites that are characteristic of the Chibcha Terrane in the Eastern Cordillera and Santander Massif, although these units crop out in the serranía de Perijá to the SE of the SNSM.

Similar to other regions, the Chibcha Terrane in the SNSM was affected by an important Permian – Triassic magmatism event, with the volcanic–sedimentary Corual and Guatapurí Formations (Tschanz et al., 1974) and vast Jurassic batholiths such as the Central, Patillal, and Pueblo Bello Batholiths dated between 189 Ma and 171 Ma (Tschanz et al., 1974). In the southernmost section of the LGP, Jurassic sedimentites from the Cuisa and Cheterló Formations (Geyer, 1973) were intruded by the Ipapure Granodiorite (Renz, 1960).

5. Yalcón Terrane

5.1. Introduction

In this study, the existence of a new terrane called "Yalcón", which is characterized by Jurassic metamorphism, is proposed. Previously, the Yalcón Terrane had not been differentiated from the Chibcha Terrane or the Tahamí Terrane. As shown below, the possibility of a new Jurassic terrane was proposed by Rodríguez et al. (2017) for the Anzoátegui region.

5.2. Discussion of the Southeastern Margin of the Central Cordillera

The metamorphic ages that were recently assessed by Ar–Ar (Blanco–Quintero et al., 2013) and U–Pb LA–MC–ICP–MS dating of the Tierradentro Gneisses and Amphibolites (Rodríguez et al., 2017) in La Cocha–Río Téllez Migmatitic Complex and Aleluya Metamorphic Complex (Hernández–González & Urueña–Suárez, 2017; Zapata et al., 2017) suggest the presence of a Jurassic metamorphic event on the western flank of the southern section of the Central Cordillera, a region that has been considered to belong to either the Chibcha Terrane or Tahamí Terrane.

Apparently, the ages that were assessed by these authors indicate that the protoliths of these metamorphic complexes have Early Triassic and Jurassic ages and that the metamorphism occurred during the Jurassic from 160 Ma to 144 Ma. This event was contemporary with the intense magmatism that affected this region, beginning with the volcanism of the Saldaña Formation and culminating with the intrusion of large batholiths, such as the Ibagué and Mocoa Batholiths and the Páez Quartz Monzodiorite, among other bodies. This observation is difficult to reconcile with the fact that Devonian sedimentites (such as those from Rovira) and Carboniferous sedimentites (including those from the Granadillo Mudstones and Limestones in the same region) have not been affected by metamorphism. The same occurs with the Triassic and Early Jurassic sedimentites in the Luisa and Payandé Formations.

In the Ibagué region, the Tierradentro Gneisses and Amphibolites, which mainly consist of quartz–feldspathic gneisses, amphibolites, hornblendic gneisses, granodioritic gneisses, and metatonalites, had been dated as Precambrian based on K–Ar dating by Barrero & Vesga (1976), with an age of 1360 ± 270 Ma, although another dating of this unit yielded an age of 171 ± 13 Ma. However, recent U–Pb–zircon datings by Bustamante et al. (2017) in this area indicated magmatic ages of 271 Ma for an orthogneiss and 234 Ma for an amphibolite. Conversely, Rodríguez et al. (2017) used the same method and found a younger age of 157.3 ± 2.6 Ma, which is considered to be an age of magmatic crystallization in amphibolites, whereas metamorphic zircon overgrowths indicated ages of 154.5 ± 3.6 Ma and 143.7 ± 1.5 Ma. These ages are close to the Ar–Ar ages by Blanco–Quintero et al. (2013) in amphiboles (146.5 ± 1.1 Ma and 157.8 ± 0.6 Ma) and phengite (146.5 ± 1.1 Ma) in the type section of the Cajamarca Complex. These data convincingly prove the existence of Jurassic metamorphism in the western portion of the Ibagué Batholith, as proposed by Blanco–Quintero et al. (2013) and Rodríguez et al. (2017). The Ibagué Batholith is intrusive in several locations in the Tierradentro Gneisses and Amphibolites and was U–Pb dated at approximately 145–138 Ma (Bustamante et al., 2017; Rodríguez et al., 2017). These data apparently contradict the very close presence of non–metamorphosed sedimentites from Rovira, which were paleontologically dated as Devonian, and the Luisa, Payandé, and Saldaña Formations, which were dated by both fossils and geochronology to the Late Triassic – Jurassic. Indeed, the Jurassic metamorphism had no effect on the Paleozoic and early Mesozoic sedimentites in the Chibcha Terrane, and the proximity of these metamorphic and sedimentary units cannot be explained by a simple lateral change in facies. The explanation for such paradoxes is one of the main characteristics of the notion of allochthonous terranes.

Rodríguez et al. (2017) postulated that the so–called Ibagué Batholith is not a single unit but actually comprises two different bodies. The first body consists of syntectonic or late tectonic intrusions called the Anzoátegui Metatonalite, which is associated with Tierradentro schists, quartzites, gneisses, and amphibolites and would have experienced metamorphism between 158.2 Ma and 150 Ma. The second body consists of granodiorites and quartz diorites called the Ibagué Tonalite, which intruded between 145 Ma and 138 Ma and did not experience metamorphism. These authors noted that the Chibcha Terrane was unaffected by Jurassic metamorphism and proposed the likely existence of a new terrane between the Chibcha Terrane and Tahamí Terrane.

Farther south, near Sibundoy, the so–called Granadillo Mudstones and Limestones, which consist of conglomerates, mudstones, limestones, and sandstones with Carboniferous fossils (Moreno–Sánchez et al., 2007), are in contact with metamorphic rocks that are attributed to the La Cocha–Río Téllez Migmatitic Complex, whose protoliths were dated by U–Pb zircon LA–ICP–MS between 235 Ma and 194 Ma, while the metamorphism was dated at 163.6 ± 4.7 Ma (Zapata et al., 2017). These results are similar to those in the Ibagué region and show an apparent geological incompatibility when disregarding the presence of two different terranes.

In the Palermo region, the Aleluya Metamorphic Complex, which is located 22 km to the west of Neiva, primarily consists of migmatites, quartzites, metasandstones, and marbles; U–Pb LA–ICP–MS dating indicated protolith ages between 235 Ma and 194 Ma, and the metamorphism of a granofels was dated at 169.1 ± 2.7 Ma (Zapata et al., 2017). The Saldaña Formation is in fault contact with the eastern edge of the Aleluya Metamorphic Complex and was U–Pb–dated between 188.9 and 172.9 Ma (Zapata et al., 2017). The Saldaña Formation is preceded in the same region by sedimentary deposits in the Luisa and Payandé Formations from the Early Triassic and Jurassic, so the hypothesis of a strong Middle Jurassic metamorphism is difficult to interpret when disregarding the presence of different terranes in this region. The precise position of the boundary between the terranes should be further studied.

García–Chinchilla & Vlach (2017) detected migrations of Mesozoic magmatic belts in the Garzón region. The oldest belt would have developed between 200 Ma and 183 Ma along the eastern flank of the Central Cordillera. Migration to the east would have subsequently occurred with intrusions between 176 Ma and 170 Ma, which would have affected the eastern portion of the Eastern Cordillera. This event would have been followed by a new event between 165 Ma and 130 Ma on the eastern flank of the Central Cordillera. These data support the hypothesis by Rodríguez et al. (2017) of the presence of two magmatic events along the eastern flank of the Central Cordillera. Based on the above, the first two events likely occurred in two different terranes, and the later event followed accretion.

On the eastern flank of the Central Cordillera, south of Mariquita, some units clearly belong to the Chibcha Terrane. On the one hand, units with low–grade metamorphism such as El Hígado and Río Nevado Formations have Ordovician protoliths that were dated by the presence of graptolites, Devonian sedimentites in La Jagua and Rovira, and Carboniferous sedimentites from the Granadillo Mudstones and Limestones. On the other hand, some medium to high–grade metamorphic rocks also belong to Chibcha. For example, La Plata granitic orthogneiss (on the eastern flank of the Central Cordillera at around 2° 30’ N), which consists of anatectic granites, quartzofeldspathic gneisses, amphibolites, and granulites, was intruded by La Plata Tonalite, which was dated at 274.8 Ma by using the U–Pb LA–MC–ICP–MS method (Leal–Mejía, 2011), indicating that the high–grade metamorphism predated the Triassic. Near El Pital, Ibañez–Mejia et al. (2011) dated El Pital Migmatite at 1000 Ma and Las Minas augen gneiss at 990 ± 7 Ma by U–Pb LA–ICP–MS. These datings permit these units to be located within the Chibcha Terrane, as described here.

The hypothesis by Rodríguez et al. (2017) for the Anzoátegui region could be generalized to the entire eastern flank of the southern section of the Central Cordillera. Accordingly, the Tierradentro metamorphic rocks, syntectonic intrusion of the Anzoátegui Metatonalite, La Cocha–Río Téllez Metamorphic Complex, and Aleluya metamorphic rocks belong to a terrane that would have experienced Jurassic metamorphism in a compressive environment at a distance from the representative units of the Chibcha Terrane, which were not affected by this event. Some or all of the metamorphic units in the Cajamarca Complex in the southern region of the Central Cordillera are probably components of this terrane. We propose naming this set the “Yalcón Terrane”, which is the name of an indigenous ethnic group led by Cacica Gaitana, who opposed the Spanish conquistadors in the Timaná region, Huila. According to this hypothesis, Jurassic metamorphism occurred in the Yalcón Terrane, whereas the western edge of the Chibcha Terrane was too far from the metamorphic zone to be affected.

A change in the tectonic regime that was related to possible changes from a head–on W–E convergence to a more oblique N–S convergence between the oceanic and continental materials to the east is one likely cause of the features between the terranes. The two terranes would have joined slightly before the Jurassic magmatism, such as the Ibagué Tonalite, which would have affected both the eastern edge of the Chibcha Terrane and the western edge of the Yalcón Terrane. Accretion may have occurred earlier in the southernmost section.

The boundary between both terranes was partially lost because of these subsequent intrusions. Later, the original boundary would have been sectioned into various segments by a N–NE fault system that included the Ibagué, Cucuana, La Plata–Chusma, Aucayao, and San Francisco–Yunguillo Faults, among others (Figure 4). Other more recent faults also affected this region. The formations shown in Figure 4, Anabá, El Imán, Luisa, and Payandé, are paleontologically well–dated sedimentary sequences that belong to the Chibcha Terrane. All of them are older than the Jurassic metamorphic event (160–140 Ma) that affected the Yalcón Terrane. The presence of older unmetamorphosed sedimentary sequences and younger metamorphic sequences in close proximity shows one of the essential characteristics of the terrane concept: this contiguity cannot be explained without the presence in this region of two different terranes, Chibcha and Yalcón; the metamorphism took place in the Yalcón Terrane before the terranes were close by, not affecting the sedimentary rocks of the Chibcha Terrane. In the southernmost section, the width of Los Andes narrows with the confluence of the three cordilleras. Apparently, the southern sections of the Chibcha and Andaquí Terranes end in this region and are not present in Ecuador. This observation would imply that the Yalcón Terrane, which is apparently correlated with the Salado Terrane in Ecuador (Litherland et al., 1994), would be in direct contact with the Amazonian Craton. Subsequent studies should more precisely determine the location of the terranes in this region.

Regardless of the proposed explanations for the Jurassic metamorphism on the eastern edge of the central Andes, the southern section of the Central Cordillera shows fundamental differences between the Yalcón Terrane and Tahamí Terrane. Thus, Permian – Triassic metamorphism is characteristic of the Tahamí Terrane, whereas Jurassic metamorphism is characteristic of the Yalcón Terrane. Subsequent studies, particularly geochronological studies, should focus on locating the boundaries between these terranes.

5.3. Yalcón Terrane's Characteristics and Boundaries

Based on the above discussion, we propose the presence of the Yalcón Terrane in the southern section of the Central Cordillera, with the following characteristics. The lithology of the Yalcón Terrane primarily consists of Jurassic metamorphic rocks that include a portion of the Cajamarca Complex, which has graphitic, chloritic, and muscovitic schists and some amphibolites, quartzites, and marbles. The rocks from this sequence were dated as Jurassic in age (Blanco–Quintero et al., 2013), as mentioned above, and include metamorphic rocks that are associated with the Tierradentro Gneisses and Amphibolites, La Cocha–Río Téllez Migmatitic Complex, metamorphic rocks from the Aleluya Metamorphic Complex, the Anzoátegui Metatonalite, and the metamorphic components of the Ibagué and Mocoa Batholiths, which have not yet been separated from their igneous sections.

As previously discussed, the boundary between the Chibcha Terrane and Yalcón Terrane is partially blurred by post–accretion Jurassic intrusions. However, this boundary may be located near the Avirama and Inzá Faults, which have early Paleozoic or Mesozoic sedimentary rocks that belong to the Chibcha Terrane on their eastern side and Jurassic metamorphic units from the Yalcón Terrane on their western side. The presence of several tectonic imbrications complicates the definition of the boundary. The original boundary was then displaced by an NNE fault system and, particularly in the southernmost region, Cenozoic faults. Accretion into the Chibcha Terrane occurred at the end of the Jurassic, probably through a network of N–NE dextral faults, which matches geotectonic models that have been proposed for that time (e.g., Pindell et al., 2012).

The western boundary of the Yalcón Terrane is represented by the Silvia–Pijao Fault, which separates this area from the Quebradagrande Terrane or some small flakes of the Tahamí Terrane.

The northern boundary with the Tahamí Terrane is difficult to locate, mostly because of the lack of reliable geochronological data for the metamorphic rocks in the Cajamarca Complex at latitudes near the Armenia–Ibagué road or farther north. Nevertheless, the data clearly indicate that the term "Cajamarca Complex" should no longer be used because this unit consists of metamorphic rocks that belong to two terranes. The Permian – Triassic metamorphic rocks in the Tahamí Terrane should be regrouped into a new lithodemic unit that we propose to denominate the "Antioquia Complex", and the metamorphic rocks in the Yalcón Terrane should be regrouped into another new unit that we propose to name the "Coello Complex", based on the name of the river that crosses the city of Cajamarca. In the Antioquia Complex, most of the rocks from the Ayurá–Montebello Group as defined by Botero (1963) would be included, but the amphibolites and the zone that comprises a portion of the Anacona Terrane would be excluded. Additionally metamorphic rocks are present in the NW section of the Central Cordillera, which were named the "Valdivia Group" by Hall et al. (1972), and the eastern side of the Central Cordillera, which were described by Feininger et al. (1972) as "Metamorphic rocks of the Central Cordillera" (west of the Otú Fault). These rocks include quartz–muscovite schists, quartz–feldspar paragneisses, granitic orthogneisses, quartzites, amphibolites, and marbles. However, some of the rocks in the southern portion of the area that were studied by these authors could belong to the Jurassic Yalcón Terrane and thus would be components of the Coello Complex.

In the Coello Complex, the majority of rocks are greenschists and quartz–muscovite schists with graphite, such as the rocks along the Armenia–Ibagué road from the Pericos Fault to La Línea pass (latitude 4° 30' N).

As originally defined along the Armenia–Ibagué highway (Maya & González, 1995), the Cajamarca Complex mostly consists of greenschist–facies metamorphic rocks, typically greenschists and graphite–quartz–muscovite schists that are

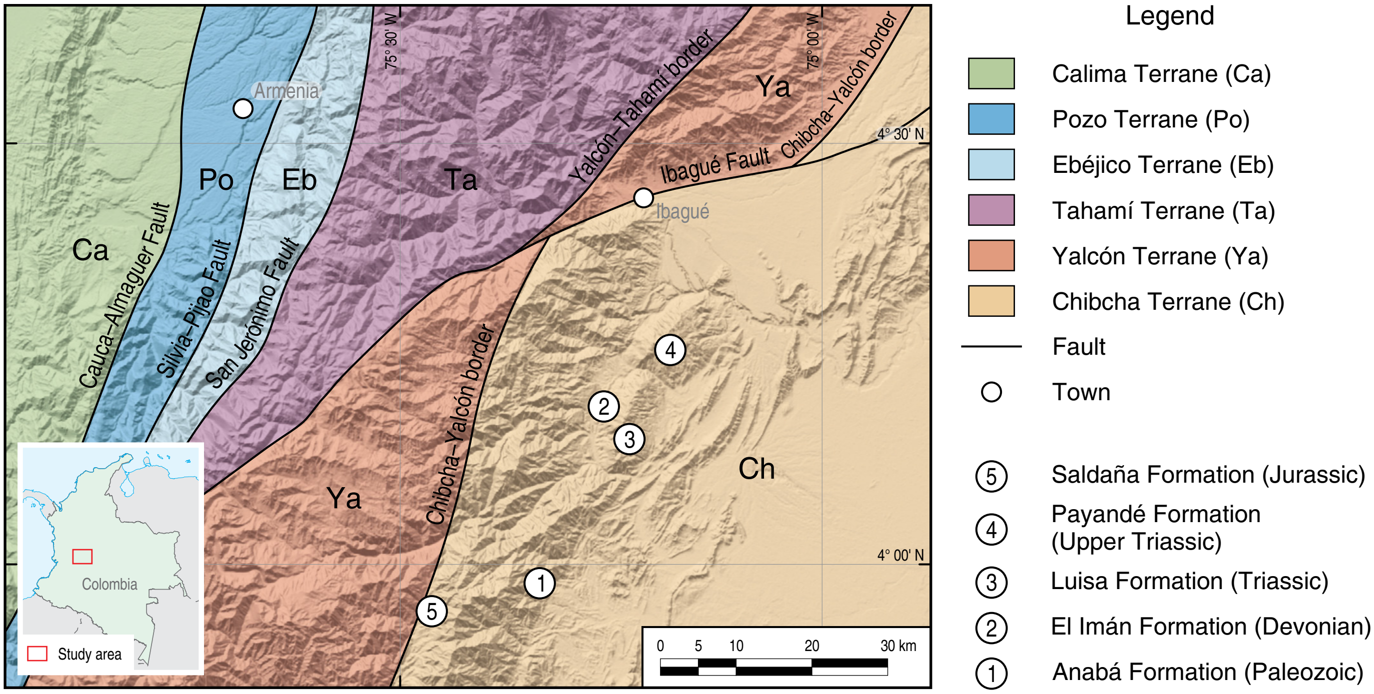

Figure 4. Schematic map of terranes and faults in the Ibagué area.

locally known as "blackschists". Rocks that were Ar–Ar dated by Blanco–Quintero et al. (2013) to the Jurassic were obtained from this sequence. More samples must be dated along this roadcut to see if the entire sequence is Jurassic or if two different units with similar aspects are present. Close to the top along the western limit, La Línea Gneissic Granite, which was dated at 236.2 ± 6.3 Ma (Cochrane, 2013), shows that this gneiss is a component of the Permian – Triassic units, so the Tahamí Terrane extends south to at least latitude 4° 28' N.

We tentatively propose that the Tahamí Terrane be restricted to the areas where Permian – Triassic metamorphic rocks are present, whereas the areas where Jurassic metamorphic rocks crop out would belong to the Yalcón Terrane. The exact boundaries of these terranes are currently uncertain.

Future studies should aim to identify the metamorphic units that were affected by Permian – Triassic metamorphism and those that were affected by Jurassic metamorphism to best define the boundary between the Tahamí and Yalcón Terranes.

6. Tahamí Terrane

6.1. Introduction

The Tahamí Terrane forms a large portion of the northern Central Cordillera, although small blocks may be present along the western flank of the southern Central Cordillera. In the first sketch of Colombian terranes that was prepared by Servicio Geológico Colombiano (Etayo-Serna et al., 1983), this area was assigned to two terranes, namely, the Puquí and Cajamarca, whereas Restrepo & Toussaint (1988) initially named this area the "Central Andean Terrane", which would comprise a polymetamorphic complex with ages ranging from the Precambrian(?) to Permian – Triassic. This terrane was later called "Tahamí" based on one of the most important indigenous cultures in the area at the arrival of the Spanish conquerors (Toussaint & Restrepo, 1989). According to Gómez et al. (2015a), the depicted Tahamí Terrane is quite similar to that proposed by Toussaint & Restrepo (1989).

6.2. Characteristics

This terrane generally consists of metamorphic rocks that were intruded by plutons with ages from the Triassic to Paleogene and minor Mesozoic sedimentary sequences. The metamorphic rocks consist of greenschists and graphite–muscovite–quartz schists (locally called "blackschists"), quartzites, and marbles. However, higher–grade rocks, mostly migmatites and amphibolites, are also present; locally, granulites are found in high–grade areas (Restrepo & Toussaint, 1985; Rodríguez et al., 2005). Syntectonic orthogneisses that were dated close to 240 Ma, such as the Samaná, Abejorral, Naranjal, and Palmitas Gneisses, intruded the metasedimentary sequence (Villagómez, 2010; Cochrane, 2013; Restrepo et al., 2011; Vinasco et al., 2006; Ibañez–Mejia et al., 2008). Although several formational names have been assigned to these metamorphic units, such as the Ayurá–Montebello Group (Botero, 1963), Cajamarca Group (Nelson, 1962), and Valdivia Group (Hall et al., 1972), the name that is presently used for these metamorphic rocks is the "Cajamarca Complex" (Maya & González, 1995). However, as previously described, the nature and extension of this complex must be reassessed.

Initial K–Ar and Rb–Sr datings for the Cajamarca metamorphic rocks yielded Permian – Triassic ages with large errors (i.e., Restrepo et al., 1991). Recent U–Pb dating in zircons yielded mostly Triassic ages for syntectonic granitic intrusions, migmatites, and amphibolites (Ibañez–Mejia et al., 2008; Restrepo et al., 2011; Cochrane et al., 2014b; Martens et al., 2014). These ages are close to 240 Ma and are interpreted as the time of the peak temperature of the metamorphism; some datings yielded younger ages close to 227 Ma, which may indicate a second metamorphic peak (Restrepo et al., 2011). In pre–tectonic intrusions, the magmatic ages in the zircons ranged from 277 to 267 Ma, whereas the metamorphic rims yielded ages from 236 to 227 Ma (Restrepo et al., 2011). With these results, the orogeny that affected the Tahamí Terrane extended at least from 277 to 227 Ma, thus confirming early assessments that this event was a Permian – Triassic orogeny (i.e., Hall et al., 1972).

A different chronological explanation was provided for these events by Vinasco et al. (2006), for whom the older ages (300–270 Ma) would be the age of metamorphism and the younger ages (ca. 250 Ma) would be magmatic ages; however, their article contained no images of the zircons to support the idea.

The great majority of these datings were undertaken on metaigneous rocks. In this sense, the dating of the metasedimentary Las Palmas Migmatite (Restrepo et al., 2011; Martens et al., 2014) is interesting in that the youngest detrital zircons indicate a maximum Carboniferous sedimentation age of 335 Ma (Restrepo et al., 2011). With this age, the proposals that the sedimentation or metamorphism was Precambrian (i.e., Nivia et al., 2006) or lower Paleozoic in age (Cediel et al., 2003) should be reevaluated. In addition, the presence of crinoids in marbles near the Palestina Fault (Patarroyo et al., 2017) precludes a Precambrian age for the protoliths (Silva–Tamayo et al., 2004).

Although a peak of approximately 240 Ma is presently widely accepted for the age of metamorphism, no datings of the metamorphism by this method have been conducted on medium–grade metasedimentary rocks. The initial metamorphism of some of these units occurred at a medium–pressure baric type followed by a low–pressure metamorphic environment (Montes & Restrepo, 2005), so two metamorphic peaks may have occurred within a short time. With a Carboniferous maximum sedimentation age, the first peak would have occurred during the Permian or Early Triassic.

The oldest post–tectonic stocks that intruded the metamorphic rocks are small granodioritic bodies such as El Buey and Montebello Stocks, which have Late Triassic ages (González, 1980; Vinasco et al., 2006). This terrane has a magmatic gap between the Jurassic and Early Cretaceous. The main intrusives are Late Cretaceous tonalites and granodiorites, including the Antioqueño Batholith (Feininger & Botero, 1982), which has an area of approximately 7000 km^2 and U–Pb ages from 93.5 to 58 Ma (Ordóñez–Carmona et al., 2008; Ibañez–Mejia et al., 2007; Restrepo–Moreno et al., 2007; Villagómez, 2010; Leal–Mejía, 2011). Some small stocks in the Medellín Valley are probably the first intrusions of this magmatism and include the Altavista Stock and San Diego Gabbro (96 Ma and 94 Ma, respectively, according to U–Pb dating; Correa et al., 2006).

Four magmatic pulses from the Late Cretaceous – Paleocene were defined by Leal–Mejía (2011): 96–92 Ma, 89–82 Ma, 81–72 Ma, and 63–58 Ma. As discussed below, the last pulse seems to have been generated by a different subduction zone, so its appurtenance to the Antioqueño Batholith proper can be questioned. Some of the small Cretaceous stocks are located on the westernmost side of the Tahamí and are cut by the Cauca–Almaguer Fault, as with the Honda Stock (76.4 Ma; Giraldo–Ramírez, 2017). On the eastern side, La Culebra Stock, which was dated at 87.5 Ma (Leal–Mejía, 2011), is truncated by the Otú Fault, indicating that the Otú Fault was still active after the beginning of the Late Cretaceous magmatism. The area where these intrusives crop out extends approximately 100 km in a W–E direction, indicating a low–angle subduction zone. As discussed below, the Tahamí Terrane was completely amalgamated into the composite craton plus the Chibcha and Yalcón Terranes during the Late Cretaceous. On the western side of the Tahamí, the Quebradagrande, Arquía, and Calima Terranes were accreted at approximately that time, and the younger magmatism was therefore generated by a more westward subduction zone, presumably with the Caribbean Plateau subducting under the Tahamí Terrane and the recently accreted terranes (Bayona et al., 2012). Paleocene – Eocene intrusives such as the Sonsón Batholith (61–56 Ma; Ordóñez–Carmona, 2001; Leal–Mejía, 2011; Cochrane, 2013), Manizales Stock (59.8 Ma; Bayona et al., 2012), El Hatillo Stock (54.6 Ma; Bayona et al., 2012), and Santa Barbara Batholith (60–58 Ma; Ordóñez–Carmona et al., 2011; Cochrane, 2013) are distributed along the entire width of the Central Cordillera, also indicating a shallow subduction zone (Bayona et al., 2012). A special mention is deserved for Paleocene intrusives within the Antioqueño Batholith (63–58 Ma; Leal–Mejía, 2011). These small intrusions are responsible for important gold mineralizations within the Antioqueño Batholith, such as Gramalote near San Roque, Antioquia (Leal–Mejía, 2011).

At the end of the Paleocene – Eocene plutonism, the area remained free of magmatism until the present volcanic chain initiated at approximately 4.3 Ma (Thouret et al., 1990) along the axis of the Central Cordillera, including the Tahamí Terrane. Small intrusions along the eastern flank of the range such as the Río Dulce Porphyries near Nariño, Antioquia, which were dated at 2.3 Ma (Leal–Mejía, 2011), may be the roots of the northern extension of this volcanism.

Locally, marine sedimentary rocks are present in the Tahamí Terrane. The oldest rocks are Late Jurassic (Tithonian) sedimentites known as the Valle Alto (González et al., 1977) and Aquitania sedimentary formations (Giraldo et al., 2015), whereas the youngest are Cretaceous in age and include La Soledad,

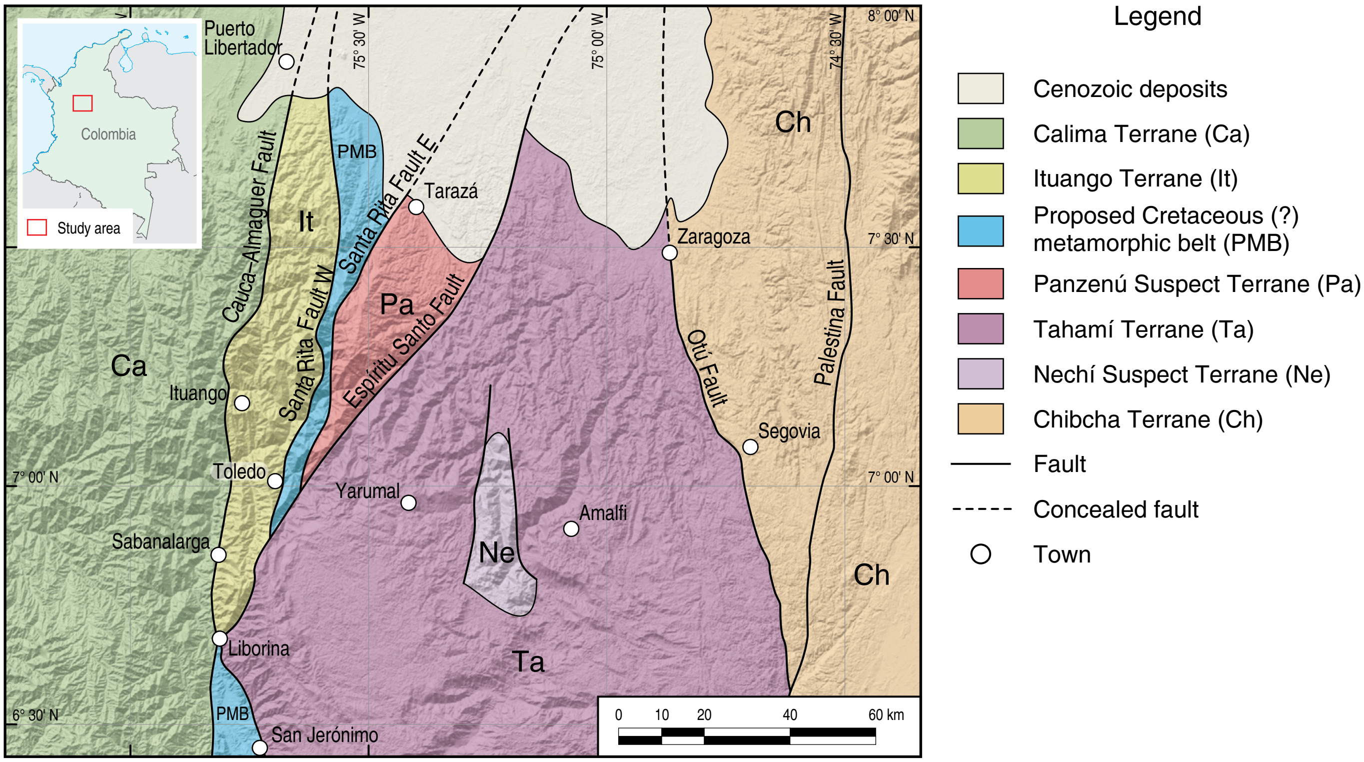

Figure 5. Schematic map of the hypothetical terranes in the northern portion of the Central Cordillera, freely adapted from Gómez et al. (2015a).

San Luis, and Abejorral Formations, which have Hauterivian to Albian ages (Bürgl & Radelli, 1962; Feininger et al., 1972); this sedimentation ceased during the Albian. Although some of the units are intensely folded, mineralogical metamorphism is not present. This compressive tectonic event occurred before the intrusion of the Antioqueño Batholith. A clearly different tectonic environment was found in the Chibcha Terrane, where thick sedimentation occurred in a distensive setting throughout the Late Cretaceous.

6.3. Extension and Boundaries

As originally defined, the Tahamí Terrane was separated in its northern section from the Chibcha Terrane to the east by the Otú Fault and at the latitude of Ibagué by the Pericos Fault, which was believed to be the southern extension of the Otú Fault (Restrepo & Toussaint, 1988). These are strike–slip faults with unknown displacements. A right–lateral displacement was assigned to the Otú Fault (Feininger, 1970). This fault was displaced around 28 km by the Palestina Fault, which is a right–lateral fault (see Feininger, 1970) and locally becomes the terrane's boundary. Many important geological differences are found on both sides of the boundary faults of the terrane, as shown in Table 1.

An area with no clarity regarding the extension and limits of the Tahamí is the exposed metamorphic rocks of the Ituango area in the NW portion of the terrane (Figure 5). On the one hand, low–grade metamorphic rocks such as metagreywackes, metasandstones, and slates with some ultramafic rocks are found at the Taque Creek, near Valle de Toledo, which could be younger than the Triassic, suggesting that the limit of the terrane is to the east of this locality. On the other hand, medium–grade metamorphic rocks are present to the west, such as the Pescadero Gneiss (Muñoz, 1980), which was dated by an Rb–Sr isochron at 253 ± 10 Ma (Restrepo et al., 1991), and "blackschists", which are similar to the Ancón Schists that consist of quartz, muscovite, and andalusite; the latter are located near Medellín and were dated by an Rb–Sr isochron at 226 ± 4 Ma (Restrepo et al., 1991). In addition, the presence of high–grade metamorphic rocks from the Panzenú Suspect

Table 1. Comparison of the main differences between the Chibcha, Yalcón, and Tahamí Terranes.

Geological units	Tahamí Terrane	Yalcón Terrane	Chibcha Terrane
Upper Cretaceous batholiths	Present	Absent	Absent
Jurassic mafic volcanic rocks	Absent	Absent	Present
Jurassic batholiths	Absent	Present	Present
Jurassic metamorphism	Absent	Present	Absent
Triassic syntectonic intrusives	Present	Absent	Absent
Upper Paleozoic metasedimentary rocks	Present	Absent	Absent
Lower Paleozoic metasedimentary rocks	Absent	Absent	Present
Precambrian metamorphic rocks	Absent	Absent	Present

Terrane to the east of this zone complicates the definition of the terranes in this area. The presence of small ultramafic lenses between these two blocks may indicate a complex limit. One possibility is that the Ituango area is a displaced Tahamí block that was moved north by transcurrent faults (Santa Rita faults?) and placed in contact with a sliver of metamorphic rocks of unknown age (Cretaceous?) that separate it from the Panzenú Terrane; several serpentinite bodies along the Santa Rita fault were indicated by Álvarez et al. (1970). In fact, west of Tarazá, small blocks of Quebradagrande–like rocks are shown in the geologic map of Colombia (Gómez et al., 2015a) to the west of the Panzenú Suspect Terrane and to the east of the metamorphic rocks of Ituango. In any case, this area must be studied in more detail to define the ages and contacts of the various metamorphic rocks and the evolution of this complex area.

Another difficulty in defining the Tahamí Terrane comes from the recent datings in the Central Cordillera, which showed the presence of Jurassic metamorphic rocks (Blanco–Quintero et al., 2013; Bustamante et al., 2017; Rodríguez et al., 2017; Zapata et al., 2017). These data challenge the assignment of a large portion of the central and southern Central Cordillera to the Tahamí Terrane. As discussed above, these new data led to the definition of a new terrane, namely, the Yalcón Terrane.

The area of the Central Cordillera south of approximately 4° 30' N has been less studied than the northern area, where most of the datings correspond to Cenozoic magmatic rocks. No Permian – Triassic datings of metamorphic rocks of what has been called the Cajamarca Complex have yet been found at this location, although metaigneous rocks of that age have been reported in the Arquía Complex to the west (Rodríguez & Arango, 2013). Although several geological facts are used to define the Tahamí Terrane, as discussed below, the presence of Permian – Triassic metamorphic rocks is an important indicator of this terrane.

The possibility that both Permian – Triassic and Jurassic metamorphic rocks with different origins are present in the Tahamí Terrane and Cajamarca Complex necessitates redefining both the terrane and the complex.

6.4. Geological History

Several models have been proposed to explain the Triassic orogeny that generated the basement of the Tahamí Terrane. A collisional model formed from the closure of Pangea was proposed by Vinasco et al. (2006). In this model, the Tahamí would have been located between Venezuela and the present Florida peninsula as a component of the Appalachians. In this context, explaining the migration of the Tahamí to its present position is difficult because this scenario implies movement contrary to that of the Caribbean Plate and the rest of terranes.

A very different model, where rifting after closure would have uplifted mantle material to heat the sedimentary sequence and produce extensional metamorphism, was proposed by Cochrane et al. (2014b). In this model, explaining the formation of the Aburrá ophiolites is difficult because a marginal basin would be required at approximately 228 Ma (Restrepo et al., 2007), when the area was supposedly completely surrounded by continental crust (Cochrane et al., 2014b). A third model positions the Tahamí along the western margin of Pangea, with an eastward–dipping subduction zone of Pacific crust (Cardona et al., 2010; Restrepo et al., 2011). This model does not exclude an extensional regime at some time.

According to the detrital zircon geochronology of Las Palmas migmatitic paragneisses, the Tahamí Terrane is related to the Loja and Amotape Terranes in Ecuador and perhaps to the Eastern Cordillera in Perú and the Chiapas Massif within the Maya Block in southern México and Guatemala (Martens et al., 2014). These terranes were probably contiguous during the closure of Pangea and were then dispersed to their present positions.

According to most models (i.e., Kennan & Pindell, 2009 and references therein), the terranes in western Colombia have moved northward from their original position in Ecuador or Perú. Thus, researchers have called the Tahamí and Chibcha "parautochthonous" terranes; however, a better designation would be "displaced" terranes because displacements occurred along transcurrent faults.

The age of the final docking of the Tahamí Terrane is believed to have been the Late Cretaceous (Toussaint & Restrepo, 1989). For example, in the northern portion of the Central Cordillera, both sides of the Otú Fault have been affected by Late Cretaceous magmatism. In the Segovia–Remedios mining district in the Chibcha Terrane, dikes that were related to Au mineralization have been dated between 89 and 85 Ma (Leal–Mejía, 2011). In the Tahamí Terrane, the Culebra Stock was dated at 87.5 Ma (Leal–Mejía, 2011). However, the truncation of the Culebra Stock indicates that the Otú Fault experienced important movements after the emplacement of this stock.

6.5. Panzenú Suspect Terrane

This suspect terrane was proposed by Ordóñez–Carmona & Pimentel (2002) for the Puquí Complex at the northern end of the Tahamí Terrane (Figure 5). This terrane consists of high–grade metamorphic rocks, including migmatites, gneisses, amphibolites, and granulites. The block is limited by the Espíritu Santo Fault to the south, the Murrucucú Fault to the north, and undetermined faults to the east and west.

The main reason for proposing this terrane seems to be the Rb–Sr isochron age for the gneiss of 306 ± 11 Ma compared to the Triassic ages found in the Tahamí Terrane. However, this terrane is herein listed as a suspect terrane until U–Pb datings for the metamorphism are available.

6.6. Possible Correlation between the Kogi Terrane in the SNSM and LGP and the Tahamí Terrane

The Kogi Terrane in the SNSM and LGP corresponds to the Sevilla Terrane and a portion of the Baja Guajira Terrane as defined by Etayo–Serna et al. (1983) and was included in the Tahamí Terrane in Toussaint & Restrepo (1989). This new terrane is proposed here because the correlation with the Tahamí Terrane is insufficiently proven.

The Kogi Terrane, which is separated from the Chibcha Terrane in the SNSM by a complex fault system that is associated in some areas with intense mylonitization, is characterized by assemblages of quartz–feldspathic gneisses, amphibolites, migmatites, schists, and marbles. These rocks are mainly the Muchachitos Gneiss, which was U–Pb dated between 276 and 288 Ma (Cardona et al., 2010); the Buritaca Gneiss, which was Ar–Ar dated at 147 ± 6 Ma (Cardona et al., 2006); the Sevilla Complex, for which a schist was Ar–Ar dated at 185.8 ± 1 Ma (Cardona et al., 2006); and the San Pedro metamorphites, which were intruded by granodiorites such as the Paleocene Buritaca and Latal plutons. In the LGP, these rocks include the Macuira Gneiss, which was dated at 265 Ma and was intruded by the Ar–Ar–dated 165.8 Ma Siapana Granodiorite (Cardona, 2003), and the Jaturuhu Schists and Uray Gneiss, which were U–Pb dated at 245.6 ± 3.9 Ma (Weber et al., 2010). These datings present a fairly large age range from the early Permian to the Late Jurassic, although these ages indicate some similarity to the Tahamí Terrane, which was also affected by Permian – Triassic metamorphism.

In the SNSM, the boundary between the Kogi and Chibcha Terranes is marked by complex tectonic imbrications that correspond to the Sevilla Fault System. These faults are a set of NW–dipping reverse faults, although dextral movements have also occurred. The great Jurassic batholiths did not affect the Kogi Terrane, in contrast to Eocene magmatism, such as that in the Buritaca Batholith, which was U–Pb dated at 50.8 Ma (Duque, 2010) and crosses the boundary. In the LGP, the boundary between the Kogi and Chibcha Terranes is marked by a set of tectonic imbrications with Cretaceous flakes of sedimentary rocks, such as those in the Poschachi Formation, thus suggesting subsequent movements in the boundary between these terranes.

In the SNSM, the Tairona Terrane is connected to the Kogi Terrane by a network of unnamed reverse faults, several of which run oblique to the original boundary. The Buritaca Pluton apparently crosses the boundary between these terranes, thus suggesting a union in the early Paleocene – Eocene range. In the LGP, the Tairona Terrane is limited to the SE side by the Simarua–Osorio Fault, which shows strong mylonitization and overthrusts onto the Kogi Terrane. Eocene reef limestones that are associated with marls, mudstone, and sandstone from the Uitpa Formation cover the boundary, which indicates that the union between the Tairona and Kogi Terranes occurred during the Late Cretaceous – Paleocene .

6.7. Continental Terranes in the Cauca–Romeral Fault Zone

The Cauca–Romeral Fault Zone is located at the boundaries between the continental and oceanic basements. Within this zone, several small terranes of both continental and oceanic nature are found. Their locations approximately correspond to the Cauca–Romeral Terrane that was mapped by Etayo–Serna et al. (1983). But this area with high–tectonic complexity, is not a terrane but an aggregate of small terranes of different ages. The continental and oceanic domains have been subjected to constant transpression and distension since the Cretaceous, and their boundaries have broken, forming a mosaic of small terranes that are separated from their places of origin. Continental terranes such as the Anacona and Amagá–Sinifaná Terranes and possible Tahamí Terrane flakes and oceanic terranes, including the Ebéjico (Quebradagrande) and Pozo (Arquía) Terranes, among others, are located in this fault zone (Figure 6). This study aims to change the names of several of these terranes to avoid confusion with the names of pre–existing formations, groups, and complexes. The continental terranes of the Cauca–Romeral Fault Zone are the Anacona, Amagá–Sinifaná, and Guaca Terranes.

The small Anacona Terrane is located approximately 25 km south of Medellín between the Tahamí and Ebéjico (Quebradagrande) Terranes (Figure 7). This terrane consists of garnetiferous amphibolites, quartzites, kyanite–staurolite–garnet–biotite schists, and chlorite–muscovite schists that were intruded by an S–type granite, which converted later into a gneiss. The magmatic stage of the gneiss yielded Ordovician ages from U–Pb zircon dating (Martens et al., 2014), whereas an Ar–Ar age of ca. 360 Ma was obtained in hornblende from the Caldas Amphibolite (Restrepo et al., 2008) and age of 344 Ma was obtained in muscovite from La Miel Gneiss (Vinasco et al., 2006). These later ages are considered to mark the time of cooling after the metamorphism that affected the granite; these Ar spectra show that the terrane was not affected by the Tahami's Triassic metamorphism. Thus, the autochthonistic hypothesis that La Miel Gneiss is the basement of the Cajamarca Complex (Villagómez et al., 2011) is not plausible. The eastern boundary with the Tahamí Terrane is marked by the Santa Isabel Fault, and the western boundary with the Ebéjico (Quebradagrande) Terrane is marked by the San Jerónimo Fault. Further discussion of this terrane is provided by Restrepo et al. (2020).

The Amagá–Sinifaná Terrane is limited by faults in the Romeral Fault Zone. The Silvia–Pijao Fault to the east separates this terrane from the Quebradagrande Terrane, and the Amagá Fault to the west separates this terrane from the Guaca Terrane. This terrane consists of very low–grade metamorphic rocks that are known as the Sinifaná Metasedimentites (González, 1980)

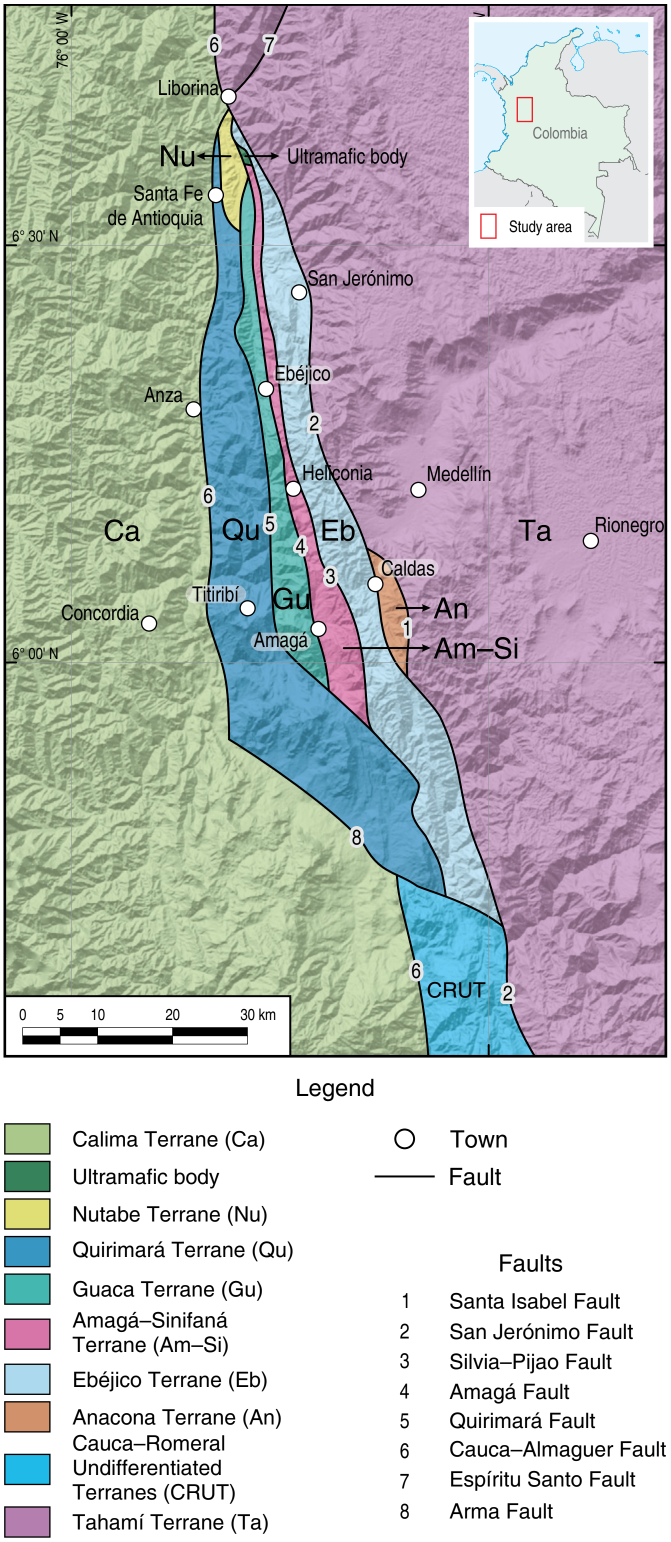

Figure 6. Schematic map of the small terranes in the Cauca–Romeral Fault Zone.

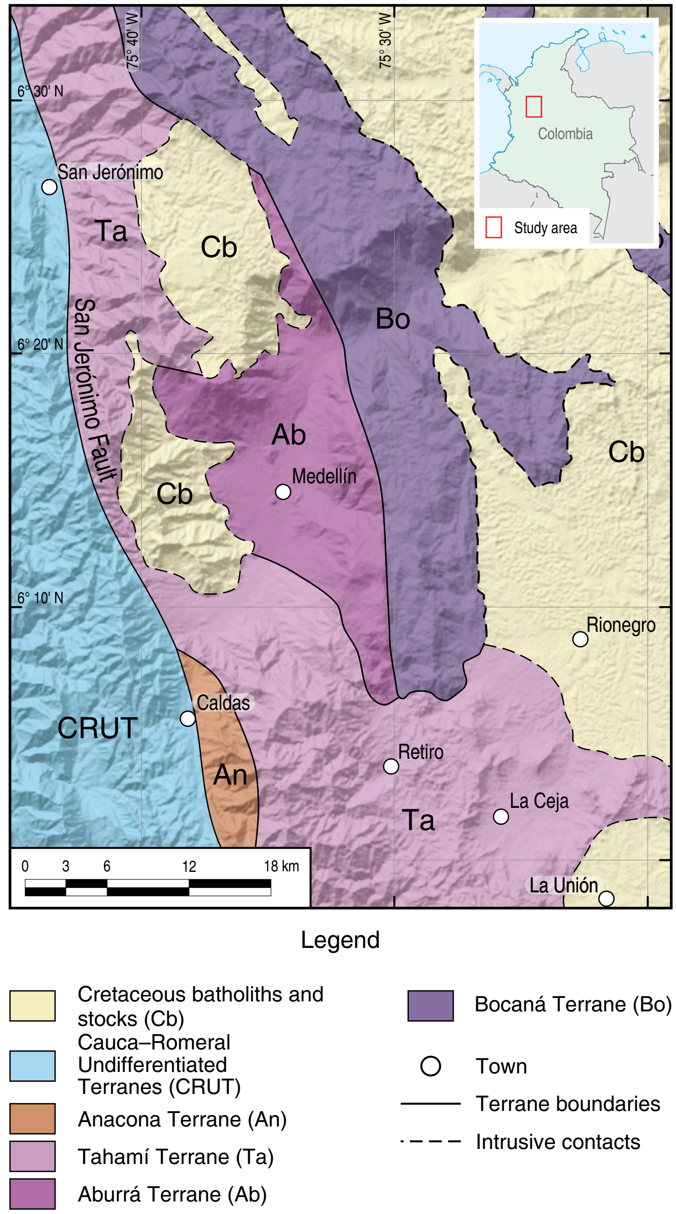

Figure 7. Schematic map of the terranes in the Medellín area.

and the Amagá granite stock, which intrudes the metasedimentites with the formation of a contact aureole. Detrital zircons from the metasedimentites were dated by Martens et al. (2012) and showed a strong affinity with zircons from the Cajamarca Complex; an Early Triassic maximum age of sedimentation was obtained. The Amagá granitic stock was dated by U–Pb in zircons with an age of 228 Ma (Vinasco et al., 2006), showing that the very low–grade metamorphism occurred between 290 and 228 Ma. Martens et al. (2012) proposed that this area is a sliver of the Cajamarca Complex that was moved northwestward by the Romeral Fault System. Amagá and Sinifaná are autochthonous indigenous names.

A somewhat similar situation is found west of Manizales, where the Chinchiná Gneiss (Mosquera, 1978; Puerta–Moreno, 1990) or Manizales Migmatite (Idárraga–García & Martínez–Uribe, 2005), which was dated at 224.7 ± 1.9 Ma (Cochrane, 2013), is in contact with the Pozo Terrane along the Silvia–Pijao Fault to the west and the Ebéjico (Quebradagrande) Terrane to the east along a nameless fault (Figure 8). In this case, within the Cauca–Rome-

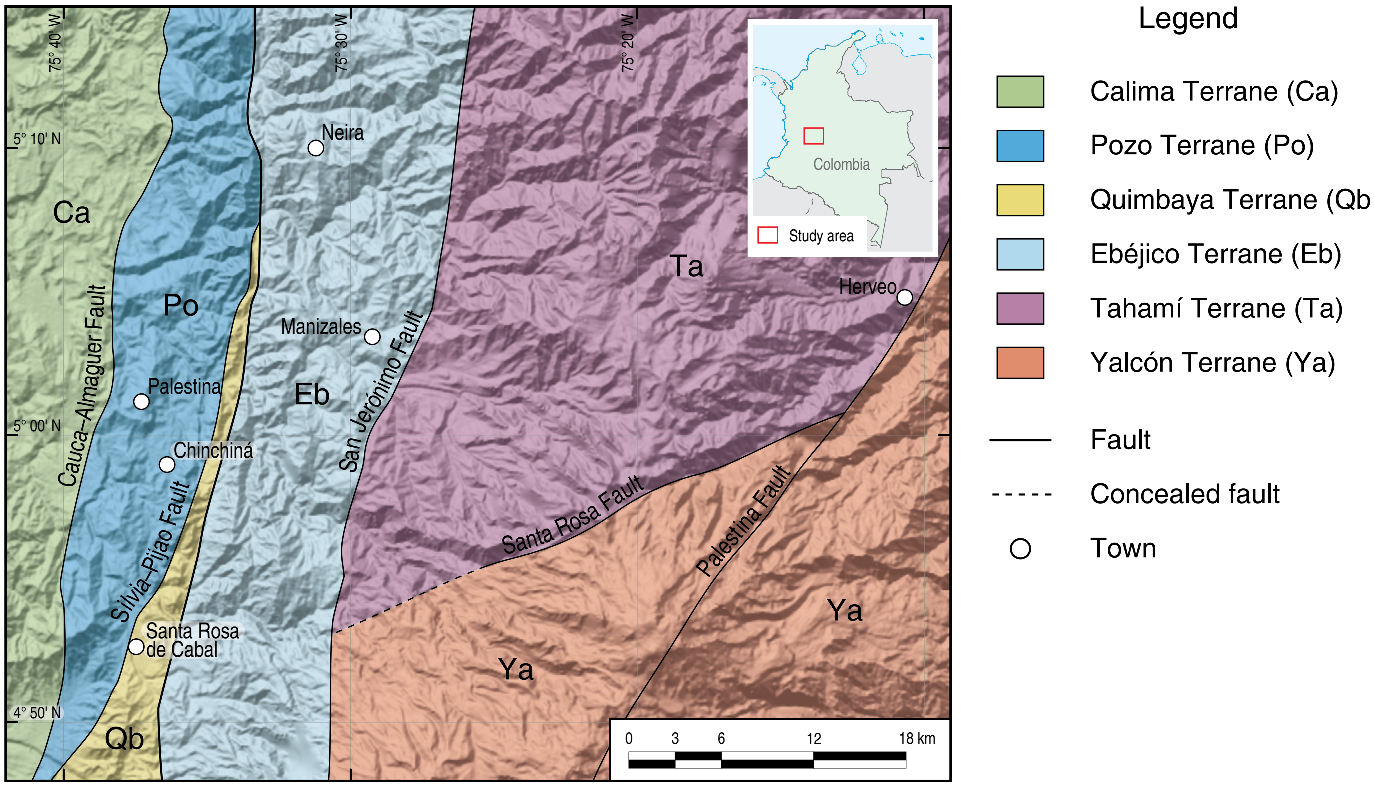

Figure 8. Schematic map of the Quimbaya Terrane in the Manizales area.

ral Fault Zone a high–grade block correlatable to the Cajamarca Complex was tectonically inserted. This block fulfills the definition of a terrane, and we propose calling this terrane the "Quimbaya Terrane" after one of the most known pre–Columbian tribes of this area.

The Guaca Terrane consists of the Pueblito Diorite within the Romeral Fault Zone and is separated from the Amagá–Sinifaná Terrane by the Amagá Fault to the east and the Quirimará oceanic Terrane (Sabaletas Schists) by the Quirimará Fault to the west. Ultramafic bodies are found along the Amagá Fault (González–Ospina, 2016). The diorite was dated by U–Pb zircons to the Triassic (233–236 Ma; Rodríguez–Jiménez, 2010). The Amagá Granite has a similar age but is geochemically an S–type granite (Vinasco et al., 2006) and is not comparable to the diorite. Guaca, an indigenous word, was the original name for the municipality of Heliconia, where most of the diorite is located.

7. Conclusions Regarding the Continental Terranes

The area within the Cauca–Romeral Fault Zone in Colombia consists of a mosaic of continental terranes, including the Andaquí, Chibcha, Yalcón, Tahamí, Kogi, and Anacona Terranes and the Panzenú Suspect Terrane. These terranes were accreted at different moments from the late Neoproterozoic to the Late Cretaceous (Figure 9). Most of the accretions involved displaced terranes: South American blocks were transported northward along transcurrent faults and are called para–autochthonous, but in a different manner to this term's usage for the Alpine overthrusts.

Some of the most characteristic features of the main terranes (Table 1) are as follows:

1. Andaquí Suspect Terrane: high–grade Putumayense basement that is covered by unmetamorphosed lower Paleozoic sedimentary rocks.
2. Chibcha Terrane: regional metamorphism of Cambrian, Ordovician and Silurian (?) sedimentary rocks, many of which were deposited over Putumayo or Grenville metamorphic basements. These metamorphic rocks were covered by Devonian and younger marine sedimentary rocks. Triassic, Jurassic, and Early Cretaceous granitoid rocks intruded some of these areas and formed extensive volcanic deposits during the Jurassic.
3. Tahamí Terrane: low– to high–grade metamorphosed metasedimentary and pre– to post–tectonic granitoid intrusions that formed during a Triassic metamorphism event. The metasedimentary rocks have a Carboniferous maximum age. The main magmatic event occurred during the Late Cretaceous.
4. Yalcón Terrane: low– to medium–grade Jurassic metamorphic rocks that were intruded by Jurassic plutons.

The newly defined Yalcón Terranes is located between the Tahamí and Ebéjico terranes to the west and the Chibcha Terrane to the east. This terrane comprises low– to medium–grade metamorphic rocks that formed during a Jurassic metamorphic

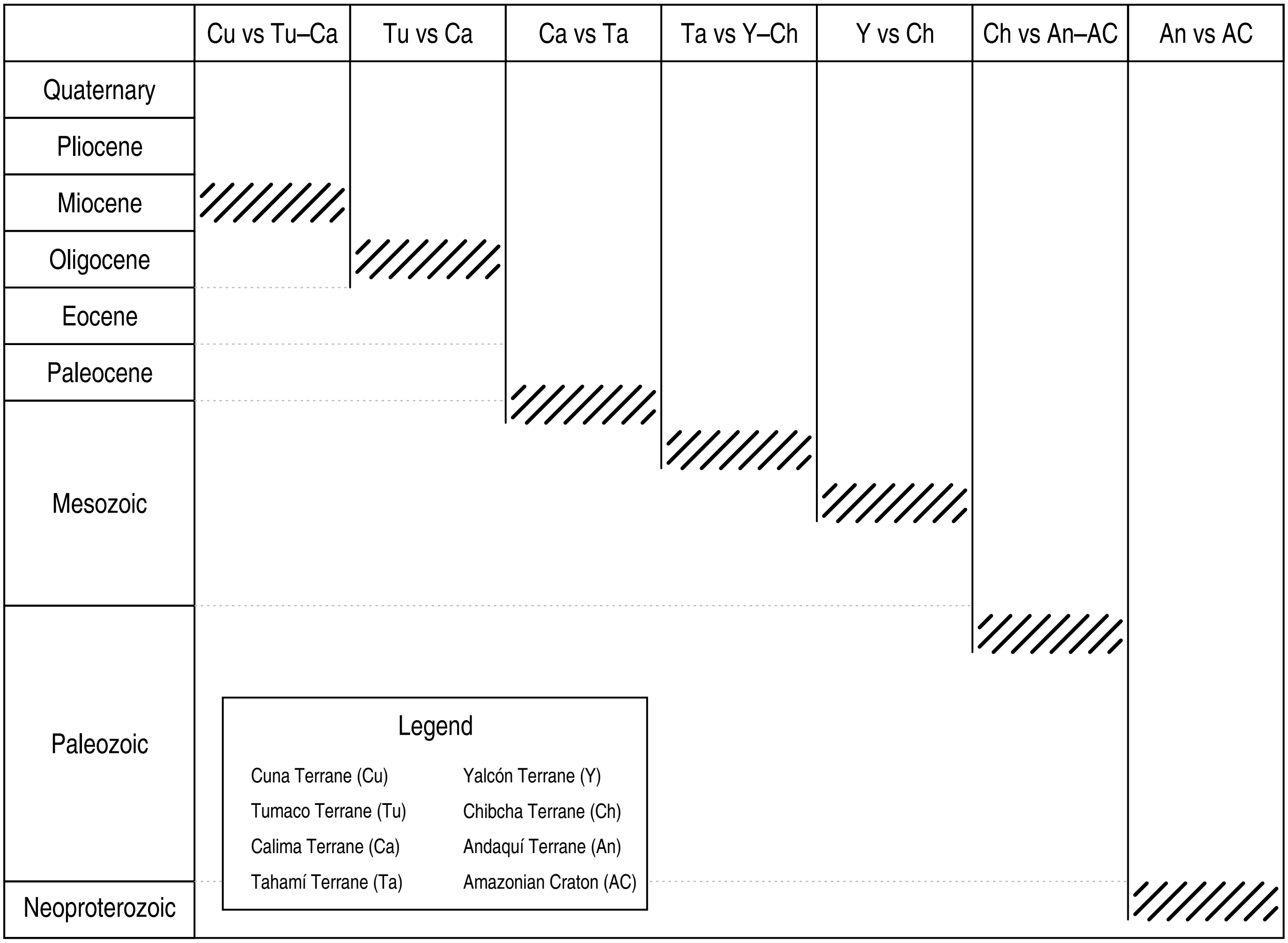

Figure 9. Timing of accretions of the Colombian terranes.

event. The Kogi Terrane in the SNSM and LGP has certain similarities to the Tahamí Terrane but is currently considered a different terrane.

The terrane concept applied to Colombian geology permits the explanation of many paradoxes that are difficult to explain from an autochthonous perspective.

Acknowledgments

Special thanks are given to Gómez et al. (2015b) for preparing the catalog of radiometric datings of Colombia. Without this catalog, the preparation of this document would have been much more time consuming. Also to Fernando ALCÁRCEL for drawing the final versions of the figures.

References

Agencia Nacional de Hidrocarburos. 2012. Cuenca de los Llanos Orientales: Integración geológica de la digitalización y análisis de núcleos. Digital Rock Physics Lab–ANH, 209 p. Bogotá.

Álvarez, J. 1981. Determinación de edad Rb/Sr en rocas del Macizo de Garzón, Cordillera Oriental de Colombia. Geología Norandina, (4): 31–38.

Álvarez, J., Rico, H., Vásquez, H. & Hall, R. 1970. Mapa geológico del cuadrángulo H–8 Yarumal y parte del H–7 Ituango, Colombia. Scale 1:100 000. Ingeominas. Bogotá.

Amaya, Z., Cramer, T., Bonilla, A., Franco, J., Campos, H., Cano, H., Castañeda, A., Roberto, O., Zuluaga, C., Zuluaga, C, Molano, J.C., Guerrero, J., Piraquive, A. & Cuellar, J. 2017. Los estratos auríferos meso–proterozóicos en los departamentos de Guainía y Vaupés, Colombia. XVI Congreso Colombiano de Geología. Memoirs, p. 995–1001. Santa Marta.

Arango, M.I., Rodríguez, G., Bermúdez, J.G. & Zapata, G. 2015. Catálogo de unidades litoestratigráficas de Colombia: Cuarzomonzonita de Anchique. Servicio Geológico Colombiano, 26 p. Bogotá.

Barrero, D. & Vesga, C. 1976. Mapa geológico del cuadrángulo K–9 Armero y mitad sur del J–9 La Dorada. Scale 1:100 000. Ingeominas. Bogotá.

Bayona, G., Cardona, A., Jaramillo, C., Mora, A., Montes, C., Valencia, V., Ayala, C., Montenegro, O. & Ibañez–Mejia, M. 2012.

Early Paleogene magmatism in the northern Andes: Insights on the effects of oceanic plateau–continent convergence. Earth and Planetary Science Letters, 331–332: 97–111. https://doi.org/10.1016/j.epsl.2012.03.015

Berg, H.C., Jones, D.L. & Coney, P.J. 1978. Map showing pre–Cenozoic tectonostratigraphic terranes of southeastern Alaska and adjacent areas. Scale 1:1 000 000. United States Geological Survey, Open–File Report 78–1085, 2 sheets. https://doi.org/10.3133/ofr781085

Blanco–Quintero, I.F., García–Casco, A., Ruiz, E.C., Toro, L.M., Moreno, M., Morata, D. & Vinasco, C.J. 2013. New petrological and geochronological data from the Cajamarca Complex (Central Cordillera, Colombia) in the Cajamarca–Ibagué region: Late Jurassic thermal resetting of Triassic metamorphic ages or Jurassic orogenic metamorphism? XIV Congreso Colombiano de Geología. Abstracts, p. 247. Bogotá.

Bogotá, J. 1982. Estratigrafía del Paleozoico inferior en el área Amazónica de Colombia. Geología Norandina, (6): 29–38.

Boinet, T., Bourgois, J., Bellon, H. & Toussaint, J.F. 1985. Age et répartition du magmatisme prémésozoïque des Andes de Colombie. Comptes Rendus des Séances de L'Académie des Sciences, 300(Serie II–10): 445–450. Paris.

Bonilla–Pérez, A., Frantz, J.C., Charão–Marques, J.C., Cramer, T., Franco–Victoria, J.A., Mulocher, E. & Amaya–Perea, Z. 2013. Petrografía, geoquímica y geocronología del Granito de Parguaza en Colombia. Boletín de Geología, 35(2): 83–104.

Bonilla, A., Frantz, J.C., Charão–Marques, J.C., Cramer, T., Franco, J.A. & Amaya, Z. 2016. Magmatismo Rapakivi en la cuenca media del río Inírida, departamento de Guainía, Colombia. Boletín de Geología, 38(1): 17–32. http://dx.doi.org/10.18273/revbol.v38n1-2016001

Botero, G. 1963. Contribución al conocimiento de la geología de la zona central de Antioquia. Universidad Nacional de Colombia, Anales de la Facultad de Minas, 57, 101 p. Medellín.

Bridger, C.S. 1982. El Paleozoico inferior de Colombia: Una revaluación en base en nuevos datos de campo. Bachelor thesis, Universidad Nacional de Colombia, 280 p. Bogotá.

Bürgl, H. & Radelli, L. 1962. Nuevas localidades fosilíferas en la Cordillera Central de Colombia (S. A.). Geología Colombiana, 3: 133–138.

Bustamante, C., Cardona, A., Bayona, G., Mora, A., Valencia, V., Gehrels, G. & Vervoort, J. 2010. U–Pb LA–ICP–MS geochronology and and regional correlation of Middle Jurassic intrusive rocks from the Garzón Massif, Upper Magdalena Valley and Central Cordillera, southern Colombia. Boletín de Geología, 32(2): 93–109.

Bustamante, C., Archanjo, C.J., Cardona, A., Bustamante, A. & Valencia, V.A. 2017. U–Pb ages and Hf isotopes in zircons from parautochthonous Mesozoic terranes in the western margin of Pangea: Implications for the terrane configurations in the northern Andes. The Journal of Geology, 125(5): 487–500. https://doi.org/10.1086/693014

Cardona, A. 2003. Correlações entre fragmentos do embasamento pré–Mesozóico da terminação setentrional dos Andes Colombianos, com base em dados isotópicos e geocronológicos. Master thesis, Universidade de São Paulo, 149 p. São Paulo. https://doi.org/10.11606/D.44.2003.tde-07042015-090410

Cardona, A., Cordani, U.G. & MacDonald, W.D. 2006. Tectonic correlations of pre–Mesozoic crust from the northern termination of the Colombian Andes, Caribbean region. Journal of South American Earth Sciences, 21(4): 337–354. https://doi.org/10.1016/j.jsames.2006.07.009

Cardona, A., Valencia, V., Garzón, A., Montes, C., Ojeda, G., Ruiz, J. & Weber, M. 2010. Permian to Triassic I to S–type magmatic switch in the northeast Sierra Nevada de Santa Marta and adjacent regions, Colombian Caribbean: Tectonic setting and implications within Pangea paleogeography. Journal of South American Earth Sciences, 29(4): 772–783. https://doi.org/10.1016/j.jsames.2009.12.005

Cawood, P.A. & Pisarevsky, S.A. 2017. Laurentia–Baltica–Amazonia relations during Rodinia assembly. Precambrian Research, 292: 386–397. https://doi.org/10.1016/j.precamres.2017.01.031

Cediel, F., Shaw, R.P. & Cáceres, C. 2003. Tectonic assembly of the northern Andean block. In: Bartolini, C., Buffler, R.T. & Blickwede, J. (editors), The circum–Gulf of Mexico and the Caribbean: Hydrocarbon habitats, basin formation, and plate tectonics. American Association of Petroleum Geologists Memoir, 79, p. 815–848. Tulsa, USA.

Cochrane, R.S. 2013. U–Pb thermochronology, geochronology and geochemistry of NW South America: Rift to drift transition, active margin dynamics and implications for the volume balance of continents. Doctoral thesis, University of Geneva, 118 p. Geneva, Switzerland. https://doi.org/10.13097/archive-ouverte/unige:30029

Cochrane, R., Spikings, R., Gerdes, A., Winkler, W., Ulianov, A., Mora, A. & Chiaradia, M. 2014a. Distinguishing between in–situ and accretionary growth of continents along active margins. Lithos, 202–203: 382–394. https://doi.org/10.1016/j.lithos.2014.05.031

Cochrane, R., Spikings, R., Gerdes, A., Ulianov, A., Mora, A., Villagómez, D., Putlitz, B. & Chiaradia, M. 2014b. Permo–Triassic anatexis, continental rifting and the disassembly of western Pangaea. Lithos, 190–191: 383–402. https://doi.org/10.1016/j.lithos.2013.12.020

Coney, P.J., Jones, D.L. & Monger, J.W.H. 1980. Cordilleran suspect terranes. Nature, 288(5789): 329–333. https://doi.org/10.1038/288329a0

Cordani, U.G., Sato, K, Teixeira, W, Tassinari, C.G.G. & Basei, M.A.S. 2000. Crustal evolution of the South American platform. In: Cordani, U.G., Milani, E.J., Thomaz–Filho, A. & Campos, D.A. (editors), Tectonic evolution of South America. 31st International Geological Congress. Proceedings, p. 19–40. Río de Janeiro, Brazil.

Cordani, U.G., Cardona, A., Jiménez, D.M., Liu, D. & Nutman, A.P. 2005. Geochronology of Proterozoic basement inliers in the Colombian Andes: Tectonic history of remnants of a fragmented Grenville belt. In: Vaughan, A.P.M., Leat, P.T. & Pankhurst, R.J. (editors), Terrane processes at the margins of Gondwana. Geological Society of London, Special Publication 246, p. 329–346. London. https://doi.org/10.1144/GSL.SP.2005.246.01.13

Cordani, U.G., Sato, K., Sproessner, W. & Fernandes, F.S. 2016. U–Pb zircon ages of rocks from the Amazonas territory of Colombia and their bearing on the tectonic history of the NW sector of the Amazonian Craton. Brazilian Journal of Geology, 46(1): 5–35. https://doi.org/10.1590/2317-4889201620150012

Correa, A.M., Pimentel, M., Restrepo, J.J., Nilson, A., Ordóñez, O., Martens, U., Laux, J.E. & Junges, S. 2006. U–Pb zircon ages and Nd–Sr isotopes of the Altavista Stock and the San Diego Gabbro: New insights on Cretaceous arc magmatism in the Colombian Andes. V South American Symposium on Isotope Geology. Abstracts in CD ROM, p. 1–3. Punta del Este, Uruguay.

Cuadros, F.A., Botelho, N.F., Ordóñez–Carmona, O. & Matteini, M. 2014. Mesoproterozoic crust in the San Lucas Range (Colombia): An insight into the crustal evolution of the northern Andes. Precambrian Research, 245: 186–206. https://doi.org/10.1016/j.precamres.2014.02.010

Dalziel, I.W.D. 1997. Overview: Neoproterozoic – Paleozoic geography and tectonics; review, hypothesis, environmental speculation. Geological Society of America Bulletin, 109(1): 16–42. https://doi.org/10.1130/0016-7606(1997)109<0016:ONPGAT>2.3.CO;2

De La Espriella, R. & Cortés, R. 1989. Contribución a la estratigrafía del Grupo Quetame. Revista del Instituto de Ciencias Naturales y Ecología, 2(1): 83–102.

Duque, J.F. 2010. Geocronología (U/Pb y ^{40}Ar/^{39}Ar) y geoquímica de los intrusivos paleógenos de la Sierra Nevada de Santa Marta y sus relaciones con la tectónica del Caribe y el arco magmático Circun–Caribeño. Master thesis, Universidad Nacional Autónoma de México, 189 p. México D. F.

Etayo–Serna, F., Barrero, D., Lozano, H., Espinosa, A., González, H., Orrego, A., Ballesteros, I., Forero, H., Ramírez, C., Zambrano–Ortiz, F., Duque–Caro, H., Vargas, R., Núñez, A., Álvarez, J., Ropaín, C., Cardozo, E., Galvis, N., Sarmiento, L., Alberts, J.P., Case, J.E., Singer, D.A., Bowen, R.W., Berger, B.R., Cox, D.P. & Hodges, C.A. 1983. Mapa de terrenos geológicos de Colombia. Publicaciones Geológicas Especiales del Ingeominas, 14(1), p. 1–135. Bogotá.

Feininger, T. 1970. The Palestina Fault, Colombia. Geological Society of America Bulletin, 81(4): 1201–1216. https://doi.org/10.1130/0016-7606(1970)81[1201:TPFC]2.0.CO;2

Feininger, T. & Botero, G. 1982. The Antioquian Batholith, Colombia. Publicaciones Geológicas Especiales del Ingeominas, 12, p. 1–50. Bogotá.

Feininger, T., Barrero, D. & Castro, N. 1972. Geología de parte de los departamentos de Antioquia y Caldas (Sub–Zona II–B). Boletín Geológico, 20(2): p. 1–67.

Forero, A. 1970. Estratigrafía del precretácico en el flanco occidental de la serranía de Perijá. Geología Colombiana, 7: 7–77.

Forero, A. 1984. Remanentes de la provincia paleobiogeográfica Frasniano–Fameniana del viejo mundo en Los Andes septentrionales. Geología Norandina, (10): 35–38.

Galvis, J., Huguett, A. & Ruge, P. 1979. Geología de la Amazonía colombiana. Boletín Geológico, 22(3): 3–86.

García–Chinchilla, D. & Vlach, S.R.F. 2017. Datación U–Pb in situ, isotopos de Hf en zircón y geoquímica de granitos y rocas relacionadas de la región de Garzón, Cordillera Oriental. XVI Congreso Colombiano de Geología. Memoirs, p. 1238–1241. Santa Marta.

Gaudette, H.E., Mendoza, V., Hurley, P.M. & Fairbairn, H.W. 1978. Geology and age of the Parguaza rapakivi granite, Venezuela. Geological Society of America Bulletin, 89(9): 1335-1340. https://doi.org/10.1130/0016-7606(1978)89<1335:GAAOTP>2.0.CO;2

Geyer, O.F. 1973. Das präkretazische Mesozoikum von Kolumbien. Geologisches Jahrbuch, 5: 1–155.

Giraldo–Ramírez, W.E. 2017. Novas idades U–Pb (LA–ICP–MS) de rochas granitoides na região de Sabanalarga (Colômbia) e sua correlação com a evolução da Placa do Caribe. Master thesis, Universidade do Estado do Rio de Janeiro, 88 p. Río de Janeiro, Brazil.

Giraldo, W., Patarroyo, P. & Restrepo, J.J. 2015. Sedimentitas de Aquitania, Antioquia: Edad y correlaciones. XV Congreso Colombiano de Geología. Memoirs, p. 1138–1140. Bucaramanga.

Goldsmith, R., Marvin, R.F. & Mehnert, H.H. 1971. Radiometric ages in the Santander Massif, Eastern Cordillera, Colombian Andes. United States Geological Survey Professional Paper, 750–D, p. D44–D49.

Gómez, J., Montes, N.E., Nivia, Á. & Diederix, H., compilers. 2015. Geological Map of Colombia 2015. Scale 1:1 000 000. Servicio Geológico Colombiano, 2 sheets. Bogotá. https://doi.org/10.32685/10.143.2015.936

Gómez, J., Montes, N.E., Alcárcel, F.A. & Ceballos, J.A. 2015b. Catálogo de dataciones radiométricas de Colombia en ArcGIS y Google Earth. In: Gómez–Tapias, J. & Almanza, M.F. (editors), Compilando la geología de Colombia: Una visión a 2015. Servicio Geológico Colombiano, Publicaciones Geológicas Especiales, 33, p. 63–419. Bogotá.

González, H. 1980. Geología de las planchas 167 Sonsón y 187 Salamina. Scale 1:100 000. Boletín Geológico, 23(1): 1–174.

González, H. 1989. Descripción petrográfica de las unidades litológicas de la serranía de Naquén (Colombia) y posibles correlaciones estratigráficas. V Congreso Colombiano de Geología. Memoirs, I, p. 31–49. Bucaramanga.

González, H., Lemoigne, I. & Martínez, J.O. 1977. Flora de la Formación Valle Alto, Jurásico en la Cordillera Central de Colombia. Boletín de Ciencias de la Tierra, 2: 107–122.

González–Ospina, L.J. 2016. Petrogénesis de los complejos ultramáficos de Heliconia–Angelópolis y del oriente de Medellín, Antioquia, Colombia. Master thesis, Universidad Nacional de Colombia, 108 p. Bogotá.

Hall, R.B., Álvarez, J. & Rico, H. 1972. Geología de parte de los departamentos de Antioquia y Caldas (Sub–Zona II–A). Boletín Geológico, 20(1): 1–85.

Harrington, H.J. & Kay, M. 1951. Cambrian and Ordovician faunas of eastern Colombia. Journal of Paleontology, 25(5): 655–668.

Hernández–González, J.S. & Urueña–Suárez, C.L. 2017. Aspectos geocronológicos y petrogenéticos del Complejo Aleluya: Implicaciones en la exploración de Mg en el norte del departamento del Huila, Colombia. XVI Congreso Colombiano de Geología. Memoirs, p. 832–838. Santa Marta.

Herrera, A. & Velásquez, B.E. 1978. Estratigrafía de la sección de Araracuara (Amazonia). Bachelor thesis, Universidad Nacional de Colombia, 82 p. Bogotá.

Ibañez–Mejia, M., Tassinari, C.C.G. & Jaramillo–Mejia, J.M. 2007. U–Pb zircon ages of the "Antioquian Batholith": Geochronological constraints of late Cretaceous magmatism in the central Andes of Colombia. XI Congreso Colombiano de Geología. Memoirs. 11 p. Bucaramanga.

Ibañez–Mejia, M., Jaramillo–Mejía, J.M. & Valencia, V. 2008. U–Th/Pb zircon geochronology by multicollector LA–ICP–MS of the Samaná Gneiss: A middle Triassic syn–tectonic body in the central Andes of Colombia related to the latter stages of Pangea assembly. VI South American Symposium on Isotope Geology San Carlos de Bariloche. Abstracts in CD ROM, p. 1–4. San Carlos de Bariloche, Argentina.

Ibañez–Mejia, M., Ruiz, J., Valencia, V.a., Cardona, A., Gehrels, G.E. & Mora, A.R. 2011. The Putumayo Orogen of Amazonia and its implications for Rodinia reconstructions: New U–Pb geochronological insights into the Proterozoic tectonic evolution of northwestern South America. Precambrian Research, 191(1–2): 58–77. https://doi.org/10.1016/j.precamres.2011.09.005

Ibañez–Mejia, M., Pullen, A., Arenstein, J., Gehrels, G.E., Valley, J., Ducea, M.N., Mora, A.R., Pecha, M. & Ruiz, J. 2015. Unraveling crustal growth and reworking processes in complex zircons from orogenic lower–crust: The Proterozoic Putumayo Orogen of Amazonia. Precambrian Research, 267: 285–310. https://doi.org/10.1016/j.precamres.2015.06.014

Ibañez–Mejia, M. & Cordani, U.G. 2020. Zircon U–Pb geochronology and Hf–Nd–O isotope geochemistry of the Paleoproterozoic to Mesoproterozoic basement in the westernmost Guiana Shield. In: Gómez, J. & Mateus–Zabala, D. (editors), The Geology of Colombia, Volume 1 Proterozoic – Paleozoic. Servicio Geológico Colombiano, Publicaciones Geológicas Especiales 35, p. 65–90. Bogotá. https://doi.org/10.32685/pub.esp.35.2019.04

Idárraga–García, J. & Martínez–Uribe, L. 2005. Petrografía y geoquímica de la Migmatita de Manizales entre el cerro Morro Gordo y el río Chinchiná, al occidente de Manizales (Caldas). Bachelor thesis, Universidad de Caldas, 63 p. Manizales.

Jaramillo, L., Escovar, R. & Vesga, C.J. 1980. Edades K/Ar de rocas con alteración hidrotermal asociadas al sistema de pórfido de cobre y molibdeno de Mocoa, Intendencia del Putumayo, Colombia. Geología Norandina, (1): 11–18.

Kennan, L. & Pindell, J.L. 2009. Dextral shear, terrane accretion and basin formation in the northern Andes: Best explained by interaction with a Pacific–derived Caribbean Plate? In: James, K.H., Lorente, M.A. & Pindell, J.L. (editors), The origin and evolution of the Caribbean Plate. Geological Society of London, Special Publication 328, p. 487–531. https://doi.org/10.1144/SP328.20

Kroonenberg, S.B. 1982a. A Grenvillian granulite belt in the Colombian Andes and its relation to the Guiana Shield. Geologie en Mijnbouw, 61(4): 325–333.

Kroonenberg, S.B. 1982b. Litología, metamorfismo y origen de las granulitas del Macizo de Garzón, Cordillera Oriental (Colombia). Geología Norandina, (6): 39–46.

Leal–Mejía, H. 2011. Phanerozoic gold metallogeny in the Colombian Andes: A tectono–magmatic approach. Doctoral thesis, Universitat de Barcelona, 989 p. Barcelona.

Litherland, M., Aspden, J.A. & Jemielita, R.A. 1994. The metamorphic belts of Ecuador. Overseas Memoir of the British Geological Survey 11, 147 p. Nottingham, England.

López, J.A.; Khurama, S.; Bernal, L.E. & Cuellar, M.A. 2007. El Complejo Mitú: Una nueva perspectiva. XI Congreso Colombiano de Geología. Memoirs, 16 p. Bucaramanga.

Manosalva, S., Mariño, J., Vlach, S., Naranjo, W. & Castillo, H. 2017. Metamorfismo de rocas pelíticas en el Macizo de Floresta, Cordillera Oriental de Colombia. XIV Congreso Latinoamericano de Geología–XIII Congreso Colombiano de Geología. Memoirs, p. 115. Medellín.

Mantilla–Figueroa, L.C., García–Ramírez, C.A. & Valencia, V.A. 2016. Propuesta de escisión de la denominada 'Formación Silgará' (Macizo de Santander, Colombia), a partir de edades U–Pb en zircones detríticos. Boletín de Geología, 38(1): 33–50. http://dx.doi.org/10.18273/revbol.v38n1-2016002

Martens, U.C., Restrepo, J.J. & Solari, L.A. 2012. Sinifaná Metasedimentites and relations with Cajamarca Paragneisses of the Central Cordillera of Colombia. Boletín de Ciencias de la Tierra, 32: 99–110.

Martens, U., Restrepo, J.J., Ordóñez–Carmona, O. & Correa–Martínez, A.M. 2014. The Tahamí and Anacona Terranes of the Colombian Andes: Missing links between South American and Mexican Gondwana margins. The Journal of Geology, 122(5): 507–530. https://doi.org/10.1086/677177

Maya, M. & González, H. 1995. Unidades litodémicas en la Cordillera Central de Colombia. Boletín Geológico, 35(2–3): 43–57.

Mojica, J. 1980. Observaciones acerca del estado actual del conocimiento de la Formación Payandé (Triásico Superior), Valle Superior del Río Magdalena, Colombia. Geología Colombiana, 11: 67–88.

Mojica, J. & Macía, C. 1981. Características estratigráficas de la Formación Yaví, Mesozoico de la región entre Prado y Dolores, Tolima, Colombia. Geología Colombiana, 12: 7–32.

Mojica, J.; Villarroel, C. & Macía, C. 1988. Nuevos afloramientos fosilíferos del Ordovícico Medio (Fm. El Hígado) al oeste de Tarqui, Valle Superior del Magdalena (Huila, Colombia). Geología Colombiana 16: 95-97.

Montes, L.F. & Restrepo, J.J. 2005. Relación entre las metamorfitas de alto y bajo grado en el sur del Valle de Aburrá, Antioquia. Boletín de Ciencias de la Tierra, (17): 9–18.

Mora–Bohórquez, J.A., Ibañez–Mejia, M., Oncken, O., de Freitas, M., Vélez, V., Mesa, A. & Serna, L. 2017. Structure and age of the lower Magdalena Valley Basin basement, northern Colombia: New reflection–seismic and U–Pb–Hf insights into the termination of the central Andes against the Caribbean Basin. Journal of South American Earth Sciences, 74: 1–26. https://doi.org/10.1016/j.jsames.2017.01.001

Moreno–Sánchez, M. & Pardo–Trujillo, A. 2003. Stratigraphical and sedimentological constraints on western Colombia: Implications on the evolution of the Caribbean Plate. In: Bartolini, C., Buffler, R.T. & Blickwede, J. (editors), The circum–Gulf of Mexico and the Caribbean: Hydrocarbon habitats, basin formation, and plate tectonics. American Association of Petroleum Geologists Memoir 79, p. 891–924. Tulsa, USA.

Moreno–Sánchez, M., Gómez–Cruz, A.J. & Castillo–González, H. 2007. Ocurrencias de fósiles paleozoicos al este de la parte norte de la Cordillera Central y discusión sobre su significado geológico. Boletín Ciencias de la Tierra, (22): 39–48.

Mosquera, D. 1978. Geología del cuadrángulo K–8 Manizales. Ingeominas, Internal report 1763, 63 p. Bogotá.

Muñoz, J. 1980. Estudio petrológico del Grupo Valdivia. Bachelor thesis, Universidad Nacional de Colombia, 108 p. Medellín.

Nelson, W.H. 1962. Contribución al conocimiento de la Cordillera Central de Colombia, sección entre Ibagué y Armenia. Boletín Geológico, 10(1–3): 161–202.

Nivia, A., Marriner, G.F., Kerr, A.C. & Tarney, J. 2006. The Quebradagrande Complex: A Lower Cretaceous ensialic marginal basin in the Central Cordillera of the Colombian Andes. Journal of South American Earth Sciences, 21(4): 423–436. https://doi.org/10.1016/j.jsames.2006.07.002

Núñez, A., Macía, C. & Mojica, J. 1984. La Fm. Amoyá: Una nueva unidad post–Precámbrica – pre–Jurásica de la Cordillera Central, al W de Chaparral, Tolima, Colombia. Newsletters on Stratigraphy, 13(2): 77. https://doi.org/10.1127/nos/13/1984/77

Ochoa, A., Ríos, P., Cardozo, A.M., Cubides, J.V., Giraldo, D.F., Rincón, H.D. & Mendivelso, D. 2012. Memoria explicativa: Cartografía geológica y muestreo geoquímico de las planchas 159, 160, 161, 179, 180 y 181 Puerto Carreño, Vichada. Servicio Geológico Colombiano, 126 p. Bogotá.

Ordóñez–Carmona, O. 2001. Caracterização isotópica Rb–Sr e Sm–Nd dos principais eventos magmáticos nos Andes colombianos. Doctoral thesis, Universidad de Brasilia, 176 p. Brasilia.

Ordóñez–Carmona, O. & Pimentel, M.M. 2002. Rb–Sr and Sm–Nd isotopic study of the Puquí Complex, Colombian Andes. Journal of South American Earth Sciences, 15(2): 173–182. https://doi.org/10.1016/S0895-9811(02)00017-2

Ordóñez–Carmona, O., Pimentel, M.M., de Moraes, R. & Restrepo, J.J. 1999. Rocas Grenvillianas en la región de Puerto Berrío–Antioquia. Revista de la Academia Colombiana de Ciencias Exactas, Físicas y Naturales, 23(87): 225–232.

Ordóñez–Carmona, O., Pimentel, M.M. & de Moraes, R. 2002. Granulitas de Los Mangos, un fragmento Grenvilliano en la parte oriental de la Sierra Nevada de Santa Marta. Revista de la Academia Colombiana de Ciencias Exactas, Físicas y Naturales, 26(99): 169–179.

Ordóñez, O., Pimentel, M.M. & Laux, J.H. 2008. Edades U–Pb del Batolito Antioqueño. Boletín de Ciencias de la Tierra, 1(22): 129–130.

Ordóñez–Carmona, O., Restrepo, J.J., de Brito, R.S.C., Martens, U. & Rodrigues, J.B. 2011. The late Paleocene age of the Santa Bárbara Batholith (Valle, Colombia) and its implications on the evolution of the Arquía Complex. XIV Congreso Latinoamericano de Geología–XIII Congreso Colombiano de Geología. Memoirs, p. 109. Medellín.

Patarroyo, P., Restrepo, J.J. & Giraldo, W. 2017. Posible presencia de fósiles de crinoides en mármoles del Complejo Cajamarca. XVI Congreso Colombiano de Geología. Memoirs, p. 428. Santa Marta.

Pindell, J., Maresch, W.V., Martens, U. & Stanek, K. 2012. The greater Antillean Arc: Early Cretaceous origin and proposed relationship to Central American subduction mélanges: Implications for models of Caribbean evolution. International Geology Review, 54(2): 131–143. https://doi.org/10.1080/00206814.2010.510008

Priem, H.N.A., Andriessen, P.A.M., Boelrijk, N.A.I.M., De Boorder, H., Hebeda, E.H., Huguett, A., Verdurmen, E.A.T. & Verschure, R.H. 1982. Geochronology of the Precambrian in the Amazonas region of southeastern Colombia (western Guiana Shield). Geologie in Mijnbouw, 61(3): 229–242.

Priem, H.N.A., Kroonenberg, S.B., Boelrijk, N.A.I.M. & Hebeda, E.H. 1989. Rb–Sr and K–Ar evidence for the presence of a 1.6 Ga basement underlying the 1.2 Ga Garzón–Santa Marta granulite belt in the Colombian Andes. Precambrian Research, 42(3–4): 315–324. https://doi.org/10.1016/0301-9268(89)90016-8

Puerta–Moreno, J.J. 1990. Estudio petrográfico del metamorfismo regional al oeste de Manizales. Bachelor thesis, Universidad Nacional de Colombia, 117 p. Medellín.

Renz, O. 1960. Geología de la parte sureste de la Península de Guajira (República de Colombia). III Congreso Geológico Venezolano. Memoirs, III, p. 317–346.

Renzoni, G. 1968. Geología del Macizo de Quetame. Geología Colombiana, 5: 75–127.

Renzoni, G. 1989. Comparación entre las secuencias metasedimentarias de la serranía de Naquén y de la Serra da Jacobina. Boletín Geológico, 30(2): 25–42.

Restrepo, J.J & Toussaint, J.F. 1985. Unidades litológicas de los alrededores de Medellín. Instituto de Ciencias Naturales y Ecología, Publicación Especial, 2: 1–31. Medellín.

Restrepo, J.J & Toussaint, J.F. 1988. Terranes and continental accretion in the Colombian Andes. Episodes. 11(3): 189–193.

Restrepo, J.J. & Toussaint, J.F. 1989. Terrenos alóctonos en los Andes colombianos: Explicación de algunas paradojas geológicas. V Congreso Colombiano de Geología. Memoirs, I, p. 92–107. Bucaramanga.

Restrepo, J.J., Toussaint, J.F., González, H., Cordani, U.G., Kawashita, K., Linares, E. & Parica, C. 1991. Precisiones geocronológicas sobre el occidente colombiano. Simposio sobre magmatismo andino y su marco tectónico. Memoirs, I, 21 p. Manizales.

Restrepo, J.J., Frantz, J.C., Ordóñez–Carmona, O., Correa, A.M., Martens, U. & Chemale Jr., F. 2007. Edad triásica de formación de la Ofiolita de Aburrá, flanco occidental de la cordillera Central. XI Congreso Colombiano de Geología. Abstracts, p. 49. Bucaramanga.

Restrepo, J.J., Dunlap, W.J., Martens, U., Ordóñez–Carmona, O. & Correa, A.M. 2008. Ar–Ar ages of amphibolites from the Central Cordillera of Colombia and their implications for tectonostratigraphic terrane evolution in the northwestern Andes. VI South American Symposium on Isotope Geology. Proceedings in CD ROM, p. 1–6. Bariloche, Argentina.

Restrepo, J.J., Ordóñez–Carmona, O., Martens, U. & Correa, A.M. 2009. Terrenos, complejos y provincias en la cordillera Central colombiana. Ingeniería, Investigación y Desarrollo, 9(2): 49–56.

Restrepo, J.J., Ordóñez–Carmona, O., Armstrong, R. & Pimentel, M.M. 2011. Triassic metamorphism in the northern part of the Tahamí Terrane of the Central Cordillera of Colombia. Journal of South American Earth Sciences, 32(4): 497–507. https://doi.org/10.1016/j.jsames.2011.04.009

Restrepo, J.J., Martens, U. & Giraldo–Ramírez, W.E. 2020. The Anacona Terrane: A small early Paleozoic peri–Gondwanan terrane in the Cauca–Romeral Fault System. In: Gómez, J. & Mateus–Zabala, D. (editors), The Geology of Colombia, Volume 1 Proterozoic – Paleozoic. Servicio Geológico Colombiano, Publicaciones Geológicas Especiales 35, p. 149–165. Bogotá. https://doi.org/10.32685/pub.esp.35.2019.08

Restrepo–Moreno, S.A., Foster, D.A. & Kamenov, G.D. 2007. Formation age and magma sources for the Antioqueño Batholith derived from LA–ICP–MS uranium–lead dating and hafnium–isotope analysis of zircon grains. Geological Society of America Annual Meeting. Session 181–28 # 186. Denver, USA.

Restrepo–Pace, P.A., Ruiz, J., Gehrels, G. & Cosca, M. 1997. Geochronology and Nd isotopic data for Grenville–age rocks in the Colombian Andes: New constraints for late Proterozoic – early Paleozoic paleocontinental reconstructions of the Americas. Earth and Planetary Science Letters, 150(3–4): 427–441. https://doi.org/10.1016/S0012-821X(97)00091-5

Rodríguez, G. & Arango, M.I. 2013. Reinterpretación geoquímica y radiométrica de las metabasitas del Complejo Arquía. Boletín de Geología, 35(2): 65–81.

Rodríguez, G., González, H. & Zapata, G. 2005. Geología de la plancha 147 Medellín Oriental. Ingeominas, 300 p. Medellín.

Rodríguez, G., Sepúlveda, J., Ramírez, C., Ortiz, F.H., Ramos, K., Bermúdez, J.G. & Sierra, M.I. 2011. Unidades, petrografía y composición química del Complejo Migmatítico de Mitú en los alrededores de Mitú. Boletín de Geología, 33(1): 27–42.

Rodríguez, G., Obando, G., Correa–Martínez, A.M., Zapata, G. Correa, T., Obando, M., Rincón, A. & Zapata, J.P. 2017. Redefinición del bloque norte del Batolito de Ibagué con base en nuevos datos de petrografía, litogeoquímica y geocronología U–Pb. XVI Congreso Colombiano de Geología. Memoirs, p. 1437–1442. Santa Marta.

Rodríguez–Jiménez, J.V. 2010. Fábrica y emplazamiento de la Diorita de Pueblito, NW Cordillera Central de Colombia: Análisis de fábrica magnética y mineral. Master thesis, Universidad Nacional de Colombia, 68 p. Medellín.

Silva–Tamayo, J.C., Sial, A.N., Ferreira, V.P. & Estrada, J.J. 2004. C–isotope stratigraphy of a Vendian carbonate succession in northwestern Andes: Implications for the NW Andes. IV Reunión de Ciencias de la Tierra. Abstracts, p. 198. Querétaro, México.

Thouret, J.C., Cantagrel, J.M., Salinas, R. & Murcia, A. 1990. Quaternary eruptive history of Nevado del Ruiz (Colombia). Journal of Volcanology and Geothermal Research, 41(1–4): 225–251. https://doi.org/10.1016/0377-0273(90)90090-3

Toussaint, J.F. & Restrepo, J.J. 1989. Acreciones sucesivas en Colombia: Un nuevo modelo de evolución geológica. V Congreso Colombiano de Geología. Memoirs, p. 127–146. Bucaramanga.

Toussaint, J.F. & Restrepo, J.J. 2020. Tectonostratigraphic terranes in Colombia: An update. Second part: Oceanic terranes. In: Gómez, J. & Pinilla–Pachon, A.O. (editors), The Geology of Colombia, Volume 2 Mesozoic. Servicio Geológico Colombiano, Publicaciones Geológicas Especiales 36, p. 237–260. Bogotá. https://doi.org/10.32685/pub.esp.36.2019.07

Trumpy, D. 1943. Pre–Cretaceous of Colombia. Geological Society of America Bulletin, 54(9): 1281–1304. https://doi.org/10.1130/GSAB-54-1281

Tschanz, C.M., Marvin, R.F., Cruz, J., Mehnert, H.H. & Cebula, G.T. 1974. Geologic evolution of the Sierra Nevada de Santa Marta, northeastern Colombia. Geological Society of America Bulletin, 85(2): 273–284. https://doi.org/10.1130/0016-7606(1974)85<273:GEOTSN>2.0.CO;2

Ulloa, C., & Rodríguez, G.I. 1982. Intrusivos ácidos Ordovícicos y post–Devónicos en la Floresta (Boyacá). IV Congreso Colombiano de Geología, Memoirs, p. 23. Cali.

Ulloa, C., Pérez, V.E. & Baldis, B. 1982. Unidades litoestratigráficas del Ordovícico de los Llanos Orientales de Colombia. V Congreso Latinoamericano de Geología. Memoirs, I, p. 109–112. Buenos Aires.

Villagómez, D.R. 2010. Thermochronology, geochronology and geochemistry of the Western and Central Cordilleras and Sierra Nevada de Santa Marta, Colombia: The tectonic evolution of NW South America. Doctoral thesis, Université de Genève, 143 p. Geneva, Switzerland. https://doi.org/10.13097/archive-ouverte/unige:14270

Villagómez, D., Spikings, R., Magna, T., Kammer, A., Winkler, W. & Beltrán, A. 2011. Geochronology, geochemistry and tectonic evolution of the Western and Central cordilleras of Colombia. Lithos, 125(3–4): 875–896. https://doi.org/10.1016/j.lithos.2011.05.003

Vinasco, C.J., Cordani, U.G., González, H., Weber, M. & Pelaez, C. 2006. Geochronological, isotopic, and geochemical data from Permo–Triassic granitic gneisses and granitoids of the Colombian central Andes. Journal of South American Earth Sciences, 21(4): 355–371. https://doi.org/10.1016/j.jsames.2006.07.007

Ward, D.E., Goldsmith, R., Cruz, J. & Restrepo, H. 1973. Geología de los cuadrángulos H–12 Bucaramanga y H–13 Pamplona, Departamento de Santander. Boletín Geológico, 21(1–3): 1–132.

Weber, M., Cardona, A., Valencia, V., García–Casco, A., Tobón, M. & Zapata, S. 2010. U/Pb detrital zircon provenance from late Cretaceous metamorphic units of the Guajira Peninsula, Colombia: Tectonic implications on the collision between the Caribbean arc and the South American margin. Journal of South American Earth Sciences, 29(4): 805–816. https://doi.org/10.1016/j.jsames.2009.10.004

Zapata, G., Rodríguez, G., Arango, M.I. & Bermúdez, J.G. 2015. Catálogo de unidades litoestratigráficas de Colombia: Cuarzomonzodiorita de Páez. Servicio Geológico Colombiano, 51 p. Bogotá.

Zapata, G., Rodríguez, G. & Arango, M.I. 2017. Petrografía, geoquímica y geocronología de rocas metamórficas aflorantes en San Francisco Putumayo y la vía Palermo–San Luis asociadas a los complejos La Cocha–Río Téllez y Aleluya. Boletín de Ciencias de la Tierra, (41): 48–65. https://doi.org/10.15446/rbct.n41.58630

Explanation of Acronyms, Abbreviations, and Symbols:

CRFZ	Cauca–Romeral Fault Zone
LA–ICP–MS	Laser ablation inductively coupled plasma mass spectrometry
LA–MC–ICP–MS	Laser ablation multi–collector inductively coupled plasma mass spectrometry
LGP	La Guajira Peninsula
SGC	Servicio Geológico Colombiano
SHRIMP	Sensitive high–resolution ion microprobe
SNSM	Sierra Nevada de Santa Marta

Authors' Biographical Notes

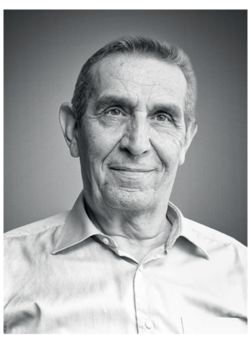

Jorge Julián RESTREPO obtained a degree in mining engineering and metallurgy at the Universidad Nacional de Colombia in 1968 and a Master of Science degree in geology at the Colorado School of Mines in 1973. He was a faculty member of the Universidad Nacional de Colombia, Sede Medellín, for over 40 years and currently holds the titles of Emeritus Professor and "Maestro Universitario". He taught Mineralogy, Metamorphic Petrology, Regional Geology, Field Geology, and Geochronology. His research focused on plate tectonics applied to the geology of Colombia, tectonostratigraphic terranes, geochronology, and the geologic evolution of metamorphic and mafic/ultramafic complexes of the Central Cordillera. Other interests are photography, genealogy, and the study of passifloras.

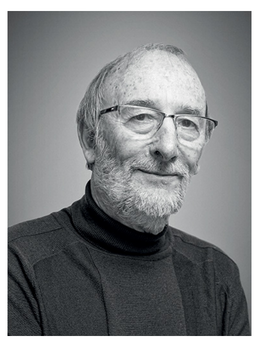

Jean–François TOUSSAINT has a Doctorate degree from the Université de Paris. After working in Bolivia for some time, he arrived at Medellín to teach at the Universidad Nacional de Colombia, Sede Medellín, where he taught courses such as Structural Geology, Geotectonics, Regional Geology, and Geology of Colombia for approximately 35 years. He was awarded the titles of Honorary Professor and "Maestro Universitario" by the Universidad Nacional. Some of his interests are the geological evolution of the Colombian Andes in terms of plate tectonics and tectonostratigraphic terranes, playing tennis, and the history of human evolution.

Volume 1

Chapter 4

Zircon U–Pb Geochronology and Hf–Nd–O Isotope Geochemistry of the Paleo– to Mesoproterozoic Basement in the Westernmost Guiana Shield

https://doi.org/10.32685/pub.esp.35.2019.04
Published online 24 November 2020

Mauricio IBAÑEZ–MEJIA[1]* and Umberto G. CORDANI[2]

1 ibanezm@arizona.edu
Department of Geosciences
University of Arizona
Tucson, Arizona, 85721, USA

2 ucordani@usp.br
Universidade de São Paulo
Instituto de Geociências
São Paulo–SP, Brasil

* Corresponding author

Abstract The crystalline basement of eastern Colombia, east of the frontal deformation zone of the north Andean Eastern Cordillera, is comprised by Precambrian igneous, metamorphic, and sedimentary rocks of the western Guiana Shield. Designated in the late seventies with the all–embracing stratigraphic name of 'Mitú Migmatitic Complex', the age, petrology, and tectonic history of the Precambrian basement in eastern Colombia has remained one of the least explored issues in South American geology. This chapter aims to present a brief overview of recent advances made to improve our general understanding of the geology of this wide region, using a compilation of the available U–Pb, Sm–Nd, Lu–Hf, and $\delta^{18}O$ isotopic data obtained using modern methods. Using all the available U–Pb geochronologic data we show that, in general: (i) The Precambrian basement of the western Guiana Shield exhibits magmatic crystallization ages in the range from ca. 1.99 to ca. 1.38 Ga, and (ii) that four broad periods of magmatic activity, two in the mid– to late–Paleoproterozoic (ca. 1.99 and ca. 1.81–1.72 Ga), one in the early Mesoproterozoic (ca. 1.59–1.50 Ga), and one in the mid Mesoproterozoic (ca. 1.41–1.39 Ga) dominate the geology of the area. The (whole–rock) Nd and combined (zircon) Hf–O datasets indicate a general lack of 'depleted mantle' like mid–Paleoproterozoic or Mesoproterozoic crust, thus indicating that either the Proterozoic sub–continental mantle in the region was not as radiogenic as global mantle evolution models would suggest, or that reworking of older crust might have played an important role in the geological and geochemical evolution of the western Guiana Shield. Therefore, although the geochronologic results confirm that most of the exposed basement in eastern Colombia can be broadly considered to be of Rio Negro–Juruena–like affinity, this belt exhibits some distinct isotopic characteristics relative to similar age domains exposed south of the Amazon Basin. Furthermore, we note that the geochronologic data obtained to this date has failed to clearly identify an early– to mid–Mesoproterozoic terrane boundary in the Colombian basement, thus opening the possibility that a Rondonian–San Ignacio–like province is not represented in the Guiana Shield. Based on these recent field, geochemical, and geochronological observations, we consider the long and extensively used term 'Mitú Migmatitic Complex' to be now inadequate and obsolete, and argue that the current state of the knowledge of the Colombian Precambrian basement is such that the community should move towards adopting

Citation: Ibañez–Mejia, M. & Cordani, U.G. 2020. Zircon U–Pb geochronology and Hf–Nd–O isotope geochemistry of the Paleo– to Mesoproterozoic basement in the westernmost Guiana Shield. In: Gómez, J. & Mateus–Zabala, D. (editors), The Geology of Colombia, Volume 1 Proterozoic – Paleozoic. Servicio Geológico Colombiano, Publicaciones Geológicas Especiales 35, p. 65–90. Bogotá. https://doi.org/10.32685/pub.esp.35.2019.04

more accurate and modern petrologic, tectonic, and stratigraphic nomenclature. Lastly, we note that the recent discovery of Cretaceous magmatism affecting the Colombian continental interior in the Araracuara basement high highlights the importance of Mesozoic tectonic reactivation in controlling the structural and landscape evolution of the Colombian Amazon. This observation indicates that future geochronologic studies aimed at better understanding the temporal history of mafic magmatism in this region will be crucial for understanding its structural and tectonic evolution.

Keywords: *Amazonian Craton, Proterozoic tectonics, U–Pb geochronology, Lu–Hf isotopes, Sm–Nd isotopes.*

Resumen El basamento cristalino del oriente colombiano, al este del frente de deformación andino de la cordillera Oriental, está compuesto por rocas ígneas, metamórficas y sedimentarias precámbricas pertenecientes al Escudo de Guayana. Agrupadas en la década de los setenta dentro de una unidad estratigráfica conocida como 'Complejo Migmatítico de Mitú', la edad, petrología, e historia tectónica de las unidades del basamento precámbrico en el oriente colombiano han permanecido como uno de los problemas menos explorados de la geología suramericana. Este capítulo tiene como objetivo presentar una revisión breve sobre los avances hechos en los últimos años para mejorar nuestro entendimiento geológico de esta amplia región, a partir de una compilación de información isotópica obtenida usando los sistemas U–Pb, Sm–Nd, Lu–Hf y $\delta^{18}O$ con métodos analíticos modernos. Considerando los datos de geocronología U–Pb disponibles observamos que en general: (1) el basamento precámbrico del límite occidental del Escudo de Guayana exhibe edades de cristalización en el rango de ca. 1,99 a ca. 1,38 Ga y (2) que cuatro principales eventos de actividad magmática, dos en el Paleoproterozoico medio a tardío (ca. 1,99 y ca. 1,81–1,72 Ga), uno en el Mesoproterozoico temprano (ca. 1,59–1,50 Ga) y uno en el Mesoproterozoico medio (ca. 1,41–1,39 Ga), dominan la geología de esta región. Las composiciones isotópicas de Nd en roca total junto con resultados conjuntos de isótopos de Hf y O en circón indican una ausencia generalizada de material directamente derivado del 'manto empobrecido' en este basamento paleo– y mesoproterozoico. Dicha observación puede deberse a dos motivos particulares: (1) que el manto sublitosférico proterozoico en la región no era tan radiogénico como la mayoría de los modelos globales de evolución mantélica sugerirían o (2) que el retrabajamiento de corteza continental más antigua podría haber jugado un papel importante en la evolución geológica y geoquímica del occidente del Escudo de Guayana. Por consiguiente, a pesar de que los resultados geocronológicos confirman que la mayor parte del basamento expuesto en el oriente colombiano puede considerarse a grandes rasgos como afín a la Provincia Río Negro–Juruena, la margen occidental del Escudo de Guayana presenta características isotópicas distintivas con respecto a los dominios de basamento de edad semejante expuestos al sur de la Cuenca del Amazonas. En adición a lo antedicho, observamos que la base de datos geocronológica existente no permite a la fecha identificar claramente una sutura mesoproterozoica temprana a media en el basamento del oriente colombiano, lo que sugiere la posibilidad de que un dominio de basamento afín a la Provincia Rondoniana–San Ignacio no este expresado en el Escudo de Guayana. Basados en las observaciones de campo, geoquímicas y geocronológicas presentadas en este capítulo consideramos que el término estratigráfico 'Complejo Migmatítico de Mitú', que ha sido ampliamente usado, resulta ahora inadecuado para describir la complejidad geológica del área y por consiguiente es obsoleto. En lugar de esto, consideramos que el estado del conocimiento geológico del oriente colombiano ha avanzado lo suficiente para permitir que una nomenclatura petrológica, tectónica y estratigráfica moderna, que describa con mayor exactitud la geología del área y por ende más apropiada, sea adoptada. Para concluir, también observamos que el descubrimiento reciente de magmatismo de edad cretácica que afecta el interior continental colombiano en el alto de basamento de Araracuara resalta la importancia que la reactivación tectónica mesozoica tuvo en el desarrollo estructural y geomorfológico de la Amazonia colombiana. Esta observación indica que los futuros estudios geocronológicos enfocados a comprender mejor la historia temporal del magmatismo máfico en esta región serán cruciales para mejorar nuestro entendimiento sobre la evolución estructural y tectónica del oriente colombiano.

Palabras clave: *Cratón Amazónico, tectónica proterozoica, geocronología U–Pb, geoquímica isotópica Lu–Hf, geoquímica isotópica Sm–Nd.*

1. Introduction

The continental basement of eastern Colombia, stretching from the Andean deformation front in the Llanos foothills to the borders with Venezuela and Brasil in the Orinoco and Amazonas territories, is comprised by Precambrian rocks of the western Guiana Shield (Figure 1; Cordani et al., 2016a; Gómez et al., 2017). Although most of the crystalline basement east of the Andes is currently buried under the thick sedimentary cover of the Putumayo and Llanos Foreland Basins, exposures of Precambrian igneous and metamorphic rocks occur in theVichada, Guainía, Vaupés, Caquetá, and Guaviare Departments (Figure 2). Difficulty of access to these areas, however, combined with the lack of roads and widespread vegetation cover, have made the geology of this region to remain relatively unexplored even to this date.

The Precambrian geology of Colombia bears great importance for understanding the growth history and paleogeography of the Amazonian Craton throughout the Proterozoic. The paleocontinent known as *Amazonia* is not only one of the largest Precambrian crustal nuclei on Earth but is also thought to have played a key role in the Precambrian supercontinent cycle (e.g., Cordani et al., 2009). Thus, understanding the construction of the Colombian Precambrian shield, and its potential correlation (or lack thereof) with crustal domains exposed south of the Amazon Basin, is a critical step toward reconstructing the tectonic history and assembly of Amazonia. Furthermore, understanding the geology of the Colombian basement is not only critical for correlating intra–cratonic structures, but also for evaluating potential connections amongst ancient orogenic belts across separate cratonic blocks that may once have been juxtaposed, therefore providing vital information for Precambrian paleogeography and supercontinent reconstructions (e.g., Li et al., 2008). All this information, however, can only be appropriately assessed if an adequate knowledge of the local geology is gained, and this is precisely why geologic, geochronologic, and isotopic studies from the eastern Colombian basement are of fundamental importance.

Over the past few years, a handful of studies have been published providing new geochronologic and isotopic data from the Precambrian basement of the westernmost Guiana Shield. These new results not only allow revisiting some of the paradigms that have prevailed in our understanding of the Colombian geology for many decades, but also to begin developing new ones. In this chapter, we provide a brief synthesis of the current state of knowledge on the geology of the Precambrian basement of the westernmost Guiana Shield, particularly focusing on the geochronologic and isotopic data obtained in Colombian territory over the last decade using modern U–Pb, Lu–Hf, and Sm–Nd methods. For a discussion of other available data using the Rb–Sr and K–Ar isotopic systems, the reader is referred to the recent comprehensive discussion provided by Cordani et al. (2016b).

2. Previous Studies and Geological Background

The first geochronologic analyses from the eastern Colombian basement were conducted by Pinson et al. (1962), where these authors performed K–Ar and Rb–Sr isotopic analyses of biotites from the San José del Guaviare syenites and porphyroblastic granitoids along the Guaviare River. They obtained ages around 1.2 Ga for the granitoids and around 460 Ma for the syenites. However, after this groundbreaking study by Pinson and co–workers, nearly two decades would have to go by before any new geochronologic data was produced.

In the late seventies, the 'Proyecto Radargramétrico del Amazonas' (PRORADAM) took place, and the results from this extensive field reconnaissance, mapping, and petrographic study were published by Galvis et al. (1979). This project also involved Rb–Sr, K–Ar, and the first U–Pb analyses performed in the area, which were conducted by the Z.W.O Isotope Geology Laboratory in Amsterdam and were published by Priem et al. (1982). These authors presented the first U–Pb concordia diagrams for ca. 1.55 Ga granitoids from the Vaupés River, identified ca. 1.8 Ga inherited components in zircons from gneisses in the Guainía River, and presented extensive Rb–Sr results suggesting the occurrence of magmatic events ca. 1.8 Ga, 1.55 Ga throughout the region. They also identified mafic rocks that defined apparent Rb–Sr isochron relations with slopes ca. 1.2 Ga, and a suite of rhyodacitic lavas from the Vaupés River with an apparent isochron age of ca. 920 Ma. This study was certain-

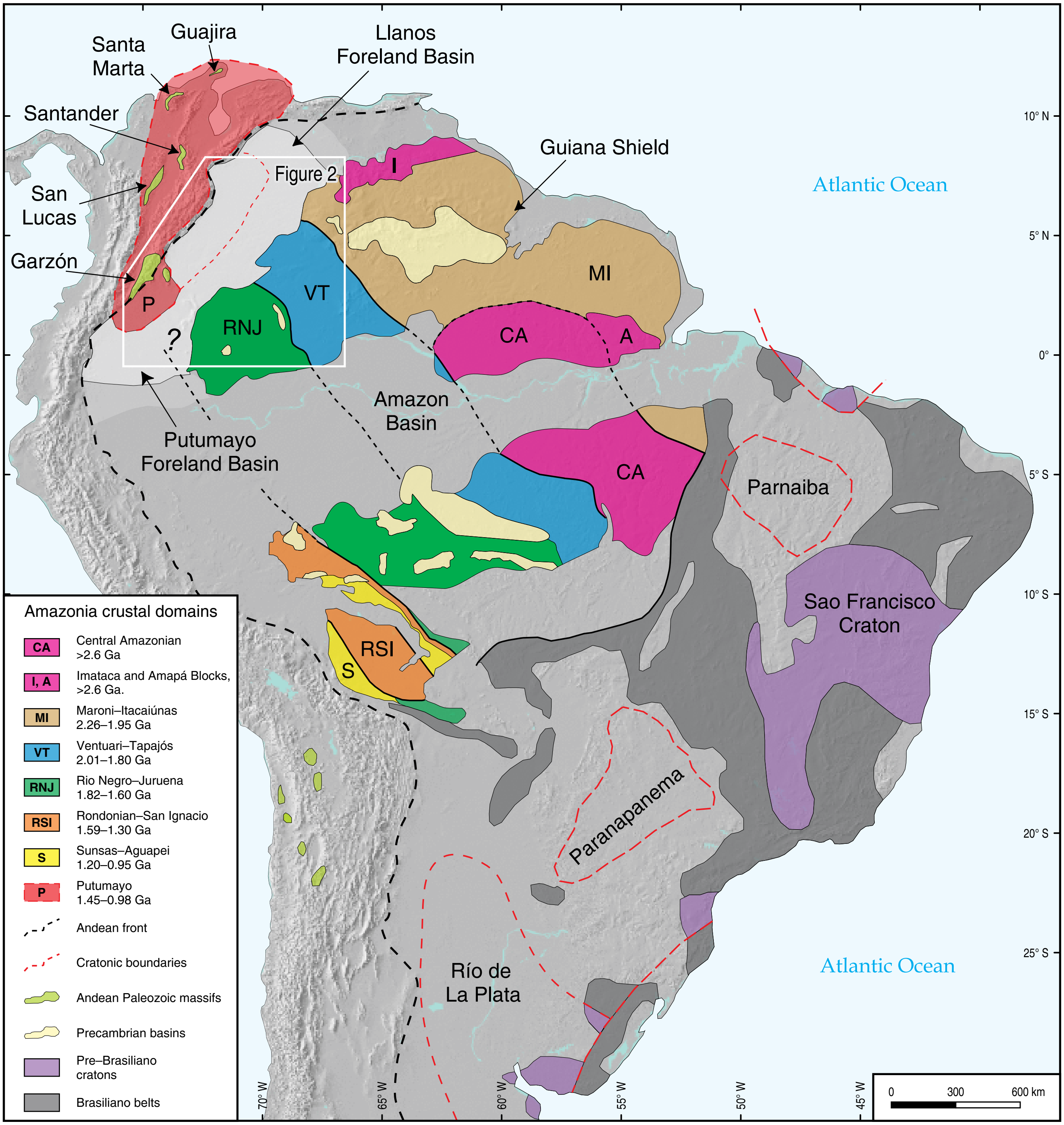

Figure 1. Simplified geo–tectonic map of South America overlaid on gray–scale shaded relief image (DEM), highlighting the approximate outline and terrane boundaries of the Amazonian Craton and the Guiana Shield. Adapted from Cordani & Teixeira (2007), Fuck et al. (2008), Ibañez–Mejia et al. (2015), Tassinari & Macambira (1999), and Teixeira et al. (2019). Shaded relief image areas with no overlay indicate younger cratonic cover or units in the Andean region. Light–gray shaded region indicates the location and extent of the north Andean Putumayo and Llanos Foreland Basins.

ly revolutionary, and set the stage for understanding the geology of eastern Colombia for the following ca. 30 years.

Although not strictly within Colombian territory, other studies conducted in SW Venezuela and NW Brasil in the late seventies and early nineties were also seminal for developing a better understanding of the geology of the western Guiana Shield; these were published by Barrios (1983), Barrios et al. (1985, 1986), Cordani et al. (1979), Fernandes et al. (1976),

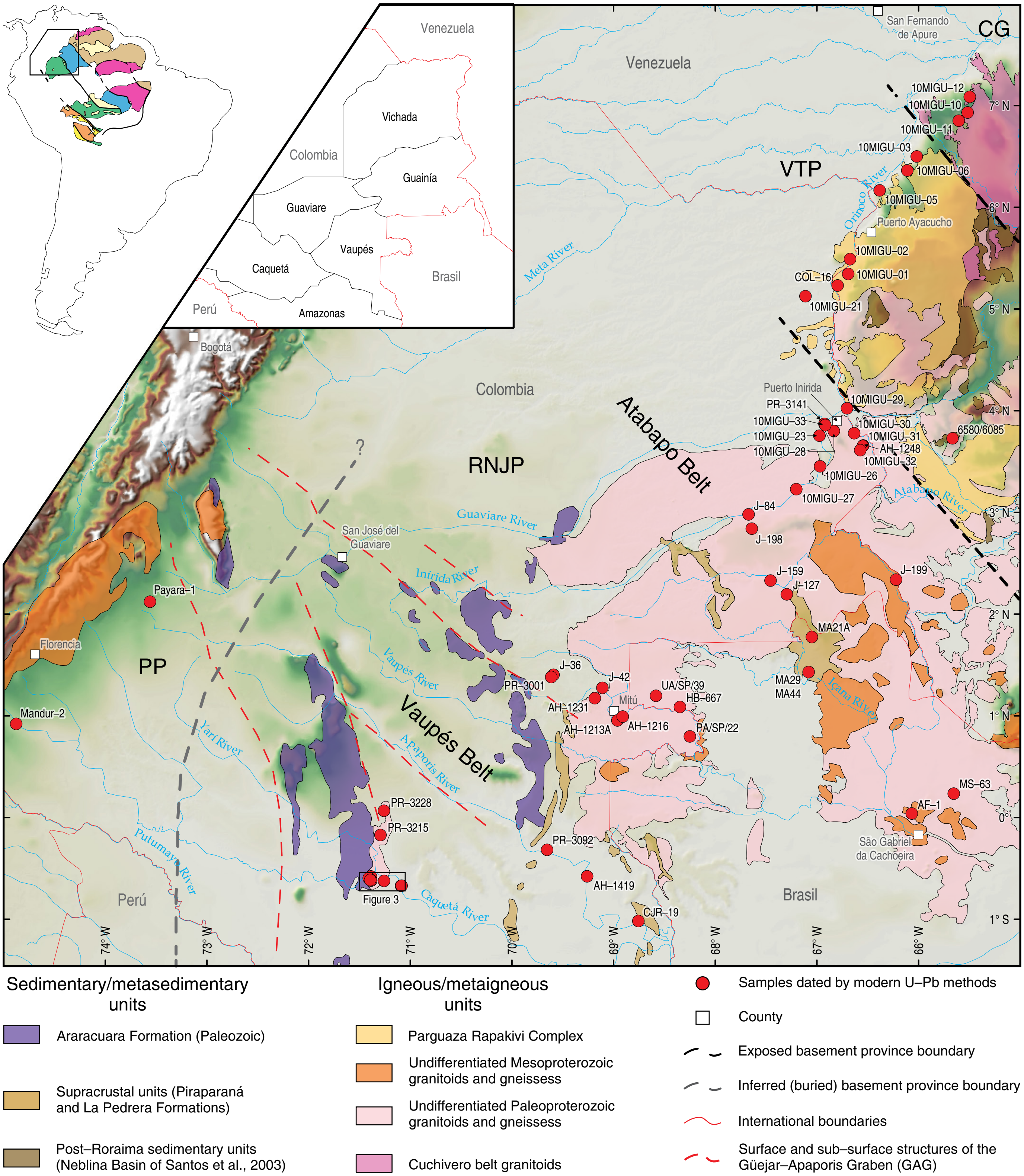

Figure 2. Simplified geologic map of the westernmost Guiana Shield, adapted from the maps of Cordani et al. (2016a) and Gómez et al. (2017). Inset shows the location and boundaries of Colombian departments mentioned throughout the text. Black dashed lines are major exposed intra–cratonic boundaries as suggested from the existing geochronologic data, namely: (1) The limit between the felsic volcanics of the Cuchivero Group (CG) in Venezuela, and the southern part of the Ventuari–Tapajós Province (VTP), and (2) the limit between VTP and Rio Negro–Juruena Province (RNJP), drawn along the Atabapo River as suggested by Cordani et al. (2016a). The dashed gray line outlines an approximate location for the suture between the RNJP and the Putumayo Province (PP), whose exact location is currently unknown. Red dashed lines reflect the approximate traces of faults associated with the intra–cratonic Güejar–Apaporis Graben (GAG).

Gaudette & Olszewski (1985), Gaudette et al. (1978), Gibbs & Barron (1993), and Pinheiro et al. (1976). Most of these studies exclusively employed Rb–Sr and K–Ar methods, with the exception of Gaudette & Olszewski (1985) and Gaudette et al. (1978) who presented the first U–Pb geochronologic result of intrusives from the Parguaza intrusive complex and the Minicia and Macabana gneisses along the Orinoco and Ventuari Rivers in Venezuela. Based on upper intercepts of discordia regressions through strongly discordant zircon U–Pb data (from dissolution of multi–grain aliquots), these authors proposed an age of ca. 1.55 Ga for the Parguaza complex and ages around 1.82 and 1.86 Ga for the Macabana and Minicia gneisses, respectively. It is worth noting that these results were obtained using a 12–inch, 60°sector mass spectrometer at Massachusetts Institute of Technology (MIT; Aldrich et al., 1953; Herzog, 1952; Shrock, 1977), which is in principle the same design that Alfred O. NIER used to separate the isotopes of uranium during World War II (Nier, 1940, 1947). Although the age results obtained using these instruments were certainly remarkable for the time, we consider them as 'legacy' data for the purposes of this discussion and only mention them here because of their particular historical significance.

In 1996, the first SHRIMP U–Pb analyses on zircons from the region were published by Tassinari et al. (1996), marking the beginning of what we here consider as 'modern methods' from a U–Pb geochronology standpoint. As mentioned previously, this chapter will not take into consideration the Rb–Sr and K–Ar databases, because a comprehensive compilation and careful analysis of these results was recently done by Cordani et al. (2016b), and because these databases have not been expanded since then. The U–Pb, Lu–Hf, and Sm–Nd datasets, on the other hand, have been moderately or significantly expanded, so the discussion provided in this chapter focuses on the data produced using these three isotopic systems as produced since 1996. Pb–Pb evaporation dates are also not considered because the geological accuracy of these dates, in and by themselves, is impossible to assess. We also make mention of the limited (but relevant) $\delta^{18}O_{Zrn}$ stable isotope results that have recently become available. Thus, the data used for the purposes of this chapter comes from the following sources (in chronologic order): Tassinari et al. (1996), Santos et al. (2000), Ibañez–Mejia et al. (2011), Bonilla–Pérez et al. (2013), Ibañez–Mejia (2014), Ibañez–Mejia et al. (2015), Cordani et al. (2016b), Veras et al. (2018). U–Pb results obtained from this compilation are listed in Table 1, along with the sample coordinates (in degrees, using the WGS84 datum), geographic locality (if known), rock–type that was analyzed, and their unique International Geo Sample Number (IGSN) identifier when available. Sm–Nd, Lu–Hf, and $\delta^{18}O_{Zrn}$ results obtained in this compilation are shown in Table 2, where only data obtained from samples with known U–Pb ages are listed and the quoted $^{143}Nd/^{144}Nd$, εNd, $^{176}Hf/^{177}Hf$, and εHf have been corrected to their initial values using the crystallization ages quoted in Tables 1, 2, and the decay constants of Lugmair & Marti (1978) and Söderlund et al. (2004).

Current models describing the growth and evolution of Amazonia indicate that, beginning at ca. 2.0 Ga, accretionary belts developed along the western margin of a cratonic nucleus that formed after the Transamazonian Orogeny. These accretionary belts are known as the Ventuari–Tapajós (ca. 2000–1800 Ma), Rio Negro–Juruena (ca. 1780–1550 Ma), and Rondonian–San Ignacio (ca. 1500–1300 Ma) (Cordani & Teixeira, 2007; Tassinari & Macambira, 1999). Continued soft–collision/accretion of these belts, driven by subduction–related processes, produced a very large "basement" in which granitoid rocks predominate, many of them with juvenile–like Nd isotopic signatures. Felsic volcanics are also widespread, and to date no clear evidence of Archean basement inliers within these tectonic provinces has been reported.

Recent geologic and geochronologic studies conducted in basement exposures found along the Caquetá, Inírida, Atabapo, and Orinoco Rivers (and vicinities) have greatly improved our understanding of the geology in eastern Colombia, thus allowing for a better interpretation of its evolution within the general tectonic framework of Amazonia and the western Guiana Shield. Outcrops along the Colombia–Venezuela border are key because they lie near the projected suture between the Ventuari–Tapajós and Rio Negro–Juruena Provinces as traced by Cordani & Teixeira (2007), thus providing an opportunity to test the predictions of their model and better understanding the nature and location of this boundary in the Guiana Shield. The Araracuara basement high is also of particular interest, mainly because it represents the westernmost basement exposure in eastern Colombia and thus allows evaluating the presence and/or location of potential Mesoproterozoic terranes and sutures in the western Guiana Shield. The sections below provide a brief summary of field observations from these two key areas, which are relevant for interpreting the geochronologic database compiled here.

2.1. Geology of the Araracuara Basement High, Caquetá River

The Araracuara High is an isolated basement exposure along the Caquetá River in SE Colombia (Figures 2, 3), which exposes a series of metasedimentary, igneous, and metaigneous rocks that uncomformably underlie mid–Paleozoic strata of the Araracuara Formation (Figure 4a, 4b). Based on field mapping and petrographic observations, the basement exposed here can be subdivided into at least four major units (Barrera, 1988; Galvis et al., 1979; Ibañez–Mejia, 2014): (i) A meta–(volcano)sedimentary unit composed predominantly by quartz–feldspar gneisses, with or without biotite, muscovite, and ± sillimanite (Figure 4a–c); (ii) equigranular and strongly

Table 1. Compilation of published geochronologic data from the westernmost Guiana Shield using modern U–Pb methods.

Sample name	Latitude	Longitude W	Locality (if know)	Rock type	Mean ± 2σ	Method	Reference	IGSN
Putumayo Basin basement								
Mandur–2 Melano	0° 55' 24.51" N	75° 52' 34.09"	Putumayo Basin well	Orthogneiss	1602 ± 16	LA–ICP–MS	Ibañez–Mejia et al. (2011, 2015)	IEURI0014
Payara–1	2° 7' 31.35" N	74° 33' 35.92"	Putumayo Basin well	Orthogneiss	1606 ± 6	LA–ICP–MS	Ibañez–Mejia et al. (2011, 2015)	IEURI0012
Araracuara basement high								
11MIAr–16	0° 36' 46.16" S	72° 23' 39.86"	Caquetá River, Araracuara	Dolerite	102.5 ± 2.3	LA–ICP–MS	Ibañez–Mejia (2014)	IEURI0048
11MIAr–18	0° 37' 17.03" S	72° 15' 29.24"	Caquetá River, Yarí Island	Porph. Syenogranite	1539 ± 20	LA–ICP–MS	Ibañez–Mejia (2014)	IEURI0049
11MIAr–22	0° 40' 8.28" S	72° 5' 7.45"	Caquetá River, Peña Roja	Foliated Syenogranite	1716 ± 16	LA–ICP–MS	Ibañez–Mejia (2014)	IEURI0050
EP–2	0° 34' 41.37" S	72° 23' 16.32"	Cañón del Diablo	Biotite gneiss	1721 ± 10	SHRIMP	Cordani et al. (2016b)	N.A.
11MIAr–07	0° 37' 0.89" S	72° 23' 10.92"	Caquetá River, Araracuara	Orthogneiss	1731 ± 16	LA–ICP–MS	Ibañez–Mejia (2014)	IEURI0046
J–263	0° 40' 10.37" S	72° 5' 26.16"	Caquetá River, Peña Roja	Syenogranite	1732 ± 17	LA–ICP–MS	Ibañez–Mejia et al. (2011)	N.A.
PR–3215	0° 10' 13.46" S	72° 17' 36.63"	Araracuara	Syenogranite	1756 ± 8	LA–ICP–MS	Ibañez–Mejia et al. (2011)	N.A.
11MIAr–02			Caquetá River, Araracuara	Paragneiss	DZ	LA–ICP–MS	Ibañez–Mejia (2014)	IEURI0044
11MIAr–06	0° 37' 3.15" S	72° 23' 2.52"	Caquetá River, Araracuara	Paragneiss	DZ	LA–ICP–MS	Ibañez–Mejia (2014)	IEURI0045
11MIAr–08	0° 35' 40.55" S	72° 24' 30.07"	Cañón del Diablo	Paragneiss	DZ	LA–ICP–MS	Ibañez–Mejia (2014)	IEURI0047
PR–3228	0° 4' 5.85"N	72° 15' 33.76"	Mesai River	Paragneiss	DZ	LA–ICP–MS	Cordani et al. (2016b)	N.A.
Apaporis River, Vaupés Department, and vicinities								
AH–1231	1° 10' 33.6" N	70° 11' 6.65"	Serranía Mitú	Monzogranite	1510 ± 26	LA–ICP–MS	Cordani et al. (2016b)	N.A.
AF–1	0° 2' 28.09" N	67° 4' 3.15"	São Gabriel	Granite with titanite	1518 ± 25	ID–TIMS	Santos et al. (2000)	N.A.
PA–22	0° 48' 0" N	69° 15' 0"	Papuri River	Granite	1521 ± 13	SHRIMP	Tassinari et al. (1996)	N.A.
AH–1419	0° 34' 35.19" S	70° 15' 38.79"	Apaporis River	Monzogranite	1530 ± 21	LA–ICP–MS	Ibañez–Mejia et al. (2011)	N.A.
AH–1216	0° 59' 42.23" N	69° 54' 37.31"	Vaupés River	Monzogranite	1574 ± 10	LA–ICP–MS	Ibañez–Mejia et al. (2011)	N.A.
PR–3092	0° 18' 57.74" S	70° 39' 15.23"	Apaporis River	Syenogranite	1578 ± 27	LA–ICP–MS	Ibañez–Mejia et al. (2011)	N.A.
CJR–19	1° 0' 59.94" S	69° 45' 24.35"	Apaporis River	Syenogranite	1593 ± 6	LA–ICP–MS	Ibañez–Mejia et al. (2011)	N.A.
UA–39	1° 12' 0" N	69° 34' 60"	Vaupés River	Quartz–diorite	1703 ± 7	ID–TIMS	Tassinari et al. (1996)	N.A.
AH–1213A	0° 57' 25.59" N	69° 57' 44.91"	Raudal Tucunare	Bt–Hnbd orthogneiss	1736 ± 19	LA–ICP–MS	Cordani et al. (2016b)	N.A.
PR–3001	1° 23' 2.76" N	70° 36' 49.25"	Caño Cuduyari	Bt–chl gneiss	1769 ± 33	SHRIMP	Cordani et al. (2016b)	N.A.
HB–667	1° 5' 23.87" N	69° 20' 51.41"	Raudal Cururu	Monzogranite	1778.8 ± 5.9	SHRIMP	Cordani et al. (2016b)	N.A.
MA44	1° 24' 7.2" N	68° 5' 31.2"	Içana River	Diatexite	1788 ± 11	LA–ICP–MS	Veras et al. (2018)	N.A.
MA29	1° 27' 36" N	68° 3' 3.6"	Içana River	Diatexite	1798 ± 11	LA–ICP–MS	Veras et al. (2018)	N.A.
MA21A	2° 9' 7.2" N	68° 3' 28.8"	Peuá Creek	Metagranite	1813 ± 19	LA–ICP–MS	Veras et al. (2018)	N.A.

Table 1. Compilation of published geochronologic data from the westernmost Guiana Shield using modern U–Pb methods (*continued*).

Sample name	Latitude	Longitude W	Locality (if know)	Rock type	Mean ± 2σ	Method	Reference	IGSN
				Apaporis River, Vaupés Department, and vicinities				
MS–63	0° 14' 13.32'' N	66° 39' 17.46''	Iã–Mirim River	Monzogranite	1810 ± 9	SHRIMP	Santos et al. (2000)	N.A.
J–42	1° 16' 41.35'' N	70° 6' 38.09''		Paragneiss	DZ	LA–ICP–MS	Cordani et al. (2016b)	N.A.
J–36	1° 24' 24.13'' N	70° 35' 28.37''		Paragneiss	DZ	LA–ICP–MS	Cordani et al. (2016b)	N.A.
				Guainía Department and vicinities				
10MIGU–27	3° 13' 58.02'' N	68° 12' 12.54''		Bt–Hnbd monzogranite	1500 ± 15	LA–ICP–MS	Ibañez–Mejia (2014)	IEURI0037
PR–3141	3° 52' 32.1'' N	67° 55' 33.81''	Caño Cuauben	Biotite gneiss	1501 ± 10	SHRIMP	Cordani et al. (2016b)	N.A.
10MIGU–23	3° 45' 33.33'' N	67° 58' 31.56''		Biotite monzogranite	1504 ± 20	LA–ICP–MS	Ibañez–Mejia (2014)	IEURI0035
J–84	2° 59' 4.83'' N	68° 40' 21.97''	Raudal Morroco	Monzogranite	1507 ± 22	SHRIMP	Cordani et al. (2016b)	N.A.
10MIGU–26	3° 27' 28.15'' N	67° 58' 9.15''	Cerros de Mavecure	Biotite syenogranite	1509 ± 14	LA–ICP–MS	Ibañez–Mejia (2014)	IEURI0036
10MIGU–33	3° 51' 48.8'' N	67° 55' 8''		Biotite granite	1516 ± 16	LA–ICP–MS	Ibañez–Mejia (2014)	IEURI0043
J–98	2° 50' 40.32'' N	68° 38' 28.4''	Caño Nabuquen	Monzogranite	1752 ± 21	LA–ICP–MS	Cordani et al. (2016b)	N.A.
J–159	2° 20' 1.19'' N	68° 27' 24.15''	Serranía de Naquén	Tonalite	1770 ± 40	LA–ICP–MS	Cordani et al. (2016b)	N.A.
J–127	2° 11' 52.96'' N	68° 17' 47.98''	Caño Naquén, Guainía River	Tonalitic orthogneiss	1775.3 ± 7.7	SHRIMP	Cordani et al. (2016b)	N.A.
10MIGU–30	3° 47' 0.2'' N	67° 38' 2.43''	Caño Chaquita	Bt–Hnbd granite	1795 ± 15	LA–ICP–MS	Ibañez–Mejia (2014)	IEURI0040
10MIGU–31	3° 39' 28.1'' N	67° 32' 54.9''	Caño Chaquita	Biotite granite	1795 ± 18	LA–ICP–MS	Ibañez–Mejia (2014)	IEURI0041
J–199	2° 20' 32.99'' N	67° 13' 20.56''	Negro River	Bt–Hnbd orthogneiss	1796.1 ± 3.7	SHRIMP	Cordani et al. (2016b)	N.A.
10MIGU–32	3° 36' 59.01'' N	67° 34' 28.62''		Biotite granite	1797 ± 17	LA–ICP–MS	Ibañez–Mejia (2014)	IEURI0042
10MIGU–29	4° 1' 42.35'' N	67° 42' 17.27''		Bt–Hnbd monzogranite	1806 ± 17	LA–ICP–MS	Ibañez–Mejia (2014)	IEURI0039
10MIGU–28	3° 48' 16.3'' N	67° 50' 2''		Biotite syenogranite	1810 ± 16	LA–ICP–MS	Ibañez–Mejia (2014)	IEURI0038
6580–6085	3° 43' 60'' N	66° 40' 0''	Casiquiare River	Tonalite	1834 ± 18	SHRIMP	Tassinari et al. (1996)	N.A.
AH–1248	3° 39' 46.54'' N	67° 32' 43.31''			DZ	LA–ICP–MS	Cordani et al. (2016b)	N.A.
				Orinoco River, Vichada Department, and vicinities				
10MIGU–03	6° 30' 24.99'' N	67° 1' 7.92''		Rapakivi granite	1388 ± 13	LA–ICP–MS	Ibañez–Mejia (2014)	IEURI0021
COL–21	5° 7' 54.1'' N	68° 6' 47.42''		Rapakivi granite	1392 ± 5	LA–ICP–MS	Bonilla–Pérez et al. (2013)	N.A.
COL–16	5° 29' 49.93'' N	67° 40' 28.19''		Rapakivi granite	1401 ± 4	LA–ICP–MS	Bonilla–Pérez et al. (2013)	N.A.
10MIGU–06	6° 22' 8.27'' N	67° 6' 41.07''		Rapakivi granite	1401 ± 14	LA–ICP–MS	Ibañez–Mejia (2014)	IEURI0023
10MIGU–05	6° 10' 23.21'' N	67° 23' 0.59''		Rapakivi granite	1402 ± 13	LA–ICP–MS	Ibañez–Mejia (2014)	IEURI0022
10MIGU–01	5° 14' 15.05'' N	67° 47' 48.89''		Rapakivi granite	1405 ± 12	LA–ICP–MS	Ibañez–Mejia (2014)	IEURI0019

Table 1. Compilation of published geochronologic data from the westernmost Guiana Shield using modern U–Pb methods (*continued*).

Sample name	Latitude	Longitude W	Locality (if know)	Rock type	Mean ± 2σ	Method	Reference	IGSN
Orinoco River, Vichada Department, and vicinities								
10MIGU–02	5° 21' 3.7" N	67° 41' 33.41"		Rapakivi granite	1408 ± 14	LA–ICP–MS	Ibañez–Mejia (2014)	IEURI0020
10MIGU–11	6° 56' 22.43" N	66° 31' 6.01"		Biotite granite	1424 ± 21	LA–ICP–MS	Ibañez–Mejia (2014)	IEURI0025
10MIGU–10	6° 51' 32.47" N	66° 36' 19.34"		Biotite leucogranite	1984 ± 18	LA–ICP–MS	Ibañez–Mejia (2014)	IEURI0024
10MIGU–12	7° 5' 37.63" N	66° 29' 49.1"		Biotite monzogranite	1989 ± 21	LA–ICP–MS	Ibañez–Mejia (2014)	IEURI0026

foliated biotite orthogneisses exposed in the Cañón del Diablo gorge and near Sumaeta and Mariñame islands (Figure 4d); (iii) coarsely porphyritic and undeformed syenogranites, best exposed near Yarí island and the Yarí River junction (Figure 4e, 4f); (iv) a younger and less deformed metasedimentary sequence that uncomformably overlies the gneissic/granitic basement, known as the La Culebra unit –not extensively exposed in map area of Figure 2–, and whose low–grade metamorphism distinguishes from the Paleozoic sedimentites of the Araracuara Formation. The first two units (i.e., paragneisses and orthogneisses) have been collectively mapped as the 'Araracuara Gneiss' unit (Figure 2). All igneous/metaigneous units are pervasively intruded by granitic dikes and sills, many of which have coarsely pegmatitic textures (e.g., Figure 4g), and a later generation of dikes and sills of doleritic composition (e.g., Figure 4h).

Samples from this uplift have been dated using zircon U–Pb geochronology by Cordani et al. (2016b), Ibañez–Mejia (2014), and Ibañez–Mejia et al. (2011), who have analyzed the (meta)granitoids outcropping along the Yarí River (sample PR–3215), the Caquetá River near the Sumaeta (J–263 and 11MIAr–22), and Yarí (11MIAr–18) islands, as well as samples taken along the Caquetá River closer to the town of Araracuara, collected from ortho– (EP–2 and 11MIAr–07) and paragneisses (11MIAr–02, –06, and –08) of the Araracuara Gneiss unit in the Cañón del Diablo gorge. These studies have found the orthogneisses in the region to yield exclusively Paleoproterozoic (ca. 1.72 to 1.76 Ga) ages for the igneous crystallization of their protoliths, while paragneisses yield unimodal detrital zircon age distributions with maximum depositional ages of around 1.73 Ga. Ibañez–Mejia (2014) interpreted the Araracuara Gneiss as reflecting: (i) A metamorphosed volcano–sedimentary sequence whose protoliths formed in a forearc basin associated with a Paleoproterozoic arc; and (ii) that these basins were rapidly buried, intruded by granitoid magmas and metamorphosed at an age that must be younger (but indistinguishable within LA–ICP–MS U–Pb age uncertainty) relative to their timing of sedimentation. No ages of metamorphism from zircon recrystallization fronts or overgrowths have yet been determined from the Araracuara Gneiss. Some of the porphyritic and unmetamorphosed syenogranites in the area, however, yield ca. 1.54 Ga U–Pb crystallization ages, which constrain the regional metamorphism that affected the Araracuara Gneiss to be older than this event.

A sample from a doleritic dike intruding the Araracuara Gneiss (11MIAr–16) dated by Ibañez–Mejia (2014) produced an Albian age of 102.5 ± 2.3 Ma, which indicates that mid Cretaceous magmatism has affected the continental interior of Colombia as far inland as Araracuara. The Cretaceous age of this dike was confirmed by Sm–Nd whole–rock isotopic analyses of the same sample, whose highly radiogenic initial $^{143}Nd/^{144}Nd$ precludes derivation from the Proterozoic mantle.

Locations of all samples that have been studied from the Araracuara High are shown in Figure 3 and their coordinates listed in Table 1. Only two granitic samples collected along the Caquetá River E of Araracuara have been analyzed for Lu–Hf isotopes in zircons following U–Pb dating, and only three Sm–Nd isotopic results from whole–rock aliquots are thus far available (Table 2).

2.2. Geology of Guainía and Vichada Near the Colombia–Venezuela Border

The most extensive outcrops of Precambrian basement in Colombia are located in the eastern and southeastern portions of the Vichada and Guainía Departments (Figure 2), along the Orinoco, Guaviare, Inírida, Atabapo, Guainía, and Negro River basins (Gómez et al., 2017). Samples dated by U–Pb methods in this region, from the studies of Bonilla–Pérez et al. (2013), Cordani et al. (2016b), and Ibañez–Mejia (2014) are mainly from outcrops located around the Orinoco, Inírida, and Atabapo Rivers. From oldest to youngest, the basement in this area is comprised by: (i) Volcanic and intrusive rocks of the Cuchivero magmatic belt (Gibbs, 1987; Teixeira et al., 2002), with crystallization ages ca. 1.99 Ga and thus presumably belonging to a broader magmatic event in the Guiana Shield known as the Orocaima event (Reis et al., 2000), which in NW Venezuela is dominantly comprised by coarse– and

Table 2. Compilation of published Sm–Nd, Lu–Hf, and O isotopic data from the westernmost Guiana Shield.

Sample name	$^{143}Nd/^{144}Nd \pm 2SE_{(t)}$	$\varepsilon Nd_{(t)} \pm 2SE$	U–Pb cryst. age	2–stage T_{DM} (Ga)	Reference	IGSN
Putumayo Basin basement Payara–1	0.510638 ± 8	+1.50 ± 0.16	1606 Ma	2.01	Ibañez–Mejia et al. (2015)	IEURI0012
Araracuara basement high 11MIAr–16	0.512722 ± 14	+4.14 ± 0.28	103 Ma	0.52	Ibañez–Mejia (2014)	IEURI0048
11MIAr–22	0.510500 ± 24	+1.60 ± 0.47	1716 Ma	2.09	Ibañez–Mejia (2014)	IEURI0050
EP–2	0.510418	+0.12	1721 Ma	2.24	Cordani et al. (2016b)	N.A.
Apaporis River, Vaupés Department, and vicinities						
AH–1231	0.510639	–0.91	1510 Ma	2.17	Cordani et al. (2016b)	N.A.
AH–1213A	0.510382	–0.20	1736 Ma	2.28	Cordani et al. (2016b)	N.A.
PR–3001	0.510388	+0.76	1769 Ma	2.22	Cordani et al. (2016b)	N.A.
HB–667	0.510329	–0.15	1779 Ma	2.31	Cordani et al. (2016b)	N.A.
Guainía Department and vicinities						
PR–3141	0.510489	–4.08	1501 Ma	2.48	Cordani et al. (2016b)	N.A.
J–84	0.510533	–3.07	1507 Ma	2.38	Cordani et al. (2016b)	N.A.
J–98	0.510331	–0.79	1752 Ma	2.36	Cordani et al. (2016b)	N.A.
J–159	0.510368	+0.41	1770 Ma	2.25	Cordani et al. (2016b)	N.A.
J–127	0.510326	–0.30	1775 Ma	2.33	Cordani et al. (2016b)	N.A.
J–199	0.510301	–0.25	1796 Ma	2.34	Cordani et al. (2016b)	N.A.

Sample name	$^{176}Hf/^{177}Hf \pm 2SD_{(t)}$	$\varepsilon Hf_{(t)} \pm 2SD$	U–Pb cryst. age	$\delta^{18}O \pm 2SD$ (‰)	Reference	IGSN
Putumayo Basin basement Mandur–2 Melano	0.281974 ± 42 (n=18)	+7.6 ± 1.5	1602 Ma	5.43 ± 0.23 (n=22)	Ibañez–Mejia et al. (2015)	IEURI0014
Payara–1	0.281796 ± 70 (n=11)	+0.8 ± 2.5	1606 Ma	ca. 9.0 to 9.4	Ibañez–Mejia et al. (2015)	IEURI0012
Araracuara basement high 11MIAr–18	0.281803 ± 46 (n=6)	–0.1 ± 1.5	1539 Ma	N.A.	Ibañez–Mejia (2014)	IEURI0049
11MIAr–22	0.281738 ± 59 (n=11)	+1.7 ± 2.0	1716 Ma	N.A.	Ibañez–Mejia (2014)	IEURI0050
Guainía Department and vicinities						
10MIGU–27	0.281686 ± 76 (n=16)	–5.1 ± 2.7	1500 Ma	8.95 ± 0.60 (n=16)	Ibañez–Mejia (2014)	IEURI0037
10MIGU–23	0.281696 ± 37 (n=16)	–4.7 ± 1.3	1504 Ma	8.41 ± 0.67 (n=14)	Ibañez–Mejia (2014)	IEURI0035
10MIGU–26	0.281667 ± 54 (n=15)	–5.6 ± 1.9	1509 Ma	9.29 ± 0.50 (n=16)	Ibañez–Mejia (2014)	IEURI0036
10MIGU–33	0.281702 ± 40 (n=16)	–4.2 ± 1.4	1516 Ma	8.27 ± 0.39 (n=12)	Ibañez–Mejia (2014)	IEURI0043
10MIGU–30	0.281634 ± 54 (n=15)	–0.2 ± 1.9	1795 Ma	8.37 ± 0.59 (n=18)	Ibañez–Mejia (2014)	IEURI0040
10MIGU–31	0.281658 ± 58 (n=15)	+0.6 ± 2.1	1795 Ma	7.09 ± 0.31 (n=13)	Ibañez–Mejia (2014)	IEURI0041
10MIGU–32	0.281614 ± 50 (n=15)	–0.9 ± 1.8	1797 Ma	7.63 ± 0.53 (n=17)	Ibañez–Mejia (2014)	IEURI0042
10MIGU–29	0.281637 ± 84 (n=17)	+0.2 ± 3.0	1806 Ma	8.52 ± 0.37 (n=12)	Ibañez–Mejia (2014)	IEURI0039
10MIGU–28	0.281633 ± 68 (n=16)	+0.1 ± 2.4	1810 Ma	7.69 ± 0.29 (n=13)	Ibañez–Mejia (2014)	IEURI0038
Orinoco River, Vichada Department, and vicinities						
10MIGU–03	0.281814 ± 50 (n=15)	–3.2 ± 1.8	1388 Ma	6.23 ± 0.30 (n=12)	Ibañez–Mejia (2014)	IEURI0021
10MIGU–06	0.281776 ± 50 (n=15)	–4.2 ± 1.8	1401 Ma	6.50 ± 0.37 (n=12)	Ibañez–Mejia (2014)	IEURI0023
10MIGU–05	0.281782 ± 57 (n=16)	–4.0 ± 2.0	1402 Ma	6.36 ± 0.26 (n=7)	Ibañez–Mejia (2014)	IEURI0022
10MIGU–01	0.281784 ± 84 (n=18)	–3.8 ± 3.0	1405 Ma	6.32 ± 0.28 (n=11)	Ibañez–Mejia (2014)	IEURI0019
10MIGU–02	0.281771 ± 77 (n=7)	–4.2 ± 2.8	1408 Ma	5.69 ± 0.55 (n=7)	Ibañez–Mejia (2014)	IEURI0020
10MIGU–11	0.281800 ± 72 (n=16)	–2.8 ± 2.6	1424 Ma	5.26 ± 0.13 (n=10)	Ibañez–Mejia (2014)	IEURI0025
10MIGU–10	0.281555 ± 51 (n=13)	+1.4 ± 1.8	1984 Ma	4.89 ± 0.37 (n=12)	Ibañez–Mejia (2014)	IEURI0024
10MIGU–12	0.281540 ± 86 (n=15)	+0.9 ± 3.1	1989 Ma	4.73 ± 0.39 (n=13)	Ibañez–Mejia (2014)	IEURI0026

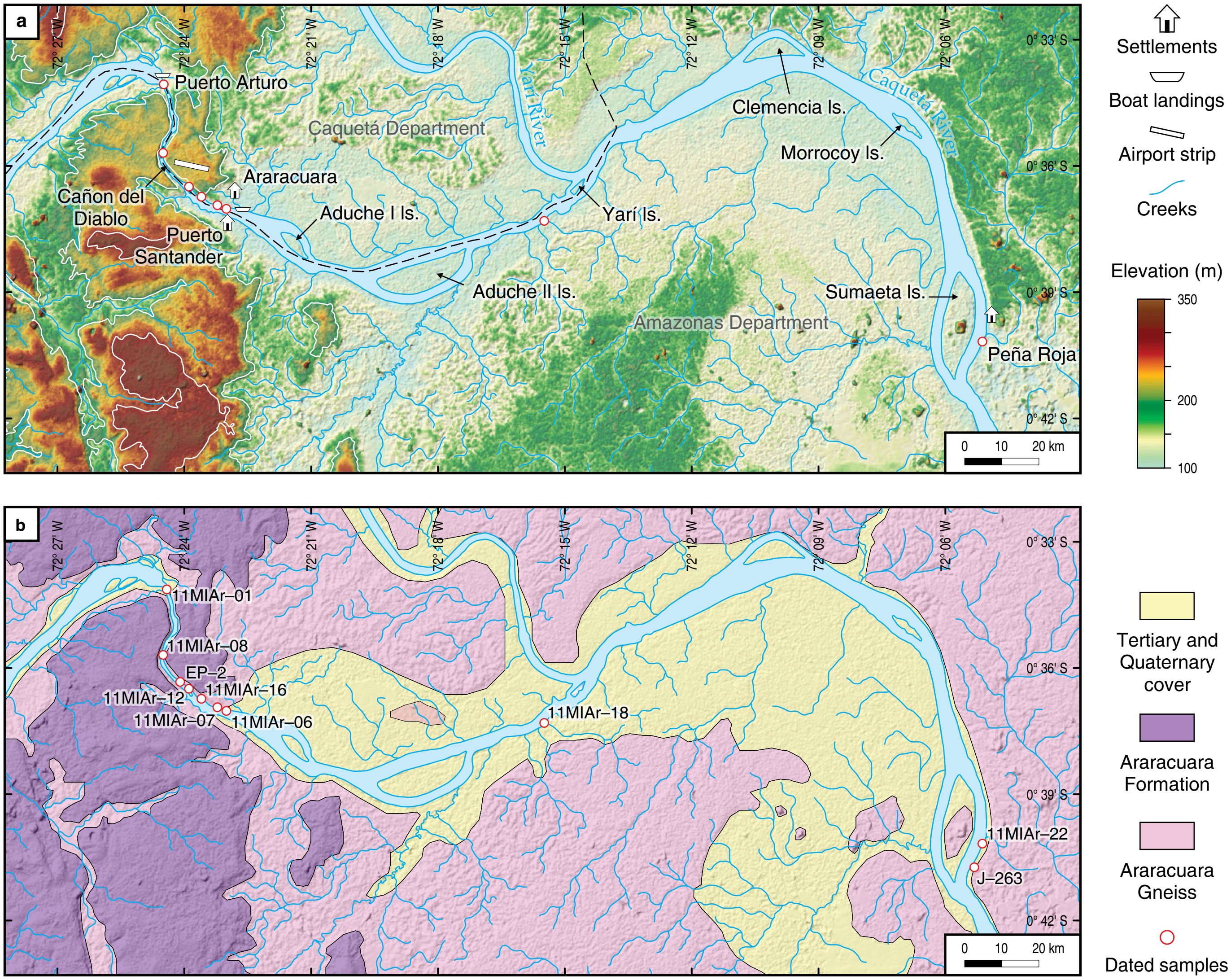

Figure 3. Topographic **(a)** and geologic **(b)** map of the Araracuara region, showing the location of samples collected and analyzed by Cordani et al. (2016b), Ibañez–Mejia (2014), and Ibañez–Mejia et al. (2011). (Is.) Island.

fine–grained biotite granitoids (e.g., Figure 5a, 5b); (ii) intermediate and granitic orthogneisses which are widespread along the Atabapo and Ventuari Rivers (e.g., Figure 5c) and yield igneous crystallization ages ca. 1.8 Ga like those of the Cauaburi Complex and Taiuaçu–Cauera diatexite in NW Brasil (Almeida et al., 2013; Veras et al., 2018). In addition to their penetrative gneissic fabric, these orthogneisses show local evidences of intense mylonitic deformation (Figure 5d); (iii) coarsely porphyritic intrusives like those that make up the "Cerros de Mavecure" inselbergs (Figure 5e, 5f) which yield U–Pb crystallization ages ca. 1.5 Ga. These intrusives can locally contain abundant metasedimentary enclaves (Figure 5g), exhibit primary magmatic fabrics denoted by alignment of orthoclase phenocrysts (Figure 5h), or have more massive, equigranular textures (Figure 5i, 5j); (iv) the Parguaza intrusive complex, which is mostly comprised by granitoids with rapakivi textures that yield U–Pb crystallization ages ca. 1.4 Ga. Outcrops of the Parguaza complex are common along the Orinoco River in Colombia and Venezuela (Figure 5k), but are best exposed in large inselbergs to the E and NE of Puerto Ayacucho (Figure 5l). Most outcrops of this unit are characterized by granitoids with fine– to coarse–grained rapakivi textures (e.g., Figure 5m, 5n).

In addition to the crystallization ages described above, Cordani et al. (2016b) obtained whole–rock Sm–Nd isotopic data from six of their dated samples, and Ibañez–Mejia (2014) obtained Lu–Hf and $\delta^{18}O_{Zrn}$ isotopic results for 17 samples from this region (Table 2). These isotopic datasets, in combination with the U–Pb dates, allow to better understand the sources of these magmas and make inferences about the processes involved in their generation and possible tectonic setting.

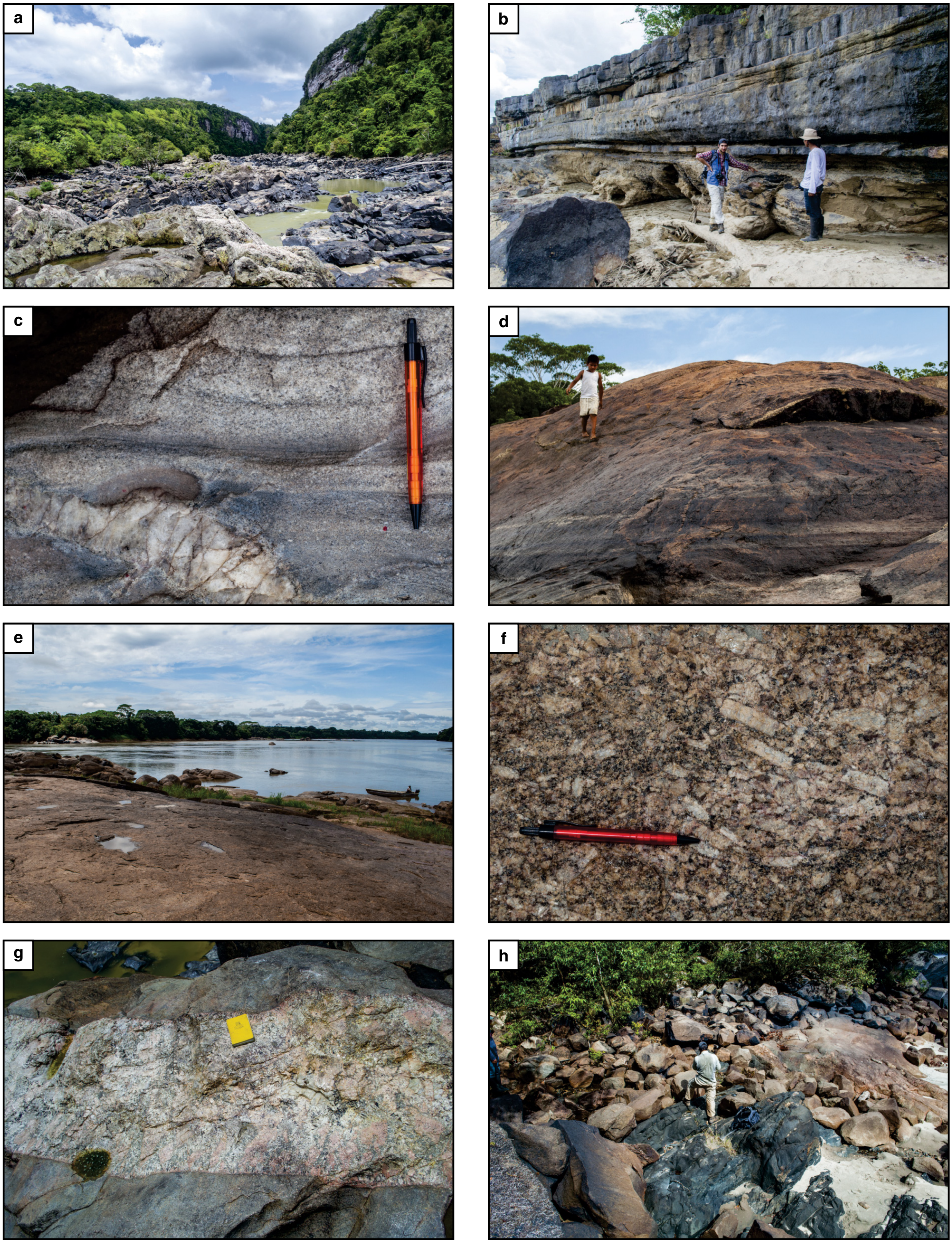
a
b
c
d
e
f
g
h

←

Figure 4. Field photographs of outcrops in the Araracuara basement high. **(a)** Caquetá river exiting through the eastern end of the Cañón del Diablo gorge, near locality 11MIAr–12 of Figure 3b; Proterozoic metasedimentary rocks of the Araracuara Gneiss appear in the foreground and Paleozoic sedimentary rocks of the Araracuara Formation in the background. **(b)** The 'Great Unconformity' of the Colombian Amazon: Paleozoic rocks of the Araracuara Formation overlie metasedimentary basement of the Araracuara Gneiss in the western end of the Cañón del Diablo gorge, near Puerto Arturo, Caquetá (locality 11MIAr–01 of Figure 3b). **(c)** Detail of layered biotite–rich and biotite–poor quartz–plagioclase metasedimentary gneisses of the Araracuara Gneiss unit, injected by coarse–grained quartz veins; sampling location 11MIAr–08, dip direction of foliation plane is 170/28. **(d)** Outcrop of foliated biotite monzogranite along the shoreline of the Caquetá River, near Sumaeta island in sampling locality 11MIAr–22 of Figure 3b. **(e)** Outcrop of coarsely porphyritic biotite monzogranite along the shoreline of the Caquetá River, near the junction of the Yarí River (sampling locality 11MIAr–18). **(f)** Detail of coarsely porphyritic biotite monzogranite in sampling locality 11MIAr–18, preserving primary magmatic fabric. **(g)** Pegmatitic dikes cross–cutting metasedimentary gneisses of the Araracuara Gneiss, near locality 11MIAr–12 of Figure 3b. **(h)** Cretaceous dolerite dike intruding metasedimentary rocks of the Araracuara Gneiss; sampling locality 11MIAr–16.

3. Discussion

3.1. It Is Time to Part with the Concept of a 'Mitú Migmatitic Complex'

The term "Mitú Migmatitic Complex" (MMC) was proposed by Galvis et al. (1979) to group all Proterozoic rocks in eastern Colombia stratigraphically underlying the so–called La Pedrera Formation. The original definition of the MMC included "metapsamites and metapelites, mafic and quartzofeldspathic metaigneous, blastomylonites, and migmatitic granitoid rocks belonging to the Guiana Shield". This definition might have been adequate in the late seventies, when exploratory mapping in the area was just starting to be performed, geochronologic information was unavailable, and modern concepts of continental construction by tectonic processes were arguably still in their infancy. However, this nomenclature results inaccurate and unpractical now, mainly because: (i) Evidently not all Precambrian rocks exposed in eastern Colombia and encompassed within this denomination are 'migmatitic' in nature (Figures 4, 5); and (ii) the growing geochronologic and isotopic database for the basement of eastern Colombia has started to shed light into the diversity of magmatic crystallization ages and possible orogenic events found in this geographically extensive region (see following sections).

Although still limited, the data compiled here allows distinct age and isotopic basement domains to be recognized and major tectonic boundaries to be sketched. Therefore, under the light of the currently available data, and with the prospect of much new geochronologic research to come, we consider the term Mitú Migmatitic Complex to be now obsolete and urge the geological community to abandon its usage, other than for historic purposes. Although it is not the objective of this chapter to propose new stratigraphic nomenclature, we believe future research efforts should be aimed at adopting a more accurate and flexible one, in line with modern geochronologic and petrologic research in the area. Using modern geochronologic and geochemical methods, it is anticipated that even individual arc sequences in this region can be identified and mapped with some detail in the future (e.g., Carneiro et al., 2017). The following sections will describe the main trends that stand out from the available geochronologic and isotopic data, and highlight recent efforts made towards adopting a modern tectonostratigraphic scheme for the basement of eastern Colombia.

3.2. Distribution of Proterozoic U–Pb Zircon Crystallization Ages in the Western Guiana Shield

The zircon U–Pb geochronologic database of eastern Colombia and adjoining regions in Venezuela and Brasil now consists of 57 published samples dated using modern methods (ID–TIMS, SHRIMP, and/or LA–ICP–MS; see Table 1 for a summary). Results from 46 of these samples interpreted as igneous crystallization ages of magmatic rocks, migmatitic leucosomes, or igneous protoliths of orthogneisses, are shown as a rank–order plot in Figure 6 and grouped by broad geographic regions. From southwest to northeast, the geographic areas used for grouping of ages are as follows: (i) Buried basement of the Putumayo Basin, which for the purposes of this chapter only includes Paleoproterozoic and early to mid–Mesoproterozoic protolith crystallization ages of orthogneisses in this region but excludes younger Proterozoic ages associated to the Putumayo orogenic cycle (discussed in Ibañez–Mejia, 2020); (ii) exposed basement of the Araracuara High, which includes all basement exposures along the Caquetá and Yarí Rivers; (iii) exposed basement outcrops along the Apaporis River, the Vaupés River, and elsewhere in the Vaupés Department and surrounding regions in Brasil (labeled 'Vaupés', for simplicity); (iv) exposed basement along the Inírida and Atabapo Rivers, elsewhere in the Guainía Department and neighboring areas in Venezuela (labeled 'Guainía'); and (v) exposed basement along the Orinoco River, the Vichada Department, and neighboring areas in Venezuela (labeled 'Orinoco').

In general, the current U–Pb geochronologic database indicates that igneous rocks from the Precambrian basement of the westernmost Guiana Shield predominantly crystallized during the Paleo– and Mesoproterozoic, between ca. 1.99 and 1.38 Ga. The oldest rock that has been dated within Colombian territory to this date is a fine–grained pink syenogranite exposed at 'Ce-

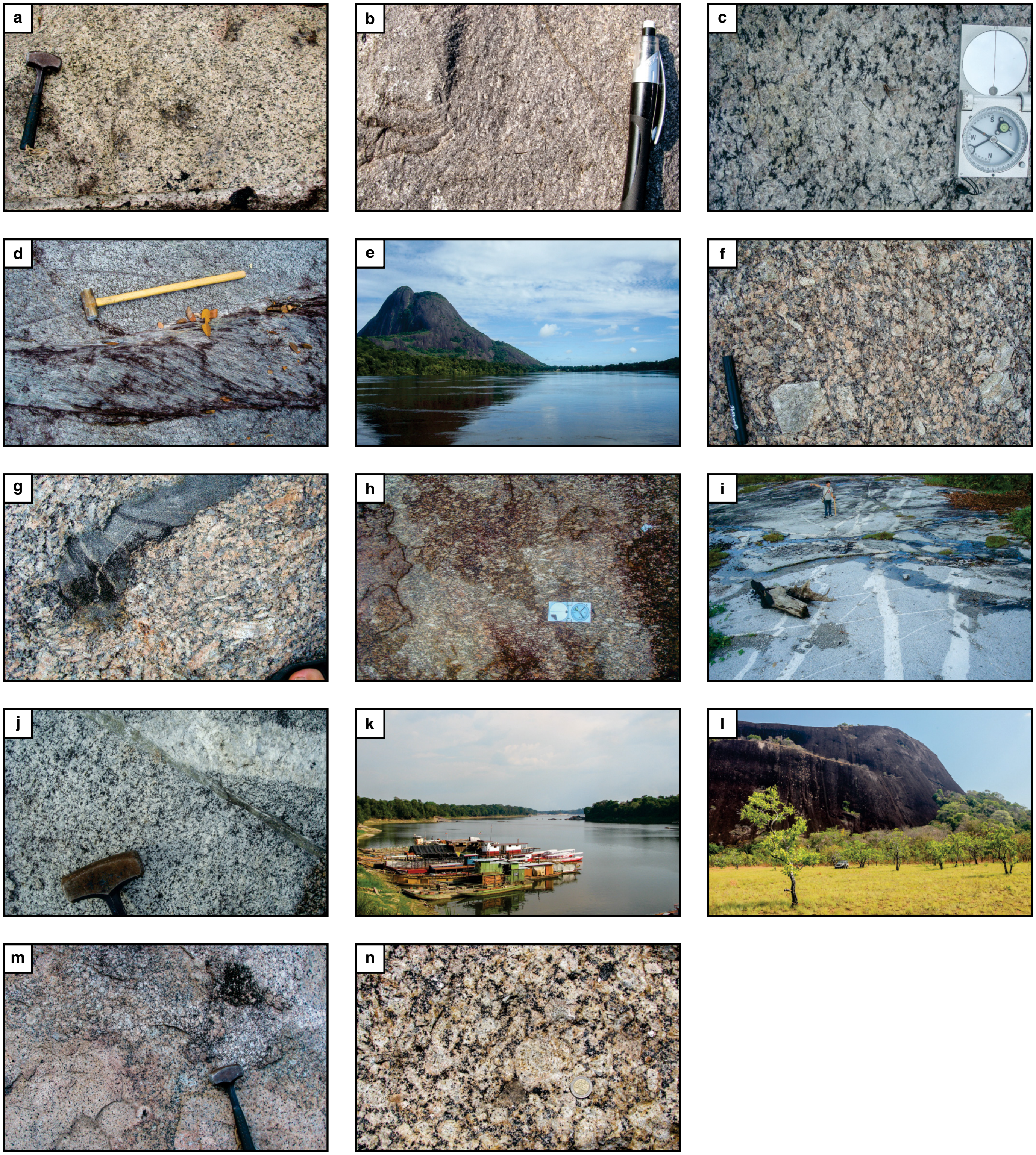

rro Vitina' in Guainía, with a U–Pb crystallization age of 1810 ± 16 Ma (sample 10MIGU–28 in Table 1), although the potential for Cuchivero–like (ca. 2.0 Ga) igneous rocks to be present in the Vichada Department, or older rocks elsewhere, still remains to be explored in more detail.

The geochronologic dataset summarized in Figure 6 defines at least four broad age clusters, which are representative of major magmatic episodes that have shaped the westernmost Guiana Shield; these are: (i) Ages around 1.99 Ga, obtained from felsic igneous rocks of the Cuchivero magmatic belt and likely belonging to the Orocaima event; (ii) a broad group of mid Paleoproterozoic ages, ranging from 1.84 to 1.72 Ga and mostly representative of igneous (protolith) crystallization ages from weakly– to strongly–foliated orthogneisses; (iii) a broad group

←

Figure 5. Field photographs of outcrops in the Guainía and Vichada Departments (and vicinities), mostly taken from outcrops along the Inírida, Atabapo, and Orinoco Rivers. **(a)** Coarse–grained, foliated biotite monzogranites of the Cuchivero Belt in Venezuela; sampling locality 10MIGU–14 (not shown in Figure 2). **(b)** Very fine–grained biotite leucogranites of the Cuchivero Belt in Venezuela; sampling locality 10MIGU–10. **(c)** Detail of ca. 1.8 Ga biotite orthogneisses from the Caño Chaquita creek tributary of the Atabapo River, defining a metamorphic foliation striking ca. 40° (azimuth); sampling location 10MIGU–31. **(d)** Meter–scale S–C mylonite cross–cutting the metamorphic foliation of 1.8 Ga orthogneisses; Caño Chaquita creek, near sampling location 10MIGU–31. **(e)** 'Cerros de Mavecure' inselbergs along the Inírida River. **(f)** Strongly porphyritic biotite syenogranite from the base of Cerros de Mavecure; sampling location 10MIGU–26. **(g)** Partially resorbed metasedimentary enclave in high $\delta^{18}O_{Zrn}$ 1.5 Ga porphyritic syenogranites of the Inírida River, near Cerros de Mavecure. **(h)** Porphyritic biotite syenogranites from the raudal Qualé, defining a magmatic orientation fabric striking ca. 140° (azimuth); sampling location 10MIGU–27. **(i)** Massive biotite granites from the 'Laja los Libertadores', near Puerto Inírida, intruded by leucocratic granite dikes; sampling location 10MIGU–33. Geologist Zeze AMAYA for scale. **(j)** Detail of biotite granites of the 'Laja los Libertadores', crosscut by discrete shear zones forming centimeter–scale cataclasites. **(k)** Exposures of the Parguaza Complex along the Orinoco River near Samariapo. Left (east) margin of the river is Venezuelan territory and right (west) margin is Colombian; photo near sampling locality 10MIGU–01. **(l)** Inselbergs of the Parguaza Complex NE of Puerto Ayacucho, Venezuela; sampling locality 10MIGU–06. **(m)** Medium–grained rapakivi granites of the Parguaza Complex; sampling locality 10MIGU–06. **(n)** Coarse–grained rapakivi granites of the Parguaza Complex; sampling locality 10MIGU–03.

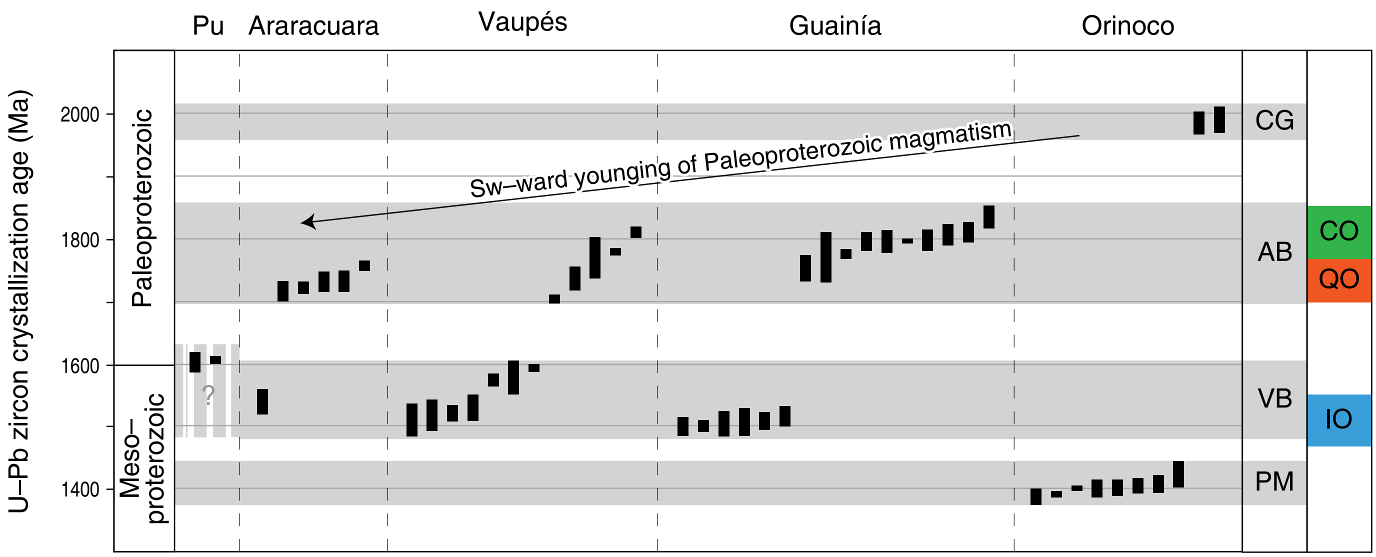

Figure 6. Rank–order plot, organized by geographic region, of the U–Pb geochronologic database available for the westernmost Guiana Shield. (Pu) includes orthogneiss protolith crystallization ages from the basement of the Putumayo Foreland Basin; (Araracuara) includes all samples dated from the Araracuara basement high; (Vaupés) includes all samples dated from the Apaporis River, Vaupés Department, and neighboring regions in Brasil; (Guainía) includes all samples dated from the Inírida and Atabapo Rivers, the Guainía Department, and neighboring regions in Venezuela; (Orinoco) includes all samples dated from the Orinoco River, the Vichada Department, and neighboring regions in Venezuela. (CG) Cuchivero Granites; (AB) Atabapo Belt; (VB) Vaupés Belt; (PM) Parguaza Massif, are after Cordani et al. (2016b). (CO) Cauaburi Orogeny; (QO) Querari Orogeny; (IO) Içana Orogeny, are after Almeida et al. (2013).

of early Mesoproterozoic ages, ranging from 1.59 to 1.50 Ga and mostly representing crystallization ages of porphyritic and/or unmetamorphosed granitoids; and (iv) mid Mesoproterozoic ages defining a tight cluster from 1.42 to 1.39 Ga, associated with the emplacement of the rapakivi granite of the Parguaza Massif.

The U–Pb data as compiled here and shown in Figure 6 confirms that widespread magmatic events coeval with what Cordani et al. (2016b) called the 'Atabapo' and 'Vaupés' Belts, with ages around 1.8 and 1.5 Ga, respectively, are indeed of great importance throughout the region. In NW Brasil, crystallization ages between ca. 1.81 and 1.75 Ga have been described for the Cumati, Cauaburi, and Querari Complexes and the Taiuaçu–Cauera diatexite; these dates have been interpreted to define the Cauaburi and Querari Orogenies (Figure 6; Almeida et al., 2013; Veras et al., 2018), whereas the younger ca. 1.5 Ga intrusives have been associated with the Içana Orogeny (Almeida et al., 2013). These orogenic events proposed in Brazilian territory have been inferred as having taken place within a series of accretionary orogens, characterized by arc–related magmatism and soft collision events along the western margin of the proto–Amazonian Craton (Almeida et al., 2013).

Similarly to the tectonic history proposed for the Cauaburi, Querari, and Içana Orogenies, Cordani et al. (2016b) proposed that the Atabapo and Vaupés Belts in eastern Colombia also reflect the successive construction of accretionary belts younging from northeast to southwest, stacked against proto–Amazonia during a long–lived convergent margin characterized by subduction–related magmatism and tectonism. What remains unclear, however, is whether these regional magmatic episodes are indeed representative of distinct crust–forming events that affected two separate geographic regions (i.e., a dominantly ca. 1.8 Ga accretionary belt in Guainía and a ca. 1.55 Ga one in Vaupés and Caquetá), or if the entire region consists essentially of Paleoproterozoic basement that was later affected by Mesoproterozoic post–tectonic or anorogenic magmatism (as previously suggested by Celada et al., 2006, and Kroonenberg & Reeves, 2011). Because the current isotopic and geochronologic database cannot unequivocally discard either of these two interpretations (see section 3.3), throughout the rest of this chapter we will consider both hypotheses as plausible and indicate that these should be the focus of continued research.

The U–Pb geochronologic data of Figure 6 shows that Paleo– and Mesoproterozoic magmatic events are not systematically clustered by geographic region as a function of their age, but rather that Paleoproterozoic basement rocks, which are typically found in the field as strongly foliated orthogneisses, are intruded throughout all eastern Colombia by Mesoproterozoic plutons. These younger ca. 1.59 to 1.38 Ga intrusives are typically less (ductilely) deformed or undeformed, and commonly exhibit strongly porphyritic (Figures 4f, 5f), rapakivi (Figure 5m, 5n), or fine–grained subvolcanic textures, with or without preservation of primary magmatic fabrics (e.g., Figure 4g, 4h). Thus, while it is clear that the Paleoproterozoic basement has been strongly deformed at mid– to high–temperatures and under high–strain conditions, it is not yet clear, but unlikely, that the Mesoproterozoic plutons have experienced a similar high–temperature deformation history.

Recently, Cordani et al. (2016b) interpreted the ca. 1.75 Ga orthogneisses in the Araracuara High as Paleoproterozoic inliers included within a Mesoproterozoic orogen. However, considering the more complete U–Pb database of Figure 6, an alternative interpretation of these data and the field observations is that the relatively undeformed ca. 1.55 Ga granitoids in Araracuara may represent post–tectonic intrusives emplaced within an older (orogenic) Paleoproterozoic basement. It is also tempting to interpret from Figure 6 that, while the ages of Paleoproterozoic magmatism become progressively younger from NE (Orinoco) to SW (Araracuara and Putumayo), thus possibly indicating the direction of arc migration throughout this period, the ages of Mesoproterozoic magmatism appear to young in the opposite direction. This migration of Mesoproterozoic magmatism towards the cratonic interior so far inland is unlike a trend that could be generated by arc–related processes, and could instead be the result of post–tectonic or anorogenic magmatic centers developing throughout the area during this time period. We note, however, that these two alternatives are difficult to disentangle using the currently available geochronologic data alone, so future research efforts aimed at testing these two hypotheses for the origin of the 'Atabapo' and 'Vaupés' magmatism will prove key for better understanding the geological evolution of eastern Colombia.

3.3. Zircon Lu–Hf and Whole–Rock Sm–Nd Constraints on Crustal Evolution

Whole–rock Sm–Nd isotopic measurements have been reported and compiled by Cordani et al. (2016b) and Lu–Hf isotopic compositions of zircon reported by Ibañez–Mejia (2014) and Ibañez–Mejia et al. (2015). A summary of all available results for both isotopic systems is presented in Table 2. In addition, $\delta^{18}O$ isotopic compositions of zircons also analyzed by U–Pb and Lu–Hf were reported for the samples studied by Ibañez–Mejia (2014) and Ibañez–Mejia et al. (2015), and are also summarized in Table 2.

Figure 7a summarizes the available Lu–Hf isotopic data available for the area, shown as mean initial $^{176}Hf/^{177}Hf$ compositions as a function of U–Pb crystallization age. In isotope–ratio vs. age space, epsilon Hf compositions (thin dashed lines) as a function of age can simply be plotted as deviations from the time–dependent chondritic reference value (thick blue line), such that both isotope–ratio and εHf values can be presented in the same diagram. This type of plot has the benefit of retaining the slope of trends in $^{176}Hf/^{177}Hf$ vs. time, which can be readily associated to apparent $^{176}Lu/^{177}Hf$ compositions of the source and/or used to easily identify the effects of zircon Pb–loss in zircon Hf data (see discussion in Ibañez–Mejia et al., 2015). Superimposed to this plot are also iso–T_{DM} contours (red thin lines) for various apparent depleted mantle 'extraction ages' (or mean crustal residence times), calculated here using the $^{176}Lu/^{177}Hf$ isotopic composition of bulk global subducted sediments (GLOOS; Plank & Langmuir, 1998) as an average composition of the bulk exposed continental crust. The Lu/Hf composition of GLOOS has an intermediate value between the bulk and lower continental crust values of Hawkesworth et al. (2010), and thus provides a good approximation of average–crust and is possibly more representative. The Mud Tank (MT) and R33 bars shown in the bottom left corner of Figure 7a reflect the external reproducibility (at 2 SD) of the $^{176}Hf/^{177}Hf$ measurements for low–rare–earth element (REE) and high–REE zircon, respectively (see Ibañez–Mejia et al., 2015 for more details) and provide a good estimate for uncertainty of mean values reported for samples.

Most of the existing zircon Lu–Hf data yield mean initial $^{176}Hf/^{177}Hf$ compositions at time of crystallization with equivalent $\varepsilon Hf_{Zrn} \leq +2$ (Figure 7a). The only exception to this generalization are zircon cores from the igneous protolith of ortho–amphibolites retrieved from the basement of the Mandur–2 well in the Putumayo basin, which have a mean εHf_{Zrn} value

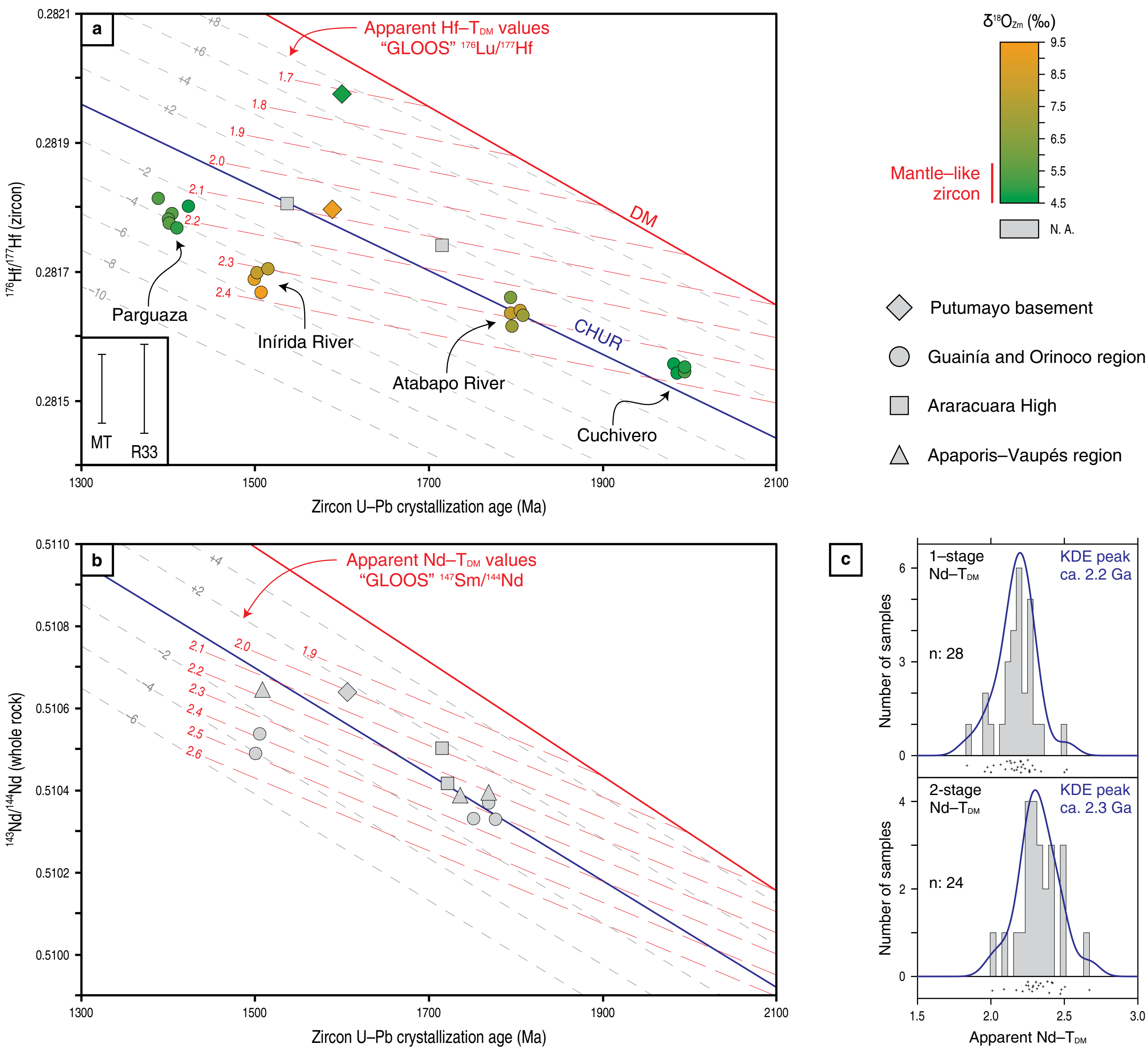

Figure 7. Summary of all available Lu–Hf and Sm–Nd isotopic data for the basement of the western Guiana Shield, corrected for radiogenic ingrowth since time of igneous crystallization. **(a)** Initial $^{176}Hf/^{177}Hf$ values vs. age diagram. Chondritic reference (CHUR) composition is after Bouvier et al. (2008); depleted mantle (DM) model curve is after Vervoort et al. (2017). Apparent iso–T_{DM} (depleted mantle average crustal residence ages) reference lines calculated using a 'GLOOS'–like Lu/Hf composition ($^{176}Lu/^{177}Hf$ = 0.0142; after Plank & Langmuir, 1998) are also shown. Gray dashed line above and below CHUR reflect positive and negative εHf deviations from a chondritic composition, respectively, plotted at +/– 2 ε intervals. $\delta^{18}O_{Zrn}$ values (in ‰, relative to VSMOW) are also shown graphically, coded using a green–to–orange gradient (see Table 2 for actual values). **(b)** Initial $^{143}Nd/^{144}Nd$ values vs. age diagram. Chondritic reference (CHUR) composition is after Bouvier et al. (2008); DM model curve is after DePaolo et al. (1991). Apparent iso–T_{DM} (depleted mantle average crustal residence ages) reference lines calculated using a 'GLOOS'–like Sm/Nd composition ($^{147}Sm/^{144}Nd$ = 0.1349; after Plank & Langmuir, 1998) are also shown. Gray dashed line above and below CHUR reflect positive and negative εNd deviations from a chondritic composition, respectively, plotted at 2 ε intervals. **(c)** Distribution of apparent depleted mantle Nd average crustal residence (Nd–T_{DM}) values for all samples analyzed from the western Guiana Shield, calculated using a 1–stage model (upper panel) and a 2–stage model (lower panel). For the 2–stage model, the second stage was calculated using a GLOOS–like Sm/Nd composition for consistency with panel B. Grey histogram reflects the distribution of data using a bin width of 50 my. Blue curve is a Gaussian Kernel Density Distribution (KDE) curve for all data, calculated using *DensityDist* (Pullen et al., 2014) and an optimized bandwidth of 70 my. See main text for details and discussion.

of +7.6 and mantle–like $\delta^{18}O_{Zrn}$ of 5.43 ± 0.23 ‰. Thus, the igneous protolith of the Mandur–2 ortho–amphibolites unambiguously reflect addition of highly radiogenic juvenile material to the Guiana Shield at the end of the Paleoproterozoic; however, all other samples analyzed thus far yield more ambiguous results, reflecting either heterogeneity of mantle sources or evidencing significant contamination with older crustal material at their time of igneous crystallization. The most unradiogenic (i.e., lowest $^{176}Hf/^{177}Hf$) intrusives yet analyzed are those exposed in the Guainía, Vichada, and Orinoco River areas (circles in Figure 7a), indicating that this region is likely underlain by the oldest continental basement. Apparent mean crustal residence (Hf–T_{DM}) values estimated for the Guainía, Vichada, and Orinoco River intrusives range from ca. 2.40 to 2.15 Ga, and exhibit no systematic dependence between mean $\delta^{18}O_{Zrn}$ and apparent Hf–T_{DM} as would be caused by contamination with subducted sediments. The Hf isotopic compositions of two intrusive samples from the Araracuara area are slightly more radiogenic, but still indicative of crustal reworking, yielding εHf_{Zrn} values between 0 and +2 at their time of crystallization and apparent Hf–T_{DM} values ca. 2.1 Ga. The latest Paleoproterozoic (Statherian) basement of the Putumayo Basin displays a more contrasting nature, with one sample clearly indicating older Paleoproterozoic crustal reworking (Payara–1 basement well; $\varepsilon Hf_t \approx 0.8$, $\delta^{18}O_{Zrn} \approx 9.2$), and one sample that reflects addition of unambiguous juvenile material at time of crystallization (Mandur–2 basement well; $\varepsilon Hf_t \approx +7.6$, $\delta^{18}O_{Zrn} \approx 5.43$ ‰).

Although far less common, Sm–Nd whole–rock isotopic data can also be displayed in isotope–ratio vs. age space, where epsilon values can be displayed as positive and negative deviations around the chondritic uniform reservoir (CHUR) composition and iso–T_{DM} contours graphed for any given $^{147}Sm/^{144}Nd$ value (e.g., Ibañez–Mejia et al., 2015). Here, we have plotted the Nd isotopic data in the same manner as the Lu–Hf results for ease of comparison. For the Nd isotopic data in Figure 7b, we have only plotted those samples for which well–determined U–Pb zircon crystallization ages are available from the same material, whereas apparent Nd–T_{DM} histograms (see further discussion below) used all the available Nd isotopic data. Apparent iso–T_{DM} contours for the Nd isotopic data have also been graphed in Figure 6b using the mean $^{147}Sm/^{144}Nd$ isotopic composition of GLOOS (Plank & Langmuir, 1998) as an average of bulk exposed continental crust and to maintain consistency with the interpretations of the Lu–Hf data. The Sm–Nd isotopic results also indicate that the Guainía and Orinoco region samples have the most unradiogenic (lowest $^{143}Nd/^{144}Nd$) initial compositions, which again suggests this area to be underlain by the oldest continental basement; apparent Nd–T_{DM} values for these samples range from ca. 2.25 to 2.50 Ga. Results from the Apaporis–Vaupés as well as the Araracuara regions further SW are again slightly more radiogenic than the Orinoco–Guainía samples on average, but still reflective of older crustal reworking. Apparent Nd–T_{DM} values for the Apaporis, Vaupés, and Araracuara samples are in the range from ca. 2.10 to 2.28 Ga. For the Putumayo Basin basement, Nd results from the Payara–1 well are also in line with the Hf results discussed above, as they indicate a Nd–T_{DM} value near 2.01 Ga and thus also highlight the presence of Paleoproterozoic basement in this region.

Another way to illustrate the Nd isotopic data is by calculating the apparent Nd–T_{DM} values (using 1– or 2–stage calculations) of samples with known $^{147}Sm/^{144}Nd_0$ and $^{143}Nd/^{144}Nd_0$, even if U–Pb crystallization ages for the same material are not available. This comparison is shown in Figure 7c, where 1–stage Nd–T_{DM} values are calculated by extrapolating the samples' isotopic composition up to the depleted mantle (DM) curve using their known $^{147}Sm/^{144}Nd_0$, and 2–stage values are calculated by using the samples' $^{147}Sm/^{144}Nd_0$ value only up to their known (or an inferred) crystallization age, and a second stage following an empirically determined $^{147}Sm/^{144}Nd$ slope (DePaolo et al., 1991). In both cases, the DM curve assumed for these calculations used the parameters of DePaolo et al. (1991), while the 2–stage model assumed a GLOOS–like $^{147}Sm/^{144}Nd$ composition for the second stage to keep results consistent with those shown in Figure 7b. Once a discrete distribution of apparent Nd–T_{DM} values is calculated using both approaches (frequency histograms in Figure 7c), a continuous probability curve can be approximated using a kernel density estimate (KDE) such that no assumptions need to be made about the uncertainty of each individual Nd–T_{DM} determination; using this approach, the 'smoothing' Kernel bandwidth is only a function of the local density of data. The KDE curves shown in Figure 7c (blue curves) were calculated using the *DensityDist* code of Pullen et al. (2014), which incorporates optimal bandwidth estimations based on the local density of points in the distribution using the algorithms of Botev et al. (2010). Using the 1–stage Nd–T_{DM} approach, KDE calculations show a maximum located at ca. 2.2 Ga, whereas 2–stage calculations display a maximum centered at ca. 2.3 Ga. By combining all available Nd isotopic data, these results indicate what the most likely value of mean residence age is for the crustal material exposed in the region. Considering the likelihood of Sm/Nd partitioning during older crustal reworking, the 2–stage calculations are considered to more closely approximate the time of mean crustal residence. Thus, the Nd data indicates that while apparent individual T_{DM} values in eastern Colombia range from ca. 2.1 to 2.4 Ga in magnitude, the most–likely value of mean crustal residence is ca. 2.3 Ga (lower panel in Figure 7c).

In summary, Lu–Hf and Sm–Nd isotopic results clearly indicate that the late–Paleo– through mid–Mesoproterozoic basement of eastern Colombia is not as radiogenic as global 'depleted mantle' models would predict for a typical juvenile terrane; however, there is no single interpretation for this observation, and we suggest that this could either reflect: (i) Derivation from heterogeneous mantle sources, which might have been affected by previous metasomatic episodes or simply not be as depleted as global MORB–based DM models suggest, or (ii) that these magmas incorporated a significant proportion of older crustal material of at least Rhyacian and potentially as old as Neoarchean age. These observations seem somewhat at odds with a simple model explaining the growth of the Amazonian Craton in this area by lateral juvenile–arc accretion, but instead suggest that crustal development was a protracted process resulting from a combination of juvenile additions and older crustal reworking. Such observations can be the end result of alternating extensional and compressional accretionary tectonics outboard a continental margin, such as has been described for the Tasmanide margin of eastern Australia (e.g., Kemp et al., 2009) and also recently for the Yavapai–Masatzal Province of Laurentia (Holland et al., 2018).

3.4. The Proterozoic of the Westernmost Guiana Shield within the Context of the Amazonian Craton

The most accepted models for the crustal evolution of the Amazonian Craton involve progressive growth by lateral accretion of Paleo– and Mesoproterozoic arc terranes onto an older Archean nucleus (e.g., Cordani & Teixeira, 2007; Tassinari & Macambira, 1999). These models describe growth as proceeding from northeast to southwest (in modern coordinates), and thus predict that crystallization ages as well as mean crustal residence values in the Guiana and Guaporé Shields should decrease towards the Andean margin of South America (Figure 1). Cordani & Teixeira (2007) proposed the limit between the mid Paleoproterozoic Ventuari–Tapajós Province (VTP) and mid Paleo– to early–Mesoproterozoic Rio Negro–Juruena Province (RNJP) in Colombia to be located near Puerto Inírida, whereas the limit between RNJP and the Rondonian–San Ignacio Province (RSIP) would project just west of Mitú (as shown in Figure 2). These hypotheses are now testable using the recent geochronologic and isotopic dataset as compiled here.

Although on a broad sense the igneous crystallization ages obtained thus far for the western Guiana Shield basement (Figure 6) are in good general agreement with existing models for the evolution of the Amazonian Craton, the new data also reveal important differences with respect to these models that are worth highlighting. For instance, as previously pointed out by Ibañez–Mejia et al. (2011, 2015), the Rondonian–San Ignacio Province appears to be absent or at least poorly represented in Colombia, as no collision–related 1.55 to 1.30 Ga tectonothermal events have been identified in the exposed craton or in the basement of the Putumayo Basin. In addition, more recently Cordani et al. (2016b) interpreted both the 'Atabapo Belt' and the 'Vaupés Belt' as belonging to the RNJP, an interpretation which implies that: (i) The RNJP–RSIP boundary is not present in Colombia just west of Mitú (or possibly even at all) as previously thought, and (ii) the areal extent of mid–Paleo– to early–Mesoproterozoic Rio Negro–Juruena–like basement domains in Colombia and the W Guiana Shield is significantly larger than previously expected.

On the other hand, the U–Pb data confirm that the expected age transition for the VTP–RNJP boundary near the Colombian–Venezuelan border is in fact present. Although previous models suggested this boundary to be west of Puerto Inírida, the new data from the Colombia–Venezuela border suggest its potential location might in fact be farther east, at least along the Atabapo River (as suggested by Cordani et al., 2016b and shown in Figure 2) or possibly to the east of the Ventuari River. Lastly, although it still remains unclear whether two distinct ca. 1.80 and ca. 1.55 Ga orogenic belts can be clearly discerned in eastern Colombia, the U–Pb data is unequivocal at pointing out the relevance of these two major magmatic episodes in shaping the Proterozoic basement of the region as interpreted by Cordani et al. (2016b).

From a crustal–growth perspective, the Hf and Nd data of Figure 7 reveal the general lack of highly radiogenic mid– to late–Paleoproterozoic crust in the region. The moderately positive to negative εHf and εNd values at time of crystallization obtained from almost all mid Paleo– to early–Mesoproterozoic intrusives in the westernmost Guiana Shield, indicate the widespread incorporation of some proportion of reworked older crustal material. Based on the apparent Hf– and Nd–T_{DM} values of samples calculated using GLOOS–like Lu/Hf and Sm/Nd compositions (Figure 7a, 7b), or the alignment of geographically associated samples in $^{176}Hf/^{177}Hf$ vs. U–Pb age space (Ibañez–Mejia, 2014), the age of the reworked crustal contaminants may range from Rhyacian to Neoarchean in age. Because accretionary belts could be the result of complex juxtaposition of tectonic units, including a great deal of intra–oceanic material with positive or slightly negative $\varepsilon Nd_{(t)}$ signatures, but also containing in places cordilleran–type granites, collisional–type belts, microcontinents, volcano–sedimentary basins, and post–tectonic to anorogenic–type complexes, we emphasize that the incorporation of older crustal material identified in the basement of eastern Colombia does not necessarily stand at odds with an accretionary tectonic model.

Mantle–derived material of "intra–oceanic" origin is difficult to be characterized solely by isotopic geochemistry. The use of $\varepsilon Nd_{(t)}$ or $\varepsilon Hf_{(t)}$ to trace juvenile processes is not completely unequivocal, because mantle sources (e.g., deep mantle material exhumed by plumes, mantle affected by metasomatism, or lithospheric mantle enriched by earlier recycling of crustal material) display varying ranges of 'depletion'. In most papers published in the last 30 years (many co–authored by Cordani), the Rio Negro–Juruena Province has been characterized as composed predominantly of granitoid rocks, deformed or not, yielding slightly positive to slightly negative $\varepsilon Nd_{(t)}$ signatures (roughly between +4.0 and –2.0);

this information has been used to suggest that juvenile accretionary events played a major role in its tectonic evolution. All samples from eastern Colombia analyzed thus far for Sm–Nd yield Paleoproterozoic Nd–T_{DM} values roughly between 1.9 and 2.5 Ga, regardless of their U–Pb zircon ages (Figure 7c; Table 2; Cordani et al. 2016b), thus suggesting the absence of a much older (Archean?) source material. Moreover, given that the $\varepsilon Nd_{(t)}$ values of the granitoid rocks are near zero or slightly positive or negative, the presence of juvenile material may have been important, and at least part of the magmatic arcs in the NW corner of the Rio Negro–Juruena Province could have been intra–oceanic. This interpretation is what is included in the Tectonic Map of South America. However, although the isotopic results shown in Figure 6 do not unequivocally show the presence of Archean crust in the region, the isotopic results in Colombia and western Venezuela seem to indicate a greater degree of older Paleoproterozoic reworking in the western Guiana Shield relative to correlative magmatic domains exposed south of the Amazon Basin.

3.5. Cretaceous Tectonic Reactivation and Thermal Effects in the Colombian Continental Interior

The recent discovery that Cretaceous mafic magmatism affected the basement of the Araracuara High (Ibañez–Mejia, 2014), expands the known extent of Mesozoic magmatic activity far beyond the easternmost locus of Cretaceous mafic intrusives known along the Eastern Cordillera axis (e.g., Vasquez et al., 2010). A dolerite dike intruding the Araracuara Gneiss yielded an age of 102.5 ± 2.2/2.3 Ma (Ibañez–Mejia, 2014) indicating that, during the Albian, this area was likely undergoing active extension and heating, synchronous to similar events occurring along the Eastern Cordillera. These results are important for two main reasons: (i) They suggest that Güejar–Apaporis Graben–related structures (Figure 2) were likely reactivated as intra–continental extensional domains during the mid–Cretaceous, coeval with extension, sedimentation, and mafic magmatism occurring along the Eastern Cordillera (e.g., Mora et al., 2009; Vasquez et al., 2010); and (ii) the age of this dolerite intrusion constrains the timing of uplift of the serranía de Chiribiquete and ultimate exhumation of the Araracuara Formation to post–Albian times, which is of importance for understanding the landscape evolution of the Colombian Amazon as well as the sedimentation history of the Late Cretaceous and Cenozoic basins of the Eastern Cordillera and its foreland (e.g., Horton et al., 2010). Although clearly outside the main scope of this chapter, we highlight the importance of this observation to argue that future efforts should be aimed at better resolving the structural as well as the temporal history of Cretaceous heating and tectonic re–activation in the eastern Colombian basement.

3.6. Future Challenges and Outstanding Questions in Colombian Precambrian Geology

This chapter presents an attempt to summarize and highlight the new advances in our understanding of the Precambrian geology of eastern Colombia, and the westernmost Guiana Shield in general. However, it should be realized that this vast area still remains one of the least explored regions in the South American continent, and thus many of the interpretations provided here are likely to be refined and modified as the geochronologic and other isotopic datasets continue to expand. Although by no means a comprehensive list, some of the main questions and/or future challenges the community needs to be address to better understand the basement in this area are:

a. We need to move past outdated stratigraphic nomenclature, and develop a local (tectono)–stratigraphic framework that is in line with modern petrologic and tectonic concepts, as well as recent geochronologic data. Although we make no attempts to propose formal modifications here, we particularly urge the community to think beyond (and ultimately abandon) the term Mitú Migmatitic Complex, to focus on developing a more accurate and detailed stratigraphic nomenclature.

b. The "granitoid basement" that cover the entire western half of the Guiana Shield remains poorly known, because geological mapping and geochemical/geochronological research has not yet progressed to a stage that would allow for a better characterization. We know that the entire region is formed by granitoid rocks (sensu lato), but it is not possible, at present, to make a clear distinction between syn–, late–, and post–tectonic, or anorogenic granitoid intrusions of various types and ages. Large parts of this province are poorly controlled by U–Pb dates and Nd–Hf isotopic constraints. More of this robust radioisotopic data, such as that compiled in this chapter, are needed.

c. The presence/absence and location of major terrane boundaries in the basement of eastern Colombia is critical for accurately placing this portion of the Guiana Shield within a larger tectonic framework. For instance, these boundaries are critical for better establishing potential correlations with the Central Brazilian Shield within the concept of a unified 'Amazonian Craton' (e.g., Cordani & Teixeira, 2007; Tassinari & Macambira, 1999), and also for evaluating the continuity of these domains to other cratons under the light of potential Columbia/Nuna and Rodinia paleogeographic configurations (e.g., Bispo–Santos et al., 2014a, 2014b; Cawood & Pisarevski, 2017; Cordani et al., 2009; D'Agrella–Filho et al., 2016; Ibañez–Mejia et al., 2011; Johansson, 2009; Li et al., 2008; Pisarevsky et al., 2014; Santos et al., 2008, among many others). The geochronologic data in this region has so far failed to identify the presence of a Rondonian–San Ignacio–like province as defined in NW Brasil and Bolivia (Bettencourt et al., 2010), but further efforts to confirm and/or negate this conclusion, as well as continue to evaluate other potential cratonic boundaries, are still necessary.

d. The combination of U–Pb, Lu–Hf and $\delta^{18}O$ isotopic information in zircon is a powerful tool to disentangle complex tectonic histories as well as revealing the mechanisms driving crustal maturation and evolution (e.g., Ibañez–Mejia, 2014; Ibañez–Mejia et al., 2015; Iizuka et al., 2017; Kemp et al., 2009; Valley et al., 2005; Vervoort & Kemp, 2016, among others). Further studies aiming to produce combined U–Pb–Hf–O datasets in zircons from the Guiana Shield offer the best path forward to resolve many of the outstanding issues of the tectonic evolution of the region.

e. There is a general dearth of geochronologic and isotopic data from mafic magmatic units in eastern Colombia and the Guiana Shield. Mafic magmatic events, in particular dike swarms potentially associated with Large Igneous Provinces (LIPs), have become a critical piece in the Precambrian tectonic puzzle. This is primordially due to their utility for providing geologic 'piercing points' amongst cratonic regions (Ernst et al., 2013) as well as acting as robust carriers of paleomagnetic information (e.g., Evans, 2013; Li et al., 2008; Pisarevsky et al., 2014). In the absence of zircon, mafic rocks can now be routinely and accurately dated using baddeleyite U–Pb geochronology by ID–TIMS (e.g., Söderlund et al., 2010), secondary ion mass spectrometry (SIMS; e.g., Chamberlain et al., 2010; Schmitt et al., 2010), or LA–ICP–MS (Ibañez–Mejia et al., 2014), and the latter approach also provides an opportunity to obtain Lu–Hf isotopic data. Future studies aimed at better understanding the mafic magmatic 'barcode' of the Guiana Shield (e.g., Reis et al., 2013; Teixeira et al., 2015) will surely bring significant advances for understanding the geology of the region and more accurately placing it within a global paleo–tectonic framework.

4. Conclusions

The U–Pb geochronologic data available for the westernmost Guiana Shield demonstrates that the basement of eastern Colombia and neighboring regions in Venezuela and Brasil is dominantly Paleo– and Mesoproterozoic in age, crystallized between ca. 1.99 and 1.38 Ga. The distribution of crystallization ages in not continuous, but rather clusters into four main periods that reflect major episodes of magmatic activity throughout the region. These are: (i) A mid–Paleoproterozoic event ca. 1.99 Ga, responsible for the development of the Cuchivero magmatic belt in Venezuela; (ii) a mid– to late–Paleoproterozoic event ranging from 1.84 to 1.72 Ga, preliminarily referred to here as the 'Atabapo Belt'; (iii) an early–Mesoproterozoic event ranging from 1.59 to 1.50 Ga, preliminarily referred to here as the 'Vaupés Belt'; and (iv) a mid–Mesoproterozoic event from 1.42 to 1.39 Ga, associated with the emplacement of the Parguaza anorogenic massif along the Colombia–Venezuela border. The combined Nd, Hf, and O isotopic systematics of granitoids in the area reveal the absence of highly radiogenic material associated with these magmatic pulses, suggesting that either: (i) The sub–continental mantle underlying the westernmost Guiana Shield was highly heterogeneous and less radiogenic than global mantle models would suggest, and/or (ii) that this basement is the result of combined juvenile additions with pervasive reworking of older crust of possible early Paleoproterozoic to late Neoarchean age.

Based on the diversity of ages, lithologies, and processes involved in shaping the geology of the eastern Colombia basement, we consider the definition of the Mitú Migmatitic Complex' to be inadequate moving forward, and urge the community to develop a more accurate and detailed nomenclature that is in line with recent geochronologic, isotopic, and petrologic research in this area.

The U–Pb and Nd isotopic result from a dolerite dike in the Araracuara area indicate that not all the magmatic activity in eastern Colombia is Precambrian in age, but reveal that Cretaceous mafic magmatism was in part responsible for controlling the geologic evolution of the area. Future studies aimed at better resolving the timing and nature of mafic magmatism in the region will thus be crucial for understanding the structural, thermal, as well as the landscape evolution of the eastern Colombian lowlands.

These are exciting times for the geology of the western Guiana Shield (!), as the development of new analytical tools for spatially–resolved geochronologic and geochemical analyses of zircon and baddeleyite now allow interrogating the geologic evolution of this complex region in greater detail than was ever possible before. We hope that the observations and ideas outlined in this chapter will serve as the launching pad for many exciting advances in understanding the geology of the western Guiana Shield in years and decades to come.

Acknowledgements

The authors would like to thank the Servicio Geologico Colombiano, particularly Jorge GÓMEZ TAPIAS and Oscar PAREDES ZAPATA for their invitation to contribute a chapter to this book. MI specially acknowledges the Guacamayo community in Araracuara, especially the Macuritofe family for their support during fieldwork, and the support that Franco URBANI, David MENDI, Zeze AMAYA, and Felipe VILLEGAS provided during various trips to the Guiana Shield in Venezuela and Colombia. UGC wishes to thank the Servicio Geologico Colombiano for the provision of samples collected during the PRORADAM. He also acknowledges the Fundação de Amparo à Pesquisa do estado de Sao Paulo for the allocation of a grant (Project 2013/12754–0) that made possible the acquisition of the geochronological analyses made on the Colombian samples. Reviewers Leda M. FRAGA and Salomon KROONENBERG are thanked for their thoughtful and in–depth comments that helped improve the final version of this chapter. Support for writing this chapter was provided to MI by the University of Rochester.

References

Aldrich, L.T., Herzog, L.F., Doak, J.B. & Davis, G.L. 1953. Variations in strontium isotope abundances in minerals part I: Mass spectrometry analysis of mineral sources of strontium. Eos, Transactions American Geophysical Union, 34(3): 457–460. https://doi.org/10.1029/TR034i003p00457

Almeida, M.E., Macambira, M.J.B., Santos, J.O.S., do Nascimento, R.S.C. & Paquette, J.L. 2013. Evolução crustal do noroeste do Cráton Amazônico, Amazonas, Brasil, baseada em dados de campo, geoquímicos e geocronológicos. 13° Simpósio de Geologia da Amazônia, Anais, p. 201–204. Belém, Brazil.

Barrera, J.I. 1988. Contribución al conocimiento y petrografía del Complejo Migmatítico de Mitú y su correlación en las localidades de Araracuara y alrededores. Bachelor thesis, Universidad Nacional de Colombia, 123 p. Bogotá.

Barrios, F.J. 1983. Caracterização geocronológica da região amazônica da Venezuela. Master thesis, Universidade de São Paulo, 123 p. Sao Paulo, Brasil. https://doi.org/10.11606/D.44.1983.tde-15072015-155335

Barrios, F., Rivas, D., Cordani, U. & Kawashita, K. 1985. Geocronología del territorio federal Amazonas. I Simposium Amazónico, Memoirs, Boletín de Geología, Publicación Especial 10: 22–31. Puerto Ayacucho, Venezuela.

Barrios, F., Cordani, U.G. & Kawashita, K. 1986. Caracterización geocronologica del territorio federal Amazonas, Venezuela. VI Congreso Geológico Venezolano, Memoirs III, p. 1432–1480. Caracas, Venezuela.

Bettencourt, J.S., Leite, Jr., W.B., Ruiz, A.S., Matos, R., Payolla, B.L. & Tosdal, R.M. 2010. The Rondonian–San Ignacio Province in the SW Amazonian Craton: An overview. Journal of South American Earth Sciences, 29(1): 28–46. http://doi.org/10.1016/j.jsames.2009.08.006

Bispo–Santos, F., D'Agrella–Filho, M.S., Trindade, R.I.F., Janikian, L. & Reis, N.J. 2014a. Was there SAMBA in Columbia? Paleomagnetic evidence from 1790 Ma Avanavero mafic sills, northern Amazonian Craton. Precambrian Research, 244: 139–155. http://doi.org/10.1016/j.precamres.2013.11.002

Bispo–Santos, F., D'Agrella–Filho, M.S., Janikian, L., Reis, N.J., Trindade, R.I.F. & Reis, M.A.A.A. 2014b. Towards Columbia: Paleomagnetism of 1980–1960 Ma Surumu volcanic rocks, northern Amazonian Craton. Precambrian Research, 244: 123–138. http://doi.org/10.1016/j.precamres.2013.08.005

Bonilla–Pérez, A., Frantz, J.C., Charão–Marques, J., Cramer, T., Franco–Victoria, J.A., Mulocher, E. & Amaya–Perea, Z. 2013. Petrografía, geoquímica y geocronología del Granito de Parguaza en Colombia. Boletín de Geología, 35(2): 83–104.

Botev, Z.I., Grotowski, J.F. & Kroese, D.P. 2010. Kernel density estimation via diffusion. The Annals of Statistics, 38(5): 2916–2957. http://doi.org/10.1214/10-AOS799

Bouvier, A., Vervoort, J.D. & Patchett, P.J. 2008. The Lu–Hf and Sm–Nd isotopic composition of CHUR: Constraints from unequilibrated chondrites and implications for the bulk composition of terrestrial planets. Earth and Planetary Science Letters, 273(1–2): 48–57. http://doi.org/10.1016/j.epsl.2008.06.010

Carneiro, M.C.R., Nascimento, R.S.C., Almeida, M.E., Salazar, C.A., da Trindade, I.R., de Oliveira–Rodrigues, V. & Passos, M.S. 2017. The Cauaburi magmatic arc: Litho–stratigraphic review and evolution of the Imeri Domain, Rio Negro Province, Amazonian Craton. Journal of South American Earth Sciences, 77: 310–326. http://doi.org/10.1016/j.jsames.2017.06.001

Cawood, P.A. & Pisarevsky, S.A. 2017. Laurentia–Baltica–Amazonia relations during Rodinia assembly. Precambrian Research, 292: 386–397. http://doi.org/10.1016/j.precamres.2017.01.031

Celada, C.M., Garzón, M., Gómez, E., Khurama, S., López, J.A., Mora, M., Navas, O., Pérez, R., Vargas, O. & Westerhof, A.B. 2006. Potencial de recursos minerales en el oriente colombiano: Compilación y análisis de la información geológica disponible (fase 0). Servicio Geológico Colombiano, unpublished report, 165 p. Bogotá.

Chamberlain, K.R., Schmitt, A.K., Swapp, S.M., Harrison, T.M., Swoboda–Colberg, N., Bleeker, W., Peterson, T.D., Jefferson, C.W. & Khudoley, A.K. 2010. In situ U–Pb SIMS (IN–SIMS) micro–baddeleyite dating of mafic rocks: Method with examples. Precambrian Research, 183(3): 379–387. http://doi.org/10.1016/j.precamres.2010.05.004

Cordani, U.G. & Teixeira, W. 2007. Proterozoic accretionary belts in the Amazonian Craton. In: Hatcher Jr, R.D., Carlson, M.P., McBride, J.H. & Martínez–Catalá, J.R. (editors), 4–D Framework of continental crust. Geological Society of America, Memoir 200, p. 297–320. https://doi.org/10.1130/2007.1200(14)

Cordani, U.G., Tassinari, C.C.G., Teixeira, W., Basei, M.A.S. & Kawashita, K. 1979. Evolução tectônica da Amazônia com base nos dados geocronológicos. II Congreso Geológico Chileno, Memoirs 4, p. 137–148. Arica, Chile.

Cordani, U.G., Teixeira, W., D'agrella–Filho, M.S. & Trindade, R.I. 2009. The position of the Amazonian Craton in supercontinents. Gondwana Research, 15(3–4): 396–407. http://doi.org/10.1016/j.gr.2008.12.005

Cordani, U.G., Ramos, V.A., Fraga, L.M., Delgado, I., de Souza, K.G., Gomes, F.E.M., Schobbenhaus, C. & Cegarra, M. 2016a. Tectonic map of South America, 2nd edition. Scale 1:5 000 000. Commission for the Geological Map of the World.

Cordani, U.G., Sato, K., Sproessner, W. & Fernandes, F.S. 2016b. U–Pb zircon ages of rocks from the Amazonas territory of Colombia and their bearing on the tectonic history of the NW sector of the Amazonian Craton. Brazilian Journal of Geology, 46(1): 5–35. http://doi.org/10.1590/2317-4889201620150012

D'Agrella–Filho, M.S., Trindade, R.I.F., Queiroz, M.V.B., Meira, V.T., Janikian, L., Ruiz, A.S. & Bispo–Santos, F. 2016. Reassessment of Aguapeí, Salto do Céu, paleomagnetic pole, Amazonian Craton and implications for Proterozoic supercontinents. Precambrian Research, 272: 1–17. http://doi.org/10.1016/j.precamres.2015.10.021

DePaolo, D.J., Linn, A.M. & Schubert, G. 1991. The continental crustal age distribution: Methods of determining mantle separation ages from Sm–Nd isotopic data and application to the southwestern United States. Journal of Geophysical Research: Solid Earth, 96(B2): 2071–2088. https://doi.org/10.1029/90JB02219

Ernst, R.E., Bleeker, W., Soderlund, U. & Kerr, A.C. 2013. Large Igneous Provinces and supercontinents: Toward completing the plate tectonic revolution. Lithos, 174: 1–14. http://doi.org/10.1016/j.lithos.2013.02.017

Evans, D.A.D. 2013. Reconstructing pre–Pangean supercontinents. Geological Society of America Bulletin, 125(11–12): 1735–1751. http://doi.org/10.1130/B30950.1

Fernandes, P.E.C.A., Pinheiro, S. da S., de Montalvão, R.M.G., Issler, R.S., Abreu, A.S. & Tassinari, C.C.G. 1976. Geologia. In: Divisão de publicação (editor), Projeto RADAMBRASIL. Levantamento de recursos naturais: Folha SA. 19 Içá, 11, p. 17–123. Rio de Janeiro, Brazil.

Fuck, R.A., Brito–Neves, B.B. & Schobbenhaus, C. 2008. Rodinia descendants in South America. Precambrian Research, 160(1–2): 108–126. http://doi.org/10.1016/j.precamres.2007.04.018

Galvis, J., Huguett, A. & Ruge, P. 1979. Geología de la Amazonia colombiana. Boletín Geológico, 22(3): 3–86.

Gaudette, H.E. & Olszewski Jr., W.J. 1985. Geochronology of the basement rocks, Amazonas territory, Venezuela and the tectonic evolution of the western Guiana Shield. Geologie en Mijnbouw, 64(2): 131–143.

Gaudette, H.E., Mendoza, V., Hurley, P.M. & Fairbairn, H.W. 1978. Geology and age of the Parguaza rapakivi granite, Venezuela. Geological Society of America Bulletin, 89(9): 1335–1340. https://doi.org/10.1130/0016-7606(1978)89<1335:GAAOTP>2.0.CO;2

Gibbs, A.K. 1987. Proterozoic volcanic rocks of the northern Guiana Shield, South America. In: Pharaoh, T.C., Beckinsale, R.D. & Rickard, D. (editors), Geochemistry and mineralization of Proterozoic volcanic suites. Geological Society of London, Special Publication 33, p. 275–288. London. https://doi.org/10.1144/GSL.SP.1987.033.01.19

Gibbs, A.K. & Barron, C.N. 1993. Geology of the Guiana Shield. Claredon Press, 245 p. New York, USA.

Gómez, J., Montes, N.E., Almanza, M.F., Alcárcel, F.A., Madrid, C.A. & Diederix, H. 2017. Geological map of Colombia 2015. Episodes, 40(3): 201–212. https://doi.org/10.18814/epiiugs/2017/v40i3/017023

Hawkesworth, C.J., Dhuime, B., Pietranik, A.B., Cawood, P.A., Kemp, A.I.S. & Storey, C.D. 2010. The generation and evolution of the continental crust. Journal of the Geological Society, 167(2): 229–248. http://doi.org/10.1144/0016-76492009-072

Herzog, L.F. 1952. Natural variations in strontium isotope abundances in minerals: A possible geologic age method. Doctoral thesis, Massachusetts Institute of Technology, 122 p. Cambridge, USA.

Holland, M.E., Karlstrom, K.E., Gehrels, G.E., Shufeldt, O.P., Begg, G., Griffin, W. & Belousova, E. 2018. The Paleoproterozoic Vishnu Basin in southwestern Laurentia: Implications for supercontinent reconstructions, crustal growth, and the origin of the Mojave crustal province. Precambrian Research, 308: 1–17. https://doi.org/10.1016/j.precamres.2018.02.001

Horton, B.K., Saylor, J.E., Nie, J., Mora, A., Parra, M., Reyes–Harker, A. & Stockli, D.F. 2010. Linking sedimentation in the northern Andes to basement configuration, Mesozoic extension, and Cenozoic shortening: Evidence from detrital zircon U–Pb ages, Eastern Cordillera, Colombia. Geological Society of America Bulletin, 122(9–10): 1423–1442. http://doi.org/10.1130/B30118.1

Ibañez–Mejia, M. 2014. Timing and rates of Precambrian crustal genesis and deformation in northern South America. Doctoral thesis, University of Arizona, 334 p. Tucson, USA.

Ibañez–Mejia, M. 2020. The Putumayo Orogen of Amazonia: A synthesis. In: Gómez, J. & Mateus–Zabala, D. (editors), The Geology of Colombia, Volume 1 Proterozoic – Paleozoic. Servicio Geológico Colombiano, Publicaciones Geológicas Especiales 35, p. 101–131. Bogotá. https://doi.org/10.32685/pub.esp.35.2019.06

Ibañez–Mejia, M., Ruiz, J., Valencia, V.A., Cardona, A., Gehrels, G.E. & Mora, A.R. 2011. The Putumayo Orogen of Amazonia and its implications for Rodinia reconstructions: New U–Pb geochronological insights into the Proterozoic tectonic evolution of northwestern South America. Precambrian Research, 191(1–2): 58–77. https://doi.org/10.1016/j.precamres.2011.09.005

Ibañez–Mejia, M., Gehrels, G.E., Ruiz, J., Vervoort, J.D., Eddy, M.E. & Li, C. 2014. Small–volume baddeleyite (ZrO_2) U–Pb geochronology and Lu–Hf isotope geochemistry by LA–ICP–MS. Techniques and applications. Chemical Geology, 384: 149–167. http://doi.org/10.1016/j.chemgeo.2014.07.011

Ibañez–Mejia, M., Pullen, A., Arenstein, J., Gehrels, G.E., Valley, J., Ducea, M.N., Mora, A.R., Pecha, M. & Ruiz, J. 2015. Unraveling crustal growth and reworking processes in complex zircons from orogenic lower–crust: The Proterozoic Putumayo Orogen of Amazonia. Precambrian Research, 267: 285–310. http://doi.org/10.1016/j.precamres.2015.06.014

Iizuka, T., Yamaguchi, T., Itano, K., Hibiya, Y. & Suzuki, K. 2017. What Hf isotopes in zircon tell us about crust–mantle evolution. Lithos, 274–275: 304–327. http://doi.org/10.1016/j.lithos.2017.01.006

Johansson, A. 2009. Baltica, Amazonia and the SAMBA connection–1000 million years of neighborhood during the Proterozoic? Precambrian Research, 175(1–4): 221–234. http://doi.org/10.1016/j.precamres.2009.09.011

Kemp, A.I.S., Hawkesworth, C.J., Collins, W.J., Gray, C.M., Blevin, P.L. & Edinburgh Ion Microprobe Facility. 2009. Isotopic evidence for rapid continental growth in an extensional accretionary orogen: The Tasmanides, eastern Australia. Earth and Planetary Science Letters, 284(3–4): 455–466. http://doi.org/10.1016/j.epsl.2009.05.011

Kronenberg, S. & Reeves, C.V. 2011. Vaupés and Amazonas Basins. In: Cediel, F. (editor), Petroleum geology of Colombia: Geology and hydrocarbon potential, 15. Agencia Nacional de Hidrocarburos and Universidad EAFIT, 103 p. Medellín.

Li, Z.X., Bogdanova, S.V., Collins, A.S., Davidson, A., de Waele, B., Ernst, R.E., Fitzsimons, I.C.W., Fuck, R.A., Gladkochub, D.P. Jacobs, J., Karlstrom, K.E., Lu, S., Natapov, L.M., Pease, V., Pisarevsky, S.A., Thrane, K. & Vernikovsky, V. 2008. Assembly, configuration, and break–up history of Rodinia: A synthesis. Precambrian Research, 160(1–2): 179–210. http://doi.org/10.1016/j.precamres.2007.04.021

Lugmair, G. W. & Marti, K. 1978. Lunar initial $^{143}Nd/^{144}Nd$: Differential evolution of the lunar crust and mantle. Earth and Planetary Science Letters, 39(3): 349–357. http://doi.org/10.1016/0012-821X(78)90021-3

Mora, A., Gaona, T., Kley, J., Montoya, D., Parra, M., Quiroz, L.I., Reyes, G. & Strecker, M. 2009. The role of inherited extensional fault segmentation and linkage in contractional orogenesis: A reconstruction of Lower Cretaceous inverted rift basins in the Eastern Cordillera of Colombia. Basin Research, 21(1): 111–137. https://doi.org/10.1111/j.1365-2117.2008.00367.x

Nier, A.O. 1940. A Mass spectrometer for routine isotope abundance measurements. Review of Scientific Instruments, 11(7): 212–216. http://doi.org/10.1063/1.1751688

Nier, A.O. 1947. A mass spectrometer for isotope and gas analysis. Review of Scientific Instruments, 18(6): 398–411. http://doi.org/10.1063/1.1740961

Pinheiro, S.S., Fernandes, P.E.C.A., Pereira, E.R., Vasconcelos, E.G., Pinto, A.C., de Montalvão, R.M.G., Issler, R.S., Dall'Agnol, R., Teixeira, W. & Fernandes, C.A.C. 1976. Geologia. In: Divisão de publicação. (editor), Projeto RADAMBRASIL. Levantamento de recursos naturais: Folha NA. 19 Pico da Neblina, 11, p. 19–137. Rio de Janeiro, Brazil.

Pinson Jr, W.H., Hurley, P.M., Mencher, E. & Fairbairn, H.W. 1962. K–Ar and Rb–Sr ages of biotites from Colombia, South America. Geological Society of America Bulletin, 73(7): 907–910. https://doi.org/10.1130/0016-7606(1962)73[907:KARAOB]2.0.CO;2

Pisarevsky, S.A., Elming, S.A., Pesonen, L.J. & Li, Z.X. 2014. Mesoproterozoic paleogeography: Supercontinent and beyond. Precambrian Research, 244: 207–225. http://doi.org/10.1016/j.precamres.2013.05.014

Plank, T. & Langmuir, C.H. 1998. The chemical composition of subducting sediment and its consequences for the crust and mantle. Chemical Geology, 145(3–4): 325–394. http://doi.org/10.1016/S0009-2541(97)00150-2

Priem, H., Andriessen, P., Boelrijk, N., De Booder, H., Hebeda, E., Huguett, A., Verdumen, E. & Verschure, R. 1982. Geochronology of the Precambrian in the Amazonas region of southeastern Colombia (western Guiana Shield). Geologie en Mijnbouw, 61(3): 229–242.

Pullen, A., Ibañez–Mejia, M., Gehrels, G.E., Ibañez–Mejia, J.C. & Pecha, M. 2014. What happens when n=1000? Creating large–n geochronological datasets with LA–ICP–MS for geologic investigations. Journal of Analytical Atomic Spectrometry, 29(6): 971–980. https://doi.org/10.1039/C4JA00024B

Reis, N.J., de Faria, M.S.G., Fraga, L.M. & Haddad, R.C. 2000. Orosirian calc–alkaline volcanism and the Orocaima event in the northern Amazonian Craton, eastern Roraima state, Brazil. Revista Brasileira de Geociencias, 30(3): 380–383.

Reis, N.J., Teixeira, W., Hamilton, M.A., Bispo–Santos, F., Almeida, M.E. & D'Agrella–Filho, M.S. 2013. Avanavero mafic magmatism, a late Paleoproterozoic LIP in the Guiana Shield, Amazonian Craton: U–Pb ID–TIMS baddeleyite, geochemical and paleomagnetic evidence. Lithos, 174: 175–195. http://doi.org/10.1016/j.lithos.2012.10.014

Santos, J.O.S., Hartmann, L.A., Gaudette, H.E., Groves, D.I., McNaughton, N.J. & Fletcher, I.R. 2000. A new understanding of the provinces of the Amazon Craton based on integration of field mapping and U–Pb and Sm–Nd geochronology. Gondwana Research, 3(4): 453–488. https://doi.org/10.1016/S1342-937X(05)70755-3

Santos, J.O.S., Potter, P.E., Reis, N.J., Hartmann, L.A., Fletcher, I.R. & McNaughton, N.J. 2003. Age, source, and regional stratigraphy of the Roraima Supergroup and Roraima–like outliers in northern South America based on U–Pb geochronology. Geological Society of America Bulletin, 115(3): 331–348. https://doi.org/10.1130/0016-7606(2003)115<0331:ASARSO>2.0.CO;2

Santos, J.O.S., Rizzotto, G.J., Potter, P.E., McNaughton, N.J., Matos, R.S., Hartmann, L.A., Cheemale, F. & Quadros, M.E.S. 2008. Age and autochthonous evolution of the Sunsás Orogen in west Amazon Craton based on mapping and U–Pb geochronology. Precambrian Research, 165(3–4): 120–152. http://doi.org/10.1016/j.precamres.2008.06.009

Schmitt, A.K., Chamberlain, K.R., Swapp, S.M. & Harrison, T.M. 2010. In situ U–Pb dating of micro–baddeleyite by secondary ion mass spectrometry. Chemical Geology, 269(3–4): 386–395. http://doi.org/10.1016/j.chemgeo.2009.10.013

Shrock, R.R. 1977. Geology at MIT 1865–1965, 1: The faculty and supporting staff. The MIT press, 1102 p. Cambridge, USA.

Söderlund, U., Patchett, P.J., Vervoort, J. & Isachsen, C.E. 2004. The ^{176}Lu decay constant determined by Lu–Hf and U–Pb isotope systematics of Precambrian mafic intrusions. Earth and Planetary Science Letters, 219(3–4): 311–324. http://doi.org/10.1016/S0012-821X(04)00012-3

Söderlund, U., Hofmann, A., Klausen, M.B., Olsson, J.R., Ernst, R.E. & Persson, P.O. 2010. Towards a complete magmatic barcode for the Zimbabwe Craton: Baddeleyite U–Pb dating of regional dolerite dyke swarms and sill complexes. Precambrian Research, 183(3): 388–398. http://doi.org/10.1016/j.precamres.2009.11.001

Tassinari, C.C.G. & Macambira, M.J.B. 1999. Geochronological provinces of the Amazonian Craton. Episodes, 22(3): 174–182.

Tassinari, C.C.G., Cordani, U.G., Nutman, A.P., van Schmus, W.R., Bettencourt, J.S. & Taylor, P.N. 1996. Geochronological systematics on basement rocks from the Rio Negro–Juruena Province, Amazonian Craton, and tectonic implications. International Geology Review, 38(2): 161–175. https://doi.org/10.1080/00206819709465329

Teixeira, W., Tassinari, C.C.G. & Mondin, M. 2002. Características isotópicas (Nd e Sr) do plutonismo intrusivo no extremo NW do Cráton Amazônico, Venezuela, e implicações para a evolução Paleoproterozóica. Revista do Instituto de Geociências da Universidade de Sao Paulo, 2(1): 131–141. https://doi.org/10.5327/S1519-874X2002000100011

Teixeira, W., Hamilton, M.A., Lima, G.A., Ruiz, A.S., Matos, R. & Ernst, R.E. 2015. Precise ID–TIMS U–Pb baddeleyite ages (1110–1112 Ma) for the Rincón del Tigre–Huanchaca Large Igneous Province (LIP) of the Amazonian Craton: Implications for the Rodinia supercontinent. Precambrian Research, 265: 273–285. http://doi.org/10.1016/j.precamres.2014.07.006

Teixeira, W., Reis, N.J., Bettencourt, J.S., Klein, E.L. & Oliveira, D.C. 2019. Intraplate Proterozoic magmatism in the Amazonian Craton reviewed: Geochronology, crustal tectonics and global barcode matches. In: Srivastava, R.K., Ernst, R.E. & Peng, P. (editors), Dyke swarms of the world: A modern perspective. Springer Geology, p. 111–154. Singapore. https://doi.org/10.1007/978-981-13-1666-1_4

Valley, J.W., Lackey, J.S., Cavosie, A.J., Clechenko, C.C., Spicuzza, M.J., Basei, M.A.S., Bindeman, I.N., Ferreira, V.P., Sial, A.N., King, E.M., Peck, W.H., Sinha, A.K. & Wei, C.S. 2005. 4.4 billion years of crustal maturation: Oxygen isotope ratios of magmatic zircon. Contributions to Mineralogy and Petrology, 150: 561–580. https://doi.org/10.1007/s00410-005-0025-8

Vasquez, M., Altenberger, U., Romer, R.L., Sudo, M. & Moreno–Murillo, J.M. 2010. Magmatic evolution of the Andean Eastern Cordillera of Colombia during the Cretaceous: Influence of previous tectonic processes. Journal of South American Earth Sciences, 29(2): 171–186. http://doi.org/10.1016/j.jsames.2009.02.003

Veras, R.da S., Nascimento, R.S.C., Almeida, M.E., Paquette, J.L. & Carneiro, M.C.R. 2018. Paleoproterozoic basement of Içana Domain, Rio Negro Province, northwestern Amazonian Craton: Geology, geochemistry and geochronology (U–Pb and Sm–Nd). Journal of South American Earth Sciences, 86: 384–409. http://doi.org/10.1016/j.jsames.2018.07.003

Vervoort, J.D. & Kemp, A.I.S. 2016. Clarifying the zircon Hf isotope record of crust–mantle evolution. Chemical Geology, 425: 65–75. http://doi.org/10.1016/j.chemgeo.2016.01.023

Vervoort, J.D., Kemp, A.I.S., Fisher, C.M. & Bauer, A.M. 2017. Growth of Earth's earliest crust: The perspective from the depleted mantle. Goldschmidt2017 Conference, Abstracts, 1 p. Paris, France.

Explanation of Acronyms, Abbreviations, and Symbols:

CG	Cuchivero Group
CHUR	Chondritic uniform reservoir
DM	Depleted mantle
GAG	Güejar–Apaporis Graben
GLOOS	Global subducted sediments
ID–TIMS	Isotope dilution thermal ionisation mass spectrometry
IGSN	International Geo Sample Number
KDE	Kernel density estimate
LA–ICP–MS	Laser ablation inductively coupled plasma mass spectrometry
LIPs	Large Igneous Provinces
MI	Mauricio IBAÑEZ–MEJIA
MMC	Mitú Migmatitic Complex
MT	Mud Tank
PP	Putumayo Province
PRORADAM	Proyecto Radargramétrico del Amazonas
REE	Rare earth element
RNJP	Rio Negro–Juruena Province
RSIP	Rondonian–San Ignacio Province
SHRIMP	Sensitive high–resolution ion microprobe
UGC	Umberto G. CORDANI
VSMOW	Vienna standard mean ocean water
VTP	Ventuari–Tapajós Province

Authors' Biographical Notes

Mauricio IBAÑEZ–MEJIA graduated as a geologist from the Universidad Nacional de Colombia, Bogotá, in 2007. He obtained MS (2010) and PhD (2014) degrees in petrology and geochemistry from the University of Arizona, USA, followed by two years as a W.O. Crosby postdoctoral fellow in the Massachusetts Institute of Technology in Cambridge, USA, and four years as an assistant professor in the Department of Earth and Environmental Sciences at University of Rochester, USA. He is currently an assistant professor in the Department of Geosciences at the University of Arizona, USA. His main research interests are in the fields of isotope geochemistry, geochronology, petrology, and crustal evolution.

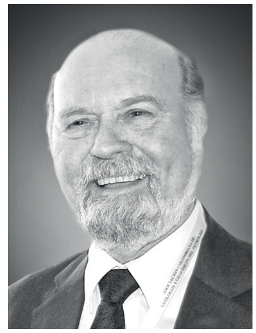

Umberto G. CORDANI graduated in geology in 1960 at the Universidade de São Paulo, Brasil, was hired as Assistant Professor by the same university and obtained his PhD in 1968. In 1980 he completed his teaching career as full professor. Retired, he continues working as Emeritus Professor. His main research interests are in geochronology applied to tectonics and crustal evolution. He had active participation in the international community and was president of the International Union of Geological Sciences (IUGS) from 1988 to 1992. He has received a few honours, including the José Bonifácio Gold Medal of the Brazilian Geological Society, and the Great Cross of Scientific Merit, the highest Brazilian award in science.

Volume 1

Chapter 5

https://doi.org/10.32685/pub.esp.35.2019.05
Published online 5 May 2020

Neoproterozoic Records of the Llanos Orientales Basin, Colombia

Hernando DUEÑAS–JIMÉNEZ[1]* and Jorge MONTALVO–JÓNSSON[2]

1 hdjbioss@yahoo.com
hduenas@sgc.gov.co
Academia Colombiana de Ciencias Exactas, Físicas y Naturales
Carrera 28A n.° 39A–63
Bogotá, Colombia
Servicio Geológico Colombiano
Dirección de Hidrocarburos
Diagonal 53 n.° 34–53
Bogotá, Colombia.

2 jemontalvom@unal.edu.co
Departamento de Geociencias
Universidad Nacional de Colombia
Carrera 30 n.° 45–03
Bogotá, Colombia

* Corresponding authorr

Abstract In the Llanos Orientales Basin of Colombia, below thick Tertiary and Cretaceous strata, Paleozoic sedimentary sequences are present, which yield good, diverse, and well–preserved assemblages of palynomorphs. In the northeastern part of the basin in the Arauca Graben, after crossing the unconformity at the base of the Cretaceous sequence, oil wells face the presence of Cambrian and Neoproterozoic (Cryogenian – Ediacaran) sedimentites deposited in low latitudes under shallow marine settings that yield abundant, diverse, poorly preserved, and dark–colored sphaeromorph acritarch assemblages.

In the Chiguiro–1, La Coral–1, and Pato–1 wells drilled in 1985–1986, the presence of Ediacaran palynomorphs was observed for the first time in Colombia. This discovery can be considered to be the oldest sedimentites dated by paleontological methods reported in Colombia. Twenty–six years later, analysis of samples from the Chilacoa–1S, Coralito–1S, Torodoi–1X, and Vaco–1X wells confirmed the presence of Ediacaran sedimentites in the Llanos Orientales Basin. All these wells are located in the Arauca Graben, which is a northeast tectonic depression that extends north, reaching Venezuelan territory.

In the Arauquita–1—Torodoi–1X seismic transect it is possible to observe the presence of a general pinch–out of Tertiary and Cretaceous stratigraphic units towards the east. Under the basal Cretaceous unconformity, all of the stratigraphic units have suffered a great tectonic activity that divides the Arauca Graben into narrow blocks, in which it is possible to observe the presence of a not yet drilled stratigraphic sequence with a thickness of several thousand feet that could involve pre–Ediacaran sedimentites. The detailed palynological analysis of those sedimentites could aid in the interpretation of the evolution of life during (acritarchs) early times.

Keywords: *acritarchs, Ediacaran, Llanos Orientales Basin, Arauca Graben.*

Resumen En la Cuenca de los Llanos Orientales de Colombia, bajo los espesos estratos del terciario y del Cretácico, se encuentran secuencias sedimentarias paleozoicas y neoproterozoicas que tienen abundantes y diversas asociaciones de palinomorfos bien preservados. En el sector nororiental de la cuenca, luego de cruzar la discordancia en la base de la secuencia cretácica, los pozos perforados dentro del Graben de Arauca registran sedimentitas del Cámbrico y Neoproterozoico (Criogeniano–Ediacariano) depositadas en latitudes bajas y en un ambiente marino somero. Estas sedimentitas neoproterozoicas contienen asociaciones de acritarcos esferomorfos abundantes, diversas, pobremente preservadas y oscurecidas.

Citation: Dueñas–Jiménez, H. & Montalvo–Jónsson, J. 2020. Neoproterozoic records of the Llanos Orientales Basin, Colombia. In: Gómez, J. & Mateus–Zabala, D. (editors), The Geology of Colombia, Volume 1 Proterozoic – Paleozoic. Servicio Geológico Colombiano, Publicaciones Geológicas Especiales 35, p. 91–99. Bogotá. https://doi.org/10.32685/pub.esp.35.2019.05

En los pozos Chiguiro–1, La Coral–1 y Pato–1, perforados en 1985–1986, se observó por primera vez en Colombia la presencia de palinomorfos ediacarianos. Este descubrimiento se puede considerar como el de las sedimentitas más antiguas datadas por métodos paleontológicos que se han reportado en Colombia. Veintiséis años después, el análisis de muestras de los pozos Chilacoa–1S, Coralito–1S, Torodoi–1X y Vaco–1X confirmó la presencia de sedimentitas ediacarianas en la Cuenca de los Llanos Orientales. Todos estos pozos están ubicados en el Graben de Arauca, una depresión tectónica de dirección noreste que se extiende hacia el norte hasta llegar a territorio venezolano.

En la transecta sísmica Arauquita–1—Torodoi–1X es posible observar un acuñamiento hacia el este de las unidades estratigráficas terciarias y cretácicas. Bajo la discordancia basal del Cretácico, todas las unidades estratigráficas han sufrido una gran deformación tectónica que divide el Graben de Arauca en bloques estrechos. En estos bloques es posible observar una secuencia estratigráfica aún no perforada de varios miles de pies de espesor que podría involucrar sedimentitas preediacarianas. El análisis palinológico detallado de estas sedimentitas podría ayudar en la interpretación de la evolución de la vida (acritarcos) durante los primeros tiempos del planeta.

Palabras clave: *acritarcos, Ediacariano, Cuenca de los Llanos Orientales, Graben de Arauca.*

1. Introduction

The Llanos Orientales is one of the largest sedimentary basins in Colombia and has been a target for oil exploration since the 1940s. Exploratory activity in this basin has been increased in the last decades, but, nevertheless, the basin still holds great possibility for new oil discoveries.

The Llanos Orientales Basin is a lowland area that covers more than 300 000 km^2 on the eastern edge of Colombia (Figure 1). It is bounded on the west by the Andean Eastern Cordillera and on the north by the Colombia–Venezuela border. It is bounded on the southwest by the serranía de La Macarena and in the southeast and east by outcrops of igneous and metamorphic rocks that belong to the Guiana Shield (Cordani et al., 2016).

The Llanos Orientales Basin is a north trending structural depression adjacent to the Eastern Cordillera. The sedimentary sequences that refill this depression are clearly divisible into three chronostratigraphic units, which have been palynologically dated to the Paleozoic, Cretaceous, and Tertiary. These units are internally separated by well–known regional unconformities and have been considered independently as oil systems.

In the main depocenters of this basin, 3D seismic surveys allow observations of Paleozoic stratigraphic sequences that can reach thicknesses exceeding 15 000 feet (Dueñas, 2001, 2011; Arminio et al. 2013). However, this sequence of marine sedimentites has received very little attention to date, probably because a low hydrocarbon potential has been wrongly assumed (Dueñas, 2002; Arminio et al. 2013).

In the eastern part of the basin (Arauca Graben), the Sun Colombia Oil Company drilled the Chiguiro–1, La Coral–1, and Pato –1 wells in 1985 (Figures 1, 2). After drilling a thick sequence of Tertiary and Cretaceous sedimentites, those wells passed through the basal Cretaceous unconformity facing Cambrian and Neoproterozoic strata (Dueñas, 2001, 2011). Later, (2011–2012), the Pacific Rubiales Company drilled four wells that confirm the presence of Ediacaran sedimentites in the basin. The Chilacoa–1, Torodoi–IX, and Vaco–IX wells at their bottoms drilled sedimentites of Ediacaran age. Palynological analysis of samples from the Coralito–1S well confirm the presence of Ediacaran sedimentites and suggest the presence of Ediacaran – Cryogenian palynomorphs (Arminio et al., 2013).

Ediacaran palynological associations similar to those reported in the Llanos Orientales have been described in many locations in Europe, Asia, and Africa (Korolev & Ogurtsova, 1983; Baudet, 1988; Palacios & Vidal, 1992; Strother, 1996), but interest in these sedimentites in Latin America has only begun recently (Dueñas, 2001, 2011; Gaucher et al., 2004; Gaucher & Sprechmann, 2009; Gaucher & Poiré, 2009; Ibañez–Mejia et al., 2011; Chiglino, 2013; Chiglino et al., 2015). Unfortunately, the efforts of Feo–Codecido et al. (1984) to study and interpret the Paleozoic rocks of the Venezuelan basins did not continue.

The main objective of this work is to analyze the palynological data obtained from the study of samples from these seven wells and improve our understanding of the diversity of the biosphere during the Ediacaran – Cryogenian in Colombian areas.

2. Palynological Data

In 1985–1986, the Sun Colombia Oil Company carried out a drilling program in the eastern part of the Llanos Orientales Basin. Three of the drilled wells with bottomed cores reported the presence of Ediacaran strata. These three wells are located in what today is known as the Arauca Graben, which is an elongated structure oriented northeast that extends to Venezuelan territory (Figure 1). The Chiguiro–1, Pato–1, and La Coral–1 wells, after crossing thick stratigraphic sequences of Tertiary and Cretaceous sedimentites, passed through the basal unconformity of the Cretaceous and began to perforate Cambrian and

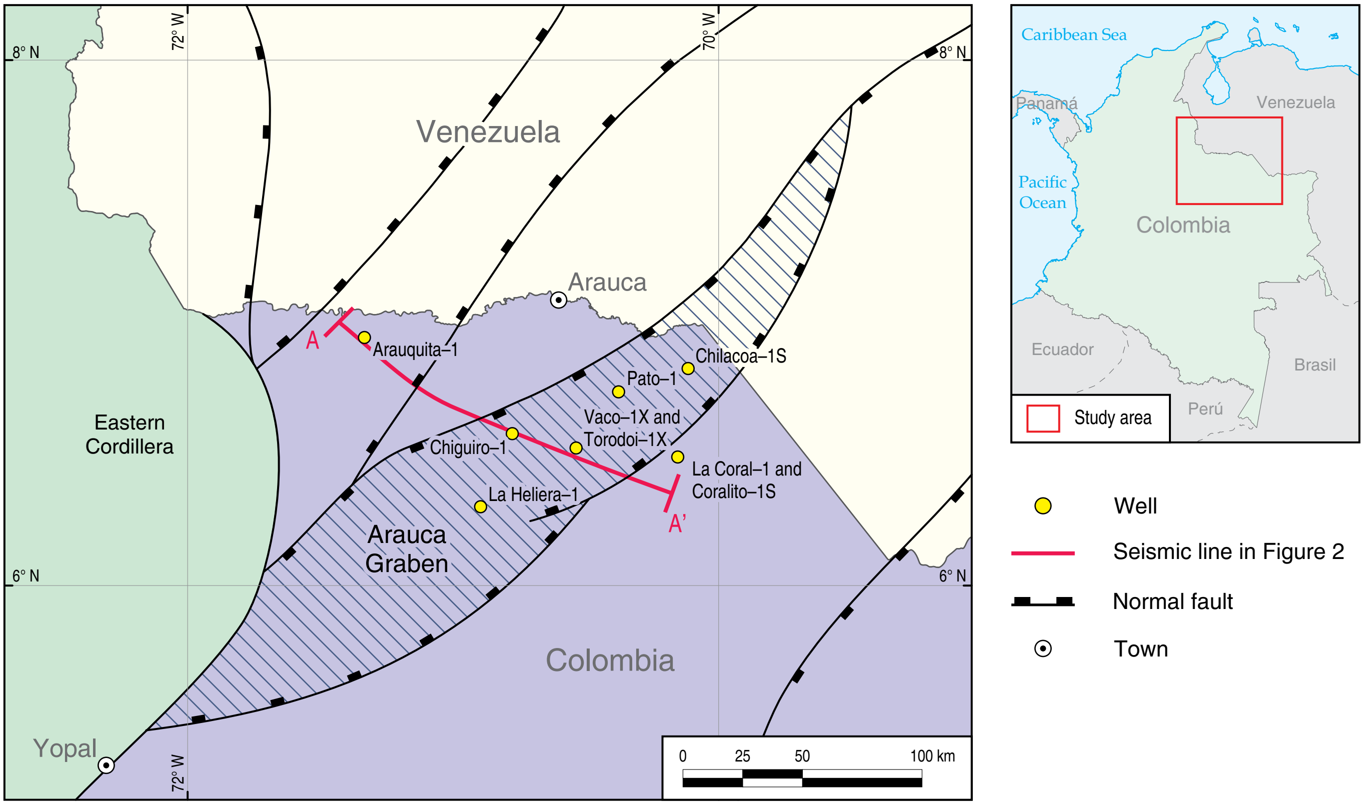

Figure 1. Map of northeastern Llanos Orientales Basin showing the locations of wells included in the text.

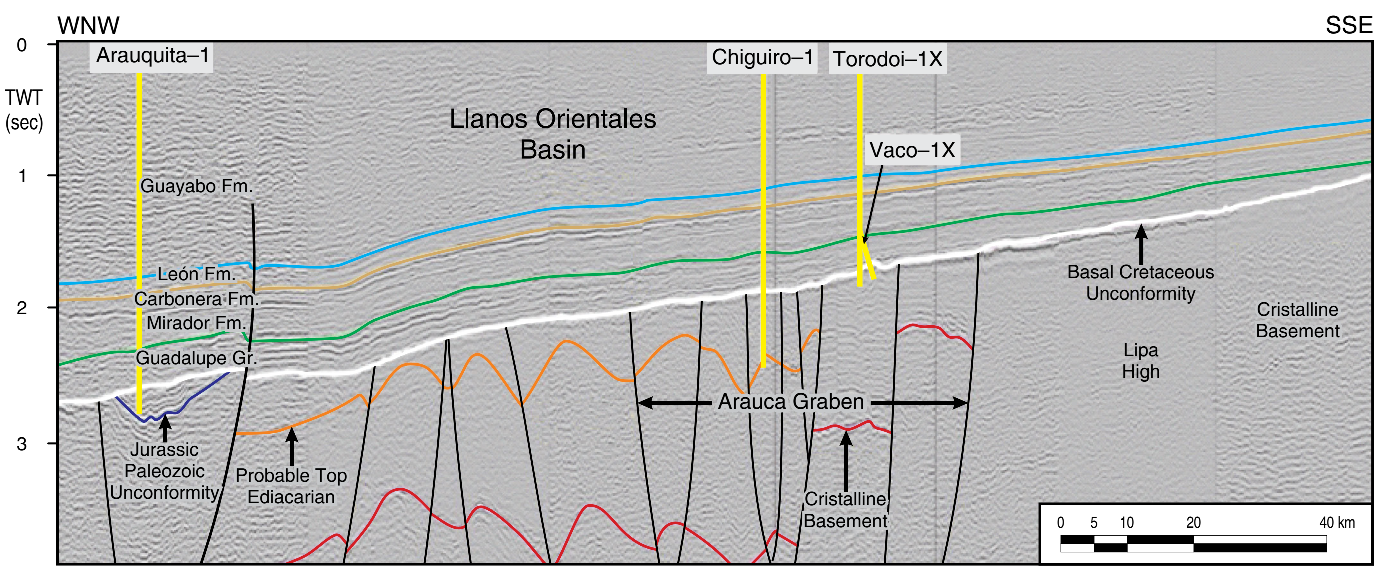

Figure 2. Seismic transect from Arauquita–1 to Torodoi–1X, in which it is possible to observe the regional pinch–out of the Tertiary and Cretaceous units towards the east as well as the tectonics of blocks related to the Arauca Graben. In the Arauquita–1 well, after drilling the unconformity at the base of the Cretaceous, the well drilled a Jurassic sequence before reaching Paleozoic sedimentites. Adapted from Arminio et al. (2013).

Ediacaran sedimentites. The Ediacarian palynological assemblages recovered from those cores samples are comprised of poorly preserved but clearly identifiable acritarch assemblages (Figures 3, 4, 5).

2.1. Chiguiro–1 Well

On 27 January 1985, the Sun Colombia Oil Company carried out a drilling program that commenced with the spudding of

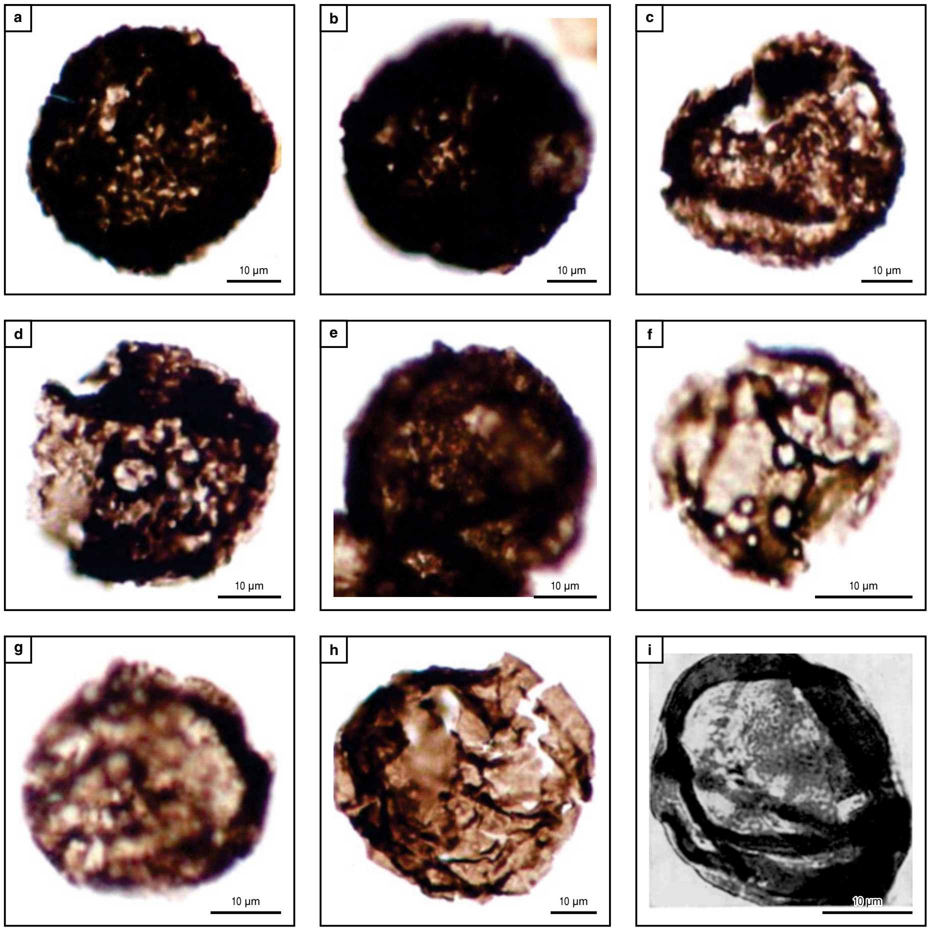

Figure 3. Neoproterozoic acritarchs found in the Llanos Orientales Basin of Colombia. Adapted from Arminio et al. (2013) and Dueñas (2011). Subfigures **(a)**, **(b)**, **(c)**, **(d)**, **(e)** display *Kildinosphaera* cf. *verrucata* whereas **(f)**, **(g)**, **(h)**, **(i)** exhibit *Kildinosphaera chagrinata*.

the Chiguiro–1 well. The primary objective of this well was a large thrusted (flowered) anticline that appeared in seismic lines below the regional unconformity of the Cretaceous. The age of the preunconformity section was not known prior to drilling, and speculations ranged from Lower Paleozoic to Lower Cretaceous.

There were no secondary objectives. After drilling 8630' feet of Tertiary and Cretaceous sedimentites, this well passed through a regional unconformity and began to drill fine, blackish, shallow marine sedimentites of Middle to Early Cambrian age and later (11 800) sedimentites of Ediacaran age (Dueñas, 2011).

Sedimentites under the unconformity are constituted by hard bioturbated siltstones with dolomitic and calcite cement. Cuttings samples were taken at 30–feet intervals. Several sidewall cores were taken, and three conventional cores were acquired towards the base of the drilled sequence.

Cuttings samples yielded Cambrian palynological assemblages, including the acritarchs *Granomarginata squamacea, Micrhystridium* sp., *Multiplicisphaeridium* sp., *Comasphaeridium strigosum, Dictyotidium birvetense, Acanthodiacrodium constrictum, Protosphaeridium* cf. *densum, Synsphaeridium conglutinatum, Baltisphaeridium pellucidum, Dasydiacrodium bicuspidatum, Tectitheca additionalis, Leiosphaeridia* sp., and *Archaeodiscina* cf. *umbonulata*. These assemblages also include Chitinozoan fragments. In the uppermost part of this Cambrian interval, the presence of *Timofeevia brevibifurcata* and *Timofeevia lancarae*, species that can reach the Upper Cambrian, was reported.

Samples from the bottom core the 1985 Chiguiro–1 well also yielded palynological assemblages characterized by the presence of *Chuaria circularis* (Figure 4), which is accompanied by *Synsphaeridium conglutinatum, Stichtosphaeridium* spp., *Kildinosphaera* spp., *Pterospermopsimorpha* sp., *Synsphaeridium* sp., and *Trematosphaeridium* sp. *Chuaria* is compared with *Leiosphaeridia* and classified with it as a sphaeromorphid acritarch (Wang et al., 2011). The presence of the sphaeromorphid *Chuaria* is indicative of Neoproterozoic strata. *Kildinosphaera* spp. are not known to occur in sedimentites above the Neoproterozoic. This acritarch assemblage is comparable to the Late Ediacarian Leiosphere Palynoflora (LELP).

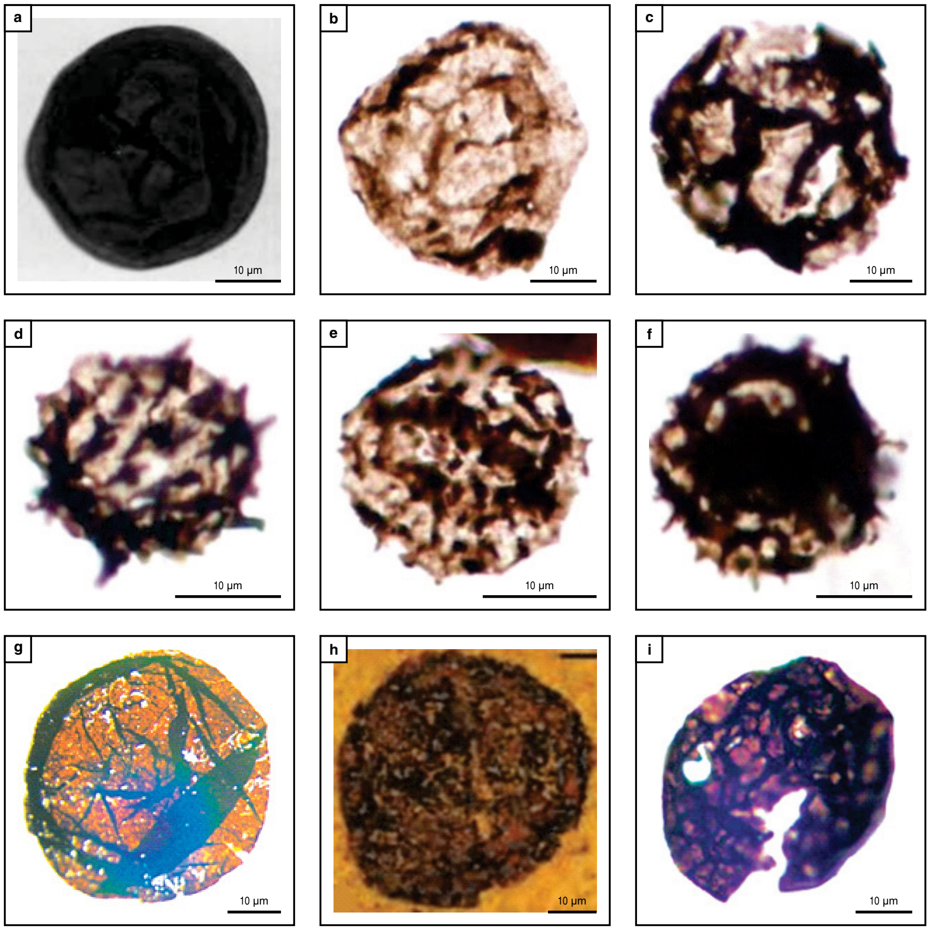

Figure 4. Neoproterozoic acritarchs found in the Llanos Orientales Basin of Colombia. Adapted from Arminio et al. (2013) and Dueñas (2011). Subfigures **(a)**, **(b)**, **(c)** display *Leiosphaeridia* sp.; **(d)**, **(e)**, **(f)** show *Michrystridium* sp. and **(g)**, **(h)**, **(i)** are *Chuaria circularis*.

2.2. Pato–1 Well

The second well drilled by the Sun Colombia Oil Company in the eastern part of the Llanos Orientales was Pato–1. This well was spudded on 19 May 1985. Under the basal unconformity of the Cretaceous, this well penetrated Cambrian – Ediacaran strata. Cuttings samples from the interval 7000'–7165' interval yielded acritarchs of Cambrian age. From the 7170'–7200' (TD) interval, cuttings samples and ten fragments of a conventional core (bottom core) were prepared and analyzed, yielding palynological associations of Ediacaran acritarchs.

Assemblages of acritarchs recovered from fragments of this conventional core include among others *Kildinosphaera chagrinata, Kildinosphaera granulata, Kildinosphaera lophostriata, Lophosphaeridium* sp., *Leiosphaeridia asperata, Protosphaeridium* sp., *Synsphaeridium* aff. *conglutinatum, Micrhystridium* sp., and *Stictosphaeridium* sp. The presence of *Kildinosphaera* spp. are not known to occur in sedimentites above the Ediacaran (LELP). These associations also indicate that these sedimentites were deposited under shallow marine conditions.

2.3. La Coral–1 Well

This well found the top of Neoproterozoic strata at 5650' and reached a total depth of 6492'. A bottom core taken in La Coral–1 encountered a pure sandstone sequence at the top that grades down to bioturbated argillaceous siltstones and sandstones. Very poor assemblages of badly preserved acritarchs were obtained from these sedimentites, which is indicative of high thermal alteration. Recovered acritarchs include *Kildinosphaera* spp., *Micrhystridium* sp., and *Leiosphaeridium* spp., which indicate an Ediacarian age (LELP) for core samples.

2.4. Coralito–1S

The Coralito–1S and the Coral–1 wells were drilled close to each other, and are located on the eastern ascending flank of the rifting system of which the Arauca Graben form part. Therefore, exhibit similar acritarchs assemblages of *Kildinosphaera* spp. and *Leiosphaeridia* spp., indicating an Ediacaran age, which is either equivalent to the Late Ediacarian Leiosphere Palynoflora (LELP).

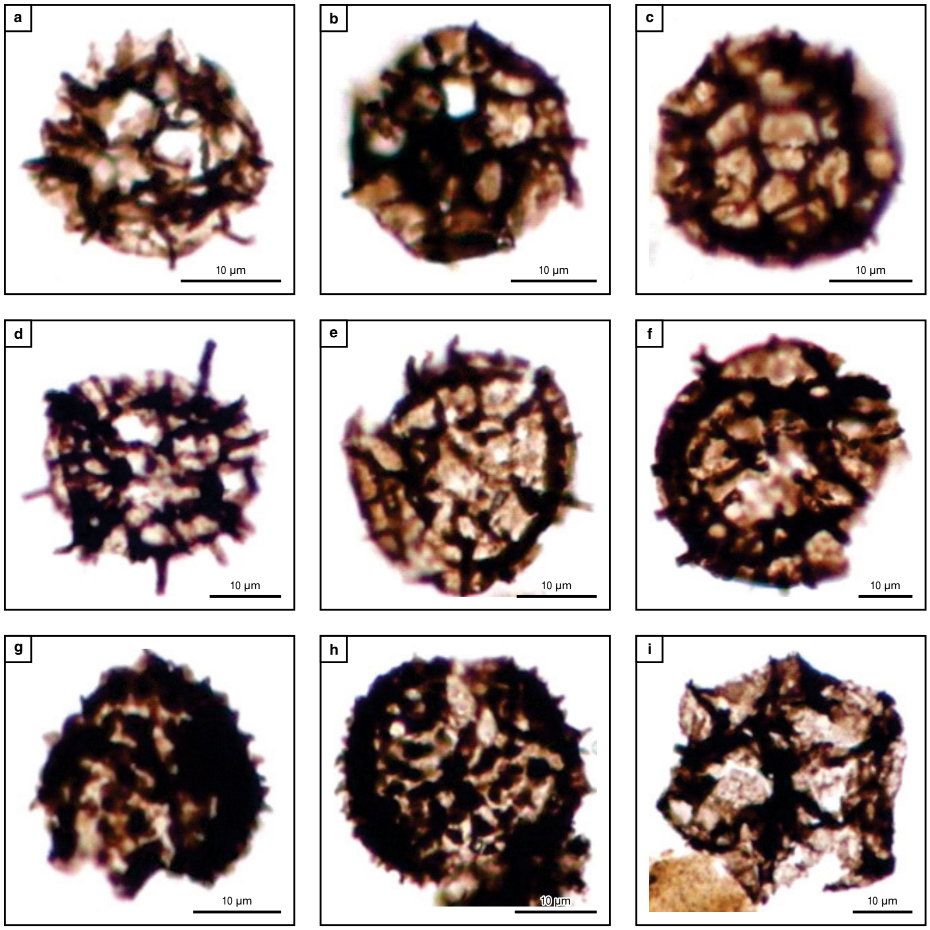

Figure 5. Neoproterozoic acritarchs found in the Llanos Orientales Basin of Colombia. Adapted from Arminio et al. (2013) and Dueñas (2011). Subfigures **(a)**, **(b)**, **(c)** show images of *Dyctiodinium* sp.; **(d)**, **(e)**, **(f)** display *acanthomorph acritarch*; **(g)**, **(h)** are *Lophosphaeridium* sp. and **(i)** *Cymatiosphera* sp.

2.5. Chilacoa–1S well

The Chilacoa–1S well drilled a total of 6745 feet, by finding the top of Ediacarian strata at 5640 feet (1105). Recovered assemblages include *Cymatiosphaera* spp., *Micrhystridium* spp., and rare *Lophosphaeridium* cf. tentativum (Figures 4, 5), suggesting a Late Neoproterozoic very close to the base of the Cambrian (Arminio et al., 2013).

2.6. Torodoi–1X Well

Samples from the interval 7200'–7327' were prepared and analyzed by palynological methods. Good assemblages of poorly preserved acritarchs were obtained from these samples, which are dominated by sphaeromorph forms. Identifiable forms include *Kildinosphaera* spp., (*K. verrucata* and *K. chagrinata*) (Figure 3) and *Leiosphaeridia* spp. This dominance of sphaeromorph acritarchs is characteristic of an Ediacaran age (LELP).

Kildinosphaera spp. (Figure 3) are not known to occur in sedimentites above the Neoproterozoic, but the base of their range is in the Tonian. Based on the recovered palynomorphs, an Ediacaran age can be assigned to these sedimentites, which were deposited under shallow marine environments.

2.7. Vaco–1X Well

This well was drilled as a sidetrack well of Torodoi–1X. Samples from 8760' to 8880' were prepared and analyzed. The abundant presence of poorly preserved, dark–colored sphaeromorph acritarchs were obtained from these samples. Identifiable forms include *Kildinosphaera* spp. (*K. verrucata* and *K. chagrinata*) with *Leiosphaeridia* spp. This dominance of sphaeromorph acritarchs is characteristic of an Ediacarian age (LELP). The Vaco–1x and Torodoi–1X acritarchs assemblages are similar. Again, *Kildinosphaera* spp. are not known to occur in sedimentites above the Neoproterozoic (Figure 3).

These taxa occur in the Neoproterozoic, certainly within the Ediacaran, but the base of their range is uncertain. A Late Tonian – Ediacaran age has been assigned to these sedimentites, which were deposited under shallow marine environments.

3. Discussion

In the northeastern part of the Llanos Orientales Basin (Figure 1), there is a tectonic depression known as the Arauca Graben. The main faults that control this graben extend towards the northeast, crossing from one side of the frontier with Venezuela to the other.

Dozens of wells have been drilled in the Arauca Graben, but only the Chiguiro–1, Chilacoa–1S, and La Heliera–1 wells were drilled with the main objective of studying the sedimentary sequence below the Cretaceous – Paleozoic unconformity (Figure 2). The other wells drilled in the Arauca Graben immediately touched the Paleozoic ended.

For a long time, Paleozoic sedimentites were mistakenly considered as metamorphic rocks and the economic basement of the Llanos Basin. Palynological determinations have allowed us to determine that both the color and the preservation of palynomorphs recovered from Paleozoic and Neoproterozoic samples are indicative that these sedimentites have experienced thermal alteration but cannot be classified as metamorphic rocks for any reason. It is also important to bear in mind that the presence of both liquid and gaseous hydrocarbons has been reported associated with Paleozoic sedimentites (La Heliera–1) in the Llanos Orientales Basin (Dueñas, 2002, 2011).

In the last two decades, extensive and detailed seismic surveys (2D + 3D) have been carried out in the Llanos Orientales Basin. Those associated with intensive drilling programs have allowed us to observe the presence of a thick Neoproterozoic sequence that could be the basis of proposing a new oil system for the Llanos Orientales Basin.

In the Arauca Graben, core samples from seven wells (Chiguiro–1, Pato–1, La Coral–1, Chilacoa–1S, Coralito–1S, Torodoi–1X, and Vaco–1X) have yielded palynomorphs assemblages indicative of an Ediacaran age and shallow marine settings. The most representative of the recovered Ediacaran acritarchs are *Kildinosphaera* sp. *Leiosphaeridia* sp., and *Chuaria circularis*. These observations should be the subject of future analysis. Undoubtedly, sedimentites analyzed from these seven wells are the oldest ones dated by biostratigraphic methods in Colombia.

From the analysis of the seismic programs obtained in the Arauca Graben as well as from the analysis of samples from the seven wells, it is clear that below the Paleozoic sedimentites there is a sedimentary sequence that until now has been sparsely scratched and that could hold the key to understanding the evolution of Acritarchs in the planet's primary times.

Acknowledgments

We wish to thank Dr. Oscar PAREDES ZAPATA, General Director of the Servicio Geológico Colombiano, for his collaboration during the preparation of this chapter. Likewise, we would like to thank Daniela MATEUS ZABALA and Alejandra CARDONA of the editorial team of The Geology of Colombia for their collaboration in editing the figures.

References

Arminio, J.F., Yoris, F., Quijada, C., Lugo, J.M., Shaw, D., Keegan, J.B. & Marshall, J.E.A. 2013. Evidence for Precambrian stratigraphy in graben basins below the Eastern Llanos Foreland, Colombia. American Association Petroleum Geologists International Conference and Exhibition. Abstracts, 35 p. Cartagena.

Baudet, D. 1988. Precambrian palynomorphs from northeast Libya. In: El–Arnauti, A., Owens, B. & Thusu, B. (editors), Subsurface palynostratigraphy of northeast Libya. Garyounis University Publications, p. 17–25. Benghazi, Libya.

Chiglino, L. 2013. Quimioestratigrafia e bioestratigrafia da Formação Frecheirinha, Grupo Ubajara–nordeste do Brasil. Doctoral thesis, Universidade Federal de Pernambuco, 101 p. Recife, Brazil.

Chiglino, L., Gaucher,C., Sial, A.N. & Ferreira, V.P. 2015. Acritarchs of the Ediacaran Frecheirinha Formation, Ubajara Group, northeastern Brazil. Anais da Academia Brasileira de Ciências, 87(2): 635–649. https://doi.org/10.1590/0001-3765201520140430

Cordani, U.G., Sato, K., Sproessner, W. & Fernandes, F.S. 2016. U–Pb zircon ages of rocks from the Amazonas territory of Colombia and their bearing on the tectonic history of the NW sector of the Amazonian Craton. Brazilian Journal of Geology, 46(Suppl 1): 5–35. https://doi.org/10.1590/2317-4889201620150012

Dueñas, H. 2001. Paleozoic palynological assemblages from the Llanos Orientales Basin, Colombia. 34th Annual Meeting American Association of Stratigraphic Palynologists. Proceedings, 16 p. San Antonio, USA.

Dueñas, H. 2002. Asociaciones palinológicas y posibilidades de hidrocarburos en el Paleozoico de la cuenca de los Llanos Orientales de Colombia. Segunda Convención Técnica Asociación Colombiana de Geólogos y Geofísicos del Petróleo. Geología y Petróleo en Colombia. Memoirs, p. 15–17. Bogotá.

Dueñas, H. 2011. The Paleozoic of the Llanos Orientales Basin, Colombia: Integration of biostratigraphic data. Report Bioss Limited 780, unpublished report, 260 p. Bogotá.

Feo–Codecido, G., Smith, F.D., Aboud, N. & Di Giacomo, E. 1984. Basement and Paleozoic rocks of the Venezuelan Llanos basins. In: Bonini, W.E., Hargraves, R.B. & Shagam, R. (editors), The Caribbean–South American Plate boundary and regional tectonics. Geological Society of America, Memoir 162, p. 175–187. https://doi.org/10.1130/MEM162-p175

Gaucher, C. & Poiré, D. 2009. Chapter 4.3 Biostratigraphy. In: Gaucher, C., Sial, A.N., Frimmel, H.E. & Halverson, G.P. (editors), Neoproterozoic – Cambrian tectonics, global change and evolution: A focus on south western Gondwana. Developments in Precambrian Geology (16), Elsevier, p. 103–114. https://doi.org/10.1016/S0166-2635(09)01606-5

Gaucher, C. & Sprechmann, P. 2009. Chapter 9.1 Neoproterozoic acritarch evolution. In: Gaucher, C., Sial, A.N., Frimmel, H.E. & Halverson, G.P. (editors), Neoproterozoic – Cambrian tectonics, global change and evolution: A focus on south western Gondwana. Developments in Precambrian Geology (16), Elsevier, p. 319–326. https://doi.org/10.1016/S0166-2635(09)01622-3

Gaucher, C., Chiglino, L. & Peçoits, E. 2004. Southernmost exposures of the Arroyo del Soldado Group (Vendian to Cambrian, Uruguay): Palaeogeographic implications for the amalgamation of W–Gondwana. Gondwana Research, 7(3): 701–714. https://doi.org/10.1016/S1342-937X(05)71057-1

Ibañez–Mejia, M., Ruiz, J., Valencia, V.A., Cardona, A., Gehrels, G.E. & Mora, A.R. 2011. The Putumayo Orogen of Amazonia and its implications for Rodinia reconstructions: New U–Pb geochronological insights into the Proterozoic tectonic evolution of northwestern South America. Precambrian Research, 191(1–2): 58–77. https://doi.org/10.1016/j.precamres.2011.09.005

Korolev, V.G. & Ogurtsova, R.N. 1983. Correlation of Vendian–Lower Cambrian boundary deposits in the Talas–Karatau zone (Malyy Karatau Range) with the reference sections in the East European and Siberian platforms. International Geology Review, 25(5): 587–595. https://doi.org/10.1080/00206818309466742

Palacios, T. & Vidal, G. 1992. Lower Cambrian acritarchs from northern Spain: The Precambrian–Cambrian boundary and biostratigraphic implications. Geological Magazine, 129(4): 421–436. https://doi.org/10.1017/S0016756800019518

Strother, P.K. 1996. Acritarchs. In: Jansonius, J. & McGregor, D.C. (editors), Palynology, principles and applications: Principles. American Association of Stratigraphic Palynologist Foundation, volume 1, chapter 5, p. 81–106. Dallas.

Wang, X., Yuan, X., Zhou, C., Du, K. & Gong, M. 2011. Anatomy and plant affinity of Chuaria. Chinese Science Bulletin, 56(12): 1256–1261. https://doi.org/10.1007/s11434-011-4370-x

Explanation of Acronyms, Abbreviations, and Symbols:

LELP	Late Ediacarian Leiosphere Palynoflora
PZ	Paleozoic
TD	Total depth

Authors’ Biographical Notes

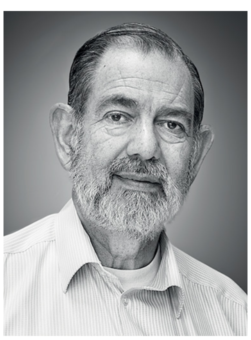

Hernando DUEÑAS–JIMÉNEZ studied geology at Universidad Nacional de Colombia, where he graduated in 1972. He later specialized in studies in geology and palynology at the Gemeente Universiteit van Amsterdam, Holland, between 1977–1979 and obtained a PhD in geological sciences in 1986 at the same institution. He was later associated with Servicio Geológico Colombiano leading the Laboratorio de Palinología between 1977 and 1978 and as the Director of the División de Estratigrafía y Paleontología between 1978 and 1980. He was a professor of Palynology in the Departamento de Geociencias, Universidad Nacional de Colombia, Sede Bogotá, between 1979 and 1981, during which time he occupied the position of geologist expert in palynology in Intercol (Exxon group). He was a palynologist in the section of regional works of the Robertson Research INC Company (Houston) between 1982 and 1983, from which he began to practice his profession independently as a consultant geologist in biostratigraphy for the Colombian petroleum industry. In 1978, he was awarded the “Best Geological Research” prize by the Board of Directors of Servicio Geológico Colombiano. He received a recognition for scientific contribution (San Cayetano Formation) from the Centro de Investigaciones del Petróleo CEINPET, Cuba, in 2003. He held the vice presidency of the Academia Colombiana de Ciencias Exactas, Físicas y Naturales (ACCEFYN) between 2000 and 2002. He is a numerical member of the ACCEFYN and Academia Colombiana de Geografía and a foreign correspondent member of the Real Academia de Ciencias Exactas, Físicas y Naturales de España. He has published more than 80 articles in indexed journals.

Jorge MONTALVO–JÓNSSON studied geology at the University of Iceland. He graduated with a BS degree in 2008, then pursued an M.Paed degree in geology at the same university, from which he graduated in 2010. Afterwards, he pursued a MS in Geology with special emphasis on the analysis of volcanic hazards. He obtained the title in 2014 from the University of Iceland. During his studies in Iceland, he worked remotely at Bioss S.A.S. as a support member in research pertaining to the regional geology of Colombia. Furthermore, he worked at ÍSOR (Icelandic Geo Survey) as an assistant geologist in the summer of 2010 and at the Icelandic Meteorological Institute (Veðurstofa Íslands) as a specialist in volcanology in 2011. Most recently, he has been pursuing a PhD degree at the Universidad Nacional de Colombia. Additionally, he has been involved in promoting ethics in geosciences as a member of the IAPG (International Association for Promoting Geoethics).

Volume 1

Chapter 6

https://doi.org/10.32685/pub.esp.35.2019.06
Published online 24 November 2020

The Putumayo Orogen of Amazonia: A Synthesis

Mauricio IBAÑEZ–MEJIA[1]*

1 ibanezm@arizona.edu
Department of Geosciences
University of Arizona
Tucson, Arizona, 85721, USA*
Corresponding author

Abstract Meso– and Neoproterozoic paleogeographic reconstructions indicate that Amazonia played an important role in the assembly of Rodinia, and that its incorporation into this supercontinent led to continent–continent collision(s) with the Grenville Orogen of Laurentia and the Sveconorwegian Orogen of Baltica. The Sunsás–Aguapeí belt of SW Amazonia has traditionally been regarded as the geological evidence of such interactions, although it is becoming increasing clear that the metamorphic and tectonic history of this margin does not match the grade and timing that would be expected from interactions with the (near)–Adirondian margin of the Grenville, or with the Sveconorwegian margin of Fennoscandia. Massifs of amphibolite– to granulite–facies basement of late Proterozoic age have been known to exist in the northern Andes for many decades, but an autochthonous late Meso– to early Neoproterozoic orogenic belt in the western Guiana Shield that is un–remobilized by Andean tectonics, remained unknown. The recent discovery of such a belt, hidden under the Putumayo Foreland Basin, allowed, for the first time, to directly link the basement inliers of the Colombian Andes with the western Guiana Shield. Furthermore, the improved geochronologic database of some cordilleran inliers and Putumayo Basin basement, using high–spatial–resolution U–Pb methods, has permitted a more complete reconstruction of their evolution. This orogenic belt, which owing to its geographical location obtained the name 'Putumayo Orogen', holds key information about Amazonia's Meso– to early Neoproterozoic tectonics and is of great geodynamic significance in understanding the role played by this craton during amalgamation of the Rodinia supercontinent. This chapter provides a brief overview of the currently available geochronologic data and hypothesized tectonic evolution of the Putumayo Orogenic Cycle, with particular emphasis on its reconstruction within a dynamic framework of Laurentia–Amazonia–Baltica interactions in the second half of the Proterozoic Eon and during Rodinia supercontinent accretion.

Keywords: *Amazonia, Putumayo Orogen, Rodinia, Proterozoic tectonics, collisional orogenesis.*

Resumen Reconstrucciones paleogeográficas de los periodos Meso– y Neoproterozoico indican que Amazonia jugó un papel importante durante la amalgamación de Rodinia, y que su incorporación al núcleo de este supercontinente involucró colisiones continente–continente con el Orógeno Grenville de Laurentia y el Orógeno Sueco–Noruego de Báltica. El cinturón orogénico Sunsás–Aguapeí en la margen SW de Amazonia ha sido tradicionalmente considerado como la principal evidencia geológica de dichas interacciones; sin embargo, cada vez es más claro que la historia metamórfica y tectónica de este orógeno no coincide ni en grado metamórfico ni en edad con lo que se esperaría si este hubiese colisionado con la margen adiron-

Citation: Ibañez–Mejia, M. 2020. The Putumayo Orogen of Amazonia: A synthesis. In: Gómez, J. & Mateus–Zabala, D. (editors), The Geology of Colombia, Volume 1 Proterozoic – Paleozoic. Servicio Geológico Colombiano, Publicaciones Geológicas Especiales 35, p. 101–131. Bogotá. https://doi.org/10.32685/pub.esp.35.2019.06

diana del Orógeno Grenville o la margen sueco–noruega de Fenoscandia. Aunque la ocurrencia de bloques de basamento con asociaciones metamórficas en facies anfibolita a granulita y edad proterozoica tardía en los Andes del norte es bien conocida desde hace varias décadas, la existencia de un cinturón orogénico autóctono mesoproterozoico tardío a neoproterozoico temprano en la margen occidental del Escudo de Guayana, el cual no haya sido retrabajado durante la Orogenia Andina, fue por mucho tiempo desconocida. El reciente descubrimiento de dicho cinturón orogénico bajo la cuña sedimentaria de la cuenca de antepaís del Putumayo ha permitido, por primera vez, una correlación directa entre los bloques de basamento expuestos en los Andes colombianos y la margen occidental del Escudo de Guayana. En adición a esto, los esfuerzos recientes realizados para expandir la base de datos geocronológica de los bloques de basamento cordilleranos y el basamento de la Cuenca del Putumayo, particularmente utilizando métodos de datación U–Pb de alta resolución espacial, han permitido realizar una reconstrucción más completa de su evolución tectónica. Este cinturón orogénico, que debido a su localización geográfica ha recibido el nombre de 'Orógeno Putumayo', contiene información crucial sobre la evolución tectónica meso– neoproterozoica temprana de Amazonia y es de gran importancia geodinámica para entender el rol de este gran bloque continental en la amalgamación del supercontinente Rodinia. El objetivo de este capítulo es proporcionar una breve síntesis de la información geocronológica existente y la evolución tectónica propuesta del Ciclo Orogénico Putumayo, haciendo énfasis particular en su reconstrucción dentro de un marco dinámico global de interacciones entre Laurentia, Amazonia y Báltica en la segunda mitad del Proterozoico y durante la acreción del supercontinente Rodinia.

Palabras clave: *Amazonia, Orógeno Putumayo, Rodinia, tectónica proterozoica, orogenia colisional.*

1. Introduction

The supercontinent cycle is thought to have exerted a major control on the development and preservation of Earth's crust through geologic time (e.g., Cawood et al., 2013; Hawkesworth et al., 2013), and is a first–order feature –and inevitable consequence– of terrestrial plate tectonics. In this cycle, continental land–masses break apart along continental rift zones, thereby opening ocean basins that separate previously adjoining continental fragments, and continental land–masses collide, thereby consuming ocean basins by subduction and resulting in pervasive deformation and high–temperature (± pressure) metamorphism of cratonic margins. Therefore, unraveling the timing, tempo, and physical conditions of these processes in ancient orogenic belts is the best–suited approach to quantitatively reconstruct the tectonic history of our planet, and to understand the chemical/structural development of Earth's lithosphere.

The Amazonian Craton is one of the largest Precambrian continental nuclei on Earth and a key piece of the supercontinent puzzle (Cordani et al., 2009). This cratonic block is thought to encompass two exposed shield areas (Figure 1), namely the Guiana Shield to the north of the Amazon Basin and the Central Brazil (or Guaporé) Shield south of the Amazon Basin. Besides preserving an extensive geological record of Proterozoic magmatism, arc development, and potentially also crustal growth (Cordani & Teixeira, 2007; Tassinari & Macambira, 1999), the craton known as Amazonia is thought to be one of the principal building blocks during the assembly of the Nuna/Columbia (e.g., Bispo–Santos et al., 2014) and Rodinia (e.g., Li et al., 2008) Proterozoic supercontinents. Although geological evicendes of Amazonia's incorporation in Rodinia are widely exposed in the eastern plains of Bolivia and in northwestern Brazil, within an orogenic belt in the Central Brazilian Shield known as the Sunsás–Aguapeí Orogen (Boger et al., 2005; Litherland & Bloomfield, 1981; Litherland et al., 1989; Sadowski & Bettencourt, 1996; Teixeira et al., 2010; among others), geological records of this period in the Guiana Shield have proven more elusive to detect. For many decades, the occurrence of Proterozoic basement inliers with upper amphibolite– to granulite–facies metamorphic assemblages has been known in the Andes of Colombia (Kroonenberg, 1982, and references therein), but their relationship with respect to the Guiana Shield remained enigmatic for a long time. Such cordilleran blocks, often grouped within the so–called Garzón–Santa Marta granulite belt (after Kroonenberg, 1982), include the Garzón and Santander Massifs in the Colombian Eastern Cordillera, Las Minas and San Lucas

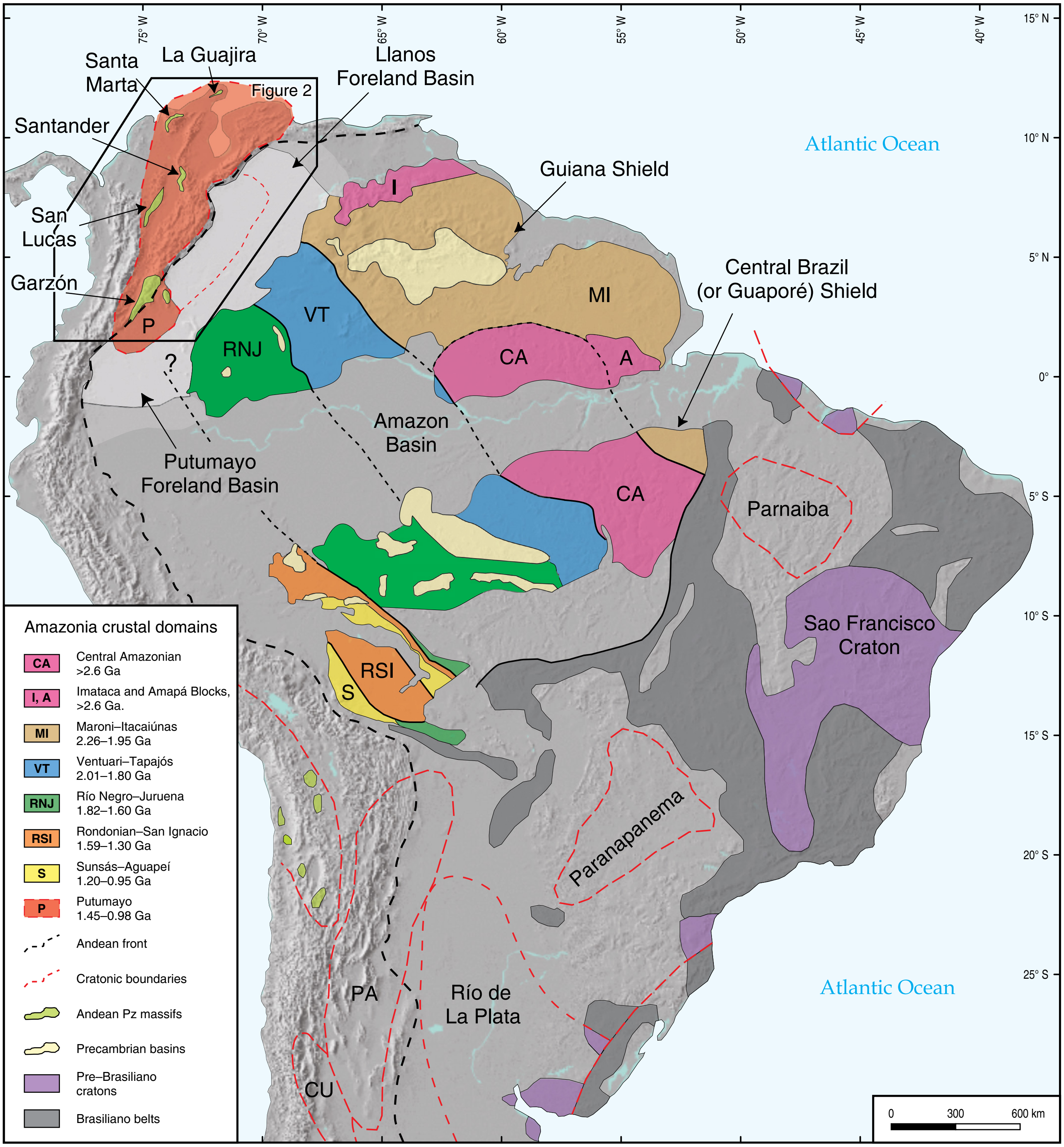

Figure 1. Simplified geo–tectonic map of South America, highlighting the approximate outline and terrane boundaries of the Amazonian Craton and the Guiana Shield. Adapted from Tassinari & Macambira (1999), Cordani & Teixeira (2007), Fuck et al. (2008), Ibañez–Mejia et al. (2015), and Teixeira et al. (2019). (CU) Cuyania Terrane, (PA) Pampia Terrane.

Massifs in the Central Cordillera, and the Sierra Nevada de Santa Marta and La Guajira Peninsula along the northernmost Colombia–Venezuela border (Figure 2).

It has also been recognized for several years that the geochronologic and geochemical record of units within the Garzón–Santa Marta granulite belt bear many similarities with the Proterozoic basement of south central Mexico, known as 'Oaxaquia' (Ortega–Gutiérrez et al., 1995). Mostly hidden underneath younger cover, Oaxaquia is exposed in various localities throughout Mexico including units known as the Novillo

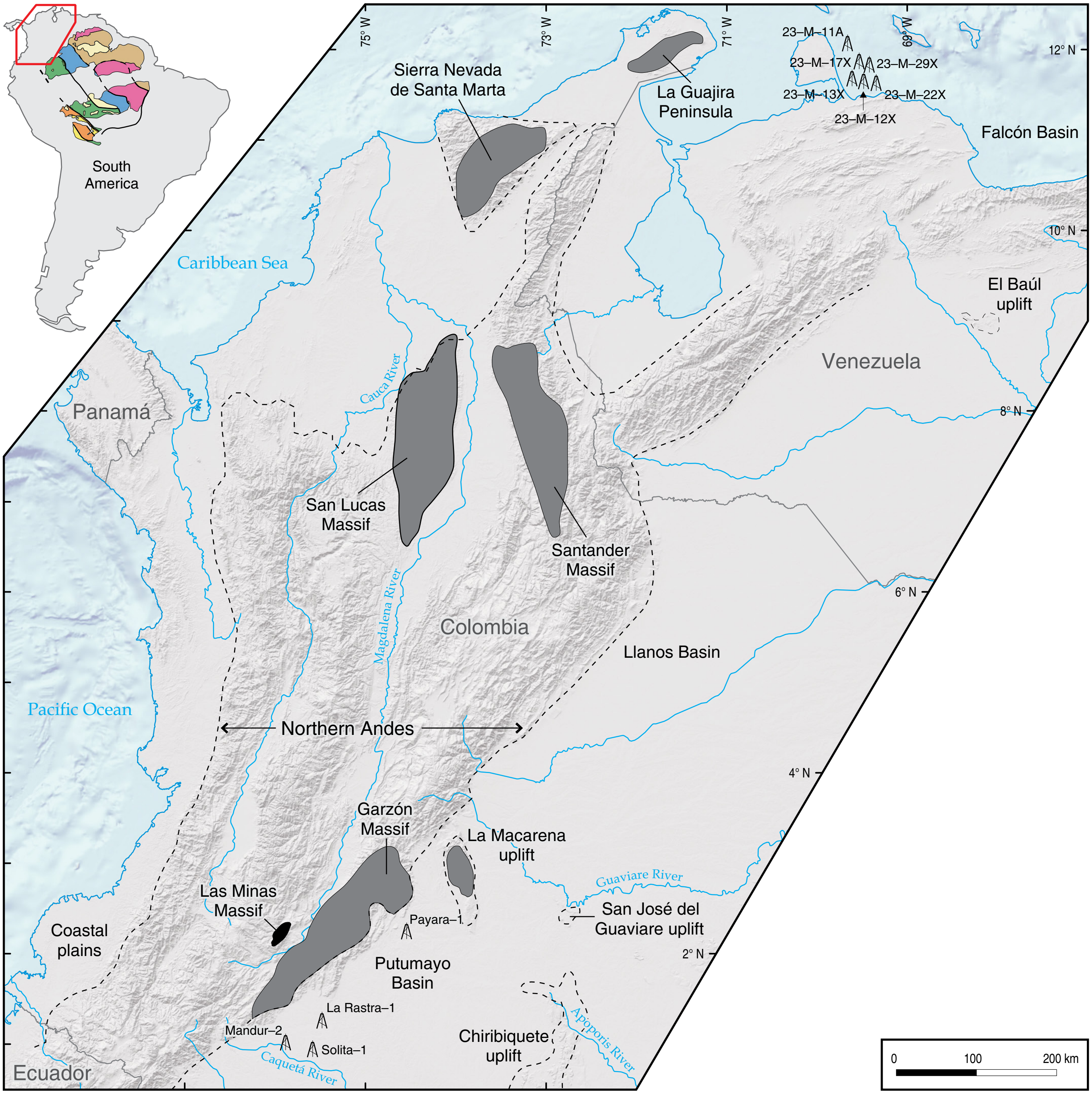

Figure 2. Simplified shaded relief image of NW South America showing the location of cordilleran basement inliers that form part of the Putumayo Orogen, and basement drilling cores in the Putumayo and Falcón Basins where late Meso– to early Neoproterozoic units have been dated using modern geochronologic methods. See Table 1 for references.

Gneiss, the Huiznopala Gneiss, the Guichicovi Complex, and the Oaxacan Complex (Ortega–Gutiérrez et al., 2018, and references therein). Based on Sm–Nd (Restrepo–Pace et al., 1997), Pb (Ruiz et al., 1999), and Lu–Hf (Weber et al., 2010) isotopic compositions, the strong geochemical resemblance between Oaxaquia and the Colombian cordilleran inliers has been well established over a decade. Nevertheless, a key part of the puzzle that was missing was a direct link to tie this now strongly dismembered 'Colombia/Oaxaquia' tectonic block back to its purported Amazonian ancestry. In 2011, dating of exploratory–borehole cores from the basement of the Putumayo Foreland Basin yielded ages similar to those found in the Garzón–Santa Marta granulite belt and Oaxaquia (Ibañez–Mejia et al., 2011), thus allowing linking these dismembered blocks (i.e., Colombia/Oaxaquia terrane) to the westernmost Guiana Shield and incorporating all these pieces into the definition of the 'Putumayo Orogen'. Since 2011, additional U–Pb, Sm–Nd, Lu–Hf, and O isotopic data from zircon and whole–rock samples have further strengthened the consanguinity of all blocks considered to form an integral part of, or be related to, the Putumayo Orogen (e.g., Baquero et al., 2015; Ibañez–Mejia et al., 2015, 2018; Solari et al., 2013; Weber & Schulze, 2014).

Although both the paleomagnetic and geochronologic datasets for Meso– and Neoproterozoic units in Oaxaquia and NW South America remain arguably very limited, the available geochronology/isotope geochemistry of the Putumayo Orogen, in concert with the existing Mesoproterozoic paleomagnetic poles available for Amazonia, are converging into a coherent tectonic picture for this time period (Cawood & Pisarevsky, 2017). This chapter presents a synthesis of the available geochronologic information for the Putumayo Orogen obtained using modern analytical methods, and their interpreted geologic significance within tectonic reconstructions at an orogen to cratonic scale. This reconstruction places particular emphasis on understanding this orogen within a continuously refining picture of Amazonia's role in Proterozoic paleogeography and the assembly of Rodinia, to elucidate possible tectonic correlations with the Grenville margin of Laurentia and/or the Sveconorwegian margin of Baltica. Nevertheless, successfully unraveling the geological history of continental collisions associated with Rodinia assembly, which are crucial for continuing to test and further enlighten plausible paleo–geographic and paleo–tectonic scenarios, will require continuous improvement of the geologic, geochronologic, petrologic, and paleomagnetic databases.

2. Summary of Available Geochronologic Data

The first geochronologic evidence for the occurrence of late Meso– to early Neoproterozoic orogenic events in NW South America date back to the seminal works of Pinson et al. (1962), MacDonald & Hurley (1969), Goldsmith et al. (1971), Tschanz et al. (1974), Alvarez & Cordani (1980), Alvarez (1981), and Priem et al. (1982, 1989). All these results, however, were obtained by means of K–Ar and Rb–Sr methods, which can be easily reset (totally or partially) by thermally–activated diffusion and/or fluid alteration even at moderate temperatures (Reiners et al., 2017). Therefore, although these results are important from an historical standpoint, they will not be considered further for the purposes of this chapter. The first zircon U–Pb results from the cordilleran basement inliers in Colombia were obtained by Restrepo–Pace et al. (1997), using the isotope dilution–thermal ionization mass spectrometry (ID–TIMS) method. Nevertheless, because of the complex growth history of zircon from the Garzón Massif, these bulk–crystal analyses yielded complex (i.e., mixed) results that prevent determining igneous protolith and/or metamorphic ages with accuracy.

Due to the textural complexity of zircon crystals in collisional orogens such as the Putumayo, where metamorphic overgrowths and/or sub–solidus recrystallization of inherited nuclei are commonplace (see Ibañez–Mejia et al., 2015 and references therein), this chapter only considers U–Pb dates obtained using spatially–resolved analytical techniques, such as secondary ion mass spectrometry (SIMS) or laser ablation–inductively coupled plasma–mass spectrometry (LA–ICP–MS). The zircon U–Pb geochronologic database for portions of the Putumayo Orogen identified to date in NW South America is summarized in Table 1. Note that, for the sake of brevity, Table 1 does not include the available geochronology from Oaxaquia; for this, the interested reader is pointed to the recent review of Ortega–Gutiérrez et al. (2018) and references therein. In chronologic order, the dataset presented here was compiled from the works of Cardona (2003), Cordani et al. (2005), Cardona et al. (2010), Ibañez–Mejia et al. (2011), Leal–Mejía (2011), Cuadros et al. (2014), Baquero et al. (2015), Ibañez–Mejia et al. (2015), Urbani et al. (2015), and van der Lelij et al. (2016). Only a handful of isochron dates obtained by the Sm–Nd and Lu–Hf methods are available for samples of the Putumayo Orogen, from the works of Cordani et al. (2005), Ordóñez–Carmona et al. (2006), and Ibañez–Mejia et al. (2018); these dates are also included in Table 1.

3. Mesoproterozoic Paleogeography and Amazonia in Rodinia

Paleogeographic reconstructions of the Proterozoic Earth commonly rely on one or several of three key sources of information: (1) robust paleomagnetic data (e.g., Evans, 2013; Pisarevsky et al., 2014), which can be used to infer the paleo–latitude of sample–sets/terranes at the time of magnetic–remanence blocking; (2) geological matching of orogenic belts, magmatic arcs, and/or basins across once adjoining cratons or crustal blocks (e.g., Dalziel, 1991; Hoffman, 1991); and/or (3) matching of mafic dike swarms or other large igneous province (LIP) features (e.g., Bleeker & Ernst, 2006; Ernst et al., 2013). Paleogeographic solutions drawn from applying each of these lines of evidence by itself can be non–unique, but solutions that take into consideration the broadest spectrum of information are more likely to approach an accurate picture (Li et al., 2008).

Laurentia (North American Craton), Baltica (East European Craton), and Amazonia (northern South American Craton) are three key Precambrian crustal nuclei thought to form the core of Rodinia (Figure 3), and their most accepted positions within the fully assembled supercontinent at ca. 1.00–0.95 Ga are shown in Figure 3a. This configuration, which remains similar to the earliest reconstructions of the late Proterozoic supercontinent now known as Rodinia (e.g., Bond et al., 1984; Hoffman,

Table 1. Compilation of published geochronologic data from the Putumayo Orogen using modern U–Pb, Sm–Nd, and Lu–Hf methods.

Sample name	Latitude N	Longitude W	Unit	Rock type	Mean	±2σ	Event	Method	Reference
				Putumayo Basin basement					
Caimán–3 (Leuco)	0° 45' 13.6"	76° 9' 45.4"	Putumayo Basin well	Leucogranite	952	± 19	Ign.	U–Pb, LA–ICP–MS	Ibañez–Mejia et al. (2011)
Caimán–3 (Metased)	0° 45' 13.6"	76° 9' 45.4"	Putumayo Basin well	Metased. migmatite	989	± 11	Met.	U–Pb, LA–ICP–MS	Ibañez–Mejia et al. (2011)
Payara–1	2° 7' 31.3"	74° 33' 35.9"	Putumayo Basin well	Metaign. migmatite	987	± 17	Met.	U–Pb, LA–ICP–MS	Ibañez–Mejia et al. (2011, 2015)
					1606	± 6	Ign.	U–Pb, LA–ICP–MS	Ibañez–Mejia et al. (2011, 2015)
Mandur–2 (Leuco)	0° 55' 24.5"	75° 52' 34.1"	Putumayo Basin well	Syenogranite	1017	± 4	Ign.	U–Pb, LA–ICP–MS	Ibañez–Mejia et al. (2011, 2015)
Mandur–2 (Melano)	0° 55' 24.5"	75° 52' 34.1"	Putumayo Basin well	Migmat. amphibolite	1019	± 8	Met.	U–Pb, LA–ICP–MS	Ibañez–Mejia et al. (2011, 2015)
					1592	± 8	Ign.	U–Pb, LA–ICP–MS	Ibañez–Mejia et al. (2011, 2015)
Solita–1	0° 52' 28.6"	75° 37' 21.3"	Putumayo Basin well	Metased. migmatite	1046	± 23	Met.	U–Pb, LA–ICP–MS	Ibañez–Mejia et al. (2011)
La Rastra–1	1° 9' 58"	75° 30' 13"	Putumayo Basin well	Metased. migmatite	1007.0	± 2.9	Cool	Sm–Nd isochron	Ibañez–Mejia et al. (2018)
					1070.8	± 5.6		Lu–Hf isochron*	Ibañez–Mejia et al. (2018)
				Falcón Basin basement in La Vela Bay					
23–M–22X–1	11° 34' 30"	69° 31' 26.4"	Falcón Basin well	Metawacke	984.8	± 6.7	Met.	U–Pb, SHRIMP	Baquero et al. (2015)
					DZ	≥1029	Sed.	U–Pb, SHRIMP	Baquero et al. (2015)
23–M–22X–3	11° 34' 30"	69° 31' 26.4"	Falcón Basin well	Metapelite	981	± 10	Met.	U–Pb, SHRIMP	Baquero et al. (2015)
					DZ	≥1044	Sed.	U–Pb, SHRIMP	Baquero et al. (2015)
23–M–22X–4	11° 34' 30"	69° 31' 26.4"	Falcón Basin well	Mafic granulite	967	± 8	Met.	U–Pb, SHRIMP	Baquero et al. (2015)
					1034	± 12	Ign.	U–Pb, SHRIMP	Baquero et al. (2015)
				Cordilleran inliers–Colombian Central and Eastern Cordilleras					
PCM–1105	7° 17' 57.8"	72° 53' 17.87"	Bucaramanga Gneiss	Biotite gneiss	DZ	≥864	Sed.	U–Pb, SHRIMP	Cordani et al. (2005)
CC–1	6° 29' 38"	74° 46' 8.71"	Nus Gneiss	Bt–Sill gneiss	DZ	≥969	Sed.	U–Pb, SHRIMP	Cardona (2003)
CB–006	2° 13' 26.5"	75° 50' 22"	Zancudo Migmatites	Metased. migmatite	972	± 12	Met.	U–Pb, LA–ICP–MS	Ibañez–Mejia et al. (2011, 2015)
MIVS–26	2° 3' 19.2"	75° 42' 47.6"	Guapotón Gneiss	Augen–gneiss	990	± 8	Met.	U–Pb, LA–ICP–MS	Ibañez–Mejia et al. (2011, 2015)
					1135	± 6	Ign.	U–Pb, LA–ICP–MS	Ibañez–Mejia et al. (2011, 2015)
MIVS–41	2° 13' 34"	75° 50' 30.3"	Las Minas Gneiss	Augen–gneiss	990	± 7	Met.	U–Pb, LA–ICP–MS	Ibañez–Mejia et al. (2011, 2015)
					1325	± 5	Ign.	U–Pb, LA–ICP–MS	Ibañez–Mejia et al. (2011, 2015)
MIVS–11	2° 9' 33.4"	75° 35' 37"	El Vergel Granulites	Felsic granulite	992	± 5	Met.	U–Pb, LA–ICP–MS	Ibañez–Mejia et al. (2011)
CB–002	2° 7' 37.7"	75° 37' 41.9"	El Vergel Granulites	Felsic paragneiss	992	± 8	Met.	U–Pb, LA–ICP–MS	Ibañez–Mejia et al. (2011)
MIVS–12	2° 9' 20.7"	75° 35' 27.4"	El Vergel Granulites	Felsic granulite	997	± 17	Met.	U–Pb, LA–ICP–MS	Ibañez–Mejia et al. (2015)
V–198	1° 49' 14.6"	75° 47' 12.6"	Guapotón Gneiss	Augen–gneiss	1000	± 25	Met.	U–Pb, SHRIMP	Cordani et al. (2005)
					1158	± 22	Ign.	U–Pb, SHRIMP	Cordani et al. (2005)
MIVS–16A	2° 8' 11.7"	75° 36' 55.7"	El Vergel Granulites	Grt–bearing leucosome	1001	± 12	Met.	U–Pb, LA–ICP–MS	Ibañez–Mejia et al. (2015)
MIVS–15A	2° 8' 28.2"	75° 36' 44.7"	El Vergel Granulites	Granitic pegmatite	1022.3	± 8.8	Ign.	U–Pb, LA–ICP–MS	Ibañez–Mejia et al. (2015)
MIVS–13	2° 8' 9"	75° 35' 22.7"	El Vergel Granulites	Felsic paragneiss	DZ	≥1000	Sed.	U–Pb, LA–ICP–MS	Ibañez–Mejia et al. (2015)
MIVS–37A	2° 15' 37.3"	75° 49' 49.9"	Pital Migmatites	Metased. migmatite	DZ	≥1005	Sed.	U–Pb, LA–ICP–MS	Ibañez–Mejia et al. (2011)
Gr–29	1° 45' 50.6"	75° 44' 8.68"	El Vergel Granulites	Enderbite	DZ	≥1005	Sed.	U–Pb, SHRIMP	Cordani et al. (2005)
Gr–15	1° 32' 31"	75° 26' 18.43"	Florencia Migmatites	Leucosome	1015	± 8	Met.	U–Pb, SHRIMP	Cordani et al. (2005)
10VDL61	7° 9' 59"	73° 5' 17"	Río Suratá granodiorite	Enclaves	1018	± 9	Ign.?	U–Pb, LA–ICP–MS	van der Lelij et al. (2016)
WR–219	7° 44' 25"	74° 29' 2"	Guamoco orthogneiss	Qz–Fsp–Bt gneiss	1048	± 24	Met.	U–Pb, LA–ICP–MS	Leal–Mejía (2011)
					1280	± 36	Ign.	U–Pb, LA–ICP–MS	Leal–Mejía (2011)
Macarena–2	3° 1' 45"	73° 52' 13.5"	La Macarena Gneiss	Felsic mylonitic gneiss	1461	± 10	Ign.	U–Pb, LA–ICP–MS	Ibañez–Mejia et al. (2011, 2015)
017–05	8° 34' 6.3"	74° 5' 44.98"	San Lucas Gneiss	Granitic gneiss	1502	± 18	Ign.	U–Pb, LA–ICP–MS	Cuadros et al. (2014)
020–03	8° 40' 25.2"	74° 5' 48.85"	San Lucas Gneiss	Metamonzogabbro	1507	± 6	Ign.	U–Pb, LA–ICP–MS	Cuadros et al. (2014)
PGG–18	8° 40' 45.6"	74° 5' 20.92"	San Lucas Gneiss	Granitic gneiss	1508	± 15	Ign.	U–Pb, LA–ICP–MS	Cuadros et al. (2014)
					1527	± 10	Ign.	U–Pb, LA–ICP–MS	Cuadros et al. (2014)

Table 1. Compilation of published geochronologic data from the Putumayo Orogen using modern U–Pb, Sm–Nd, and Lu–Hf methods (*continued*).

Sample name	Latitude N	Longitude W	Unit	Rock type	Mean	±2σ	Event	Method	Reference
			Cordilleran inliers–Colombian Central and Eastern Cordilleras						
022–01	8° 39' 5"	74° 5' 39.4"	San Lucas Gneiss	Granitic gneiss	1527	± 14	Ign.	U–Pb, LA–ICP–MS	Cuadros et al. (2014)
020–02	8° 40' 25.2"	74° 5' 48.85"	San Lucas Gneiss	Metamonzogabbro	1530	± 11	Ign.	U–Pb, LA–ICP–MS	Cuadros et al. (2014)
D–982	2° 9' 35.7"	75° 29' 47"	El Vergel Granulites	Garnet gneiss	925	± 7	Cool	Sm–Nd isochron**	Cordani et al. (2005)
V–332	1° 46' 56.9"	75° 46' 2.34"	El Vergel Granulites	Charnockite	935	± 5	Cool	Sm–Nd isochron**	Cordani et al. (2005)
C–32	1° 42' 49.8"	75° 18' 30.94"	Florencia Migmatites	Paragneiss	990	± 8	Cool	Sm–Nd isochron**	Cordani et al. (2005)
Gr–15p	1° 32' 31.7"	75° 26' 18.43"	Florencia Migmatites	Paragneiss	1034	± 6	Cool	Sm–Nd isochron**	Cordani et al. (2005)
			Cordilleran inliers–Sierra Nevada de Santa Marta						
A–49	11° 12' 24.3"	73° 12' 37.16"	Dibulla Gneiss	Biotite gneiss	991	± 12	Met.	U–Pb, SHRIMP	Cordani et al. (2005)
					1374	± 13	Ign.	U–Pb, SHRIMP	Cordani et al. (2005)
JRG–20–96	N.R.	N.R.	Los Mangos Granulites	Paragneiss	991	± 12	Met.	U–Pb, LA–ICP–MS	Cardona et al. (2010)
GRM–10	N.R.	N.R.	Los Mangos Granulites	Garnet gneiss	971	± 8	Cool	Sm–Nd isochron**	Ordóñez–Carmona et al. (2006)
			Cordilleran inliers–La Guajira Peninsula and Venezuelan Cordillera de La Costa						
Jojon–1	11° 52' 13.92"	72° 1' 26.58"	Jojoncito Gneiss	Qz–Fsp gneiss	916	± 19	Met.?	U–Pb, SHRIMP	Cordani et al. (2005)
Ya–235B	N.R.	N.R.	El Guayabo Complex	Charnockite	986	± 5	Met.	U–Pb, SHRIMP	Urbani et al. (2015)
					1167	± 7	Ign.	U–Pb, SHRIMP	Urbani et al. (2015)
08VDL11	8° 41' 41"	70° 53' 31"	Micarache orthogneiss	Sillimanite gneiss	1009	± 7	Ign.?	U–Pb, LA–ICP–MS	van der Lelij et al. (2016)
Zu–6	11° 40' 60"	71° 46' 60"	Atuschon Gneiss	Qz–Fsp gneiss	1028.7	± 4.4	Met.	U–Pb, SHRIMP	Baquero et al. (2015)

*Isochron affected by Lu–Hf diffusive decoupling–see reference for details.

**2–point isochrons. Rarely reliable.

N.R.: Sampling coordinates not reported.

Cool: Cooling age; DZ: Detrital zircon; Ign: Age of igneous crystallization; Met: Age of metamorphism; Sed: Maximum age of sedimentation from DZ U–Pb results.

1991), has stood the test of time and to date remains the most plausible and widely–accepted reconstruction (Cawood & Pisarevski, 2017; D'Agrella–Filho et al., 2016a; Li et al., 2008; Weil et al., 1998). Some key aspects of this reconstruction, and the relative role of these three major cratons just prior to and during the assembly of Rodinia, are summarized below.

D'Agrella–Filho et al. (2016a) presented a recent up–to–date discussion of the paleomagnetic poles available for Amazonia, and interested readers are referred to their work for an in–depth discussion. In brief, robust paleo–magnetic constraints for the position of Amazonia within Rodinia come from two key poles in NW Brazil: (1) The Nova Floresta pole (Tohver et al., 2002), dated at ca. 1.2 Ga; and (2) the Fortuna pole of the Aguapeí Group (D'Agrella–Filho et al., 2008), dated at 1149 ± 7 Ma. Both of these poles are consistent with SW Amazonia as being positioned near the Grenville margin of North America during the Stenian, therefore confirming previous reconstructions (e.g., Hoffman, 1991; Weil et al., 1998) in which Amazonia's position was inferred from other lines of geological evidence since no paleomagnetic information was then available. The relative positions of the Nova Floresta and Fortuna poles indicate that an oblique collision between Amazonia and Laurentia took place in the Mesoproterozoic (Cordani et al., 2009; D'Agrella–Filho et al., 2016a; Tohver et al., 2002, 2004), and these results have been used to infer that collision first took place between the Llano and Sunsás–Aguapei margins of Laurentia and Amazonia, respectively (Figure 3b), followed by sinistral strike–slip displacement between the two cratons (Figure 3c) until these attained their final Rodinia configuration (Figure 3a).

The relative position of Baltica within Rodinia and with respect to Laurentia during the second half of the Mesoproterozoic, as inferred from paleomagnetic data, is well established (Li

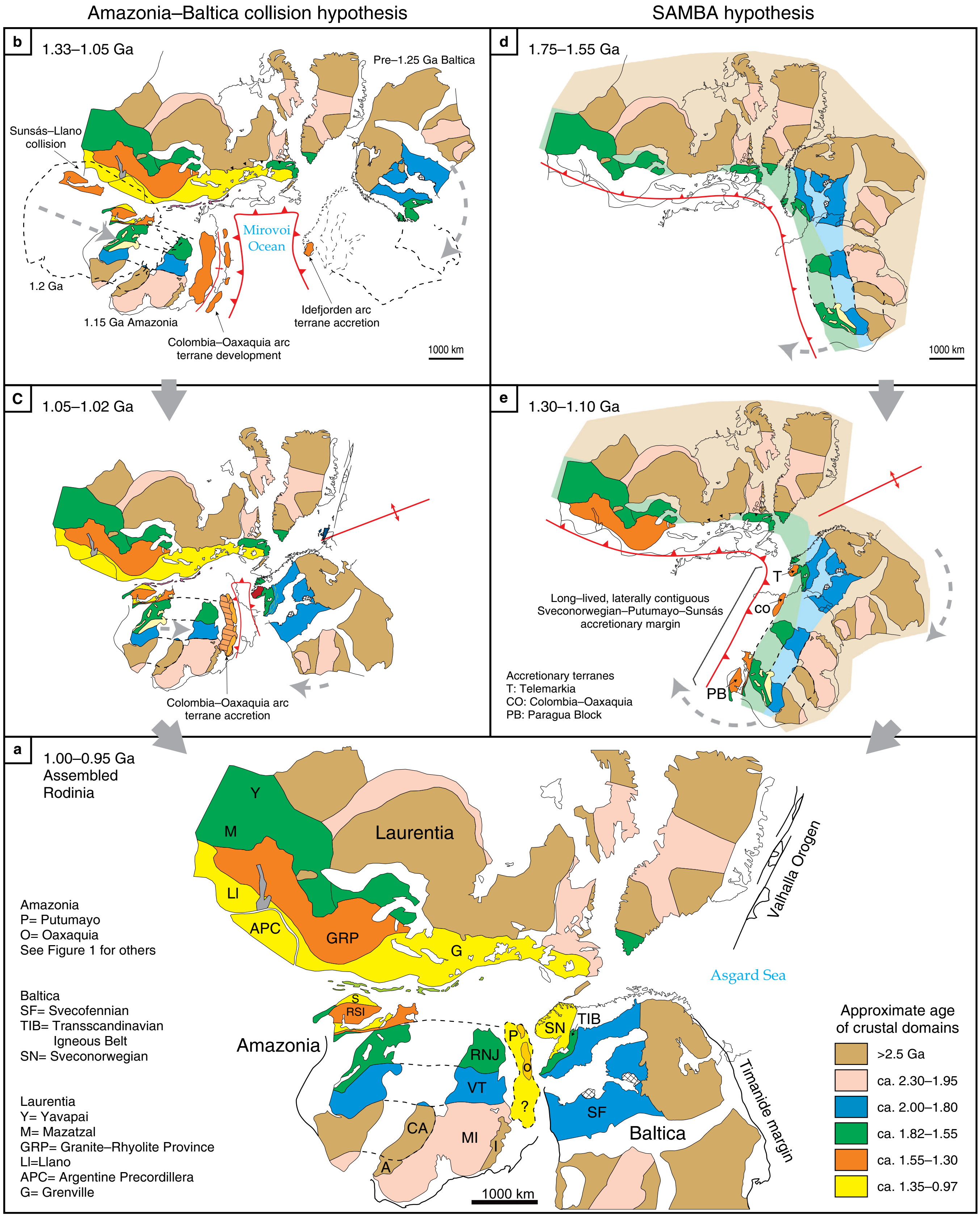

Figure 3. Two possible tectonic reconstructions for Laurentia–Amazonia–Baltica interactions in the Mesoproterozoic leading to the assembly of Rodinia. Panel **(a)** show the most widely accepted configuration of these three cratons within Rodinia. Panels **(b)** and **(c)** illustrate the Amazonia–Baltica collision reconstruction (preferred model discussed in this chapter), while panels **(d)** and **(e)** illustrate two snapshots of the SAMBA reconstruction (no Amazonia–Baltica collision). See text for details and references.

et al., 2008; Pisarevsky et al., 2014). Paleomagnetic and geologic data indicate that, prior to ca. 1265 Ma, the northern margin of Baltica lay adjacent to modern Eastern Greenland (Figure 3b; Cawood and Pisarevsky, 2006; Cawood et al., 2010), and the available poles between ca. 1265 and 1000 Ma indicate that northern Baltica rifted away from Laurentia during the Mesoproterozoic, causing a clockwise oroclinal rotation with NW Fennoscandia as the approximate fulcrum (Figure 3c). The geological expression of this rotation is recorded in the opening of the Asgard Sea and initiation of the Valhalla Orogen in NE Laurentia (Cawood et al., 2010). At approximately 1 Ga, Baltica reached its final position within Rodinia (Figure 3a), with the Sveconorwegian margin laterally adjacent to the Grenville Province and directly facing Amazonia.

These paleomagnetic reconstructions for the incorporation of Amazonia and Baltica within Rodinia were used by Bogdanova et al. (2008) to suggest that the Stenian – Tonian contractional deformation of the Sveconorwegian margin was a result of collisional interactions with Amazonia. This 'oblique collision' model, suggested by the limited paleomagnetic database from Amazonia, results in several other important (and testable) geological predictions such as: (1) An early collision between Laurentia and Amazonia should have occurred prior to final Rodinia assembly (e.g., Tohver et al., 2002); (2) an ocean basin would have been closed between Amazonia and Baltica as they approached their final positions within Rodinia, implying that both (or at least one) of their leading margins experienced a long history of subduction–driven accretionary tectonics; (3) closure of an ocean basin would culminate with continental collision between Amazonia and Baltica, so their margins would exhibit a congruent collisional tectono–metamorphic history; and (4) if correct, this scenario would lead to the development of two separate orogenic belts in Amazonia, reflecting its two–stage collisional incorporation into Rodinia by early interactions with Laurentia (Sunsás–Aguapeí) and later by collision with Baltica (Putumayo–Oaxaquia).

An alternative model for Laurentia, Baltica, and Amazonia interactions leading to Rodinia assembly postulates that Amazonia and Baltica never collided during the Meso– Neoproterozoic, but instead that they behaved coherently as a single tectonic plate (along with West Africa) since at least the Paleoproterozoic and throughout Meso– Neoproterozoic supercontinent assembly; this idea is known as the SAMBA (South America Baltica) connection (Johansson, 2009). In this model, the (modern) northern margin of Amazonia and southern margin of Baltica were purportedly connected from at least 2 Ga onwards (Johansson, 2009), and evolution of the joint Ventuari–Tapajós (Am) – Svecoffenian (Ba) and Río Negro–Juruena (Am) – Gothian/Transscandinavian Igneous Belt (Ba) provinces would have taken place along a common, long–lived accretionary margin (Figure 3d). At approximately 1.3 Ga, rifting would have initiated along the Laurentia–Baltica margin, opening the Asgard Sea –thus satisfying the clockwise rotation of Baltica constrained from robust paleomagnetic data (Cawood et al., 2010)– while keeping Baltica–Amazonia as a coherent plate (Figure 3e). This rotation would have driven compressional accretionary tectonics along the western Amazonian margin, driving the docking of para–autochthonous Amazonian crust such as the Paragua Block (Figure 3e; Johansson, 2009) and culminating with continental collision along the Sunsás–Grenville margin. Although appealing for its simplicity, the SAMBA model has multiple issues, namely: (1) It does not explain the disparate tectonometamorphic history of the Sunsás and Putumayo Orogens of Amazonia (Ibañez–Mejia et al., 2011); (2) it violates paleomagnetic constraints on the location of Amazonia during the Stenian placed by the Nova Floresta and Fortuna Formation poles (D'Agrella–Filho et al., 2016a); and (3) it also violates early Mesoproterozoic poles for Baltica and Amazonia at ca. 1.42 Ga (i.e., Indiavaí; D'Agrella–Filho et al., 2012 and Nova Guarita; Bispo–Santos et al., 2012), which indicate significant distance between Amazonia and Baltica during the Calymmian following the break–up of Nuna/Columbia.

Considering the current paleomagnetic and geochronologic databases, the only scenario under which both the SAMBA and the Amazonia–Baltica collision hypotheses could be simultaneously satisfied is if the northern portion of the Amazonian Craton (i.e., Guiana Shield) and the southern portion (i.e., Central Brazil Shield) did not behave as a single tectonic block through most of the Mesoproterozoic. Because both the Nova Floresta and Fortuna Formation poles were obtained from localities in NW Brazil, strictly speaking these results only constrain the Stenian paleolatitude of the Central Brazil Shield. Therefore, one could argue that no paleomagnetic data yet exist for determining the Stenian paleolatitude of the Guiana Shield. Under this scenario, it is at least permissible to consider that the two shields could have had different paleogeographic histories prior to the assembly of Rodinia, with the Guiana Shield attached to Baltica and co–evolving with it in a SAMBA–like configuration, while the Central Brazilian Shield was colliding obliquely with Laurentia along the Sunsás–Aguapeí and Llano margins. This scenario has some partial support from the dissimilar paleolatitudes of the coeval 1.79 Ga Colider (Central Brazilian shield; Bispo–Santos et al., 2008) and Avanavero (Guiana; Bispo–Santos et al., 2014; Reis et al., 2013) poles, and the seemingly contrasting geologic histories of the Guiana and Central Brazilian Shields in the early– to mid–Mesoproterozoic (e.g., lack of a clear Rondonia–San Ignacio–like province in the Guiana Shield; Ibañez–Mejia et al., 2011, 2015; see also chapter 4 in this volume by Ibañez–Mejia & Cordani, 2020). This alternative, however, would make the Proterozoic tectonic evolution of 'Amazonia' far more complex than currently accepted, e.g., by requiring a hitherto unknown Mesoproterozoic collisional belt between the Guiana and Central Brazil Shields to be present, and is thus beyond the scope of this chapter. Nevertheless, future studies should be aimed at obtaining robust Mesoproterozoic paleomagnetic records for the Guiana Shield to independently constrain its paleolatitude and compare them with the record from the Central Brazil Shield.

Following the discussion above, the SAMBA model as proposed by Johansson (2009) is considered here to be unsupported, and instead it is argued that the Amazonia–Baltica collision (Figure 3b, 3c) remains a more feasible dynamic model to explain the evolution of the Putumayo Orogen (see discussion below) as well as all the existing paleomagnetic data (Cawood & Pisarevsky, 2017; D'Agrella–Filho et al., 2016a). Consequently, the rest of this chapter will be developed using the Amazonia–Baltica collision model (Figure 3a–c) as the global dynamic framework leading to Rodinia assembly.

4. The Putumayo Orogenic Cycle and its Geologic Components

Orogenic belts are comprised by several recognizable tectonic–stratigraphic elements, each one of key importance to decipher the history of mountain building and, in collisional settings, their pre–collisional architecture. The existing geochronologic data from different units of the Putumayo Orogen can be used for reconstructing portions of its Mesoproterozoic tectonic history and place this margin of Amazonia within a global tectonic framework prior to, and during, its collisional incorporation into Rodinia. In the sections below, a reconstruction of the Putumayo Orogen is presented, based on interpretations of the available isotopic and geochronologic data. As will be shown below, given the similar geologic histories of Oaxaquia and fragments of the Putumayo Orogen preserved in NW South America, Oaxaquia will be treated as an integral part of the Putumayo Orogen throughout this chapter. Figure 4 shows a series of schematic cross–sections summarizing the tectonic history of the Putumayo Orogen as currently understood and its interactions with the Sveconorwegian margin of Baltica. The time snapshots in these cross sections will be used as a guide for the discussion below. For more details about different aspects of the interpretations below, the interested reader is referred to the original works of Cardona et al. (2010), Weber et al. (2010), Ibañez–Mejia et al. (2011, 2015, 2018), Solari et al. (2013), Weber & Schultze (2014), and references therein. The tectonic evolution of Baltica in Figure 4 is based on data and reconstructions by Bogdanova et al. (2008), Bingen et al. (2008a), Cawood & Pisarevsky (2017), and Bingen & Viola (2018).

4.1. Pre–Putumayo Architecture (>1.46 Ga)

The westernmost exposed extension of the Guiana Shield in South America is comprised of late Paleo– and early Mesoproterozoic basement, presumably belonging to the Río Negro–Juruena (RNJ) Province of the Amazonian Craton (see Chapter 4 in this volume by Ibañez–Mejia & Cordani, 2020). Mesoproterozoic units dated in the exposed portions of the Guiana Shield in eastern Colombia consist of ca. 1.60 to 1.50 Ga deformed biotite granites, and ca. 1.4 Ga anorogenic granites associated with the Parguaza Intrusive Complex (Ibañez–Mejia & Cordani, 2020). Due to the still limited basement–core repository from the north Andean foreland basins, it remains uncertain whether basement of this age continues all the way to the Andean deformation front underneath the Llanos Basin. Nevertheless, two basement cores from the Putumayo Foreland Basin, namely the Payara–1 and Mandur–2 (Figure 2), have retrieved orthogneisses with protolith ages of 1606 ± 6 Ma and 1592 ± 8 Ma, respectively (Table 1; Ibañez–Mejia et al., 2011, 2015). Consequently, the current geochronologic dataset allows inferring that RNJ–type basement extends under the Putumayo Foreland Basin, implying that: (1) the Putumayo Orogen was initially developed in juxtaposition to, and thus likely reworked, Mesoproterozoic basement of the RNJ (Figure 4a), and (2) a Rondonian–San Ignacio (RSI)–type province, as exposed along the western Central Brazilian Shield (Bettencourt et al., 2010) appears to be absent in the Guiana Shield (see Ibañez–Mejia & Cordani, 2020 for additional discussion). Further evidence for the reworking of Mesoproterozoic basement of possible RNJ affinity within the Putumayo Orogen is provided by orthogneisses exposed in the San Lucas Massif (Figure 2), which yield protolith crystallization ages between 1.53 and 1.50 Ga and metamorphic overgrowths at ca. 1.01–0.99 Ga (Cuadros et al. 2014).

4.2. Proto–Putumayo and Proto–Oaxaquia Phase (ca. 1.46 to 1.33 Ga)

The precise timing of initiation of the Putumayo Orogenic Cycle, which began as an accretionary orogen along a convergent plate margin, remains uncertain. This is due to the limited exposures along the westernmost Guiana Shield (i.e., basement remains buried underneath the thick Putumayo and Llanos Foreland Basins; see Figure 1 and Ibañez–Mejia & Cordani, 2020) and the still limited geochronologic/geochemical database. Within the cordilleran inliers of the northern Andes, at least within those that contain an extensive record of Ectasian to Stenian arc building, the oldest igneous protoliths dated thus far yielded an age of 1461 ± 10 Ma and correspond to mylonitic orthogneisses of the serranía de La Macarena (Ibañez–Mejia et al., 2011). Based on zircon $^{176}Hf/^{177}Hf$ and $\delta^{18}O$ data, Ibañez–Mejia et al. (2015) suggested that the igneous protolith of La Macarena gneisses may correspond to an early pulse of magmatism associated with the nascent arc of the Putumayo Orogen. The relatively low initial $^{176}Hf/^{177}Hf$ composition of La Macarena gneiss protolith, which yields an $\varepsilon Hf_{(t)} = +0.6 \pm 2.2$, indicates significant reworking of crustal components (Figure 5a; Table 2; Ibañez–Mejia et al., 2015). Furthermore, the 'heavy' oxygen isotopic composition of these zircons, with

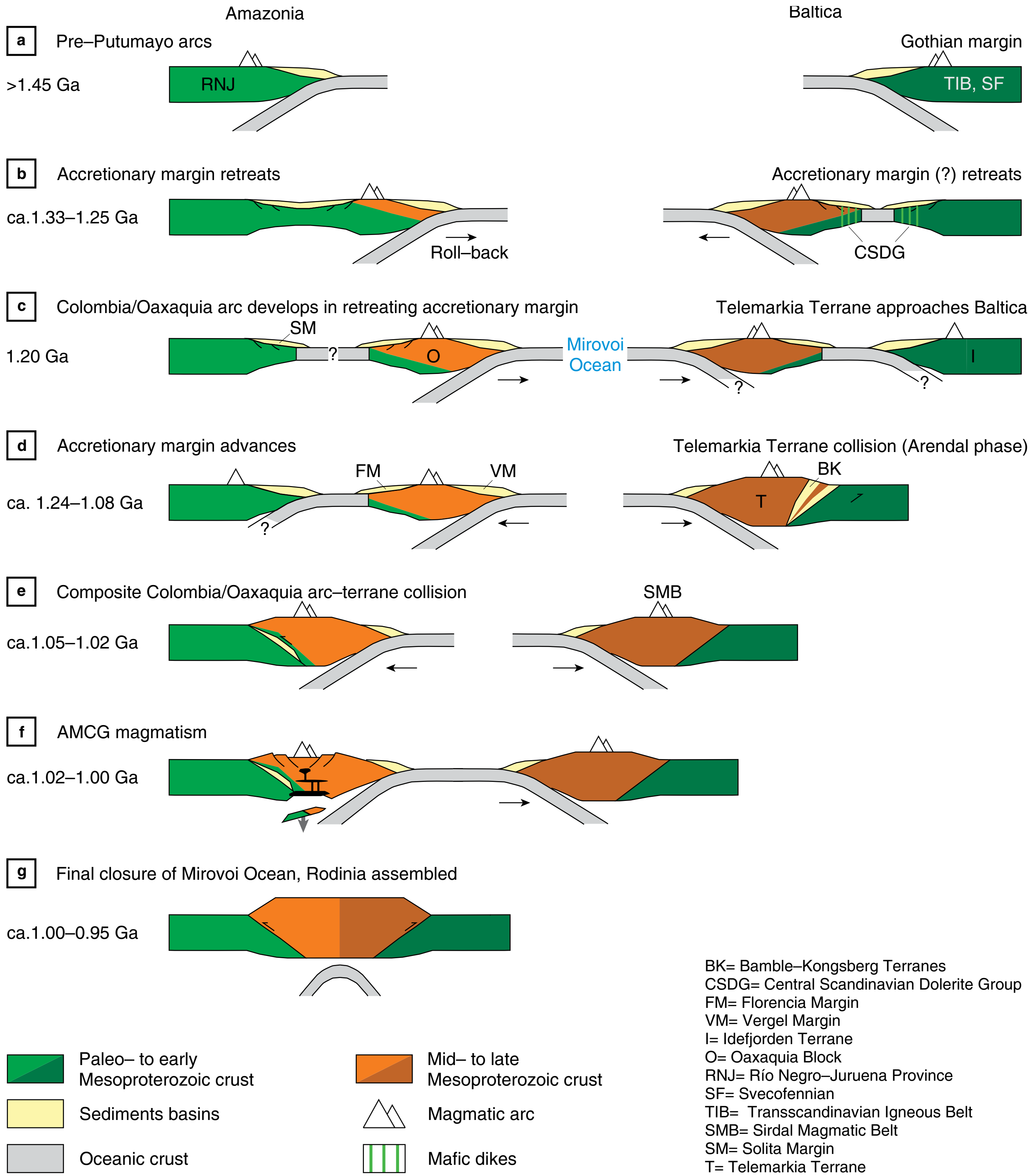

Figure 4. Schematic orogen–scale cross–sections illustrating the tectonic history of the Putumayo Orogen of Amazonia as discussed throughout the text. The tectonic evolution of Baltica is based on Bogdanova et al. (2008), Bingen et al. (2008a), Cawood & Pisarevsky (2017), and Bingen & Viola (2018).

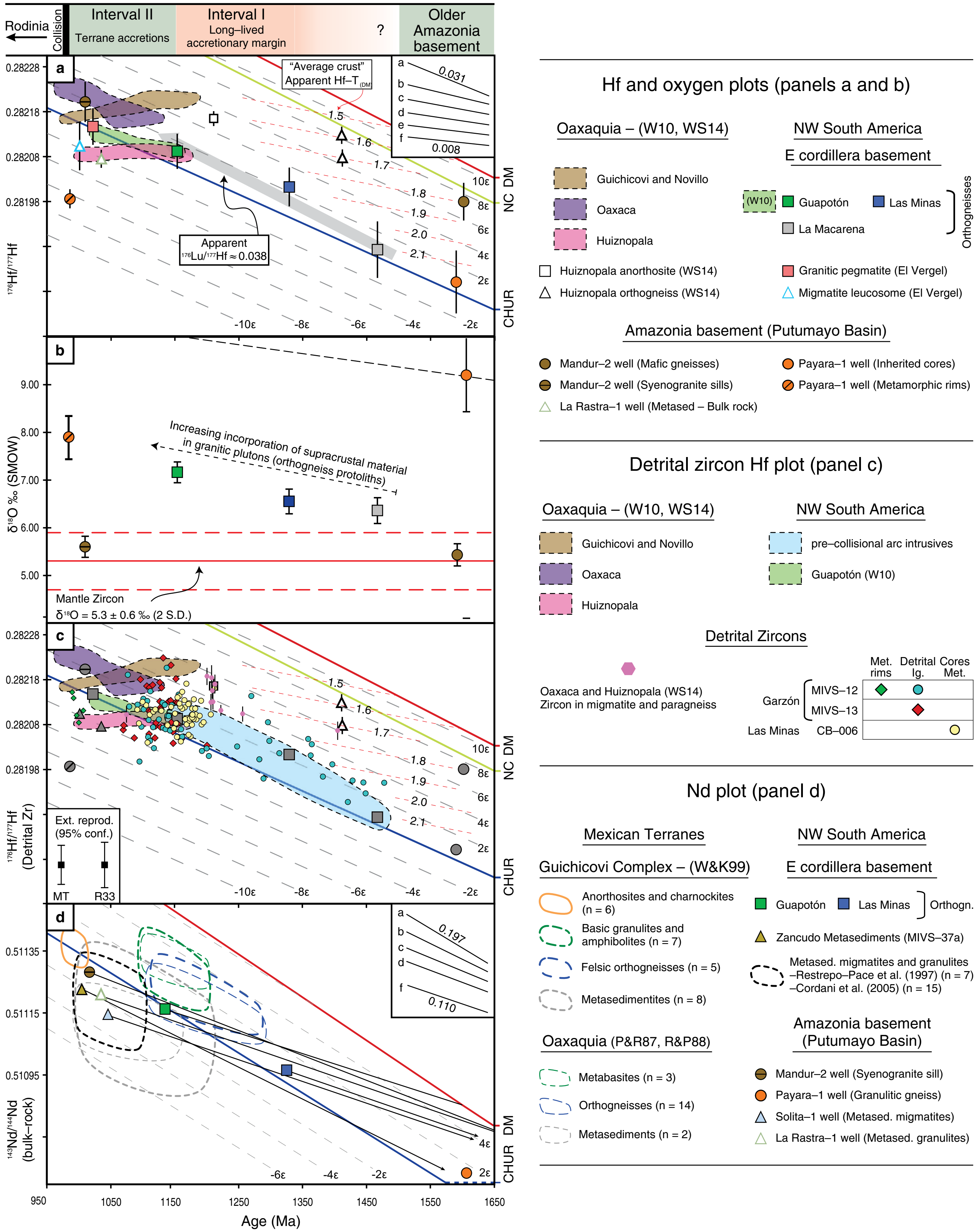
Rodinia
Collision
Interval II
Terrane accretions
Interval I
Long–lived accretionary margin
?
Older Amazonia basement
a
"Average crust" Apparent Hf–T(DM)
0.031
0.008
1.5
1.6
1.7
1.8
1.9
2.0
2.1
10ε
8ε
6ε
4ε
2ε
-10ε
-8ε
-6ε
-4ε
-2ε
NC DM
CHUR
Apparent 176Lu/177Hf ≈ 0.038
176Hf/177Hf
0.28228
0.28218
0.28208
0.28198
b
Increasing incorporation of supracrustal material in granitic plutons (orthogneiss protoliths)
δ18O ‰ (SMOW)
9.00
8.00
7.00
6.00
5.00
Mantle Zircon
δ18O = 5.3 ± 0.6 ‰ (2 S.D.)
c
176Hf/177Hf (Detrital Zr)
Ext. reprod. (95% conf.)
MT
R33
d
0.197
0.110
143Nd/144Nd (bulk-rock)
0.51135
0.51115
0.51095
-6ε
-4ε
-2ε
DM
950
1050
1150
1250
1350
1450
1550
1650
Age (Ma)
Hf and oxygen plots (panels a and b)
Oaxaquia – (W10, WS14)
NW South America
E cordillera basement
Guichicovi and Novillo
Oaxaca
Huiznopala
(W10)
Guapotón
Las Minas
La Macarena
Orthogneisses
Huiznopala anorthosite (WS14)
Huiznopala orthogneiss (WS14)
Granitic pegmatite (El Vergel)
Migmatite leucosome (El Vergel)
Amazonia basement (Putumayo Basin)
Mandur–2 well (Mafic gneisses)
Mandur–2 well (Syenogranite sills)
La Rastra–1 well (Metased – Bulk rock)
Payara–1 well (Inherited cores)
Payara–1 well (Metamorphic rims)
Detrital zircon Hf plot (panel c)
Oaxaquia – (W10, WS14)
NW South America
Guichicovi and Novillo
Oaxaca
Huiznopala
pre–collisional arc intrusives
Guapotón (W10)
Detrital Zircons
Oaxaca and Huiznopala (WS14)
Zircon in migmatite and paragneiss
Met. rims
Detrital Cores
Ig.
Met.
Garzón
MIVS–12
MIVS–13
Las Minas
CB–006
Nd plot (panel d)
Mexican Terranes
Guichicovi Complex – (W&K99)
Anorthosites and charnockites (n = 6)
Basic granulites and amphibolites (n = 7)
Felsic orthogneisses (n = 5)
Metasedimentites (n = 8)
Oaxaquia (P&R87, R&P88)
Metabasites (n = 3)
Orthogneisses (n = 14)
Metasediments (n = 2)
NW South America
E cordillera basement
Guapotón
Las Minas
Orthogn.
Zancudo Metasediments (MIVS–37a)
Metased. migmatites and granulites
–Restrepo–Pace et al. (1997) (n = 7)
–Cordani et al. (2005) (n = 15)
Amazonia basement (Putumayo Basin)
Mandur–2 well (Syenogranite sill)
Payara–1 well (Granulitic gneiss)
Solita–1 well (Metased. migmatites)
La Rastra–1 well (Metased. granulites)

Figure 5. U–Pb age, Lu–Hf, Sm–Nd, and O isotopic data from basement igneous, metaigneous, and metasedimentary rocks of the Putumayo Orogen. **(a)** Age–corrected $^{176}Hf/^{177}Hf$ vs. U–Pb age for granitoids, orthogneisses, and migmatites. εHf values plotted with respect to CHUR (Bouvier et al., 2008). Red dotted lines are apparent iso–T_{DM} contours, showing values for the apparent model ages calculated by assuming a reservoir Lu/Hf composition of 'average crust' (i.e., $^{176}Lu/^{177}Hf$ = 0.015; Condie et al., 2005). Other reservoir slopes shown in inset are: (a) Island arc crust (Hawkesworth et al., 2010); (b) bulk lower–crust (Rudnick & Gao, 2014); (c) global subducting sediments (GLOOS; Plank & Langmuir, 1998); (d) bulk continental crust (Rudnick & Gao, 2014); (e) average Precambrian granites (Vervoort & Patchett, 1996); (f) bulk upper–crust (Rudnick & Gao, 2014). DM is the juvenile–crust depleted mantle model using the data of Vervoort & Blichert–Toft (1999); NC is the 'New Crust' model of Dhuime et al. (2011). Fields for different terranes within Oaxaquia are from Weber et al. (2010), and individual orthogneiss protoliths and anorthosite samples from the Huiznopala Complex are from Weber & Schulze (2014). **(b)** $\delta^{18}O$ zircon compositions vs. age for granitoids and orthogneisses. **(c)** $^{176}Hf/^{177}Hf$ vs. apparent $^{207}Pb/^{206}Pb$ date of detrital zircons from metasedimentary granulites and migmatites of the Garzón and Las Minas Massifs from the Colombian Andes, and from migmatites and metasedimentites of the Oaxaca and Huiznopala Complexes (Weber & Schulze, 2014). External reproducibility (at 95% confidence) of low Yb (Mud Tank) and high Yb (R33) values from zircon crystals are shown as reference for the typical uncertainty bars of individual analyses. **(d)** $^{143}Nd/^{144}Nd$ vs. age for metasedimentary (plotted at their age of metamorphism) and metaigneous units of the north Andean basement massifs and the basement of the Putumayo Basin. Analogous to the Hf plots, the y–axis of this plot is in $^{143}Nd/^{144}Nd$ values and εNd values are also shown as deviations in +2 and –2 increments around the CHUR composition. Slopes for the evolution of different reservoirs as a function of their Sm/Nd compositions (inset) follow the same nomenclature as panel (a). Fields for the different units and lithologies within Oaxaquia are recalculated from: P&R87 – Patchett & Ruiz (1987); R&P88 – Ruiz et al. (1988); W&K99 – Weber & Köhler (1999). The composition of metasedimentary migmatites and granulites of the north Andean Precambrian basement massifs are recalculated after Restrepo–Pace et al. (1997) and Cordani et al. (2005). Figure reproduced with modifications from Ibañez–Mejia et al. (2015), with permission of Elsevier.

Table 2. Compilation of published $^{176}Hf/^{177}Hf$, εHf, and O isotopic data from the Putumayo Orogen.

Sample name	$^{176}Hf/^{177}Hf_{(t)}$ ± 2SD	$\varepsilon Hf_{(t)}$ ± 2SD	U–Pb cryst. age	$\delta^{18}O$ ± 2SD (‰)	Reference
Putumayo Basin basement					
Mandur–2_Leuco	0.282197 ± 45 (n = 12)	+ 2.0 ± 1.6	1017 Ma	5.60 ± 0.22 (n = 11)	Ibañez–Mejia et al. (2015)
Mandur–2 Melano	0.281974 ± 42 (n = 18)	+ 7.6 ± 1.5	1602 Ma	5.43 ± 0.23 (n = 22)	Ibañez–Mejia et al. (2015)
Payara–1	0.281981 ± 21 (n = 4)	– 6.4 ± 0.8	986 Ma	– 6.4 ± 0.8 (n = 6)	Ibañez–Mejia et al. (2015)
Payara–1	0.281796 ± 70 (n = 11)	+ 0.8 ± 2.5	1606 Ma	ca. 9.0 to 9.4	Ibañez–Mejia et al. (2015)
La Macarena, Garzón, and Las Minas Massifs					
MIVS–26	0.282087 ± 39 (n = 10)	+ 1.2 ± 1.4	1135 Ma	7.16 ± 0.22 (n = 8)	Ibañez–Mejia et al. (2015)
MIVS–41	0.282007 ± 43 (n = 12)	+ 2.4 ± 1.5	1325 Ma	6.55 ± 0.26 (n = 8)	Ibañez–Mejia et al. (2015)
Macarena–2	0.281868 ± 63 (n = 13)	+ 0.6 ± 2.2	1461 Ma	6.36 ± 0.27 (n = 10)	Ibañez–Mejia et al. (2015)
MIVS–15A	0.282141 ± 40 (n = 23)	+ 0.1 ± 1.4	1022 Ma	–	Ibañez–Mejia et al. (2015)
MIVS–16A	0.282099 ± 54 (n = 10)	– 1.9 ± 1.9	1001 Ma	–	Ibañez–Mejia et al. (2015)

$\delta^{18}O$= +6.36 ± 0.27 ‰ (Figure 5b; Table 2), also reflects incorporation of supracrustally altered material (Valley et al., 2005), in agreement with the above interpretation.

Within Oaxaquia, orthogneisses with protolith crystallization ages between 1.44 and 1.39 Ga are known from the Huiznopala Gneiss, Guichicovi Complex, and Oaxaca Complex (Schulze, 2011; Solari et al. 2003; Weber & Schulze, 2014). Hafnium isotopic compositions of zircons from these orthogneisses reflect a combination of juvenile ($\varepsilon Hf_{(t)} \approx +8$) and more evolved ($\varepsilon Hf_{(t)} \approx +3$) sources (Figure 5a; Weber & Schulze, 2014), indicating that the early phases of the Oaxaquia arc involved both the generation of juvenile crust –presumably in an intra–oceanic and/or extensional arc setting– but also reworked older crustal material. Weber & Schulze (2014) interpreted this early phase of magmatism with juvenile components to represent an early phase of arc construction, which they termed proto–Oaxaquia. Similarly, it is possible that the ca. 1.46 Ga La Macarena orthogneiss protolith reflects the construction of a proto–Putumayo arc onto a continental margin (Ibañez–Mejia et al., 2015), but for which no juvenile components have yet been clearly identified.

4.3. Main Arc Development Phase (ca. 1.33 to 1.08 Ga)

For at least half of the Ectasian and most of the Stenian Periods, the Putumayo/Oaxaquia margin was characterized by subduction–driven magmatism and deformation, likely within a fringing arc–type accretionary margin (Figure 4b, 4c; Ibañez–Mejia et al., 2011). Several lines of geochemical and geochronologic evidence support this assertion: Within the Proterozoic basement inliers of the Eastern Cordillera of Colombia, orthogneisses with protolith crystallization ages between 1.33 and 1.15 Ga are present in Las Minas and Garzón Massifs (Ibañez–Mejia et al., 2011, 2015), the Colombian Central Cordillera (Leal–Mejía, 2011), the Yarucuy state in Venezuela (Urbani et al., 2015), and the basement of the Falcón Basin offshore northwestern Venezuela (Baquero et al., 2015). Orthogneisses from basement inliers comprising the Oaxaquia Terrane exhibit a similar range of igneous protolith crystallization ages (Cameron et al., 2004; Weber & Schulze, 2014; Weber et al., 2010). A progressive increase in initial $^{176}Hf/^{177}Hf$ compositions of inherited zircons from orthogneiss in the Colombian inliers as a function of younging age, along a trend with an apparent $^{176}Lu/^{177}Hf$ = 0.038 (Figure 5a), cannot be simply explained by radiogenic ingrowth and/or intra–crustal reworking (Ibañez–Mejia et al., 2015), but instead requires that this period was characterized by progressive rejuvenation of the arc–crust by addition of more radiogenic melts from the underlying mantle wedge. The concomitant increase in $^{176}Hf/^{177}Hf_{(t)}$ of orthogneiss protoliths of the Colombian inliers contrasts with their marked increase in (zircon) $\delta^{18}O$ compositions (Figure 5b), which implies that, in concert with the net new crustal additions needed to explain the $^{176}Hf/^{177}Hf$ data, this period also saw a progressive increase in the magnitude of supracrustally–altered material being reworked within the magmatic arc. This apparent dichotomy can result from increasing sediment underplating via subduction and/or enhanced tectonic erosion of a sediment–filled trench (and possibly also forearc crust), in a scenario akin to that of the modern Aleutian subduction zone (Scholl & von Huene, 2009) or the Paleozoic Tasmanide Orogen (Kemp et al., 2009). If the sediments comprising the prism are primarily derived from the arc itself instead of having a significant component of detritus sourced from an older cratonic interior (i.e., older Amazonia basement), then enhanced sedimentary reworking could lead to isotopically heavier $\delta^{18}O$ in magmas without driving the initial $^{176}Hf/^{177}Hf$ compositions towards less radiogenic values.

The sedimentary record and Nd isotopic compositions of units within the Putumayo/Oaxaquia composite arc are also in agreement with, and further support, paleogeographic connections between these now dispersed tectonic blocks as well as the inferences described above regarding the fringing arc nature of this composite margin (Figure 5c, 5d). High–grade metasedimentary units of the Santa Marta, Las Minas, and Garzón Massifs, as well as metasedimentary gneisses from Oaxaquia, contain a detrital zircon cargo with U–Pb ages dominantly in the range from 1.45 to 0.97 Ga (Ibañez–Mejia et al., 2011, 2015; Solari et al. 2013; Weber & Schulze, 2014) which excludes significant input of coarse–grained detritus from cratonic Amazonia (Figure 5c). Nevertheless, the presence of older continental material in Putumayo/Oaxaquia, possibly in the form of reworked crust within the arc, is evident from metaigneous and metasedimentary units with relatively unradiogenic $^{143}Nd/^{144}Nd$ initial compositions and crustal residence values generally greater than 1.45 Ga (Figure 5d).

Figure 6 summarizes the U–Pb detrital zircon age spectra (and metamorphic ages, if calculated by the authors) of Putumayo/Oaxaquia metasedimentary gneisses. In the case of Oaxaquia's detrital zircon U–Pb data of Solari et al. (2013), no cathodoluminescence images or spot–by–spot annotations were reported, so a distinction between inherited (detrital) xenocrysts, metamorphic rims, and/or mixed analyses cannot be made here. Thus, in an attempt to minimize the effects that the high–grade metamorphic overprint would have on the detrital–age probability density function, the Oaxaquia results shown in Figure 6 were filtered to exclude all spots which are younger than, or overlap within 2σ uncertainty, the metamorphic age of ca. 985 ± 10 Ma that is representative of Oaxaquian granulites (Ortega–Gutiérrez et al., 2018). Note, however, that this filtering is unlikely to remove all 'mixed' spot analyses, and that any inadvertent ablation mixtures would systematically bias the $^{207}Pb/^{206}Pb$ dates of individual spots/grains towards younger apparent dates.

Despite the limitations of the existing data, the detrital zircon spectra shown in Figure 6 clearly illustrate that ages older than ca. 1.45 Ga are virtually absent from Oaxaquia and the Colombian cordilleran inliers, thus indicating that cratonic Amazonia (or any other older continental nuclei, for that matter) was not a major source of coarse–grained detritus for the basins where the metasedimentary protoliths were deposited. The strongly quartzofeldspathic nature of the metasedimentary granulites and gneisses of El Vergel Unit in the Garzón Massif, along with the observation that most samples contain oscillatory–zoned xenocrystic zircon cores with dates that just precede the age of their metamorphic overgrowths outside of uncertainty (Figure 6), were used by Ibañez–Mejia et al. (2011) to infer that these units were deposited in close proximity to a volcanic arc, possibly in the forearc basin of a 'Colombia/Oaxaquia' fringing arc system. This interpretive forearc basin sequence is schematically depicted in Figure 4d and is termed the Vergel Margin (VM).

An exception to the above–mentioned provenance characteristics of metasedimentites from the Colombian inliers was recently discovered in the Florencia Migmatites of the eastern Garzón Massif by Restrepo & Giraldo (2018). A paleosome from a migmatitic paragneiss yielded a provenance spectrum characterized by two dominant modes, one at ca. 1.2 Ga and another one at ca. 1.6 Ga, with additional minor components ranging in age up to ca. 1.9 Ga (Figure 6). The younger zircon population was likely derived from the Colombia/Oaxaquia arc system, but the older group clearly denotes sourcing from Amazonia's cratonic interior. These older ages are similar to detrital zircon populations found in metasedimentites from the Putumayo Basin basement, thus indicating that coarse–grained

→

Figure 6. Probability density functions for U–Pb dates obtained from the detrital zircon components of Mesoproterozoic metasedimentary units included within the Putumayo Orogen, indicating their respective ages of metamorphism measured by zircon U–Pb and calculated protolith maximum depositional ages. In addition to the metasedimentary samples, the inherited component of anatectic leucogranites found in the Caimán–3 basement well is also plotted. The upper portion of the plot shows the age ranges of relevant magmatic activity from the Proterozoic of Mexico and Colombia. Colored columns reflect the age ranges of crustal provinces of the Amazonian Craton found in the Guiana Shield (see Ibañez–Mejia & Cordani, 2020), and have the same color–coding as Figure 1. Figure reproduced with modifications from Ibañez–Mejia et al. (2011), with permission of Elsevier.

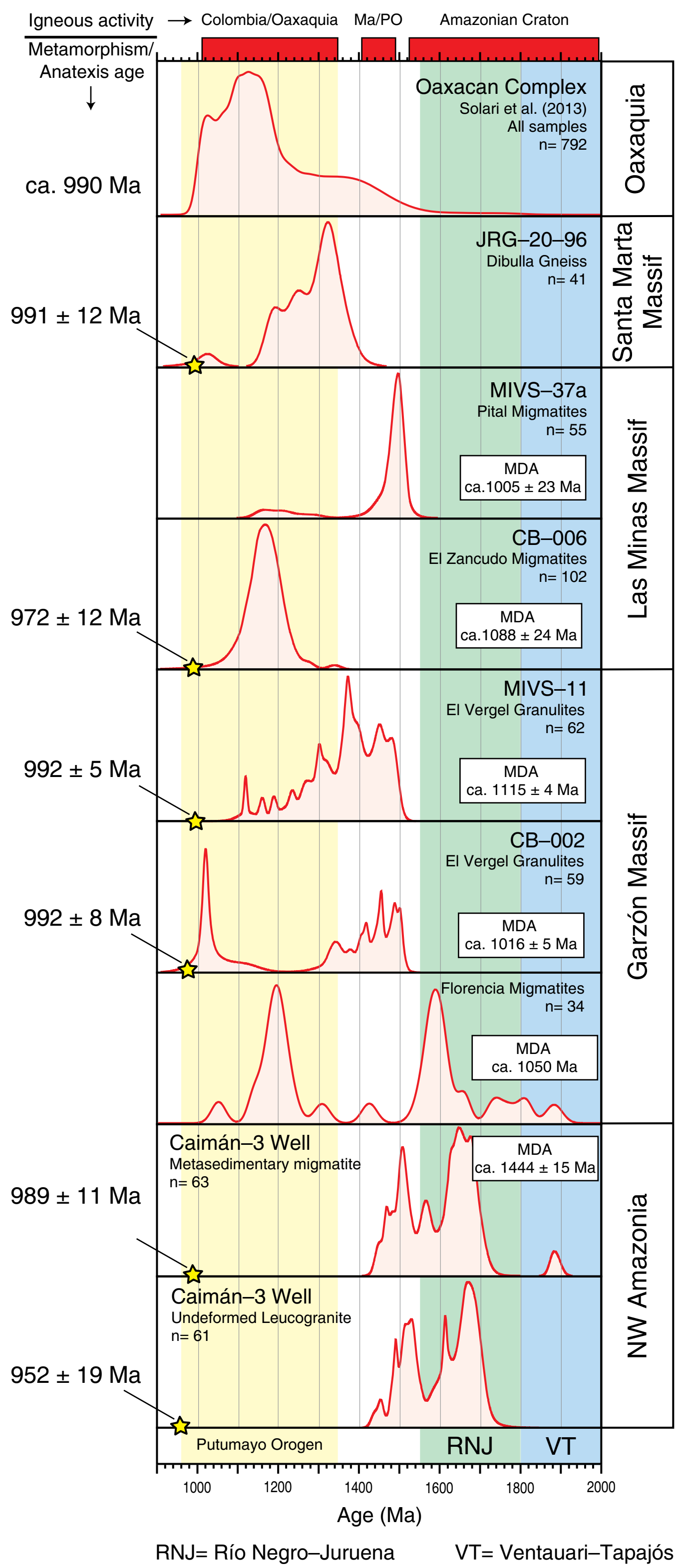

detritus with a cratonic–source component were deposited in the basin where the sedimentary protoliths of the Florencia Migmatites were formed. This suggests that, in contrast to the VM described above, the sedimentary protoliths of the Florencia Migmatites could represent the sedimentary infill of a back–arc basin to the Colombia/Oaxaquia fringing arc system (i.e., the 'Florencia Margin', FM in Figure 4d). The age of metamorphism of the Florencia Migmatites, as determined from U–Pb analyses of zircon overgrowths (sample Gr–15 of Cordani et al., 2005), is 1015 ± 8 Ma, which is distinctly older than the pervasive granulite–forming event around 990 Ma dated in the Vergel Granulites, as will be further discussed below (sections 4.4 and 4.5). There are, therefore, increasing observations suggesting that El Vergel Granulites and Florencia Migmatites might not only have different metamorphic histories, but may also preserve contrasting (and complementary) tectonic information for reconstructing the evolution of the Putumayo Orogen. If this were indeed the case, then the original definition of the Garzón Group, which includes metasedimentites of both El Vergel and Florencia Units (Jiménez–Mejia et al., 2006; Kroonenberg, 1982; Restrepo–Pace et al., 1997), is no longer adequate and needs to be re–visited. It is emphasized, however, that this interpretation currently relies on the results of only two samples from the Florencia Migmatites, dated by Cordani et al. (2005) and Restrepo & Giraldo (2018). Therefore, further geochronologic and isotopic studies will be necessary to confirm or negate the preliminary interpretations provided here.

Contrasting with the U–Pb age spectra of metasedimentites from the Andean inliers and Oaxaquia, detrital zircons from metasedimentites of the Putumayo Basin basement indicate an entirely different provenance. Metasedimentary migmatites and leucogranites recovered from the basement of the Solita–1, La Rastra–1, and Caimán–3 wells, have xenocrystic cores with ages exclusively older than 1.4 Ga and as old as ca. 2.0 Ga (Figure 6), which are unlike those that could be sourced from the Colombia/Oaxaquia arc terranes. Instead, these dates reflect sediment sources from the continental interior of Amazonia and are in good agreement with the age of Meso– and Paleoproterozoic basement domains of the westernmost Guiana Shield (Ibañez–Mejia & Cordani, 2020). Such provenance signatures indicate that the protoliths of these metasedimentites were deposited in a basin associated with cratonic Amazonia but disconnected from the arc system; such basins are schematically shown in Figure 4c as resting upon the rifted continental–margin of a wide back–arc basin, and are referred here as the 'Solita Margin' (SM in Figure 4). However, it should be noted that because these sediments were likely sourced from the cratonic interior and did not receive a significant proportion of detritus from active arc sources, xenocrystic zircon cores of detrital origin from these metasedimentites are unlikely to approach the age of sediment deposition (e.g., Cawood et al., 2012). As such, the youngest zircon populations in the detrital zircon U–Pb record of the Putumayo basement metasedimentites do not accurately constrain protolith deposition and thus the age of sediment accumulation in the SM is only a maximum estimate.

In summary, although the exact timing and magnitude of retreat of the Putumayo/Oaxaquia arc crust depicted in Figure 4b is not exactly known, it can be argued that extension was likely the driver of rapid crustal rejuvenation by mantle–derived magmatic fluxing (e.g., Kemp et al., 2009) and was responsible for maintaining the arc–proximal basins 'disconnected' from cratonic coarse–sediment sources. Two key pieces to this reconstruction that remain unknown are: (1) how wide was the back–arc basin between the Colombia/Oaxaquia arc and cratonic Amazonia? (Figure 4c); and (2) when the arc system was thrown back into compression, was the back–arc basin wide enough to initiate subduction of oceanic crust underneath Amazonia's cratonic margin as the arc system approached the continent prior to collision? (Figure 4d). Although no evidence currently exists to support the occurrence of a subduction margin along Amazonia's cratonic edge *(*i.e., in the modern Putumayo Basin basement) during the latest Mesoproterozoic (e.g., as depicted in Weber et al., 2010 and Cawood & Pisarevsky, 2017, and shown with a question mark in Figure 4d), this possibility certainly remains open but will necessitate further geochronologic research in the autochthonous Putumayo basement to be properly addressed.

4.4. Collision Initiation by Arc–Terrane Accretion (ca. 1.05 to 1.02 Ga)

Near the end of the Stenian Period, as Amazonia and Baltica approached their final positions within an assembled Rodinia configuration (Figure 3), the intervening ocean basin between these cratons, known as the Mirovoi Ocean (Cawood & Pisarevsky, 2017), was consumed, and the Colombia/Oaxaquia arc systems that had previously developed along Amazonia's leading edge switched from an extensional to a compressional regime. These arc terranes were ultimately docked against the continental margin prior to, or some fragments possibly during, final closure of the Mirovoi Ocean (Figure 4e). Accretion of arc terranes would have resulted in the closure of the back–arc basin(s) to the Colombia/Oaxaquia arc discussed in the previous section, thus resulting in tectonic burial and metamorphism of sedimentary sequences of the Solita, Florencia, and possibly also the Vergel Margins (Figure 4e). Indeed, Cordani et al. (2005) and Ibañez–Mejia et al. (2011, 2015) have identified an 'early' metamorphic event from zircon overgrowths found in amphibolite–facies metasedimentary units throughout the Putumayo Orogen, which Ibañez–Mejia et al. (2011, 2015) interpreted as reflecting a phase of basin closure and tectonic burial by arc–terrane accretion prior to final continent–continent collision. This event is constrained to have occurred in the time interval from ca. 1.05 to 1.02 Ga by: (i) U–Pb dating of zircon overgrowths in metasedimentary migmatites of the Solita–1 well (1046 ± 23 Ma; Ibañez–Mejia et al., 2011), (ii) a migmatitic ortho–amphibolite and associated syenogranitic injections in the Mandur–2 well (1019 ± 8 Ma and 1017 ± 4 Ma, respectively; Ibañez–Mejia et al., 2011), (iii) a metasedimentary migmatite of the Florencia Migmatites (1015 ± 8 Ma; Cordani et al., 2005), (iv) metasedimentary migmatites within El Vergel Granulites unit (1022 ± 9 Ma; Ibañez–Mejia et al., 2015), and (v) an orthogneiss from the Novillo Gneiss unit in Oaxaquia (1026 ± 9 Ma; Weber et al., 2010). Currently, little is known about the precise pressure–temperature conditions responsible for this metamorphic episode, so these remain a prime target for future research.

Metamorphic events associated with arc accretion episodes prior to continental collision are widespread in other collisional settings. For instance, in Laurentia, Mesoproterozoic arc terrane docking during the Grenville Orogenic Cycle in its (modern) northern segment has been well–documented and is responsible for what is locally known as the Shawinigan Orogeny (McLelland et al., 2010, and references therein; Rivers & Corrigan, 2000). This event is characterized by accretion of the Elzevirian arcs, Frontenac Terrane, and Adirondack highlands against the (proto–Grenville) Laurentian continental margin (Gower & Krogh, 2002; McLelland et al., 1996), resulting in widespread deformation and metamorphism of the central metasedimentary belt domain, a sedimentary sequence deposited in a back–arc basin behind the fringing arc terranes of the pre–collisional Grenville margin (McLelland et al., 2010). The reconstruction for the Putumayo Orogen shown in Figure 4 envisions a similar tectonic scenario and significance for the FM and SM (Figure 4c, 4d) as that of the Grenville Supergroup in the Adirondack Lowlands (e.g., Chiarenzelli et al., 2015) and other units included within the Central Metasedimentary Belt of Laurentia. Similarly, metasedimentary units were also metamorphosed along the Sveconorwegian margin of Baltica during the pre–collisional accretion of the Telemarkia Terrane at ca. 1.14–1.12 Ga (i.e., metasedimentites included within the Bamble and Kongsberg Terranes, metamorphosed during the Arendal phase; Figure

4d; Bingen et al., 2008a, 2018b), indicating this is a common phenomenon in collisional margins.

4.5. Anorthosite–Mangerite–Charnockite–Granite (AMCG) Magmatism (ca. 1.02 to 1.00 Ga)

Following arc–terrane accretion but prior to final continent–continent collision, widespread anorthosites and associated charnockitic magmas were emplaced throughout Oaxaquia between 1.02 and 1.00 Ga (Cameron et al., 2004; Cisneros de León et al., 2017; Keppie et al., 2003; Weber & Schulze, 2014; Weber et al., 2010). However, although a significant portion of the exposed Oaxaquian basement consists of these AMCG–type units, similar intrusives do not appear, at least to date, to be as abundant in the Colombian Proterozoic basement inliers. Although anorthosites are known to occur in association with Los Mangos Granulites in the Sierra Nevada de Santa Marta (Tschanz et al., 1969, 1974; Cardona et al., 2010), their age of igneous emplacement remains unconstrained, and no other AMCG–type bodies have yet been mapped in the Garzón, Santander, San Lucas, La Guajira, or Las Minas Massifs. There are two potential explanations for this apparent discrepancy: (1) detailed geologic mapping of most Colombian basement inliers remains arguably very limited, and thus these units may in fact be present but not yet clearly identified; or (2) following arc–terrane accretion, intrusions of AMCG–type magmas may have been focused on the portion of the Putumayo Orogen that is now represented by the Oaxaquia Terrane, and may mostly be absent –or present only in small volumes– in the limited basement exposures represented by the Colombian basement inliers. At any rate, future investigations of the Proterozoic basement of the Colombian Andes, including mapping and additional petrologic/geochronologic work, should place attention on documenting the occurrence (and field relations, if present) of AMCG–type intrusives.

Traditionally, massif–type anorthosites and AMCG complexes have been regarded as ‘anorogenic’ in nature (e.g., Anderson, 1983; Ashwal, 1993; Emslie, 1991; amongst many others), which has posed complexities for interpreting the AMCG magmatism within Oaxaquia (see discussion in Weber et al., 2010). Nevertheless, recent advances in our understanding of AMCG associations and their relationship with regional tectonic regimes using modern geochronologic methods, are shifting this long–standing view in favor a convergent (i.e., Andean–type) margin for their origin (e.g., Ashwal & Bybee, 2017; Bybee et al., 2019). Indeed, voluminous AMCG magmatism at 1.08–1.03 in the Grenville Orogen post–dates arc accretion (Shawinigan event) and predates collisional orogenesis (Ottawan event), and evidently took place within a convergent margin (e.g., Bickford et al., 2010; Hamilton et al., 2004; McLelland et al., 2004, 2010). Because it is widely agreed that AMCG magmatism requires some sort of extensional tectonic regime, particularly for allowing the ascent of plagioclase–rich (anorthositic) mushes from the lower crust to their final emplacement levels (see Ashwal & Bybee, 2017, and references therein), it has been suggested that the origin of the Grenville anorthosites is related to transient events of regional extension, driven by the convective removal of the lower lithosphere following compressional crustal thickening (e.g., Corrigan & Hanmer, 1997; McLelland et al., 2004). Thus, considering that, much as in the Grenville, AMCG magmatism in the Putumayo Orogen post–dates arc accretion (section 4.4) but pre–dates the main collisional event (section 4.6), the AMCG magmatism expressed in Oaxaquia also most likely took place in a convergent tectonic environment. It is suggested here that, following the orogenic event at ca. 1.05–1.02 Ga and associated crustal thickening due to arc accretion, gravitational, and/or convective removal of the lower lithosphere could have triggered regional extension within the Putumayo/Oaxaquia arc crust at ca. 1.02 to 1.00 Ga (Figure 4f), driving asthenospheric upwelling, regional basaltic underplating, and providing the necessary conditions for massif–type anorthosites and other charnockitic magmas to be developed and emplaced.

4.6. Main Collisional Event (ca. 1.00 to 0.95 Ga)

Final closure of the Mesoproterozoic ocean basins that once separated Laurentia, Baltica, and Amazonia (Li et al., 2008; Pisarevsky et al., 2014) brought about a series of continent–continent collisions at the heart of an assembling Rodinia (Figures 3, 4g). Collisions amongst the various segments of the 1000s–of–km–long margins comprising this Laurentia–Baltica–Amazonia orogenic ‘triple–junction’ were diachronous in nature, and the relative timing of metamorphic events amongst them is an important tectonic discriminator for establishing inter–cratonic correlations amongst the orogenic belts that developed.

On the Amazonian side of this collision, a widespread granulite–forming event at ca. 990–970 Ma has been dated by multiple groups in various units within Oaxaquia and northwestern South America. In Colombia and Venezuela, granulite–facies rocks around this age, dated by U–Pb methods, are known from the Garzón Massif (Cordani et al., 2005; Ibañez–Mejia et al., 2011, 2015; Weber et al., 2010), Las Minas Massif (Ibañez–Mejia et al., 2011, 2015), the Colombian Central Cordillera (Leal–Mejía, 2011), the Serranía de San Lucas Massif (Cuadros et al., 2014), the basement of the Putumayo Foreland Basin (Ibañez–Mejia et al., 2011, 2015), La Guajira Peninsula (Baquero et al., 2015), the Venezuelan Cordillera de la Costa (Urbani et al., 2015), and the offshore basement of the Falcón Basin (Baquero et al., 2015). In Mexico, this event is locally known as the Zapotecan Orogeny (Solari et al., 2003) and has been recognized in units from the Oaxacan Complex (Shchepetilnikova et al., 2015; Solari et al., 2003, 2013; Weber & Schulze, 2014; Weber et al., 2010), the Guichicovi Complex (Weber & Kohler, 1999; Weber & Schulze, 2014; Weber et al., 2010), the Huiznopala Gneiss (Lawlor et al., 1999; Weber & Schulze, 2014), and the Novillo Gneiss (Cameron et al., 2004; Weber & Schulze, 2014). This regionally coherent tectonothermal event has been interpreted as reflecting the climax of collisional metamorphism in the Putumayo/Oaxaquia margin during Amazonia's incorporation to Rodinia (Cardona et al., 2010; Cawood & Pisarevski, 2017; Cordani et al., 2005; Ibañez–Mejia et al., 2011, 2015; Li et al., 2008; Solari et al., 2003; Weber et al., 2010; among others).

Potential conjugate margins to the Putumayo/Oaxaquia margin based on recent tectonic reconstructions (Figure 3) are either the Grenville Orogen of Laurentia (e.g., Gower et al., 2008; McLelland et al., 1996, 2010) or the Sveconorwegian Orogen of Baltica (e.g., Bingen et al., 2008a; Bogdanova et al., 2008). In order to resolve this paleogeographic conundrum, possibly the best approach is to take the timing of regional tectonometamorphic events associated with collision in the Grenville and Sveconorwegian Orogens, and compare them with events identified in Putumayo/Oaxaquia in order to determine which margin is most likely to be its collisional conjugate.

In Laurentia, the major regional metamorphic event associated with continental collision took place during the 1.09–1.02 Ga interval and is locally known as the Ottawan Orogeny. This event, based on U–Pb dating of zircon (e.g., McLelland et al., 2001, 2004), U–Pb in monazite (e.g., Heumann et al., 2006), and U–Pb in titanite (e.g., Bonamici et al., 2015; Mezger et al., 1991) is thought to have attained its peak at ca. 1050 Ma before starting to cool slowly, presumably during exhumation and orogenic collapse. U–Pb zircon dates of an undeformed pegmatite dike in the Adirondack highlands (1034 ± 8 Ma; McLelland et al., 2001), and syn–kinematic granite injections associated with normal–fault displacement along the Carthage–Colton shear zone (1047 ± 5; Selleck et al., 2005) place a lower age limit of ca. 1047 Ma for Ottawan contractional deformation in this portion of the Grenville Orogen. The Ottawan event was followed by a phase known as the Rigolet phase, which lasted from 1011 to 980 Ma and is commonly associated with ubiquitous extensional deformation and channel–flow in the front of the Grenville orogenic plateau, marking widespread orogenic collapse (Rivers, 2008).

In Baltica, following the arc–accretion–related orogenesis of the Arendal phase, the main continent–continent collisional episode is thought to have taken place in the interval from 1.05 to 0.98 Ga and is locally known as the Agder phase (Bingen et al., 2008a; Bogdanova et al., 2008). This event induced metamorphism and magmatism in the Idefjorden and Telemarkia Terranes, with high–pressure (1.0–1.5 GPa) amphibolite– to granulite–facies conditions affecting the Idefjorden and moderate pressure (0.6–0.8 GPa) amphibolite– to granulite–facies conditions and penetrative deformation affecting Telemarkia (Bingen et al., 2008b). Following the regionally extensive Arendal tectonometamorphic event, Sveconorwegian deformation migrated towards the foreland, to affect primarily the so–called 'Eastern Segment' during an event known as the Falkenberg phase. This event is associated with local eclogite and regional high–P granulite–facies metamorphism with peak pressures of ca. 1.5 GPa and 'clockwise' P–T paths, presumably reflecting deep burial of Fennoscandian crust due to overthrusting of the Sveconorwegian hinterland (Johansson et al., 2001; Möller, 1998). Following this final phase of convergence, the Sveconorwegian Orogen entered a phase of extensional deformation during tectonic relaxation and gravitational collapse; this phase is locally known as the Dalane phase, and is marked by post–collisional magmatism in the time interval from 0.97 to 0.90 Ga (Bingen et al., 2008a; Bogdanova et al., 2008). During this period, rapid exhumation of high–pressure metamorphic rocks took place at ca. 960 Ma in the footwall of the mylonite zone (Möller, 1999), shallow plutons were emplaced in a brittle regime between 0.97 and 0.93 Ga (e.g., Hellstrom et al., 2004), and, finally, between 0.93–0.92 Ga, voluminous plutonic rocks including AMCG complexes, such as the Rogaland Complex (e.g., Westphal et al., 2003), were emplaced, marking the end of the Sveconorwegian Orogeny.

Using a compilation of the available geochronologic data from the Grenville, Sveconorwegian, Sunsás–Aguapeí, Oaxaquia, and Putumayo, and particularly from observations regarding the timing of peak metamorphism described above, Ibañez–Mejia et al. (2011) concluded that the Sveconorwegian is a more likely conjugate margin to explain the timing of collisional deformation of the Putumayo Orogen and Oaxaquia than the Grenville. In this framework, the Sunsás–Aguapeí Orogen was developed by early oblique collision between Amazonia and the Llano segment of the Grenville Province (Tohver et al., 2002, 2005) and thus reflects the onset of collisional incorporation of Amazonia into an assembling Rodinia, but not final supercontinent amalgamation. The hypothesis of a frontal Amazonia–Baltica collision to explain the Arendal and Falkenberg phases of the Sveconorwegian Orogen had previously been suggested by Bogdanova et al. (2008), based on other paleogeographic and paleomagnetic arguments (see section 3), but the new geochronologic data that has since emerged from the Putumayo Orogen has not only re–affirmed such correlations but also significantly improved our understanding of the tectonic processes and dynamics that led to Rodinia assembly in this complex orogenic 'triple–junction'.

4.7. Collapse of the Orogenic Plateau and Supercontinent Breakup (<0.97 Ga)

It is thought that through the major collisional events that occurred along the Grenville, Putumayo, and Sveconorwegian margins, the core of Rodinia was fully assembled (Cawood &

Pisarevski, 2017; Li et al., 2008), and a large, high–standing orogenic plateau akin to the Tibetan Plateau in the India–Asia collision zone (Dewey et al., 1988; Royden et al., 2008) developed in the Rodinian orogenic hinterland (e.g., Rivers, 2008, 2012). This feature has been suggested to set the Grenville–Sveconorwegian–Putumayo Orogen apart from all older orogens associated with pre–Rodinian supercontinents (i.e., Nuna/Columbia and Superia/Sclavia; Hawkesworth et al., 2013), in that this represents the first known occurrence of a long–lived, possibly high–standing orogenic plateau in the geological record. If true, this apparently simple feature marks a dramatic shift in the geologic evolution of our planet, given the strong impact that plateau development has in modulating continental weathering and tectonic forcing of global climate (Edmond, 1992; Garzione, 2008; Raymo & Ruddiman, 1992).

Following the lithospheric thickening that occurs along collisional orogens by rapid structural shortening, advective thinning of the thermal boundary layer in the lower lithosphere, coupled with isotherm relaxation, inevitably leads to extensional orogenic collapse (Dewey, 1988). In NW South America, units belonging to the Putumayo Orogenic Cycle yield biotite, hornblende, feldspar, and phlogopite Ar–Ar (plateau) cooling dates ranging mainly from ca. 970 to 870 Ma (Baquero et al., 2015; Cordani et al., 2005; Fournier et al., 2017; Restrepo–Pace et al., 1997), indicating that significant exhumation and cooling of the lower crustal orogenic roots took place within this time interval. Older cooling dates in the range from 1007 and 1045 Ma (Ar–Ar plateau ages from biotite and hornblende) occur exclusively in the Florencia Migmatites unit of the eastern Garzón Massif (Margaritas Gneiss of Cordani et al., 2005), which is consistent with an early onset of their exhumation associated with the 1.05 to 1.02 Ga metamorphism by arc–continent collision (see section 4.4) rather than orogen–wide extensional collapse.

To this date, little is known about the ultimate demise of the Putumayo Orogen and events associated with the onset of Iapetus Ocean opening in NW South America. In the Grenville and Sveconorwegian margins, opening of the Iapetus Ocean is constrained by ca. 570 Ma rift–related structures and magmatism in the Newfoundland margin (Cawood et al., 2001), and emplacement of the Egersund dike swarm in southern Norway at ca. 616 Ma (Bingen et al., 1998). The best constraints from the Amazonia side of this rift come from: (1) Plume-related dikes intruded into the Novillo Gneiss in northern Oaxaquia, dated to 619 ± 9 Ma using U–Pb in micro–baddeleyite (Weber et al., 2019); and (2) El Triunfo Complex in the Chiapas Massif of southern Mexico (González–Guzmán et al., 2016; Weber et al., 2018), where amphibolite layers with E–MORB geochemical characteristics are found within the Ediacaran Jocote metasedimentary unit and in Oaxaca–type orthogneiss and anorthosite (Weber et al., 2018); and (3) metamorphic zircon overgrowths ca. 600 Ma in Oaxaquian anorthosites from the Chiapas Massif, which Cisneros de León et al. (2017) suggested were formed due to anorthosite reheating during intra–plate rifting and mafic magma intrusions. These observations unambiguously indicate a Neoproterozoic age for rift–related magmatism on the Oaxaquian (Amazonian) margin of the Iapetus rift zone. Further efforts focused on finding the evidence of orogenic collapse and supercontinent break–up in the exposed basement inliers of the northern Andes and autochthonous Putumayo basement is an important target for future research.

5. The P–T–t History of Continent–Continent Collisions

Reconstructing the pressure–temperature–time (P–T–t) paths of metamorphic rocks is key for understanding the rates and mechanisms of orogenic development and reconstructing the tectonic history of metamorphic belts throughout the geologic record (Brown & Johnson, 2018; England & Thompson, 1984; Thompson & England, 1984). Quantitative P–T estimates (e.g., using mineral thermodynamics) of Putumayo–related metamorphic assemblages in NW South America remain limited, restricted to the works of Jiménez–Mejia et al. (2006), Altenberger et al. (2012), and Ibañez–Mejia et al. (2018). Jiménez–Mejia et al. (2006) applied multi–equilibrium thermodynamic calculations to samples from El Vergel Granulites and Florencia Migmatites of the Garzón Massif, using the TWQ software and thermodynamic database of Berman (1991). These authors determined peak conditions around 750 ºC and 0.6 GPa for a charnockitic gneiss of El Vergel unit, and conditions between 680–830 ºC and 0.6–0.9 GPa for the Florencia unit. These results are broadly indicative of metamorphism having taken place at ca. 22–30 km depths and under upper–amphibolite to granulite–facies conditions. On the other hand, based on exsolution textures in feldspars and pyroxenes and Ti–in–quartz thermometry, Altenberger et al. (2012) suggested that El Vergel unit was metamorphosed at (or near) ultra–high temperature (UHT) conditions ca. 900–1000 ºC. These authors hypothesized that the UHT metamorphic event in El Vergel unit must have resulted from high heat–flow provided by an episode of arc magmatism and back–arc extension that shortly pre–dated continental collision, in agreement with the tectonic history of the Putumayo Orogen as described in the previous sections (e.g., potentially in association with AMCG–related magmatism). One sample from the Florencia Migmatites studied by Altenberger et al. (2012) yielded lower peak temperatures ca. 760 ºC, in agreement with the results of Jiménez–Mejia et al. (2006) for the same unit.

Of all the samples analyzed for geothermobarometry by Jiménez–Mejia et al. (2006) and Altenberger et al. (2012), only sample Gr–15 of Jiménez–Mejia et al. (2006) from the Florencia Migmatites has been dated using U–Pb geochronology of metamorphic zircon overgrowths, yielding a mean $^{207}Pb^{*}/^{206}Pb^{*}$ date of 1015 ± 8 Ma (Cordani et al., 2005), and a two–point garnet–whole rock Sm–Nd isochron (1034 ± 6 Ma; Cordani et al., 2005). Thus, the general disconnect that exists between the currently available thermobarometric and geochronologic datasets precludes using most of the existing P–T data to robustly constrain the time–temperature history of events within the Putumayo Orogenic Cycle. Nevertheless, from a qualitative standpoint, based on regional mapping and petrographic observations made by Kroonenberg (1982), Restrepo–Pace et al. (1997), Jiménez–Mejia et al. (2006), Altenberger et al. (2012), and Ibañez–Mejia et al. (2011, 2015), two generalizations can be made: (1) it seems likely that (volcano)–sedimentary units that in the field appear as stromatic metatexites were metamorphosed during the early orogenic episode at ca. 1.05–1.02 Ga and dominantly recrystallized under upper–amphibolite to granulite facies conditions, and (2) the massive felsic and mafic granulites were dominantly recrystallized during the main collisional event at ca. 1.0 to 0.95 Ga. In the Garzón Massif, amphibolite–facies stromatic metatexites are found both within the Florencia Migmatites and El Vergel Granulites units (e.g., Altenberger et al., 2012; Ibañez–Mejia et al., 2015) whereas massive granulites seem to be restricted to El Vergel Granulites unit only (as mapped by Rodríguez et al., 2003).

More recently, Ibañez–Mejia et al. (2018) performed a detailed high–temperature thermochronologic study of a metasedimentary granulite with migmatitic textures from La Rastra–1 well of the Putumayo Basin basement. The chemical composition of co–existing garnet, orthopyroxene, and plagioclase in the melanosome indicated peak P–T conditions of approximately 680 ºC and 0.62 GPa, by simultaneously solving the net–transfer GAPES geobarometer of Eckert et al. (1991) and the garnet–orthopyroxene Fe–Mg exchange geothermometer of Ganguly et al. (1996). Garnets in contact with biotite exhibit conspicuous retrograde Fe–Mg zoning profiles, which were used to determine an initial cooling rate of ca. 5 K/my from peak conditions using diffusion–based geospeedometry (Lasaga, 1983) and a numerically optimized solution to the 1–D diffusion equation (after Ganguly et al., 2000). Garnets with a narrow grain–size distribution of 100 ± 20 μm in diameter where hand–picked and analyzed for their Sm–Nd and Lu–Hf isotopic compositions (Figure 7a, 7b), resulting in a five–point Sm–Nd isochron of 1007.0 ± 2.9 Ma (2σ, MSWD = 1.3) and a six–point Lu–Hf isochron of 1070.8 ± 5.6 Ma (2σ, MSWD = 0.84). This discrepancy in apparent ages was explained by Ibañez–Mejia et al. (2018) in terms of the different diffusivities of Sm–Nd and Lu–Hf in garnets (determined experimentally by Bloch et al., 2015, 2020; Ganguly et al., 1998; Tirone et al., 2005; van Orman et al., 2002), and was solved numerically to invert a time–temperature history that satisfied the thermobarometry, initial cooling rate, grain–size–age relation of Sm–Nd and Lu–Hf isochrons, and a garnet Sm–Nd bulk closure temperature of 560 ºC independently calculated using the analytical formulations of Ganguly & Tirone (1999). The results of this numerical inversion are shown graphically in Figure 7c, which represents what is currently the best (and only) estimate for the time–temperature history of the metamorphic basement of the Putumayo Basin. Comparison of this T–t history with trajectories reconstructed for metasedimentites of the Great Himalayan Sequence in the India–Asia collision zone are in good agreement (Figure 7d), thus indicating that the tectonic processes resulting in metamorphism of La Rastra–1 well basement were likely similar to those operating in modern collisional orogenic settings (see Ibañez–Mejia et al., 2018 for further discussion).

Other garnet Sm–Nd dates for samples from the Colombian cordilleran inliers have been published by Cordani et al. (2005) and Ordóñez–Carmona et al. (2006). These studies obtained two–point (garnet–whole–rock) isochron dates for two samples of the Florencia Migmatites in the Garzón Massif (1034 ± 6 Ma and 990 ± 8 Ma; Cordani et al., 2005), two samples of El Vergel Granulites in the W Garzón Massif (935 ± 5 Ma and 925 ± 7 Ma; Cordani et al., 2005), and one sample of Los Mangos Granulites in the Sierra Nevada de Santa Marta (971 ± 8 Ma; Ordóñez–Carmona et al., 2002, 2006). Nevertheless, these ages –and their assigned uncertainties– must be interpreted cautiously, as two–point isochrons are not always reliable and the uncertainties associated to linear regressions through only two points are rarely an accurate approximation of the true geological uncertainty of an isochron age. Qualitatively, however, these results appear to agree with an early metamorphic event for metasedimentites from the Florencia Migmatites unit (Sm–Nd dates between 1.05 and 0.99 Ga), and a younger cooling of higher–grade units such as El Vergel and Los Mangos granulites (e.g., during exhumation after the 0.99 Ga peak metamorphism). Nevertheless, neither of these two studies obtain peak T conditions of the dated samples, cooling rates, or described the dimensions of the garnets that were analyzed. Without such data, it is not possible to calculate the effective closure temperature of the Sm–Nd system in the analyzed garnets, and thus these dates cannot be utilized to quantitatively constrain the T–t path of the studied units.

In summary, considering the reconstruction of the Putumayo Orogen as presented in section 4 of this chapter and the numerically modeled peak metamorphic date for La Rastra–1 basement (i.e., 1035 +8/–6 Ma; Figure 7c), it is possible that the basement drilled by the La Rastra–1 well represents a slice of metasedimentites underthrusted to mid–crustal depths and exhumed during arc–terrane accretion (Figure 4e), but that subsequently sat at a structural level that did not experience significant burial during continent–continent collision (unlike the basement of the Payara–1 well). Nevertheless, discerning the significance of La Rastra–1 thermal path within the tectonic history of the Putumayo remains mostly hypothetical until additional studies combining thermobarometry and high–temperature thermochronology are performed throughout the orogen. Particularly, units yielding ca. 990 Ma zircon U–Pb ages,

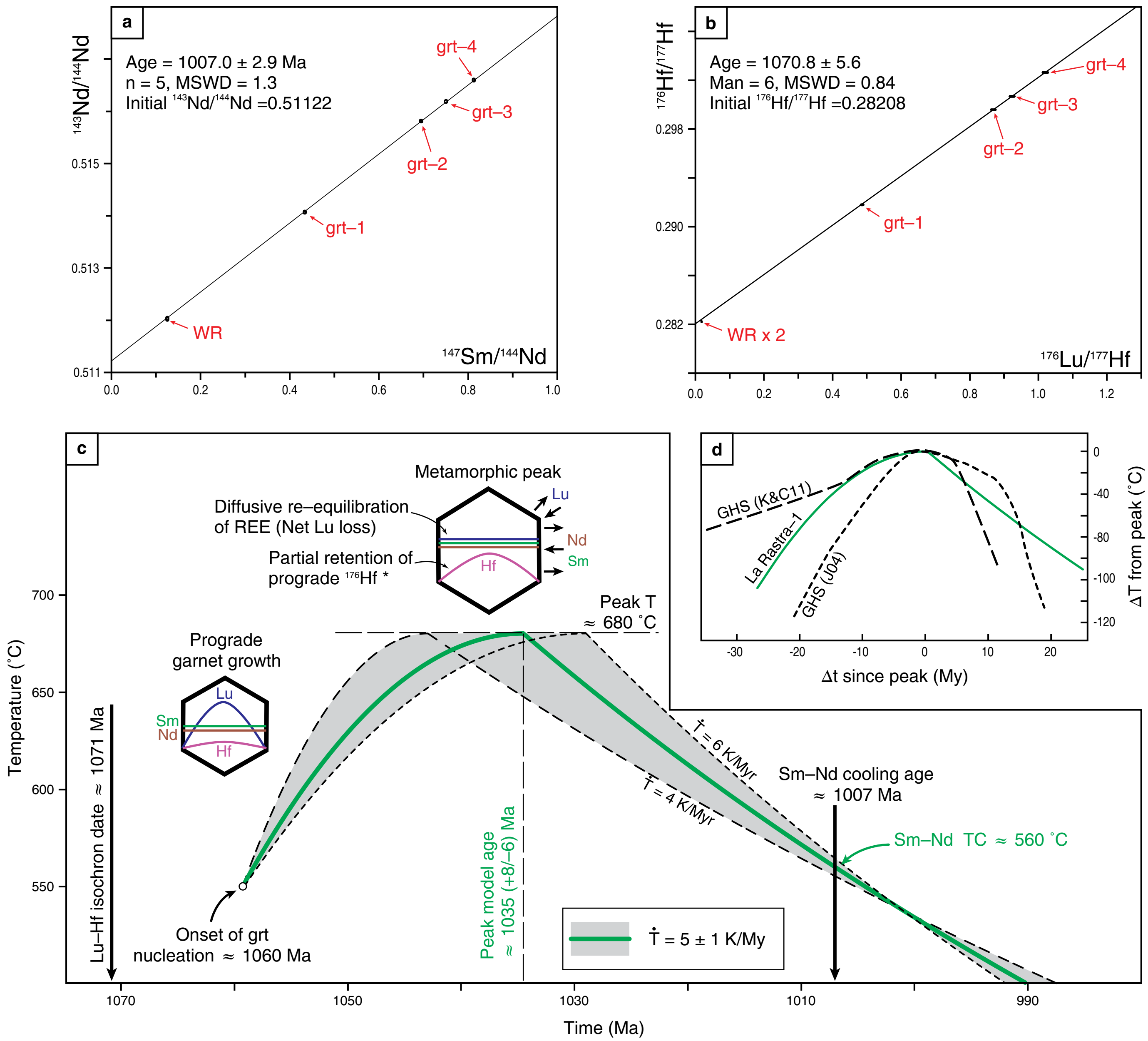

Figure 7. (a) Sm–Nd, **(b)** Lu–Hf internal isochron diagrams and calculated dates for analyzed garnet and whole–rock fractions of La Rastra–1 basement. **(c)** Time–temperature (T–t) evolution model reconstructed for the basement of La Rastra–1 well in the Putumayo Basin by Ibañez–Mejia et al. (2018). Hexagons present a conceptual representation of the Lu–Hf diffusive decoupling issue in prograde garnet crystals; see text and Ibañez–Mejia et al. (2018) for further details. **(d)** Comparison of the (idealized) T–t path reconstructed for La Rastra–1 with paths reconstructed for the Greater Himalayan Sequence (GHS) of the Indo–Asian collision zone by means of titanite U–Pb thermochronology and Zr thermometry (K&C11 curve, after Kohn & Corrie, 2011), and thermo–mechanical numerical modeling (J04 curve, after Jamieson et al., 2004). See Ibañez–Mejia et al. (2018) for further details. Figures reproduced from Ibañez–Mejia et al. (2018), with permission of Elsevier.

such as El Vergel Granulites, are an important target for future high–temperature thermochronology studies. Beyond allowing a more complete P–T–t reconstruction of the Putumayo Orogen to be achieved, such studies will be crucial for better understanding the structural role that the Amazonian cratonic margin played in the series of collisional events leading to the assembly of Rodinia.

6. Outstanding Challenges and Future Outlook

Despite significant advances made over the last two decades in understanding the Meso–Neoproterozoic orogenic events that took place in (modern) NW South America during Amazonia's incorporation into Rodinia, the existing geochronologic, thermochronologic, and thermobarometric databases remain limited. This is due to multiple factors, but particularly problematic are the limited exposure (i.e., most of the Putumayo Orogen is buried under younger Andean hinterland and foreland cover), and the difficulty of access to many regions where portions of this orogenic belt are exposed. Nevertheless, recent developments in micro–analytical techniques for the geochemical and isotopic study of geological samples are constantly expanding the spectrum of information that can be gleaned from the tiniest mineral fragments, and even small samples can now be investigated to extract a wealth of chronologic and thermal history information (e.g., Ibañez–Mejia et al., 2018). Further applications of state–of–the–art analytical techniques for studying the Proterozoic basement of NW South America and southern Mexico have the potential to provide a wealth of new information that will certainly improve and/or modify the ideas presented throughout this chapter.

In particular, some key outstanding issues and therefore aspects where further research could be deeply transformative for the ideas presented here are:

1. Although the probability of finding extensive outcrops of Putumayo–related rocks in the westernmost exposed Guiana Shield in Colombia is rather low (see Ibañez–Mejia & Cordani, 2020 in this volume), the possibility that even limited outcrops can be found remains plausible. Such exposures could be located in proximity of the serranía de La Macarena and San José del Guaviare uplifts (Figure 2), where the thickness of the Llanos and Putumayo Andean Foreland Basins tapers and basement rocks are exposed.
2. The existing geochronologic database is, for most practical purposes, devoid of a robust petrologic context. For instance, thermobarometric information of dated samples remains scarce, and no trace element data for zircon domains dated by U–Pb methods yet exist, therefore precluding linking these (re)crystallization dates with the petrologic history of their host rocks (e.g., DesOrmeau et al., 2015; Kohn et al., 2015). Further application of methods that allow linking metamorphic temperatures and/or phase assemblages with dates (e.g., Engi et al., 2017; Ibañez–Mejia et al., 2018; Kohn, 2016) will allow more robust time–temperature histories for the different phases of the Putumayo Orogenic Cycle to be reconstructed.
3. In detail, structural models of the Grenville–Putumayo–Sveconorwegian collision remain relatively poorly developed. For instance, it remains unclear which margins were underthrusted or thrusted–on–top–of other(s) during collision, and petrologic studies from the Grenville, Putumayo, and Sveconorwegian have generally resulted in conflicting hypotheses as to which margin acted as a 'lower plate' during collision (e.g., Bingen et al., 2008a; Gower et al., 2008; McLelland et al., 1996; Weber et al., 2010). Further thermobarometric, geochemical, and geo–thermochronologic work from all three margins is necessary to arrive at a plausible structural configuration that explains the P–T trajectories and thermal histories of these orogenic belts.
4. Although most lines of paleogeographic and geochronologic evidence suggest that the Putumayo and Sveconorwegian margins collided near the end of the Stenian and beginning of the Tonian Periods, recent studies have challenged the collisional nature of the Sveconorwegian Orogen (Coint et al., 2015; Slagstad et al., 2013a, 2017), a scenario which would render the collisional model between Amazonia and Baltica as depicted in Figure 3a–c inaccurate. Although debate still persists regarding the nature and causes of the contractional deformation within tectonic units of the Sveconorwegian (e.g., Bingen & Viola, 2018; Möller et al., 2013; Slagstad et al., 2013b), resolving this discrepancy will have a major impact on reconstructions of Rodinia and the Putumayo Orogen.
5. The apparent lack of voluminous AMCG–type intrusives in the Colombian cordilleran inliers contrasts with their widespread occurrence in Oaxaquia. This stark difference not only requires further explanation in order to validate the hypothesis that Oaxaquia was integral part of the Putumayo Orogen (as suggested in this chapter), but the petrologic and tectonic significance of the Oaxaquian AMCG massifs, emplaced just prior to continent–continent collision, remains to be better understood.
6. The paleo–latitude of the Guiana Shield in the Meso– and Neoproterozoic remains, strictly speaking, almost entirely unconstrained. All of Amazonia's paleomagnetic poles in this time period with a quality factor (Q) of 4 or greater, and robust age constrains, namely the Guadalupe (1.53 Ga; Bispo–Santos et al., 2012), Rio Branco (1.54 – 1.44 Ga; D'Agrella–Filho et al., 2016b), Salto do Céu (1.44 Ga; D'Agrella–Filho et al., 2016b), Nova Guarita (1.42 Ga; Bispo–Santos et al., 2012), Indiavaí (1.42 Ga; D'Agrella–Filho et al., 2012), Nova Floresta (1.2 Ga; Tohver et al., 2002), and Fortuna (1.15 Ga; D'Agrella–Filho et al., 2008) poles, have been obtained from localities in the Central Brazil Shield (see recent review by D'Agrella–Filho et al., 2016a). Therefore, obtaining robust paleomagnetic information from Meso– Neoproterozoic units of the Guiana Shield is a most needed objective in order to better constrain its position during the Meso– and Neoproterozoic and further corroborate (or challenge) the ideas presented here and the concept of a unified 'Amazonia'.

7. Summary

Significant advances in the geologic and geochronologic knowledge of NW South America's basement over the last 15 years have, in concert with the growing paleomagnetic database, allowed for a better understanding of: (1) the timing and nature of the Meso– Neoproterozoic orogenic events that have affected the westernmost Guiana Shield, and (2) the role that Amazonia played prior to, and during, the amalgamation of the supercontinent Rodinia. These reconstructions have led to the idea of a 'Putumayo Orogen', underscoring the importance that these series of tectonic events have in our understanding of the geologic evolution of Amazonia.

The Putumayo Orogenic Cycle, as summarized here, records a protracted (ca. 400 my) history of convergence and arc–related magmatism and sedimentation along the leading margin of Amazonia, prior to continent–continent collision at the heart of an assembling Rodinia. Therefore, continuing to refine the timing and physical conditions of the events described herein will continue to provide insights for reconstructing the tectonic history of the Putumayo Orogen, the westernmost Guiana Shield, and perhaps more crucially, for refining the paleogeographic role of Amazonia in global tectonic reconstructions of the Proterozoic Earth. Lastly, notwithstanding the lack of widespread AMCG magmatism in NW South America during the late Mesoproterozoic, the congruence in geologic histories between the Putumayo Basin basement, the north Andean Proterozoic basement inliers, and Oaxaquia, suggests that the latter is an integral part of the Putumayo Orogen.

Acknowledgements

The author thanks Jorge GÓMEZ TAPIAS and Oscar PAREDES ZAPATA for their invitation to write this chapter. The ideas presented here are the result of multiple collaborations and insightful discussions with many colleagues over the years, particularly with Joaquin RUIZ, George GEHRELS, John VALLEY, Jibamitra GANGULY, Jon PATCHETT, Agustin CARDONA, Andres MORA, Victor VALENCIA, and Elias BLOCH; however, any omissions or mistakes remain the sole responsibility of the author. Support for writing this chapter was provided by the University of Rochester. Access to core samples from the Putumayo Foreland Basin was facilitated by the Instituto Colombiano del Petróleo (ICP–ECOPETROL) and the Litoteca Nacional de Colombia. The author is thankful for the very insightful reviews provided by Bodo WEBER, Simon WILDE, and Victor RAMOS, which improved the clarity and accuracy of this chapter.

References

Altenberger, U., Jiménez–Mejia, D.M., Günter, C., Rodríguez–Sierra, G.I., Scheffler, F. & Oberhänsli, R. 2012. The Garzón Massif, Colombia: A new ultrahigh–temperature metamorphic complex in the early Neoproterozoic of northern South America. Mineralogy and Petrology, 105(3–4): 171–185. https://doi.org/10.1007/s00710-012-0202-1

Alvarez, J. 1981. Determinación de edad Rb/Sr en rocas del Macizo de Garzón, Cordillera Oriental de Colombia. Geología Norandina, (4): 31–38.

Alvarez, J. & Cordani, U.G. 1980. Precambrian basement within the septentrional Andes: Age and geological evolution. 26th International Geological Congress. Abstracts 1, p. 18–19. Paris, France.

Anderson, J.L. 1983. Proterozoic anorogenic granite plutonism of North America. In: Medaris, L.G., Jr., Byers, C.W., Mickelson, D.M. & Shanks, W.C. (editors), Proterozoic geology selected papers from an International Proterozoic Symposium. Geological Society of America, Memoir 161: p. 133–154. https://doi.org/10.1130/MEM161-p133

Ashwal, L.D. 1993. Anorthosites. Springer–Verlag, 422 p. Berlin, Heidelberg, Germany. https://doi.org/10.1007/978-3-642-77440-9

Ashwal, L.D. & Bybee, G.M. 2017. Crustal evolution and the temporality of anorthosites. Earth–Science Reviews, 173, 307–330. https://doi.org/10.1016/j.earscirev.2017.09.002

Baquero, M., Grande, S., Urbani, F., Cordani, U. G., Hall, C. & Armstrong, R. 2015. New evidence for Putumayo crust in the basement of the Falcon Basin and Guajira Peninsula, Northwestern Venezuela. In: Bartolini, C. & Mann, P. (editors), Petroleum Geology and Potential of the Colombian Caribbean Margin, American Association Petroleum Geologists, Memoir 108, p. 105–136. https://doi.org/10.1306/13531933M1083639

Berman, R.G. 1991. Thermobarometry using multi–equilibrium calculations: A new technique, with petrological applications. Canadian Mineralogist, 29(4): 833–855.

Bettencourt, J.S., Leite, Jr., W.B., Ruiz, A.S., Matos, R., Payolla, B.L. & Tosdal, R.M. 2010. The Rondonian–San Ignacio Province in the SW Amazonian Craton: An overview. Journal of South American Earth Sciences, 29(1): 28–46. https://doi.org/10.1016/j.jsames.2009.08.006

Bickford, M.E., McLelland, J.M., Mueller, P.A., Kamenov, G.D. & Neadle, M. 2010. Hafnium isotopic compositions of zircon from Adirondack AMCG suites: Implications for the petrogenesis of anorthosites, gabbros, and granitic members of the suites. Canadian Mineralogist, 48(4): 751–761. https://doi.org/10.3749/canmin.48.2.751

Bingen, B. & Viola, G. 2018. The early–Sveconorwegian Orogeny in southern Norway: Tectonic model involving delamination of the sub–continental lithospheric mantle. Precambrian Research, 313: 170–204. https://doi.org/10.1016/j.precamres.2018.05.025

Bingen, B., Demaiffe, D. & van Breemen, O. 1998. The 616 Ma Old Egersund Basaltic Dike Swarm, SW Norway, and Late Neoproterozoic opening of the Iapetus Ocean. Journal of Geology, 106(5): 565–574. https://doi.org/10.1086/516042

Bingen, B., Nordgulen, O. & Viola, G. 2008a. A four–phase model for the Sveconorwegian Orogeny, SW Scandinavia. Norwegian Journal of Geology, 88(1): 43–72.

Bingen, B., Davis, W.J., Hamilton, M.A., Engvik, A.K., Stein, H.J., Skår, Ø. & Nordgulen, O. 2008b. Geochronology of high–grade metamorphism in the Sveconorwegian belt, S Norway: U–Pb, Th–Pb and Re–Os data. Norwegian Journal of Geology, 88(1): 13–42.

Bispo–Santos, F., D'Agrella–Filho, M.S. Pacca, I.I.G., Janikian, L., Trindade, R.I.F., Elming, S.A., Silva, J.A., Barros, M.A.S. & Pinho, F.E.C. 2008. Columbia revisited: Paleomagnetic results from the 1790 Ma colider volcanics (SW Amazonian Craton, Brazil). Precambrian Research, 164(1–2): 40–49. https://doi.org/10.1016/j.precamres.2008.03.004

Bispo–Santos, F., D'Agrella–Filho, M.S., Trindade, R.I.F., Elming, S.–A., Janikian, L., Vasconcelos, P.M., Perillo, B.M., Pacca, I.I.G., da Silva, J.A. & Barros, M.A.S. 2012. Tectonic implications of the 1419 Ma Nova Guarita mafic intrusives paleomagnetic pole (Amazonian Craton) on the longevity of Nuna. Precambrian Research, 196–197: 1–22. https://doi.org/10.1016/j.precamres.2011.10.022

Bispo–Santos, F., D'Agrella–Filho, M.S., Trindade, R.I.F., Janikian, L. & Reis, N.J. 2014a. Was there SAMBA in Columbia? Paleomagnetic evidence from 1790 Ma Avanavero mafic sills, northern Amazonian Craton. Precambrian Research, 244: 139–155. https://doi.org/10.1016/j.precamres.2013.11.002

Bleeker, W. & Ernst, R. 2006. Short–lived mantle generated magmatic events and their dyke swarms: The key unlocking Earth's paleogeographic record back to 2.6 Ga. In: Hanski, E., Mertanen, S., Rämö, T. & Vuollo, J. (editors), Dyke Swarms—Time Markers of Crustal Evolution. A.A. Balkema Publishers, p. 3–26. Rotterdam, the Netherlands.

Bloch, E., Ganguly, J., Hervig, R. & Cheng, W. 2015. ^{176}Lu–^{176}Hf geochronology of garnet I: Experimental determination of the diffusion kinetics of Lu^{3+} and Hf^{4+} in garnet, closure temperatures and geochronological implications. Contributions to Mineralogy and Petrology, 169(2): 1–18. https://doi.org/10.1007/s00410–015–1109–8

Bloch, E.M., Jollands, M.C., Devoir, A., Bouvier, A.S., Ibañez–Mejia, M. & Baumgartner, L.P. 2020. Multispecies diffusion of yttrium, rare earth elements and hafnium in garnet. Journal of Petrology, egaa055, p. 1–77. https://doi.org/10.1093/petrology/egaa055

Bogdanova, S.V., Bingen, B., Gorbatschev, R., Kheraskova, T.N., Kozlov, V.I., Puchkov, V.N. & Volozh, Y.A. 2008. The East European Craton (Baltica) before and during the assembly of Rodinia. Precambrian Research, 160(1–2): 23–45. https://doi.org/10.1016/j.precamres.2007.04.024

Boger, S.D., Raetz, M., Giles, D., Etchart, E. & Fanning, C.M. 2005. U–Pb age data from the Sunsas region of eastern Bolivia, evidence for the allochthonous origin of the Paragua Block. Precambrian Research, 139(3–4): 121–146. https://doi.org/10.1016/j.precamres.2005.05.010

Bonamici, C.E., Fanning, C.M., Kozdon, R., Fournelle, J.H. & Valley, J.W. 2015. Combined oxygen–isotope and U–Pb zoning studies of titanite: New criteria for age preservation. Chemical Geology, 398: 70–84. https://doi.org/10.1016/j.chemgeo.2015.02.002

Bond, G.C., Nickeson, P.A. & Kominz, M.A. 1984. Breakup of a supercontinent between 625 Ma and 555 Ma: New evidence and implications for continental histories. Earth and Planetary Science Letters, 70(2), 325–345. https://doi.org/10.1016/0012–821X(84)90017–7

Bouvier, A., Vervoort, J.D. & Patchett, P.J. 2008. The Lu–Hf and Sm–Nd isotopic composition of CHUR: Constraints from unequilibrated chondrites and implications for the bulk composition of terrestrial planets. Earth and Planetary Science Letters, 273(1–2): 48–57. https://doi.org/10.1016/j.epsl.2008.06.010

Brown, M. & Johnson, T. 2018. Secular change in metamorphism and the onset of global plate tectonics. American Mineralogist, 103(2): 181–196. https://doi.org/10.2138/am-2018-6166

Bybee, G.M., Hayes, B., Owen–Smith, T.M., Lehmann, J., Ashwal, L.D., Brower, A M., Hill, C.M., Corfu, F. & Manga, M. 2019. Proterozoic massif–type anorthosites as the archetypes of long–lived (≥100 Myr) magmatic systems—New evidence from the Kunene Anorthosite Complex (Angola). Precambrian Research, 332, 105393: 1–16. https://doi.org/10.1016/j.precamres.2019.105393

Cameron, K.L., Lopez, R., Ortega–Gutiérrez, F., Solari, L.A., Keppie, J.D. & Schulze, C. 2004. U–Pb geochronology and Pb isotope compositions of leached feldspars: Constraints on the origin and evolution of Grenvillian rocks from eastern and southern Mexico. In: Tollo, R.P., Corriveau, L., McLelland, J.M. & Bartholomew, M.J. (editors), Proterozoic Tectonic Evolution of the Grenville Orogen in North America. Geological Society of America, Memoir 197, p. 755–769. https://doi.org/10.1130/0-8137-1197-5.755

Cardona, A. 2003. Correlações entre fragmentos do embasamento pré–Mesozóico da terminação setentrional dos Andes Colombianos, com base em dados isotópicos e geocronológicos. Master thesis, Universidade de São Paulo, 149 p. São Paulo. https://doi.org/10.11606/D.44.2003.tde-07042015-090410

Cardona, A., Chew, D., Valencia, V.A., Bayona, G., Mišković, A. & Ibañez–Mejia, M. 2010. Grenvillian remnants in the northern Andes: Rodinian and Phanerozoic paleogeographic perspectives. Journal of South American Earth Sciences, 29(1): 92–104. https://doi.org/10.1016/j.jsames.2009.07.011

Cawood, P.A. & Pisarevsky, S.A. 2006. Was Baltica right–way–up or upside–down in the Neoproterozoic? Journal of the Geological Society, 163(5): 753–759. https://doi.org/10.1144/0016-76492005-126

Cawood, P.A. & Pisarevsky, S.A. 2017. Laurentia–Baltica–Amazonia relations during Rodinia assembly. Precambrian Research, 292: 386–397. https://doi.org/10.1016/j.precamres.2017.01.031

Cawood, P.A., McCausland, P. & Dunning, G.R. 2001. Opening Iapetus: Constraints from the Laurentian margin in Newfoundland.

GSA Bulletin, 113(4): 443–453. https://doi.org/10.1130/0016-7606(2001)113<0443:OICFTL>2.0.CO;2

Cawood, P.A., Strachan, R., Cutts, K., Kinny, P.D., Hand, M. & Pisarevsky, S. 2010. Neoproterozoic orogeny along the margin of Rodinia: Valhalla Orogen, North Atlantic. Geology, 38(2): 99–102. https://doi.org/10.1130/G30450.1

Cawood, P.A., Hawkesworth, C.J. & Dhuime, B. 2012. Detrital zircon record and tectonic setting. Geology, 40(10): 875–878. https://doi.org/10.1130/G32945.1

Cawood, P.A., Hawkesworth, C.J. & Dhuime, B. 2013. The continental record and the generation of continental crust. GSA Bulletin, 125(1–2): 14–32. https://doi.org/10.1130/B30722.1

Chiarenzelli, J., Kratzmann, D., Selleck, B. & deLorraine, W. 2015. Age and provenance of Grenville supergroup rocks, Trans–Adirondack Basin, constrained by detrital zircons. Geology, 43(2): 183–186. https://doi.org/10.1130/G36372.1

Cisneros de León, A., Weber, B., Ortega–Gutiérrez, F., González–Guzmán, R., Maldonado, R., Solari, L., Schaaf, P. & Manjarrez–Juárez, R. 2017. Grenvillian massif–type anorthosite suite in Chiapas, Mexico: Magmatic to polymetamorphic evolution of anorthosites and their Ti–Fe ores. Precambrian Research, 295: 203–226. https://doi.org/10.1016/j.precamres.2017.04.028

Coint, N., Slagstad, T., Roberts, N.M.W., Marker, M., Røhr, T. & Sørensen, B.E. 2015. The late Mesoproterozoic Sirdal Magmatic Belt, SW Norway: Relationships between magmatism and metamorphism and implications for Sveconorwegian orogenesis. Precambrian Research, 265: 57–77. https://doi.org/10.1016/j.precamres.2015.05.002

Condie, K.C., Beyer, E., Belousova, E., Griffin, W.L. & O'Reilly, S.Y. 2005. U–Pb isotopic ages and Hf isotopic composition of single zircons: The search for juvenile Precambrian continental crust. Precambrian Research, 139(1–2): 42–100. https://doi.org/10.1016/j.precamres.2005.04.006

Cordani, U.G. & Teixeira, W. 2007. Proterozoic accretionary belts in the Amazonian Craton. In: Hatcher Jr, R.D., Carlson, M.P., McBride, J.H. & Martínez–Catalá, J.R. (editors), 4–D Framework of continental crust. Geological Society of America, Memoir 200, p. 297–320. https://doi.org/10.1130/2007.1200(14)

Cordani, U.G., Cardona, A., Jiménez, D.M., Liu, D. & Nutman, A.P. 2005. Geochronology of Proterozoic basement inliers in the Colombian Andes: Tectonic history of remnants of a fragmented Grenville belt. In: Vaughan, A.P.M., Leat, P.T. & Pankhurst, R.J. (editors), Terrane processes at the margins of Gondwana. Geological Society of London, Special Publication 246, p. 329–346. London. https://doi.org/10.1144/GSL.SP.2005.246.01.13

Cordani, U.G., Teixeira, W., D'Agrella–Filho, M.S. & Trindade, R.I. 2009. The position of the Amazonian Craton in supercontinents. Gondwana Research, 15(3–4): 396–407. https://doi.org/10.1016/j.gr.2008.12.005

Corrigan, D. & Hanmer, S. 1997. Anorthosites and related granitoids in the Grenville Orogen: A product of convective thinning of the lithosphere? Geology, 25(1): 61–64. https://doi.org/10.1130/0091-7613(1997)025<0061:AARGIT>2.3.CO;2

Cuadros, F.A., Botelho, N.F., Ordóñez–Carmona, O. & Matteini, M. 2014. Mesoproterozoic crust in the San Lucas Range (Colombia): An insight into the crustal evolution of the northern Andes. Precambrian Research, 245: 186–206. https://doi.org/10.1016/j.precamres.2014.02.010

Dalziel, I.W.D. 1991. Pacific margins of Laurentia and east Antarctica–Australia as a conjugate rift pair: Evidence and implications for an Eocambrian supercontinent. Geology, 19(6): 598–601. https://doi.org/10.1130/0091-7613(1991)019<0598:PMOLAE>2.3.CO;2

D'Agrella–Filho, M.S., Tohver, E., Santos, J.O.S., Elming, S.Å., Trindade, R.I.F., Pacca, I.I.G. & Geraldes, M.C. 2008. Direct dating of paleomagnetic results from Precambrian sediments in the Amazon Craton: Evidence for Grenvillian emplacement of exotic crust in SE Appalachians of North America. Earth and Planetary Science Letters, 267(1–2): 188–199. https://doi.org/10.1016/j.epsl.2007.11.030

D'Agrella–Filho, M.S., Trindade, R.I.F., Elming, S.Å., Teixeira, W., Yokoyama, E., Tohver, E., Geraldes, M.C., Pacc, I.I.G., Barros, M.A.S. & Ruiz, A.S. 2012. The 1420 Ma Indiavaí Mafic Intrusion (SW Amazonian Craton): Paleomagnetic results and implications for the Columbia supercontinent. Gondwana Research, 22(3–4): 956–973. https://doi.org/10.1016/j.gr.2012.02.022

D'Agrella–Filho, M. S., Bispo–Santos, F., Trindade, R. I. F. & Antonio, P. Y. J. 2016a. Paleomagnetism of the Amazonian Craton and its role in paleocontinents. Brazilian Journal of Geology, 46(2):275–299. http://doi.org/10.1590/2317-4889201620160055

D'Agrella–Filho, M.S., Trindade, R.I.F., Queiroz, M.V.B., Meira, V.T., Janikian, L., Ruiz, A.S. & Bispo–Santos, F. 2016b. Reassessment of Aguapeí, Salto do Céu, paleomagnetic pole, Amazonian Craton and implications for Proterozoic supercontinents. Precambrian Research, 272: 1–17. http://doi.org/10.1016/j.precamres.2015.10.021

DesOrmeau, J.W., Gordon, S.M., Kylander–Clark, A.R.C., Hacker, B.R., Bowring, S.A., Schoene, B. & Samperton, K.M. 2015. Insights into (U)HP metamorphism of the Western Gneiss Region, Norway: A high–spatial resolution and high–precision zircon study. Chemical Geology, 414: 138–155. https://doi.org/10.1016/j.chemgeo.2015.08.004

Dewey, J.F. 1988. Extensional collapse of orogens. Tectonics, 7(6): 1123–1139. https://doi.org/10.1029/TC007i006p01123

Dewey, J.F., Shackleton, R.M., Chengfa, C. & Yiyin, S. 1988. The tectonic evolution of the Tibetan Plateau. Philosophical Transactions of the Royal Society A, Memoir 327: 379–413. https://doi.org/10.1098/rsta.1988.0135

Dhuime, B., Hawkesworth, C. & Cawood, P. 2011. When continents formed. Science, 331(6014): 154–155. https://doi.org/10.1126/science.1201245

Eckert, J.O., Newton, R.C. & Kleppa, O.J. 1991. The ΔH of reaction and recalibration of garnet–pyroxene–plagioclase–quartz geobarometers in the CMAS system by solution calorimetry. American Mineralogist, 76(1–2): 148–160.

Edmond, J.M. 1992. Himalayan tectonics, weathering processes, and the strontium isotope record in marine limestones. Science, 258(5088): 1594–1597. https://doi.org/10.1126/science.258.5088.1594

Emslie, R.F. 1991. Granitoids of rapakivi granite–anorthosite and related associations. Precambrian Research, 51(1–4): 173–192. https://doi.org/10.1016/0301-9268(91)90100-O

Engi, M., Lanari, P. & Kohn, M.J. 2017. Significant Ages—An Introduction to Petrochronology. Reviews in Mineralogy and Geochemistry, 83(1): 1–12. https://doi.org/10.2138/rmg.2017.83.1

England, P.C. & Thompson, A.B. 1984. Pressure—temperature—time paths of regional metamorphism I. Heat transfer during the evolution of regions of thickened continental crust. Journal of Petrology, 25(4): 894–928. https://doi.org/10.1093/petrology/25.4.894

Ernst, R.E., Bleeker, W., Soderlund, U. & Kerr, A.C. 2013. Large Igneous Provinces and supercontinents: Toward completing the plate tectonic revolution. Lithos, 174: 1–14. http://doi.org/10.1016/j.lithos.2013.02.017

Evans, D.A.D. 2013. Reconstructing pre–Pangean supercontinents. Geological Society of America Bulletin, 125(11–12): 1735–1751. http://doi.org/10.1130/B30950.1

Fournier, H.W., Lee, J.K.W., Urbani, F. & Grande, S. 2017. The tectonothermal evolution of the Venezuelan Caribbean Mountain System: $^{40}Ar/^{39}Ar$ age insights from a Rodinian–related rock, the Cordillera de la Costa and Margarita Island. Journal of South American Earth Sciences, 80: 149–173. http://doi.org/10.1016/j.jsames.2017.09.015

Fuck, R.A., Brito–Neves, B.B. & Schobbenhaus, C. 2008. Rodinia descendants in South America. Precambrian Research, 160(1–2): 108–126. http://doi.org/10.1016/j.precamres.2007.04.018

Ganguly, J. & Tirone, M. 1999. Diffusion closure temperature and age of a mineral with arbitrary extent of diffusion: Theoretical formulation and applications. Earth and Planetary Science Letters, 170(1–2): 131–140. https://doi.org/10.1016/S0012-821X(99)00089-8

Ganguly, J., Cheng, W. & Tirone, M. 1996. Thermodynamics of aluminosilicate garnet solid solution: New experimental data, an optimized model, and thermometric applications. Contributions to Mineralogy and Petrology, 126(1–2): 137–151.

Ganguly, J., Tirone, M. & Hervig, R.L. 1998. Diffusion kinetics of samarium and neodymium in garnet, and a method for determining cooling rates of rocks. Science, 281(5378): 805–807. https://doi.org/10.1126/science.281.5378.805

Ganguly, J., Dasgupta, S., Cheng, W. & Neogi, S. 2000. Exhumation history of a section of the Sikkim Himalayas, India: Records in the metamorphic mineral equilibria and compositional zoning of garnet. Earth and Planetary Science Letters, 183(3–4): 471–486. https://doi.org/10.1016/S0012-821X(00)00280-6

Garzione, C.N. 2008. Surface uplift of Tibet and Cenozoic global cooling. Geology, 36(12): 1003–1004. https://doi.org/10.1130/focus122008.1

Goldsmith, R., Marvin, R.F. & Mehnert, H.H. 1971. Radiometric ages in the Santander Massif, Eastern Cordillera, Colombian Andes. United States Geological Survey Professional Paper, 750–D, p. D44–D49.

González–Guzmán, R., Weber, B., Manjarrez–Juárez, R., Cisneros de León, A., Hecht, L. & Herguera–García, J.C. 2016. Provenance, age constraints and metamorphism of Ediacaran metasedimentary rocks from the El Triunfo Complex (SE Chiapas, Mexico): Evidence for Rodinia breakup and Iapetus active margin. International Geology Review, 58(16): 2065–2091. https://doi.org/10.1080/00206814.2016.1207208

Gower, C.F. & Krogh, T.E. 2002. A U–Pb geochronological review of the Proterozoic history of the eastern Grenville Province. Canadian Journal of Earth Sciences, 39(5): 795–829. https://doi.org/10.1139/E01–090

Gower, C.F., Kamo, S. & Krogh, T. E. 2008. Indentor tectonism in the eastern Grenville Province. Precambrian Research, 167(1–2): 201–212. https://doi.org/10.1016/j.precamres.2008.08.004

Hamilton, M. A., McLelland, J. & Selleck, B. 2004. SHRIMP U–Pb zircon geochronology of the anorthosite–mangerite–charnockite–granite suite, Adirondack Mountains, New York: Ages of emplacement and metamorphism. In: Tollo, R.P., Corriveau, L., McLelland, J.M. & Bartholomew, M.J. (editors), Proterozoic Tectonic Evolution of the Grenville Orogen in North America. Geological Society of America, Memoir 197, p. 337–355. https://doi.org/10.1130/0-8137-1197-5.337

Hawkesworth, C.J., Dhuime, B., Pietranik, A.B., Cawood, P.A., Kemp, A.I.S. & Storey, C.D. 2010. The generation and evolution of the continental crust. Journal of the Geological Society, 167(2): 229–248. http://doi.org/10.1144/0016-76492009-072

Hawkesworth, C., Cawood, P. & Dhuime, B. 2013. Continental growth and the crustal record. Tectonophysics, 609(C): 651–660. https://doi.org/10.1016/j.tecto.2013.08.013

Hellström, F.A., Johansson, Å.E., Larson, S. Å. 2004. Age and emplacement of late Sveconorwegian monzogabbroic dykes, SW Sweden. Precambrian Research, 128(1–2): 39–55. https://doi.org/10.1016/S0301-9268(03)00194-3

Heumann, M.J., Bickford, M.E., Hill, B.M., McLelland, J.M., Selleck, B.W. & Jercinovic, M.J. 2006. Timing of anatexis in metapelites from the Adirondack lowlands and southern highlands: A manifestation of the Shawinigan Orogeny and subsequent anorthosite–mangerite–charnockite–granite magmatism. GSA Bulletin, 118(11–12): 1283–1298. https://doi.org/10.1130/B25927.1

Hoffman, P.F. 1991. Did the breakout of Laurentia turn Gondwanaland inside–out? Science, 252(5011): 1409–1412. https://doi.org/10.1126/science.252.5011.1409

Ibañez–Mejia, M. & Cordani, U.G. 2020. Zircon U–Pb geochronology and Hf–Nd–O isotope geochemistry of the Paleoproterozoic to Mesoproterozoic basement in the westernmost Guiana Shield. In: Gómez, J. & Mateus–Zabala, D. (editors), The Geology of Colombia, Volume 1 Proterozoic – Paleozoic. Servicio Geológico Colombiano, Publicaciones Geológicas Especiales 35, p. 65–90. Bogotá. https://doi.org/10.32685/pub.esp.35.2019.04

Ibañez–Mejia, M., Ruiz, J., Valencia, V.A., Cardona, A., Gehrels, G.E. & Mora, A.R. 2011. The Putumayo Orogen of Amazonia and its implications for Rodinia reconstructions: New U–Pb geochronological insights into the Proterozoic tectonic evolution of northwestern South America. Precambrian Research, 191(1–2): 58–77. https://doi.org/10.1016/j.precamres.2011.09.005

Ibañez–Mejia, M., Pullen, A., Arenstein, J., Gehrels, G., Valley, J., Ducea, M., Mora, A., Pecha, M. & Ruiz, J. 2015. Unraveling crustal growth and reworking processes in complex zircons from orogenic lower–crust: The Proterozoic Putumayo Orogen of Amazonia. Precambrian Research, 267: 285–310. https://doi.org/10.1016/j.precamres.2015.06.014

Ibañez–Mejia, M., Bloch, E.M. & Vervoort, J.D. 2018. Timescales of collisional metamorphism from Sm–Nd, Lu–Hf and U–Pb thermochronology: A case from the Proterozoic Putumayo Orogen of Amazonia. Geochimica Et Cosmochimica Acta, 235: 103–126. http://doi.org/10.1016/j.gca.2018.05.017

Jamieson, R.A., Beaumont, C., Medvedev, S. & Nguyen, M.H. 2004. Crustal channel flows: 2. Numerical models with implications for metamorphism in the Himalayan–Tibetan Orogen. Journal of Geophysical Research: Solid Earth, 109(B6): 1–24. https://doi.org/10.1029/2003JB002811

Jiménez–Mejía, D.M., Juliani, C. & Cordani, U.G. 2006. P–T–t conditions of high–grade metamorphic rocks of the Garzón Massif, Andean basement, SE Colombia. Journal of South American Earth Sciences, 21(4): 322–336. https://doi.org/10.1016/j.jsames.2006.07.001

Johansson, A. 2009. Baltica, Amazonia and the SAMBA connection–1000 million years of neighborhood during the Proterozoic? Precambrian Research, 175(1–4): 221–234. http://doi.org/10.1016/j.precamres.2009.09.011

Johansson, L., Möller, C. & Söderlund, U. 2001. Geochronology of eclogite facies metamorphism in the Sveconorwegian Province of SW Sweden. Precambrian Research, 106(3–4): 261–275. https://doi.org/10.1016/S0301-9268(00)00105-4

Kemp, A.I.S., Hawkesworth, C.J., Collins, W.J., Gray, C.M., Blevin, P.L. & Edinburgh Ion Microprobe Facility. 2009. Isotopic evidence for rapid continental growth in an extensional accretionary orogen: The Tasmanides, eastern Australia. Earth and Planetary Science Letters, 284(3–4): 455–466. https://doi.org/10.1016/j.epsl.2009.05.011

Keppie, J.D., Dostal, J., Cameron, K.L., Solari, L.A., Ortega–Gutiérrez, F. & Lopez, R. 2003. Geochronology and geochemistry of Grenvillian igneous suites in the northern Oaxacan Complex, southern Mexico: Tectonic implications. Precambrian Research, 120(3–4): 365–389. https://doi.org/10.1016/S0301-9268(02)00166-3

Kohn, M.J. 2016. Metamorphic chronology—a tool for all ages: Past achievements and future prospects. American Mineralogist, 101(1): 25–42. https://doi.org/10.2138/am-2016-5146

Kohn, M.J. & Corrie, S.L. 2011. Preserved Zr–temperatures and U–Pb ages in high–grade metamorphic titanite: Evidence for a static hot channel in the Himalayan Orogen. Earth and Planetary Science Letters, 311(1–2): 136–143. https://doi.org/10.1016/j.epsl.2011.09.008

Kohn, M.J., Corrie, S.L. & Markley, C. 2015. The fall and rise of metamorphic zircon. American Mineralogist, 100(4): 897–908. https://doi.org/10.2138/am-2015-5064

Kroonenberg, S.B. 1982. A Grenvillian granulite belt in the Colombian Andes and its relation to the Guiana Shield. Geologie en Mijnbouw, 61(4): 325–333.

Lasaga, A.C. 1983. Geospeedometry: An extension of geothermometry. In: Saxena, S.K. (editor), Kinetics and Equilibrium in Mineral Reactions. Springer, p. 81–114. New York, USA. https://doi.org/10.1007/978-1-4612-5587-1_3

Lawlor, P.J., Ortega–Gutiérrez, F., Cameron, K.L., Ochoa–Camarillo, H., Lopez, R. & Sampson, D.E. 1999. U–Pb geochronology, geochemistry, and provenance of the Grenvillian Huiznopala Gneiss of eastern Mexico. Precambrian Research, 94(1–2): 73–99. https://doi.org/10.1016/S0301-9268(98)00108-9

Leal–Mejía, H. 2011. Phanerozoic gold metallogeny in the Colombian Andes: A tectono–magmatic approach. Doctoral thesis, Universitat de Barcelona, 989 p. Barcelona.

Li, Z.X., Bogdanova, S.V., Collins, A.S., Davidson, A., de Waele, B., Ernst, R.E., Fitzsimons, I.C.W., Fuck, R.A., Gladkochub, D.P. Jacobs, J., Karlstrom, K.E., Lu, S., Natapov, L.M., Pease, V., Pisarevsky, S.A., Thrane, K. & Vernikovsky, V. 2008. Assembly, configuration, and break–up history of Rodinia: A synthesis. Precambrian Research, 160(1–2): 179–210. http://doi.org/10.1016/j.precamres.2007.04.021

Litherland, M. & Bloomfield, K. 1981. The Proterozoic history of eastern Bolivia. Precambrian Research, 15(2): 165–179. https://doi.org/10.1016/0301-9268(81)90027-9

Litherland, M., Annells, R.N., Darbyshire, D.P.F., Fletcher, C.J.N., Hawkins, M.P., Klinck, B.A., Mitchell, W.I., O'Connor, E.A., Pitfield, P.E.J., Power, G. & Webb, B.C. 1989. The Proterozoic of eastern Bolivia and its relationship to the Andean Mobile Belt. Precambrian Research, 43(3): 157–174. https://doi.org/10.1016/0301-9268(89)90054-5

MacDonald, W.D. & Hurley, P.M. 1969. Precambrian gneisses from northern Colombia, South America. Geological Society of America Bulletin, 80(9): 1867–1872. https://doi.org/10.1130/0016-7606(1969)80[1867:PGFNCS]2.0.CO;2

McLelland, J.M., Daly, J.S. & McLelland, J.M. 1996. The Grenville Orogenic Cycle (ca 1350–1000 Ma): An Adirondack perspective. Tectonophysics, 265(1–2): 1–28. https://doi.org/10.1016/S0040-1951(96)00144-8

McLelland, J.M., Hamilton, M., Selleck, B., McLelland, J., Walker, D. & Orrell, S. 2001. Zircon U–Pb geochronology of the Ottawan Orogeny, Adirondack Highlands, New York: Regional and tectonic implications. Precambrian Research, 109(1–2): 39–72. https://doi.org/10.1016/S0301-9268(01)00141-3

McLelland, J.M., Bickford, M.E., Hill, B.M., Clechenko, C.C., Valley, J.W. & Hamilton, M.A. 2004. Direct dating of Adirondack massif anorthosite by U–Pb SHRIMP analysis of igneous zircon: Implications for AMCG complexes. GSA Bulletin, 116(11–12): 1299–1317. https://doi.org/10.1130/B25482.1

McLelland, J.M., Selleck, B.W. & Bickford, M.E. 2010. Review of the Proterozoic evolution of the Grenville Province, its Adirondack outlier, and the Mesoproterozoic inliers of the Appalachians. In: Tollo, R.P., Bartholomew, M.J., Hibbard, J.P. & Karabinos, P.M. (editors), From Rodinia to Pangea: The Lithotectonic Record of the Appalachian Region. Geological Society of America, Memoir 206, p. 21–49. Boulder, USA. https://doi.org/10.1130/2010.1206(02)

Mezger, K., Rawnsley, C.M., Bohlen, S.R. & Hanson, G.N. 1991. U–Pb garnet, sphene, monazite, and rutile ages: Implications for the duration of high–grade–metamorphism and cooling histories, Adirondack Mts., New York. The Journal of Geology, 99(3): 415–428. https://doi.org/10.1086/629503

Möller, C. 1998. Decompressed eclogites in the Sveconorwegian (–Grenvillian) Orogen of SW Sweden: Petrology and tectonic implications. Journal of Metamorphic Geology 16(5): 641–656. https://doi.org/10.1111/j.1525-1314.1998.00160.x

Möller, C. 1999. Sapphirine in SW Sweden: A record of Sveconorwegian (–Grenvillian) late–orogenic tectonic exhumation. Journal of Metamorphic Geology 17(1): 127–141. https://doi.org/10.1046/J.1525-1314.1999.00184.X

Möller, C., Bingen, B., Andersson, J., Stephens, M.B., Viola, G. & Scherstén, A. 2013. A non–collisional, accretionary Sveconorwegian Orogen–Comment. Terra Nova 25(2): 165–168. https://doi.org/10.1111/ter.12029

Ordóñez–Carmona, O., Pimentel, M.M. & De Moraes, R. 2002. Granulitas de Los Mangos: Un fragmento grenviliano en la parte oriental de la Sierra Nevada de Santa Marta. Revista de la Academia Colombiana de Ciencias Exactas, Físicas y Naturales, 26(99): 169–179.

Ordóñez–Carmona, O., Restrepo, J.J. & Pimentel, M.M. 2006. Geochronological and isotopical review of pre–Devonian crustal basement of the Colombian Andes. Journal of South American Earth Sciences, 21(4): 372–382. https://doi.org/10.1016/j.jsames.2006.07.005

Ortega–Gutiérrez, F., Ruiz, J. & Centeno–García, E. 1995. Oaxaquia: A Proterozoic microcontinent accreted to North America during the late Paleozoic. Geology, 23(12): 1127–1130. https://doi.org/10.1130/0091-7613(1995)023<1127:OAPMAT>2.3.CO;2

Ortega–Gutiérrez, F., Elías–Herrera, M., Morán–Zenteno, D.J., Solari, L., Weber, B. & Luna–González, L. 2018. The pre–Mesozoic metamorphic basement of Mexico, 1.5 billion years of crustal evolution. Earth–Science Reviews, 183: 2–37. https://doi.org/10.1016/j.earscirev.2018.03.006

Patchett, P.J. & Ruiz, J. 1987. Nd isotopic ages of crust formation and metamorphism in the Precambrian of eastern and southern Mexico. Contributions to Mineralogy and Petrology, 96(4): 523–528. http://doi.org/10.1007/BF01166697

Pinson Jr, W.H., Hurley, P.M., Mencher, E. & Fairbairn, H.W. 1962. K–Ar and Rb–Sr ages of biotites from Colombia, South America. Geological Society of America Bulletin, 73(7): 907–910. https://doi.org/10.1130/0016-7606(1962)73[907:KARAOB]2.0.CO;2

Pisarevsky, S.A., Elming, S.A., Pesonen, L.J. & Li, Z.X. 2014. Mesoproterozoic paleogeography: Supercontinent and beyond. Precambrian Research, 244: 207–225. http://doi.org/10.1016/j.precamres.2013.05.014

Plank, T. & Langmuir, C.H. 1998. The chemical composition of subducting sediment and its consequences for the crust and mantle. Chemical Geology, 145(3–4): 325–394. http://doi.org/10.1016/S0009-2541(97)00150-2

Priem, H., Andriessen, P., Boelrijk, N., De Booder, H., Hebeda, E., Huguett, A., Verdumen, E. & Verschure, R. 1982. Geochronology of the Precambrian in the Amazonas region of southeastern Colombia (western Guiana Shield). Geologie en Mijnbouw, 61(3): 229–242.

Priem, H.N.A., Kroonenberg, S.B., Boelrijk, N.A.I.M. & Hebeda, E.H. 1989. Rb–Sr and K–Ar evidence for the presence of a 1.6 Ga basement underlying the 1.2 Ga Garzón–Santa Marta granulite belt in the Colombian Andes. Precambrian Research, 42(3–4): 315–324. https://doi.org/10.1016/0301-9268(89)90016-8

Raymo, M.E. & Ruddiman, W.F. 1992. Tectonic forcing of late Cenozoic climate. Nature, 359(6391): 117–122. https://doi.org/10.1038/359117a0

Reiners, P.W., Carlson, R.W., Renne, P.R., Cooper, K.M., Granger, D.E., McLean, N.M. & Schoene, B. 2017. Geochronology and thermochronology. American Geophysical Union–John Wiley & Sons Ltd., 480 p.

Reis, N.J., Teixeira, W., Hamilton, M.A., Bispo–Santos, F., Almeida, M.E. & D'Agrella–Filho, M.S. 2013. Avanavero mafic magmatism, a late Paleoproterozoic LIP in the Guiana Shield, Amazonian Craton: U–Pb ID–TIMS baddeleyite, geochemical and paleomagnetic evidence. Lithos, 174: 175–195. http://doi.org/10.1016/j.lithos.2012.10.014

Restrepo, J.L. & Giraldo, O.A. 2018. Petrografía y geocronología (U–Pb) de las Migmatitas de Florencia, en el Complejo Garzón, departamento de Caquetá. Bachelor thesis, Universidad de Caldas, 126 p. Manizales, Colombia.

Restrepo–Pace, P.A., Ruiz, J., Gehrels, G. & Cosca, M. 1997. Geochronology and Nd isotopic data of Grenville–age rocks in the Colombian Andes: New constraints for late Proterozoic – early Paleozoic paleocontinental reconstructions of the Americas. Earth and Planetary Science Letters, 150(3–4): 427–441. https://doi.org/10.1016/S0012-821X(97)00091-5

Rivers, T. 2008. Assembly and preservation of lower, mid, and upper orogenic crust in the Grenville Province–Implications for the evolution of large hot long–duration orogens. Precambrian Research, 167(3–4): 237–259. https://doi.org/10.1016/j.precamres.2008.08.005

Rivers, T. 2012. Upper–crustal orogenic lid and mid–crustal core complexes: Signature of a collapsed orogenic plateau in the hinterland of the Grenville Province. Canadian Journal of Earth Sciences, 49(1): 1–42. https://doi.org/10.1139/e11-014

Rivers, T. & Corrigan, D. 2000. Convergent margin on southeastern Laurentia during the Mesoproterozoic: Tectonic implications. Canadian Journal of Earth Sciences, 37(2–3): 359–383. https://doi.org/10.1139/e99-067

Rodríguez, G., Zapata, G., Velásquez, M.E., Cossio, U. & Londoño, A.C. 2003. Memoria explicativa: Geología de las planchas 367 Gigante, 368 San Vicente del Caguán, 389 Timaná, 390 Puerto Rico, 391 Lusitania (parte noroccidental) y 414 El Doncello. Scale 1:100 000. Ingeominas, 166 p. Bogotá.

Royden, L.H., Burchfiel, B.C. & van der Hilst, R.D. 2008. The geological evolution of the Tibetan Plateau. Science, 321(5892): 1054–1058. https://doi.org/10.1126/science.1155371

Rudnick, R.L. & Gao, S. 2014. Composition of the Continental Crust. In: Holland, H.D. & K.K. Turekian (editors), Treatise on Geochemistry: The Crust, 4. Elsevier, p. 1–51. https://doi.org/10.1016/B978-0-08-095975-7.00301-6

Ruiz, J., Patchett, P.J. & Ortega–Gutiérrez, F. 1988. Proterozoic and Phanerozoic basement terranes of Mexico from Nd isotopic studies. GSA Bulletin, 100(2): 274–281. https://doi.org/10.1130/0016-7606(1988)100<0274:PAPBTO>2.3.CO;2

Ruiz, J., Tosdal, R.M., Restrepo, P.A. & Murillo–Muñetón, G. 1999. Pb isotope evidence for Colombia–southern México connections in the Proterozoic. In: Ramos, V.A. & Keppie, J.D. (editors), Laurentia–Gondwana connections before Pangea. Geological Society of America, Special Paper 336, p. 183–197. https://doi.org/10.1130/0-8137-2336-1.183

Sadowski, G.R. & Bettencourt, J.S. 1996. Mesoproterozoic tectonic correlations between eastern Laurentia and the western border of the Amazon Craton. Precambrian Research, 76(3–4): 213–227. https://doi.org/10.1016/0301-9268(95)00026-7

Scholl, D.W. & von Huene, R. 2009. Implications of estimated magmatic additions and recycling losses at the subduction zones of accretionary (non–collisional) and collisional (suturing) orogens. Geological Society, London, Special Publications 318, p. 105–125. https://doi.org/10.1144/SP318.4

Schulze, C. 2011. Petrología y geoquímica de las rocas del área de Pluma Hidalgo, Oaxaca e implicaciones tectónicas para el Proterozoico de Oaxaquia. Doctoral thesis, Universidad Autónoma Nacional de México, 311 p. México D.F., México.

Selleck, B., McLelland, J.M. & Bickford, M.E. 2005. Granite emplacement during tectonic exhumation: The Adirondack example. Geology, 33(10): 781–784. https://doi.org/10.1130/G21631.1

Shchepetilnikova, V., Solé, J., Solari, L.A. & Abdullin, F. 2015. A chronological and chemical zircon study of some pegmatite dikes and lenses from the central part (Ayoquezco–Ejutla) of the Oaxacan Complex, southern Mexico. Revista Mexicana Ciencias Geológicas, 32 (1): 123–143.

Slagstad, T., Roberts, N.M.W., Marker, M., Røhr, T.S. & Schiellerup, H. 2013a. A non–collisional, accretionary Sveconorwegian Orogen. Terra Nova, 25(1): 30–37. https://doi.org/10.1111/ter.12001

Slagstad, T., Roberts, N.M.W., Marker, M., Røhr, T.S. & Schiellerup, H. 2013b. A non– collisional, accretionary Sveconorwegian Orogen–Reply. Terra Nova 25(2): 169–171. https://doi.org/10.1111/ter.12028

Slagstad, T., Roberts, N.M.W. & Kulakov, E. 2017. Linking orogenesis across a supercontinent; the Grenvillian and Sveconorwegian margins on Rodinia. Gondwana Research, 44: 109–115. https://doi.org/10.1016/j.gr.2016.12.007

Solari, L.A., Keppie, J.D., Ortega–Gutiérrez, F., Cameron, K.L., Lopez, R. & Hames, W.E. 2003. 990 and 1100 Ma Grenvillian tectonothermal events in the northern Oaxacan Complex, southern Mexico: roots of an orogen. Tectonophysics, 365(1–4): 257–282. https://doi.org/10.1016/S0040-1951(03)00025-8

Solari, L.A., Ortega–Gutiérrez, F., Elías–Herrera, M., Ortega–Obregón, C., Macías–Romo, C. & Reyes–Salas, M. 2013. Detrital provenance of the Grenvillian Oaxacan Complex, southern Mexico: a zircon perspective. International Journal of Earth Sciences, 103(5): 1301–1315. https://doi.org/10.1007/s00531-013-0938-9

Tassinari, C. & Macambira, M. 1999. Geochronological provinces of the Amazonian Craton. Episodes, 22(3): 174–182.

Teixeira, W., Geraldes, M.C., Matos, R., Ruiz, A.S., Saes, G. & Vargas–Mattos, G. 2010. A review of the tectonic evolution of the Sunsás Belt, SW Amazonian Craton. Journal of South American Earth Sciences, 29(1): 47–60. https://doi.org/10.1016/j.jsames.2009.09.007

Teixeira, W., Reis, N.J., Bettencourt, J.S., Klein, E.L. & Oliveira, D.C. 2019. Intraplate Proterozoic magmatism in the Amazonian Craton reviewed: Geochronology, crustal tectonics and global barcode matches. In: Srivastava, R.K., Ernst, R.E. & Peng, P. (editors), Dyke swarms of the world: A modern perspective. Springer Geology, p. 111–154. Singapore. https://doi.org/10.1007/978-981-13-1666-1_4

Thompson, A.B. & England, P.C. 1984. Pressure—Temperature—Time paths of regional metamorphism II. Their inference and interpretation using mineral assemblages in metamorphic rocks. Journal of Petrology, 25(4): 929–955. https://doi.org/10.1093/petrology/25.4.929

Tirone, M., Ganguly, J., Dohmen, R., Langenhorst, F., Hervig, R. & Becker, H.W. 2005. Rare earth diffusion kinetics in garnet: Experimental studies and applications. Geochimica et Cosmochimica Acta, 69(9): 2385–2398. https://doi.org/10.1016/j.gca.2004.09.025

Tohver, E., van der Pluijm, B.A., van der Voo, R., Rizzotto, G. & Scandolara, J.E. 2002. Paleogeography of the Amazon Craton at 1.2 Ga: Early Grenvillian collision with the Llano segment of Laurentia. Earth and Planetary Science Letters, 199(1–2): 185–200. https://doi.org/10.1016/S0012-821X(02)00561-7

Tohver, E., Bettencourt, J.S., Tosdal, R., Mezger, K., Leite, W.B. & Payolla, B.L. 2004. Terrane transfer during the Grenville Orogeny: Tracing the Amazonian ancestry of southern Appalachian basement through Pb and Nd isotopes. Earth and Planetary Science Letters, 228(1–2): 161–176. https://doi.org/10.1016/j.epsl.2004.09.029

Tohver, E., van der Pluijm, B.A., Scandolâra, J. & Essene, E.J. 2005. Late Mesoproterozoic deformation of SW Amazonia (Rondônia, Brazil): Geochronological and structural evidence for collision with southern Laurentia. Journal of Geology, 113(3): 309–323. https://doi.org/10.1086/428807

Tschanz, C.M., Jimeno, A. & Cruz, J. 1969. Geology of the Sierra Nevada de Santa Marta area (Colombia): Preliminary report. Ingeominas, 288 p. Bogotá.

Tschanz, C.M., Marvin, R.F., Cruz, J., Mehnert, H.H. & Cebula, G.T. 1974. Geologic evolution of the Sierra Nevada de Santa Marta, northeastern Colombia. Geological Society of America Bulletin, 85(2): 273–284. https://doi.org/10.1130/0016-7606(1974)85<273:GEOTSN>2.0.CO;2

Urbani, F., Baquero, M., Grande, S., Valencia, V., Martens, U., Pindell, J., Mendi, D. & Gomez, A. 2015. Nuevas edades U–Pb de rocas ígneo–metamórficas el Estado Yaracuy. Boletín de La Academia de Ciencias Físicas, Matemáticas y Naturales, LXXV(2): 33–52.

Valley, J.W., Lackey, J.S., Cavosie, A.J., Clechenko, C.C., Spicuzza, M.J., Basei, M.A.S., Bindeman, I.N., Ferreira, V.P., Sial, A.N., King, E.M., Peck, W.H., Sinha, A.K. & Wei, C.S. 2005. 4.4 billion years of crustal maturation: Oxygen isotope ratios of magmatic zircon. Contributions to Mineralogy and Petrology, 150: 561–580. https://doi.org/10.1007/s00410–005–0025–8

van der Lelij, R., Spikings, R., Ulianov, A., Chiaradia, M. & Mora, A. 2016. Palaeozoic to Early Jurassic history of the northwestern corner of Gondwana, and implications for the evolution of the Iapetus, Rheic and Pacific Oceans. Gondwana Research, 31: 271–294. https://doi.org/10.1016/j.gr.2015.01.011

van Orman, J.A., Grove, T.L., Shimizu, N. & Layne, G.D. 2002. Rare earth element diffusion in a natural pyrope single crystal at 2.8 GPa. Contributions to Mineralogy and Petrology, 142(4): 416–424. https://doi.org/10.1007/s004100100304

Vervoort, J.D. & Blichert–Toft, J. 1999. Evolution of the depleted mantle: Hf isotope evidence from juvenile rocks through time. Geochimica et Cosmochimica Acta, 63(3–4): 533–556. https://doi.org/10.1016/S0016–7037(98)00274–9

Vervoort, J. & Patchett, P. 1996. Behavior of hafnium and neodymium isotopes in the crust: Constraints from Precambrian crustally derived granites. Geochimica Et Cosmochimica Acta, 60(19): 3717–3733.

Weber, B. & Köhler, H. 1999. Sm–Nd, Rb–Sr and U–Pb geochronology of a Grenville terrane in southern Mexico: Origin and geologic history of the Guichicovi Complex. Precambrian Research, 96(3–4): 245–262. https://doi.org/10.1016/S0301-9268(99)00012-1

Weber, B. & Schulze, C.H. 2014. Early Mesoproterozoic (>1.4 Ga) ages from granulite basement inliers of SE Mexico and their implications on the Oaxaquia concept: Evidence from U–Pb and Lu–Hf isotopes on zircon. Revista Mexicana de Ciencias Geológicas, 31(3): 377–394.

Weber, B., Scherer, E.E., Schulze, C., Valencia, V.A., Montecinos, P., Mezger, K. & Ruiz, J. 2010. U–Pb and Lu–Hf isotope systematics of lower crust from central–southern Mexico: Geodynamic significance of Oaxaquia in a Rodinia Realm. Precambrian Research, 182(1–2): 149–162. https://doi.org/10.1016/j.precamres.2010.07.007

Weber, B., González–Guzmán, R., Manjarrez–Juárez, R., Cisneros de León, A., Martens, U., Solari, L., Hecht, L., Valencia, V. 2018. Late Mesoproterozoic to early Paleozoic history of metamorphic basement from the southeastern Chiapas Massif Complex, Mexico, and implications for the evolution of NW Gondwana. Lithos, 300–301: 177–199. https://doi.org/10.1016/j.lithos.2017.12.009

Weber, B., Schmitt, A.K., Cisneros de León, A. & González–Guzmán, R. 2019. Coeval early Ediacaran breakup of Amazonia, Baltica, and Laurentia: Evidence from micro–baddeleyite dating of dykes from the Novillo Canyon, Mexico. Geophysical Research Letters, 46(4): 2003–2011. https://doi.org/10.1029/2018GL079976

Weil, A.B, van der Voo, R., Mac Niocaill, C. & Meert, J. 1998. The Proterozoic supercontinent Rodinia: Paleomagnetically derived reconstructions for 1100 to 800 Ma. Earth and Planetary Science Letters, 154(1–4): 13–24. https://doi.org/10.1016/S0012-821X(97)00127-1

Westphal, M., Schumacher, J.C. & Boschert, S. 2003. High–temperature metamorphism and the role of magmatic heat sources at the Rogaland Anorthosite Complex in Southwestern Norway. Journal of Petrology, 44(6): 1145–1162. http://doi.org/10.1093/petrology/44.6.1145

Explanation of Acronyms, Abbreviations, and Symbols:

AMCG	Anorthosite–Mangerite–Charnockite–Granite
CHUR	Chondritic uniform reservoir
E–MORB	Enriched–mid ocean ridge basalt
FM	Florencia Margin
GAPES	Garnet–Pyroxene–Plagioclase–Quartz geobarometer of Eckert et al. (1991)
GHS	Greater Himalayan Sequence
GLOOS	Global subducting sediments
LA–ICP–MS	Laser ablation–inductively coupled plasma–mass spectrometry
LIP	Large igneous province
RNJ	Río Negro–Juruena
RSI	Rondonian–San Ignacio
SAMBA	South America Baltica
SIMS	Secondary ion mass spectrometry
SM	Solita Margin
TIMS	Thermal ionization mass spectrometry
TWQ	Software and thermodynamic database of Berman (1991)
UHT	Ultra–high temperature
VM	Vergel Margin

Author's Biographical Notes

Mauricio Ibañez–MEJIA graduated as a geologist from the Universidad Nacional de Colombia, Bogotá, in 2007. He obtained MS (2010) and PhD (2014) degrees in petrology and geochemistry from the University of Arizona, USA, followed by two years as a W.O. Crosby postdoctoral fellow in the Massachusetts Institute of Technology in Cambridge, USA, and four years as an assistant professor in the Department of Earth and Environmental Sciences at University of Rochester, USA. He is currently an assistant professor in the Department of Geosciences at the University of Arizona, USA. His main research interests are in the fields of isotope geochemistry, geochronology, petrology, and crustal evolution.

Volume 1

Chapter 7

Paleontology of the Paleozoic Rocks of the Llanos Orientales Basin, Colombia

https://doi.org/10.32685/pub.esp.35.2019.07
Published online 2 June 2020

Hernando DUEÑAS–JIMÉNEZ[1*], Victoria Elena CORREDOR–BOHÓRQUEZ[2], and Jorge MONTALVO–JÓNSSON[3]

1 hdjbioss@yahoo.com
hduenas@sgc.gov.co
Academia Colombiana de Ciencias Exactas, Físicas y Naturales
Carrera 28A n.° 39A–63
Bogotá, Colombia
Servicio Geológico Colombiano
Dirección de Hidrocarburos
Diagonal 53 n.° 34–53
Bogotá, Colombia

2 vcorredor@sgc.gov.co
Servicio Geológico Colombiano
Dirección de Geociencias Básicas
Diagonal 53 n.° 34–53
Bogotá, Colombia

3 jemontalvom@unal.edu.co
Departamento de Geociencias
Universidad Nacional de Colombia
Carrera 30 n.° 45–03
Bogotá, Colombia

* Corresponding author

Abstract Paleontological data on Paleozoic fossils in the Llanos Orientales Basin of Colombia are presented here. Some of these data have not been published previously and come from technical reports prepared for Oil Operators that now form part of the Servicio Geológico Colombiano library. These data contribute to a better understanding of the Paleozoic Era in Colombia. During the Devonian Period, some organisms managed to occupy terrestrial environments. Before that, life occurred exclusively in marine environments. This progression of life included terrestrial plants that produced fern spores. In the principal depocenters of the Llanos Orientales Basin, up to 6000 m of Paleozoic sedimentites are present. They include (1) Cambrian strata, determined by associations of acritarchs; (2) Ordovician strata, identified in many wells by the presence of acritarchs, chitinozoans, very well–preserved trilobites (*Jujuyaspis* spp., *Helieranella negritoensis*, and *Triarthus* sp.), and graptolites (*Janagraptus* sp., *Didymograptus extensus*, and *Dictyonema* spp.); (3) Silurian by the presence of acritarchs *Domasia bispinosa*, *Dactylofusa* spp. and *Eupoikilofusa* spp.; and finally, (4) Devonian and Carboniferous strata, which are erosional remnants that contain characteristic associations of trilete spores and acritarchs. Sedimentites from the Permian have not been in the basin, most likely because they were periods of erosion or nondeposition. The good preservation of the palynomorphs is evidence that the Paleozoic rocks in the Llanos Orientales Basin are not metamorphosed and should not be considered as the economic basement of the basin.

Keywords: *Paleozoic, palynomorphs, acritarchs, trilobites, Llanos Basin.*

Resumen Se presenta información paleontológica sobre los fósiles paleozoicos del subsuelo de la Cuenca de los Llanos Orientales de Colombia. Parte de esta información no ha sido publicada previamente y proviene de reportes técnicos preparados para Operadores Petroleros que hoy en día forman parte de la biblioteca del Servicio Geológico Colombiano. Estos datos contribuyen a comprender mejor la era paleozoica en Colombia. Durante el Devónico, algunos organismos lograron ocupar el medio terrestre. Antes de eso, la vida ocurría exclusivamente en ambientes marinos. Esta progresión de la vida incluyó plantas terrestres que producían esporas de helechos. En los principales depocentros de la Cuenca de los Llanos Orientales se presentan hasta 6000 m de rocas sedimentarias de edad paleozoica. Estas incluyen (1) estratos cámbricos, determinados con base en asociaciones de acritarcos; (2) estratos ordovícicos, identificados en un gran número de pozos por la presencia de acritarcos, quitinozoarios, trilobites muy

Citation: Dueñas–Jiménez, H., Corredor–Bohórquez, V.E. & Montalvo–Jónsson, J. 2020. Paleontology of the Paleozoic rocks of the Llanos Orientales Basin, Colombia. In: Gómez, J. & Mateus–Zabala, D. (editors), The Geology of Colombia, Volume 1 Proterozoic – Paleozoic. Servicio Geológico Colombiano, Publicaciones Geológicas Especiales 35, p. 133–148. Bogotá. https://doi.org/10.32685/pub.esp.35.2019.07

bien conservados (*Jujuyaspis* spp., *Helieranella negritoensis* y *Triarthus* sp.) y graptolites (*Janagraptus* sp., *Didymograptus extensus* y *Dictyonema* spp.); (3) sedimentitas silúricas caracterizadas por la presencia de los acritarcos *Domasia bispinosa*, *Dactylofusa* spp., y *Eupoikilofusa* spp.; y finalmente, (4) estratos devónicos y carboníferos, que se presentan como pequeños remanentes erosionales y contienen asociaciones características de esporas triletes y acritarcos. Sedimentitas del Pérmico no han sido reportadas en la cuenca, muy probablemente porque fueron periodos de erosión o no depósito de sedimentos. El buen estado de conservación de los palinomorfos permite determinar que las rocas paleozoicas en la Cuenca de los Llanos Orientales no se encuentran metamorfizadas y por ello no deben ser consideradas como el basamento económico de la cuenca.
Palabras clave: *Paleozoico, palinomorfos, acritarcos, trilobites, Cuenca de los Llanos.*

1. Introduction

During the Paleozoic Era, life moved from being exclusively marine dwellers to occupying terrestrial environments, especially during the Devonian Period (Buatois et al., 1998). In the early Paleozoic, trilobites, graptolites, and crinoids dominated the oceans; however, in the late Paleozoic, terrestrial plants, fish, and reptiles already shared the world. The Paleozoic featured two of the most important events in the history of life on planet Earth: the Cambrian faunal explosion (e.g., Erwin et al., 2011; Marshall, 2006; Shu, 2008) and the Permian mass extinction, which resulted in the loss of approximately 90% of marine organisms (e.g., Burgess et al., 2014; Payne & Clapham, 2012; Raup, 1979; Raup & Sepkoski, 1982).

Multicellular organisms, which began their evolution during the Precambrian, experienced a sudden increase in quantity and diversity at the beginning of the Cambrian Period (Erwin et al., 2011). This incremental diversification of organisms strengthened life on the planet. Most of the phyla appeared within a few millions of years, and by the Cambrian Period, all the phyla that live today had appeared. The explosion of life in the Cambrian has been called "The Dilemma of Charles Darwin", who could not fit it into his theory of evolution by natural selection (Darwin, 1859).

The colonization of the continents began slowly during the late Silurian Period and became entrenched during the Devonian Period (Buatois et al., 1998). During the Carboniferous Period, the vegetation was quite abundant in large marshes, especially in Europe and North America; thus, plant remains were deposited and gave rise to thick coal deposits (e.g., Ogg et al., 2016).

During the Paleozoic, the Amazonian Craton became one of the continental nuclei (Cordani et al., 2009), around which very thick sedimentary sequences accumulated (peri–Gondwanic). These Paleozoic strata have been preserved in the Eastern and Western Venezuela (Barinas and Apure Basins) and in the Llanos, Colombia. These Paleozoic sequences form a belt that partly coincides with what Feo–Codecido et al. (1984) and Sinanoglu (1984) called the Cambrian belt.

2. Paleozoic in the Llanos Orientales Basin

In the Llanos Orientales Basin as well as in the Eastern Venezuela Basin, Paleozoic strata are widely distributed as a basal sedimentary sequence. They occur in large subsurface structures, as can be observed in the seismic lines Q–85–1275 and RLJ–2040 (Figure 1).

The correlations between Paleozoic sequences in the Llanos Orientales and Paleozoic outcrops in the Eastern Cordillera are very imprecise. The Paleozoic outcrops in the Eastern Cordillera appear as patches in the geological scheme without direct connection with the regional geology. Furthermore, the Paleozoic sedimentites of the Eastern Cordillera have suffered very strong thermal alterations, which contrasts with the weak thermal alteration of the Paleozoic sedimentites in the Llanos Orientales Basin. The scarce stratigraphic information from the Paleozoic outcrops in the Eastern Cordillera does not allow a trustworthy correlation between the two Paleozoic sequences.

Cuttings samples from the Negritos–1 well at 2698 m yielded an association of Ordovician (Tremadocian) palynomorphs (Figure 2), while at a depth of 3206.2 m, the well reached the top of the igneous–metamorphic basement. The two above mentioned surfaces can be readily followed on the seismic lines. Furthermore, with the interpretation of seismic lines, it was estimated that the thickness of the Paleozoic sedimentites in the Quenane area may exceed 6000 m (Dueñas, 2002).

On the RLJ–2040 seismic line (Figure 3) from the Eastern Venezuela Basin, it is possible to observe, highlighted in green, the unconformity at the top of the Paleozoic strata and Paleozoic structural folds due to compression. The thickness of these Paleozoic strata is ca. 2700 m, and these strata include the Carrizal and Hato Viejo Formations, which were considered by Feo–Codecido et al. (1984) to be Cambrian or older sedimentites. From Figures 2 and 3, it is possible to deduce the presence of thick coeval Paleozoic sedimentary successions in the Llanos Basin of Colombia and the Barinas Basin of Venezuela.

Traditionally, the Paleozoic sedimentites in the Llanos Orientales Basin have received little attention because they

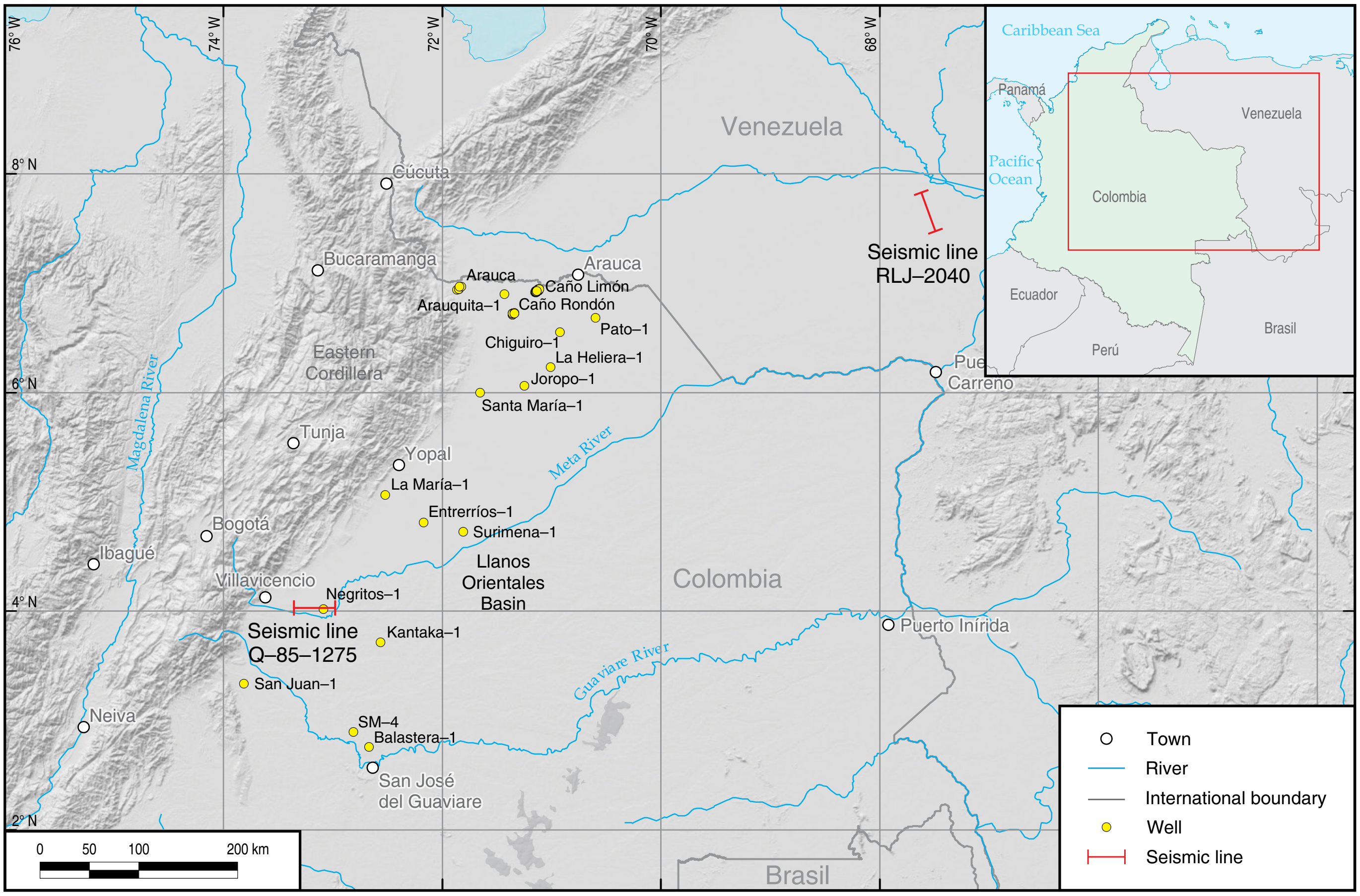

Figure 1. Locations of seismic lines Q–85–1275 and RLJ–2040 and some of the wells in which Paleozoic fossils have been recovered in the Llanos Orientales Basin.

were erroneously considered metamorphic rocks and therefore the economic basement of the basin. Many wells ended immediately after reaching the top of the Paleozoic strata that were assumed to be metamorphic. Thus, no analysis (biostratigraphic or geochemical) was carried out on the Paleozoic samples. In the central part of the basin in the Rancho Hermoso field, the color and excellent preservation of the Ordovician acritarchs indicate that these sedimentites have reached the oil generation window. Lithological and geochemical data suggest that these Paleozoic sedimentites can be interpreted as source and reservoir rocks (Arminio et al., 2013; Dueñas, 2001, 2002).

2.1. Cambrian

It has been hypothesized that during the Cambrian Period, sea level was relatively low (Haq & Schutter, 2008; Maruyama et al., 2014) and that the climate was cold. However, the climate was significantly warmer than in previous times, during which the planet suffered intense global glaciations (Maruyama & Santosh, 2008).

The Cambrian rocks are the oldest rocks in which it is possible to find abundant fossils of multicellular organisms that are more complex than sponges or jellyfishes (e.g., Shu, 2008; Zhang et al., 2014). Most of the current phyla appeared suddenly at the beginning of the Cambrian, during the greatest diversification of live in the history of the planet (Smith & Harper, 2013). Trilobites appeared in the oceans during this period (Briggs, 2015). During the Cambrian, the environment became more hospitable to life than that in the previous Ediacaran.

The Chiguiro–1 well (Figure 1) drilled in the northeastern part of the basin encountered Cambrian sedimentites at a depth between 2578.6 and 3602.7 m. Cuttings samples, as well as conventional cores, yielded Cambrian palynological associations that were characterized by the presence of *Retisphaeridium dichamerum*, *Crystallinium ovillense*, *C. cambriense*, *Satka colonialica*, *Cymatiosphaera postii*, *Trachysphaeridium laminarum*, *Leiosphaeridia* spp., *Archaeotrichion* spp., and others. These strata deposited in a marginal marine environment have been dated as middle to late Cambrian. The sedimentites between 2932.2 and 3340.6 m presented acritarch associations with *Adara matutina, Micrhystridinium lubomiense*, *M. notatum*,

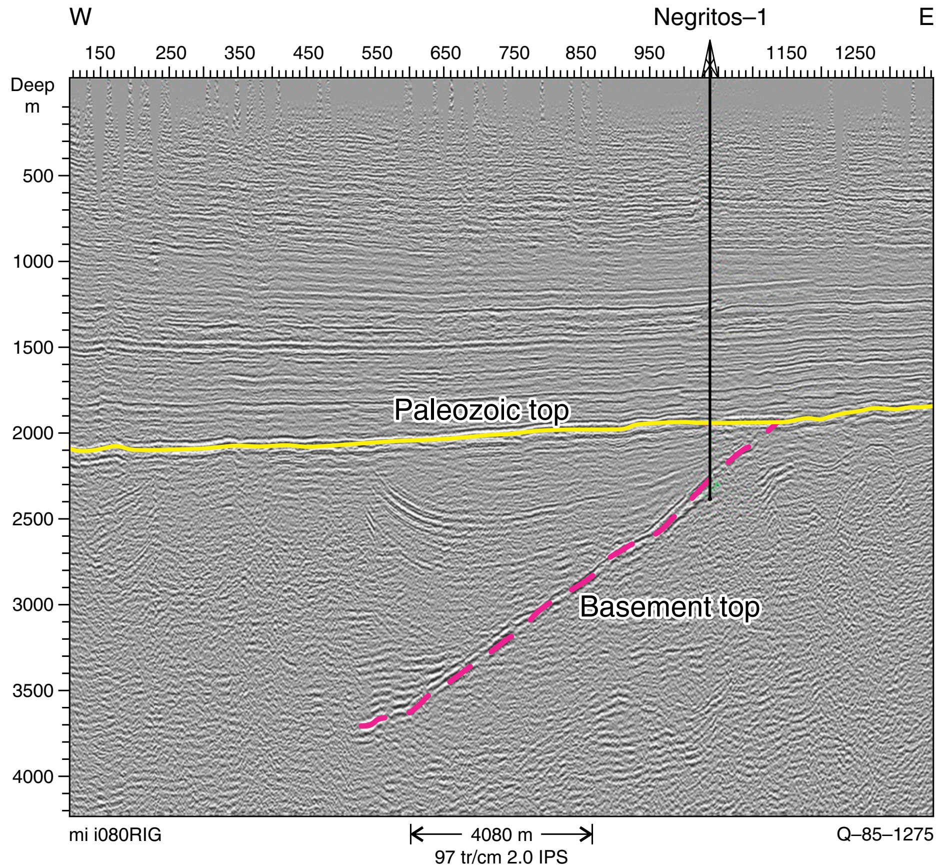

Figure 2. Seismic line Q–85–1275 including the Negritos–1 well, adapted from Dueñas (2002). The position of the top of the Paleozoic is highlighted in yellow, and the position of the top of the basement is highlighted in pink, showing a wedge of Paleozoic sedimentites that can reach 6000 m in thickness.

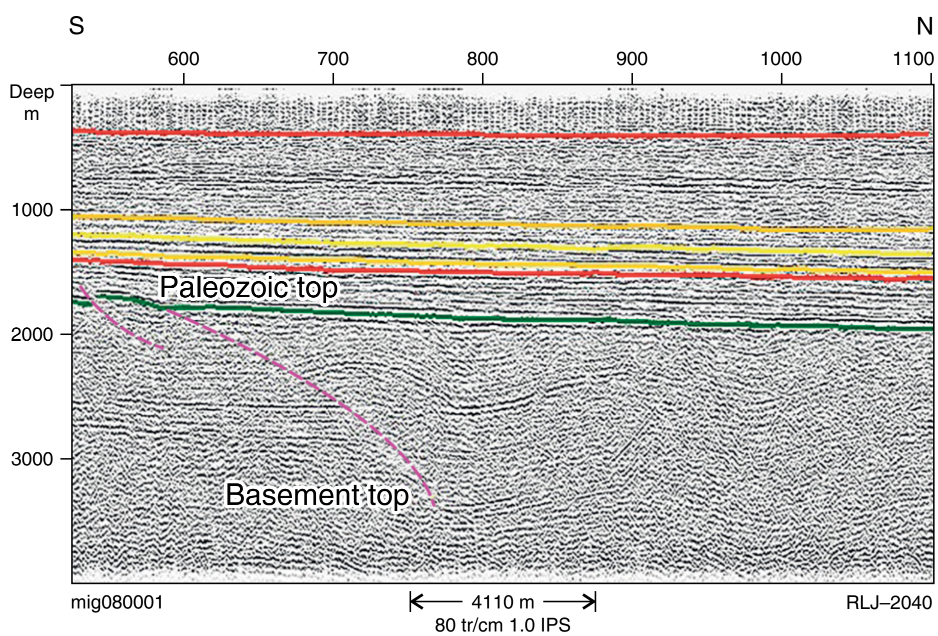

Figure 3. Seismic line RLJ–2040. The unconformity at the top of the Paleozoic sedimentites is highlighted in green and the top of the basement is highlighted in pink.

M. multipliciflagellata, *Synsphaeridium conglutinatum*, *Comasphaeridium stigosum*, *Dictyotidium birvetense*, *Cymatiosphaera ovillensis*, and *Timofeevia brevibifurcata*. This acritarch association represents a marginal marine depositional environment and indicates an early to middle Cambrian age. Associations of palynomorphs between 3368 and 3602.7 m present an abundant acritarch recovery that included *Zonhosphaeridium ovillensis*, *Tasmanites* cf. *bobrowskii*, *Micrhystridium paucoloquetrum,* and *Acrum* cf. *cylindricum* of early Cambrian age, which were deposited in a shallow marine environment. It is important to note that in deeper sedimentites, it is possible to determine the presence of Ediacaran rocks (Dueñas–Jiménez & Montalvo–Jónsson, 2020). This is the only well in the Llanos Orientales Basin in which the systematic study of samples allowed us to obtain a biostratigraphic subdivision of the Cambrian.

The Pato–1 in the northeastern side of the Llanos Orientales Basin (Figure 1) meets Paleozoic sedimentites at depths between 2133.6 and 2194.6 m. The cuttings samples between 2133.6 and 2183.9 m yielded very poor associations of palynomorphs that represent a marine depositional environment and a Cambrian age. Conventional core samples between depths of 2185.4 and 2194.6 m yielded Ediacaran palynomorphs (Dueñas, 2011). The Chiguiro–1 well and the Pato–1 well are located in the northeastern part of the basin and are related to the so–called Arauca Graben (Arminio et al., 2013).

In the Eastern Venezuela Basin, Sinanoglu (1984) reported Cambrian and shallow marine depositional environments in core samples from the Carrizal Formation. The acritarch associations from these samples are characterized by the presence of *Archaediscin umbonulata*, *Granomarginata* spp., *Skiagia ciliosa*, *S.* cf. *ornata*, *S. compressa,* and *Baltisphaeridium compressum*.

2.2. Ordovician

In several parts of the world, global sea level was significantly higher than at present (Miller, 1997), representing the greatest transgression of the Paleozoic Era (Vail et al., 1977). During the Ordovician, the Amazonian Craton was located in the Southern Hemisphere near the pole, while the Northern Hemisphere was practically an open sea (Torsvik & Cocks, 2013). The most evolved organisms that diversified during the Cambrian continued to flourish, increasing their diversity in what is known as the Great Ordovician Biodiversification Event (Webby et al., 2004).

In the Llanos Orientales Basin, a large number of wells have been drilled through Ordovician strata. Dueñas (2011) reported the presence of Ordovician acritarchs and chitinozoans in the wells and in the depths listed in Table 1. Ordovician strata occur throughout the Llanos Orientales Basin. These Paleozoic strata are characterized by an abundance of well–preserved marine palynomorphs (acritarchs and chitinozoans) and graptolites.

In a large number of old biostratigraphic reports related to the Llanos Orientales Basin, the English nomenclature was used for the Ordovician. It is therefore difficult to equate the data obtained at that time with the International Chronostratigraphic Chart (Figure 4a, 4b) (Cohen et al., 2013). Figure 4b presents a comparison between the names used in England and those used by the International Stratigraphic Commission for the Ordovician (Bergström et al., 2009).

An intense glacial period occurred in the Late Ordovician (Finnegan et al., 2011) during the Hirnantian Age at ca. 445.2 Ma (see compilation in Sheehan, 2001). That event has been associated with the mass extinction at the end of the Ordovician (Delabroye & Vecoli, 2010), which was the first of the great Phanerozoic extinctions (Sepkoski, 1996). Between 60 and 85% of taxa were lost (e.g., Delabroye & Vecoli, 2010; Isaza & Campos, 2007). No strata of glacial origin have been reported in the Llanos Orientales Basin. The Ordovician Period was very active tectonically around the world (e.g., Torsvik & Cocks, 2013), and the fact that no strata of the Upper Ordovician interval have been found in the Llanos Orientales Basin would indicate that during this interval, there was a period of erosion or nondeposition.

2.3. Silurian

The Silurian has been considered a period of erosion or nondeposition in the Llanos Orientales Basin. However, recent publications (Cediel, 2019; Kroeck et al., 2019) mention that the San Juan–1 well, drilled by Nomeco Latin America in 1988 near the serranía de La Macarena, reported the presence of *Domasia bispinosa*, a restricted Silurian acritarch, at 6905 ft.

Ecopetrol (2010) carried out palynological analysis in cuttings samples from the Paso Real–1 well, located in the southwestern part of the Llanos Basin. From 2140 to 2360 ft eight samples were prepared that yielded good acritarchs assemblages characterized by the presence of *Dactilofusa marahensis, D. oblancae*, *Eupoikiofusa cabottii*, *E. cantábrica*, *Neoveryhachium tentaculiformis*, *N. carminae*, and *Villasacapsula* spp., among others. An Early Silurian age and marine environments of deposit were assigned to this interval.

2.4. Devonian – Carboniferous

These periods cover the interval between ca. 419.2 and 298.9 Ma BP (Cohen et al., 2013). The Devonian is known as the age of the fish, in reference to the great diversification of fish during the Devonian (Benton, 1986, 2005). However, other very significant events also occurred, including the evolution of the first tetrapods, the evolution of terrestrial plants, the appearance of the first gymnosperms, and the evolution of insects and other terrestrial and marine animals. During these periods, the take-

Table 1. Wells and depth intervals where Ordovician acritarchs and chitinozoans were found. Adapted from Dueñas (2011).

Oil well name	Total deep (ft)	Terrane elevation (ft)	Latitude N	Longitude W
Almagro–1	7000	665.85	3° 54’ 7.17”	72° 39’ 45.16”
Apiay–4	12 065	950	4° 4’ 53.64”	73° 23’ 16.48”
Camoa–1	7492	936.23	3° 38’ 18.35”	73° 23’ 54.11”
Caño Cumare–1	10 583	783.62	6° 16’ 48.07”	71° 14’ 57.57”
Caño Duya–1	6196	132.89	4° 56’ 44.48”	71° 22’ 58.15”
Chavivia–1	7824	653.61	4° 13’ 25.41”	72° 13’ 52.81”
Cocli SW–1	940	647.29	4° 20’ 6.92”	71° 22’ 56.11”
Entrerrios–1	10 714.1	557.51	4° 48’ 12.97”	72° 10’ 28.6”
Fuente–1X (1821–1X)	9168	966.01	3° 29’ 12.16”	73° 36’ 41.46”
Guariloque–3	6900	479	4° 51’ 56.25”	71° 36’ 54.13”
Joropo–1	8200	328.79	6° 4’ 17.01”	71° 14’ 20.02”
Kantaka–1	5676	603	3° 42’ 40.39”	72° 33’ 53.22”
La Cabaña–1	17 569	650.03	5° 2’ 51.67”	72° 27’ 15.53”
La Heliera–1	8961	439.69	6° 14’ 47.95”	70° 59’ 57.36”
Metica–1	11 171	548.42	4° 16’ 4.64”	72° 50’ 34.41”
Negritos–1	10 452.5	611.87	4° 1’ 40.43”	73° 4’ 36.07”
Ocelote–1	4817	649.39	4° 16’ 25.24”	71° 35’ 40.92”
Rancho Hermoso–1	10 710	169	5° 1’ 45.39”	71° 58’ 33.6”
Rondón–1	8134	447	5° 27’ 14.57”	71° 14’ 30.62”
S–11A (X–R–859) (STRAT–XR–11A)	8544	531.99	4° 29’ 57.23”	71° 37’ 14.75”
San Juan–1	6965	1459.97	3° 22’ 35.71”	73° 51’ 07.65”
Santa María–1	13 582	857.19	6° 0’ 31.1”	71° 38’ 34.17”
Simón–1	5780	558.6	4° 30’ 21.22”	71° 37’ 12.98”
Surimena–1	8324	486.24	4° 44’ 21.75”	71° 47’ 58.2”
Valdivia–1	6120	642.68	3° 54’ 34.41”	72° 39’ 36.85”

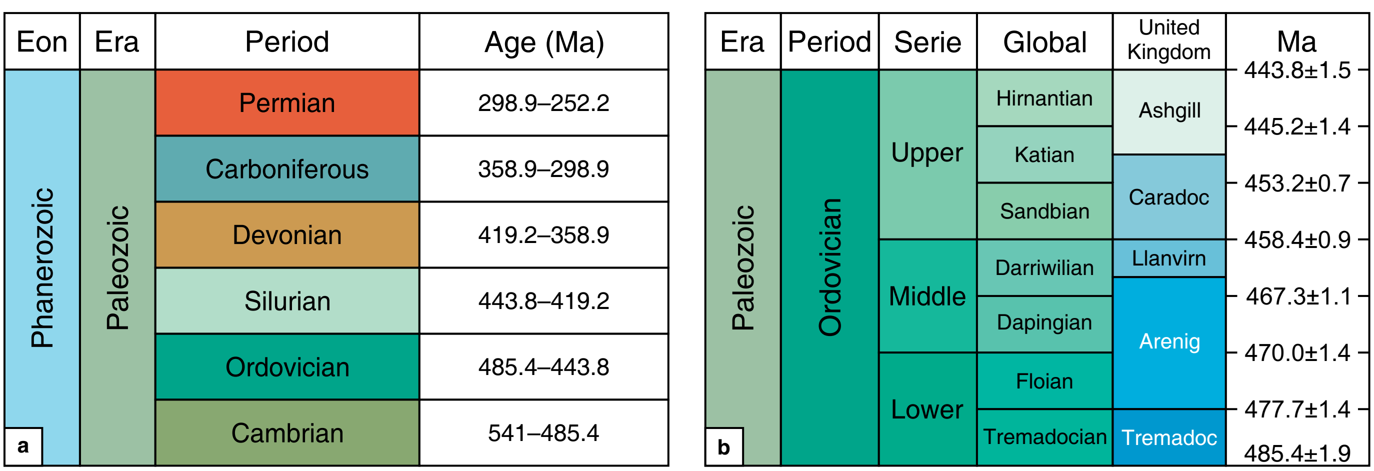

Figure 4. (a) Chronostratigraphic subdivisions of the Paleozoic. Adapted from Cohen et al. (2013). **(b)** Correlation between the current global nomenclature of 2017 and the classic Ordovician nomenclature used in the United Kingdom. Adapted from Bergström et al. (2009).

over of the continents by complex life forms progressed (e.g., Algeo & Scheckler, 1998; Davies & Gibling, 2013).

In the Llanos Orientales Basin, Dueñas (2001, 2011) reported the presence of Devonian strata in the Balastera–1, SM–4 (728.5–899.2 m), Surimena–1 and La Maria–1 (5273–5291.3 m) wells.

The cuttings samples from La María–1 well presented poor associations of trilete spores of genera *Archaeozonotriletes* and *Grandispora* with acritarchs of genera *Veryhachium*, *Baltisphaeridium,* and *Micrhystridium*, which indicates a Devonian age (Dueñas, 2001, 2011).

A very rich and diverse association of palynomorphs was recovered from cuttings samples of the SM–4 well (Figure 1), within which the presence of trilete spores and their association with acritarchs are highlighted (Dueñas & Césari, 2005, 2006). The analysis of these associations of palynomorphs permits assigning an early Carboniferous age to the 579.7–713.2 m interval, whereas from 713.2 to 906.8 m, the sedimentites drilled were assigned a Late Devonian age (Dueñas & Césari, 2006). The early Carboniferous trilete spores assemblages included *Spelaeotriletes triangulus*, *Retusotriletes crassus, Prolycospora rugulosa*, *Indotriradites dolianitii*, *Auroraspora solisorta*, *Apiculiretusispora multiseta*, *Vallatisporites* sp., *Anapiculatisporites concinnus*, *Grandispora spiculifera*, *Verrucosisporites nitidus*, *Spelaeotriletes pretiosus*, among others. Devonian trilete assemblages included *Teichertospora torquata*, *Ancyrospora* sp., and *Hystricosporites* spp. The SM–4 well is the only published record in which sedimentites of early Carboniferous age have been identified in the Llanos Orientales Basin. The assemblages of trilete spores and acritarchs are illustrated in Figures 5, 6, 7.

In the Eastern Venezuela Basin, Sinanoglu (1984) mentioned that several samples from the post–Carrizal unit in the Carrizal–1X, Tres Matas–X, Socorro–1X, Hato Viejo–1X, and Zuata–1X wells yielded palynological associations of Late Devonian – early Carboniferous age, which allows a correlation with the Llanos Orientales Basin of Colombia, based on the age reported for the SM–4 well.

2.5. Permian

No Permian strata have been reported in the Llanos Orientales Basin. The Permian was probably a time of nondeposition or intense erosion.

3. The Fauna of La Heliera–1 and Negritos–1 Wells

La Heliera–1 well is located in the northwestern part of the Llanos Orientales Basin (Figure 1). The well was drilled by Mobil Oil Company in 1959. After traversing 2499.4 m of a sequence of Cenozoic and Cretaceous strata, it cut Paleozoic strata, reaching a total depth of 2729.5 m (Dueñas, 2011). Within the Paleozoic sequence, two conventional cores were taken, the first one (Core 1) between depths of 2618.8 and 2628 m and the second (Core 2) between depths of 2728 and 2731.3 m. Several cuttings samples and some fragments of conventional cores were analyzed using palynological methods, yielding associations of acritarchs, chitinozoans, and graptolites of Early Ordovician age (Tremadocian) (Dueñas, 2011).

Core 1 showed an abundant, diverse, very well–preserved, and identifiable association of trilobites, some dendroid graptolites, and an orthid brachiopod of Early Ordovician age (Tremadocian). Core 2 did not present any identifiable fauna, but fragments of this core yielded Tremadocian palynomorphs.

Eighteen black–and–white photographs of the Tremadocian fauna have been preserved, some of which are reproduced in this chapter (Figures 8, 9, 10). The complete set of photographs and related reports have been delivered to the Museo Geológico Nacional José Royo y Gómez for preservation and consultation. The photographs of this fauna were analyzed by Clark (1960) and by Hughes (1980, 1982), who identified the trilobite *Jujuyaspis keideli* and the graptolite *Dictyonema* sp. It is necessary to bear in mind that several of the names assigned by Clark (1960), Hughes (1980, 1982), and Baldis et al. (1984), to the fauna found in these cores require a taxonomic revision based on modern criteria. The taxonomic revision of these names, as well as the description of new material found in the geological museum of the Universidad Nacional de Colombia, is in progress.

Based on the information from La Heliera–1 and Negritos–1 wells, Ulloa et al. (1982) presented a stratigraphic subdivision of the Ordovician in the Llanos Orientales Basin, establishing the Negritos Formation, which is composed of the Casanare, La Heliera, and Puerto López Members. In the Negritos–1 well, between depths of 2781 and 2784 m, a core (Core 2) was cut in which it was possible to identify the presence of the trilobite *Triarthus* sp., the graptolites *Janagraptus* sp. and *Didymograptus extensus,* and the brachiopod *Acotetra* sp. Dueñas (2011) reported that cuttings samples from Negritos–1 well located between 2743.2 and 3200.4 m presented quite abundant, well–preserved, and diverse associations of palynomorphs (acritarchs and chitinozoans) and graptolites of Tremadocian age deposited in near–shore sea environments.

Using black–and–white photographs of Core 1 from La Heliera–1 well, Baldis et al. (1984) determined the presence of the new genus *Helieranella*, which is represented by the species *Helieranella negritoensis* and the presence of the dendroid graptolite *Dictyonema flabeliforme*. They also described the trilobites *Jujuyaspis truncaticonis* and *Jujuyapsis colombiana* as new species. The association of trilobites allows a Tremadocian age to be

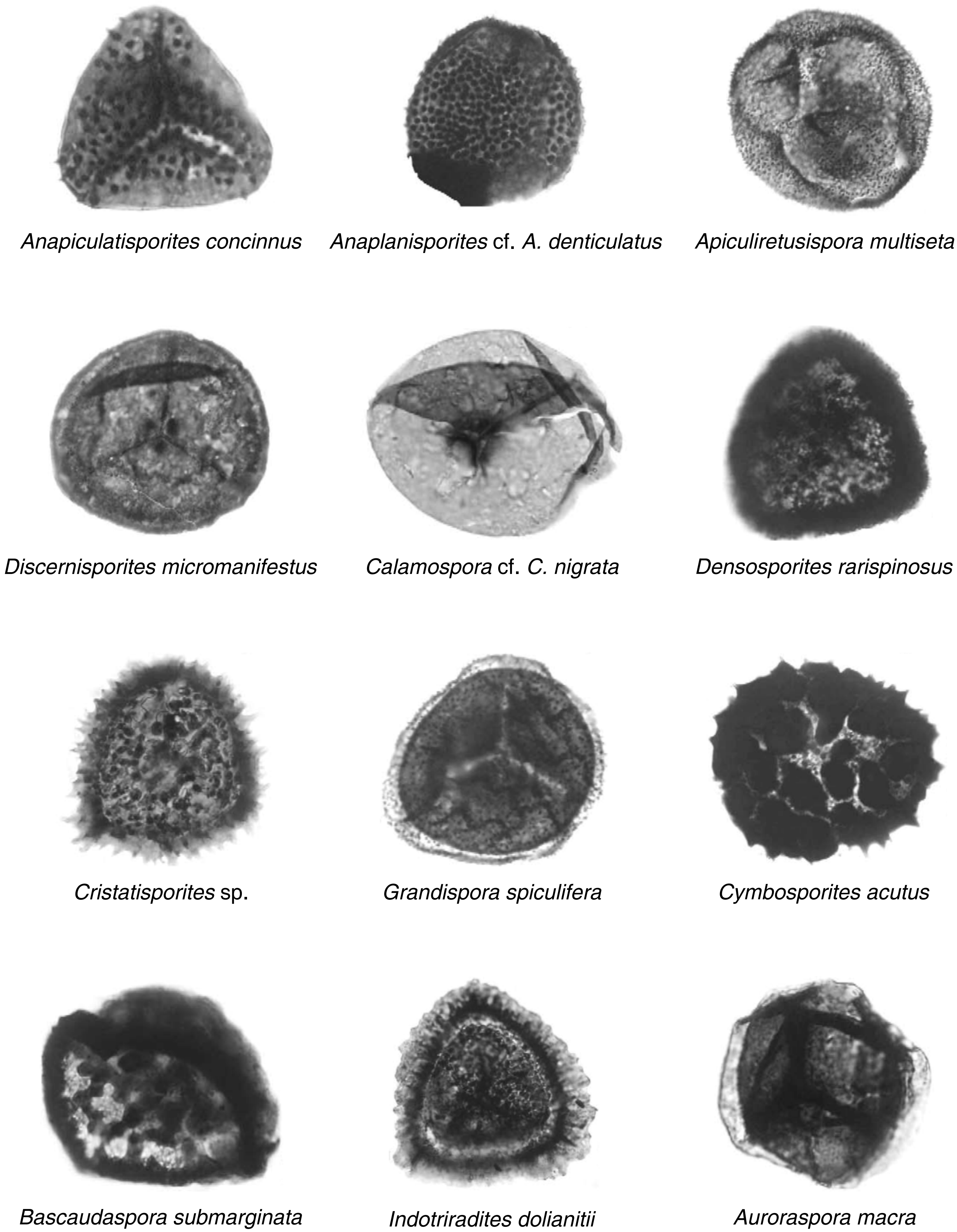

Figure 5. Carboniferous palynomorphs, SM–4 well. Adapted from Dueñas & Césari (2006). Photos without scale.

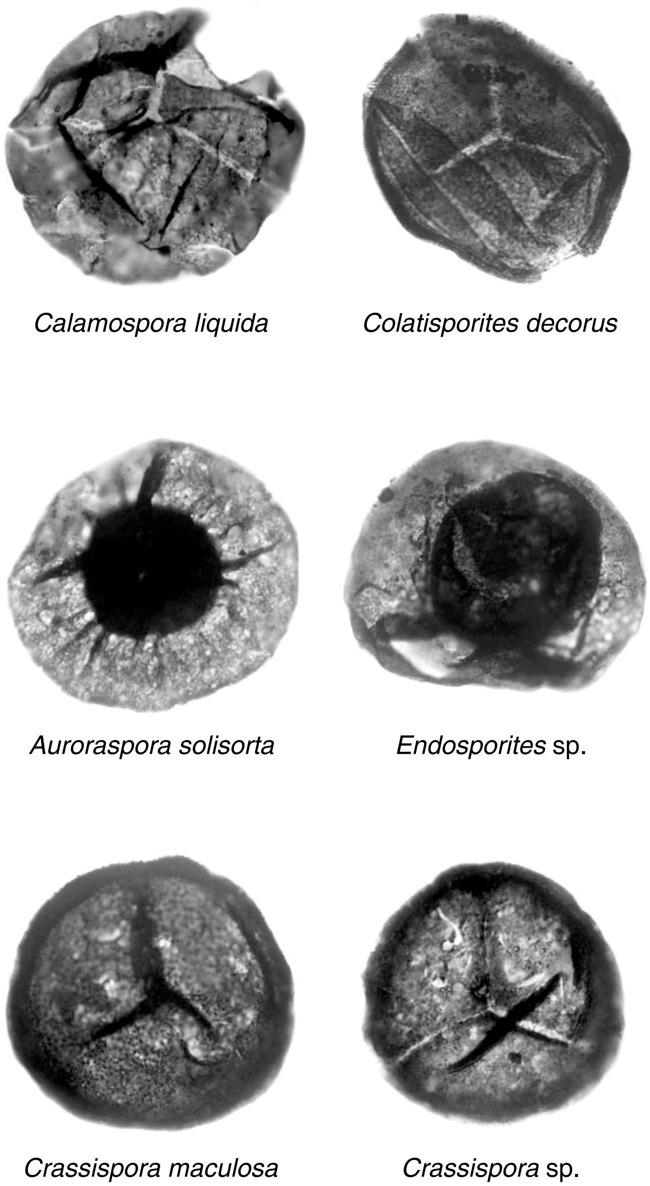

Figure 6. Carboniferous palynomorphs, SM–4 well. Adapted from Dueñas & Césari (2006). Photos without scale.

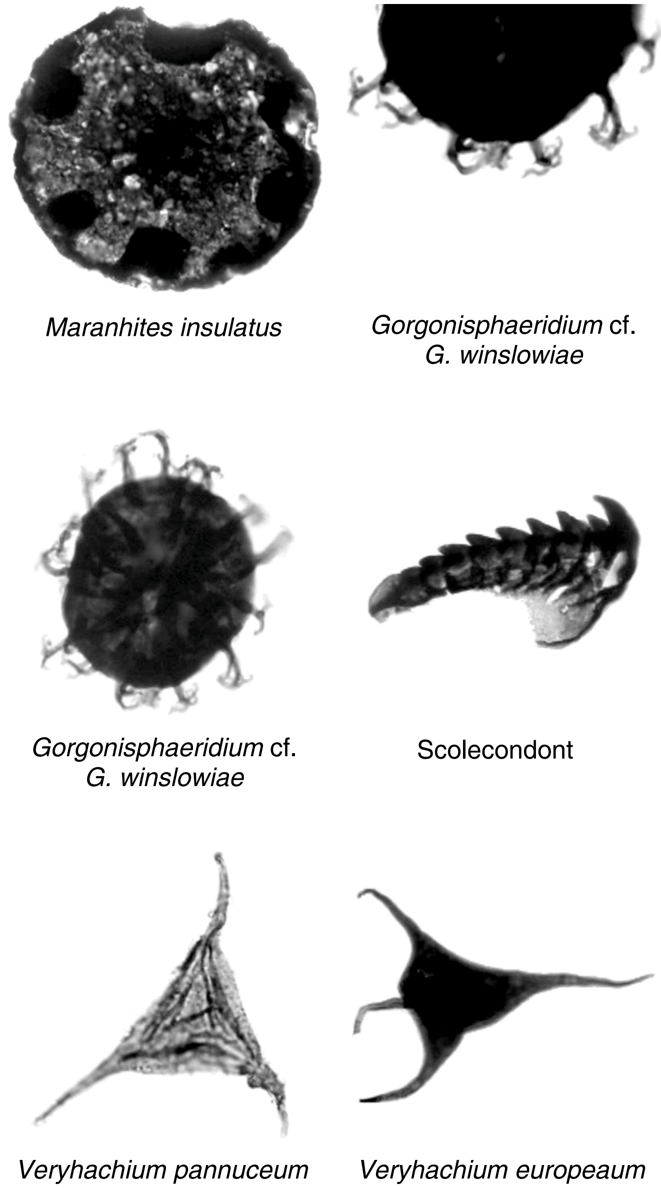

Figure 7. Carboniferous palynomorphs, SM–4 well. Adapted from Dueñas & Césari (2006). Photos without scale.

assigned to Core 1. Sedimentites from the Core 1 are part of La Heliera Member of the Negritos Formation, according to Ulloa et al. (1982), who also mentioned that sedimentites containing *Jujuyaspis* occur in Argentina, Bolivia, Colombia, and Venezuela.

4. Acritarchs and Other Fossils from the Araracuara Region

In the western part of the serranía de Chiribiquete, south of the Llanos Orientales Basin near the town of Araracuara, along the Caquetá River (Figure 11), a sandy section with sporadic presence of clays crops out and can reach more than 500 m in thickness (Bogotá, 1982; Galvis et al., 1979). From these clays, Théry et al. (1986) recovered abundant and well–preserved assemblages of acritarchs, including *Cymatiogalea cuvillieri, Acanthodiacrodium angustum*, *Acanthodiacrodium constrictum*, *Acanthodiacrodium lineatum*, *Acanthodiacrodium simplex*, *Acanthodiacrodium* cf. *filiferum*, *Veryhachium valiente*, *Veryhachium trispinosum*, *Dactylofusa striata*, *Leiosphaeridia* spp., *Priscogalea cortinula*, *Priscotheca raia*, *Dasydiacrodium eichwaldi*, *Dasydiacrodium* spp., and *Polygonium spinosum*. Théry et al. (1986) assigned an Ordovician age and a near–shore depositional environment to these sedimentites. This publication became the first record of acritarch associations in

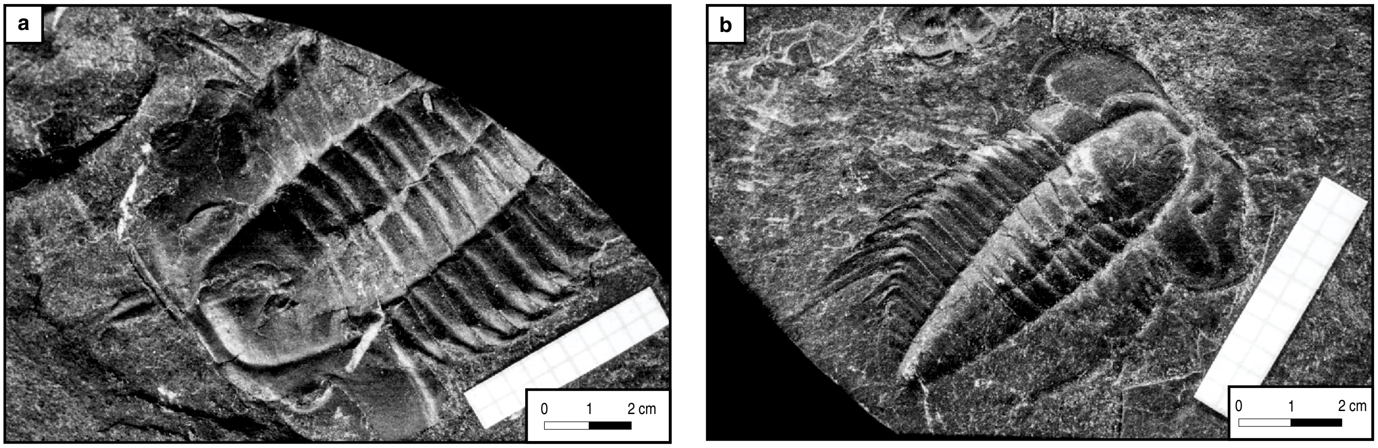

Figure 8. Tremadocian trilobites from La Heliera–1 well. **(a)** and **(b)** *Jujuyaspis truncaticonis.*

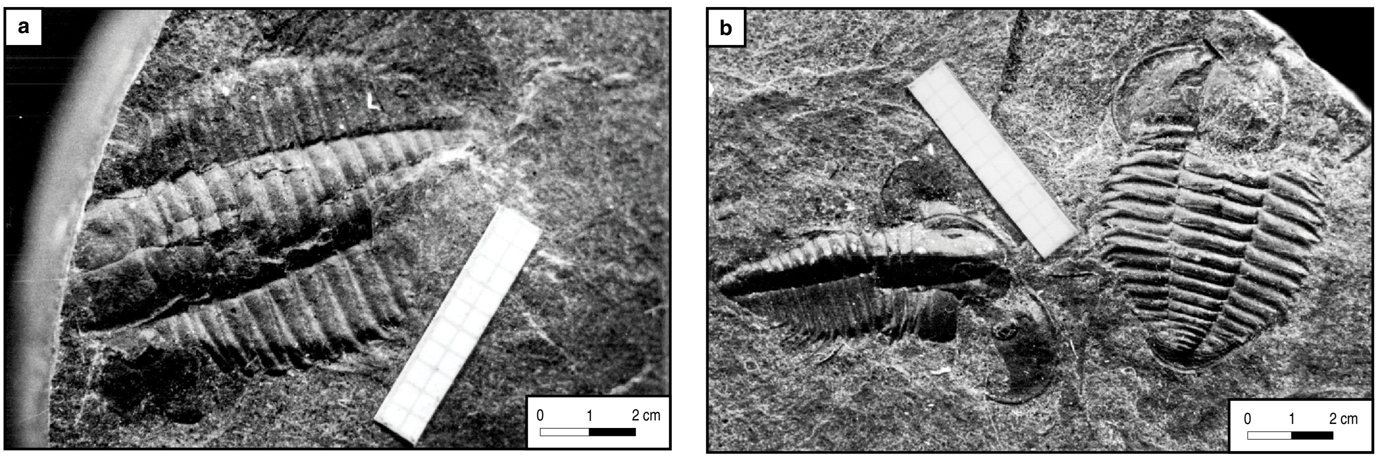

Figure 9. Tremadocian trilobites from La Heliera–1 well. **(a)** *Jujuyaspis colombiana*. **(b)** From left to right: *Jujuyaspis truncaticonis* and *Jujuyaspis colombiana*.

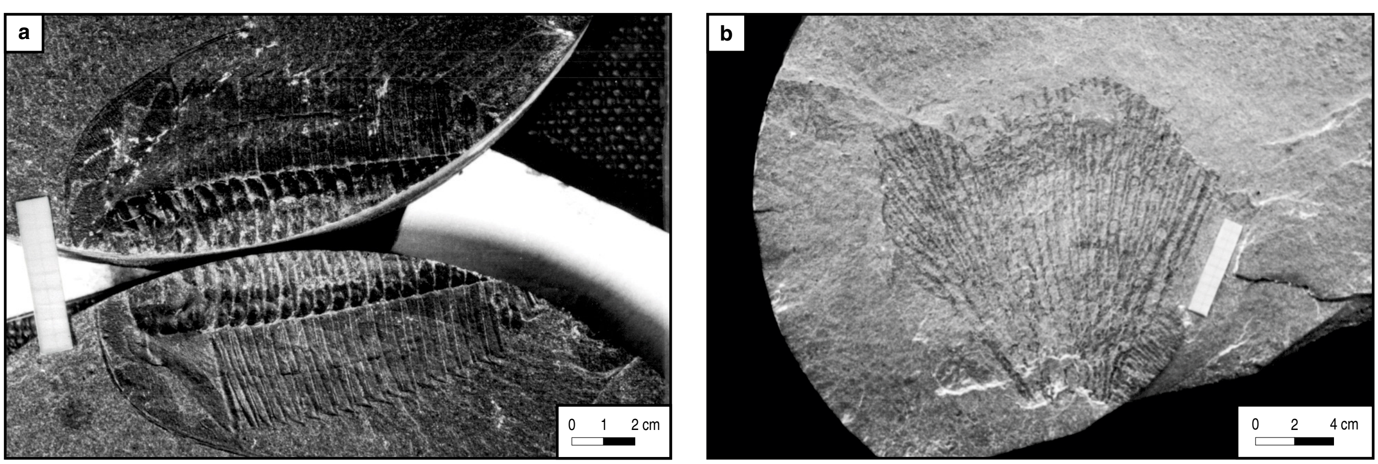

Figure 10. Tremadocian fossils from La Heliera–1 well. **(a)** Trilobite *Helieranella negritoensis* and **(b)** graptolite *Dictyonema flabelliforme*.

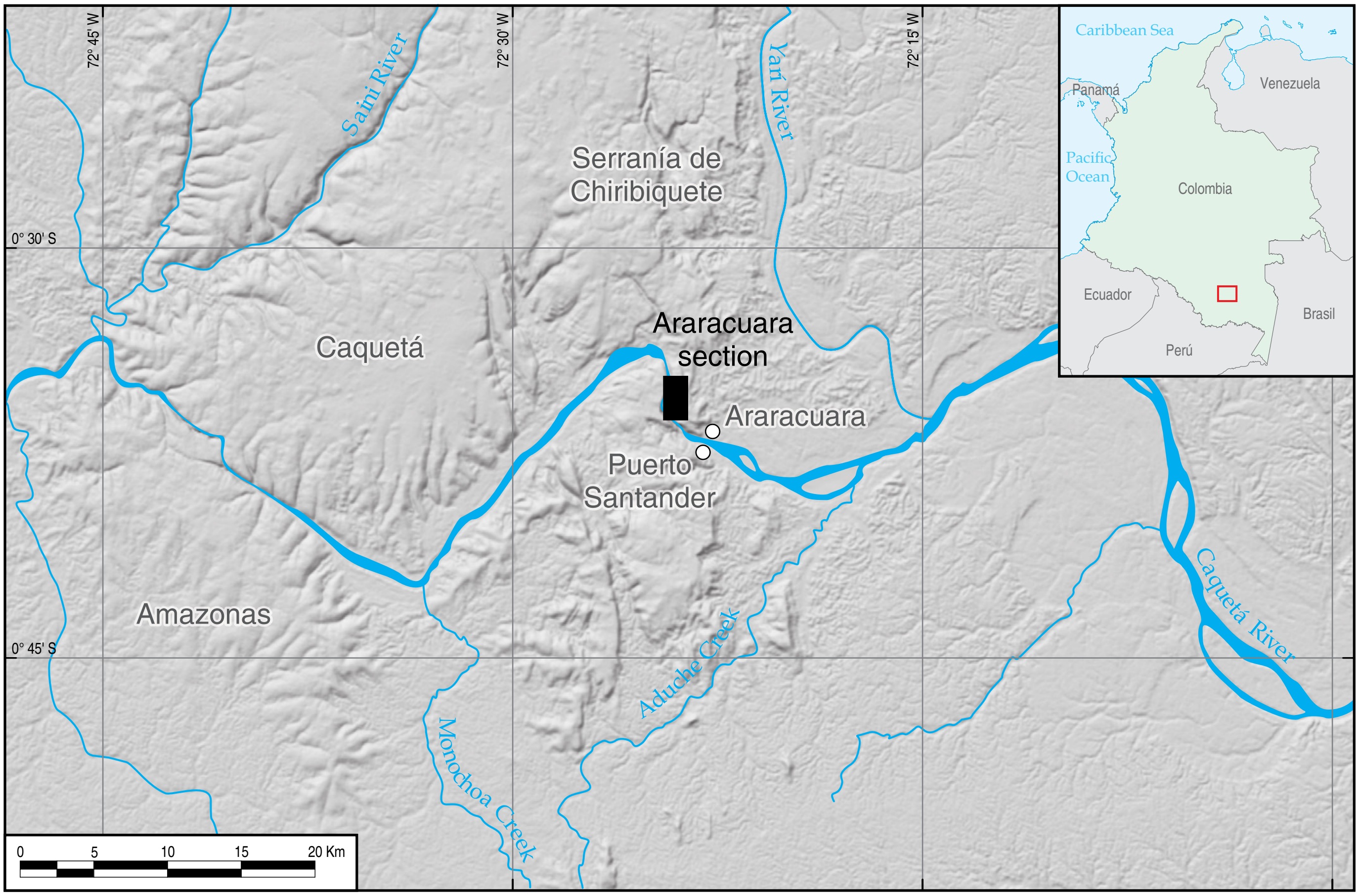

Figure 11. Location of the Araracuara section on the banks of the Caquetá River, northwest of the town of Araracuara. Adapted from Théry et al. (1986).

Colombia. Some of the cited palynomorphs are illustrated in Figure 12. Currently, this sandy section is being studied by the Servicio Geológico Colombiano.

Associations of Ordovician acritarchs, similar to those reported by Théry et al. (1986), were reported by Martinez–Aguirre (2011) in the Kantaka–1 well and by Dueñas (1984) in the Entrerrios–1 well, which are located in the central part of the Llanos Orientales Basin.

It is important to mention that Mojica & Villarroel (1990) reported an Arenigian age for the Araracuara region based on the presence of trace fossils (*Cruziana*, *Skolithos*, *Fucoides*), inarticulate brachiopods (*Lingulella*? sp.), and unidentified trilobites. Unfortunately, the exact locations of these samples are not known. These fossil remains allow us to correlate the Araracuara sandy section with the Negritos Formation in the Negritos–1 well.

5. Discussion and Conclusions

Despite the inclusion of these paleontological data, especially palynomorphs and some trilobites, information remains very fragmented for establishing biostratigraphic subdivisions of the Paleozoic in the Llanos Orientales Basin of Colombia. The associations of acritarchs, chitinozoans, and trilobites have allowed the Cambrian, the Silurian, the Devonian, and the Carboniferous Periods, and and the Early and Middle Ordovician Epochs to be differentiated in wells in the Llanos Orientales Basin. However, Upper Ordovician and Permian strata have not been reported in the basin, apparently due to periods of erosion or no sedimentation.

The Paleozoic sequence of the Llanos Orientales Basin of Colombia may show thicknesses of up to 20 000 ft of organic–rich marine mudstones, which cover thousands of square kilometers. These sedimentites are characterized by the presence of very well–preserved palynomorphs that indicate moderate thermal alteration. The presence of hydrocarbons in the Paleozoic sedimentites has been detected in several wells. The Paleozoic strata in the Llanos Orientales Basin can be considered an oil exploration target.

Acknowledgments

We would like to thank geologists Alberto OCHOA YARZA and Jorge GÓMEZ TAPIAS, without whose collaboration it

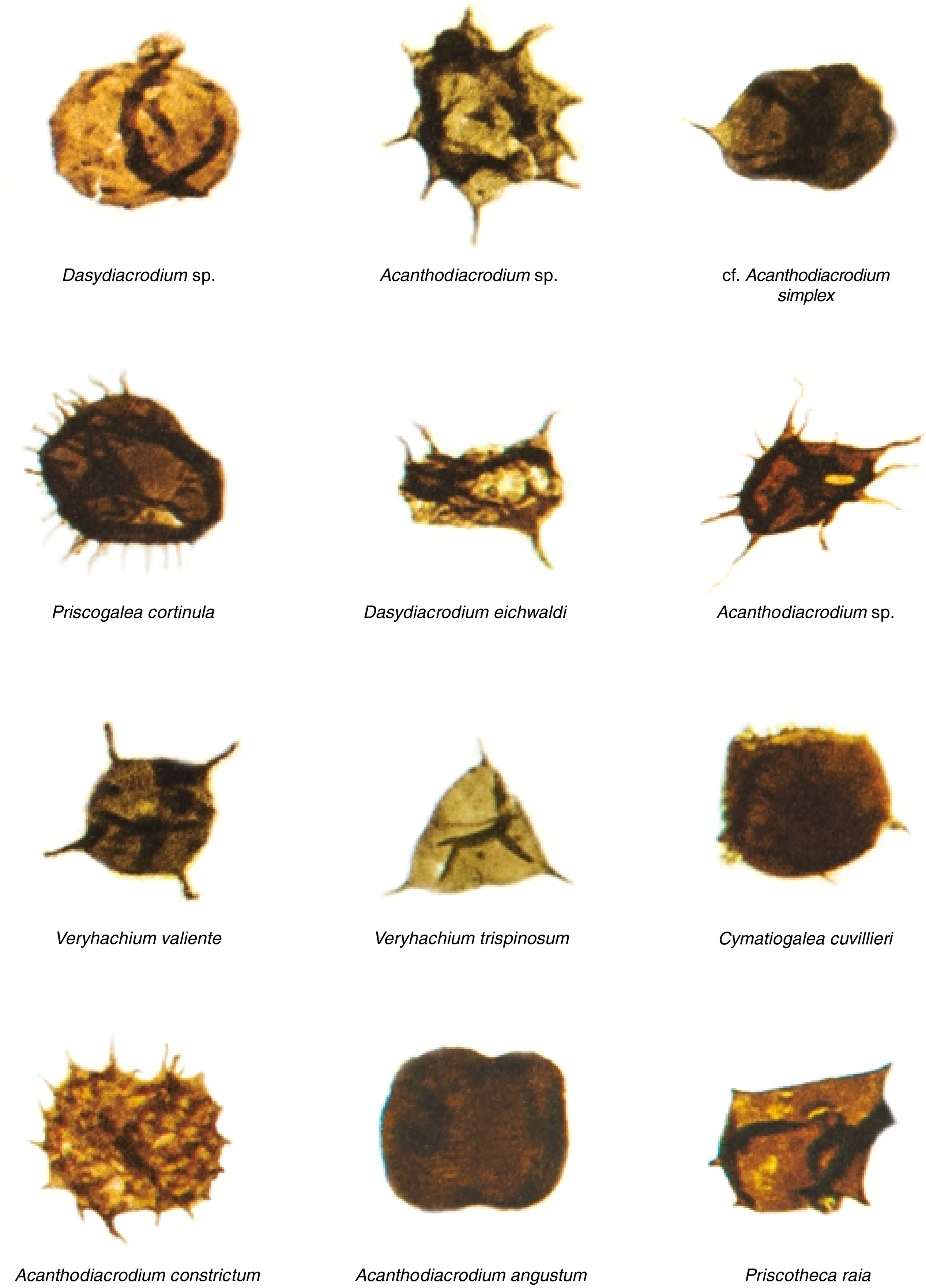

Figure 12. Ordovician acritarchs from the Araracuara section samples. Adapted from Théry et al. (1986). Photos without scale.

would have been very difficult to complete this manuscript. We would also like to thank geologist Fernando ALCÁRCEL GUTIÉRREZ, and photographer and graphic designer Alejandra CARDONA MAYORGA for their collaboration during the editing of the figures and tables.

References

Algeo, T.J. & Scheckler, S.E. 1998. Terrestrial–marine teleconnections in the Devonian: links between the evolution of land plants, weathering processes, and marine anoxic events. Philosophical Transactions of the Royal Society of London. Series B, Biological Sciences 353: 113–130. https://doi.org/10.1098/rstb.1998.0195

Arminio, J.F., Yoris, F., Quijada, C., Lugo, J.M., Shaw, D., Keegan, J.B. & Marshall, J.E.A. 2013. Evidence for Precambrian stratigraphy in graben basins below the Eastern Llanos Foreland, Colombia. American Association of Petroleum Geologists International Conference and Exhibition. Abstracts, 35 p. Cartagena.

Baldis, B.A., González, S.B. & Pérez, V.E. 1984. Trilobites tremadocianos de la Formación Negritos ("perforación La Heliera"), Llanos de Colombia. III Congreso Latinoamericano de Paleontología. Memoirs, p 28–41. México.

Benton, M.J. 1986. The evolutionary significance of mass extinctions. Trends in Ecology and Evolution 1(5): 127–130. https://doi.org/10.1016/0169-5347(86)90007-8

Benton, M.J. 2005. Vertebrate Paleontology, 3rd edition. Blackwell Science Ltd. 472 p. Bristol, UK.

Bergström, S.M., Chen, X., Gutiérrez–Marco, J.C. & Dronov, A. 2009. The new chronostratigraphic classification of the Ordovician System and its relations to major regional series and stages and to δ13C chemostratigraphy. Lethaia, 42(1): 97–107. https://doi.org/10.1111/j.1502–3931.2008.00136.x

Bogotá, J. 1982. Estratigrafía del Paleozoico inferior en el área Amazónica de Colombia. Geología Norandina, 6: 29–38.

Briggs, D.E.G. 2015. The Cambrian explosion. Current Biology, 25(19): R864–R868. https://doi.org/10.1016/j.cub.2015.04.047

Buatois, L.A., Mángano, M.G., Genise, J.F. & Taylor, T.N. 1998. The ichnologic record of the continental invertebrate invasion: Evolutionary trends in environmental expansion, ecospace utilization, and behavioral complexity. Palaios, 13(3): 217–240. http://dx.doi.org/10.2307/3515447

Burgess, S.D., Bowring, S. & Shen, S. 2014. High–precision timeline for Earth's most severe extinction. Proceedings of the National Academy of Sciences of the United States of America, 111(9): 3316–3321.

Cediel, F. 2019. Phanerozoic Orogens of northwestern South America: Cordilleran–Type Orogens. Taphrogenic tectonics. The Maracaibo Orogenic Float. The Chocó–Panamá Indenter. In: Cediel, F. & Shaw, R.P. (editors), Geology and Tectonics of northwestern South America: The Pacific–Caribbean–Andean junction. Frontiers in Earth Sciences. Springer Nature Switzerland, p. 3–95. https://doi.org/10.1007/978-3-319-76132-9_1

Clark, E.W. 1960. Petroleum development in South America and Caribbean area in 1959. American Association of Petroleum Geologists Bulletin, 44(7): 1014–1057. https://doi.org/10.1306/0BDA60F2-16BD-11D7-8645000102C1865D

Cohen, K.M., Finney, S.C., Gibbard, P.L. & Fan, J.X. 2013. The ICS International Chronostratigraphic Chart. Episodes, 36(3): 199–204. https://doi.org/10.18814/epiiugs/2013/v36i3/002

Cordani, U.G., Teixeira, W., D'Agrella–Filho, M.S. & Trindade, R.I. 2009. The position of the Amazonian Craton in supercontinents. Gondwana Research, 15(3–4): 396–407. https://doi.org/10.1016/j.gr.2008.12.005

Darwin, C. 1859. On the origin of species by means of natural selection. John Murray, 502 p. London.

Davies, N.S. & Gibling, M.R. 2013. The sedimentary record of Carboniferous rivers: Continuing influence of land plant evolution on alluvial processes and Palaeozoic ecosystems. Earth–Science Reviews, 120: 40–79. https://doi.org/10.1016/j.earscirev.2013.02.004

Delabroye, A. & Vecoli, M. 2010. The end–Ordovician glaciation and the Hirnantian Stage: A global review and questions about Late Ordovician event stratigraphy. Earth–Science Reviews, 98(3–4): 269–282. https://doi.org/10.1016/j.earscirev.2009.10.010

Dueñas, H. 1984. Análisis palinológicos de muestras del pozo Entrerrios–1. Cuenca de los Llanos Orientales. Informe preparado por Geoconsulta Ltda. para Empresa Colombiana de Petróleos "Ecopetrol". 13 p. Bogotá.

Dueñas, H. 2001. Paleozoic palynological assemblages from the Llanos Orientales Basin, Colombia. 34th Annual Meeting of the American Association of Stratigraphic Palynologists. Proceedings, 16 p. San Antonio, USA.

Dueñas, H. 2002. Asociaciones palinológicas y posibilidades de hidrocarburos en el Paleozoico de la Cuenca de los Llanos Orientales de Colombia. Segunda Convención Técnica Asociación Colombiana de Geólogos y Geofísicos del Petróleo. Geología y Petróleo en Colombia. Memoirs, p. 15–17. Bogotá.

Dueñas, H. 2011. The Paleozoic of the Llanos Orientales Basin, Colombia: Integration of biostratigraphic data. Report Bioss Limited 780, unpublished report, 260 p. Bogotá.

Dueñas, H. & Césari, S.N. 2005. Systematic study of Early Carboniferous palynological assemblages from the Llanos Orientales Basin, Colombia. Revista del Museo Argentino de Ciencias Naturales, 7(2): 139–152. https://doi.org/10.22179/REVMACN.7.331

Dueñas, H. & Césari, S.N. 2006. Palynological evidence of Early Carboniferous sedimentation in the Llanos Orientales Basin, Colombia. Review of Palaeobotany and Palynology, 138(1): 31–42. https://doi.org/10.1016/j.revpalbo.2005.10.002

Dueñas–Jiménez, H. & Montalvo–Jónsson, J. 2020. Neoproterozoic records of the Llanos Orientales Basin, Colombia. In: Gómez, J. & Mateus–Zabala, D. (editors), The Geology of Colombia, Volume 1 Proterozoic – Paleozoic. Servicio Geológico Colombiano, Publicaciones Geológicas Especiales 35, p. 91–99. Bogotá. https://doi.org/10.32685/pub.esp.35.2019.05

Ecopetrol. 2010. Biostratigraphic evaluation of selected wells from the Llanos Orientales Basin. Unpublished report, 42 p. Bogotá.

Erwin, D.H., Laflamme, M., Tweedt, S.M., Sperling, E.A., Pisani, D. & Peterson, K.J. 2011. The Cambrian conundrum: Early divergence and later ecological success in the early history of animals. Science, 334(6059): 1091–1097. https://doi.org/10.1126/science.1206375

Feo–Codecido, G., Smith, F.D., Aboud, N. & Di Giacomo, E. 1984. Basement and Paleozoic rocks of the Venezuelan Llanos basins. In: Bonini, W.E., Hargraves, R.B. & Shagam, R. (editors), The Caribbean–South American Plate boundary and regional tectonics. Geological Society of America, Memoir 162, p. 175–187. https://doi.org/10.1130/MEM162-p175

Finnegan, S., Bergmann, K., Eiler, J.M., Jones, D.S., Fike, D.A., Eisenman, I., Hughes, N.C., Tripati, A.K. & Fischer, W.W. 2011. The magnitude and duration of Late Ordovician – Early Silurian glaciation. Science, 331(6019): 903–906. https://doi.org/10.1126/science.1200803

Galvis, J., Huguett, A. & Ruge, P. 1979. Geología de la Amazonia colombiana. Boletín Geológico, 22(3): 3–86.

Haq, B.U. & Schutter, S.R. 2008. A chronology of Paleozoic sea–level changes. Science, 322(5898): 64–68. https://doi.org/10.1126/science.1161648

Hughes, C.P. 1980. A brief review of the Ordovician faunas of northern South America. II Congreso Argentino de Paleontología y Bioestratigrafía y I Congreso Latinoamericano de Paleontología. Memoirs, p. 11–22. Buenos Aires.

Hughes, C.P. 1982. The Tremadoc rocks of South America with special reference to those of Bolivia. Special Papers in Palaeontology, 30: 9–14.

Isaza, J.F. & Campos, D. 2007. Cambio climático: Glaciaciones y calentamiento global. Universidad de Bogotá Jorge Tadeo Lozano, 294 p. Bogotá.

Kroeck, D.M., Pardo–Trujillo, A., Plata–Torres, A., Romero–Baéz, M & Servais, T. 2019. Peri–Gondwanan acritarchs from the Ordovician of the Llanos Orientales Basin, Colombia. Palynology: 1–14 p. https://doi.org/10.1080/01916122.2019.1624279

Martinez–Aguirre, F. 2011. Informe geológico final pozo exploratorio Kantaka–1. Cuenca de los Llanos Orientales, Bloque CPO 11. Preparado por Unión Temporal GEXDES–CSI para Ecopetrol. 77 p. Bogotá.

Marshall, C.R. 2006. Explaining the Cambrian "explosion" of animals. Annual Review of Earth and Planetary Sciences, 34: 355–384. https://doi.org/10.1146/annurev.earth.33.031504.103001

Maruyama, S. & Santosh, M. 2008. Snowball Earth to Cambrian explosion. Gondwana Research, 14: 1–4. https://doi.org/10.1016/j.gr.2008.02.001

Maruyama, S., Sawaki, Y., Ebisuzaki, T., Ikoma, M., Omori, S. & Komabayashi, T. 2014. Initiation of leaking Earth: An ultimate trigger of the Cambrian explosion. Gondwana Research, 25(3): 910–944. https://doi.org/10.1016/j.gr.2013.03.012

Miller, A.I. 1997. Dissecting global diversity patterns: Examples from the Ordovician radiation. Annual Review of Ecology and Systematics, 28: 85–104. https://doi.org/10.1146/annurev.ecolsys.28.1.85

Mojica, J. & Villarroel, C. 1990. Sobre la distribución y facies del Paleozoico inferior sedimentario en el extremo NW de Sudamérica. Geología Colombiana, 17: 219–226.

Ogg, J.G., Ogg, G.M. & Gradstein, F.M. 2016. A concise geologic time scale. Elsevier, 240 p. https://doi.org/10.1016/c2009-0-64442-1

Payne, J.L. & Clapham, M.E. 2012. End–Permian mass extinction in the oceans: An ancient analog for the twenty–first century? Annual Review of Earth and Planetary Sciences, 40: 89–111. https://doi.org/10.1146/annurev-earth-042711-105329

Raup, D.M. 1979. Size of the Permo–Triassic bottleneck and its evolutionary implications. Science, 206(4415): 217–218. https://doi.org/10.1126/science.206.4415.217

Raup, D.M. & Sepkoski Jr., J.J. 1982. Mass extinctions in the marine fossil record. Science, 215(4539): 1501–1503. https://doi.org/10.1126/science.215.4539.1501

Sepkoski Jr., J.J. 1996. Patterns of Phanerozoic extinction: A perspective from global data bases. In: Walliser, O.H. (editor), Global events and event stratigraphy in the Phanerozoic. Springer, p. 35–51. Berlin.https://doi.org/10.1007/978-3-642-79634-0_4

Sheehan, P.M. 2001. The Late Ordovician mass extinction. Annual Review of Earth and Planetary Sciences, 29: 331–364. https://doi.org/10.1146/annurev.earth.29.1.331

Shu, D.G. 2008. Cambrian explosion: Birth of tree of animals. Gondwana Research, 14: 219–240. https://doi.org/10.1016/j.gr.2007.08.004

Sinanoglu, E. 1984. Estudio palinológico de los sedimentos pre–cretáceos (Formación Carrizal) en el área de Zuata, Venezuela oriental. Revista Técnica INTEVEP, 6(1): 67–89.

Smith, M.P. & Harper, D.A.T. 2013. Causes of the Cambrian explosion. Science, 341(6152): 1355–1356. https://doi.org/10.1126/science.1239450

Torsvik, T.H. & Cocks, L.R.M. 2013. Gondwana from top to base in space and time. Gondwana Research, 24(3–4): 999–1030. https://doi.org/10.1016/j.gr.2013.06.012

Théry, J.M., Peniguel, T. & Haye, G. 1986. Descubrimiento de acritarcos del Arenigiano cerca a Araracuara (Caquetá–Colombia). Ensayo de reinterpretación de esta región de la saliente del Vaupés. Geología Norandina, (9): 3–17.

Ulloa, C., Pérez, V.E. & Baldis, B. 1982. Unidades litoestratigráficas del Ordovícico de los Llanos Orientales de Colombia. V Congreso Latinoamericano de Geología. Memoirs, I, p. 109–120. Buenos Aires.

Vail, P.R., Mitchum Jr., R.M. & Thompson III, S. 1977. Seismic stratigraphy and global changes of sea level. Part 4: Global cycles of relative changes of sea level. In: Payton, C.E. (editor), Seismic stratigraphy–applications to hydrocarbon exploration. American Association of Petroleum Geologists. Memoirs 26, p. 83–97.

Webby, B.D., Paris, F., Droser, M.L. & Percival, I.G. 2004. The great Ordovician biodiversification event. Columbia University Press, 496 p. New York. https://doi.org/10.7312/webb12678

Zhang, X., Shu, D., Han, J., Zhang, Z., Liu, J. & Fu, D. 2014. Triggers for the Cambrian explosion: Hypotheses and problems. Gondwana Research, 25(3): 896–909. https://doi.org/10.1016/j.gr.2013.06.001

Explanation of Acronyms, Abbreviations, and Symbols:

BP	Before present	ft	Foot

Authors' Biographical Notes

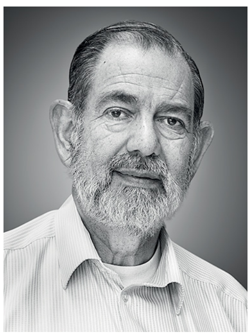

Hernando DUEÑAS–JIMÉNEZ studied geology at Universidad Nacional de Colombia, where he graduated in 1972. He later specialized in studies in geology and palynology at the Gemeente Universiteit van Amsterdam, Holland, between 1977–1979 and obtained a PhD in geological sciences in 1986 at the same institution. He was later associated with Servicio Geológico Colombiano leading the Laboratorio de Palinología between 1977 and 1978 and as the Director of the División de Estratigrafía y Paleontología between 1978 and 1980. He was a professor of Palynology in the Departamento de Geociencias, Universidad Nacional de Colombia, Sede Bogotá, between 1979 and 1981, during which time he occupied the position of geologist expert in palynology in Intercol (Exxon group). He was a palynologist in the section of regional works of the Robertson Research INC Company (Houston) between 1982 and 1983, from which he began to practice his profession independently as a consultant geologist in biostratigraphy for the Colombian petroleum industry. In 1978, he was awarded the "Best Geological Research" prize by the Board of Directors of Servicio Geológico Colombiano. He received a recognition for scientific contribution (San Cayetano Formation) from the Centro de Investigaciones del Petróleo CEINPET, Cuba, in 2003. He held the vice presidency of the Academia Colombiana de Ciencias Exactas, Físicas y Naturales (ACCEFYN) between 2000 and 2002. He is a numerical member of the ACCEFYN and Academia Colombiana de Geografía and a foreign correspondent member of the Real Academia de Ciencias Exactas, Físicas y Naturales de España. He has published more than 80 articles in indexed journals.

Victoria Elena CORREDOR–BOHÓRQUEZ completed her studies in geology at the Universidad Nacional de Colombia in 2008. She has worked with consulting companies in geology in the areas of sedimentology, stratigraphy, and cartography. Between 2008 and 2009, she worked for the company Geostratos Ltda., and between 2012 and 2014, she worked for the company Paleoexplorer S.A.S., undertaking descriptive and sedimentological analyses and paleoenvironmental interpretations of drill cores and stratigraphic columns in the field for different Colombian basins. In 2010 and 2011, she joined the research group of the Museo Geológico Nacional José Royo y Gómez, supporting stratigraphic paleontological explorations and collaborating with the curatorship of the micropaleontological collections of foraminifera. She is currently a candidate for the Master of Science–Geology at the Universidad Nacional de Colombia, with a project on the Cretaceous foraminifera, and has worked in the Servicio Geológico Colombiano within the Grupo de Cartografía and the Grupo de Estratigrafía of the Dirección de Geociencias Básicas since 2014.

Jorge MONTALVO–JÓNSSON studied geology at the University of Iceland. He graduated with a BS degree in 2008, then pursued an M.Paed degree in geology at the same university, from which he graduated in 2010. Afterwards, he pursued a MS in Geology with special emphasis on the analysis of volcanic hazards. He obtained the title in 2014 from the University of Iceland. During his studies in Iceland, he worked remotely at Bioss S.A.S. as a support member in research pertaining to the regional geology of Colombia. Furthermore, he worked at ÍSOR (Icelandic Geo Survey) as an assistant geologist in the summer of 2010 and at the Icelandic Meteorological Institute (Veðurstofa Íslands) as a specialist in volcanology in 2011. Most recently, he has been pursuing a PhD degree at the Universidad Nacional de Colombia. Additionally, he has been involved in promoting ethics in geosciences as a member of the IAPG (International Association for Promoting Geoethics).

Chapter 8

The Anacona Terrane: A Small Early Paleozoic Peri–Gondwanan Terrane in the Cauca–Romeral Fault System

https://doi.org/10.32685/pub.esp.35.2019.08
Published online 21 May 2020

Jorge Julián RESTREPO[1]*, Uwe MARTENS[2], and Wilmer E. GIRALDO–RAMÍREZ[3]

1 jjrestrepoa@gmail.com
Universidad Nacional de Colombia
Sede Medellín
GEMMA Research Group
Medellín, Colombia

2 umartens@s2sgeo.com
S2SGeo
1315 Alma Ave Ste 134, Walnut Creek, CA 94596, USA

3 wegirald@gmail.com
Alcaldía de Marinilla
Calle 30 n.° 30–13
Marinilla, Antioquia, Colombia

* Corresponding author

Abstract The Anacona Terrane is a small terrane south of Medellín that underwent a geologic history dissimilar to that of the adjacent Tahamí Terrane to the east and the Quebradagrande (Ebéjico) Terrane to the west. The metamorphic basement of the Anacona Terrane is relatively old, comprising amphibolites and metasedimentary rocks, with probable late Neoproterozoic depositional ages, and granitic orthogneisses, with Ordovician magmatic ages. The age of the last metamorphic event to affect the Anacona Terrane is constrained to the Devonian or earliest Carboniferous, while Triassic metamorphism, which is widespread in the Tahamí Terrane, has not been documented in the Anacona Terrane, indicating that the terranes were amalgamated during or after the Triassic. Correlatives of the terrane are the Acatlán Complex in southern México and the Marañón Complex and coastal islands in Perú; we surmise that the Anacona Terrane may have originated in a southerly position and migrated northwards, similar to the motion of the Caribbean Plate relative to the South American margin.
Keywords: *Anacona, tectonostratigraphic terranes, Colombian Andes, Proterozoic sedimentation, garnet amphibolites.*

Resumen El Terreno Anacona es un pequeño terreno localizado al sur de Medellín que presenta una historia geológica diferente a la de los terrenos adyacentes, el Tahamí al este y el Quebradagrande (Ebéjico) al oeste. El basamento metamórfico del Terreno Anacona es relativamente antiguo, comprende anfibolitas y rocas metasedimentarias, con probable edad de depositación neoproterozoica tardía, y ortogneises graníticos con edades magmáticas ordovícicas. La edad del último evento metamórfico que afectó al Terreno Anacona está restringida al Devónico o Carbonífero temprano, mientras que el metamorfismo triásico, presente en el Terreno Tahamí, no ha sido registrado en el Terreno Anacona. Lo anterior indica que estos terrenos se amalgamaron durante o después del Triásico. El Complejo Acatlán en el sur de México y el Complejo Marañón y las islas costeras en Perú son equivalentes del Terreno Anacona; proponemos que el Terreno Anacona podría haberse originado en una posición al sur y migrado al norte, siguiendo el desplazamiento de la Placa del Caribe con relación al margen suramericano.
Palabras clave: *Anacona, terrenos tectonoestratigráficos, Andes colombianos, sedimentación proterozoica, anfibolitas granatíferas.*

Citation: Restrepo, J.J., Martens, U. & Giraldo–Ramírez, W.E. 2020. The Anacona Terrane: A small early Paleozoic peri–Gondwanan terrane in the Cauca–Romeral Fault System. In: Gómez, J. & Mateus–Zabala, D. (editors), The Geology of Colombia, Volume 1 Proterozoic – Paleozoic. Servicio Geológico Colombiano, Publicaciones Geológicas Especiales 35, p. 149–165. Bogotá. https://doi.org/10.32685/pub.esp.35.2019.08

1. Introduction

The basement of the Central Cordillera of Colombia comprises low– to high–grade metamorphic rocks of diverse age locally intruded by Triassic, Cretaceous, and Paleogene plutons. Initial studies regarded the metamorphic basement as a single unit, the Ayurá–Montebello Group (Botero, 1963), but it soon became apparent that several metamorphic events had affected this group of rocks. This led to the proposal that the metamorphic basement of the Central Cordillera was a polymetamorphic unit (Restrepo & Toussaint, 1984) and that this metamorphic basement formed the "backbone" of the Tahamí Terrane (Toussaint & Restrepo, 1989; see also Restrepo & Toussaint, 2020).

Mapping conducted in the 1970s and 1980s revealed in detail the nature of the metamorphic basement exposed around the county of Caldas, ca. 20 km south of Medellín (Echeverría, 1973; Sepúlveda & Saldarriaga, 1980; Patiño & Noreña, 1984; Maya & Escobar, 1985). Unlike the majority of the metamorphic basement in the Central Cordillera, which is characterized by low–P assemblages (e.g., Echeverría, 1973), the rocks near Caldas include garnet–bearing amphibolites and kyanite–bearing metapelites indicative of medium–pressure metamorphism (Restrepo & Toussaint, 1977). Furthermore, geochronologic work consistently yielded older ages than the Permian – Triassic metamorphic events detected in the rest of the Tahamí Terrane (Restrepo & Toussaint, 1978; Restrepo et al., 1991). The first Precambrian K–Ar hornblende age of 1650 ± 500 Ma (Restrepo & Toussaint, 1978) was discarded after the same sample was dated again by the same method, yielding ages between 254 ± 9 Ma and 319 ± 48 Ma; in contrast, a K–Ar muscovite age from the granitic orthogneiss yielded an age 343 ± 12 Ma, older than all the other mica ages from gneisses in the Central Cordillera (Restrepo et al., 1991). Recently, more robust U–Pb and ^{40}Ar–^{39}Ar geochronology has confirmed that the metamorphic basement in the Caldas area underwent a different geological evolution compared with the rest of the metamorphic basement of the Tahamí Terrane. It was therefore separated as an independent unit termed the Anacona Terrane (Figure 1; Martens et al., 2014; Restrepo et al., 2009).

Despite its relatively small size, approximately 45 km^2, the Anacona Terrane satisfies the definition of tectonostratigraphic terrane (Coney et al., 1980; Jones et al., 1983); it is a fault–bounded geologic entity or fragment that is characterized by a distinctive geologic history that differs markedly from that of adjacent terranes. Detailed mapping has shown that the Anacona–Tahamí Terrane boundary is a regional north–south trending ductile fault zone, the Santa Isabel Fault (Figure 2; Giraldo–Ramírez, 2013), which is characterized by mylonites and tectonic breccias.

2. Lithology of Units

The two main rock units of the Anacona Terrane are the Caldas Amphibolite and La Miel Orthogneiss (Figure 3a, 3b). The amphibolite is a polyphase metamorphic rock composed mainly of blue–green hornblende + almandine–rich garnet + plagioclase. Unlike the nearby amphibolites of the Tahamí Terrane, the amphibolites in the Anacona Terrane are rich in garnet, up to 30% by volume (Figure 3a). The garnet porphyroblasts are characterized by coronas of hornblende + plagioclase + quartz. Peak amphibolite facies pressure and temperature (PT) conditions were estimated at 1.35 GPa, 630 °C (Bustamante, 2003). These PT conditions are consistent with those established for the mineral assemblages in the metasedimentary schists that are locally interbedded with the amphibolite. These assemblages contain kyanite, garnet, and staurolite, indicating medium–pressure, lower–amphibolite facies conditions. The schists are also polyphase, showing evidence for at least three metamorphic phases (Restrepo, 1986).

Some features are suggestive of the Caldas garnet amphibolite being a retrogressed eclogite: the high garnet content is more typical of eclogite than amphibolite; symplectites of hornblende and plagioclase are common; corona textures of garnet producing amphibole + plagioclase are suggestive of retrogression by decompression (Figure 4). However, despite detailed thin section petrography, it has not been possible to identify relict sodic clinopyroxene (omphacite) in this unit (Martens et al., 2014).

Geochemical analyses of the Caldas Amphibolite (Giraldo–Ramírez, 2013) show a predominance of basaltic protoliths. The rare earth element (REE) patterns (Figure 5) are slightly enriched in light REE, with Ta and Nb anomalies suggesting the presence of subduction–related fluids in the melted source. The REE patterns are transitional between continental arc and E–MORB or continental tholeiite. The trace element geochemistry is inconsistent with the generation of the amphibolite protolith in a typical mid–ocean ridge; instead, it has been proposed that the basaltic protoliths formed in a continental arc (Giraldo–Ramírez, 2013). These features contrast with the geochemical character of Tahamí Terrane amphibolites, which are predominantly MORB tholeiites (Correa–Martínez et al., 2005; Vinasco et al., 2006; Restrepo, 2008; Giraldo, 2010). Sm–Nd isotopic analyses of Caldas Amphibolite are presented in Table 1, showing positive εNd ranging from 2.6 and 5.8 and model ages between 0.89 and 1.19 Ga.

The second major geologic unit in the Anacona Terrane is the granitic, S–type La Miel Orthogneiss, which is composed of quartz + plagioclase + K–feldspar + muscovite + biotite ± garnet. The K–feldspar is mainly orthoclase that has been inverted to microcline. The foliation of the rock is defined by the muscovite and biotite, and locally, a primary mineral tabular

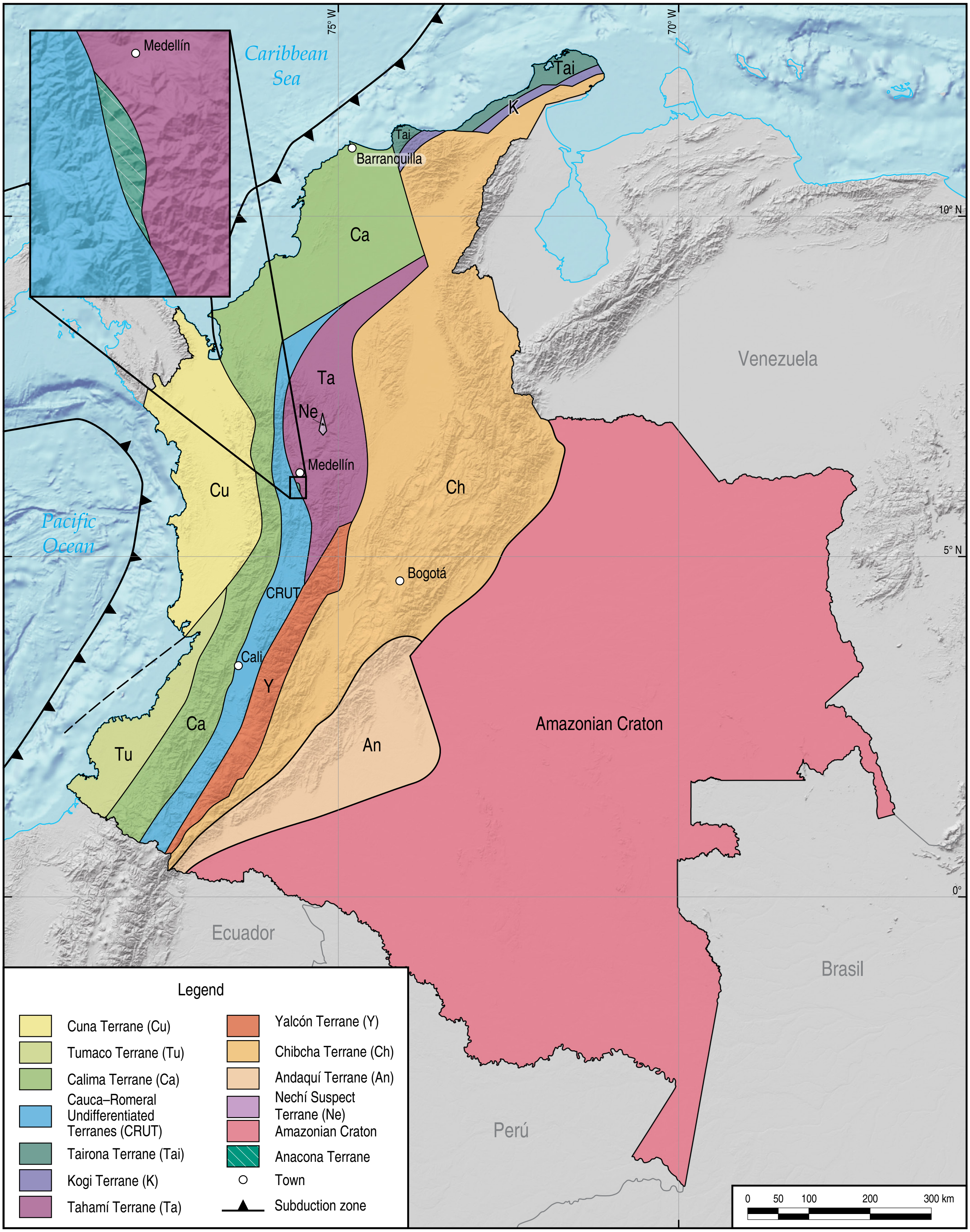

Figure 1. Tectonostratigraphic terranes of Colombia (after Restrepo & Toussaint, 2020).

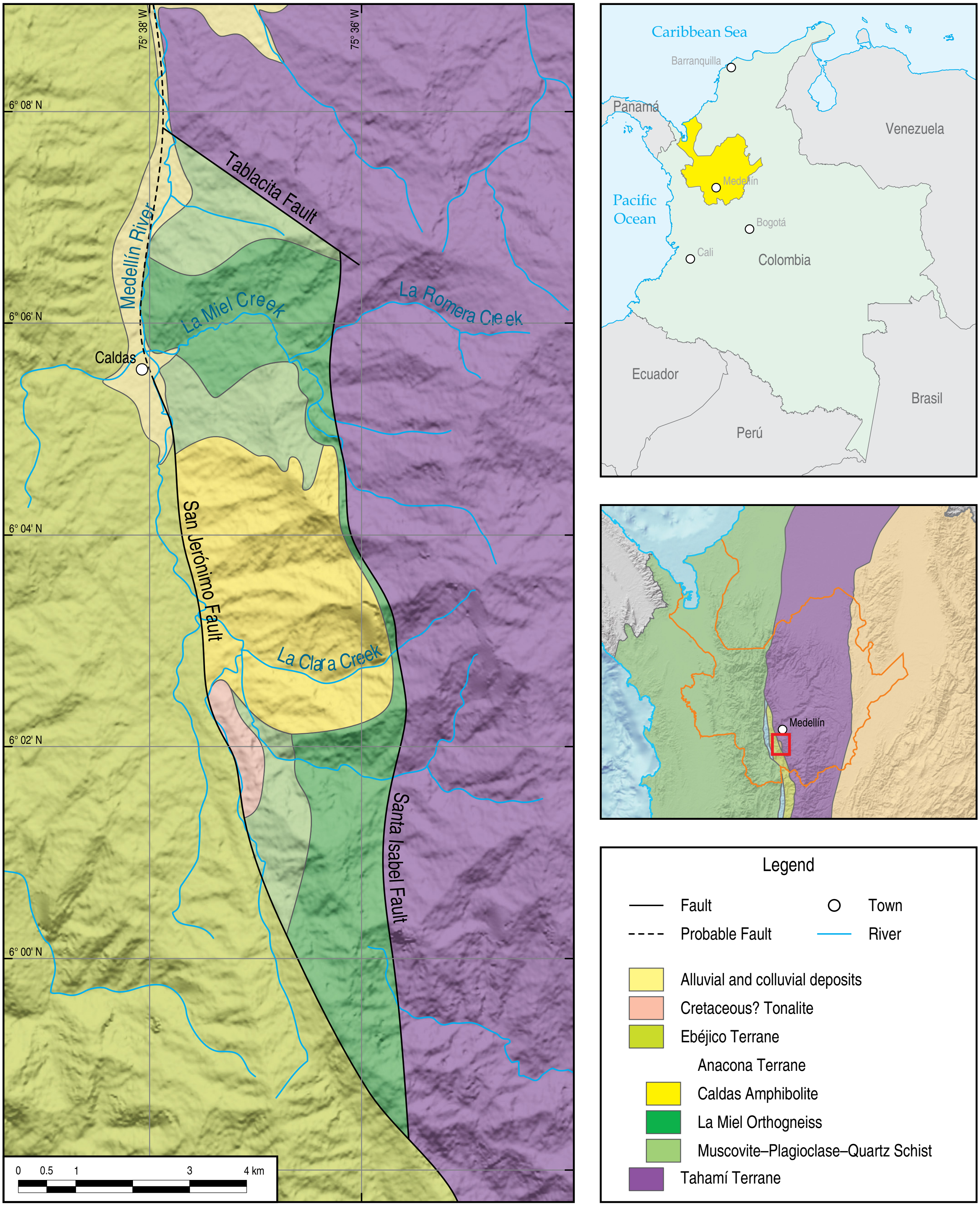

Figure 2. Geologic map of the Anacona Terrane, modified from Giraldo–Ramírez (2013).

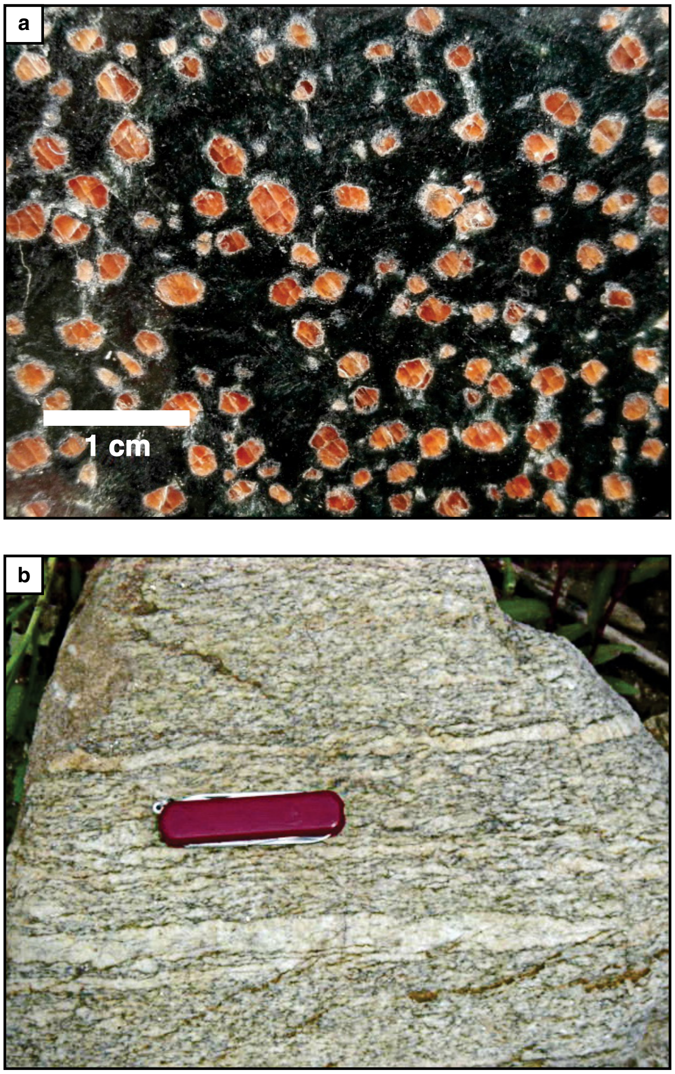

Figure 3. (a) Photographs of a polished slab of the Caldas Amphibolite **(b)** and La Miel Granitic Orthogneiss.

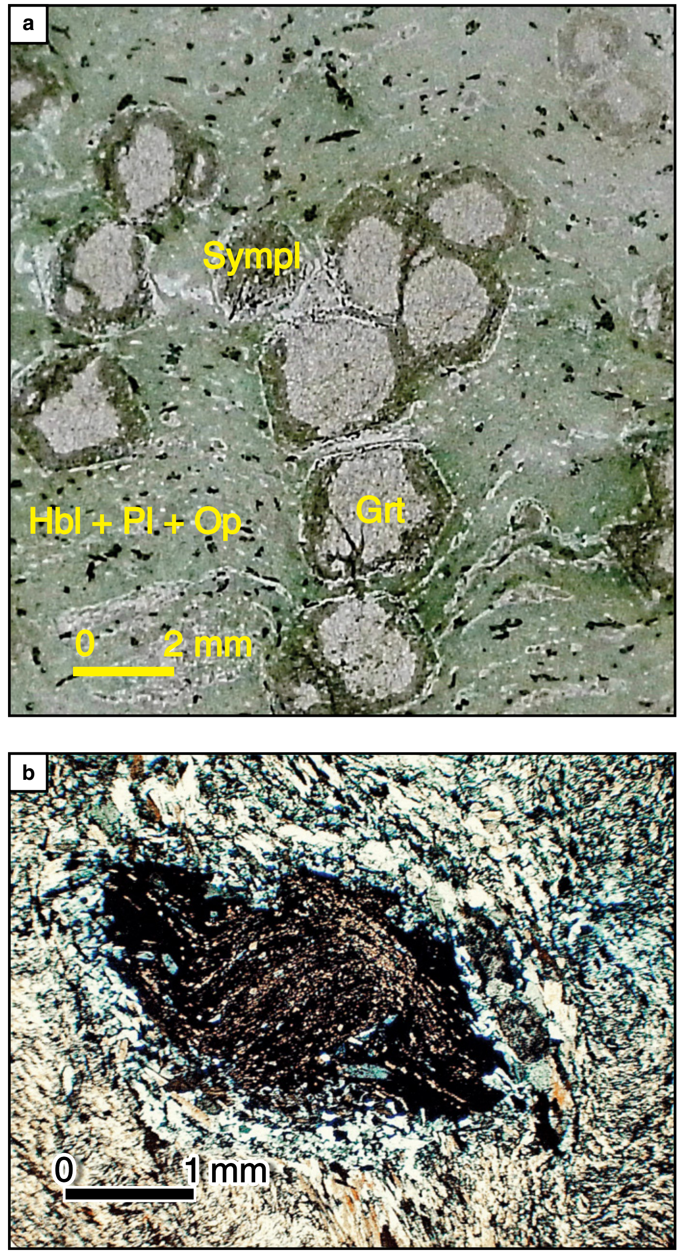

Figure 4. (a) Garnet replaced by a symplectite of plagioclase and hornblende; photomicrograph in plane light (Grt) garnet, (Sympl) symplectite, (Hbl) hornblende, (Pl) plagioclase, (Op) Opaque mineral. **(b)** Garnet with rotational structure and rims replaced by plagioclase and hornblende; photomicrograph in crossed–polarized light (from Restrepo, 1986).

orientation of feldspar is preserved (Figure 3b). Field relations clearly show that La Miel granitic protolith intruded the amphibolites and the associated metamorphic units.

U–Pb zircon geochronology of La Miel Orthogneiss has yielded Ordovician crystallization ages of approximately 445 Ma and 480 Ma in two different samples (Martens et al., 2014), implying an even older protolith age for the Caldas Amphibolite and their associated metasedimentites. ^{40}Ar–^{39}Ar white mica ages of the orthogneiss yielded an age of ca. 345 Ma (Vinasco et al., 2006), which is the best available age constraint for the timing of metamorphism in the Anacona Terrane. This age is consistent with the maximum age of ca. 360 Ma obtained from a U–shaped ^{40}Ar–^{39}Ar hornblende spectrum, which may reflect the incorporation of excess argon (Restrepo et al., 2008). Importantly, none of the ^{40}Ar–^{39}Ar step–heating experiments have revealed any Triassic component, indicating that the Anacona Terrane basement has not experienced the ubiquitous Triassic metamorphism characteristic of the Tahamí Terrane. It therefore seems unlikely that the Anacona Terrane was adjacent to the Tahamí Terrane during high–grade Triassic metamorphism or that it forms the basement to the Tahamí Terrane (Cajamarca Complex), as proposed by Villagómez et al. (2011).

Although less abundant, quartz + muscovite + garnet–bearing quartzites and mica schists are also present in the Anacona Terrane. They occur as metapelitic layers interbedded with the

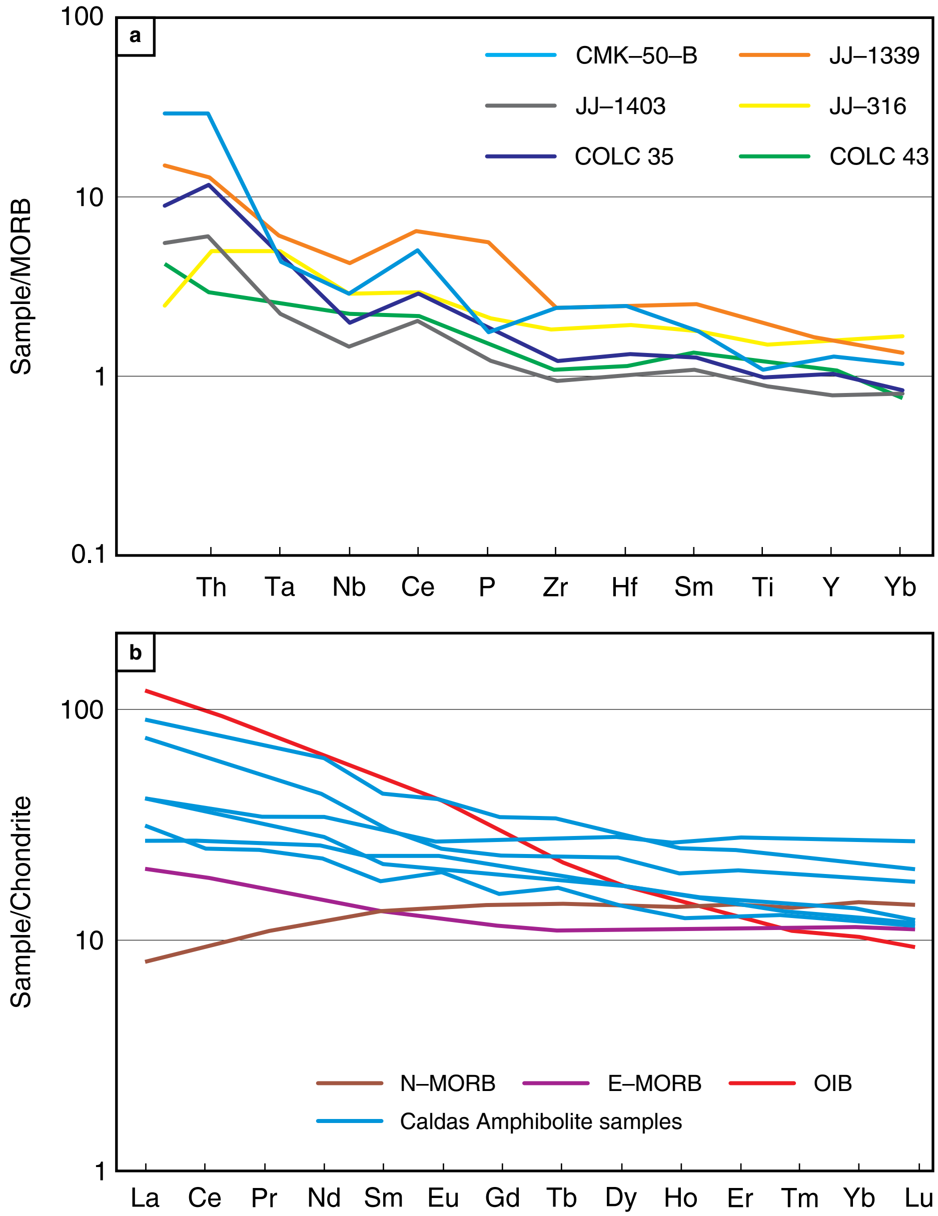

Figure 5. (a) N–MORB (Hofmann, 1988) normalized analyses of the Caldas Amphibolite. Modified from Giraldo–Ramírez (2013). Samples CMK–50–B, JJ–316, JJ–1339 and JJ–1403 from Giraldo–Ramírez (2013) and COLC 35 and COLC 43 from Giraldo (2010). **(b)** Chondrite–normalized Caldas Amphibolite (Boynton, 1984; blue) in comparison with N–MORB, E–MORB and OIB (Sun & McDonough, 1989). Modified from Giraldo–Ramírez (2013).

Table 1. εNd and model ages for three samples of Caldas Amphibolite

Sample	(^{143}Nd/^{144}Nd) 0	(^{147}Sm/^{144}Nd) 0	(^{143}Nd/^{144}Nd)	εNd (700 Ma)	T dm (Ga)
MIG 1	0.513	0.152	0.512	2.612	1.192
MIG 2	0.513	0.172	0.512	5.799	0.891
WG	0.513	0.158	0.512	3.428	1.135

Source: Samples MIG 1 and 2 from Giraldo (2010); sample WG from Giraldo–Ramírez (2013).

Note: Assumed values: (^{143}Nd/^{144}Nd)CHUR = 0.512638, (^{147}Sm/^{144}Nd)CHUR = 0.1967 (De Paolo, 1981).

Present–day composition of the DM: ^{147}Sm/^{144}Nd = 0.222 and ^{143}Nd/^{144}Nd = 0.513114 (Michard et al., 1985).

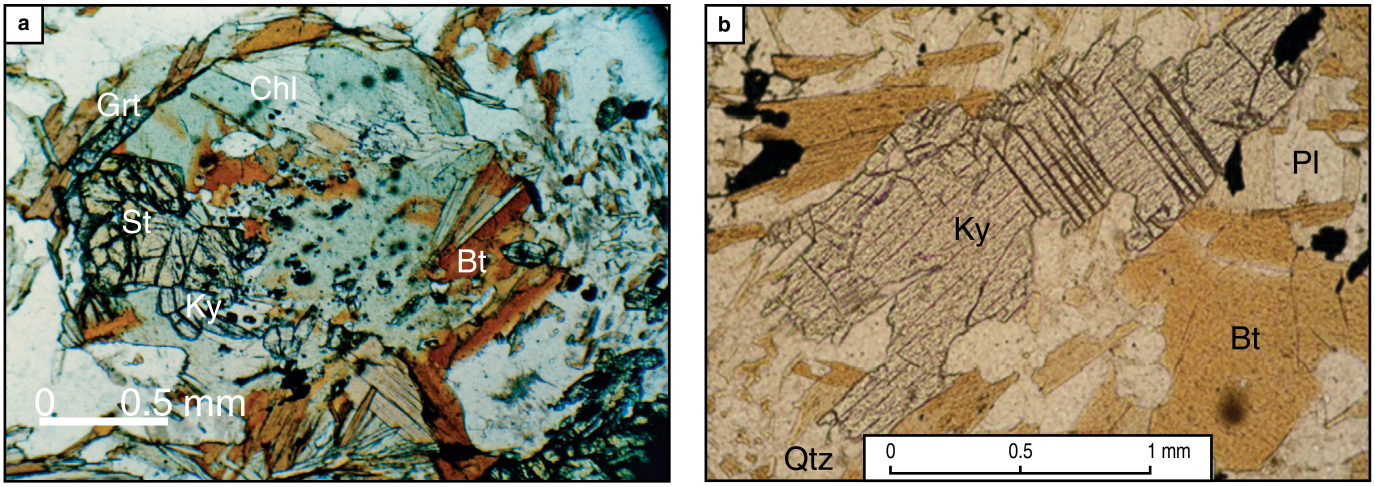

Figure 6. (a) Photomicrograph of pelitic schist interbedded within the Caldas Amphibolite, showing staurolite (St), kyanite (Ky), garnet (Grt), and chloritized (Chl) biotite (Bt). The garnet was partially replaced by biotite. (Mineral abbreviations following Siivola & Schmid, 2007). Taken from Restrepo (1986). **(b)** Kyanite (Ky) crystal with biotite (Bt), quartz (Qtz) and plagioclase (Pl).

amphibolites, and both are intruded by La Miel Orthogneiss. The paragenesis of the pelitic schist includes staurolite, kyanite, garnet, and chloritized biotite (Figure 6). This amphibolite–pelite association likely reflects a volcano–sedimentary sequence metamorphosed under medium pressure, lower–amphibolite facies conditions. The microstructures of the pelitic schist more clearly show the polyphase metamorphic character of the unit (Figure 4b), which underwent at least three tectonic phases (Restrepo, 1986).

Porphyritic dikes of an intermediate composition locally intrude the metamorphic basement of the Anacona Terrane, and range in thickness from 0.5–40 m; a tonalitic pluton also intrudes the metamorphic rocks on the western side. Their ages have yet to be determined. In fact, establishing whether the intrusions are related to magmatism in the Central Cordillera or to magmatic units east of the San Jerónimo Fault would be important in further constraining the geologic evolution of the Anacona Terrane.

3. Terrane Boundaries

To the east, the Santa Isabel Fault separates the Anacona Terrane from the Tahamí Terrane, whereas to the west, the San Jerónimo Fault, the easternmost fault of the Romeral Fault System, separates the Anacona Terrane from the low–grade volcanosedimentary rocks of the Quebradagrande Complex (Figure 2). Both faults run predominantly N–S in the region and define a narrow, near rhombic block at least 20 km long and only 4 km wide at its maximum extent. Mapping by González (1980) suggests that the Anacona Terrane may extend 60 km southwards. The NW–trending Tablacita Fault cuts the Santa Isabel Fault along the northern terrane boundary.

The San Jerónimo Fault, the easternmost strand of the Romeral Fault System, was initially described as an east–dipping reverse fault (Grosse, 1926). At present, most authors regard the San Jerónimo as a dextral strike–slip fault with a reverse component (e.g., Maya & González, 1995). The San Jerónimo Fault exhibits fault–gouge zones up to 3 meters thick (Patiño & Noreña, 1984) along the extent of the Anacona Terrane and a variable trend ranging from N25ºW in the southern segment to N–S in the central and northern segments. The age of movement on the San Jerónimo Fault is constrained by the accretion of the Quebradagrande Complex to the Tahamí Terrane, which is estimated to have occurred at 117–107 Ma (Villagómez et al, 2011), 73–65 Ma (Jaramillo et al., 2017) or 70–58 Ma (Zapata & Cardona, 2017). The timing of accretion of the Anacona Terrane to the Tahamí Terrane is post–Triassic in age, probably occurring in the Late Cretaceous – Paleocene as a consequence of the northward displacement of the Ebéjico and Caribbean Terranes. The Santa Isabel Fault was first mapped by Sepúlveda & Saldarriaga (1980) and Patiño & Noreña (1984). The fault is a strike–slip, mainly ductile structure with a N–S trend and a vertical to 80°W dip. It can be traced from the Versalles–Montebello road in the south (Patiño & Noreña, 1984) to the north, where it ends against the Tablacita Fault. Locally, the fault is characterized by a brittle–ductile tectonic breccia with rock fragments ranging from 1–15 mm in size and embedded in a dark–gray schistose matrix. The breccia fragments include rocks typical of both the Anacona and Tahamí Terranes; some clasts belong to La Miel Orthogneiss, while others are andalusite–bearing schist fragments that are likely derived from the Tahamí Terrane (Giraldo–Ramírez, 2013).

The Tablacita Fault was mapped by Maya & Escobar (1985) and was defined as a terrane boundary by Giraldo–Ramírez (2013). It is a ductile fault trending N55ºW. The fault separates units of the Anacona Terrane to the SW from those of the Tahamí Terrane to the NE. Kinematic indicators show sinistral strike–slip movement and possibly a younger phase of fault movement than that on the Santa Isabel Fault. The Santa Isabel

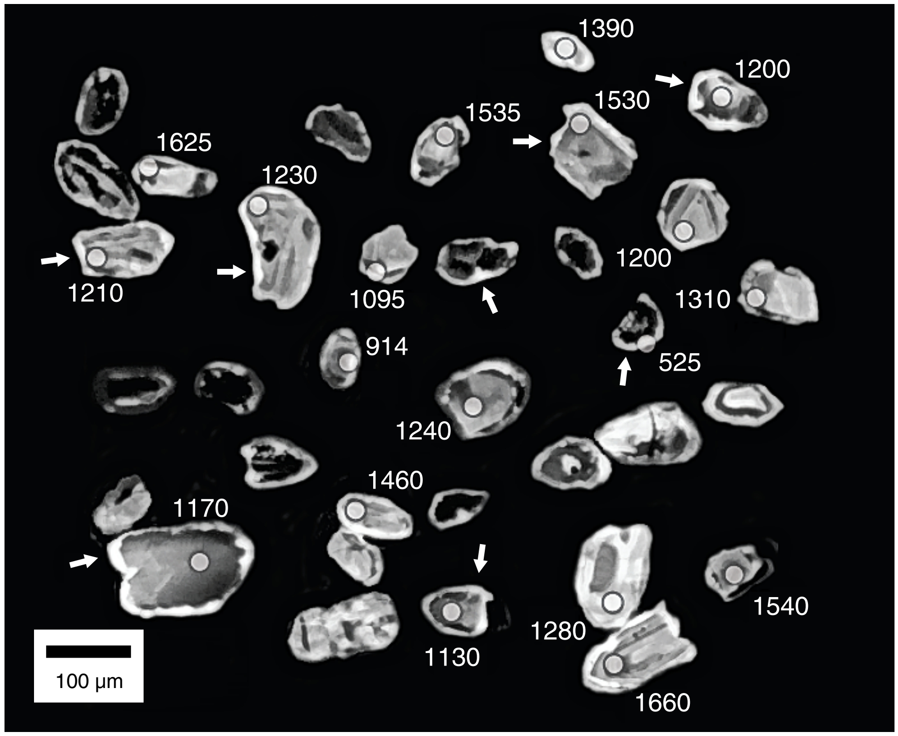

Figure 7. CL imaging of sample AC–1 zircon grains. The numbers are U–Pb ages in Ma. Arrows point to thin metamorphic rims.

and the Tablacita Faults are predominantly ductile in character. They likely formed at a depth greater than 10 km with minor brittle reactivations; there is no evidence for present–day seismic activity (Giraldo–Ramírez, 2013).

4. New Detrital Zircon Geochronology

U–Pb zircon ages were obtained from an Anacona Terrane quartzite collected at the junction between La Romera Creek and La Miel Creek (6° 5' 54'' N, 75° 36' 52'' W). Zircon grains in the sample are anhedral and rounded, and their sizes range from 50–200 μm along their longest dimension (Figure 7). The cathodoluminescence (CL) textures vary from grain to grain and include homogeneous luminescence, concentric zoning, sector zoning, and irregular zones of low luminescence, among others. The roundness and the variety in size and texture attest to the variable nature of the detrital zircon population in the sample. Importantly, CL images reveal thin, luminous, homogenous rims in many of the zircon grains (Figure 7). These rims were likely produced by Paleozoic metamorphism in the Anacona Terrane, but they were too thin to be dated by the method used.

U–Pb geochronology was conducted by LA–ICP–MS at the Laboratorio de Estudios Isotópicos, Centro de Geociencias, UNAM, following the methods described in Solari et al. (2010). Isotopic ratios were corrected for common Pb using the method of Andersen (2002). Ninety–eight grains were dated (Table 2), and they yielded Precambrian ages; hence, $^{207}Pb/^{206}Pb$ ages were preferred. Eight analyses were disregarded because they yielded uncertainties greater than 5%, discordance greater than 4%, or reverse discordance greater than 2%. Hence, 90 analyses were used to construct the probability density diagram in Figure 8.

The detrital zircon signature of the quartzite sample is characterized by a spread in ages from 850 Ma to 1700 Ma. Most of the zircon ages range from 1575–1425 Ma and 1250–1125 Ma. The former population is mostly absent from Laurentian sources (Hoffman, 1989; Martens et al., 2010) but is abundant in Amazonia (Tassinari et al., 2000), a strong indication that the Anacona Terrane is of Gondwanan affinity. The mid–Mesoproterozoic population points to provenance from a Grenville source within Gondwana, such as the Oaxaquia microcontinent (Ortega–Gutiérrez et al., 1995), the Putumayo Orogen (Ibañez–Mejia et al., 2011), or the Arequipa Massif (Wasteneys et al., 1995). A similar feature has been previously observed in the xenocrystic zircon component of La Miel Orthogneiss (Martens et al., 2014, Figure 9).

An important constraint from the geochronology is the time of deposition of the sedimentary protolith of the quartzite. The youngest dated spot yielded an age of 540 ± 75 Ma. However, this age does not necessarily imply a Paleozoic depositional age, because it may correspond to a mixture between a detrital core and a Paleozoic metamorphic rim (see spot in Figure 7). Indeed, the analysis was conducted on an external zone involving part of the detrital core, the metamorphic rim, and epoxy. Furthermore, the Th/U ratio is relatively low, suggestive of a metamorphic isotopic component. It is therefore plausible to in-

Table 2. Corrected zircon U–Pb isotopic ratios, ages, and chondrite–normalized REE concentrations of sample AC–1 (an Anacona Terrane quartzite).

				Corrected ratios[2]									Corrected Ages (Ma)						Chondrite–normalized REE concentrations												
	U (ppm)[1]	Th (ppm)[1]	Th/U	$^{207}Pb/^{206}Pb$	±2s abs	$^{207}Pb/^{235}U$	±2s abs	$^{206}Pb/^{238}U$	±2s abs	$^{208}Pb/^{232}Th$	±2s abs	Rho	$^{206}Pb/^{238}U$	±2s	$^{207}Pb/^{235}U$	±2s	$^{207}Pb/^{206}Pb$	±2s	La	Ce	Pr	Nd	Sm	Eu	Gd	Tb	Dy	Ho	Er	Yb	Lu
Zircon_001	945	381	0.40	0.0751	0.0018	1.715	0.051	0.1640	0.0025	0.04933	0.00081	0.45	979	14	1014	19	1088	57	1.11E+01	3.05E+01	1.16E+01	2.12E+01	7.28E+01	1.56E+01	2.24E+02	4.29E+02	7.16E+02	1.24E+03	1.91E+03	3.59E+03	4.64E+03
Zircon_002	243	154	0.63	0.0782	0.0006	2.149	0.039	0.1980	0.0022	0.05980	0.00180	0.51	1165	12	1167	12	1151	16	1.90E+00	2.46E+01	5.17E+00	1.20E+01	6.31E+01	4.21E+00	2.04E+02	3.63E+02	5.98E+02	9.96E+02	1.45E+03	2.52E+03	3.11E+03
Zircon_003	773	240	0.31	0.0859	0.0007	2.800	0.033	0.2325	0.0023	0.06680	0.00200	0.29	1347	12	1355.5	8.9	1336	16	6.92E-01	2.63E+01	2.30E+00	3.54E+00	1.28E+01	7.99E+00	5.33E+01	1.12E+02	2.04E+02	3.52E+02	5.28E+02	9.66E+02	1.27E+03
Zircon_004	111	35	0.31	0.0795	0.0041	2.230	0.130	0.2028	0.0031	0.06100	0.00140	0.41	1190	17	1188	41	1180	100	4.98E-01	1.08E+01	9.70E-01	3.48E+00	1.71E+01	5.86E+00	7.49E+01	1.52E+02	2.78E+02	4.91E+02	7.61E+02	1.51E+03	1.90E+03
Zircon_005	83	47	0.57	0.0833	0.0057	2.650	0.200	0.2305	0.0042	0.06870	0.00130	0.63	1337	22	1312	57	1260	140	1.86E+00	8.56E+00	6.90E+00	1.68E+01	7.30E+01	1.69E+01	2.35E+02	3.78E+02	6.02E+02	9.27E+02	1.27E+03	2.08E+03	2.52E+03
Zircon_006	431	182	0.42	0.0955	0.0012	3.466	0.054	0.2650	0.0031	0.07890	0.00240	0.76	1515	16	1519	12	1537	23	1.43E+02	1.27E+02	7.87E+01	7.09E+01	8.58E+01	9.06E+00	2.65E+02	4.69E+02	8.20E+02	1.40E+03	2.09E+03	3.74E+03	4.52E+03
Zircon_007	152	45	0.29	0.0873	0.0019	2.650	0.120	0.2219	0.0066	0.06970	0.00490	0.84	1291	35	1313	33	1364	42	2.32E-01	9.23E+00	9.48E-01	2.30E+00	1.51E+01	4.19E+00	6.98E+01	1.38E+02	2.51E+02	4.60E+02	7.29E+02	1.42E+03	1.85E+03
Zircon_008	243	102	0.42	0.0805	0.0009	2.293	0.057	0.2051	0.0022	0.06170	0.00160	0.54	1203	12	1209	18	1208	22	1.73E+01	3.30E+01	2.35E+01	4.05E+01	1.22E+02	3.14E+01	4.27E+02	6.95E+02	1.13E+03	1.80E+03	2.45E+03	3.80E+03	4.79E+03
Zircon_009	136	59	0.44	0.0760	0.0013	1.935	0.051	0.1845	0.0031	0.05660	0.00200	0.61	1091	17	1092	18	1099	37	1.77E-01	8.19E+00	4.25E+00	1.49E+01	7.16E+01	1.12E+01	2.36E+02	3.96E+02	6.51E+02	1.03E+03	1.46E+03	2.45E+03	3.09E+03
Zircon_010	1766	606	0.34	0.0780	0.0006	2.074	0.028	0.1925	0.0030	0.05950	0.00300	0.66	1135	16	1140.2	9.3	1147	16	6.96E-01	4.40E+01	3.20E+00	1.22E+01	8.24E+01	4.07E+00	2.79E+02	5.72E+02	9.92E+02	1.70E+03	2.61E+03	4.75E+03	5.69E+03
Zircon_011	744	295	0.40	0.0776	0.0008	2.082	0.030	0.1941	0.0018	0.05780	0.00074	0.55	1144	10	1142.4	9.9	1136	22	5.53E+02	2.90E+02	3.02E+02	2.74E+02	2.77E+02	1.01E+02	3.72E+02	5.60E+02	9.02E+02	1.46E+03	2.26E+03	4.73E+03	6.38E+03
Zircon_012	240	71	0.29	0.0786	0.0005	2.226	0.027	0.2042	0.0021	0.06100	0.00170	0.29	1198	11	1188.9	8.6	1162	12	1.35E-01	2.89E+01	1.64E+00	6.21E+00	3.76E+01	3.37E+00	1.46E+02	2.72E+02	4.88E+02	8.39E+02	1.26E+03	2.31E+03	2.83E+03
Zircon_013	451	203	0.45	0.0699	0.0020	1.562	0.040	0.1654	0.0034	0.05030	0.00120	0.45	987	19	955	16	923	58	6.96E-01	1.29E+01	1.84E+00	5.47E+00	3.34E+01	1.37E+01	1.66E+02	3.44E+02	6.43E+02	1.19E+03	1.88E+03	3.83E+03	5.03E+03
Zircon_014	825	189	0.23	0.0708	0.0015	1.230	0.029	0.1270	0.0018	0.03854	0.00052	0.13	771	10	814	13	949	44	1.56E+01	3.12E+01	1.45E+01	1.95E+01	4.21E+01	3.43E+01	7.49E+01	1.43E+02	2.60E+02	4.33E+02	7.55E+02	1.97E+03	3.12E+03
Zircon_015	719	110	0.15	0.0937	0.0005	3.363	0.028	0.2610	0.0025	0.07610	0.00210	0.56	1495	13	1496.8	6.2	1502	9.2	4.60E-01	5.63E+00	1.62E+00	5.10E+00	3.80E+01	1.94E+00	1.80E+02	4.52E+02	9.51E+02	1.81E+03	3.04E+03	6.30E+03	8.15E+03
Zircon_016	225	79	0.35	0.0734	0.0009	1.751	0.036	0.1738	0.0018	0.05170	0.00150	0.46	1033	10	1027	13	1023	24	3.46E-01	1.35E+01	4.22E+00	1.29E+01	6.68E+01	1.97E+01	2.56E+02	4.56E+02	7.46E+02	1.25E+03	1.77E+03	2.98E+03	3.81E+03
Zircon_017	291	62	0.21	0.0743	0.0005	1.798	0.040	0.1766	0.0027	0.05390	0.00190	0.80	1048	15	1044	14	1049	12	1.52E-01	1.57E+01	1.44E+00	4.27E+00	2.40E+01	4.14E+00	8.85E+01	1.79E+02	3.20E+02	5.72E+02	8.93E+02	1.77E+03	2.38E+03
Zircon_018	334	160	0.48	0.0939	0.0006	3.430	0.036	0.2667	0.0026	0.07840	0.00190	0.61	1524	13	1510.9	8.3	1506	13	4.85E-01	1.51E+01	1.89E+00	5.05E+00	2.37E+01	3.61E+00	1.08E+02	2.07E+02	3.70E+02	6.45E+02	9.64E+02	1.66E+03	2.02E+03
Zircon_019	133	97	0.73	0.1005	0.0007	3.982	0.067	0.2884	0.0036	0.08280	0.00250	0.65	1633	18	1630	14	1633	12	1.81E-01	5.69E+01	1.07E+00	3.87E+00	1.97E+01	9.79E+00	7.31E+01	1.35E+02	2.46E+02	4.32E+02	7.06E+02	1.51E+03	2.05E+03
Zircon_020	302	100	0.33	0.0814	0.0005	2.292	0.022	0.2063	0.0018	0.06150	0.00150	0.26	1209.3	9.7	1210.8	6.6	1230	12	7.55E-01	2.07E+01	1.22E+00	4.16E+00	2.38E+01	3.57E+00	1.02E+02	2.01E+02	3.72E+02	6.58E+02	1.01E+03	1.93E+03	2.44E+03
Zircon_021	386	164	0.43	0.0937	0.0006	3.396	0.035	0.2634	0.0028	0.07830	0.00120	0.61	1507	14	1503.3	8	1501	13	1.60E-01	1.40E+01	1.68E+00	5.84E+00	3.21E+01	2.97E+00	1.46E+02	2.82E+02	4.99E+02	8.94E+02	1.37E+03	2.44E+03	3.06E+03
Zircon_022	114	43	0.38	0.0786	0.0009	2.119	0.047	0.1983	0.0027	0.05870	0.00190	0.38	1166	15	1154	15	1162	22	1.14E-01	1.52E+01	1.25E+00	2.98E+00	1.69E+01	7.99E+00	7.61E+01	1.49E+02	2.78E+02	4.96E+02	8.02E+02	1.63E+03	2.13E+03
Zircon_023	401	133	0.33	0.0962	0.0006	3.486	0.033	0.2660	0.0026	0.07720	0.00240	0.37	1520	13	1523.8	7.5	1551	11	3.29E-01	7.13E+00	1.08E+00	4.09E+00	2.33E+01	2.86E+00	1.19E+02	2.57E+02	4.80E+02	8.74E+02	1.35E+03	2.58E+03	3.35E+03
Zircon_024	195	134	0.69	0.0917	0.0008	3.144	0.057	0.2505	0.0024	0.07330	0.00210	0.70	1441	12	1443	14	1461	17	4.22E-01	1.98E+01	5.18E+00	1.84E+01	8.85E+01	1.71E+01	2.91E+02	4.88E+02	7.63E+02	1.23E+03	1.74E+03	2.82E+03	3.51E+03
Zircon_025	505	119	0.23	0.0810	0.0005	2.298	0.025	0.2067	0.0020	0.06440	0.00240	0.68	1211	11	1212.9	7.3	1221	13	1.35E-01	3.22E+01	8.62E-01	3.74E+00	2.36E+01	2.22E+00	1.19E+02	2.39E+02	4.65E+02	8.32E+02	1.29E+03	2.41E+03	2.86E+03
Zircon_026	1031	158	0.15	0.0674	0.0018	1.089	0.033	0.1173	0.0039	0.03580	0.00140	0.74	715	23	748	16	849	55	2.38E+01	7.88E+01	5.36E+01	5.91E+01	1.53E+02	9.43E+01	2.09E+02	3.48E+02	4.73E+02	6.87E+02	1.07E+03	2.50E+03	3.70E+03
Zircon_027	664	483	0.73	0.0935	0.0040	2.960	0.120	0.2298	0.0043	0.06760	0.00150	0.62	1333	23	1397	30	1495	78	1.18E+00	8.97E+01	1.12E+01	2.54E+01	7.70E+01	8.21E+01	2.33E+02	3.55E+02	5.61E+02	8.94E+02	1.34E+03	2.66E+03	3.72E+03
Zircon_028	395	129	0.33	0.0995	0.0006	3.904	0.057	0.2866	0.0042	0.07850	0.00160	0.74	1624	21	1614	12	1615	11	3.97E-01	5.29E+00	4.85E+00	1.95E+01	9.39E+01	1.47E+01	4.02E+02	8.09E+02	1.48E+03	2.36E+03	3.38E+03	5.53E+03	6.59E+03
Zircon_029	186	58	0.31	0.0795	0.0006	2.205	0.036	0.2018	0.0020	0.06000	0.00180	0.45	1185	11	1184	11	1185	16	1.22E-01	1.05E+01	1.24E+00	3.57E+00	2.20E+01	5.42E+00	1.13E+02	2.20E+02	4.06E+02	6.94E+02	1.06E+03	1.90E+03	2.46E+03
Zircon_030	446	253	0.57	0.0960	0.0012	3.554	0.056	0.2697	0.0030	0.07930	0.00099	0.76	1539	15	1539	12	1546	24	7.97E-01	2.46E+01	1.44E+00	5.05E+00	2.67E+01	1.08E+01	1.57E+02	3.34E+02	6.70E+02	1.28E+03	2.16E+03	4.58E+03	6.33E+03
Zircon_031	237	133	0.56	0.0776	0.0022	2.009	0.068	0.1879	0.0026	0.05635	0.00080	0.66	1110	14	1117	23	1155	56	6.96E-01	3.34E+01	3.16E+00	1.11E+01	4.81E+01	1.07E+01	1.85E+02	3.14E+02	5.40E+02	9.14E+02	1.32E+03	2.43E+03	3.20E+03
Zircon_032	354	119	0.34	0.0951	0.0009	3.408	0.052	0.2612	0.0029	0.07840	0.00360	0.30	1496	15	1506	12	1529	18	1.22E+00	4.32E+01	7.11E+00	1.25E+01	4.21E+01	2.77E+01	1.40E+02	2.28E+02	3.95E+02	6.83E+02	1.04E+03	2.01E+03	2.72E+03
Zircon_033	1240	398	0.32	0.0795	0.0008	2.152	0.038	0.1974	0.0021	0.06020	0.00310	0.87	1161	11	1168	11	1184	20	8.73E-01	4.18E+01	2.41E+00	5.80E+00	2.73E+01	6.96E+00	1.16E+02	2.26E+02	4.54E+02	8.65E+02	1.52E+03	3.47E+03	4.74E+03
Zircon_034	271	90	0.33	0.0805	0.0006	2.261	0.040	0.2030	0.0022	0.06130	0.00200	0.35	1191	12	1200	12	1207	16	1.14E-01	2.12E+01	1.09E+00	4.20E+00	2.18E+01	2.88E+00	9.20E+01	1.77E+02	3.27E+02	5.81E+02	9.01E+02	1.76E+03	2.31E+03
Zircon_035	408	103	0.25	0.0869	0.0006	2.664	0.049	0.2249	0.0030	0.06770	0.00230	0.77	1308	16	1324	16	1358	13	1.47E+00	2.18E+01	1.52E+00	5.16E+00	1.85E+01	4.26E+00	6.43E+01	1.47E+02	2.65E+02	4.71E+02	7.32E+02	1.44E+03	1.91E+03
Zircon_036	76	43	0.56	0.0749	0.0041	1.850	0.110	0.1816	0.0035	0.05530	0.00140	0.63	1076	19	1061	40	1040	120	1.51E+00	7.78E+00	4.53E+00	1.37E+01	6.28E+01	1.99E+01	1.86E+02	3.16E+02	5.20E+02	8.15E+02	1.12E+03	1.91E+03	2.32E+03
Zircon_037	516	84	0.16	0.0832	0.0009	2.468	0.043	0.2167	0.0023	0.06453	0.00061	0.71	1264	12	1263	13	1272	21	9.11E+00	7.55E+00	4.91E+00	8.75E+00	3.86E+01	5.06E+00	1.95E+02	4.09E+02	6.82E+02	1.05E+03	1.51E+03	2.80E+03	3.39E+03
Zircon_038	748	155	0.21	0.0784	0.0035	1.722	0.086	0.1585	0.0025	0.03830	0.00870	0.66	948	14	1016	32	1149	89	3.76E+00	2.14E+01	1.56E+01	2.91E+01	9.39E+01	5.68E+01	1.79E+02	3.16E+02	5.73E+02	8.75E+02	1.34E+03	2.88E+03	3.78E+03
Zircon_039	95	20	0.21	0.0832	0.0021	2.550	0.096	0.2228	0.0045	0.06800	0.00340	0.60	1296	24	1285	28	1271	49	3.59E-01	7.72E+00	1.19E+00	2.60E+00	1.66E+01	3.61E+00	6.73E+01	1.15E+02	2.17E+02	3.62E+02	5.73E+02	1.06E+03	1.37E+03

Devonian Carboniferous

Table 2. Corrected zircon U–Pb isotopic ratios, ages, and chondrite–normalized REE concentrations of sample AC–1 (an Anacona Terrane quartzite) (*continued*).

				Corrected ratios[2]									Corrected Ages (Ma)						Chondrite–normalized REE concentrations													
	U (ppm)[1]	Th (ppm)[1]	Th/U	$^{207}Pb/^{206}Pb$	±2s abs	$^{207}Pb/^{235}U$	±2s abs	$^{206}Pb/^{238}U$	±2s abs	$^{208}Pb/^{232}Th$	±2s abs	Rho	$^{206}Pb/^{238}U$	±2s	$^{207}Pb/^{235}U$	±2s	$^{207}Pb/^{206}Pb$	±2s	La	Ce	Pr	Nd	Sm	Eu	Gd	Tb	Dy	Ho	Er	Yb	Lu
Zircon_040	314	107	0.34	0.0928	0.0013	3.144	0.075	0.2471	0.0033	0.07250	0.00140	0.80	1423	17	1443	19	1491	30	1.73E-01	1.95E+01	1.14E+00	2.80E+00	1.50E+01	1.01E+01	5.98E+01	1.16E+02	2.26E+02	4.34E+02	7.67E+02	2.13E+03	3.17E+03
Zircon_041	291	56	0.19	0.0719	0.0007	1.605	0.027	0.1616	0.0018	0.04880	0.00140	0.49	966	10	972	11	981	18	1.27E-01	9.72E+00	7.33E-01	3.33E+00	1.77E+01	5.84E+00	6.93E+01	1.29E+02	2.26E+02	3.70E+02	5.39E+02	9.43E+02	1.21E+03
Zircon_042	342	153	0.45	0.0955	0.0007	3.443	0.035	0.2642	0.0029	0.07750	0.00250	0.50	1511	15	1515.8	8.4	1538	14	5.02E-01	1.54E+01	5.55E+00	1.93E+01	1.07E+02	2.08E+01	4.15E+02	7.15E+02	1.22E+03	2.00E+03	2.82E+03	4.42E+03	5.36E+03
Zircon_043	697	51	0.07	0.0929	0.0023	3.260	0.110	0.2547	0.0046	0.07490	0.00130	0.79	1462	24	1472	26	1485	47	1.31E+00	2.46E+00	3.02E+00	4.88E+00	4.59E+01	3.75E+00	2.31E+02	4.28E+02	7.21E+02	9.73E+02	1.28E+03	2.09E+03	2.50E+03
Zircon_044	877	48	0.05	0.0933	0.0007	3.131	0.028	0.2474	0.0035	0.07240	0.00190	0.42	1425	18	1440.3	6.9	1493	14	-8.08E-05	1.96E+00	8.30E-01	3.61E+00	1.89E+01	3.91E+00	8.19E+01	1.44E+02	2.34E+02	4.01E+02	6.98E+02	2.09E+03	3.04E+03
Zircon_045	1018	334	0.33	0.0856	0.0011	2.345	0.036	0.1992	0.0020	0.05895	0.00077	0.58	1171	11	1226	11	1330	24	3.84E+01	7.50E+01	4.20E+01	5.51E+01	1.09E+02	5.63E+00	3.95E+02	6.98E+02	1.16E+03	2.00E+03	2.86E+03	4.57E+03	5.78E+03
Zircon_046	529	62	0.12	0.0937	0.0004	3.436	0.042	0.2657	0.0040	0.07530	0.00320	0.77	1519	20	1512.3	9.6	1501	8.3	1.81E-01	3.23E+00	1.44E+00	6.13E+00	6.75E+01	2.86E+00	3.04E+02	5.24E+02	6.61E+02	7.20E+02	7.53E+02	8.94E+02	9.67E+02
Zircon_047	447	84	0.19	0.0789	0.0028	1.751	0.074	0.1609	0.0032	0.04819	0.00094	0.44	962	18	1027	27	1168	70	6.46E+00	3.08E+02	2.37E+01	3.44E+01	1.36E+02	9.77E+01	5.85E+02	1.14E+03	1.93E+03	3.04E+03	4.48E+03	7.71E+03	9.53E+03
Zircon_048	384	193	0.50	0.0791	0.0004	2.160	0.025	0.1993	0.0022	0.05690	0.00150	0.56	1172	12	1168.1	8.1	1173	11	8.52E-01	2.10E+01	4.91E+00	1.39E+01	6.28E+01	9.79E+00	2.13E+02	3.85E+02	6.26E+02	1.03E+03	1.49E+03	2.56E+03	3.08E+03
Zircon_049	361	102	0.28	0.0801	0.0006	2.306	0.037	0.2083	0.0023	0.06230	0.00190	0.69	1220	12	1214	11	1200	15	7.59E-02	1.92E+01	8.84E-01	2.95E+00	1.61E+01	1.47E+00	6.65E+01	1.30E+02	2.44E+02	4.29E+02	6.96E+02	1.38E+03	1.74E+03
Zircon_050	375	176	0.47	0.0804	0.0006	2.243	0.036	0.2039	0.0023	0.06150	0.00200	0.80	1196	12	1194	11	1209	13	4.10E+00	2.43E+01	4.62E+00	1.15E+01	5.91E+01	1.03E+01	2.67E+02	4.85E+02	8.46E+02	1.40E+03	2.05E+03	3.55E+03	4.33E+03
Zircon_051	367	223	0.61	0.1001	0.0010	3.857	0.077	0.2798	0.0029	0.08210	0.00220	0.39	1591	15	1604	16	1625	19	3.25E-01	4.32E+01	3.13E+00	1.15E+01	5.20E+01	2.79E+01	1.58E+02	2.97E+02	4.94E+02	8.52E+02	1.29E+03	2.48E+03	3.31E+03
Zircon_052	153	47	0.31	0.0794	0.0015	2.260	0.068	0.2052	0.0025	0.06310	0.00280	0.88	1203	13	1198	21	1189	36	1.43E-01	8.91E+00	9.59E-01	3.39E+00	1.95E+01	4.09E+00	8.94E+01	1.69E+02	2.97E+02	5.18E+02	7.93E+02	1.50E+03	1.91E+03
Zircon_053	317	107	0.34	0.0806	0.0005	2.363	0.032	0.2112	0.0021	0.06250	0.00200	0.26	1235	11	1231.2	9.5	1212	12	1.18E-01	2.77E+01	1.41E+00	4.79E+00	2.55E+01	2.63E+00	1.23E+02	2.39E+02	4.22E+02	7.45E+02	1.13E+03	2.15E+03	2.77E+03
Zircon_054	241	93	0.39	0.0813	0.0009	2.300	0.047	0.2063	0.0021	0.06210	0.00150	0.39	1209	11	1215	13	1229	22	4.89E+00	2.12E+01	4.09E+00	5.71E+00	1.97E+01	3.32E+00	8.04E+01	1.50E+02	2.80E+02	5.02E+02	7.86E+02	1.60E+03	2.08E+03
Zircon_055	429	78	0.18	0.0760	0.0006	1.887	0.022	0.1812	0.0019	0.05490	0.00160	0.39	1073	10	1076.3	7.9	1095	15	2.15E-01	1.72E+01	1.48E+00	3.79E+00	2.05E+01	4.51E+00	9.50E+01	1.87E+02	3.54E+02	6.17E+02	9.58E+02	1.76E+03	2.24E+03
Zircon_056	292	51	0.17	0.0954	0.0007	3.548	0.057	0.2708	0.0036	0.08270	0.00270	0.78	1545	18	1537	13	1536	15	2.36E-01	7.81E+00	1.57E+00	4.27E+00	2.78E+01	5.35E+00	1.18E+02	2.30E+02	4.04E+02	7.16E+02	1.07E+03	1.95E+03	2.52E+03
Zircon_057	559	189	0.34	0.0803	0.0006	2.210	0.042	0.2033	0.0025	0.06140	0.00210	0.25	1193	13	1184	13	1205	16	-7.59E-05	3.61E+01	2.03E+00	5.03E+00	3.82E+01	4.26E+00	1.71E+02	3.45E+02	6.26E+02	1.10E+03	1.70E+03	3.07E+03	3.63E+03
Zircon_059	990	419	0.42	0.0884	0.0010	2.706	0.046	0.2220	0.0034	0.06570	0.00150	0.96	1292	18	1330	13	1391	20	8.10E+00	5.22E+01	3.01E+01	5.58E+01	1.74E+02	1.44E+02	4.02E+02	6.79E+02	1.13E+03	1.82E+03	2.61E+03	4.88E+03	6.79E+03
Zircon_060	305	106	0.35	0.0951	0.0008	3.606	0.047	0.2728	0.0029	0.08100	0.00230	0.39	1555	15	1551	10	1533	15	4.22E-01	7.10E+00	2.66E+00	9.45E+00	5.28E+01	1.08E+01	1.97E+02	3.45E+02	5.72E+02	9.38E+02	1.38E+03	2.48E+03	3.21E+03
Zircon_061	1665	74	0.04	0.0910	0.0007	2.979	0.031	0.2389	0.0032	0.06920	0.00180	0.84	1381	17	1402.3	8	1445	14	9.11E+00	9.74E+00	1.02E+01	1.41E+01	4.35E+01	2.82E+01	1.37E+02	3.47E+02	7.22E+02	1.30E+03	2.22E+03	5.02E+03	6.90E+03
Zircon_062	163	58	0.35	0.0802	0.0012	2.349	0.053	0.2108	0.0031	0.06470	0.00210	0.29	1233	16	1227	16	1202	31	5.91E-02	1.53E+01	8.30E-01	2.78E+00	1.50E+01	2.68E+00	5.93E+01	1.13E+02	2.11E+02	3.66E+02	5.88E+02	1.14E+03	1.54E+03
Zircon_063	790	52	0.07	0.0584	0.0020	0.697	0.038	0.0846	0.0035	0.02620	0.00110	0.75	524	21	537	23	541	74	1.98E+02	1.68E+02	1.26E+02	1.16E+02	1.12E+02	6.71E+01	1.34E+02	2.22E+02	2.93E+02	4.36E+02	6.19E+02	1.43E+03	2.41E+03
Zircon_064	315	98	0.31	0.0968	0.0013	3.660	0.054	0.2748	0.0035	0.08120	0.00220	0.42	1565	18	1563	12	1563	26	2.36E+01	5.22E+01	4.31E+01	5.03E+01	8.31E+01	3.46E+01	2.15E+02	3.38E+02	5.34E+02	8.70E+02	1.25E+03	2.35E+03	3.12E+03
Zircon_065	311	78	0.25	0.0847	0.0014	2.683	0.055	0.2295	0.0032	0.06830	0.00270	0.09	1332	17	1323	15	1309	32	1.35E-01	1.86E+01	2.06E+00	9.39E+00	3.56E+01	3.91E+00	1.78E+02	3.04E+02	5.29E+02	8.90E+02	1.27E+03	2.17E+03	2.86E+03
Zircon_066	285	83	0.29	0.0800	0.0005	2.330	0.032	0.2104	0.0024	0.06330	0.00220	0.27	1231	13	1221.4	9.7	1197	12	1.43E+01	3.25E+01	2.11E+01	3.26E+01	7.30E+01	1.99E+01	2.13E+02	3.60E+02	6.30E+02	1.04E+03	1.57E+03	2.71E+03	3.37E+03
Zircon_067	714	197	0.28	0.0690	0.0014	1.369	0.035	0.1442	0.0022	0.04381	0.00050	0.66	869	12	876	15	896	43	7.22E+00	3.13E+01	2.45E+01	4.73E+01	1.80E+02	1.05E+02	4.19E+02	7.29E+02	1.15E+03	1.72E+03	2.40E+03	4.11E+03	5.08E+03
Zircon_068	105	73	0.70	0.0690	0.0012	1.487	0.040	0.1564	0.0022	0.04710	0.00140	0.37	937	12	924	16	896	35	5.15E-01	2.76E+01	7.06E+00	2.24E+01	8.68E+01	5.15E+01	2.56E+02	3.77E+02	5.62E+02	8.15E+02	1.08E+03	1.66E+03	2.04E+03
Zircon_069	1930	1056	0.55	0.0790	0.0003	2.164	0.026	0.1984	0.0021	0.06220	0.00170	0.77	1167	11	1169.2	8.2	1171.6	7.6	1.05E+02	1.66E+02	6.90E+01	6.56E+01	1.51E+02	1.85E+01	5.78E+02	1.09E+03	1.95E+03	3.32E+03	4.95E+03	8.11E+03	9.63E+03
Zircon_070	963	92	0.10	0.0835	0.0007	2.562	0.039	0.2216	0.0027	0.06790	0.00250	0.81	1290	14	1289	11	1281	16	2.56E+00	2.23E+01	1.15E+01	2.23E+01	8.11E+01	5.52E+01	1.87E+02	2.96E+02	4.11E+02	5.07E+02	6.13E+02	8.45E+02	9.35E+02
Zircon_071	390	12	0.03	0.0701	0.0004	1.574	0.028	0.1611	0.0016	0.05140	0.00290	0.80	962.9	8.8	960	11	931	12	1.52E-01	2.79E+00	4.09E-01	1.20E+00	4.46E+00	6.75E+00	1.98E+01	3.17E+01	4.65E+01	6.28E+01	8.09E+01	1.18E+02	1.43E+02
Zircon_072	855	215	0.25	0.0766	0.0004	1.996	0.024	0.1881	0.0017	0.05660	0.00160	0.63	1111.2	9	1114	8.1	1111	11	4.39E-01	1.44E+01	1.61E+00	2.19E+00	8.31E+00	1.12E+01	3.39E+01	8.28E+01	1.89E+02	4.18E+02	8.05E+02	2.27E+03	3.28E+03
Zircon_073	1503	121	0.08	0.0933	0.0006	3.131	0.038	0.2458	0.0036	0.07480	0.00530	0.85	1417	18	1444	11	1493	13	8.82E+00	1.56E+01	1.50E+01	2.39E+01	7.77E+01	4.80E+01	2.65E+02	6.10E+02	1.23E+03	2.09E+03	3.19E+03	6.16E+03	7.67E+03
Zircon_074	567	191	0.34	0.0784	0.0010	2.204	0.041	0.2041	0.0021	0.06050	0.00180	0.17	1198	11	1182	13	1156	25	1.48E-01	3.18E+01	9.38E-01	3.35E+00	2.77E+01	1.33E+00	1.32E+02	2.70E+02	4.72E+02	8.33E+02	1.29E+03	2.47E+03	3.11E+03
Zircon_075	1437	200	0.14	0.0688	0.0003	1.457	0.020	0.1521	0.0019	0.03930	0.00110	0.62	912	10	912.5	8.2	893.9	8.6	2.53E-01	5.02E+00	1.10E+00	6.08E+00	3.92E+01	8.88E+00	1.63E+02	2.78E+02	3.82E+02	4.76E+02	5.51E+02	6.99E+02	7.92E+02
Zircon_076	362	130	0.36	0.0788	0.0006	2.111	0.030	0.1956	0.0019	0.05780	0.00110	0.54	1152	10	1151.9	9.7	1165	14	3.04E-01	2.42E+01	1.64E+00	4.22E+00	2.30E+01	3.23E+00	1.05E+02	2.04E+02	3.73E+02	6.55E+02	1.04E+03	2.02E+03	2.56E+03
Zircon_077	962	252	0.26	0.0733	0.0012	1.663	0.020	0.1652	0.0020	0.04970	0.00085	0.16	986	11	994.4	7.7	1021	32	9.54E-01	2.89E+01	4.63E+00	1.14E+01	6.42E+01	1.35E+01	2.77E+02	5.01E+02	8.62E+02	1.54E+03	2.36E+03	4.32E+03	5.49E+03
Zircon_079	405	134	0.33	0.0788	0.0008	2.267	0.048	0.2067	0.0026	0.06090	0.00190	0.28	1211	14	1202	15	1167	19	1.39E-01	2.88E+01	1.06E+00	4.20E+00	2.76E+01	2.01E+00	1.28E+02	2.62E+02	4.67E+02	8.14E+02	1.24E+03	2.42E+03	3.01E+03
Zircon_080	605	138	0.23	0.0779	0.0003	2.103	0.015	0.1953	0.0018	0.05850	0.00170	0.66	1150	9.7	1149.8	5	1146.1	9.1	9.28E-02	2.71E+01	8.41E-01	2.54E+00	1.16E+01	4.44E+00	5.83E+01	1.26E+02	2.59E+02	4.82E+02	8.25E+02	1.92E+03	2.63E+03

Table 2. Corrected zircon U–Pb isotopic ratios, ages, and chondrite–normalized REE concentrations of sample AC–1 (an Anacona Terrane quartzite) (*continued*).

				Corrected ratios[2]									Corrected Ages (Ma)						Chondrite–normalized REE concentrations													
	U (ppm)[1]	Th (ppm)[1]	Th/U	$^{207}Pb/^{206}Pb$	±2s abs	$^{207}Pb/^{235}U$	±2s abs	$^{206}Pb/^{238}U$	±2s abs	$^{208}Pb/^{232}Th$	±2s abs	Rho	$^{206}Pb/^{238}U$	±2s	$^{207}Pb/^{235}U$	±2s	$^{207}Pb/^{206}Pb$	±2s	La	Ce	Pr	Nd	Sm	Eu	Gd	Tb	Dy	Ho	Er	Yb	Lu
Zircon_081	300	77	0.26	0.0774	0.0009	2.213	0.043	0.2047	0.0027	0.05530	0.00160	0.18	1201	14	1185	14	1132	22	5.49E-01	1.45E+01	1.13E+00	3.17E+00	1.07E+01	1.79E+00	5.06E+01	1.05E+02	2.14E+02	3.97E+02	6.28E+02	1.30E+03	1.70E+03
Zircon_082	172	63	0.36	0.0917	0.0008	3.205	0.057	0.2521	0.0042	0.07480	0.00230	0.70	1449	22	1461	15	1461	16	1.39E+01	3.03E+01	2.16E+01	2.69E+01	3.31E+01	7.82E+00	1.09E+02	1.95E+02	3.60E+02	6.20E+02	9.29E+02	1.74E+03	2.24E+03
Zircon_083	349	77	0.22	0.0696	0.0012	1.472	0.030	0.1529	0.0017	0.04642	0.00059	0.37	917.4	9.5	919	12	914	35	7.17E-02	7.83E+00	4.74E-01	8.75E-01	3.18E+00	6.20E+00	1.67E+01	3.57E+01	6.79E+01	1.33E+02	2.26E+02	5.78E+02	9.31E+02
Zircon_084	213	74	0.35	0.0819	0.0030	2.197	0.066	0.1986	0.0038	0.05928	0.00086	0.28	1168	21	1180	21	1238	70	2.24E-01	1.90E+01	1.65E+00	4.81E+00	2.85E+01	8.35E+00	1.08E+02	2.14E+02	3.94E+02	7.01E+02	1.10E+03	2.17E+03	2.80E+03
Zircon_085	265	86	0.32	0.0817	0.0014	2.348	0.063	0.2082	0.0024	0.06220	0.00250	0.43	1219	13	1226	19	1237	33	1.10E-01	1.58E+01	1.13E+00	3.33E+00	1.91E+01	2.42E+00	8.99E+01	1.87E+02	3.24E+02	5.51E+02	8.53E+02	1.64E+03	2.11E+03
Zircon_086	251	43	0.17	0.0888	0.0007	3.005	0.060	0.2448	0.0029	0.08060	0.00390	0.06	1412	15	1408	15	1399	16	3.80E-02	1.76E+01	9.27E-01	3.54E+00	2.45E+01	1.49E+01	9.35E+01	1.82E+02	3.26E+02	5.71E+02	9.04E+02	1.86E+03	2.68E+03
Zircon_087	141	36	0.26	0.0835	0.0012	2.640	0.063	0.2285	0.0031	0.06680	0.00230	0.23	1326	16	1311	17	1279	29	3.29E+00	1.47E+01	3.23E+00	4.16E+00	1.01E+01	1.08E+00	3.77E+01	7.98E+01	1.61E+02	3.16E+02	5.39E+02	1.19E+03	1.67E+03
Zircon_088	307	177	0.58	0.1020	0.0017	3.412	0.069	0.2442	0.0040	0.07120	0.00160	0.71	1408	21	1507	16	1659	30	1.73E+00	3.37E+01	4.59E+00	9.02E+00	2.77E+01	1.71E+01	8.59E+01	1.45E+02	2.78E+02	5.11E+02	8.99E+02	2.25E+03	3.43E+03
Zircon_089	114	59	0.51	0.0905	0.0012	3.161	0.061	0.2510	0.0031	0.07340	0.00210	0.41	1443	16	1447	15	1435	24	2.57E-01	1.08E+01	1.06E+00	4.70E+00	2.78E+01	5.63E+00	1.21E+02	2.26E+02	4.00E+02	7.07E+02	1.06E+03	1.92E+03	2.56E+03
Zircon_090	170	66	0.39	0.0964	0.0007	3.613	0.041	0.2724	0.0027	0.08130	0.00250	0.38	1553	14	1552.1	9.1	1556	13	1.90E-01	1.77E+01	1.37E+00	3.94E+00	2.15E+01	6.77E+00	8.67E+01	1.70E+02	3.09E+02	5.26E+02	8.14E+02	1.49E+03	1.93E+03
Zircon_091	551	71	0.13	0.0956	0.0011	3.583	0.045	0.2712	0.0026	0.09340	0.00520	0.59	1547	13	1546.9	9.6	1543	21	2.36E-02	1.52E+00	8.84E-01	2.67E+00	2.68E+01	1.28E+00	1.62E+02	4.18E+02	8.38E+02	1.55E+03	2.43E+03	4.52E+03	5.72E+03
Zircon_092	290	98	0.34	0.0792	0.0006	2.218	0.039	0.2029	0.0025	0.06170	0.00160	0.70	1191	13	1186	12	1177	16	5.44E-01	2.15E+01	1.70E+00	5.73E+00	2.96E+01	6.16E+00	1.27E+02	2.34E+02	4.10E+02	7.10E+02	1.08E+03	2.02E+03	2.57E+03
Zircon_093	745	199	0.27	0.0919	0.0025	3.150	0.130	0.2489	0.0046	0.07300	0.00140	0.83	1433	24	1443	31	1464	51	3.76E-01	1.18E+01	1.52E+00	3.61E+00	2.09E+01	1.01E+01	1.26E+02	2.54E+02	5.00E+02	8.81E+02	1.42E+03	2.77E+03	3.69E+03
Zircon_094	616	640	1.04	0.1024	0.0004	4.051	0.042	0.2885	0.0028	0.08390	0.00250	0.78	1634	14	1644.3	8.3	1667.3	6.7	7.51E+00	1.16E+02	1.77E+01	3.06E+01	1.09E+02	5.81E+01	3.77E+02	6.68E+02	1.20E+03	2.05E+03	3.08E+03	5.98E+03	7.98E+03
Zircon_095	707	118	0.17	0.0787	0.0004	2.134	0.025	0.1973	0.0020	0.06180	0.00220	0.73	1161	11	1159.7	8.1	1163.3	9.3	-6.21E-05	9.89E+00	4.42E-01	7.88E-01	3.85E+00	4.83E+00	1.85E+01	3.82E+01	8.50E+01	1.70E+02	3.25E+02	9.53E+02	1.59E+03
Zircon_096	289	139	0.48	0.0883	0.0009	2.935	0.052	0.2400	0.0025	0.06930	0.00210	0.46	1387	13	1391	13	1389	19	3.92E-01	1.76E+01	4.09E+00	1.54E+01	8.63E+01	2.63E+01	3.81E+02	7.03E+02	1.24E+03	2.14E+03	3.15E+03	5.29E+03	6.62E+03
Zircon_097	524	233	0.44	0.0951	0.0020	2.845	0.053	0.2170	0.0024	0.06371	0.00076	0.73	1266	13	1367	14	1529	39	2.83E+00	3.94E+01	7.87E+00	1.37E+01	4.39E+01	2.82E+01	1.63E+02	2.76E+02	5.18E+02	8.53E+02	1.35E+03	2.64E+03	3.44E+03
Zircon_098	227	54	0.24	0.0788	0.0008	2.161	0.064	0.2007	0.0037	0.06320	0.00320	0.40	1179	20	1168	20	1166	19	1.39E-01	1.49E+01	1.23E+00	4.25E+00	1.68E+01	4.80E+00	9.10E+01	1.80E+02	3.38E+02	5.99E+02	8.69E+02	1.78E+03	2.31E+03
Zircon_099	175	36	0.21	0.0853	0.0014	2.637	0.077	0.2256	0.0040	0.06880	0.00370	0.85	1311	21	1314	21	1319	32	1.90E-01	6.36E+00	5.06E-01	2.54E+00	1.22E+01	3.52E+00	6.48E+01	1.24E+02	2.33E+02	4.21E+02	6.49E+02	1.25E+03	1.69E+03
Zircon_100	992	722	0.73	0.0882	0.0033	2.840	0.110	0.2335	0.0036	0.06910	0.00130	0.39	1353	19	1366	28	1387	72	1.52E-01	1.70E+02	3.57E+00	1.20E+01	7.50E+01	5.88E+01	2.43E+02	4.38E+02	8.20E+02	1.39E+03	2.29E+03	5.18E+03	7.07E+03

Note: $^{207}Pb/^{206}Pb$ ratios, ages, and errors are calculated according to Petrus & Kamber (2012).
Analyzed spots were 23 micrometers, using an analytical protocol modified from Solari et al.
Data measured employing a Thermo Xseries QICPMS coupled to a Resonetics, Resolution M050 excimer laser workstation.
[1]U and Th concentrations are calculated employing an external standard zircon as in Paton et al. (2010).
[2]2 sigma uncertainties propagated according to Paton et al., 2010.

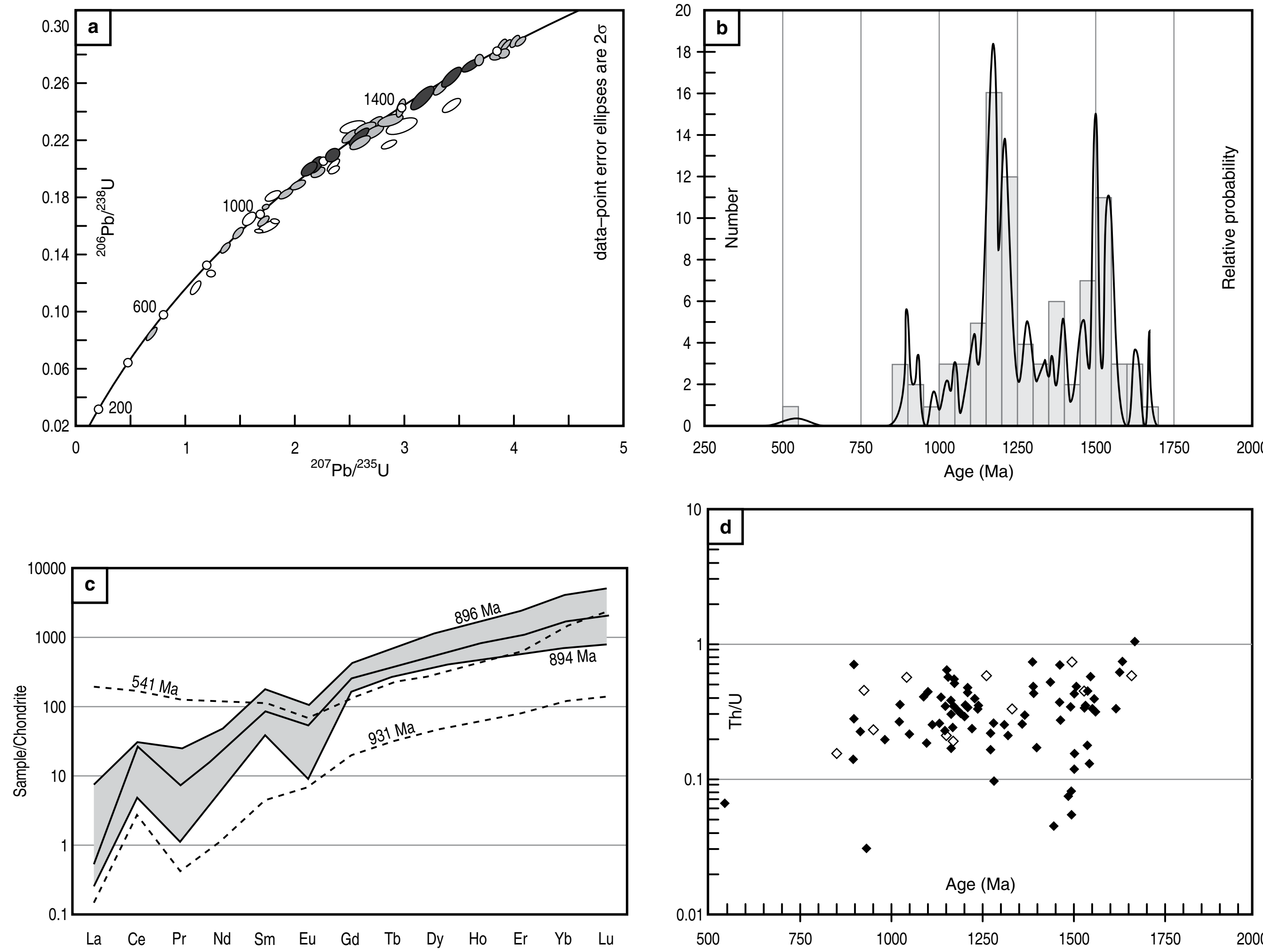

Figure 8. (a) Wetherill concordia diagram of dated zircon spots; dark, filled ellipses correspond to analyses selected for the probability density diagram. **(b)** Probability density plot. **(c)** Chondrite–normalized REE patterns of youngest zircon grains, used to constrain the protolith age. **(d)** Th/U versus age (Ma) diagram; filled symbols correspond to analyses selected for the probability density diagram.

terpret this analysis as reflecting an isotopic mixture between an inherited core and the Paleozoic metamorphism of the sample. A more robust constraint on the depositional age is the youngest population of zircon, which includes three grains that yielded near–identical ages with a mean of 894 ± 8 Ma (MSWD = 0.01). It is therefore likely that the sedimentary protolith of the quartzites and the basic protolith of the interbedded amphibolites of the Anacona Terrane may be Neoproterozoic in age.

5. Comparison with Adjacent Terranes

The main characteristics that allow differentiating the Anacona Terrane from the neighboring Ebéjico and Tahamí Terranes are presented in Table 3. In terms of the basement, the Anacona Terrane is characterized by pre–Carboniferous metamorphic rocks (e.g., the Caldas Amphibolite and its associated metasedimentites); no rocks as old as these are present in the predominantly Permian – Triassic basement of the Tahamí Terrane, while the volcano–sedimentary Ebéjico Terrane lacks medium– or high–grade metamorphic basement. The Ordovician granites present in the Anacona Terrane (e.g., La Miel Orthogneiss) are also absent in the Tahamí and Ebéjico Terranes (Restrepo et al., 2009).

Triassic metamorphic rocks are widespread in the Tahamí Terrane (e.g., Las Palmas Gneiss) but are unknown or not present in either the Cretaceous–aged Ebéjico Terrane or Anacona Terrane. The Tahamí Terrane has well–documented Cretaceous sedimentary cover units (e.g., the Abejorral, San Luis, and San Pablo Formations), and the Ebéjico Terrane is composed of Cretaceous volcano–sedimentary successions. In contrast, no such sedimentary sequences are present in the Anacona Terrane. Finally, the presence of spilites and other low–grade mafic rocks is only reported in the Ebéjico Terrane (Table 3).

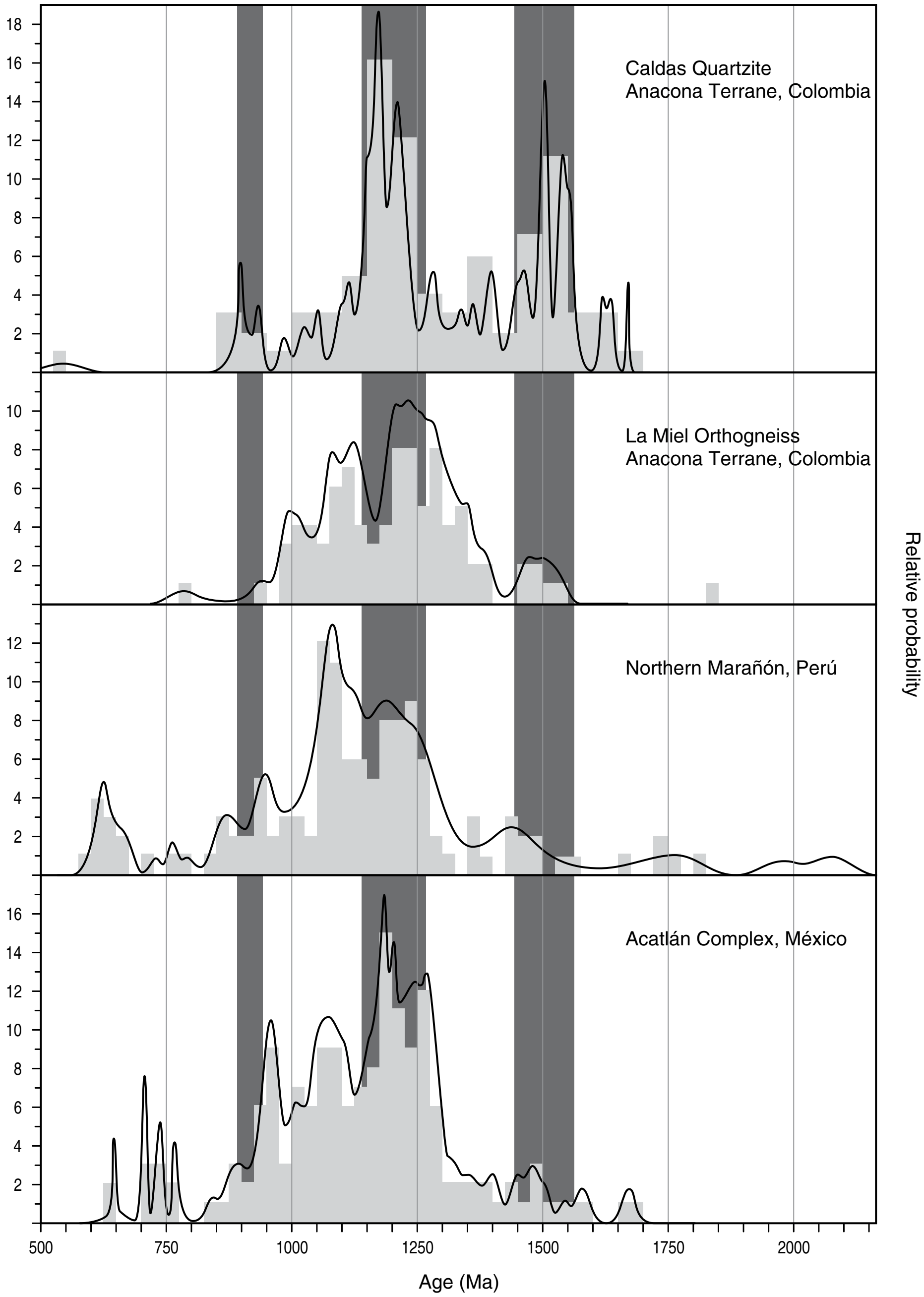

Figure 9. Comparison of probability density plots of quartzite AC–1 and the xenocrystic component in granites of the Acatlán Complex in México, the Marañón Complex in Perú, and the Anacona Terrane in Colombia (modified from Martens et al., 2014 and references therein).

6. Correlatives of the Anacona Terrane in Perú and México

Previous work has correlated the Anacona Terrane with peri–Gondwanan terranes containing relics of an Ordovician magmatic belt that fringed Gondwana (Martens et al., 2014). This Famatinian Orogen is present in South America from Argentina to Venezuela (Ramos, 2018). Potential correlatives are the Mixteca Terrane and the Acatlán Complex in southern México, which initially made part of Gondwana, the early Paleozoic component of the western Marañón Complex in Perú, and the Famatinian magmatic rocks found on the islands off the coast of Perú (Romero et al., 2013). This correlation is supported by the similarity in the ages of xenocrystic zircons from these Ordovician granites in each of these terranes (Figure 9). In the case of the Mexican terranes, the Gondwanan origin has been shown paleontologically (Robison & Pantoja–Alor, 1968; Sánchez–Zavala et al., 1999; Stewart et al., 1999).

Given that no basement rocks similar to those in the Anacona Terrane are known from Ecuador and that the general

Table 3. Comparison between the main characteristics of the Anacona, Ebéjico, and Tahamí Terranes.

Units	Ebéjico	Anacona	Tahamí
Pre–Carboniferous metamorphic rocks	Absent	Present	Absent
Ordovician granites	Absent	Present	Absent
Triassic metamorphic rocks	Absent	Absent	Present
Cretaceous sedimentary rocks	Present	Absent	Present
Spilites and other mafic rocks	Present	Absent	Absent

trend of tectonic transport by the collision of the Caribbean with the South American margin was northward, it is likely that the Anacona Terrane formed further south (in present–day Perú) during the Ordovician, being transported by the north–moving transcurrent faults related to the Cauca–Romeral Fault System. Amalgamation with the Tahamí Terrane occurred at some time between the Jurassic and the end of the Cretaceous (Martens et al., 2014). Given its allochthonous or parautochthonous nature in relation to the Central and Eastern Colombian Andes, all the blocks west of the Anacona Terrane are also necessarily allochthonous or parautochthonous.

7. History of Accretion

The Anacona Terrane does not record a Triassic thermal perturbation of the $^{40}Ar–^{39}Ar$ hornblende or biotite systems. This result indicates that during the main stage of Triassic orogenesis that substantially reworked the Tahamí Terrane, the Anacona Terrane was not nearby. This constraint provides an upper temporal limit on the juxtaposition of the two terranes. Based on the geochronological and field data, we conclude that the Ordovician intrusion of La Miel granite occurred when the amphibolite and biotite schists had already undergone a phase of regional metamorphism as shown by xenoliths of foliated amphibolite within the gneiss. A second phase of metamorphism resulted in the formation of a gneissic foliation in La Miel unit. The timing of this second metamorphic phase has not yet been constrained by U–Pb geochronology, but a $^{40}Ar–^{39}Ar$ hornblende age yields a maximum age constraint of 360 Ma (Restrepo et al., 2008), along with an $^{40}Ar–^{39}Ar$ white mica age of ca. 345 Ma (Vinasco et al., 2006); these mineral ages are currently the best constraints for the onset of cooling following this second metamorphic event. These ages imply that the Anacona Block was not adjacent to the Tahamí Terrane during regional Permian – Triassic metamorphism, and so the terrane docking is post–Triassic.

The Ebéjico Terrane is formed by mafic volcanic rocks interbedded with sedimentary rocks (González, 2001; Jaramillo et al., 2017). The accretion of this block to the Anacona and Tahamí Terranes is thought to have occurred during the Late Cretaceous – Paleogene, dated at 73–65 Ma by Jaramillo et al. (2017) and 70–58 Ma by Zapata & Cardona (2017).

8. Conclusion

The recognition of the Anacona Terrane is significant, despite its relatively small size. It lies along the eastern Cauca–Romeral Fault Zone, a major tectonic boundary in the Colombian Andes that separates a domain of predominantly oceanic affinity in the west from a continental–dominated domain in the east. The terrane is unlike others in the Western or Central Cordilleras, comprising basement rocks with a geologic history spanning the Neoproterozoic – Ordovician. Its medium–pressure metamorphism, xenocrystic and detrital zircon age spectra, and early Paleozoic metamorphism contrast with the low–pressure, Triassic metamorphic basement of the adjacent and much larger Tahamí Terrane. The closest correlative Gondwanan terranes of the Anacona Terrane are in México and Perú. The initial accretion of the Anacona and the Tahamí Terranes occurred in the latest Triassic or later, and we surmise that from a southerly position, the Anacona Terrane was pushed northwards along the Cauca–Romeral Fault by the oblique convergence of the Caribbean Plate located to the northwest.

Acknowledgments

We are grateful to David M. CHEW and Victor A. RAMOS, who improved the manuscript considerably with their suggestions and corrections as reviewers.

References

Andersen, T. 2002. Correction of common lead in U–Pb analyses that do not report ^{204}Pb. Chemical Geology, 192(1–2): 59–79. https://doi.org/10.1016/S0009-2541(02)00195-X

Botero, G. 1963. Contribución al conocimiento de la geología de la zona central de Antioquia. Universidad Nacional de Colombia, Anales de la Facultad de Minas, 57, 101 p. Medellín.

Boynton, W.V. 1984. Cosmochemistry of the rare earth elements: Meteorite studies. Developments in Geochemistry, 2: 63–114. https://doi.org/10.1016/B978-0-444-42148-7.50008-3

Bustamante, A. 2003. Definição das trajetórias P–T–t em rochas metamórficas do flanco ocidental da Cordilheira Central da Colômbia, nas regiões de Caldas e El Retiro. Master thesis, Universidade de São Paulo, 107 p. São Paulo. https://doi.org/10.11606/D.44.2003.tde-26012011-135543

Coney, P.J., Jones, D.L. & Monger, J.W.H. 1980. Cordilleran suspect terranes. Nature, 288(5789): 329–333. https://doi.org/10.1038/288329a0

Correa–Martínez, A.M., Martens, U., Restrepo, J.J., Ordóñez–Carmona, O. & Martins–Pimentel, M. 2005. Subdivisión de las metamorfitas básicas de los alrededores de Medellín–cordillera Central de Colombia. Revista de la Academia Colombiana de Ciencias Exactas, Físicas y Naturales, 29(112): 325–344.

De Paolo, D.J. 1981. Trace element and isotopic effects of combined wallrock assimilation and fractional cristallization. Earth and Planetary Science Letters, 53(2): 189–202. https://doi.org/10.1016/0012-821X(81)90153-9

Echeverría, L.M. 1973. Zonación de las rocas metamórficas del valle de Aburrá y sus alrededores. Bachelor thesis, Universidad Nacional de Colombia, 124 p. Medellín.

Giraldo, M.I. 2010. Esquema geodinámico de la parte noroccidental de la cordillera Central de Colombia. Master thesis, Universidad Nacional de Colombia, 146 p. Medellín.

Giraldo–Ramírez, W. 2013. Caracterización estructural y geoquímica del bloque Anacona. Bachelor thesis, Universidad Nacional de Colombia, 91 p. Medellín.

González, H. 1980. Geología de las planchas 167 Sonsón y 187 Salamina. Scale 1:100 000. Ingeominas, Internal report 1760, 262 p. Medellín.

González, H. 2001. Memoria explicativa: Mapa geológico del departamento de Antioquia. Scale 1:400 000. Ingeominas, 240 p. Medellín.

Grosse, E. 1926. Estudio geológico del terciario carbonífero de Antioquia en la parte occidental de la cordillera Central de Colombia, entre el río Arma y Sacaojal, ejecutado en los años de 1920–1923. Dietrich Reimer, 361 p. Berlin.

Hoffman, P.F. 1989. Precambrian geology and tectonic history of North America. In: Bally, A.W. & Palmer, A.R. (editors), The geology of North America–An overview. Geological Society of America, A: 447–511. Boulder, USA. https://doi.org/10.1130/DNAG-GNA-A.447

Hofmann, A.W. 1988. Chemical differentiation of the Earth: The relationship between mantle, continental crust, and oceanic crust. Earth and Planetary Science Letters, 90(3): 297–314. https://doi.org/10.1016/0012-821X(88)90132-X

Ibañez–Mejia, M., Ruiz, J., Valencia, V.A., Cardona, A., Gehrels, G.E. & Mora, A. 2011. The Putumayo Orogen of Amazonia and its implications for Rodinia reconstructions: New U–Pb geochronological insights into the Proterozoic tectonic evolution of northwestern South America. Precambrian Research, 191(1–2): 58–77. https://doi.org/10.1016/j.precamres.2011.09.005

Jaramillo, J.S., Cardona, A., León, S., Valencia, V. & Vinasco, C. 2017. Geochemistry and geochronology from Cretaceous magmatic and sedimentary rocks at 6° 35' N, western flank of the Central Cordillera (Colombian Andes): Magmatic record of arc growth and collision. Journal of South American Earth Sciences, 76: 460–481. https://doi.org/10.1016/j.jsames.2017.04.012

Jones, D.L., Howell, D.G., Coney, P.J. & Monger, J.W.H. 1983. Recognition, character and analysis of tectonostratigraphic terranes in western North America. Journal of Geological Education, 31(4): 295–303.

Martens, U., Weber, B. & Valencia, V. 2010. U/Pb geochronology of Devonian and older Paleozoic beds in the southeastern Maya Block, Central America: Its affinity with peri–Gondwanan terranes. Geological Society of America Bulletin, 122(5–6): 815–829. https://doi.org/10.1130/B26405.1

Martens, U., Restrepo, J.J., Ordóñez–Carmona, O. & Correa–Martínez, A.M. 2014. The Tahamí and Anacona Terranes of the Colombian Andes: Missing links between South American and Mexican Gondwana margins. The Journal of Geology, 122(5): 507–530. https://doi.org/10.1086/677177

Maya, M. & Escobar, A. 1985. Estudio de las rocas metamórficas entre el Ancón sur y la quebrada La Miel, Caldas, Antioquia. Bachelor thesis, Universidad Nacional de Colombia, 160 p. Medellín.

Maya, M. & González, H. 1995. Unidades litodémicas en la cordillera Central de Colombia. Boletín Geológico, 35(2–3): 43–57.

Michard, A., Gurriet, P., Soudant, M. & Albarede, F. 1985. Nd isotopes in French Phanerozoic shales: External vs. internal aspects of crustal evolution. Geochimica et Cosmochimica Acta, 49(2): 601–610. https://doi.org/10.1016/0016-7037(85)90051-1

Ortega–Gutiérrez, F., Ruiz, J. & Centeno–García, E. 1995. Oaxaquia: A Proterozoic microcontinent accreted to North America during the late Paleozoic. Geology, 23(12): 1127–1130. https://doi.org/10.1130/0091-7613(1995)023<1127:OAPMAT>2.3.CO;2

Patiño, J.J. & Noreña, J.A. 1984. Estudio de las rocas metamórficas en la parte sur del municipio de Caldas, Antioquia. Bachelor thesis, Universidad Nacional de Colombia, 154 p. Medellín.

Paton, C., Woodhead, J.D., Hellstrom, J.C., Hergt, J.M., Greig, A. & Maas, R. 2010. Improved laser ablation U–Pb zircon geochronology through robust downhole fractionation correction. Geochemistry, Geophysics, Geosystems, 11(3): 1–36. https://doi.org/10.1029/2009GC002618

Petrus, J.A. & Kamber, B.S. 2012. VizualAge: A novel approach to laser ablation ICP–MS U–Pb geochronology data reduction. Geostandards and Geoanalytical Research, 36(3): 247–270. https://doi.org/10.1111/j.1751-908X.2012.00158.x

Ramos, V.A. 2018. The Famatinian orogen along the protomargin of western Gondwana: Evidence for a nearly continuous Ordovician magmatic arc between Venezuela and Argentina. In: Folguera, A., Contreras–Reyes, E., Heredia, N., Encinas, A., Iannelli, S.B., Oliveros, V., Dávila, F.M., Collo, G., Giambiagi, L., Maksymowicz, A., Iglesia–Llanos, M.P., Turienzo, M., Naipauer, M., Orts, D., Litvak, V., Alvarez, O., Arriagada, C. (editors), The evolution of the Chile–Argentinean Andes. Springer Earth System Sciences. Springer, p. 133–161. https://doi.org/10.1007/978-3-319-67774-3_6

Restrepo, J.J. 1986. Metamorfismo en el sector norte de la cordillera Central de Colombia. Universidad Nacional de Colombia, Trabajo presentado como requisito parcial para la promoción a Profesor Titular. Unpublished report, 195 p. Medellín.

Restrepo, J.J. 2008. Obducción y metamorfismo de ofiolitas triásicas en el flanco occidental del Terreno Tahamí, cordillera Central de Colombia. Boletín Ciencias de la Tierra, (22): 49–100.

Restrepo, J.J. & Toussaint, J.F. 1977. Anfibolitas granatíferas de Caldas, Antioquia. Boletín Ciencias de la Tierra, (2): 147–154.

Restrepo, J.J. & Toussaint, J.F. 1978. Ocurrencia de Precámbrico en las cercanías de Medellín, cordillera Central de Colombia. Publicaciones Especiales de Geología, 12: 1–11.

Restrepo, J.J. & Toussaint, J.F. 1984. Unidades litológicas de los alrededores de Medellín. Primera conferencia sobre riesgos geológicos del valle de Aburrá. Sociedad Colombiana de Geología. Memoirs, p. 1–26. Medellín.

Restrepo, J.J. & Toussaint, J.F. 2020. Tectonostratigraphic terranes in Colombia: An update. First part: Continental terranes. In: Gómez, J. & Mateus–Zabala, D. (editors), The Geology of Colombia, Volume 1 Proterozoic – Paleozoic. Servicio Geológico Colombiano, Publicaciones Geológicas Especiales 35, p. 37–63. Bogotá. https://doi.org/10.32685/pub.esp.35.2019.03

Restrepo, J.J., Toussaint, J.F., González, H., Cordani, U., Kawashita, K., Linares, E. & Parica, C. 1991. Precisiones geocronológicas sobre el occidente colombiano. Simposio sobre magmatismo andino y su marco tectónico, Programa Internacional de Ciencias Geológicas. Memoirs, I, p. 1–21. Manizales.

Restrepo, J.J., Dunlap, W.J., Martens, U., Ordóñez–Carmona, O. & Correa–Martínez, A.M. 2008. Ar–Ar ages of amphibolites from the Central Cordillera of Colombia and their implications for tectonostratigraphic terrane evolution in the northwestern Andes. VI South American Symposium on Isotope Geology. Proceedings CD ROM, p. 1–6. Bariloche, Argentina.

Restrepo, J.J., Ordóñez–Carmona, O., Martens, U. & Correa–Martínez, A.M. 2009. Terrenos, complejos y provincias en la cordillera Central de Colombia. Ingeniería, Investigación y Desarrollo, 9(2): 49–56.

Robison, R.A. & Pantoja–Alor, J. 1968. Tremadocian trilobites from the Nochixtlán region, Oaxaca, Mexico. Journal of Paleontology, 42(3): 767–800.

Romero, D., Valencia, K., Alarcón, P., Peña, D. & Ramos, V.A. 2013. The offshore basement of Perú: Evidence for different igneous and metamorphic domains in the forearc. Journal of South American Earth Sciences, 42: 47–60. https://doi.org/10.1016/j.jsames.2012.11.003

Sánchez–Zavala, J.L., Centeno–García, E. & Ortega–Gutiérrez, F. 1999. Review of Paleozoic stratigraphy of México and its role in the Gondwana–Laurentia connections. In: Ramos, V.A. & Keppie, J.D. (editors), Laurentia–Gondwana connections before Pangea. Geological Society of America, Special Paper 336, p. 211–226. https://doi.org/10.1130/0-8137-2336-1.211

Sepúlveda, R.D. & Saldarriaga, S.M. 1980. Metamorfismo de las rocas del oriente del municipio de Caldas, Antioquia. Bachelor thesis, Universidad Nacional de Colombia, 115 p. Medellín.

Siivola, J. & Schmid, R. 2007. List of mineral abbreviations. In: Fettes, D. & Desmons, J. (editors), Metamorphic rocks: A classification and glossary terms. Cambridge University Press, p. 93–110.

Solari, L., Gómez–Tuena, A., Bernal, J.P., Pérez–Arvizu, O. & Tanner, M. 2010. U–Pb zircon geochronology with an integrated LA–ICP–MS microanalytical workstation: Achievements in precision and accuracy. Geostandards and Geoanalytical Research, 34(1): 5–18. https://doi.org/10.1111/j.1751-908X.2009.00027.x

Stewart, J.H., Blodgett, R.B., Boucot, A.J., Carter, J.L. & López, R. 1999. Exotic Paleozoic strata of Gondwanan provenance near Ciudad Victoria, Tamaulipas, México. In: Ramos, V.A. & Keppie, J.D. (editors), Laurentia–Gondwana connections before Pangea. Geological Society of America, Special Paper 336, p. 227–252. https://doi.org/10.1130/0-8137-2336-1.227

Sun, S.S. & McDonough, W.F. 1989. Chemical and isotopic systematics of oceanic basalts: Implications for mantle composition and processes. In: Saunders, A.D. & Norry, M.J. (editors), Magmatism in the ocean basins. Geological Society of London, Special Publication 42, p. 313–345. https://doi.org/10.1144/GSL.SP.1989.042.01.19

Tassinari, C.C.G., Bettencourt, J.S., Geraldes, M.C., Macambira, M.J.B. & Lafon, J.M. 2000. The Amazonian Craton. In: Cordani, U.G., Milani, E.J., Thomaz–Filho, A. & Campos, D.A. (editors), Tectonic evolution of South America. 31st International Geological Congress. Proceedings, p. 41–95. Rio de Janeiro, Brazil.

Toussaint, J.F. & Restrepo, J.J. 1989. Acreciones sucesivas en Colombia: Un nuevo modelo de evolución geológica. V Congreso Colombiano de Geología. Memoirs, I, p. 127–146. Bucaramanga.

Villagómez, D., Spikings, R., Magna, T., Kammer, A., Winkler, W. & Beltrán, A. 2011. Geochronology, geochemistry and tectonic evolution of the Western and Central Cordilleras of Colombia. Lithos, 125(3–4): 875–896. https://doi.org/10.1016/j.lithos.2011.05.003

Vinasco, C.J., Cordani, U.G., González, H., Weber, M. & Peláez, C. 2006. Geochronological, isotopic, and geochemical data from Permo–Triassic granitic gneisses and granitoids of the Colombian central Andes. Journal of South American Earth Sciences, 21(4): 355–371. https://doi.org/10.1016/j.jsames.2006.07.007

Wasteneys, H.A., Clark, A.H., Farrar, E. & Langridge, R.J. 1995. Grenvillian granulite–facies metamorphism in the Arequipa Massif, Peru: A Laurentia–Gondwana link. Earth and Planetary Science Letters, 132(1–4): 63–73. https://doi.org/10.1016/0012-821X(95)00055-H

Zapata, J.P. & Cardona, A. 2017. Unidades miloníticas asociadas a eventos colisionales del Cretácico Superior en el margen occidental de la cordillera Central. XVI Congreso Colombiano de Geología and III Simposio de Exploradores. Memoirs, p. 1889–1891. Santa Marta.

Explanation of Acronyms, Abbreviations, and Symbols:

CL	Cathodoluminescence
E–MORB	Enriched mid–ocean ridge basalt
LA–ICP–MS	Laser ablation inductively coupled plasma mass spectrometry
Low–P	Low pressure
MORB	Mid–ocean ridge basalt
MSWD	Mean square weighted deviation
N–MORB	Normal mid–ocean ridge basalt
OIB	Ocean island basalt
PT	Pressure and temperature
REE	Rare earth element
UNAM	Universidad Nacional Autónoma de México

Authors' Biographical Notes

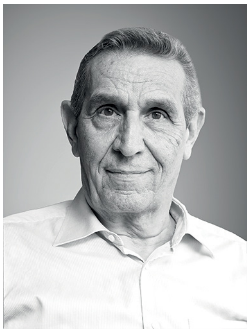

Jorge Julián RESTREPO obtained a degree in mining engineering and metallurgy at the Universidad Nacional de Colombia in 1968 and a Master of Science degree in geology at the Colorado School of Mines in 1973. He was a faculty member of the Universidad Nacional de Colombia Sede Medellín, for over 40 years and currently holds the titles of Emeritus Professor and "Maestro Universitario". He taught Mineralogy, Metamorphic Petrology, Regional Geology, Field Geology, and Geochronology. His research focused on plate tectonics applied to the geology of Colombia, tectonostratigraphic terranes, geochronology, and the geologic evolution of metamorphic and mafic/ultramafic complexes of the Central Cordillera. Other interests are photography, genealogy, and the study of passifloras.

Uwe MARTENS graduated with a degree in geological engineering from the Universidad Nacional de Colombia, Sede Medellín, and a PhD in geological and environmental science from Stanford University. He has taught at the Universidad Nacional de Colombia, San Carlos National University in Guatemala, and Stanford University. He currently is a visiting researcher at Centro de Geociencias, UNAM, México and works as an independent consultant in the field of source–to–sink analysis.

Wilmer E. GIRALDO–RAMÍREZ is a geological engineer who graduated from the Universidad Nacional de Colombia Sede Medellín (2014) and has a Master of Science degree in basins and mobile belt analysis from the Universidade do Estado do Rio de Janeiro (2017). He has worked at institutions such as the Universidad Nacional de Colombia, Universidad Católica de Oriente, Corporación Autónoma Regional de las Cuencas de los Ríos Negro y Nare "Cornare" and city of Marinilla. His main interests are the geodynamic evolution of the northern Andes, and he has secondary interests in the land use planning of eastern Antioquia, biology of *Passiflora* and sports including rugby and Brazilian jiu–jitsu.

Carboniferous

Devonian

Chapter 9

Paleozoic of Colombian Andes: New Paleontological Data and Regional Stratigraphic Review

https://doi.org/10.32685/pub.esp.35.2019.09
Published online 19 May 2020

Mario MORENO–SÁNCHEZ[1]*, Arley GÓMEZ–CRUZ[2], and José BUITRAGO–HINCAPIÉ[3]

1 mario.moreno@ucaldas.edu.co
Universidad de Caldas
Facultad de Ciencias Exactas y Naturales
Departamento de Ciencias Geológicas
Calle 65 n° 26–10
Manizales, Colombia

2 arley.gomez@ucaldas.edu.co
Universidad de Caldas
Facultad de Ciencias Exactas y Naturales
Departamento de Ciencias Geológicas
Calle 65 n° 26–10
Manizales, Colombia

3 jbuitrago@sgc.gov.co
Servicio Geológico Colombiano
Dirección de Geociencias Básicas
Diagonal 53 n° 34–53
Bogotá D. C., Colombia

* Corresponding author

Abstract The continental basement, east of the Otú–Pericos Fault, is made up of two sectors with different geological histories. The western sector, comprised of Payandé, and Payandé San Lucas blocks, are considered here as a part of the autochthonous basement of South America. The autochthonous basement is composed of high–grade metamorphic rocks with Grenvillian and Amazonian ages. The basal sedimentary cover includes marine deposits that span from Ediacaran to Ordovician in the Llanos Basin, and from the Ordovician, in the La Macarena and Magdalena Valley. The Eastern Cordillera consists of an allochthonous tectonic block (Quetame–Mérida Terrane) where several phases of metamorphism are identified. The Bucaramanga Gneiss and Silgará Schists (sensu stricto) were formed during the Precambrian. The Chicamocha Schists originated from a sedimentary protolith of Cambrian age. The identification of bioturbation in metamorphic rocks of the Quetame Massif confirms the existence of Phanerozoic rocks in the area. In the Eastern Cordillera, an Ordovician magmatic phase associated with the Famatinian Orogeny (Taconic) is recognized. Orogenic metamorphism and its termination are associated with the collision of the Quetame–Mérida Terrane against the pericratonic margin of South America. An erosive phase at the end of the Ordovician and the beginning of the Silurian separated a brief marine incursion during the Ludlow. In northern South America, Devonian sedimentation spans from the Emsian to the ends of the Famennian. The Devonian marine fauna is similar to the marine fauna of eastern North America. The flora tends to be cosmopolitan (several species of *Archaeopteris*) with elements common to Laurussia. However, fossil fish show elements of both Gondwana and Laurussia. The Carboniferous series is extended from the Sierra Nevada of Santa Marta to the south of Colombia. The fossils indicate that the sedimentation, limestones and mudstones of the shallow marine platform, spans from the Bashkirian to the Moscovian. The Permian sedimentation starts with basal conglomerates and continues with platform limestone deposits. The fossils indicate a range of sedimentation that spans from the Cisuralian to the Guadalupian. A tectonic phase (the assemblage of the Pangea) creates the hiatus between the late Permian (Lopingian) and the Middle Triassic. This phase results in magmatic activity and metasomatism in the Magdalena Valley (Payandé and Payandé–San Lucas).

Keywords: *fossils, tectonic provinces, Payandé and Payandé San Lucas Terranes, Quetame–Mérida Terrane.*

Citation: Moreno–Sánchez, M., Gómez–Cruz, A. & Buitrago–Hincapié, J. 2020. Paleozoic of Colombian Andes: New paleontological data and regional stratigraphic review. In: Gómez, J. & Mateus–Zabala, D. (editors), The Geology of Colombia, Volume 1 Proterozoic – Paleozoic. Servicio Geológico Colombiano, Publicaciones Geológicas Especiales 35, p. 167–203. Bogotá. https://doi.org/10.32685/pub.esp.35.2019.09

Resumen El zócalo continental, al este de la Falla de Otú–Pericos, se compone de dos sectores con diferentes historias geológicas. El sector occidental, conformado por los bloques Payandé y Payandé–San Lucas, se considera aquí como parte del basamento autóctono de Suramérica. El zócalo autóctono se compone de rocas metamórficas de alto grado con edades grenvillianas y amazónicas. La cubierta sedimentaria basal incluye depósitos marinos que abarcan desde el Ediacariano hasta el Ordovícico en la Cuenca de los Llanos y desde el Ordovícico en La Macarena y el valle del Magdalena. La cordillera Oriental está constituida por un bloque tectónico alóctono (Terreno Quetame–Mérida) en el cual se identifican varias fases de metamorfismo. El Gneis de Bucaramanga y los Esquistos del Silgará (*sensu stricto*) se formaron durante el Precámbrico. Los Esquistos del Chicamocha se originaron a partir de un protolito sedimentario de edad cámbrica. La identificación de bioturbación en rocas metamórficas del Macizo de Quetame confirma la existencia de rocas fanerozoicas en el área. En la cordillera Oriental se reconoce una fase magmática ordovícica asociada con la Orogenia Famatiniana (Tacónica). El metamorfismo orogénico y su terminación se asocian con la colisión del Terreno Quetame–Mérida contra el margen pericratónico de Suramérica. Una fase erosiva al final del Ordovícico y el comienzo del Silúrico creó una breve incursión marina durante el Ludloviano. La sedimentación del Devónico en el norte de Suramérica abarca desde el Emsiano hasta el final del Famenniano. La fauna marina del Devónico es similar a la del este de Norteamérica. La flora tiende a ser cosmopolita (varias especies de *Archaeopteris*) con elementos en común con Laurusia. Sin embargo, los peces fósiles muestran elementos tanto de Gondwana como de Laurusia. La serie carbonífera se extiende desde la Sierra Nevada de Santa Marta hasta el sur de Colombia. Los fósiles indican que la sedimentación, calizas y lodolitas de plataforma marina somera, abarca desde el Bashkiriano al Moscoviano. La sedimentación del Pérmico comienza con conglomerados basales y continúa con depósitos de calizas de plataforma. Los fósiles indican un rango de sedimentación que abarca desde el Cisuraliano hasta el Guadalupiano. Una fase tectónica (el ensamblaje de Pangea) crea el hiato entre el Pérmico tardío (Lopingiano) y el Triásico Medio. Esta fase da como resultado actividad magmática y metasomatismo en el valle del Magdalena (Payandé y Payandé–San Lucas).

Palabras clave: *fósiles, provincias tectónicas, terrenos Payandé y Payandé–San Lucas, Terreno Quetame–Mérida.*

1. Introduction

A divergent evolution and structure characterize the mountain ranges that divide the Andes in Colombia. The Western Cordillera (western mountain range) on the Pacific Ocean and the Cauca Valley domain consist largely of Cretaceous oceanic crust (Figure 1). This tectonic block that includes Calima, Cuna, and Gorgona Terranes (Toussaint & Restrepo, 1993, 1994) will not be considered in this work nor will the Chocó Block (Duque–Caro, 1990), since during the Paleozoic, they were not yet formed. The Central Cordillera (central mountain range) is an assemblage of Mesozoic and Paleozoic metamorphic terranes (Figure 2). The central and northern part of this range belongs to the Tahamí Terrane (Toussaint & Restrepo, 1994), including the Cajamarca Complex (Maya & González, 1995), which is a tectonic assemblage of pre–Cretaceous metamorphic rocks. The Tahamí Terrane is composed of low grade metaigneous and metasedimentary rocks whose chronological ranges extend from Devonian (Anacona Terrane) to Jurassic (Blanco–Quintero et al., 2014; Restrepo et al., 2009; Spikings et al., 2015; Vinasco et al., 2006). To date, Precambrian rocks have not been found in this terrane (Ordoñez–Carmona et al., 2006). Both Western and Central Cordilleras were affected by Cretaceous and Paleogene magmatism (Maya, 1992). The oldest fossiliferous rocks in the Tahamí Terrane are those of the Early Cretaceous age of Valle Alto and Berlin areas (Barrero & Vesga, 1976; Etayo–Serna, 1985). Nelson (1957) discovered a rich fossil flora in the Valle Alto region that is attributed to the Early Cretaceous (Wealden facies). Nevertheless, Lemoigne (1984) proposes a Jurassic age based on the additional material. The above–mentioned age was controverted by Etayo–Serna (1985), who referred to a Lower Cretaceous mollusks fauna from the same deposits cited by Lemoigne (1984). Additionally, Vakhrameev (1991) subsequently checked the flora species studied by LEMOIGNE and concluded that the most convenient age for the fossil material is Early Cretaceous,

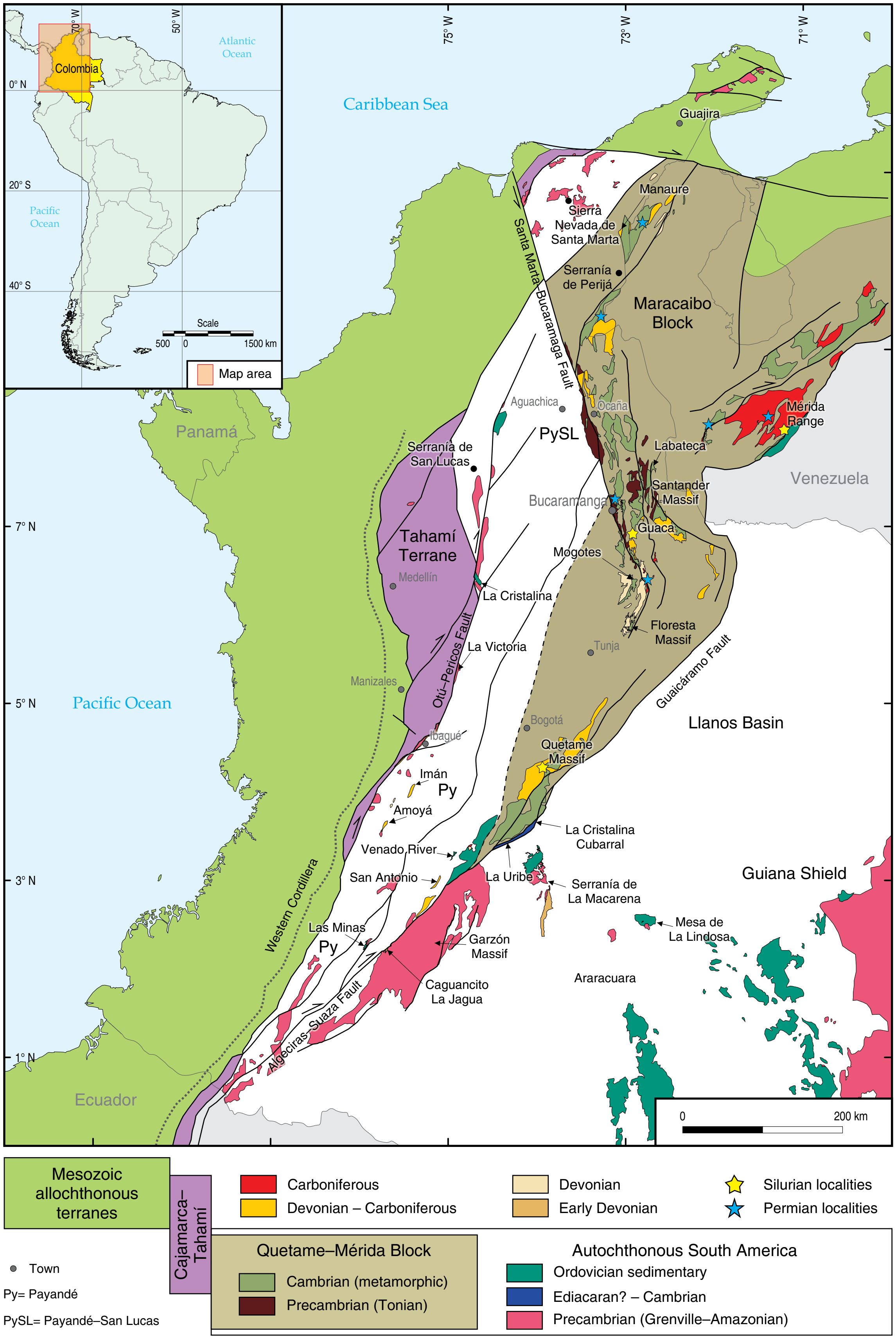

Figure 1. Geological sketch map of the northern Andes showing the main tectonic blocks.

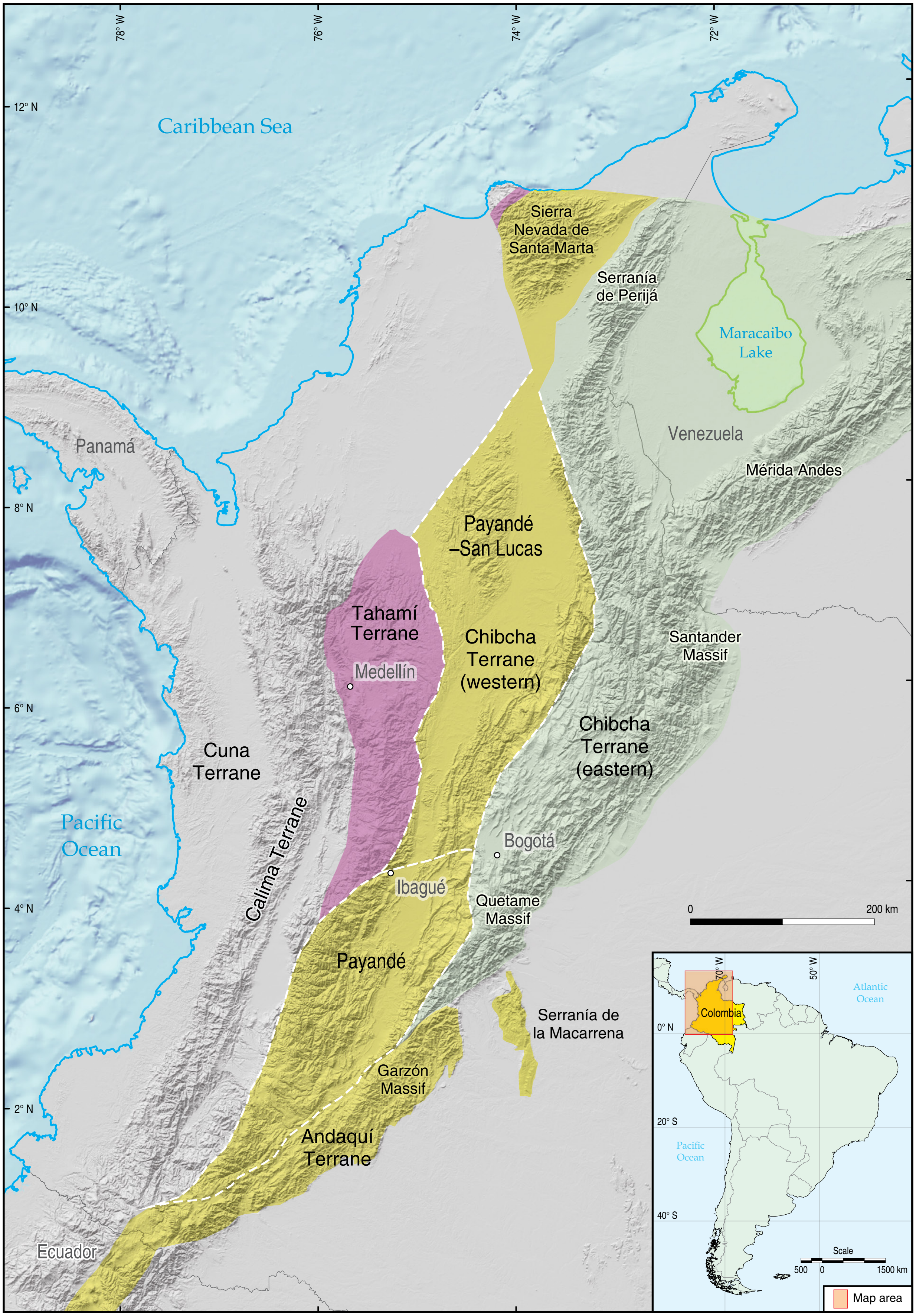

Figure 2. Geological terrane map and relief of Colombia and neighboring jurisdictions. Modified from Restrepo & Toussaint (1988).

which is in agreement with the Etayo–Serna's conclusions. To date, no pre–Cretaceous sedimentary rocks have been found in the Tahamí Terrane.

The Chibcha Terrane (Restrepo et al., 2009) is a geologic province located between the Otú–Pericos and Guaicáramo Faults (Borde Llanero Fault), which comprises the Sierra Nevada de Santa Marta, Magdalena Valley, the eastern slope of the Central Cordillera, Quetame and Santander Massifs, Mérida Andes, and the serranía de Perijá. The Magdalena Valley and the eastern slope of the Central Cordillera, included in the Payandé and Payandé–San Lucas Terranes sensu Etayo–Serna et al. (1983), has a Mesoproterozoic (Grenvillian) basement similar to the basement reported in the serranía de La Macarena, Sierra Nevada de Santa Marta, and Garzón Massifs (Kroonenberg, 1982; Ramos, 2010). Like serranía de La Macarena, the oldest sedimentary rocks from Magdalena Valley are lower and late Paleozoic age. Middle Ordovician graptolites are reported in the El Hígado (Borrero et al., 2007; Mojica et al., 1988) and La Cristalina Formations (Feininger et al., 1972) at the domain of the Payandé and Payandé–San Lucas Terranes.

In this work, the west part of the Chibcha Terrane of Restrepo et al. (2009), including the Payandé and Payandé–San Lucas Terranes of Etayo–Serna (1985), is provisionally called "Western Chibcha Terrane". We consider that the Western Chibcha Terrane has a geologic genesis distinct from the geologic genesis of the eastern Chibcha Terrane. Western Chibcha Terrane, with Grenvillian basement and covered with early Paleozoic sedimentary rocks, shares a tectonic history like the tectonic history of the serranía de La Macarena and Llanos Basin.

The eastern sector of the Chibcha Terrane ("Eastern Chibcha Terrane" in this work) is composed of a Proterozoic crystalline basement (Bucaramanga Gneiss) covered by Tonian–age schists (Silgará), Cambrian–age schists (Quetame, Perijá Series and Chicamocha Schists) and cut by Ordovician (Famatinian) granitoids. In addition, there is a cover of metasedimentites ("Filitas de San Pedro", Guaca Metasedimentites, and "Susumuco Silurian beds") of Silurian age (Forero, 1990; Grösser & Prössl, 1991; Mantilla–Figueroa et al., 2016).

Famatinian (Taconic) age arc granitoids, affecting low grade metamorphic rocks, are common along the Eastern Cordillera and Mérida Andes (Restrepo–Pace & Cediel, 2010). The oldest sedimentary rocks in the Eastern Cordillera are commonly cited as Devonian, suggesting that the metamorphic event of the Eastern Cordillera predates the Devonian (Renzoni, 1968; Stibane, 1968; Trumpy, 1943). However, in the Mogotes–Santa Bárbara area (Santander Massif), low grade metamorphic rocks with late Paleozoic fossils (Moreno–Sánchez et al., 2005; Ward et al., 1977) and Early Devonian zircons are reported (Mantilla–Figueroa & García–Ramírez, 2018). Additionally, Silurian (Ludlow) spores occur in weakly metamorphosed rocks of the Quetame Massif (Grösser & Prössl, 1991) and the Silurian brachiopod *Aenigmastrophia* sp. was recovered from low grade metamorphic rocks near Guaca town at the Santander Massif (Forero, 1990). Early Paleozoic igneous and metamorphic events are absent in the basement of Magdalena Valley (Payandé and Payandé–San Lucas Terranes sensu Etayo–Serna, 1985).

Based on the above, we consider that the pre–Devonian geological history of western and eastern Chibcha Terrane is not similar and, therefore, both crustal blocks could consider tectonic blocks that evolved independently from Precambrian to Ordovician times.

Minor occurrences of Devonian and Carboniferous sequences are known in the serranía de La Macarena and the Garzón Massif. To the west, from the Otú–Pericos System Fault to the Cauca Valley, Paleozoic sedimentary rocks are unknown. This area, integrated into the Tahamí Terrane by Restrepo et al. (2009), has undergone the effect of metamorphic events during the late Paleozoic and early Mesozoic, and all this region can be considered an allochthonous terrane.

The Quetame, Perijá, Santander, and Mérida Massifs are part of a tectonic block (abbreviated: Quetame–Mérida Terrane or Eastern Chibcha Terrane) affected by a mid–Ordovician orogenic greenschist event referred to as the Quetame–Caparonensis Orogeny by some authors (Mantilla–Figueroa et al., 2016; Restrepo–Pace, 1995). The Quetame–Caparonensis Orogeny is the northern extension of the Famatinian Orogeny that affected the western margin of South America during the Ordovician period (Mantilla–Figueroa et al., 2016; Ramos, 2015; van der Lelij, 2013; van der Lelij et al., 2016a). Late Paleozoic sedimentary sequences are known in the Llanos Basin but are not included in this study, as they are extensively studied in another chapter.

The first Paleozoic rocks of Colombia were recognized in the Floresta Massif (Figure 1). The discovery of Devonian strata in Colombia is a credit to Axel A. OLSSON and Parke A. DICKEY, geologists of the International Petroleum Company. The Devonian fossils, collected by OLSSON and DICKEY at the north of the Floresta town (Department of Boyacá), were studied by Caster (1939) and McNair (1940).

The Floresta Series (Olsson & Caster, 1937), then Floresta Formation (Botero, 1950), was divided into three units: The basal El Tíbet Formation, the Floresta Formation in the middle, and the Cuche Formation at the top (Mojica & Villarroel, 1984).

The oldest sedimentary unit of the Floresta Massif is the Emsian El Tíbet Formation. This formation covers unconformably Ordovician granites and early Paleozoic metamorphic rocks. The unit consists of a succession of conglomerates, sandstones, and gray–colored interbedded shales. The El Tíbet was initially included by Cediel (1969) as a member of the Floresta Formation but was later established as a separate formation by Mojica & Villarroel (1984). The Cuche Formation, previously considered a Carboniferous ensemble, is a clastic succession with Late Devonian fossils of a continental and transitional marine environment (Berry et al., 2000; Janvier & Villarroel, 2000; Moreno–Sánchez, 2004). The Devonian sequence extends from La Jagua, south of the Garzón village (Stibane & Forero, 1969), to the serranía de Perijá (Forero, 1970, 1991).

Scattered sedimentary Carboniferous rocks crop out from southern Colombia (Dickey, 1941; Mojica et al., 1987a) to the Sierra Nevada de Santa Marta (Gansser, 1955) and are also recognized in the subsoil of the Llanos Basin (Dueñas, 2001; Dueñas & Césari, 2003, 2006). The Carboniferous system in the Andean region is dominated by shallow carbonate marine deposits. At the Llanos Basin, Dueñas & Césari (2006) found a Late Devonian pollen assemblage (characterized by spores *Hystricosporites* spp., *Ancyrospora* spp., and *Teichertospora torquata*) in a sequence of siliciclastic nature that reaches the lower Carboniferous (Tournaisian – Visean).

The Permian record is limited to outcrops on the northern Andean region: the Santander Massif, serranía de Perijá, and Mérida Andes in Venezuela (Arnold, 1966; García–Jarpa, 1972; Hea & Whitman, 1960). The Permian sequences originate on a carbonate platform in shallow and warm marine waters. At the Mérida Andes, Permian Carache and Palmarito Formations preserve a floral assemblage characterized by the remains of *Delnorti*a, a gigantopterid fossil plant common in the Road Canyon Formation of Texas (Ricardi–Branco, 2008; Ricardi–Branco et al., 2005). At the serranía de Perijá, the Fusulinid *Paraschwagerina yabei* and presence of the ammonoids genus *Perrinites hilli*, *Medlicottia* sp., and *Titanoceras* sp. suggest an Artinskian – Kungurian age (Miller & Williams, 1945; Trumpy, 1943).

In recent years, new geochronological information has been presented, but this information has rarely been contrasted with the paleontological and stratigraphic data. The main purpose of this contribution is to present an integration of the paleontological and regional information to clarify the geological history of Colombia during the Paleozoic era. In this chapter, we included some of the most characteristic Paleozoic formations to the east of the Otú–Pericos Fault but not the Paleozoic formations in the Llanos Basin. Here, we present new paleontological data with geographic coordinates, along with a summarized stratigraphic framework and distribution of upper Paleozoic sedimentary sequences of the Andean region of Colombia. Additionally, the new geological data are used to discuss the ages of the metamorphic basement of the Chibcha Terrane (Restrepo, 1983; Restrepo & Toussaint, 1988).

2. Materials and Methods

Most of the original material cited in this work was collected during field campaigns conducted by the authors and students of the Universidad de Caldas. The samples and the geological sections were located by GPS (Garmin Map 64s). Fossils were prepared in the laboratory of paleontology. Some samples were cut and polished into thin sections. The petrographic thin sections were analyzed using a polarizing microscope (Nikon Eclipse E–200) with the camera adapter. A Nikon D610 camera assisted by the Helicon remote and Helicon focus 6 software was used to obtain net photographs of the macrofossils.

3. Serranía de Perijá

The serranía de Perijá, at the border between Colombia and Venezuela, includes the northernmost Paleozoic deposits of South America. The basement is constituted of weakly metamorphosed sedimentary rocks of the early Paleozoic age consisting of metapelites and quartzite of the Perijá Series (Forero, 1970). An angular unconformity separates metamorphic rocks from sedimentary sequences of the Devonian age. Gaps in the fossil succession suggest that separation surfaces, between Devonian, Carboniferous, and Permian strata, are disconformities (Forero, 1970) (Figure 3). Devonian strata, near 1300 m thick, are composed of a siliciclastic sequence of quartzite conglomerates, sandstones, and mudstones of shallow marine origin. The brachiopod fauna age of serranía de Perijá from Emsian?, Middle Devonian, and Frasnian is due to the presence of *Nervostrophia rockfordensis* (Forero, 1970).

The Carboniferous sequence, with a thickness close to 300 meters in the section of Manaure, is composed of conglomerates, red sandstones, and shallow platform limestones. The fossil fauna, containing brachiopods, mollusks, and bryozoans, indicates a Middle to Late Pennsylvanian age (Forero, 1970). The sedimentary rocks on the eastern side of the serranía de Perijá are correlated with the Lower and Middle Pennsylvanian Caño Indio and Río Palmar Formations of Venezuela (Benedetto, 1978).

Perijá Permian is made up of facies like those of the upper Carboniferous. The first mention of the presence of the Permian sequences in the serranía de Perijá is due to Trumpy (1943), who cites (from fossils collected to the east of Manaure by RENZ) Artinskian – Kungurian ammonites (*Perrinites hilli*, *Medlicottia* sp., and *Titanoceras* sp.), crinoids, brachiopods, and mollusks (*Bellerophon*). The Palmarito Formation, their stratigraphic equivalent on the Venezuelan flank of Perijá, has fauna in the range of Leonardian to Guadalupian (early to middle Permian).

From limestone material collected on the Colombian side of the serranía, east of the population of Manaure (10° 21’ 25.31” N, 73° 00’ 11.11” W), a fusulinid assemblage constituted of *Praeskinnerella hedbergi*, *Schwagerinoidea* sp., *Pseudoschwagerina dalmussi*, and *Climacammina* sp. (Figure 4) was recovered. The material, identified by Daniel VACHARD, is Sakmarian age (late Wolfcampian). At serranía de Perijá, the age of the Permian sequences lies between the lower Cisuralian (Sakmarian) and Guadalupian.

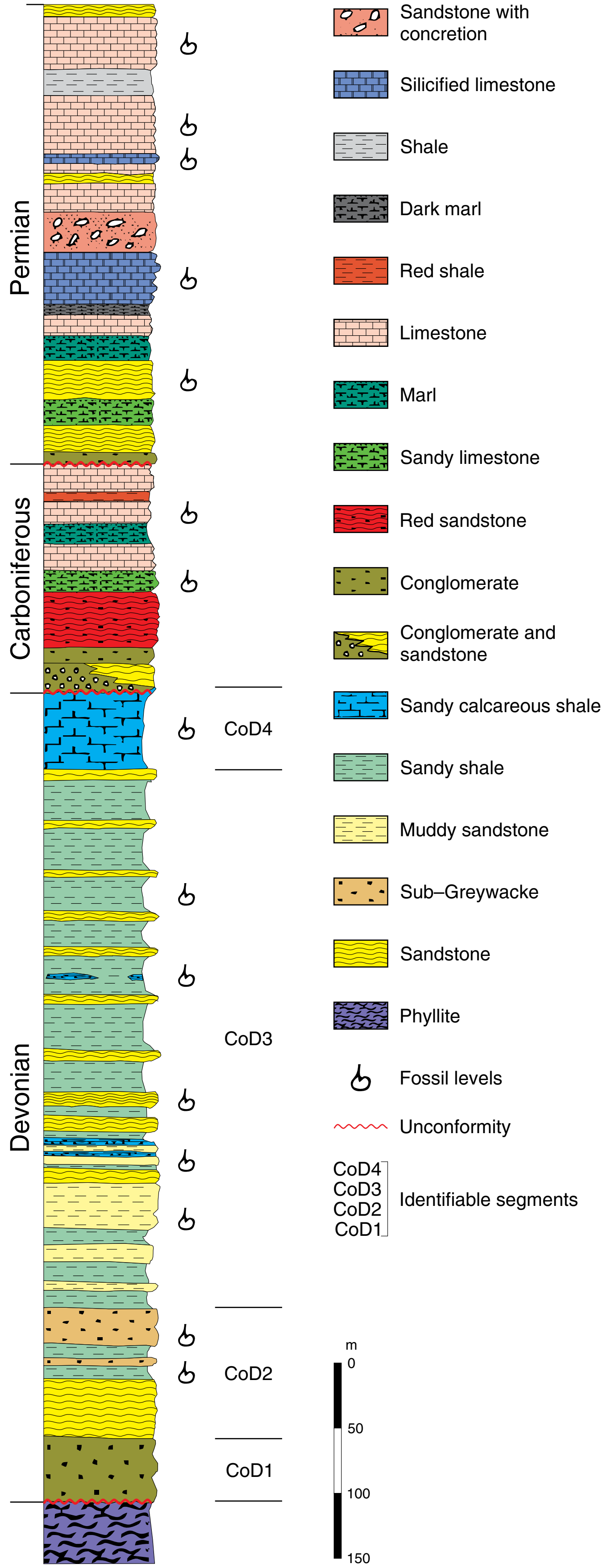

Figure 3. Geologic columns from serranía de Perijá (Forero 1970). Devonian sedimentary rocks cover unconformably early Paleozoic metamorphic basement (Perijá Series).

4. Santander Massif

The oldest rocks of the Santander Massif correspond to the Precambrian Bucaramanga Gneiss and the schists of the Silgará Formation (Ward et al., 1973, 1977). In the Chitagá River gorge (N 7° 16’ 25.81”, W 72° 32’ 52.48”), Devonian sandstones unconformable overlie low grade metamorphic basement constituted of quartzites and cordieritic metapelitic rocks of the Silgará Formation (sensu Royero & Zambrano, 1987). Metapelitic horizons still preserve traces of bioturbation (*Paleophycus* and *Teichichnus*), suggesting a post–Ediacaran age (Figure 5).

Along the Chitagá River, on the road that goes from Pamplona to Labateca, more than 700 meters of Devonian and Carboniferous sedimentary sequences are exposed. The Devonian deposits, unlike those of the Floresta Massif, are dominated by sandstones. Middle Devonian fossils occur at the base of the sequence, which includes *Eodevonaria imperialis*, *Mucrospirifer mucronatus*, “*Camarotoechia*”? cf., *C. sappho*, *Devonochonetes* sp., *D. coronatus*, and *D. mediolatus*, and *Leptaena* sp. (Boinet et al., 1986).

From loose material, Boinet et al. (1986) identify some fossil plants including *Platyphyllum* cf. *williamsonii*, *Taeniocrada decheniana*, cf. *Stockmansella* (*Taeniocrada*) *langii* in association with palinomorphs *Ancyrospora* sp., *Acanthotriletes* cf. *horridus*, *Auroraspora* sp., *Cirratriradites* sp., *Geminospora lemurata*, *Grandispora macrotuberculata, Hystrichosporites corystus*, *Leiotriletes ornatus*, *Raistrickia* sp., *Retusotriletes rugulatus*, *Rhabdosporites langii*, and *Spinizonotriletes* cf. *echinatus.* Additionally, BOINET report brachiopods *Devonochonetes* sp., *D. coronatus*, and *D. mediolatus*, *Eodevonaria imperialis*, *Leptaena* sp., *Mucrospirifer mucronatus*, and “*Camarotoechia*”? cf. C. *sappho*. The entire association points to a Middle to Late Devonian age. At the reddish sandstone and shales at the top of the Devonian sequence, the horizons contain flabellate leaves of genus form *Platyphyllum* (possibly detached leaves of *Archaeopteris obtusa*). These red beds, correlated with Cuche Formation of the Floresta Massif, are separated in this work from the Diamante Formation sensu Royero & Zambrano (1987). A disconformity surface separates the Carboniferous sandstone stratum from the underlying red beds of the Cuche Formation. We use Labateca Formation for the Carboniferous sedimentary succession composed of sandstones, limestones, and dark shales that crop out between the red beds of the Cuche Formation and the Girón Formation (Figure 6). At the Carboniferous occurs the rugose coral *Aulophyllum* sp. Permian fossils were not found in this formation.

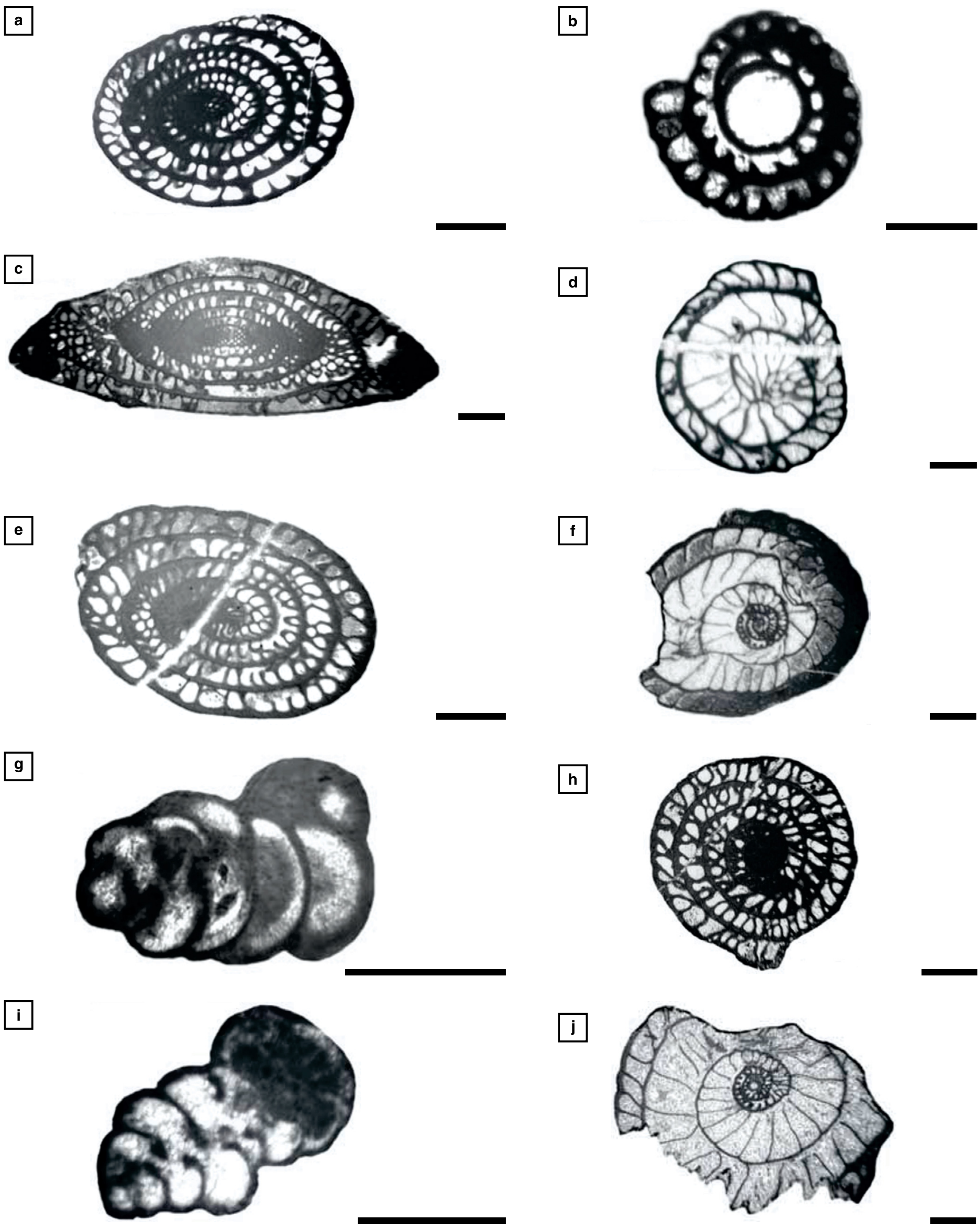

Figure 4. Fusulinids from Manaure (serranía de Perijá): **(a, c, e)** and **(h)** *Schwagerina? hedbergi* Thompson & Miller (1949); **(b)** *Schwagerinoidea* (indet.); **(d, f, j)** *Pseudoschwagerina dallmusi* Thompson & Miller (1949); **(g, i)** *Climacammina* sp. Sakmarian (late Wolfcampian) age. Scale bar is 1000 µm.

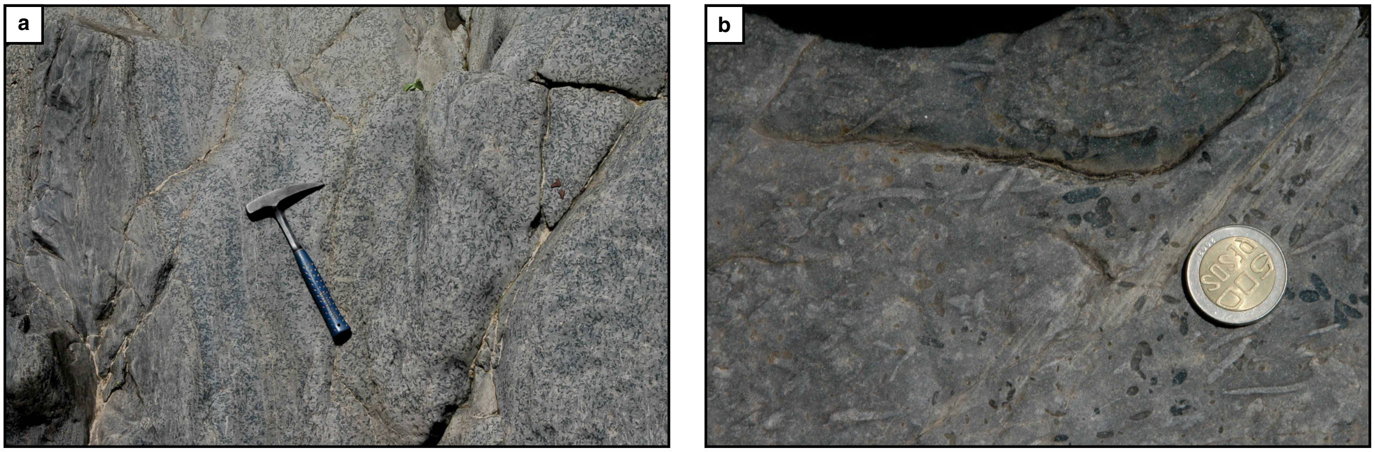

Figure 5. Metapelitic rocks at Chitagá River (Labateca). Floresta sedimentary rocks cover unconformably early Paleozoic metamorphic basement (Chicamocha Formation). **(a)** Cordieritic bands in stratified metapelite; **(b)** *Paleophycus* burrows preserved in metapelite. The dark patches are cordierite crystals.

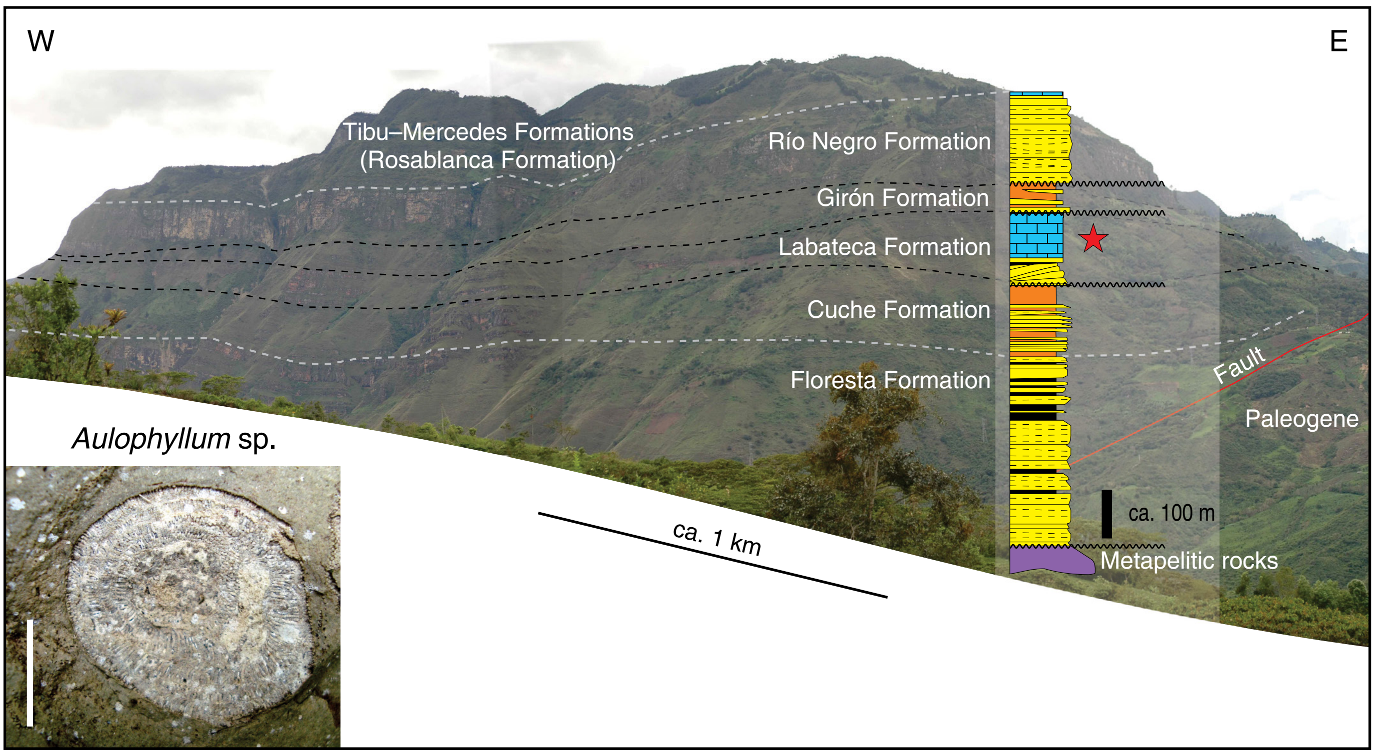

Figure 6. Paleozoic sedimentary succession at Chitagá River, near Labateca. Lower image, Carboniferous rugose coral *Aulophyllum* sp., the stratigraphic position is indicated by the red star. Scale represents 1 cm.

In the core of the Santander Massif, as in the sierra de Mérida, metamorphic rocks of Carboniferous age are exposed. The term "Metamorphosed Floresta Formation" is applied to a group of weakly metamorphosed rocks exposed between the towns of Santa Bárbara and Mogotes in the core of the Bucaramanga Massif (Ward et al., 1977). These rocks include Carboniferous low–grade metamorphic rocks of Mogotes, without relation to the true Floresta Formation (Moreno–Sánchez et al., 2005) and the "metasedimentary series of Guaca", where Forero (1990) identified *Aenigmastrophia* sp., a Silurian (Ludlowvian) brachiopod. The "Metamorphosed Floresta Formation" was dated Devonian based on bryozoans found in the metasedimentites. Diana GUTIÉRREZ (in Ward et al., 1977) identified Devonian Fenestellidae. Nevertheless, these fossils were not suitable for classification nor did they delimit a specific range of time since they are affected by metamorphism.

The "Metamorphosed Floresta Formation" is truly an association constituted of least by two lithological entities with a low degree of metamorphism:

- The youngest sequence, a succession of slates and weakly metamorphosed calcareous horizons (locally, marbles) that crop out near to Mogotes (6° 26' 02.29'' N, 72° 54' 46.77'' W) (Moreno–Sánchez et al., 2005), contains Carboniferous brachiopods (*Derbya* sp., and *Linoproductus*?) replaced partially by mica (Figure 7). At the Alto el Portachuelo hill (Molagavita, 6° 38' 26.80'' N, 72° 51' 18.90'' W and 6° 39' 55.30'' N, 72° 50' 44.50'' W), where Ward et al. (1977) found the fossils used to define the age of the unity, the metalimestone preserving the remains of brachiopods, trilobites (*Paladin* sp.), bryozoans, and crinoids. This upper calcareous segment, due to the paleontological and facial characteristics, can be correlated with the Carboniferous of Mogotes but not with the true Floresta Formation (Moreno–Sánchez et al., 2005).
- The oldest metasedimentary sequence, underlying the metalimestones, is composed of a succession of gray metamudstones and quartzites. The only fossiliferous locality in this unit is located north of Guaca and contains trilobites, crinoids, and brachiopods. The Silurian brachiopod *Aenigmastrophia* sp. occurs in distorted gray slates (Forero, 1990).

In the area between Tipacoque and Soatá (southern Santander Massif), Guaca and Mogotes metamorphic rocks are overlain in angular unconformity by the sedimentary sequence of the Río Nevado Formation, with the age between the Pennsylvanian and the Permian (Stibane & Forero, 1969). According to Stibane & Forero (1969), on the road that leads from the Chicamocha River to the Cocuy village near the Totumo bridge, the Río Nevado Formation composed of conglomerates, red and gray shales, sandstone and limestone of Pennsylvanian – lower Permian age (Figure 8).

To the east of the Bocas village (7° 13' 22.99'' N, 73° 08' 27.35'' W), in a calcareous section attributed to the base of the Bocas Formation, the foraminifers *Cuniculinella* ex gr. *fusiformis* that point to a lower Artinskian age (Figure 9) occur. In the same area, a calcareous bed also contains Wolfcampian conodonts (Rabe, 1974). Thus, adding the new material, the range of this segment would be Sakmarian to Artinskian. This segment, consisting of thick limestone packages, should be excluded from the Bocas Formation (sensu Remy et al., 1975) and included as an upper part of the Suratá Group of Dickey (1941; Navas, 1962). It is necessary to clarify that the siliciclastic segments of the Bocas Formation contain fossil flora that points to an early Mesozoic age (Remy et al., 1975; Ward et al., 1977).

Under the Carboniferous limestones (Suratá Group), between the Suratá River and Bocas village, a wedge of sandstone and mudstone with a fossil fauna consisting of brachiopods, trilobites, and crinoids that point to a late Middle Devonian age correlated to Floresta Formation (Rabe, 1974).

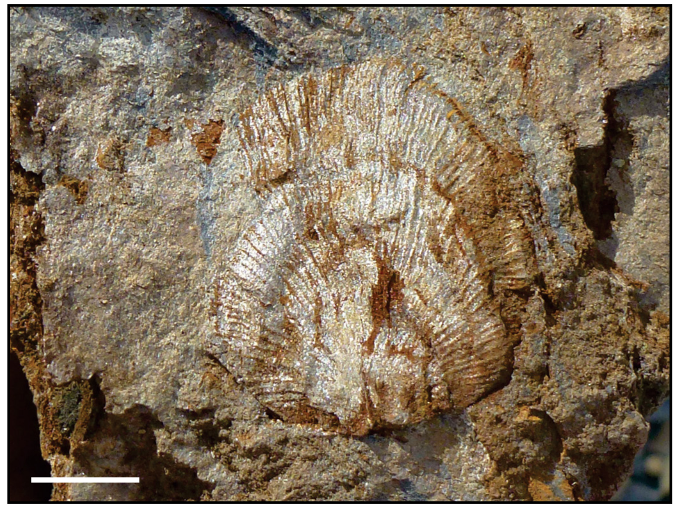

Figure 7. Pennsylvanian brachiopod *Derbyia* sp. From the Mogotes locality. The shell was partially replaced by muscovite. Scale represents 1 cm.

Figure 8. Carboniferous to Permian deposits of Río Nevado Formation at Totumo Bridge.

Pennsylvanian conodonts are found at the Suratá Group in northern Bucaramanga (Rabe, 1974). The assemblage contains *Adetognathus inflexus*, *Adetognathus lautus*, *Adetognathus spathus*, *Anchignathodus coloradoensis*, *Anchignathodus minutus*, *Gnathodus bassleri symmetricus*, *Gnathodus bassleri* n. subsp. *A., Gnathodus lateralis, Gnathodus noduliferus*, *Gnathodus roundyi, Gondolella clarki*, *Hindeodella* sp., *Idiognathodus delicatus*, *Idiognathoides sinuatus*, *Ligonodina* sp.*,* *Lonchodina* sp., *Metalonchodina* sp.*,* *Neoprioniodus*? *expandofundus*, *Ozarkodina delicatula*, *Ozarkodina* sp., *Streptognathodus expansus, Streptognathodus* sp. According to Rabe (1974), the assemblage suggests a Morrowan to Desmoinesian age (Bashkirian to Moscovian).

South of the same section (upper Suratá Group, Figure 10), at the Diamante Formation (lower part of the Suratá Group),

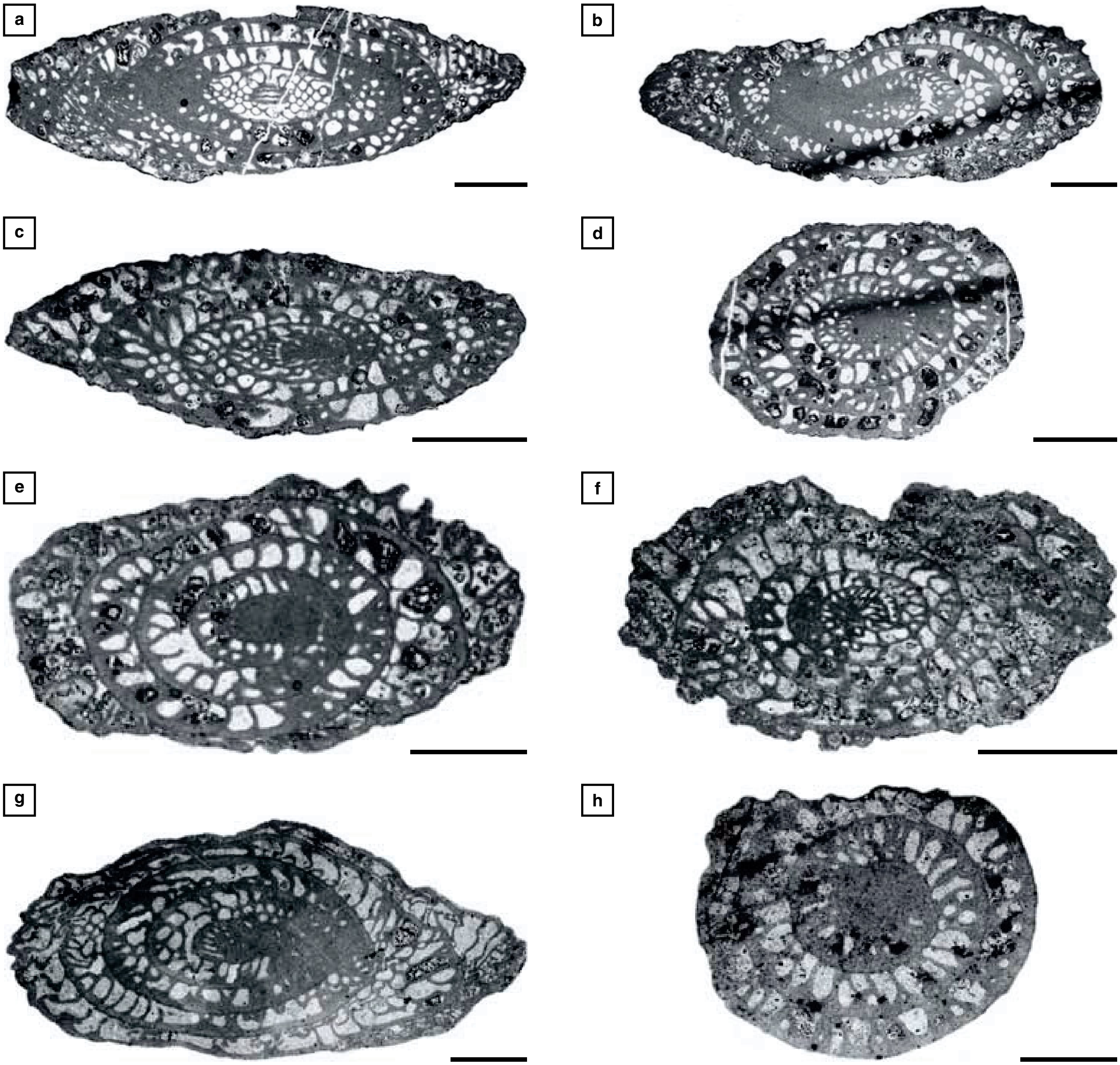

Figure 9. Permian Suratá Group foraminifer: **(a–h)** *Cuniculinella* ex gr. *fusiformis* Skinner & Wilde (1965). Early Artinskian age. Scale bar is 1000 µm.

Permian conodonts have been recovered (Rabe, 1974): *Anchignathodus* aff. *typicalis*, *Gnathodus bucaramangus* n. sp., *Gnathodus whitei*, *Gondolella* sp., *Hindeodella* sp., *Lonchodina* sp., *Ozarkodina* sp., *Streptognathodus elongatus*, *Streptognathodus sulcoplicatus*. According to (Rabe, 1974), this assemblage points to Wolfcampian to Guadalupian age (nearly Cisuralian to Guadalupian). The Diamante Formation (Dickey, 1941) is made up of 440 meters of sandstones, mudstones, and slightly recrystallized limestones. The unit outcrops along the old Rionegro–Bucaramanga road to the north of Bucaramanga city, particularly in the "Cementos Diamante" quarry where it takes its name. Fossils of Permian age including brachiopods (*Meekella* sp., cf. *Orthotichia* sp.) and fusulinids (Ward et al., 1973) occur at the formations.

5. Floresta Massif

A complete section of the Devonian in the Floresta Massif is found in the Potrero Rincón locality (Figure 11). The core of the Floresta Massif is formed by granitoids, phyllites, and slates of Cambrian – Ordovician age. The El Tíbet Formation (Cediel,

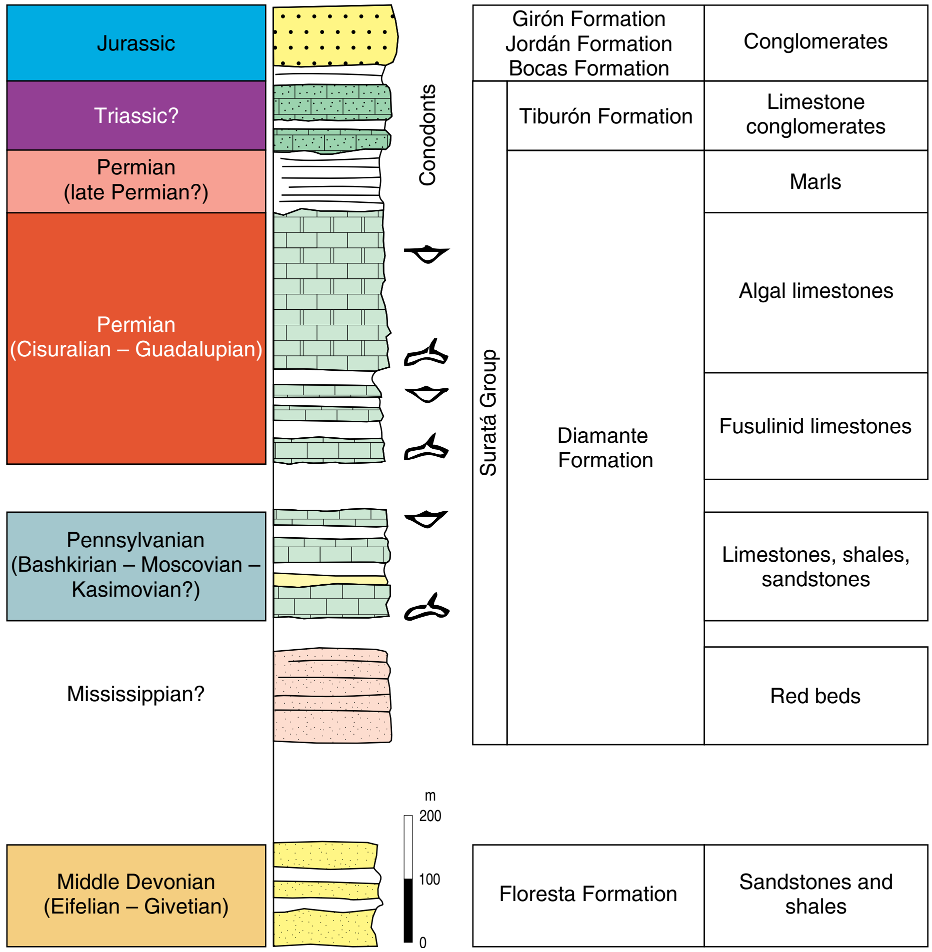

Figure 10. Stratigraphic chart of Suratá Group at the Santander Massif (Rabe, 1974).

1969; Mojica & Villarroel, 1984), separated from the metamorphic and igneous rocks by an unconformity, is a sedimentary succession composed of micaceous sandstones, conglomerates and thin layers of gray mudstones. At the Potrero Rincón, the thickness of this formation varies between 40 and 60 meters.

Fossils are rare, although towards the base, at a 4–meter clay level, brachiopods and plant remains have been found. The most common fossils of invertebrates in the El Tíbet Formation correspond to inarticulate brachiopods of the family Discinidae (*Schizobolus?* sp.) (Figure 12) and spiriferida brachiopods. Fossil plants (at 5° 49' 25.92'' N, 72° 55' 14.47'' W) correspond to fragmentary remains, something carbonized, where it is possible to identify the parenchymatous land plant *Spongiophyton* sp. (Moreno–Sánchez, 2004). U–Pb detrital zircon, recovered from the El Tíbet Formation, points to a maximum Early Devonian depositional age (414 Ma age peak) (Cardona et al., 2016). However, spores recovered from this formation indicate an Emsian age (Grösser & Prössl, 1994).

At the Floresta Massif, the El Tíbet Formation has a thickness that varies between 30 and 600 meters (Cediel, 1969), suggesting that during Early Devonian times in the region, there was a rugged paleotopography. The El Tíbet Formation was deposited in a coastal siliciclastic transgressive environment during the Emsian age.

The Floresta Formation mudstones, near 500 meters thick, conformably overlie the sandstones of the El Tíbet Formation. Floresta lithology consists mainly of mudstones and dark shales with some sandstone intercalations, to the base where thin ferruginous ooid strata occur. In all the studied sections, the richest fossil interval is very close to the base of the sedimentary sequence (e.g., Potrero Rincón A, Figure 11). The fossils, originally of carbonates, correspond now to molds, consisting of bryozoans, trilobites, tabulata (*Favosites* sp., *Pleurodictyum* sp.) rugose corals, brachiopods, crinoids, and mollusks (gastropods and bivalves). From the lower Floresta Formation, Trapp (1968) quotes *Hoareicardia cunea* ("*Conocardium cuneus*"), the first Rostroconchia from Colombia. Some dacryoconarid remains (Figure 13), semi–infaunal shelly fossils of unknown affinities, are found in the transition from the gray to the dark shales. On the argillaceous part, black shales with a few interbedded limestones predominate to the top of the formation.

At the Potrero Rincón B (5° 49' 41.48'' N, 72° 55' 35.71'' W; Figure 11), thin limestone layers, always weathered, con-

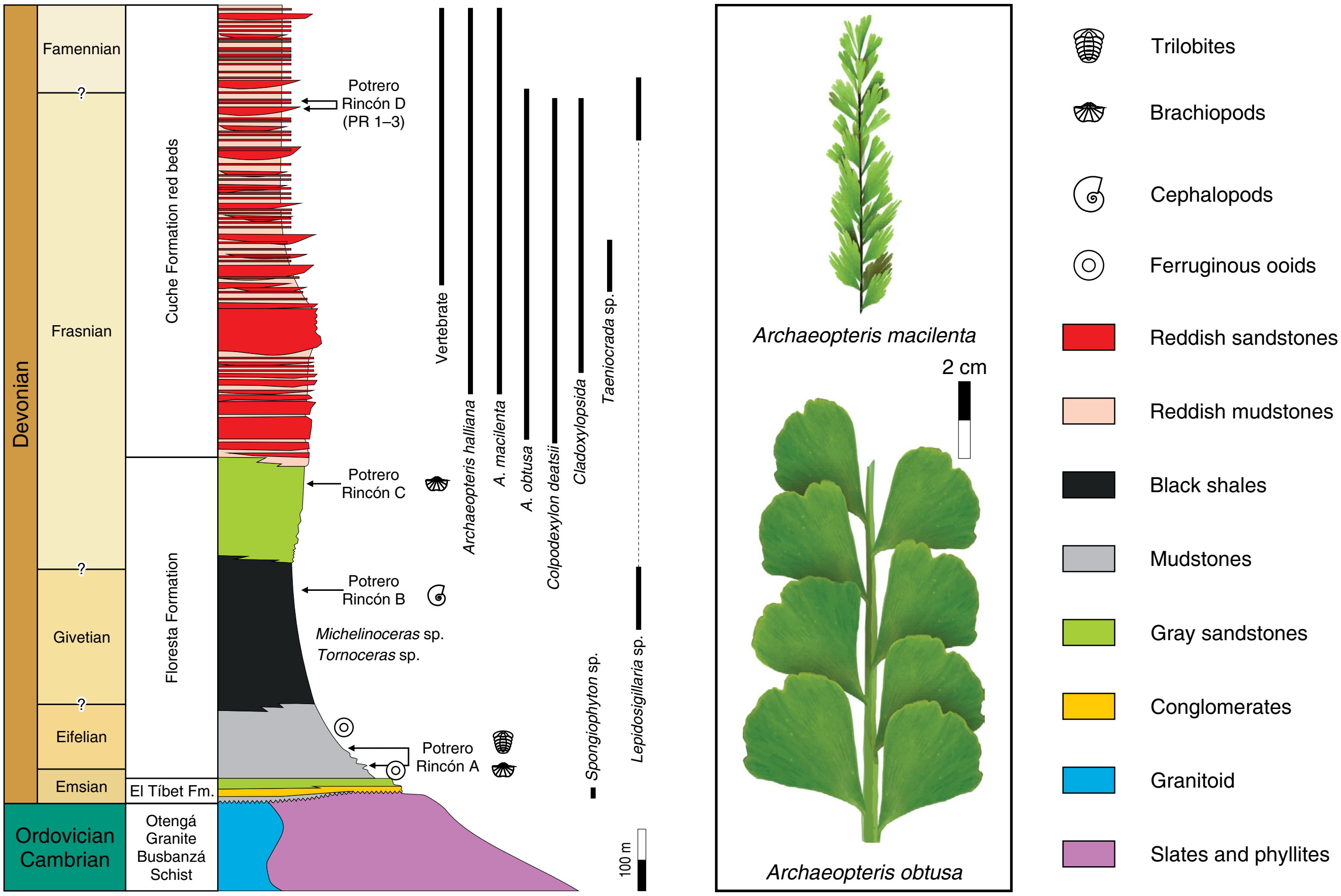

Figure 11. A geologic column of Devonian formations at Potrero Rincón locality (Floresta Massif).

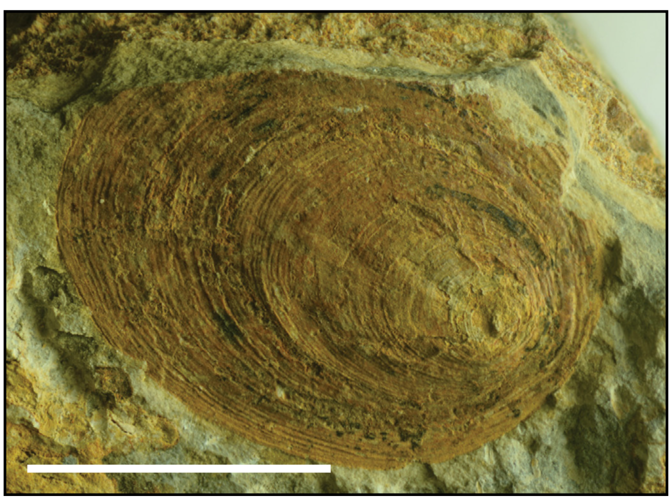

Figure 12. Inarticulate brachiopod (*Schizobolus?* sp.) recovered from the base of El Tíbet Formation. Scale bar represents 1 cm.

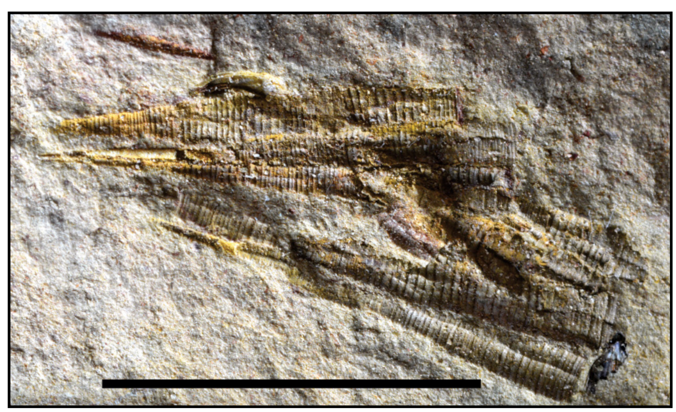

Figure 13. Dacryoconarids remains from the middle part of Floresta Formation. Scale bar represents 1 cm.

tain cephalopods of the genus *Michelinoceras* and *Tornoceras*) mixed with remains of Phyllocarida crustaceans (Figure 14). At the top of Floresta Formation, the silty sandstone beds contain the brachiopod *Composita* sp., that indicates a Frasnian age for this segment (Potrero Rincón C; Figure 11).

The fauna of Floresta Formation, quoted by Caster (1939), McNair (1940), Morales (1965), and Barrett (1988), shows similarities to the Onondaga Formation and Hamilton Group of eastern North America, suggesting an Eifelian to Givetian age. Based on trilobites and brachiopods, Morzadec et al. (2015)

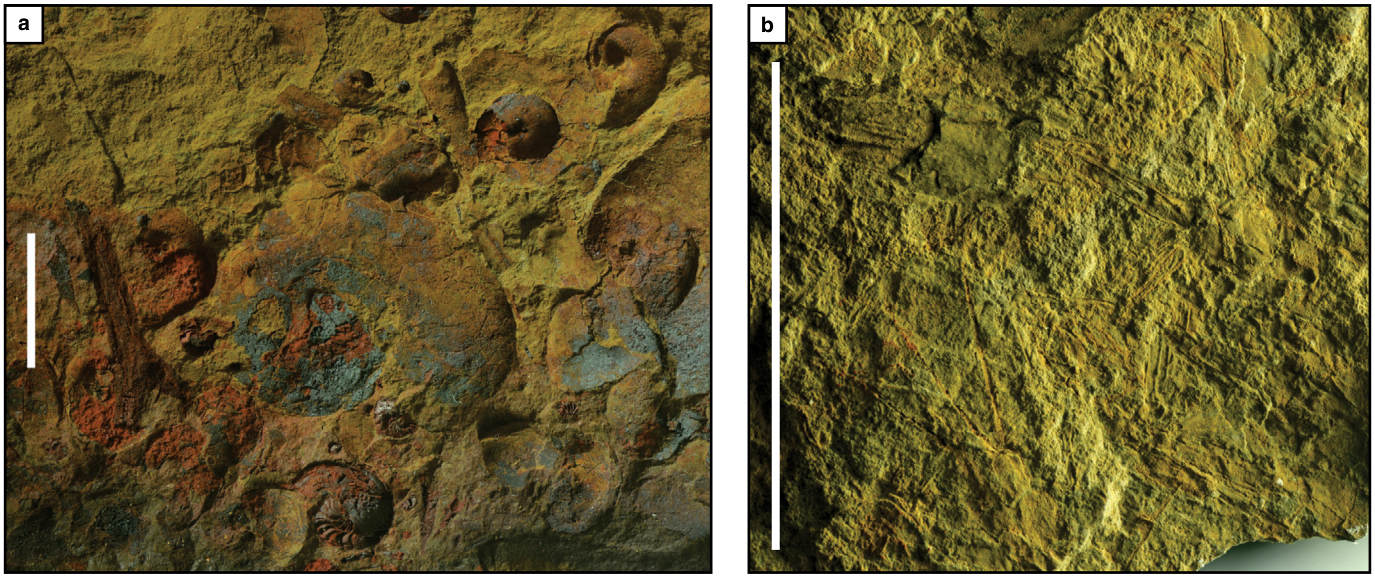

Figure 14. (a) Cephalopods *Tornoceras* sp. from the Floresta Formation; **(b)** phyllocarid remains. Scale bar represents 1 cm.

propose a late Emsian age for the lower part and a Givetian age for the upper part of the formation. Fragments of the plates of placoderm fishes (order Rhenanida) have been found in the lower part of the Floresta Formation (Janvier & Villarroel, 1998, 2000). The Floresta Formation was deposited in an epicontinental marine environment. Rich fossil assemblages in the Potrero Rincón A locality (Figure 11) indicate a shallow marine environment. Cephalopods in the black shales (Potrero Rincón B) suggest a maximum flooding surface at the middle part of the Floresta Formation. Ferruginous ooid beds are interpreted as non–deposition conditions in a low–energy marine environment (Burkhalter, 1995).

The Cuche Formation, approximately 750 meters thick, is composed of red and gray sandstones interbedded with reddish mudstones originating in a deltaic and fluvial environment (Moreno–Sánchez, 2004). Petrographically, the sandstones are classified as litharenites whose source, according to Dickinson (1985), is the one of a recycled orogen (Cardona et al., 2016). The formation covers conformably the epeiric marine layers of the Floresta Formation. The Cuche Formation red beds contain vertebrates and plant remains often found in the muddy intervals of the unit. At the Potrero Rincón D beds (at 5° 49' 08.30'' N, 72° 56' 29.71'' W; Figure 11), Janvier & Villarroel (2000) found fish remains that include *Cheiracanthoides*? sp., *Antarctilamna*? sp., placoderms (*Bothriolepis* sp., *Asterolepis*? sp.), and sarcopterygians (*Holoptychius*, *Strepsodus*? sp.). The fish assemblage shows Laurussian affinities, but *Antarctilamna* is a Gondwanan chondrichthyan; Burrow et al. (2003) also quote other species such as *Nostolepis gaujensis* and *Florestacanthus morenoi* (Figure 15). The age of the fish assemblage of Potrero Rincón D (PR 1–3) is late Frasnian (Janvier & Villarroel, 2000).

The most common fossil plant in the red beds of the Cuche Formation is *Archaeopteris* (Figure 16), a sporangiate tree with pycnoxylic wood similar to that of some conifers. *A. obtusa*, a species with the largest leaves, and *A. notosaria* are the most common plants in the lower part of the formation. *Archaeopteris halliana* and *A. macilenta* are the dominant plants towards the upper part of the Cuche Formation, originating possibly in a drained portion of a floodplain. Almost every *Archaeopteris* species has a global distribution, although *A. notosaria* is known only from the Upper Devonian from South Africa (Anderson et al., 1995). All recognized *Archaeopteris* species are constrained to the Frasnian – Famennian (Fairon–Demaret, 1986). Impressions of detached fan–shaped leaves with parallel bifurcating veins of *Ginkgophytopsis* (*Ginkgophyton*) and *Platyphyllum* genus are common throughout the unit. Fossil assemblages of Cuche Formation include highly dissected isolate leaves, often confused with *Baiera*, which are ascribable to the Paleozoic genus *Ginkgophyllum*. Remains of Cladoxylopsida–like plants, *Colpodexylon deatsii*, and arborescent lycopsida (*Lepidosigillaria* sp.) are found in association with channel margin and lacustrine deposits (Moreno–Sánchez, 2004). Sandstones of the El Tíbet, Floresta, and Cuche Formations are composed of arkosic and lithic siliciclastic components (Cardona et al., 2016), but there are no primary volcanic deposits attributable to proximal volcanism. The abundance of muscovite flakes in the sandstones (especially in the El Tíbet Formation) suggests that a large part of the detrital components of these units comes from the erosion of a metamorphic massif.

In South America, the Cuche Formation is the equivalent of the Catskill Formation of the eastern North America. The Cuche Formation correlates with the Frasnian age Campo Chico Formation (Harvey, 1999) at the serranía de Perijá (Colombia–Venezuela border). The Campo Chico Formation yields a Phyllolepid fish fauna composed of Gondwanan and Laurussian elements (Young & Moody, 2002a, 2002b).

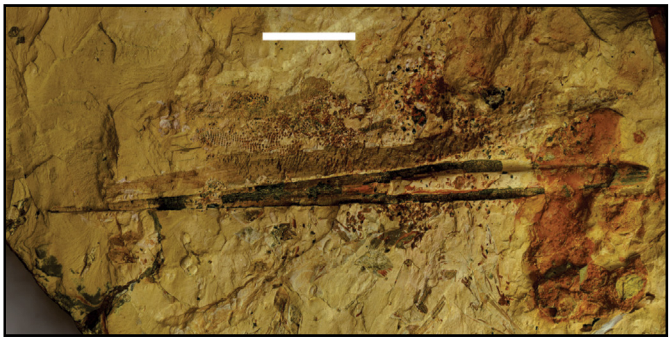

Figure 15. *Florestacanthus morenoi* from the fish assemblage of Potrero Rincón D (PR 1–3). Scale bar represents 1 cm.

6. Quetame Massif

The oldest rocks reported in the Quetame Massif that crop out on the Bogotá–Villavicencio highway, correspond to quartzitic conglomerates, phyllites, and schists originally described by Hettner (1892). Trumpy (1943, 1945), based on lithological comparisons, suggests that the metamorphic rocks of the Quetame Massif are the time equivalent to the sedimentary succession of the Güejar River canyon in the serranía de La Macarena. Therefore, after the publication of the work of Trumpy (1943), a Cambrian – Ordovician age has been assumed for the sedimentation of similar rocks on the Eastern Cordillera (Campbell & Bürgl, 1965; Renzoni, 1968; Stibane, 1968). Trapp (1968) brings together the different metamorphic units of the massif (conglomerates, quartzites, and gray and greenish phyllites) in the so–called "Quetame Group", which includes rocks characterized by penetrative planar fabric.

At the Casa de Teja Creek site (Bogotá–Villavicencio road, 4° 11' 55.87" N, 73° 46' 24.98" W), despite the penetrative foliation (S_1 average: 310°/70°) that affects the Quetame Group rocks, the bedding is still visible. The phyllites expose sectors with a high degree of bioturbation (Figure 17). Thus, the presence of ichnofossil burrows such as ichnogenus *Teichichnus*, in agreement with the invertebrate evolution, discards a Precambrian age (Gradstein et al., 2012) for the phyllites and quartzites of Guayabetal Formation (part of the Quetame Group). The finding of Silurian palynomorphs in a sequence of clastic rocks (conglomerates, sandstones, and mudstones), slightly metamorphosed and lithologically different from those of the underlying Quetame Group, indicates that the main phase of the Quetame metamorphism is older than the Silurian (Grösser & Prössl, 1991).

All the Paleozoic sedimentary formations of the Quetame Massif (from the Devonian to the Carboniferous) were gathered by Braun (1979) within the Farallones Group. The Areniscas de Gutiérrez and Pipiral Formations (Middle Devonian), composed of sandstones, siltstones and black mudstones, correlate with the El Tíbet and Floresta Formations in the Macizo de Floresta. Towards the upper part of the group is the Capas Rojas de Guatiquía Formation, of Pennsylvanian age, composed of siltstones, red and green pale beds, and limestones (Braun, 1979; Pulido & Gómez, 2001; Pulido et al., 1998). Trapp (1968) mentions Mississippian deposits; however, this has not been confirmed by biostratigraphic data.

The Farallones Group, at Guateque–Santa María road, includes a sequence of conglomerates, sandstones, and mudstones of middle Devonian age (Segovia & Renzoni, 1965). The most common fossils are brachiopods, tentaculites, and bivalves. *Orthonata undulata* (4° 53' 33.72" N, 73° 17' 11.94" W, Figure 18), a Givetian razor clam, is reported in the mudstones.

Limestones collected by Fernando ETAYO–SERNA from the Farallones Group, to the north of Quetame Massif (4° 43' 16.20" N, 73° 21' 37.79" W), contain foraminifers identified by Daniel VACHARD as an assemblage of Middle Pennsylvanian age (Moscovian: late Atokan or Kashirian – Podolskian): *Fusulinella* ex gr. *thompsoni*, *Schubertellina* sp., *Fusulinella* sp., *Pseudoacutella* cf. *grozdilovae*, *Planoendothyra* sp., *Palaeotextularia* sp., *Millerella* sp., *Climacammina* sp., and *Plectomillerella* sp. (Figure 19).

7. Late Paleozoic Sedimentary Rocks on the Eastern Flank of the Central Cordillera

To the west of Ibagué city (Chapetón neighborhood), a strip of limestone and marble crops out, cited by Nelson (1957) as part of the Cajamarca Series. These late Paleozoic marbles, cropping out to the east of the Otú–Pericos Fault, are constituted of thick layers of crinoidal limestones (Gómez & Bocanegra, 1999; Moreno–Sánchez et al., 2008a). The Carboniferous limestones at Ibagué are correlated with other marmorized limestones cropping out along the eastern flank of the Central Cordillera. The marbles, some of them included in the Aleluya Complex (Ferreira et al., 2002), are thermally affected by Mesozoic intrusives. Hernández–González & Urueña–Suárez (2017) dated the biotite of the marbles and obtain a $^{40}Ar/^{39}Ar$ age of 211.2 ± 1.18 Ma (Triassic) attributed to a metasomatic event.

In the El Imán Creek, near Rovira in the eastern foothills of the Central Cordillera, there is a sedimentary sequence consisting of conglomerates, sandstones, and fossiliferous shales (Núñez & Murillo, 1982). Fossil (bryozoans and brachiopods) age ranges from the Middle Devonian to Carboniferous (Tournaisian), the latter suggested by the presence of the brachiopod *Ericiatia* (Forero, 1986). The fossil fauna of Rovira contains elements common to New Mexico, which, according to Forero (1986), suggest that the northern South America platform was in a latitudinal position similar to that of the Old–World Province (sensu Johnson & Boucot, 1973). The fossil assemblage includes *Adolfia* cf. *A. deflexa, Cariniferella alleni*, *Cryptothyrella* cf. *C. cylindrica*, *Devonoproductus intermedius*, *Eleuterocoma* cf. *E. beardi*, *Laminatia*

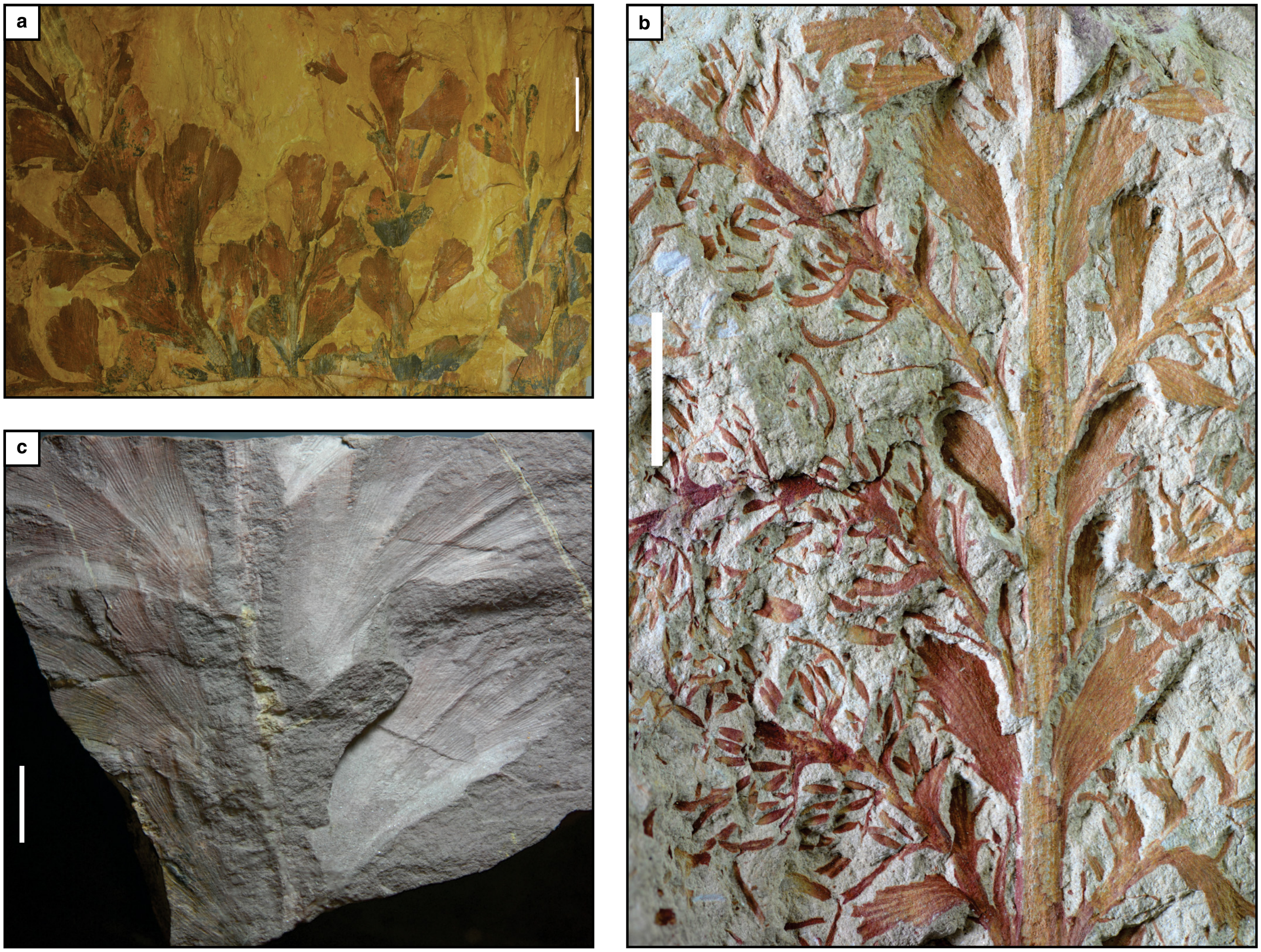

Figure 16. Plant remains from the Cuche Formation. **(a)** *Archaeopteris obtusa*; **(b)** A. *macilenta*; **(c)** *A.* cf. *notosaria*. Scale bar represents 1 cm.

laminata, Schizophoria amanuensis, *Strophopleura notabilis*, besides the genera *Cyrtina*, *Eostrophalosia, Schelwienella,* and *Tylothyris*.

At the Amoyá Formation (Núñez et al., 1984), constituted of a failed sequence of black shales with intercalations of sandstones exposed on the eastern flank of Central Cordillera, *Cymbosporites catillus*, *Stenozonotriletes inequaemarginalis*, *Dibolisporites abitibiensis*, and *Apiculiretusispora pygmaea* were recovered. The aforementioned pollen assemblage indicates, at the place of sampling (near to 3° 46' 54.41'' N, 75° 33' 33.16'' W), an Eifelian age (Prössl & Grösser, 1995). Sedimentary facies at Amoyá and Rovira (Forero, 1986) indicate near shore marine environments during the Middle and Late Devonian.

To the east of San Antonio on the border of Garzón Massif, a Pennsylvanian sequence composed of siliceous mudstones, quartzites, and oolitic limestones crops out. The rocks are thermally affected by Jurassic intrusives that locally generate marbles. The limestones contain crinoids and brachiopods. A limestone was sampled (2° 54' 51.00'' N, 75° 05' 12.96'' W) and contained *Seminovella* sp., an early Bashkirian (Morrowan) Millerellinae foraminifer (Figure 20). The carboniferous Formation of San Antonio is correlated with the nearby Cerro Neiva Formation (Mojica et al., 1987a).

8. La Jagua (Huila)

Stibane & Forero (1969) use the term "Paleozoic of the La Jagua" to refer to a sedimentary section exposed near La Yunga farm. However, detailed field geological work has determined that, in the vicinity of the farm outcrops mentioned above, the Gualanday Group is of Paleogene age. Carboniferous deposits of the La Jagua (Stibane & Forero, 1969) crop out along the Caguancito Creek, southwest of the municipality of Garzón, Huila. The occurrence of the brachiopod *Acrospirifer olssoni* (Stibane & Forero, 1969) and tentaculitids in the shales exposed to the west of the section of Caguancito indicates the presence of Devonian in this area.

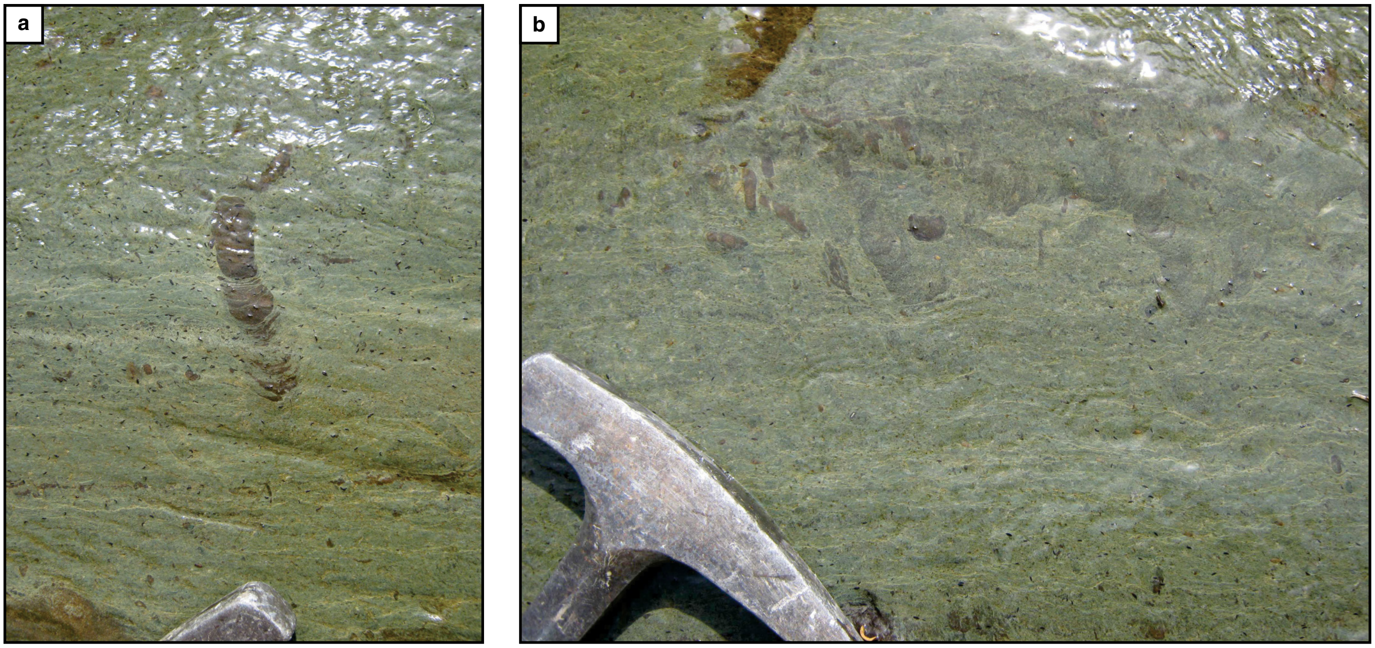

Figure 17. Fossil traces at the Quetame Massif. **(a)** *Teichichnus* isp.; **(b)** pervasive bioturbation at the Quetame phyllites.

Figure 18. Bivalve *Orthonata undulata* from the Farallones Group. Scale bar represents 1 cm.

At the Caguancito Creek, a tributary of Aguas Calientes River (5 km to the southeast of the La Yunga farm), the most continuous outcrops of the Carboniferous on the Garzón Massif occur. The section, according to Velandia et al. (1996), is 660 m thick, measured at the junction with the Aguas Calientes Creek (2° 06' 13.94'' N, 75° 39' 14.77'' W).

In the Caguancito Creek, it is possible to recognize repetitive sequences in which layers of continental origin alternate with marine deposits (Figure 21) indicating cyclic sea level changes characteristic of Carboniferous global glaciations (Heckel, 2008). The segments of marine origin are characterized by calcareous levels, sometimes oolitic, and gray to black shales, with a fauna consisting mainly of brachiopods, crinoids, conulariids, bryozoans, and mollusks. Goniatitid ammonoidea (*Gastrioceras* sp.) are present at the dark shale segments (e.g., 2° 06' 27.00'' N, 75° 38' 56.30'' W). The continental deposits are characterized by desiccation cracks, rain drop marks, eurytopic leaioid conchostracan (*Hemicycloleaia* sp.) and fossil plants such as *Calamites* sp., *Odontopteris* sp., and seed impressions (*Samariopsis* sp.) (Figure 22). The presence of dolomites with pseudomorphs of anhydrite suggests sedimentation under dry climatic conditions and high temperatures (Gómez–Cruz & Chevalier, 2003).

Several samples of limestone were studied in this section by Daniel VACHARD, providing an association of foraminifera composed of *Millerella* sp., *Asteroarchaediscus*? sp., *Calcivertella* sp., *Planoendothyra* sp., *Glovivalvulina* sp., *Millerella* sp. 1., *Millerella* sp. 2., *Tetrataxis* sp., *Tubispirodiscus*? sp., *Planoendothyra aljutovica* (Figure 23). The assemblage age is Lower Pennsylvanian (Bashkirian). The Pennsylvanian deposits of La Jagua are correlated with the "Calizas y Arenitas de La Batalla" at Las Minas.

9. The Problem of Crystalline Basements of Eastern Cordillera and Magdalena Valley

During the Precambrian and early Paleozoic, the stratigraphic and tectonic history of the Eastern Cordillera (Quetame–Mérida Terrane) differs clearly from the stratigraphic and tectonic history of the Magdalena Valley (Payandé and Payandé–San Lucas Terranes sensu Etayo–Serna et al., 1983).

Bucaramanga Gneiss is the oldest metamorphic rock at the Santander Massif. Cordani et al. (2005) report U–Pb zircon ages between 1558 and 864 Ma, Ward et al. (1973) quote a 945 ± 40 Ma K/Ar age, and Restrepo–Pace (1995) give $^{40}Ar/^{39}Ar$

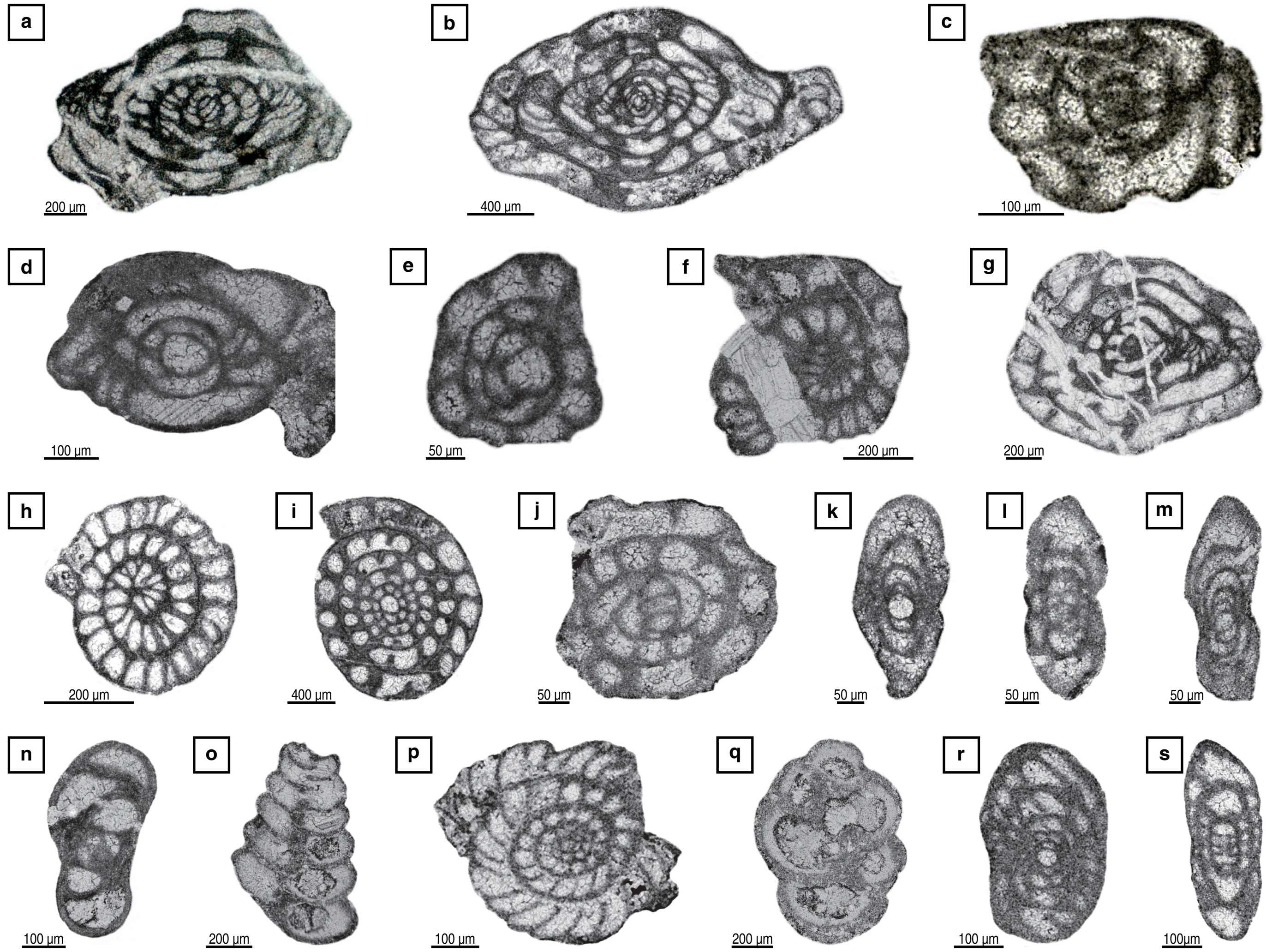

Figure 19. Pennsylvanian foraminifers from Mámbita (Quetame Massif): **(a, b)** *Fusulinella* ex gr. Thompsoni Skinner & Wilde (1954); **(c, d, e)** *Schubertellina* sp.; **(f, g, h, i, j)** *Fusulinella* sp.; **(k, l, m)** *Pseudoacutella* cf. *grozdilovae* Maslo & Vachard (1997); **(n)** *Planoendothyra* sp. Skinner & Wilde (1954); **(o)** *Palaeotextularia* sp.; **(p)** *Millerella* sp.; **(q)** *Climacammina* sp.; **(r, s)** *Plectomillerella* sp. Early Moscovian (Kashirian and /or Podolskian) age.

ages between 850–800 Ma. At the same locality where Ward et al. (1973) report the K/Ar samples, Ordóñez–Carmona et al. (2006) obtained a 1.71 Ga for the protolith sedimentation based on Sr and Nd isotopic analyses. However, due to the sample location on a tectonic wedge placed along the Bucaramanga Fault between Aguachica and Ocaña, it is not reliable that gneisses can be included safely either in the Santander Massif or in the Payandé–San Lucas Block (Figure 1).

The Silgará Formation includes sequences of metamorphosed clastic rocks consisting of schists, slates, phyllites, siltstones, sandstones, and calcareous phyllites. Based on petrographic features and detrital zircons, Mantilla–Figueroa et al. (2016) split off the older Silgará Formation (sensu Ward et al., 1973) into three different units.

- The Silgará Formation sensu stricto is restricted to the type section of the Silgará Formation (Santander Massif, Matanza–Cachirí area), which contains detrital zircons with peaks of Precambrian U–Pb ages approximately 940, 1010 and 1248 Ma (Mantilla–Figueroa et al., 2016).
- The Chicamocha Schists, with a maximum depositional age of 506.7 ± 9.3 Ma (middle Cambrian), is constituted of the schists and quartzites that crop out at the Chicamocha canyon on the Piedecuesta–Aratoca section. Chicamocha Schists are intruded by Ordovician foliated granitoids (orthogneisses) (Mantilla–Figueroa et al., 2016).
- The San Pedro Phyllites, cropping out at the Piedecuesta–Aratoca sector, contain the youngest zircons of 451.6 ± 7.7 Ma (Mantilla–Figueroa et al., 2016), suggesting a maximum depositional age near the Ordovician – Silurian boundary.

The Chicamocha Schists can be correlated with the Quetame Group and with the metasedimentary rocks with fossil traces of Labateca (Silgará Schists sensu Royero & Zambrano, 1987). Quetame and Chicamocha units, with *Teichichnus* that suggest

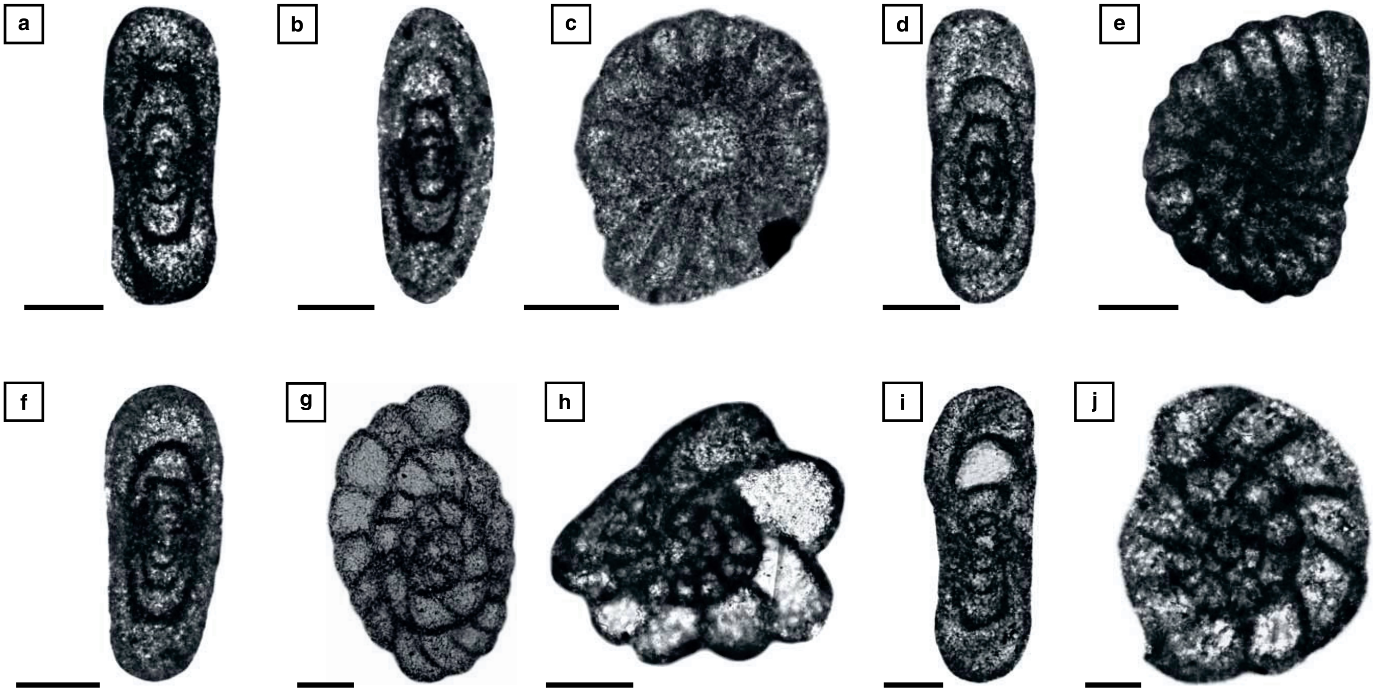

Figure 20. Early Bashkirian (Morrowan) Millerellinae foraminifer from San Antonio: **(a–i)** Seminovella sp. Maslo & Vachard (1997). Scale bar is 20 µm.

a post–Ediacaran age, are intruded by Early to Middle Ordovician granitoids (Horton et al., 2010; Mantilla–Figueroa et al., 2016). The San Pedro phyllites can be correlated with the lower part of "metamorphosed Floresta Formation" and could be equivalent to the Silurian metasedimentary rocks of Guaca.

At the Quetame, Floresta, Santander, and Perijá areas, the late Paleozoic sedimentary sequences were deposited over a basement constituted of Precambrian to early Paleozoic metamorphic rocks intruded by Ordovician granitoids (e.g., Boinet et al., 1985; Cardona et al., 2016; Goldsmith et al., 1971; Horton et al., 2010).

The upper Paleozoic sedimentary sequences in the Eastern Cordillera unconformably cover lower Paleozoic metamorphic rocks. The highest degree of burial is presumed to occur where the Carboniferous metasedimentary rocks (Mogotes–Mucuchachí) were latter exhumed were exhumed. Late Pennsylvanian low–grade metamorphism was developed in the core of the Santander Massif and the Mérida Andes. At the Mérida Andes, the Mucuchachí Formation is composed of green to black slates, metavolcanic rocks, and phyllites, which yield fossil plants of the Pennsylvanian age (Odreman & Wagner, 1979; Pfefferkorn, 1977). Volcanic rocks of the Mucuchachí Formation could be correlated with magmatism present in the Pennsylvanian series on the Maya Block (e.g., Bateson, 1972). At Santander Massif and Mérida Andes, metamorphic rocks of the Carboniferous age precede deposition of Sabaneta and Río Nevado sequences. The Mucuchachí Formation is covered unconformably by Permian conglomerates of the Sabaneta Formation. Additionally, compared with the Santander Massif, a lower exhumation degree in the Quetame Massif is suggested by the absence of Precambrian gneisses and the presence of Ordovician unfoliated granitoids.

The analysis of detrital zircons on early Paleozoic rocks from the Santander Massif and Mérida Andes suggests that they come from sources within the Amazonian Craton (Horton et al., 2010; Mantilla–Figueroa et al., 2016; van der Lelij et al., 2016b).

Contrasting with the data mentioned above, there are no early Paleozoic events recorded in the rocks of the Magdalena Valley (Payandé and Payandé–San Lucas), as well as in the Llanos Basin and the La Macarena mountain range. The basement at serranía de La Macarena is composed of Precambrian gneisses (Calymmian?) and Ediacaran syenites. Buchely et al. (2015a) quote a 1528 Ma U–Pb age from a quartzofeldspathic gneiss outcropping at Caño Rojo (serranía de La Macarena). Gneisses of the serranía de La Macarena are intruded by syenites with a 600 Ma U–Pb peak age (Buchely et al., 2015a). To the south of the La Macarena (San José del Guaviare), U–Pb dating on nepheline syenite indicates a crystallization age 577.8 +6.3/–9 Ma (Arango et al., 2012). Both dates on syenites suggest an event of crustal stretching during the Ediacaran.

Geochronological data from high–grade metamorphic rocks at the Garzón Massif range between 1200 to 900 Ma (Cordani et al., 2005); similar data have been obtained in the Sierra Nevada de Santa Marta and the La Guajira Peninsula. The high–grade metamorphic rocks of the Garzón Massif, as well as part of the Sierra Nevada de Santa Marta, were included in the same Grenvillian belt by Kroonenberg (1982).

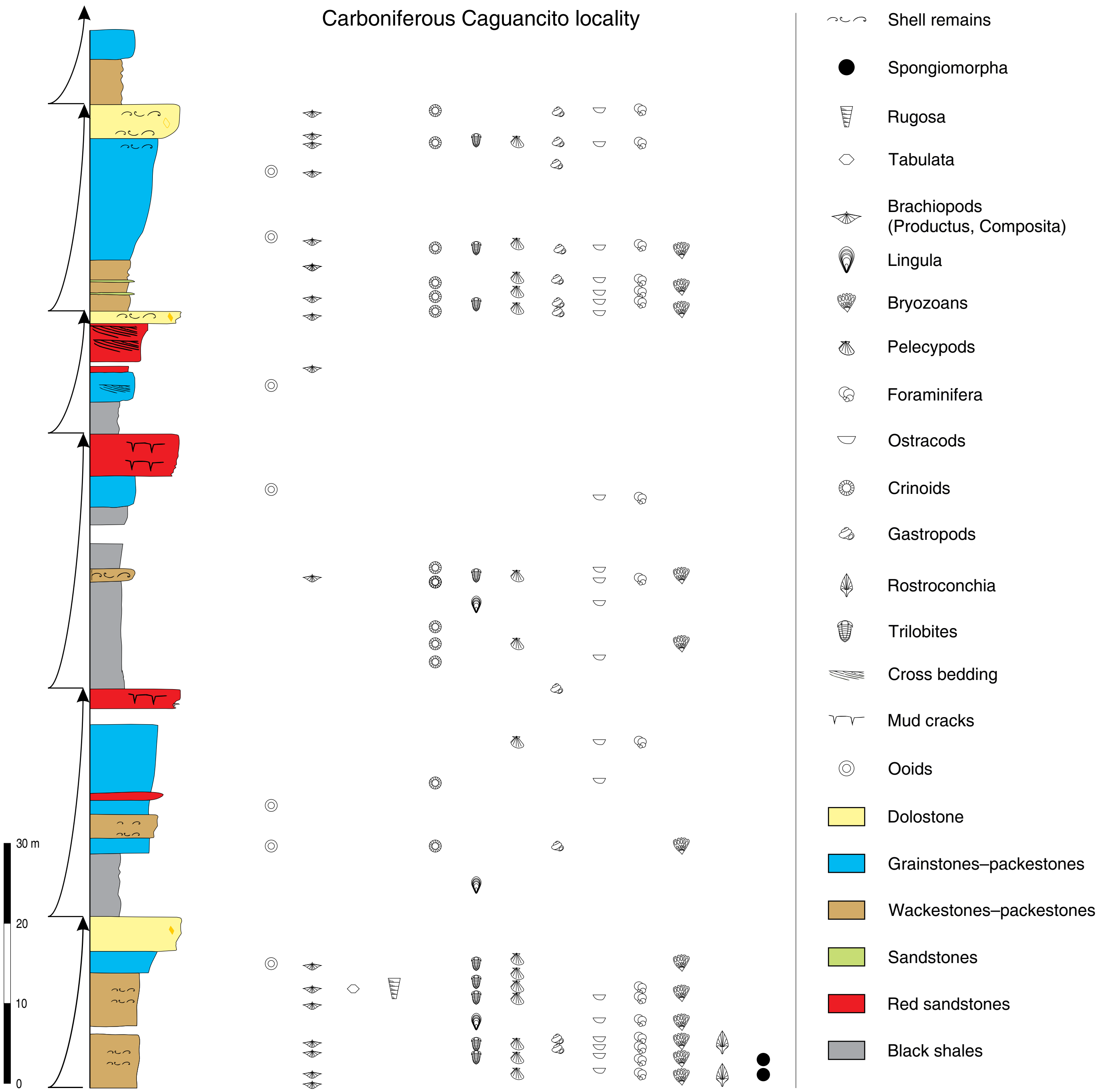

Figure 21. Repetitive sequences at Caguancito Creek in which layers of continental origin alternate with marine deposits indicating cyclic eustatic changes of sea level.

The El Vapor Mylonitic Gneisses under the La Cristalina Formation (Figure 1), indicates an age Rb/Sr isochron of 894 ± 36 Ma (Ordóñez–Carmona et al., 1999). La Cristalina Formation is a sequence of sandstones and mudstones with graptolites of Middle Ordovician age (Gutiérrez–Marco et al., 2006). At La Victoria (Figure 1), on the eastern flank of the Central Cordillera, a metamorphic complex cited as Tierradentro Gneisses and Amphibolites with 1360 ± 270 Ma K/Ar age is exposed (Barrero & Vesga, 1976; Marquínez & Núñez, 1998; Vesga & Barrero, 1978). Santa Marta and La Victoria (Caldas) include the only two known reports of anorthosites in Colombia (Figure 24).

At Las Minas area (Figure 1), Restrepo–Pace et al. (1997) quote a $^{40}Ar/^{39}Ar$ hornblende age of 911 ± 2 Ma for amphibolites that underlie the Ordovician El Hígado Formation (Mojica et al., 1987b, 1988). The preceding information suggests that the basement of the Magdalena Valley (Payandé, and Payandé–San Lucas Terranes) is typically Grenvillian with strong affinities with the autochthonous block (serranía de La Macarena, Garzón,

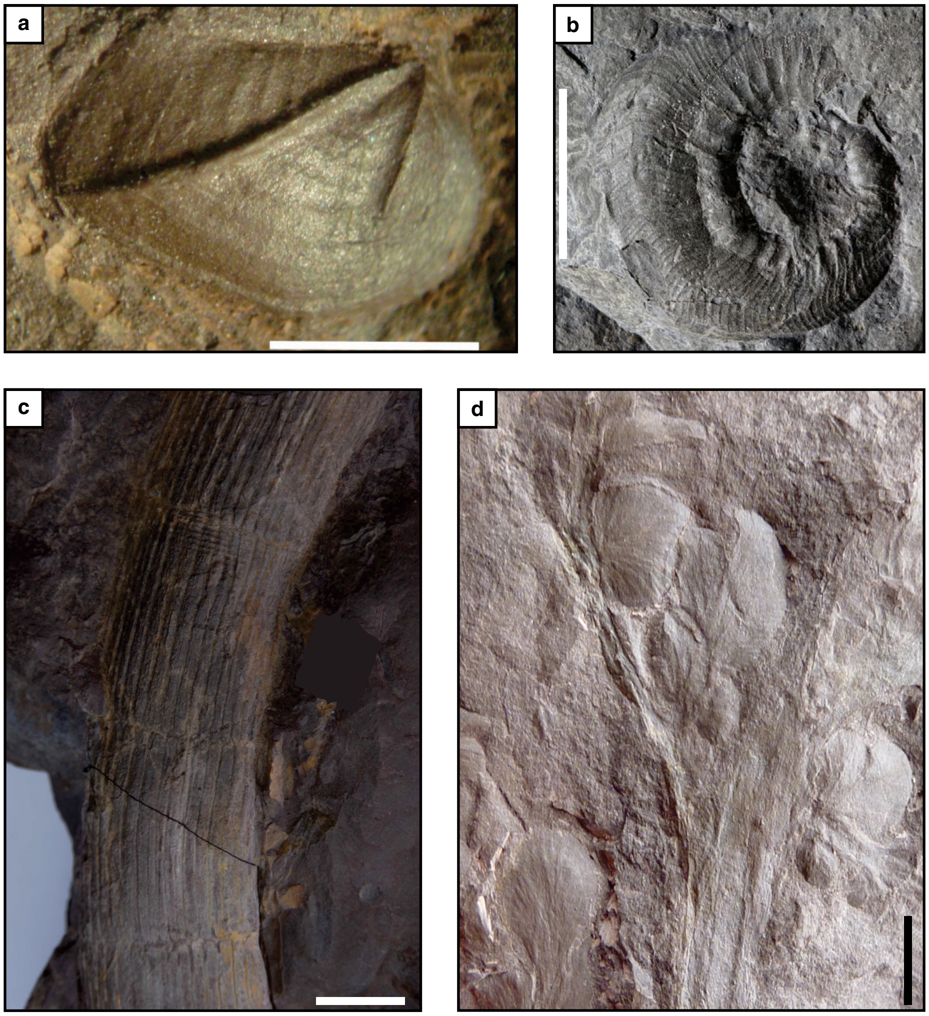

Figure 22. Caguancito Creek fossils: **(a)** *Hemicycloleaia* sp., a leaioid conchostracan; **(b)** *Gastrioceras* sp.; **(c)** *Calamites* sp.; **(d)** *Odontopteris* sp. Scale bar for a is 2 mm.; scale bar for b, c, and d is 1 cm.

Amazonian Terranes, and Llanos Basin basement) and Santa Marta. However, the oldest sedimentary rocks of the Magdalena Valley correspond to the Ordovician sequence that is exposed in La Cristalina, Río Venado, and serranía de las Minas.

At the serranía de las Minas, the fossil assemblage of the El Hígado Formation contains Tremadocian conodonts (probably winnowed) of the biozones of *Paltodus deltifer* and *Paroistodus proteus*. Graptolites and conodonts of *Lenodus variabilis* and *Eoplacognathus suecicus* biozones suggest that sedimentation reaches the lower Darriwilian (Borrero et al., 2007; Gutiérrez–Marco et al., 2007). At the Venado and Ambicá Rivers (Figure 1), a turbiditic sequence correlated with Zanza Formation (La Macarena) contains a Floian assemblage composed of *Acrograptus filiformis*, *Baltograptus kurcki*, *Phyllograptus* cf. *ilicifolius*, and *Expansograptus* cf. *extensus* (Buchely et al., 2015a; Moreno–Sánchez et al., 2008b, 2014).

Similarly, Ordovician sedimentary rocks are widespread in most of the subsoil of the Llanos Basin, although Ediacaran and Cambrian sequences are known in the north of the basin (Arauca Graben). Towards the Amazon region, in the Araracuara area, Ordovician sandstones (Théry et al., 1984) emerge, forming table–top mountains (tepuis).

The sedimentary cycle of the Llanos Basin begins with the Ediacaran marine deposits reported in the Chigüiro–1 and Strat–11a oil wells. At the Chigüiro–1 oil well (to the north of the Llanos Basin), an Ediacaran microfossil assemblage occurs, composed of *Chuaria circularis*, *Synsphaeridium conglutinatum*, *Stichtosphaeridium* spp., *Kildinella* sp., *Pterospermopsimorpha* sp., *Synsphaeridium* sp., and *Trematosphaeridium* sp. (Dueñas, 2001).

The early to middle Cambrian fossil assemblage at Chigüiro–1 oil well contains microfossils, including *Acanthodiacrodium constrictum*, Acritarch *Acrum* cf. *cylindricum*, *Archaediscina* cf. *umbonulata, Baltisphaeridinium pellicidum*, *Comasphaeridium stigosum*, *Dasydiacrodium bicuspidata, Granomarginata squamacea*, *Dictyotidium birvetense*, *Leio-*

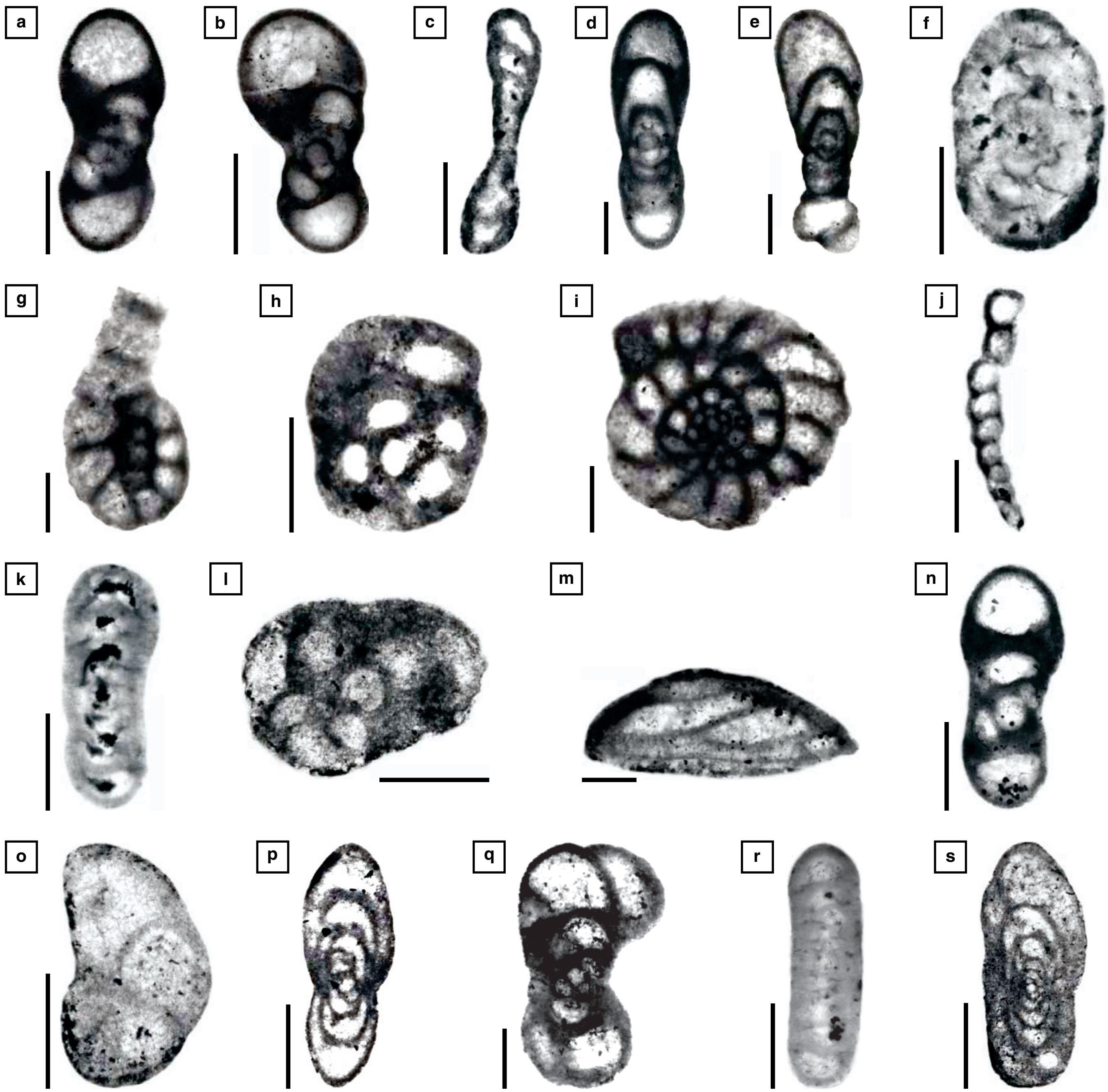

Figure 23. Pennsilvanian foraminifers from Caguancito: **(a, b, n)** *Planoendothyra* sp.; **(c)** *Cornuspira* sp.; **(d, e)** *Millerella marblensis*. Thompson (1942); **(f)** *Asteroarchaediscus* ex gr. *Rugosus* Rauzer–Chernousova (1948); **(g)** *Endothyranella* sp.; **(h, l)** undeterminate calcivertelid; **(i)** *Millerella* sp.; **(j)** *Calcivertella* sp.; **(k)** *Asteroarchaediscus?* sp.; **(m)** *Tetrataxis* sp.; **(o)** *Globivalvulina* sp.; **(p)** *Millerella* sp. 1; **(q)** *Planoendothyra aljutovica* Reitlinger (1950); **(r)** *Tubispirodiscus?* sp.; **(s)** *Millerella* sp. 2. Bashkirian (Morrowan) age. Scale bar represents 50 µm for c and f, scale bar for s is 200 µm and 100 µm for the others.

sphaeridia sp., *Micrhystridium lubomlense*, *Micrhystridium notatum*, *Micrhystridium multipliciflagellata*, *Protosphaeridinium* cf. *densum, Tasmanites* cf. *bobrowskii, Synsphaeridinium conglutinatum,* and *Tectitheca additionalis* (Dueñas, 2001). Upper Cambrian samples yielded palynological assemblages composed of *Timofeevia brevibifurcata* and *Timofeevia lancarae,* and including *Acanthodiacrodium costata*, *A. latizonale*, *Archaeotrichion* sp., *Cristallinium ovillense*, *Leiofusa* sp., *Leiosphaeridia* sp., *Lophodiacrodium* sp., *Pterospermopsimorpha* sp., *Protosphaeridium* sp., *Retisphaeridium dichamerum*, *Synsphaeridium conglutinatum*, and *Trachysphaeridium laminarum* (Dueñas, 2001). The Negritos Formation, distributed through the subsurface of the Llanos Basin (e.g., Negritos–1 and Heliera–1 wells), consists of calcareous sandstones with intercalations of fossiliferous dark and gray shales of Early to Middle Ordovician age. The Heliera Member contains

Figure 24. Anorthosites (An) in the Tierradentro Gneisses and Amphibolites Metamorphic Complex near La Victoria (Payandé Terrane).

Janograptus sp. and Didymograptus sp., Triarthus sp. and Acrotreta sp., these fossils are restricted to an Early Ordovician age (Ulloa et al., 1982).

At the serranía de La Macarena, Ordovician platform deposits cover unconformably Precambrian metamorphic rocks (syenites and amphibolites). In silty shales sequence, in the central and northern of serranía de La Macarena, an Early Ordovician fossils assemblage is reported, including Dichograptus octobrachiatus (Hall), *Didymograptus* sp., *Tetragraptus* sp., aff. *T. bigsbyi* (Hall), *"Obulus"* sp. cf. *Elkania ambigua* (Walcott), *"Lingula"* sp. cf. *Obolus elongatus* (Harrington), *Caryocaris* sp. (Trumpy,1943). Near the locality mentioned above, an association of Tremadocian brachiopods is reported. This includes *Acrotreta aequatorialis n.* sp., *Lingulella* cf. *desiderata*, *Nanorthis?* sp., and the trilobites *Geragnostus tilcuyensis*, *Kainella colombiana*, *Parabolinopsis* sp., and cf. *Pseudokainella* sp. (Harrington & Kay 1951). The fossil assemblage, contained in quartz silty sequence of upper Tremadocian age, includes, *Apheoorthis?* sp., *Basiliella trumpyi n.* sp., *Megalaspis* sp. cf. *M. planilimbata Angelin, Raphiophorus? pyrus* n. sp., *Tropidopyge stenorhachis* n. gen., n. sp., Cytid plate, Bellerophontid gastropod. This fossil assemblage were reported by Trumpy, (1943) and Harrington & Kay (1951). At the north of the La Macarena, at the Zanza Creek (3° 16' 24.14'' N, 73° 55' 16.48'' W) and La Recebera locality (3° 20' 28.98'' N, 73° 56' 28.89'' W), a turbiditic sequence with the Floian graptolite Baltograptus cf. turgidus is exposed (Buchely et al., 2015a; Gutiérrez–Marco et al., 2006).

Therefore, the remnants of the Ordovician sedimentary sequence of the Magdalena Valley are stratigraphically correlated with the remnants of the Ordovician sedimentary sequence of the serranía de La Macarena. The sedimentary rocks of the Ordovician age of the Magdalena Valley (El Hígado Formation, Río Venado, Ambicá, and La Cristalina), Llanos Basin, and La Macarena were deposited on a continental platform in a shallow marine environment without volcanic influence.

Mid–Cambrian trilobites were recovered from a locality near the Uribe, on the Duda Formation (Bridger, 1981). The material, studied by Rushton (1963), contained *Paradoxides* sp., *Peronopsis* sp., *Ehmania akanthophora*, a genus of common occurrence in the Avalonian Terranes. Duda Formation, at the Cristalina Creek (Cubarral), is a sedimentary succession composed of diamictites, feldspathic conglomerates, and sandstones originated by submarine mass flows due to tectonic activity (Buchely et al., 2015a). Underlying the Duda Formation, the Ariari and Guape Formations (Ediacaran? – Cambrian) are exposed. Guape is a sedimentary formation composed of sandstones, black shales, thin limestones beds, and volcanic deposits (Bridger, 1982; Buchely et al., 2015b; Toro et al., 2014).

10. Discussion

The metamorphic basement of the Magdalena Valley (Western Chibcha Terrane or Payandé and Payandé–San Lucas Blocks) was affected by the Grenvillian event in the same way that the Garzón Massif and the Sierra Nevada de Santa Marta (Álvarez, 1981; Kroonenberg, 1982; Ordóñez–Carmona et al., 1999; Priem et al., 1989; Ramos, 2010; Restrepo–Pace et al., 1997) were affected. A nonconformity surface separates the Grenvillian rocks from the Ordovician siliciclastic marine deposits. Shallow marine deposits at La Cristalina, El Hígado (Las Minas), Río Venado, and Ambicá contain Early to Middle Ordovician graptolites. Ordovician sequences of Magdalena Valley can be understood as an extension of platform deposits of serranía de La Macarena and Llanos. The Ordovician magmatic event (Famatinian–Caparonensis), common to Quetame–Mérida Terrane, is not recorded at Garzón Massif, serranía de La Macarena, Magdalena Valley (Western Chibcha Terrane or Payandé San Lucas and Payandé–San Lucas Blocks), and the Santa Marta area.

Traditionally, it has been accepted that the Chibcha Terrane was a single geologic block with an active margin to the east, with Cambrian to Silurian arc volcanism and metamorphism (Ramos, 2010; Restrepo & Toussaint, 1988). Thus, Payandé and Payandé–San Lucas (Western Chibcha) can be explained as the trailing age of the Quetame–Mérida Crustal Block (Eastern Chibcha). Although this model seems to be a simpler explanation, it does not explain the greater complexity that the eastern block (Eastern Chibcha) presents and that can be summarized as follows:

- The Chibcha Terrane has a Grenville basement. However, the Quetame–Mérida Crustal Block has a Tonian sedimentary cycle (Silgará Formation) not registered in the Payandé Block (Western Chibcha).

- The Eastern Chibcha has a Cambrian sedimentary sequence with volcanic rocks (Chicamocha Formation and Quetame Group). This cycle is absent in the western block.
- The Silurian age sedimentary cycle is only registered in the Eastern Chibcha Terrane.
- Ordovician rocks are without signs of volcanism in the western block. The Ordovician conglomerates of the Venado Formation are composed of clasts of gneisses and granulites. No volcanic debris are reported.

On the eastern slope of the Central Cordillera, Tierradentro Gneisses and Amphibolites unity (Marquínez & Núñez, 1998), truly a geologic complex with a complex thermal history, have a wide range of lithologies including ortho– and paragneisses, amphibolites, minor granulites, metagabbros, anorthosites, migmatites, and mylonitic rocks. The Tierradentro Complex is located to the east of the Otú–Pericos Fault. Therefore, the Tierradentro Complex is incorporated as the Precambrian basement of the western part of the Chibcha Terrane (Payandé and Payandé–San Lucas Terranes). Bustamante et al. (2017) propose, based on U–Pb data of zircons (271 and 234 Ma), that the high–grade metamorphic rocks in this complex were formed during a Permian to Triassic event. However, the Bustamante et al. (2017) interpretation ignores the regional geologic data and field observations. Additional issues could be the result of bias in the sample collection or thermal episodes (including metasomatism), taking as orogenic metamorphic events or loss of radiogenic lead related to uplifting and eroding of the crystalline basement. The conclusions of Bustamante et al. (2017) are in conflict with the following facts:

- Occurrence, on the eastern slope of the Central Cordillera, of Ordovician sedimentary sequences such as La Cristalina and El Hígado Formations (Las Minas).
- Occurrence, near Ibagué city, of Devonian (Imán and Amoyá) and Triassic (Luisa and Payandé Formations) sedimentary sequences. Luisa Formation (Geyer, 1973), underlying Payandé Formation, is a continental sequence composed of red sandstones and matrix–supported conglomerates with clasts of granites.
- The occurrence of crinoidal Carboniferous metalimestones and marbles cropping out to the west of Ibagué city (Gómez & Bocanegra, 1999; Moreno–Sánchez et al., 2008a) in the area of Bustamante et al. (2017) sampling.
- Record of Triassic metasomatism on marbles and metalimestones (Aleluya Complex) on the eastern slope of Central Cordillera is dated as a Triassic intrusive event (Hernández–González & Urueña–Suárez, 2017).

However, the Quetame, Santander, Perijá, and the Mérida Cordillera have experienced complex metamorphic histories. On the Santander Massif, the oldest metamorphic rocks are of Tonian age, although it has been proposed that these are the result of rejuvenation of Grenvillian–age rocks (Ordóñez–Carmona et al., 2006). The low–grade metamorphic rocks, such as the Perijá Series, the Chicamocha and the Quetame Schists, originated in a terrane not too far from Gondwana, since they have detrital zircons derived from sources on the South American Craton (van der Lelij, 2013). Cambrian sedimentary rocks were later metamorphosed and thermally affected by Ordovician intrusives (Famatinian–Caparonensis or Taconian event).

The Ediacaran – Cambrian oceanic gabbros (Ariari Metagabbro) and basalts (Guape Formation) covering by submarine mass flow deposits (diamictites) of Duda Formation suggest an extended continental margin. The recognition of Ediacaran – Cambrian remnants of oceanic gabbros and basalts between the Eastern Cordillera (at the La Cristalina, Cubarral locality) and Llanos Basin let us infer that, during the Ediacaran – Cambrian, the early Palaeozoic proto–Andean margin of South America (Iapetus coast?) was near this modern tectonic limit (Bridger, 1982; Buchely et al., 2015b; Toro et al., 2014). Syenites of the Ediacaran age (Arango et al., 2012; Buchely et al., 2015a) intruding basement rocks at the serranía de La Macarena and western Llanos Basin record the extension of the proto–Andean margin during the aperture of the Iapetus Ocean.

During Cambrian to Ordovician times, the proto–Andean margin in northern South America was a subsiding passive platform in front of an ocean basin and not too far from a volcanic arc formed in a peri–Gondwana microcontinent (Quetame–Mérida Terrane). The Quetame–Mérida volcanic arc could have been the prolongation towards the north of the volcanic chain developed to the west of South America during the Ordovician (e.g., Benedetto et al., 2009). The basement of Eastern Cordillera and Mérida Andes, a continental fragment, was accreted to the pericratonic platform of Gondwana during the Late Ordovician or early Silurian times. The microcontinent and its volcanic arc (e.g., Forero, 1990) collided against the proto–Andean margin, leaving a remnant of transitional oceanic crust in the region of the Cristalina (Cubarral). During the closure of the basin (fore–arc to continental platform), oceanic crust sank into the mantle along a subduction zone with a westward–dipping orientation (Figure 25).

The modern position of Payandé, Payandé–San Lucas, Santa Marta, and portions of the La Guajira Peninsula can be interpreted as a geologic artifact result of strike–slip displacements (e.g., Bayona et al., 2010; Scott, 1978) produced by the oblique subduction during late Paleozoic or Mesozoic times. These lithospheric clasts are interpreted as Grenvillian fragments detached from the pericratonic margin of Gondwana and dragged to the north and then superimposed on the front of the Quetame–Mérida Terrain.

We proposed, as has been suggested in other works (Aleman & Ramos, 2000; Bellizzia & Pimentel, 1994; Forero, 1990; Restrepo et al., 2009; Restrepo & Toussaint, 1988), that a large part of the Eastern Chibcha Terrane were part of an allochthonous continental fragment that was accreted on the pericratonic South American margin during the Paleozoic period. However,

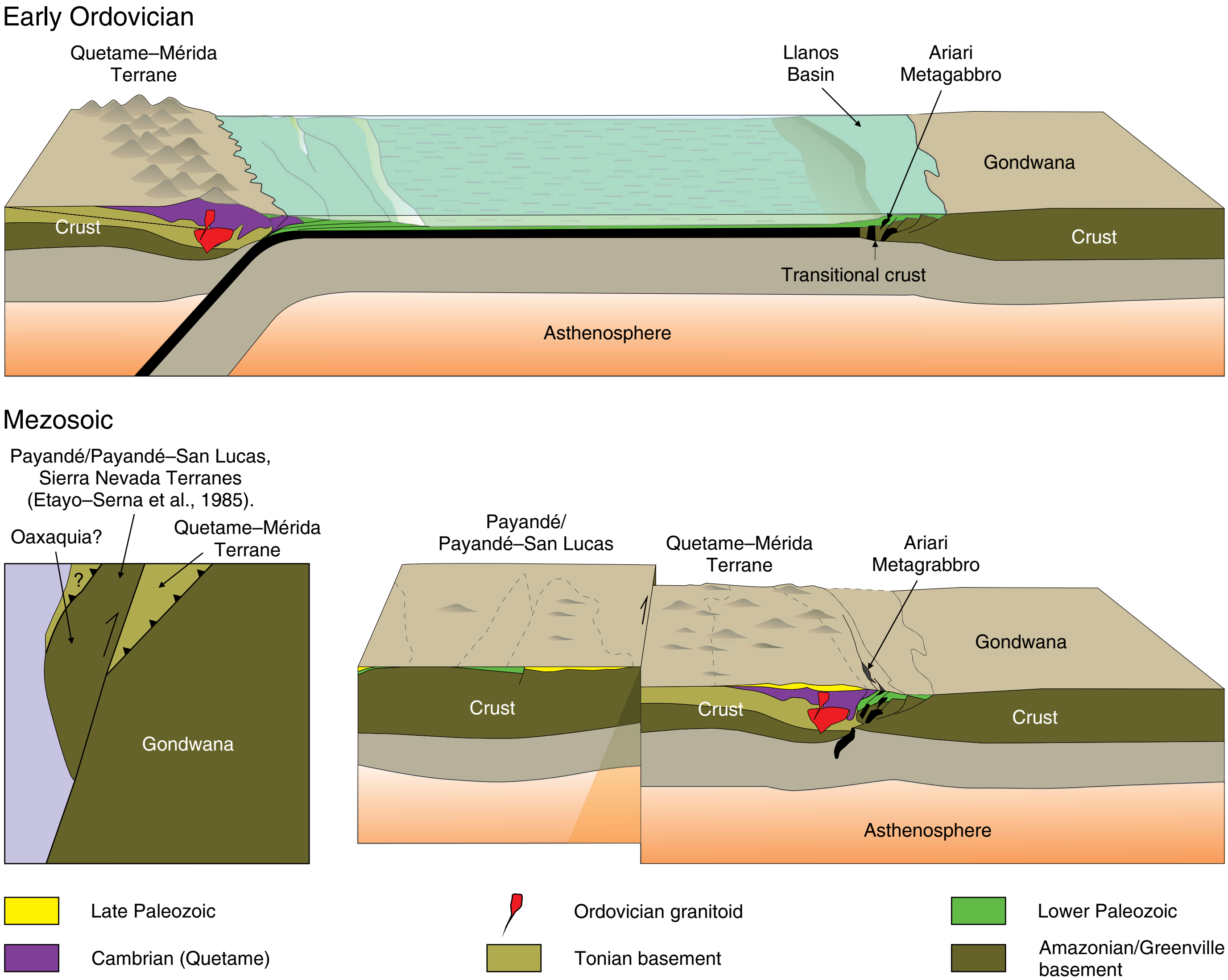

Figure 25. Geological evolution of the terranes east of the Otú–Pericos fault. Western Chibcha Terrane (Payandé) can be explained as being the trailing age of Eastern Chibcha Terrane (Quetame crustal block). However, based on the stratigraphic differences, we propose that this area is made up of at least two tectonic blocks with dissimilar geologic histories.

we suggest that Payandé and Payandé–San Lucas Blocks (Western Chibcha Terrane) should be included in the autochthonous basement and not as part of the Chibcha Terrane (sensu Restrepo & Toussaint, 1988).

The Trilobites (*Paradoxides* sp., *Peronopsis* sp., *Ehmania akanthophora*) of the Duda Formation (see Rushton, 1963) suggest the presence of tectonic blocks located in front of the prism of the Quetame–Caparo arc that may have had a platform connection with the Avalonia continent during the Cambrian. Metamorphism of the Quetame Group, Chicamocha Schists, and Perijá Series is constrained between the igneous activity (Caparo–Famatinian or Taconic event) and the erosive phase of the Late Ordovician and early Silurian during the closure of the marine basin located between the Quetame–Caparo Terrane and the pericratonic margin of Gondwana (Figure 25). Bordonaro (1992) attributes the fossils of cited by Rushton (1963) to the serranía de La Macarena and the Llanos Basin. However, the *Paradoxides* locality is actually found in the Eastern Cordillera at the Duda Formation (Figure 1). The Duda Formation is a very thick accumulation (more than a thousand meters) of diamictites, sandstones, and mudstones, with evidence of tectonic stacking, which may include sediments from both the continental margin of South America and the Quetame Block (Chibcha Terrane).

During Precambrian and Ordovician times, the geologic history of South America remains closely similar to the Oaxaquia Terrane in Mexico (Restrepo–Pace et al., 1997; Ruiz et al., 1999; Sedlock et al., 1993). The geological evidence indicates that some tectonic blocks, now belonging to Mexico and Central America (Maya and Chortis), during Precambrian and early Paleozoic times were part of the proto–Andean margin of South America.

The Silurian sequence of the north of South America was deposited after the collision of the Quetame–Mérida Block. Additionally, the Silurian fossil assemblages between those areas show connection during that time interval. The braquiopod assemblage of El Horno Formation (Venezuela) is similar to the braquiopod assemblage of the Ciudad Victoria (Mexico) and Rhenish–European Province (Boucot et al., 1972, 1997; Stewart et al., 1999).

Late Silurian to Pragian rocks are not known in the Eastern Cordillera. The Angosturas Formation (Buchely et al., 2015a) corresponds to a remnant of Lower Devonian shales and sandstones that crops out to the south of the serranía de La Macarena but without any relation to the Eastern Cordillera deposits. In Perijá, Santander, and Quetame Massifs, the marine to continental sequences range from Emsian to Famennian (Tournaisian at El Iman). Lochkovian – Pragian deposits are absent. The Devonian record, as observed in the Floresta Massif, begins with a transgressive cycle with a maximum marine invasion towards the upper part of the Floresta Formation. The regressive phase culminates with the deltaic deposition of the Cuche Formation.

Santa Marta Fault has an accumulated horizontal offset of 120 km (Dewey & Pindell, 1985), but when restored to the pre–Miocene position, Floresta Massif rests to the west of the Labateca area. Middle Devonian sandstones at Labateca suggest the proximity of the basin margin. Frasnian – Famennian continental deposits of the Cuche Formation are coeval with the marine deposits of the El Iman Formation (Payandé Terrane), suggesting that the source area of the sedimentites had to be located to the east, towards the South American Craton.

Despite the presence of magmatic zircons (Cardona et al., 2016; Horton et al., 2010), there are no proofs of volcanic deposits attributable to proximal volcanism in the Devonian El Tíbet, Floresta, and Cuche Formations. The detrital zircons detected in the sedimentites could come from reworked deposits outside of the basin or from ash rains coming from a distant volcanic source. Lithic sandstones (Cardona et al., 2016) and detrital muscovite on the Devonian formations point to an erosion of the metamorphic basement.

The biogeographical data point to a proximity or a connection between South America (west Gondwana) and Laurussia during Devonian times. The late Lochkovian terrestrial paleoflora assemblage from Brazil and Argentina (SW Gondwana) shows close similarities to the Laurussia Province (Edwards et al., 2009). Additionally, in northern South America, the number of species in common with Europe is sizable for the Middle and Upper Devonian interval (Berry, 1997; Berry & Fairon–Demaret, 2001; Meyer–Berthaud et al., 2003). Early and Middle Devonian brachiopod associations of northern South America show common elements with southern North America and are included in the Eastern Americas Realm (Barrett, 1985) or Appalachian Province (Boucot, 1985). However, Devonian fossil fish from the Perijá and Floresta deposits indicate a connection with Laurussia but still present elements in common with Gondwana (Burrow et al., 2003; Janvier & Villarroel, 2000; Young & Moody, 2002a).

The climate during the Devonian, at least for the north of South America, was characterized by being relatively warm (greenhouse climate) with increasing temperatures during the Famennian (Joachimski et al., 2002). According to most of the paleogeographic reconstructions of Gondwana (Barrett, 1985; Barret & Isaacson, 1988; Heckel & Witzke, 1979; Scotese et al., 1979), Colombia and Venezuela would be close to 40° S latitude and would have a wet temperate climate (Barrett, 1985). For Laurussia, we prefer a paleogeographic position close to the north of Gondwana such as the Barrett (1985) reconstruction, which is more in line with the biogeographical data (Figure 26).

A hiatus, that covers much of the Mississippian time, separates the Devonian and Carboniferous sequences. San Antonio, Caguancito Creek, Cerro Neiva, and "Calizas y Arenitas de La Batalla" are the southern remnants of a late Carboniferous shallow marine basin that extended from the northern margin of Colombia and Venezuela to Ecuador (Macuma Formation). The Carboniferous and Permian systems in northern South America, unlike the Devonian, are characterized by the presence of large beds of limestones and occasional evaporitic bodies. Carboniferous magmatism of Venezuela and Central America (Maya Block) suggests the closure of a remnant ocean basin between North and South America.

The Bocas Formation age is an Early Jurassic sequence since *Piazopteris branneri* (*Phlebopteris branneri*), a matoniaceae fern, and *Classopollis* sp. occur in this formation (Remy et al., 1975). Ambiguous ages (Carboniferous to Permian) obtained in the Bocas Formation are apparently the result of ill–defined mapping contacts between Paleozoic and Mesozoic deposits.

In comparison to the Devonian climate, the Carboniferous was dominantly cool (icehouse) with alternating warming and cooling stages. During the Moscovian – Kasimovian, the climatic tendency was towards the decreasing temperatures, but during the Kasimovian – Gzhelian, the trend is to cooler temperatures (Bruckschen et al., 1999). The upper Paleozoic of northern South America was characterized by sedimentation in a coastal domain with alternating marine and continental influences. According to the reconstruction of Raymond et al. (1985) and despite the global cooling of the climate, the north of South America enjoyed a warmer climate due to the displacement towards latitudes close to 15–20°S. Braun (1979) suggests that the largest fluctuations are related to epeirogenic movements and the minor phases were produced by climatic influence. The geological section of Caguancito could be considered the typical example of the Pennsylvanian cyclothemes. At the interglacial stages, the dominant deposits were marine carbonates with oolitic layers. During the cold stages, deltaic deposits occurred associated with red beds and plant macrofossils.

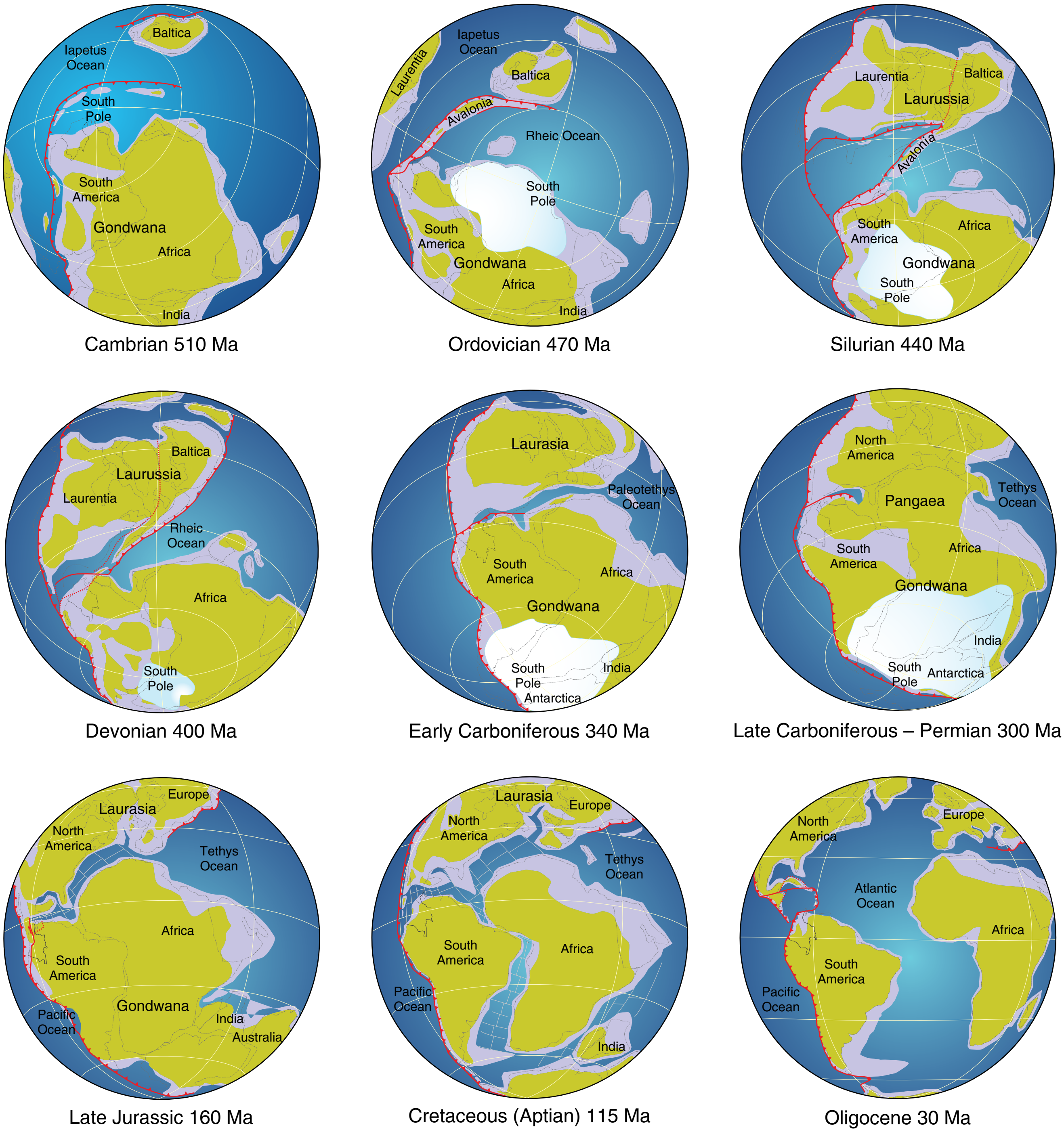

Figure 26. Paleogeographic reconstructions of Gondwana (modified of Barret & Isaacson, 1988; Barrett, 1985; Heckel & Witzke, 1979; Scotese et al., 1979).

The Tahamí Terrane (Cajamarca) is separated from the Payandé Terrane (Western Chibcha Terrane) by the Otú–Pericos dextral Fault. The activity of this tectonic structure is presumed to be Late Jurassic or Early Cretaceous because the fault affects Jurassic intrusives (Gómez & Bocanegra, 1999). Therefore, the Tahamí Terrane should be located farther south of their present position. For the Tahamí Terrane and western Payandé Terrane, Cochrane et al. (2014) suggest a first compressive event during middle Permian to Early Triassic (275–240 Ma) related to the amalgamation of western Pangea. This event can be associated with the phase of uplift and erosion that creates the erosive hiatus, from Lopingian (late Permian) to Middle Triassic, recorded in the Santander Massif.

The Permian record of northern Colombia and Venezuela, limited to the Cisuralian to Guadalupian, is made up of thick basal conglomerate layers covered by platform limestones, shales, evaporites, and sandstones. The sandstones, which are interpreted as sea level fall deposits, contain a fossil macroflora similar to the Road Canyon Formation of Texas (Ricardi–Branco et al., 2005). Eustatic changes of climatic origin begin to lose influence at the end of the Permian due to the rapid retreat of the glaciers in Gondwana (Crowell, 1995). The Lopingian (late Permian) to Middle Triassic hiatus is interpreted as the result of uplift and erosion associated with regional compression during the formation of Pangea. Additionally, Cochrane et al. (2014) deduce a rifting event during Middle to Late Triassic (240 to 225 Ma), an event that coincides with the start of sedimentation of the Luisa and Payandé Formations (Middle? to Late Triassic of Payandé and Payandé San Lucas Terranes).

There are no known fossiliferous Permian deposits in the Magdalena Valley. The Luisa Formation, underlying the Payandé Formation of the Late Triassic, is a continental succession constituted of sandstones, reddish shales, and matrix–supported conglomerates with clasts of granites. This formation, apparent unfossiliferous, correlated with the El Sudán Formation on the Payandé–San Lucas Block that is attributed to the Permian – Triassic lapse by Geyer (1982).

11. Conclusions

The lower Paleozoic sedimentary sequences of the Llanos Basin and the La Macarena and Magdalena Valleys (Payandé and Payandé–San Lucas Terranes) were deposited on the pericratonic margin of South America. During the early Paleozoic, the Quetame–Mérida Terrane (eastern part of the Chibcha Terrane) developed a more complex tectonic and thermal history than the Payandé and Payandé–San Lucas Terranes (Figure 27).

The record at the Cubarral region of the Ediacaran sienites and Ediacaran – Cambrian gabbros (MORB), suggests the opening of an ocean basin during the formation of the southern Iapetus Ocean on the current boundary between the Eastern Cordillera and the Llanos Basin controlled by the detachment of Avalonia.

The Sierra Nevada, Payandé, and Payandé–San Lucas Terranes (Etayo–Serna et al., 1983) are interpreted as Grenvillian lithospheric clasts detached from the pericratonic margin of Gondwana (autochthonous basement) and dragged to the north along strike–slip faults and then superimposed on the front of the Quetame–Mérida Terrane.

U–Pb zircon ages of Tierradentro Gneisses and Amphibolites, Aleluya Complex, and Payandé Granitoids (Cochrane et al., 2014; Hernández–González & Urueña–Suárez, 2017) suggest Permian – Triassic thermal events spanning the west of the Payandé Terrane. A Permian to Triassic age for the Tierradentro Gneisses and Amphibolites, as interpreted by Bustamante et al. (2017), should be revised because it is not supported by field observations and local stratigraphy.

According to geochronological and paleontological data, the metamorphic rocks of the Quetame Group and the Chicamocha Schists (Santander Massif) would be of Cambrian age. The Quetame–Mérida Terrane (Eastern Chibcha) was an allochthonous microcontinent based on high–grade metamorphic rocks of Tonian age. The microcontinent and its volcanic arc along with a west–dipping subduction zone collide against the eastern pericratonic margin of South America at the end of the Ordovician times. An episode of magmatism and regional metamorphism (Quetame–Caparonensis, Famatinian or Taconic event) culminates during the continental collision and then is followed by a phase of erosion interrupted by a marine invasion during the middle Silurian. Similarities of Silurian fossil assemblages from Venezuela (El Horno) prove the geographical connection with eastern Mexico (Ciudad Victoria). During Pridoli to early Emsian, the area to the west of the Guicáramo Fault (suture zone of Quetame–Caparo Terrane) was affected by exhumation and erosion. However, there are marine incursions towards the south of the Llanos Basin (Angosturas Formation).

The Devonian deposition begins at the Emsian during a transgressive phase that reaches its maximum during the Frasnian. During the Frasnian – Famennian interval, a delta was formed, progradating to the west. Limestones are rare in the Devonian record of northern South America. The Devonian flora and fauna of Colombia and Venezuela maintained close ties with the Old–World Realm (Laurussia).

At the beginning of the Pennsylvanian in the Andean region of northern South America, there was an erosive phase. The initial flooding of the region produced the sandstones and mudstones at the base of the Pennsylvanian sequence. The sedimentation is followed by a succession of fossiliferous limestones and shales. During the Carboniferous, northern South America moved towards the equator, thus, the climate was warmer than during the Devonian. The sedimentation was influenced by the rise and fall of the sea level linked to the advances and retreats of glaciers in the polar areas. Despite the intermittence, Devonian and Carboniferous records in the northern Andes apparently extended from the Otú–Pericos Fault to the western limit of the Llanos Basin.

Evidence for a Late Pennsylvanian tectonic event is preserved in the core of the Santander Massif and Mérida Andes. This evidence consists of weakly metamorphosed sedimentary rocks covered unconformably by thick layers of early Permian conglomerates. In the north of South America, the Permian record is limited to areas in the Santander Massif, serranía de Perijá and the Mérida Andes. The Permian record consists mainly of limestones accumulated on a shallow marine platform and in warm weather conditions. The Pennsylvanian deposition cycle is interrupted at the Kasimovian and resumed at the beginning of the Sakmarian (early Permian).

The geochronology based on zircons is a set of high precision methods used for dating rocks inaccessible by other tech-

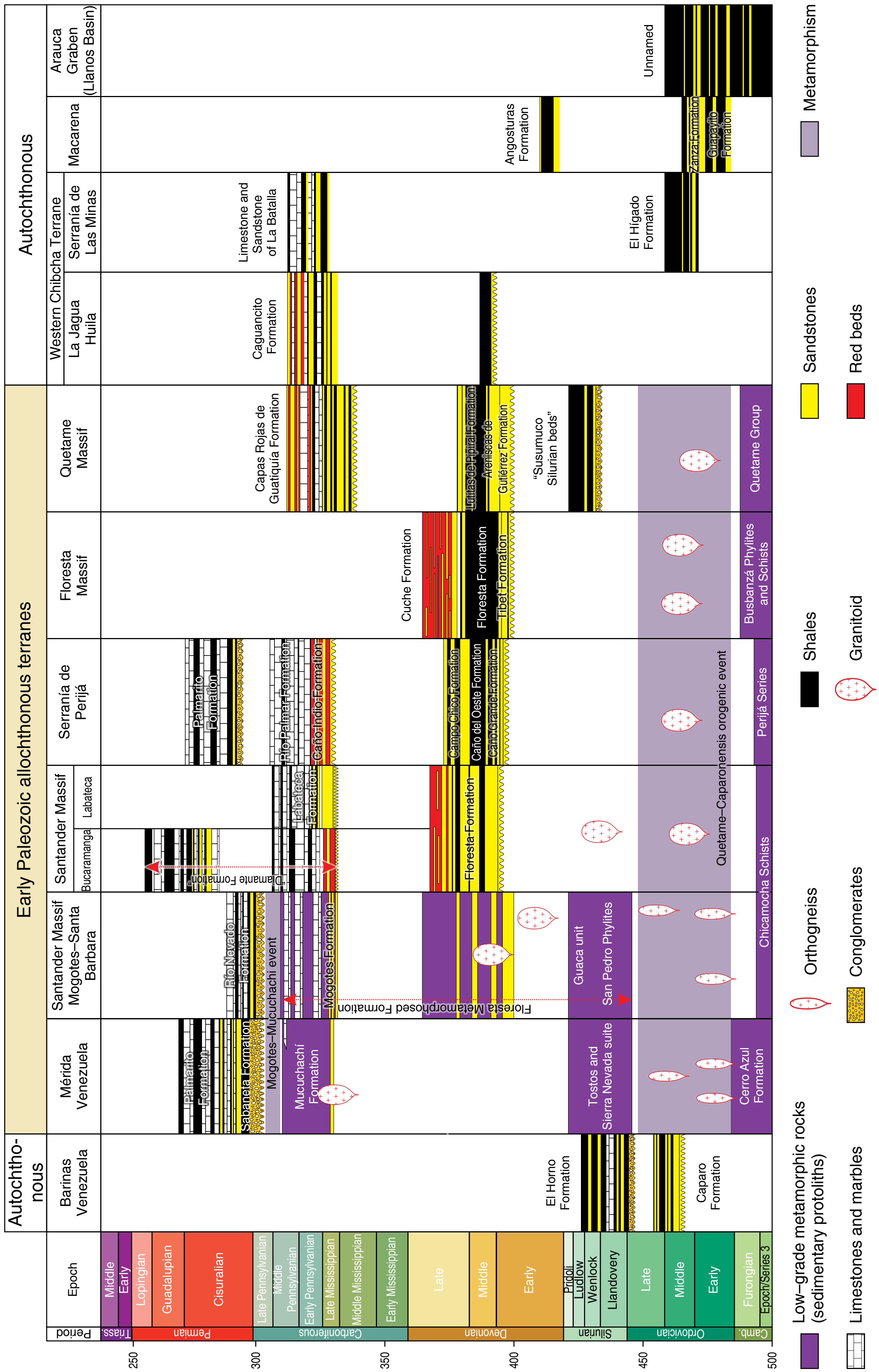

Figure 27. The chronostratigraphic chart that summarizes the main events east of the Otú–Pericos Fault.

Cambrian Ordovician Silurian Devonian Carboniferous Permian niques. Zircon methods have become an essential tool in Earth science. However, the interpretation of long thermal structure and tectonothermal histories for igneous–metamorphic complexes should be contrasted using stratigraphic and paleontological data.

Acknowledgments

Two institutions have contributed to the discussion and presentation of this work, the Universidad de Caldas and the Servicio Geológico Colombiano through the Dirección de Geociencias Básicas; thanks to them. We also want to acknowledge Victor A. RAMOS and Stanley C. FINNEY for reviews that greatly improved the manuscript.

References

Aleman, A. & Ramos, V.A. 2000. Northern Andes. In: Cordani, U.G., Milani, E.J., Thomaz–Filho, A. & Campos, D.A. (editors), Tectonic evolution of South America. 31st International Geological Congress. Proceedings, p. 453–480. Rio de Janeiro, Brazil.

Álvarez, J. 1981. Determinación de la edad Rb/Sr en rocas del Macizo de Garzón, cordillera Oriental de Colombia. Geología Norandina, (4): 31–38.

Anderson, H.M., Hiller, N. & Gess, R.W. 1995. *Archaeopteris* (Progymnospermopsida) from the Devonian of southern Africa. Botanical Journal of the Linnean Society, 117(4): 305–320. https://doi.org/10.1006/bojl.1995.0021

Arango, M.I., Zapata, G. & Martens, U. 2012. Caracterización petrográfica, geoquímica y edad de la Sienita Nefelínica de San José del Guaviare. Boletín de Geología, 34(1): 15–26.

Arnold, H.C. 1966. Upper Paleozoic Sabaneta–Palmarito sequence of Mérida Andes, Venezuela. American Association of Petroleum Geologists Bulletin, 50(11): 2366–2387. https://doi.org/10.1306/5D25B769-16C1-11D7-8645000102C1865D

Barrero, D. & Vesga, C.J. 1976. Mapa geológico del cuadrángulo K–9 Armero y mitad sur del J–9 La Dorada. Scale 1:100 000. Ingeominas. Bogotá.

Barrett, S.F. 1985. Early Devonian continental positions and climate: A framework for paleophytogeography. In: Tiffney, B. (editor), Geological Factors and the Evolution of Plants. Yale University Press, p. 93–127. New Haven, USA.

Barrett, S.F. 1988. The Devonian system in Colombia. In: McMillan, N.J., Embry, A.F. & Glass, D.J. (editors), Devonian of the world. Proceedings of the Second International Symposium on the Devonian System. Canadian Society of Petroleum Geologists, Memoir 14, p. 705–717. Calgary, Canada.

Barrett, S.F. & Isaacson, P.E. 1988. Devonian paleogeography of South America. In: McMillan, N.J., Embry, A.F. & Glass, D.J. (editors), Devonian of the world. Proceedings of the Second International Symposium on the Devonian System. Canadian Society of Petroleum Geologists, Memoir 14, p. 655–667. Calgary, Canada.

Bateson, J.H. 1972. New interpretation of geology of Maya Mountains, British Honduras. American Association of Petroleum Geologists Bulletin, 56(5): 956–963. https://doi.org/10.1306/819A40A0-16C5-11D7-8645000102C1865D

Bayona, G., Jiménez, G., Silva, C., Cardona, A., Montes, C., Roncancio, J. & Cordani, U. 2010. Paleomagnetic data and K–Ar ages from Mesozoic units of the Santa Marta Massif: A preliminary interpretation for block rotation and translations. Journal of South American Earth Sciences, 29(4): 817–831. https://doi.org/10.1016/j.jsames.2009.10.005

Bellizzia, A. & Pimentel, N. 1994. Terreno Mérida: Un cinturón alóctono herciniano en la cordillera de los Andes de Venezuela. V Simposio Bolivariano Exploración Petrolera en las Cuencas Subandinas. Proceedings, p. 271–290. Caracas.

Benedetto, G.A. 1978. Evidencias bioestratigráficas para la correlación de las unidades paleozoicas de los flancos venezolano y colombiano de la sierra de Perijá. II Congreso Colombiano de Geología. Memoirs, p. 39. Bogotá.

Benedetto, J.L., Vaccari, N.E., Waisfeld, B.G., Sánchez, T.M. & Foglia, R.D. 2009. Cambrian and Ordovician biogeography of the South American margin of Gondwana and accreted terranes. In: Bassett, M.G. (editor), Early Palaeozoic peri–Gondwana terranes: New insights from tectonics and biogeography. Geological Society of London, Special Publication 325, p. 201–232. https://doi.org/10.1144/SP325.11

Berry, C.M. 1997. Devonian plants from the eastern Andean Terrane (western Venezuela, Colombia): Laurentian or Gondwanan? First International Conference on North Gondwanan mid–Palaeozoic Biodynamics. Proceedings, 10, IGCP Project 421. Vienna, Austria.

Berry, C.M. & Fairon–Demaret, M. 2001. The Middle Devonian flora revisited. In: Gensel, P. & Edwards, D. (editors), Plants invade the land: Evolutionary and environmental perspectives. Columbia University Press, p. 120–139. New York. https://doi.org/10.7312/gens11160-008

Berry, C.M., Morel, E., Mojica, J. & Villarroel, C. 2000. Devonian plants from Colombia, with discussion of their geological and palaeogeographical context. Geological Magazine, 137(3): 257–268. https://doi.org/10.1017/S0016756800003964

Blanco–Quintero, I.F., García–Casco, A., Toro, L.M., Moreno, M., Ruiz, E.C., Vinasco, C.J., Cardona, A., Lázaro, C. & Morata, D. 2014. Late Jurassic terrane collision in the northwestern margin of Gondwana (Cajamarca Complex, eastern flank of the Central Cordillera, Colombia). International Geology Review, 56(15): 1852–1872. https://doi.org/10.1080/00206814.2014.963710

Boinet, T., Bourgois, J., Bellon, H. & Toussaint, J.F. 1985. Age et repartition du magmatism premesozoique des Andes de Colombie. Comptes Rendus Hebdomadaires des séaces de l´Académie des Sciences, Série D: Sciences Naturalles, 300(II): 445–450.

Boinet, T., Babin, C., Bourgois, J., Broutin, J., Lardeux, H., Pons, D. & Racheboeuf, P. 1986. Les grandes étapes de l´évolution paléozoïque du Massif de Santander (Andes de Colombie): Signification de la discordance du Dévonien moyen. Comptes Rendus de l´Académie des Sciences, série II, 303(8): 707–712.

Bordonaro, O.L. 1992. El Cámbrico de Sudamérica. In: Gutiérrez–Marco, J.C., Saavedra, J. & Rábano, I. (editors), Paleozoico inferior de Ibero–América. Universidad de Extremadura, p. 69–84. Mérida, Spain.

Borrero, C., Sarmiento, G.N., Gómez–González, C. & Gutiérrez–Marco, J.C. 2007. Los conodontos de la Formación El Hígado y su contribución al conocimiento del metamorfismo y la paleogeografía del Ordovícico en la cordillera Central colombiana. Boletín de Geología, 29(2): 39–46.

Botero, G. 1950. Reconocimiento geológico del área comprendida por los municipios de Belén, Cerinza, Corrales, Floresta, Nobsa y Santa Rosa de Viterbo, departamento de Boyacá. Compilación de los Estudios Geológicos Oficiales en Colombia, 8: 245–311.

Boucot, A.J. 1985. Late Silurian – early Devonian biogeography, provincialism, evolution and extinction. Philosophical Transactions of the Royal Society of London, 309(1138): 323–339. https://doi.org/10.1098/rstb.1985.0089

Boucot, A.J., Johnson, J.G. & Shagam, R. 1972. Braquiópodos silúricos de los Andes Merideños de Venezuela. IV Congreso Geológico Venezolano. Proceedings, II, p. 585–727. Caracas.

Boucot, A.J., Blodgett, R.B. & Stewart, J.H. 1997. European province Late Silurian brachiopods from the Ciudad Victoria area, Tamaulipas, northeastern Mexico. In: Klapper, G., Murphy, M.A. & Talent, J.A. (editors), Paleozoic sequence stratigraphy, biostratigraphy, and biogeography: Studies in honor of J. Granville ("Jess") Johnson. Geological Society of America, Special Paper 321, p. 273–293. https://doi.org/10.1130/0-8137-2321-3.273

Braun, R. 1979. Le Paléozoïque Supérieur du Quetame (cordillère Orientale, Colombie): Un exemple de sédimentation fluvio–deltaïque sur une bordure de craton. Doctorade thesis, Université de Droit D'Économie et des Sciences D'Aix, 157 p. Marseille.

Bridger, C.S. 1981. The Cambrian in Colombia: A new vision of an old theme. III Congreso Colombiano de Geología. Abstracts, p. 29. Medellín.

Bridger, C.S. 1982. El Paleozoico inferior de Colombia: Una revaluación en base en nuevos datos de campo. Bachelor thesis, Universidad Nacional de Colombia, 280 p. Bogotá.

Bruckschen, P., Oesmann, S. & Veizer, J. 1999. Isotope stratigraphy of the european Carboniferous: Proxy signals for ocean chemistry, climate and tectonics. Chemical Geology, 161(1–3): 127–163. https://doi.org/10.1016/S0009-2541(99)00084-4

Buchely, F., Gómez, L., Buitrago, J., Cristancho, A., Moreno–Sánchez, M., Aranzazu, J.M.H., Castelblanco, E., Tovar, A., Ramos, J., Ojeda, C., Facio–Lince, I. & Quiñones, C. 2015a. Memoria explicativa: Geología de la plancha 326 Vista Hermosa. Scale 1:100 000. Servicio Geológico Colombiano, 119 p. Bogotá.

Buchely, F., Gómez, L., Moreno–Sánchez, M., Hincapié, G., Buitrago, J., Cristancho, A., Aranzazu, J.M., Patiño, A., Quiñonez, C. & Buitrago, J. 2015b. Memoria explicativa: Geología de la plancha 285 San Martín. Scale 1:100 000. Servicio Geológico Colombiano, 144 p. Bogotá.

Burkhalter, R.M. 1995. Ooidal ironstones and ferruginous microbialites: Origin and relation to sequence stratigraphy (Aalenian and Bajocian, Swiss Jura mountains). Sedimentology, 42(1): 57–74. https://doi.org/10.1111/j.1365-3091.1995.tb01271.x

Burrow, C.J., Janvier, P. & Villarroel, C. 2003. Late Devonian acanthodians from Colombia. Journal of South American Earth Sciences, 16(2): 155–161. https://doi.org/10.1016/S0895-9811(03)00026-9

Bustamante, C., Archanjo, C.J., Cardona, A., Bustamante, A. & Valencia, V.A. 2017. U–Pb ages and Hf isotopes in zircons from parautochthonous Mesozoic terranes in the western margin of Pangea: Implications for the terrane configurations in the northern Andes. The Journal of Geology, 125(5): 487–500. https://doi.org/10.1086/693014

Campbell, C.J. & Bürgl, H. 1965. Section through the Eastern Cordillera of Colombia, South America. Geological Society of America Bulletin, 76(5): 567–590. https://doi.org/10.1130/0016-7606(1965)76[567:STTECO]2.0.CO;2

Cardona, A., Valencia, V.A., Lotero, A., Villafañez, Y. & Bayona, G. 2016. Provenance of middle to late Palaeozoic sediments in the northeastern Colombian Andes: Implications for Pangea reconstruction. International Geology Review, 58(15): 1914–1939. https://doi.org/10.1080/00206814.2016.1190948

Caster, K.E. 1939. A Devonian fauna from Colombia. Bulletins of American Paleontology, 24(83): 101–318.

Cediel, F. 1969. Geología del Macizo de Floresta: Nota explicativa del mapa geológico. Scale: 1:50 000. Primer Congreso Colombiano de Geología. Memoirs, p. 17–29. Bogotá.

Cochrane, R., Spikings, R., Gerdes, A., Ulianov, A., Mora, A., Villagómez, D., Putlitz, B. & Chiaradia, M. 2014. Permo–Triassic anatexis, continental rifting and the disassembly of western Pangaea. Lithos, 190–191: 383–402. https://doi.org/10.1016/j.lithos.2013.12.020

Cordani, U.G., Cardona, A., Jiménez, D.M., Liu, D. & Nutman, A.P. 2005. Geochronology of Proterozoic basement inliers in the Colombian Andes: Tectonic history of remnants of a fragmented Grenville belt. In: Vaughan, A.P.M., Leat, P.T. & Pankhurst, R.J. (editors), Terrane processes at the margins of Gondwana. Geological Society of London, Special Publication 246, p. 329–346. London. https://doi.org/10.1144/GSL.SP.2005.246.01.13

Crowell, J.C. 1995. The ending of the Late Paleozoic ice age during the Permian period. In: Scholle, P.A., Peryt, T.M. & Ulmer–Scholle, D.S. (editors), The Permian of northern Pangea. Volume 1: Paleogeography, Paleoclimates, Stratigraphy. Springer, p. 62–74. Berlin–Heidelberg. https://doi.org/10.1007/978-3-642-78593-1_5

Dewey, J.F. & Pindell, J.L. 1985. Neogene block tectonics of eastern Turkey and northern South America: Continental applications of the finite difference method. Tectonics, 4(1): 71–83. https://doi.org/10.1029/TC004i001p00071

Dickey, P.A. 1941. Pre–Cretaceous sediments in cordillera Oriental of Colombia. American Association of Petroleum Geologists Bulletin, 25(9): 1789–1795.

Dickinson, W.R. 1985. Interpreting provenance relations from detrital modes of sandstones. In: Zuffa, G.G. (editor), Provenance of arenites. Springer, p. 333–361. Netherlands https://doi.org/10.1007/978-94-017-2809-6_15

Dueñas, H. 2001. Paleozoic palynological assemblages from the Llanos Orientales Basin, Colombia. 34th Annual Meeting of the American Association of Stratigraphic Palynologists. Proceedings, 16 p. San Antonio, USA.

Dueñas, H. & Césari, S.N. 2003. Primer registro palinológico del Carbonífero Inferior en la Cuenca de los Llanos Orientales de Colombia. Ameghiniana, 40: 20–21.

Dueñas, H. & Césari, S.N. 2006. Palynological evidence of early Carboniferous sedimentation in the Llanos Orientales Basin, Colombia. Review of Palaeobotany and Palynology, 138(1): 31–42. https://doi.org/10.1016/j.revpalbo.2005.10.002

Duque–Caro, H. 1990. El Bloque Chocó en el noroccidente suramericano: Implicaciones estructurales, tectonoestratigráficas y paleogeográficas. Boletín Geológico, 31(1): 48–71.

Edwards, D., Poiré, D.G., Morel, E.M. & Cingolani, C.A. 2009. Plant assemblages from SW Gondwana: Further evidence for high–latitude vegetation in the Devonian of Argentina. In: Bassett, M.G. (editor), Early Palaeozoic peri–Gondwana terranes: New insights from tectonics and biogeography. Geological Society of London, Special Publication 325, p. 233–255. https://doi.org/10.1144/SP325.12

Etayo–Serna, F. 1985. Documentación paleontológica del Infracretácico de San Felix y Valle Alto, cordillera Central. In: Etayo–Serna, F. & Laverde, F. (editors), Proyecto Cretácico: Contribuciones. Publicaciones Geológicas Especiales del Ingeominas 16, p. XXV1–XXV7. Bogotá.

Etayo–Serna, F., Barrero, D., Lozano, H., Espinosa, A., González, H., Orrego, A., Ballesteros, I., Forero, H., Ramírez, C., Zambrano–Ortiz, F., Duque–Caro, H., Vargas, R., Núñez, A., Álvarez, J., Ropaín, C., Cardozo, E., Galvis, N., Sarmiento, L., Alberts, J.P., Case, J.E., Singer, D.A., Bowen, R.W., Berger, B.R., Cox, D.P. & Hodges, C.A. 1983. Mapa de terrenos geológicos de Colombia. Publicaciones Geológicas Especiales del Ingeominas 14, p. 1–235. Bogotá.

Fairon–Demaret, M. 1986. Some uppermost Devonian megafloras: A stratigraphical review. Annales de la Société Géologique de Belgique, 109: 43–48.

Feininger, T., Barrero, D. & Castro, N. 1972. Geología de parte de los departamentos de Antioquia y Caldas (sub–zona II–B). Boletín Geológico, 20(2): 1–173.

Ferreira, P., Núñez, A. & Rodríguez, M.A. 2002. Memoria explicativa: Levantamiento geológico de la plancha 323 Neiva. Ingeominas, 100 p. Bogotá.

Forero, A. 1970. Estratigrafía del pre–Cretácico en el flanco occidental de la serranía de Perijá. Geología Colombiana, (7): 7–77.

Forero, A. 1986. Remanentes de la provincia paleobiogeográfica Frasniano–Fameniana del viejo mundo en los Andes septentrionales. Geología Norandina, (10): 35–38.

Forero, A. 1990. The basement of the Eastern Cordillera, Colombia: An allochthonous terrane in northwestern South America. Journal of South America Earth Sciences, 3(2–3): 141–151. https://doi.org/10.1016/0895-9811(90)90026-W

Forero, A. 1991. Distribución de las rocas del Devónico en los Andes colombianos. Revista Técnica de Yacimientos Petrolíferos Fiscales Bolivianos, 12(1): 101–111.

Gansser, A. 1955. Ein Beitrag zur Geologie und Petrographie der Sierra Nevada de Santa Marta (Kolumbien, Südamerika). Schweizerische Mineralogische und Petrographische Mitteilungen, 35(2): 209–279.

García–Jarpa, R. 1972. El Permo–Carbonífero en Venezuela. Boletín de la Sociedad Venezolana de Geólogos, 7(3): 203–214.

Geyer, O.F. 1973. Das präkretazische Mesozoikum von Kolumbien. Geologisches Jahrbuch, 5: 1–155.

Geyer, O.F. 1982. Comparaciones estratigráficas y faciales en el Triásico norandino. Geología Norandina, (5): 27–31.

Goldsmith, R., Marvin, R.F. & Mehnert, H.H. 1971. Radiometric ages in the Santander Massif, Eastern Cordillera, Colombian Andes. U. S. Geological Survey, Professional Paper, 750–D: D44–D49.

Gómez, J. & Bocanegra, A. 1999. Estudio geológico–estructural de la Falla Otú–Pericos al W de la ciudad de Ibagué. Bachelor thesis, Universidad de Caldas, 116 p. Manizales.

Gómez–Cruz, A.d.J. & Chevalier, E.C. 2003. Sedimentology and paleontology of the Carboniferous of La Jagua, Huila, Colombia. 15th International Congress on Carboniferous and Permian Stratigraphy. Proceedings, p. 185. Utrecht, the Netherlands.

Gradstein, F.M., Ogg, J.G., Schmitz, M.D. & Ogg, G.M. 2012. The Geologic Time Scale 2012-2 Volume Set. Elsevier Science Ltd., 1176 p. Boston.

Grösser, J.R. & Prössl, K.F. 1991. First evidence of the Silurian in Colombia: Palynostratigraphic data from the Quetame Massif, Cordillera Oriental. Journal of South American Earth Sciences, 4(3): 231–238. https://doi.org/10.1016/0895-9811(91)90033-H

Grösser, J.R. & Prössl, K.F. 1994. Palynologische untersuchungen der Devonbasis im Floresta Massiv, Ostkordillere, Kolumbien, Südamerika. Giessener Geologische Schriften, (51): 105–121.

Gutiérrez–Marco, J.C., Gómez–González, C. & Sarmiento, G.N. 2006. El Ordovícico de la cordillera Central colombiana y su correlación con Perú. XIII Congreso Peruano de Geología. Sociedad Geológica del Perú. Publicación Especial 7, 623–626. Lima.

Gutiérrez–Marco, J.C., Sarmiento, G.N. & Gómez–González, C. 2007. First Ordovician conodonts from Colombia. Acta Paleontologica Sinica, 6: 170–175.

Harrington, H., & Kay, M. 1951. Cambrian and Ordovician faunas of Eastern Colombia. Journal of Paleontology, 25(5): 655–668.

Harvey, C. 1999. Middle and Upper Devonian palynology of the sierra de Perijá, western Venezuela. Palaeontological Association Newsletter, 42: 17–18.

Hea, J.P. & Whitman, A.B. 1960. Estratigrafía y petrología de los sedimentos pre–cretácicos de la parte norte central de la sierra de Perijá, estado Zulia, Venezuela. III Congreso Geológico Venezolano. Proceedings, 1, p. 351–376. Caracas.

Heckel, P.H. 2008. Pennsylvanian cyclothems in midcontinent North America as far–field effects of waxing and waning of Gondwana ice sheets. In: Fielding, C.R., Frank, T.D. & Isbell, J.L. (editors), Resolving the late Paleozoic ice age in time and space. Geological Society of America, Special Paper 441, p. 275–289. https://doi.org/10.1130/2008.2441(19)

Heckel, P.H. & Witzke, B.J. 1979. Devonian world palaeogeography determined from distribution of carbonates and related lithic paleoclimatic indicators. In: House, M.R., Scrutton, C.T. & Bassett, M.G. (editors), The Devonian System. Special Papers in Palaeontology (23), p. 99–123. London.

Hernández–González, J.S. & Urueña–Suárez, C.L. 2017. Aspectos geocronológicos y petrogenéticos del Complejo Aleluya: Implicaciones en la exploración de Mg en el norte del departamento del Huila, Colombia. XVI Congreso Colombiano de Geología y III Simposio de Exploradores. Memoirs, p. 832–838. Santa Marta.

Hettner, A. 1892. Die Kordillere von Bogotá. Gotha: Justus Perthes, 131 p.

Horton, B.K., Saylor, J.E., Nie, J., Mora, A., Parra, M., Reyes–Harker, A. & Stockli, D.F. 2010. Linking sedimentation in the northern Andes to basement configuration, Mesozoic extension, and Cenozoic shortening: Evidence from detrital zircon U–Pb ages, Eastern Cordillera, Colombia. Geological Society of America Bulletin, 122(9–10): 1423–1442. https://doi.org/10.1130/B30118.1

Janvier, P. & Villarroel, C. 1998. Los peces devónicos del Macizo de Floresta (Boyacá, Colombia): Consideraciones taxonómicas, bioestratigráficas, biogeográficas y ambientales. Geología Colombiana, (23): 3–18.

Janvier, P. & Villarroel, C. 2000. Devonian vertebrates from Colombia. Paleontology, 43(4): 729–763.

Joachimski, M.M., Pancost, R.D., Freeman, K.H., Ostertag–Henning, C. & Buggisch, W. 2002. Carbon isotope geochemistry of the Frasnian – Famennian transition. Palaeogeography, Palaeoclimatology, Palaeoecology, 181(1–3): 91–109. https://doi.org/10.1016/S0031-0182(01)00474-6

Johnson, J.G. & Boucot, A.J. 1973. Devonian brachiopods. In: Hallam, A. (editor), Atlas of palaeobiogeography. Elsevier, p. 89–96. Amsterdam.

Kroonenberg, S.B. 1982. A Grenvillian granulite belt in the Colombian Andes and its relation to the Guiana Shield. Geologie en Mijnbouw, 61(4): 325–333.

Lemoigne, Y. 1984. Données nouvelles sur la paléoflore de Colombie. Geobios, 17(6): 667–707. https://doi.org/10.1016/S0016-6995(84)80115-1

Mantilla–Figueroa, L.C. & García–Ramírez, C.A. 2018. Geología y geocronología de las litologías aflorantes en el tramo Mogotes–San Joaquín (sector SW del Macizo de Santander). Boletín de Geología, 40(1): 123–144. https://doi.org/10.18273/revbol.v40n1-2018008

Mantilla–Figueroa, L.C., García–Ramírez, C.A. & Valencia, V.A. 2016. Propuesta de escisión de la denominada 'Formación Silgará' (Macizo de Santander, Colombia), a partir de edades U–Pb en zircones detríticos. Boletín de Geología, 38(1): 33–50. https://doi.org/10.18273/revbol.v38n1-2016002

Marquínez, G. & Núñez, A. 1998. Catálogo de unidades litoestratigráficas de Colombia: Neises y Anfibolitas de Tierradentro, cordillera Central. Ingeominas, 26 p. Bogotá.

Maslo, A. & Vachard, D. 1997. Inventaire critique des eostaffellinae (foraminifères) du Carbonifère. Revue de Micropaléontologie, 40(1): 39–69. https://doi.org/10.1016/S0035-1598(97)90094-5

Maya, M. 1992. Catálogo de dataciones isotópicas en Colombia. Boletín Geológico, 32(1–3): 127–187.

Maya, M. & González, H. 1995. Unidades litodémicas en la cordillera Central de Colombia. Boletín Geológico, 35(2–3): 43–57.

McNair, A.H. 1940. Devonian Bryozoa from Colombia. Bulletins of American Paleontology, 25(93): 1–34.

Meyer–Berthaud, B., Fairon–Demaret, M., Steemans, P., Talent, J.A. & Gerrienne, P. 2003. The plant *Leclercqia* (Lycopsida) in Gondwana: Implications for reconstructing Middle Devonian palaeogeography. Geological Magazine, 140(2): 119–130. https://doi.org/10.1017/S0016756802007276

Miller, A.K. & Williams, J.S. 1945. Permian cephalopods from northern Colombia. Journal of Paleontology, 19(4): 347–349.

Mojica, J. & Villarroel, C. 1984. Contribución al conocimiento de las unidades paleozoicas del área de Floresta (cordillera Oriental colombiana; departamento de Boyacá) y en especial de la Formación Cuche. Geología Colombiana, (13): 55–79.

Mojica, J., Villarroel, C. & Bayer, K. 1987a. Afloramientos del Paleozoico superior en el Macizo de Garzón (cordillera Oriental) y el Valle Superior del Magdalena, Colombia. Geología Colombiana, (16): 99–104.

Mojica, J., Villarroel, C. & Macía, C. 1987b. Nuevos afloramientos fosilíferos del Ordovícico Medio (Fm. El Hígado) al oeste de Tarqui, Valle Superior del Magdalena (Huila, Colombia). Geología Colombiana, (16): 95–97.

Mojica, J., Villarroel, C., Cuerda, A. & Alfaro, M.A. 1988. La fauna de graptolites de la Formación El Hígado (Llanvirniano?–Llandeiliano), serranía de Las Minas, Valle Superior del Magdalena, Colombia. V Congreso Geológico Chileno. Memoirs, II, p. 189–202. Santiago.

Morales, P.A. 1965. A contribution to the knowledge of the Devonian faunas of Colombia. Boletín de Geología, (19): 51–111.

Moreno–Sánchez, M. 2004. Devonian plants from Colombia: Geologic framework and paleogeographic implications. Doctorade thesis, Université de Liège, 108 p. Liège, Belgium.

Moreno–Sánchez, M., Gómez–Cruz, A.d.J. & Castillo–González, H. 2005. La "Formación Floresta metamorfoseada" (sensu Ward et al., 1973) no es la Formación Floresta sin metamorfosear. X Congreso Colombiano de Geología. Abstracts, p. 124. Bogotá.

Moreno–Sánchez, M., Gómez–Cruz, A.d.J. & Castillo–González, H. 2008a. Ocurrencias de fósiles paleozoicos al este de la parte norte de la cordillera Central y discusión sobre su significado geológico. Boletín de Ciencias de la Tierra, (22): 39–47.

Moreno–Sánchez, M., Gómez–Cruz, A. de J. & Castillo–González, H. 2008b. Graptolitos del Ordovícico y geología de los afloramientos del río Venado (norte del departamento del Huila). Boletín de Geología, 30(1): 9–19.

Moreno–Sánchez, M., Gómez–Cruz, A.d.J. & Gutiérrez–Marco, J.C. 2014. New data lower Ordovician graptolites from Colombia and their correlation around the Gondwanan margin of South America. Gondwana 15th International Symposium. Proceedings, p. 112. Madrid.

Morzadec, P., Mergl, M., Villarroel, C., Janvier, P. & Racheboeuf, P. 2015. Trilobites and inarticulate brachiopods from the Devonian Floresta Formation of Colombia: A review. Bulletin of Geosciences, 90(2): 331–358. https://doi.org/10.3140/bull.geosci.1515

Navas, J. 1962. Geología del Carbonífero al N. de Bucaramanga. Boletín de Geología, (11): 23–34.

Nelson, H.W. 1957. Contribution to the geology of the Central and Western Cordilleras of Colombia in the sector between Ibagué and Cali. Leidse Geologische Mededelingen, 22: 1–75.

Núñez, A. & Murillo, A. 1982. Memoria explicativa: Geología y prospección geoquímica de las planchas 244 Ibagué y 263 Ortega. Ingeominas, Informe interno 1879, 388 p. Ibagué.

Núñez, A., Macía, C. & Mojica, J. 1984. La Formación Amoyá: Una nueva unidad post–pre–Cámbrica pre–Jurásica de la cordillera Central, al W de Chaparral, Tolima, Colombia. Newsletters on Stratigraphy, 13(2): 77–87. https://doi.org/10.1127/nos/13/1984/77

Odreman, O. & Wagner, R.H. 1979. Precisiones sobre algunas floras carboníferas y pérmicas de los Andes venezolanos. Boletín Geológico, Caracas, 13(25): 77–79.

Olsson, A.A. & Caster, K.E. 1937. Devonian fauna from Colombia, South America. Geological Society of America. Proceedings, p. 369–370.

Ordóñez–Carmona, O. Pimentel, M.M., de Moraes, R. & Restrepo, J.J. 1999. Rocas grenvilianas en la región de Puerto Berrío, Antioquia. Revista de la Academia Colombiana de Ciencias Exactas, Físicas y Naturales, 23(87): 225–232.

Ordóñez–Carmona, O., Restrepo, J.J. & Pimentel, M.M. 2006. Geochronological and isotopical review of pre–Devonian crustal basement of the Colombian Andes. Journal of South American Earth Sciences, 21(4): 372–382. https://doi.org/10.1016/j.jsames.2006.07.005

Pfefferkorn, H.W. 1977. Plant megafossils in Venezuela and their use in geology. V Congreso Geológico Venezolano. Boletín Geológico, Publicación Especial 8, p. 407–414. Caracas.

Priem, H.N.A., Kroonenberg, S.B., Boelrijk, N.A.I.M. & Hebeda, E.H. 1989. Rb–Sr and K–Ar evidence for the presence of a 1.6 Ga basement underlying the 1.2 Ga Garzón–Santa Marta granulite belt in the Colombian Andes. Precambrian Research, 42(3–4): 315–324. https://doi.org/10.1016/0301-9268(89)90016-8

Prössl, K.F. & Grösser, J.R. 1995. The age of the Formación Amoyá, Upper Magdalena Valley: Another piece in the Paleozoic stratigraphic puzzle of Colombia. Newsletters on Stratigraphy, 32(2): 91–101. https://doi.org/10.1127/nos/32/1995/91

Pulido, O. & Gómez, L.S. 2001. Memoria explicativa: Geología de la plancha 266 Villavicencio. Scale 1:100 000. Ingeominas, 52 p. Bogotá.

Pulido, O., Gómez, L.S. & Marín, P. 1998. Geología de la plancha 266 Villavicencio. Scale 1:100 000. Ingeominas. Bogotá.

Rabe, H.E. 1974. Zur Stratigraphie des ostandinen Raumes von Kolumbien. I: Die Abfolge Devon bis Perm der Ost–Kordillere nördlich von Bucaramanga. Doctorade thesis, Justus–Liebig–Univeritãt, 46 p. Giessen, Germany.

Ramos, V.A. 2010. The Grenville–age basement of the Andes. Journal of South American Earth Sciences, 29(1): 77–91. https://doi.org/10.1016/j.jsames.2009.09.004

Ramos, V.A. 2015. La orogenia Famatiniana (Ordovícico Medio a Tardío) en el margen continental protoandino de América del Sur: Nuevas evidencias y sus implicancias tectónicas. XIV Congreso Geólogico Chileno. Memoirs, p. 106–109. La Serena, Chile.

Rauzer–Chernousova, D.M. 1948. Material and foraminiferal fauna from the Carboniferous deposits of central Kazakhstan. Akademia Nauk SSSR, Trudy Institut Geologicheskii Nauk 66, Geologicheskaya Seria, 21: 1–27.

Raymond, A., Parker, W.C. & Parrish, J.T. 1985. Phytogeography and paleoclimate of the Early Carboniferous. In: Tiffney, B.H. (editor), Geological factors and evolution of plants. Yale University Press, p. 169–222. New Haven, Connecticut.

Reitlinger, E.A. 1950. Foraminifera of middle Carboniferous strata of central part of the Russian Platform (excepting the family Fusulinidae). Akademia Nauk SSSR, Trudy Institut Geologicheskii Nauk 126, Geologicheskaya Seria, 47: 1–127.

Remy, W., Remy, R., Pfefferkorn, H.W., Volkheimer, W. & Rabe, E. 1975. Neueinstufung der Bocas–Folge (Bucaramanga, Kolumbien) in den unteren Jura anhand einer Phlebopteris–branneri–und Classopollis–Flora. Argumenta Paleobotanica, 4: 55–77.

Renzoni, G. 1968. Geología del Macizo de Quetame. Geología Colombiana, (5): 75–127.

Restrepo, J.J. 1983. Guía para la geología del flanco noroccidental de la cordillera Central: Carretera Medellín–Amagá–Albania–Bolombolo. Boletín de Ciencias de la Tierra, (7–8): 168–187.

Restrepo, J.J. & Toussaint, J.F. 1988. Terranes and continental accretion in the Colombian Andes. Episodes, 11(3): 189–193.

Restrepo, J.J., Ordóñez–Carmona, O., Martens, U. & Correa–Martínez, A.M. 2009. Terrenos, complejos y provincias en la cordillera Central de Colombia. Ingeniería, Investigación y Desarrollo, 9(2): 49–56.

Restrepo–Pace, P.A. 1995. Late Precambrian to early Mesozoic tectonic evolution of the Colombian Andes, based on new geochronological, geochemical and isotopic data. Doctoral thesis, University of Arizona, 195 p. Tucson, Arizona.

Restrepo–Pace, P.A. & Cediel, F. 2010. Northern South America basement tectonics and implications for paleocontinental reconstructions of the Americas. Journal of South American Earth Sciences, 29(4): 764–771. https://doi.org/10.1016/j.jsames.2010.06.002

Restrepo–Pace, P.A., Ruiz, J., Gehrels, G. & Cosca, M. 1997. Geochronology and Nd isotopic data of Grenville–age rocks in the Colombian Andes: New constraints for late Proterozoic – early Paleozoic paleocontinental reconstructions of the Americas. Earth and Planetary Science Letters, 150(3–4): 427–441. https://doi.org/10.1016/S0012-821X(97)00091-5

Ricardi–Branco, F. 2008. Venezuelan paleoflora of the Pennsylvanian – Early Permian: Paleobiogeographical relationships to central and western equatorial Pangea. Gondwana Research, 14(3): 297–305. https://doi.org/10.1016/j.gr.2008.02.007

Ricardi–Branco, F., Rösler, O. & Odreman, O. 2005. La flora euroamericana de Carache (Carbonífero Tardío–Pérmico temprano), municipio de Carache, noroeste de Venezuela. Plántula, 3(3): 153–167.

Royero, J.M. & Zambrano, J.E. 1987. Geología de la plancha 111 Toledo, Norte de Santander. Ingeominas, Internal report 2039, 227 p. Bucaramanga.

Ruiz, J., Tosdal, R.M., Restrepo, P.A. & Murillo–Muñetón, G. 1999. Pb isotope evidence for Colombia–southern México connections in the Proterozoic. In: Ramos, V.A. & Keppie, J.D. (editors), Laurentia–Gondwana connections before Pangea. Geological Society of America, Special Paper 336, p. 183–197. https://doi.org/10.1130/0-8137-2336-1.183

Rushton, A.W.A. 1963. Paradoxides from Colombia. Geological Magazine, 100(3): 255–257. https://doi.org/10.1017/S0016756800055199

Scotese, C.R., Bambach, R.K., Barton, C., van der Voo, R. & Ziegler, A.M. 1979. Paleozoic base maps. The Journal of Geology, 87(3): 217–277. https://doi.org/10.1086/628416

Scott, G.R. 1978. Translation of accretionary slivers: Triassic results from the Central Cordillera of Colombia. EOS–Transactions Fall meeting supplements, 59(12): 1058–1059.

Sedlock, R.L., Ortega–Gutiérrez, F. & Speed, R.C. 1993. Tectonostratigraphic terranes and tectonic evolution of Mexico. Geological Society of America, Special Paper 278, 153 p. https://doi.org/10.1130/SPE278

Segovia, A. & Renzoni, G. 1965. Geología del cuadrángulo L–12 Medina. Scale 1:200 000. Servicio Geológico Nacional & Inventario Minero Nacional. Bogotá.

Skinner, J.W. & Wilde, G.L. 1954. Early Pennsylvanian fusulinids from Texas. Journal of Paleontolology, 28(6): 796-803.

Skinner, J.W. & Wilde, G.L. 1965. Permian biostratigraphy and fusulinid faunas of the Shasta Lake area, northern California. The University of Kansas Paleontological Contributions, Protozoa, 6: 1–98.

Spikings, R., Cochrane, R., Villagómez, D., van der Lelij, R., Vallejo, C., Winkler, W. & Beate, B. 2015. The geological history of northwestern South America: From Pangaea to the early collision of the Caribbean Large Igneous Province (290–75 Ma). Gondwana Research, 27(1): 95–139. https://doi.org/10.1016/j.gr.2014.06.004

Stewart, J.H., Blodgett, R.B., Boucot, A.J., Carter, J.L. & López, R. 1999. Exotic Paleozoic strata of Gondwanan provenance near Ciudad Victoria, Tamaulipas, México. In: Ramos, V.A. & Keppie, J.D. (editors), Laurentia–Gondwana connections before Pangea. Geological Society of America, Special Paper 336, p. 227–252. https://doi.org/10.1130/0-8137-2336-1.227

Stibane, F. 1968. Zur Geologie von Kolumbien, Südamerika: Das Quetame und Garzón Massiv. Geotektonische Forschungen, 30(1–2): 1–85.

Stibane, F. & Forero, A. 1969. Los afloramientos del Paleozoico en la Jagua (Huila) y río Nevado (Santander del Sur). Geología Colombiana, (6): 31–66.

Théry, J.M., Peniguel, G. & Haye, G. 1984. Descubrimiento de acritarcos del Arenigiano cerca de Araracuara (Caquetá, Colombia): Ensayo de reinterpretación de esta región de la saliente del Vaupés. Geología Norandina, (9): 3–17.

Thompson, M.L. 1942. New genera of Pennsilvanian fusulids. American Journal of Science, 240(6): 403–420. https://doi.org/10.2475/ajs.240.6.403

Thompson, M.L. & Miller, A.K. 1949. Permian fusulinids and cephalopods from the vicinity of the Maracaibo Basin in northern South America. Journal of Paleontology, 23(1): 1–24.

Toro, L.M., Moreno–Sánchez, M. & Gómez–Cruz, A.d.J. 2014. Metagabro del Ariari, plutonismo MORB, cordillera Oriental de Colombia. Boletín de Geología, 36(2): 15–24.

Toussaint, J.F. & Restrepo, J.J. 1993. Tectónica de terrenos durante el Cretácico en Colombia. VI Congreso Colombiano de Geología. Memoirs, I, p. 97–114. Medellín.

Toussaint, J.F. & Restrepo, J.J. 1994. The Colombian Andes during Cretaceous times. In: Salfity, J.A. (editor), Cretaceous tectonics of the Andes. Earth Evolution Sciences. Vieweg & Sohn Verlagsgesellschafl mbH, p. 61–100. /Wiesbaden, Germany. https://doi.org/10.1007/978-3-322-85472-8_2

Trapp, D. 1968. Das Paläozoikum und Frühmesozoikum im nördlichen Quetame–und westlichen Santander massiv der Ostkordillere Kolumbiens, Südamerike. Giessen editorial, 452 p. Giessen, Germany.

Trumpy, D. 1943. Pre–Cretaceous of Colombia. Geological Society of America Bulletin, 54(9): 1281–1304. https://doi.org/10.1130/GSAB-54-1281

Trumpy, D. 1945. El pre–Cretáceo de Colombia. Instituto Colombiano de Petróleos. Informe técnico 9, 15 p. Bogotá.

Ulloa, C.E., Pérez, V.E. & Baldis, B.A. 1982. Unidades litoestratigráficas del Ordovícico de los Llanos Orientales de Colombia. V Congreso Latinoamericano de Geología. Memoirs, I, p. 109–120. Buenos Aires.

Vakhrameev, V.A. 1991. Jurassic and Cretaceous floras and climates of the Earth. Cambridge University Press, 340 p. New York.

van der Lelij, R. 2013. Reconstructing north–western Gondwana with implications for the evolution of the Iapetus and Rheic Oceans: A geochronological, thermochronological and geochemical study. Doctorade thesis, University of Geneva, 248 p. Geneva. https://doi.org/10.13097/archive-ouverte/unige:31653

van der Lelij, R., Spikings, R.A. & Mora, A. 2016a. Thermochronology and tectonics of the Mérida Andes and the Santander Massif, NW South America. Lithos, 248–251: 220–239. https://doi.org/10.1016/j.lithos.2016.01.006

van der Lelij, R., Spikings, R., Ulianov, A., Chiaradia, M. & Mora, A. 2016b. Paleozoic to Early Jurassic history of the northwestern corner of Gondwana, and implications for the evolution of the Iapetus, Rheic and Pacific Oceans. Gondwana Research, 31: 271–294. https://doi.org/10.1016/j.gr.2015.01.011

Velandia, F., Ferreira, P., Rodríguez, G. & Núñez, A. 1996. Memoria explicativa: Levantamiento geológico de la plancha 366 Garzón, Huila. Ingeominas, internal report 2321, 121 p. Bogotá.

Vesga, C.J. & Barrero, D. 1978. Edades K/Ar en rocas ígneas y metamórficas de la cordillera Central de Colombia y su implicación geológica. II Congreso Colombiano de Geología. Abstracts, p. 19. Bogotá.

Vinasco, C.J., Cordani, U.G., González, H., Weber, M. & Peláez, C. 2006. Geochronological, isotopic, and geochemical data from Permo–Triassic granitic gneisses and granitoids of the Colombian central Andes. Journal of South American Earth Sciences, 21(4): 355–371. https://doi.org/10.1016/j.jsames.2006.07.007

Ward, D.E., Goldsmith, R., Cruz, J. & Restrepo, H. 1973. Geología de los cuadrángulos H–12 Bucaramanga y H–13 Pamplona, departamento de Santander. Boletín Geológico, 21(1–3): 132 p.

Ward, D.E., Goldsmith, R., Cruz, J., Téllez, N. & Jaramillo, L. 1977. Mapa geológico de San Gil y Málaga (parte de los cuadrángulos I–12 y I–13), Colombia. Scale 1:100 000. Ingeominas. Bogotá.

Young, G.C. & Moody, J.M. 2002a. A Middle–Late Devonian fish fauna from the sierra de Perijá, western Venezuela, South America. Fossil Record, 5(1): 155–206. https://doi.org/10.1002/mmng.20020050111

Young, G.C. & Moody, J.M. 2002b. A Middle–Late Devonian fish fauna from the sierra de Perijá, western Venezuela, South America. Mitteilungen aus dem Museum für Naturkunde in Berlin. Geowissenschaftliche Reihe 5, p. 155–206.

Authors' Biographical Notes

Mario MORENO–SÁNCHEZ is a Colombian geologist, paleontologist (focused on the paleoflora of the Paleozoic period) and professor at the Universidad de Caldas (Manizales, Colombia). He has taught earth sciences disciplines including stratigraphy, sedimentology and paleontology. He has made contributions to the cartography of the serranía de La Macarena and the Guape–Duda region. His experience in field geology includes studies in the Paleozoic units of Venezuela, Morocco, and various areas of Colombia (Guajira, the Upper Magdalena Valley, and the Santander, Floresta and Quetame Massifs).

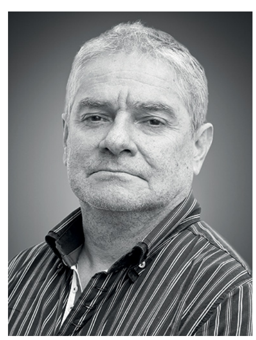

Arley GÓMEZ–CRUZ, geologist at the Universidad de Caldas, Manizales, Colombia. MS of the University of Liege, Belgium. Professor at the Universidad de Caldas since 1989. He has taught earth sciences disciplines including stratigraphy, sedimentology, historical geology, marine geology, field geology, and paleontology. Member of the working group of the Laboratory of Paleontological Studies (LEP) of the Universidad de Caldas. He has made contributions to the cartography of the Manizales area (Quebradagrande Complex). His experience in field geology include studies in the Paleozoic units of the Floresta Massif and Garzón Massif (La Jagua Formation).

José BUITRAGO–HINCAPIÉ is a Colombian field geologist and is currently working for the Servicio Geológico Colombiano. His contributions to the geology of Colombia have been the regional geological mapping of a sector of the cordillera Oriental and its foothills. His geological works also include mapping the Tumaco onshore and the Caguán–Putumayo Basin. His stratigraphic studies cover the Paleozoic units of the Quetame Massif, the Guape–Duda area (cordillera Oriental foothill), serranía de La Macarena, and the serranía de Chiribiquete (Amazon region).

Chapter 10

Fragments of a Permian Arc on the Western Margin of the Neoproterozoic Basement of Colombia

https://doi.org/10.32685/pub.esp.35.2019.10
Published online 26 September 2019

Gabriel RODRÍGUEZ–GARCÍA[1]*, Ana María CORREA–MARTÍNEZ[2], Juan Pablo ZAPATA–VILLADA[3], and Gloria OBANDO–ERAZO[4]

1 grodriguez@sgc.gov.co
Servicio Geológico Colombiano
Dirección de Geociencias Básicas
Grupo de Estudios Geológicos Especiales
Calle 75 n.° 79A–51
Medellín, Colombia

2 amcorrea@sgc.gov.co
Servicio Geológico Colombiano
Dirección de Geociencias Básicas
Grupo de Estudios Geológicos Especiales
Calle 75 n.° 79A–51
Medellín, Colombia

3 jpzapata@sgc.gov.co
Servicio Geológico Colombiano
Dirección de Geociencias Básicas
Grupo de Estudios Geológicos Especiales
Calle 75 n.° 79A–51
Medellín, Colombia

4 gobando@sgc.gov.co
Servicio Geológico Colombiano
Dirección de Geociencias Básicas
Grupo de Estudios Geológicos Especiales
Calle 75 n.° 79A–51
Medellín, Colombia

* Corresponding author

Supplementary Information:

S: https://www.sgc.gov.co/LibroGeologiaColombia/tgc/sgcpubesp35201910s.pdf

Abstract New petrographic, whole–rock geochemical, and U–Pb–zircon geochronologic data combined with data from previous studies enabled identification of a fragmented Permian magmatic arc with ages ranging from 294 to 260 Ma in the Colombian Andes. The arc is exposed along the southeastern slope of the Central Cordillera towards the Upper Magdalena Valley, serranía de San Lucas, and Sierra Nevada de Santa Marta.

The arc fragments consist of plutons on the western margin of the Neoproterozoic basement and show wide lithological variation in both igneous (monzodiorites, quartz monzonites, tonalites, granodiorites, monzogranites, and syenogranites) and metamorphic (migmatites, gneisses, and mylonitic gneisses) rocks. The granites have a metaluminous to peraluminous character and correspond to calc–alkaline to high–potassium calc–alkaline series formed in a continental arc environment. Some bodies are associated with metamorphic rocks (La Plata Granite and Icarco Complex), which may correspond to the roots of the arc, and others show superimposed dynamic metamorphism (the Nechí Gneiss and El Encanto Orthogneiss). The Permian plutons, unidentified in previous studies because of their lithological similarities to the volume of magmatism that occurred during the Early to Middle Jurassic, are dispersed along with the Neoproterozoic basement. The Permian plutonism that intruded the basement of the northern Andes possibly originated in a subduction zone located on the western margin of Gondwana.

Keywords: *geochemistry, U–Pb geochronology, Colombian Andes, igneous and metamorphic rocks.*

Resumen Nuevos datos de petrografía, geoquímica de roca total y geocronología U–Pb en circón junto con la reinterpretación de datos reportados en trabajos previos permitieron identificar en los Andes colombianos un arco magmático fragmentado con actividad entre 294 y 260 Ma. Este arco está expuesto a lo largo del flanco suroriental de la cordillera Central en el Valle Superior del Magdalena, la serranía de San Lucas y la Sierra Nevada de Santa Marta.

Los fragmentos de arco consisten en plutones localizados en la margen occidental del basamento neoproterozoico y presentan una amplia variación litológica entre ro-

Citation: Rodríguez–García, G., Correa–Martínez, A.M., Zapata–Villada, J.P. & Obando–Erazo, G. 2019. Fragments of a Permian arc on the western margin of the Neoproterozoic basement of Colombia. In: Gómez, J. & Mateus–Zabala, D. (editors), The Geology of Colombia, Volume 1 Proterozoic – Paleozoic. Servicio Geológico Colombiano, Publicaciones Geológicas Especiales 35, p. 205–239. Bogotá. https://doi.org/10.32685/pub.esp.35.2019.10

cas ígneas (monzodioritas, cuarzomonzonitas, tonalitas, granodioritas, monzogranitos y sienogranitos) y metamórficas (migmatitas, gneises y gneises miloníticos). Los granitos son de carácter metaluminoso a peraluminoso y corresponden a la serie calcoalcalina a calcoalcalina alta en potasio, formados en un ambiente de arco de margen continental. Algunos cuerpos presentan rocas metamórficas asociadas (Granito de La Plata y Complejo Icarco) que pueden corresponder a las raíces del arco, mientras que otros exhiben metamorfismo dinámico sobreimpuesto (Gneis de Nechí y Ortogneis El Encanto). Los plutones pérmicos están dispersos con el basamento neoproterozoico y no se habían identificado en trabajos anteriores debido a sus similitudes litológicas con el magmatismo que ocurrió durante el Jurásico Temprano a Medio. El plutonismo pérmico que intruye el basamento de los Andes del norte posiblemente se originó en una zona de subducción localizada en la margen occidental de Gondwana.

Palabras clave: *geoquímica, geocronología U–Pb, Andes colombianos, rocas ígneas y metamórficas.*

1. Introduction

Permian age rocks in Colombia have been described in the core of the Central Cordillera, in the serranía de San Lucas and in the Sierra Nevada de Santa Marta, without clear differentiation between metamorphic belts, granitoids, and peraluminous granitic gneisses (Cardona et al., 2010a, 2010b; Cochrane et al., 2014; Leal–Mejía, 2011; Restrepo et al., 2011; Spikings et al., 2015; Vinasco et al., 2006).

Different models have been proposed for the formation of these units: (i) a Permian – Triassic collisional orogen (Tahamí Terrane; Restrepo & Toussaint, 1989; Martens et al., 2014) that formed during the development of Pangea (Vinasco et al., 2006), (ii) a continental arc followed by anatexis during the Triassic (Spikings et al., 2015), (iii) a post–collisional anatectic event that formed granites at 280 Ma (Piraquive, 2017) and 228 Ma (Vinasco et al., 2006), and (iv) a continental arc that was along the western boundary of the Neoproterozoic basement (Cardona et al., 2010b; Rodríguez et al., 2014, 2017).

The description of plutons that comprise the Permian arc on the western boundary of the Chibcha Terrane presented in this study was conducted by the Servicio Geológico Colombiano (SGC) and from a compilation of previous studies (Cardona et al., 2010b; Leal–Mejía, 2011; Piraquive, 2017; Restrepo et al., 2011; Rodríguez et al., 2014, 2017; Villagómez, 2010). The plutons that form the Permian arc defined in this study are along the eastern margin of the Central Cordillera and in the Upper Magdalena Valley (La Plata Granite sensu Rodríguez, 1995a; Leal–Mejía, 2011; Rodríguez et al., 1998, 2017; Velandia et al., 1999, 2001a; the Ortega Granite, this study), serranía de San Lucas (Nechí Gneiss sensu Restrepo et al., 2011; Leal–Mejía, 2011; Rodríguez et al., 2014), and Sierra Nevada de Santa Marta (mylonitic granitoids sensu Cardona et al., 2010b, subsequently named El Encanto Orthogneiss sensu Piraquive, 2017).

We describe a new unit termed the Ortega Granite and characterize and compare the different Permian plutons using petrographic, whole–rock geochemical, and zircon U–Pb laser ablation inductively coupled plasma mass spectrometry (LA–ICP–MS) geochronological data. Regional geologic maps have been improved, and the spatial distribution of the Permian arc blocks was determined.

2. Geologic Setting

The Neoproterozoic basement of the Colombian Andes consists of blocks and tectonically scattered outcrops in the Upper Magdalena Valley (UMV), Eastern Cordillera, serranía de San Lucas, Sierra Nevada de Santa Marta, and La Guajira (Figure 1). These blocks are included in the Chibcha Terrane (Restrepo & Toussaint, 1989; Restrepo et al., 2009), recently described as the Putumayo Orogen (Ibañez–Mejia et al., 2011, 2015). Paleozoic marine sedimentary sequences overlie this basement. These rocks are intruded by Carboniferous arc plutons, such as the Carmen Stock (Leal–Mejía, 2011), and by Permian arc plutons, such as La Plata Granite (Leal–Mejía, 2011; Rodríguez et al., 2017), the Nechí Gneiss (Restrepo et al., 2011; Rodríguez et al., 2014), and the mylonitic granitoids of the Sierra Nevada de Santa Marta (Cardona et al., 2010b; Piraquive, 2017). The available geochronological data of the Permian magmatism in Colombia are outlined in Table 1. Subsequent to intrusion, local continental and marine sequences were deposited during the Triassic.

→

Figure 1. (a) Occurrences of Permian igneous rocks in the Colombian Andes. Modified from Gómez et al. (2015a). Data source: U–Pb zircon ages from Cardona et al. (2010b), Cochrane (2013), Cochrane et al. (2014), Gómez et al. (2015b), Leal–Mejía (2011), Piraquive, (2017), Restrepo et al. (2011), Rodríguez et al. (2017), Villagómez (2010), and this study. **(b)** Proposed distribution of metamorphic basement units in the regions related to Permian magmatism.

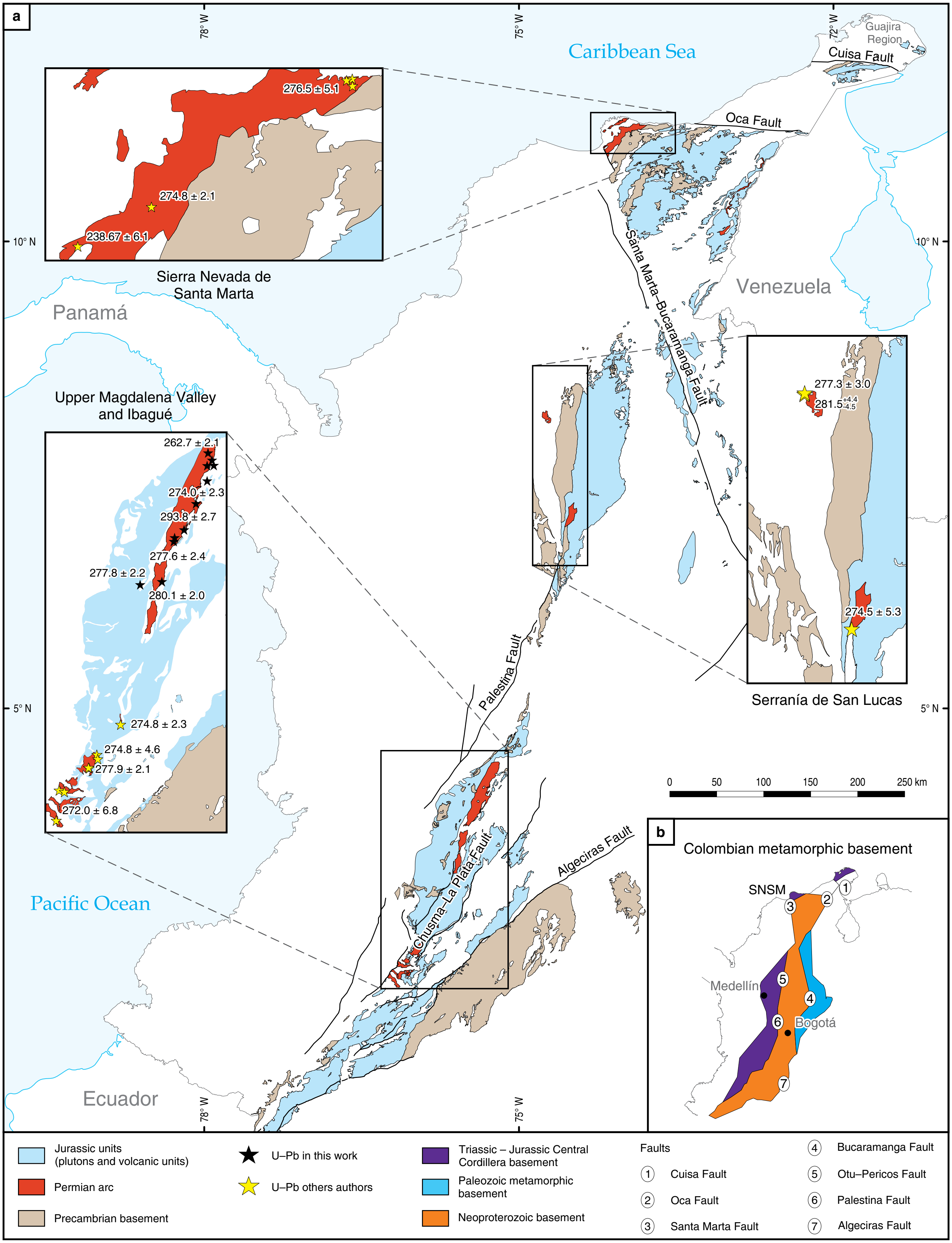
a
Caribbean Sea
Guajira Region
Cuisa Fault
Oca Fault
276.5 ± 5.1
274.8 ± 2.1
238.67 ± 6.1
Sierra Nevada de Santa Marta
Panamá
Venezuela
Santa Marta–Bucaramanga Fault
Upper Magdalena Valley and Ibagué
262.7 ± 2.1
274.0 ± 2.3
293.8 ± 2.7
277.6 ± 2.4
277.8 ± 2.2
280.1 ± 2.0
274.8 ± 2.3
274.8 ± 4.6
277.9 ± 2.1
272.0 ± 6.8
277.3 ± 3.0
281.5 +4.4 -4.5
274.5 ± 5.3
Serranía de San Lucas
Palestina Fault
Chusma–La Plata Fault
Algeciras Fault
Pacific Ocean
Ecuador
78° W
75° W
72° W
10° N
5° N
0 50 100 150 200 250 km
b
Colombian metamorphic basement
SNSM
Medellín
Bogotá
1 2 3 4 5 6 7
Jurassic units (plutons and volcanic units)
Permian arc
Precambrian basement
U–Pb in this work
U–Pb others authors
Triassic – Jurassic Central Cordillera basement
Paleozoic metamorphic basement
Neoproterozoic basement
Faults
1 Cuisa Fault
2 Oca Fault
3 Santa Marta Fault
4 Bucaramanga Fault
5 Otu–Pericos Fault
6 Palestina Fault
7 Algeciras Fault

Permian

Table 1. Previous geochronology of Permian units in Colombia.

Sample	Lithology	Latitude N	Longitude W	$^{238}U/^{206}Pb$ age (Ma) ± 2σ	MSWD	Inheritance ages (Ma)	Author
				Upper Magdalena Valley			
La Plata Granite							
JGB–373	Cpx–Bt–Kfs–Pl–Qtz granofels	2° 44' 32.83"	76° 11' 47.07"	268.3 ± 2.0	1.4	1140 ± 130, n = 1; 960 ± 100, n = 1	Rodríguez et al. (2017)
GR–6655	Monzogranite	2° 30' 19.78"	76° 25' 09.78"	269.0 ± 3.0	1.09	841.43 ± 64.1, n = 1	Rodríguez et al. (2017)
MIA–516	Granite	2° 32' 16.85"	76° 25' 45.69"	270.0 ± 2.7	1.06	309.55 ± 13.7, n = 1; 297 ± 11, n = 2	Rodríguez et al. (2017)
MIA–531	Quartz monzonite	2° 29' 13.03"	76° 36' 29.77"	272.0 ± 6.8	0.34	903 ± 79, n = 3	Rodríguez et al. (2017)
GR–6631	Kfs–Pl–Qtz granofels (monzogranite)	2° 41' 36.21"	76° 16' 54.62"	273.2 ± 4.1	3.5	1781 ± 66, n = 5; 1401 ± 50, n = 2; 972, n = 2; 534 ± 34, n = 5; 393 ± 14, n = 2; 315 ± 15, n = 6	Rodríguez et al. (2017)
GR–6632	Kfs–Pl–Qtz granofels (sienogranite)	2° 41' 22.12"	76° 16' 36.09"	277.9 ± 2.1	2.5	314.9 ± 4.5, n = 2; 295.8 ± 3.7, n = 3	Rodríguez et al. (2017)
GR–6643	Monzogranite	2° 53' 30.57"	76° 00' 28.91"	274.8 ± 2.3	1.9	304 ± 6.5, n = 1; 291.3 ± 3.1, n = 4	Rodríguez et al. (2017)
WR–290	Tonalite	2° 26' 10.30"	75° 54' 48.60"	274.8 ± 4.6	0.024	ca. 750	Leal–Mejía (2011)
				Ortega Pluton			
DV82	Granite	4° 17' 15.50"	75° 13' 59.20"	271.9 ± 3.7	1.2	309 to 299	Villagómez (2010)
10RC04	Metagranite	4° 19' 24.00"	75° 12' 07.00"	277.6 ± 1.6	1.2	Not reported	Cochrane (2013)
				Serranía de San Lucas			
Nechí Gneiss							
GN–1	Gneiss	8° 10' 13.00"	74° 46' 55.00"	277.3 ± 3.0	1.4		Restrepo et al. (2011)
NSE–1C	Migmatite gneiss	8° 09' 57.70"	74° 46' 43.00"	281.5 +4.4/–4.5		ca. 320	Leal–Mejía (2011)
Remedios							
12023251	Hornblende biotite diorite	6° 57' 27.50"	74° 32' 29.80"	274.5 ±5.3	0.67	ca. 1200–1000	Leal–Mejía (2011)
Puerto Nare							
WR–244	Hornblende granodiorite	6° 27' 11.90"	74° 38' 57.10"	262.9 ± 4.5	1.4	ca. 1200–1000; 600; 400	Leal–Mejía (2011)
				Sierra Nevada de Santa Marta			
Northern part of the Sierra Nevada de Santa Marta							
A14	Granitoid	11° 14' 26.23"	73° 47' 50.45"	288.1 ± 4.5	0.96	1210 ± 69; 800 ± 32; 730 ± 10; 615 ± 11	Cardona et al. (2010b)
A48	Granitoid	11° 14' 14.40"	73° 48' 32.56"	276.5 ± 5.1	1.8		Cardona et al. (2010b)
EAM–12–05	Mylonite	11° 14' 24.27"	73° 48' 23.99"	264.9 ± 5.1	0.0102	Significant amount: early Paleozoic and Grenvillian ages	Cardona et al. (2010b)
				Inner Santa Marta Metamorphic Belt			
MPR–33A	El Encanto Orthogneiss	11° 04' 13.58"	74° 04' 04.89"	274.8 ± 2.1		543 ± 14; 310–302	Piraquive (2017)
GLV–11	Garnet–mica schist	11° 01' 2.13"	74° 09' 59.11"	283.67 ± 6.1 (recrystallized rim over a Carboniferous core)		1. One zircon: 2235 ± 58 2. A Neoproterozoic population at 900–1200 3. Pan–African/Brasiliano 522–655 population 4. Four crystals: 463–284.2	Piraquive (2017)
MG–063	Gaira Schists (Hbl–Bt–Pl–Ms gneiss)	11° 14' 44.15"	73° 44' 26.56"	261.46 ± 2.6		Populations at around 950, 655–850, and 270. One age of ca. 468.9 ± 7.1	Piraquive (2017)

A continental volcanic arc developed in the previously described rock assemblage during the Early to Middle Jurassic and was active for approximately 30 Ma (Rodríguez et al., 2018). This arc is represented by volcanic units (Saldaña, Noreán, La Quinta, Guatapurí, and Golero Formations sensu Tschanz et al., 1969; Rodríguez et al., 2016); batholiths (Mocoa, Páez, Altamira, Algeciras, Norosí, and Pueblo Bello Batholiths sensu Hubach & Alvarado, 1932; Arango et al., 2015; Bogotá & Aluja, 1981; Rodríguez et al., 1998, 2015; Tschanz et al., 1969; Zapata et al., 2015); and smaller intrusive bodies (Figure 1).

2.1. Upper Magdalena Valley (UMV)

The Upper Magdalena Valley corresponds to a geographical division of the Magdalena River Valley, spanning from Honda, Tolima to the Magdalena River source, south of San Agustín, Huila between the Colombian Eastern and Central Cordilleras.

The UMV is underlain by a Neoproterozoic metamorphic basement that outcrops as tectonically uplifted blocks consisting of migmatites, granofels, granulites, anatectic granites, and gneisses, in granulite to high amphibolite facies, grouped in units such as the Garzón Group, Guapotón and Mancagua Gneisses, Las Minas Migmatites, and El Recreo Granite (Ibañez–Mejia et al., 2011, 2015; Jiménez–Mejía et al., 2006; Kroonenberg & Diederix, 1992; Rodríguez, 1995a, 1995b; Rodríguez et al., 2003; Velandia et al., 1996, 2001a, 2001b). Paleozoic sedimentary rocks, such as the Granadillo Limestones, La Jagua Paleozoic Group, El Hígado Formation, Cerro Neiva Sedimentary Rocks, La Batalla Limestones and Sandstones, and El Imán Formations (Cárdenas et al., 1998; Mojica et al., 1988; Núñez et al., 1984a; Stibane & Forero, 1969; Velandia et al., 1999, 2001b; Villarroel & Mojica, 1988), discordantly overlie the Neoproterozoic crystalline basement.

Permian arc granitoids (Figure 2), including La Plata Granite (Leal–Mejía, 2011; Rodríguez, 1995a; Rodríguez et al., 1998, 2017; Velandia et al., 2001a) and the southern Rovira Granitic Stocks (Cochrane, 2013; Núñez et al., 1984a; Villagómez, 2010) (Table 1), intruded the basement and the Paleozoic sedimentary rocks.

In early studies, La Plata Granite, previously termed “La Plata Massif” (Grosse, 1931; Rodríguez, 1995a) or “La Plata Orthogranite” (Velandia et al., 1999, 2001a, 2001b), was considered to be a high–grade metamorphic unit, primarily consisting of anatectic granites, migmatitic gneisses, amphibolites, and quartz–feldspar granulites, with a predominance of granites with homophonous and nebulitic structures (Rodríguez, 1995a; Velandia et al., 2001a, 2001b). However, Rodríguez et al. (2017), based on zircon morphologies and ages, suggest that these rocks belong to the roots of an extinct continental arc.

Triassic limestones and clastic sedimentites (Luisa and Payandé Formations) were deposited atop these previous units (Cediel et al., 1980; Geyer, 1973; Mojica, 1980; Núñez et al., 1984b), and Jurassic plutons and Lower to Middle Jurassic volcanic rocks (Rodríguez et al., 2018) (Figure 2) intruded and overlie the uplifted blocks delimited by thrust and strike–slip faults.

2.2. Serranía de San Lucas (SSL)

The serranía de San Lucas is northeast of the Central Cordillera and forms a rhombic N–S–trending tectonic block delimited by the Otú Fault to the west (separating it from the metamorphic basement of the Central Cordillera), recent Magdalena River deposits to the east, the Cimitarra Fault to the south, and the Espíritu Santo Fault to the north (Figures 1, 3).

This block consists of a Neoproterozoic metamorphic basement (the San Lucas Gneiss sensu Cuadros, 2012; Cuadros et al., 2014), including quartz–feldspar gneisses with amphibolite and marble lenses (Bogotá & Aluja, 1981; Feininger et al., 1972), locally covered by Paleozoic sedimentary rocks, represented by mudstones, claystones, limestones, shales, and sandstones of La Cristalina Formation (Botero, 1940; Feininger et al., 1972). These rocks are intruded by Carboniferous (Carmen Stock sensu Leal–Mejía, 2011), Permian (Nechí Gneiss and the diorite near Remedios) (Leal–Mejía, 2011; Restrepo et al., 2011; Rodríguez et al., 2014) (Figure 3; Table 1), and Lower Jurassic (Norosí Batholith sensu Ordóñez–Carmona et al., 2009; Leal–Mejía, 2011) arc plutons.

The Nechí Gneiss was initially described as the “Quartz Feldspar and Aluminous Gneiss” (González, 2001). Subsequently, it was renamed as the Nechí Gneiss (Restrepo et al., 2011) and the Metatonalitic Gneiss of the Nechí Facies (Leal–Mejía, 2011). This unit forms a 35 km long, 10 km wide strip to the east of the Nechí county (Figure 3). The unit consists of phaneritic, isotropic rocks with an igneous aspect that are white with black spots and have a medium–grained granular texture. They range between quartz diorite, tonalite, and granodiorite (Table 2) and include banded to locally folded rocks with centimeter–scale to decimeter–scale well–defined and diffuse bands. The rocks correspond to gneisses and quartz–feldspar granofels with amphibole and biotite or their igneous equivalents, such as meta–tonalites, meta–quartz diorites, and meta–granodiorites with gneissic and granofelsic structures (Rodríguez et al., 2014) (Figure 4). Rodríguez et al. (2014) identified plagioclase, alkali feldspar, quartz, hornblende, zircon, and allanite to be igneous minerals inherited from the protolith. The quartz, plagioclase, biotite, epidote, sphene, and apatite are metamorphic minerals (Table 2) that define the gneissic structure of the rock. This unit corresponds to an igneous body affected by ductile dynamic metamorphism in low amphibolite facies with non–penetrative schistosity

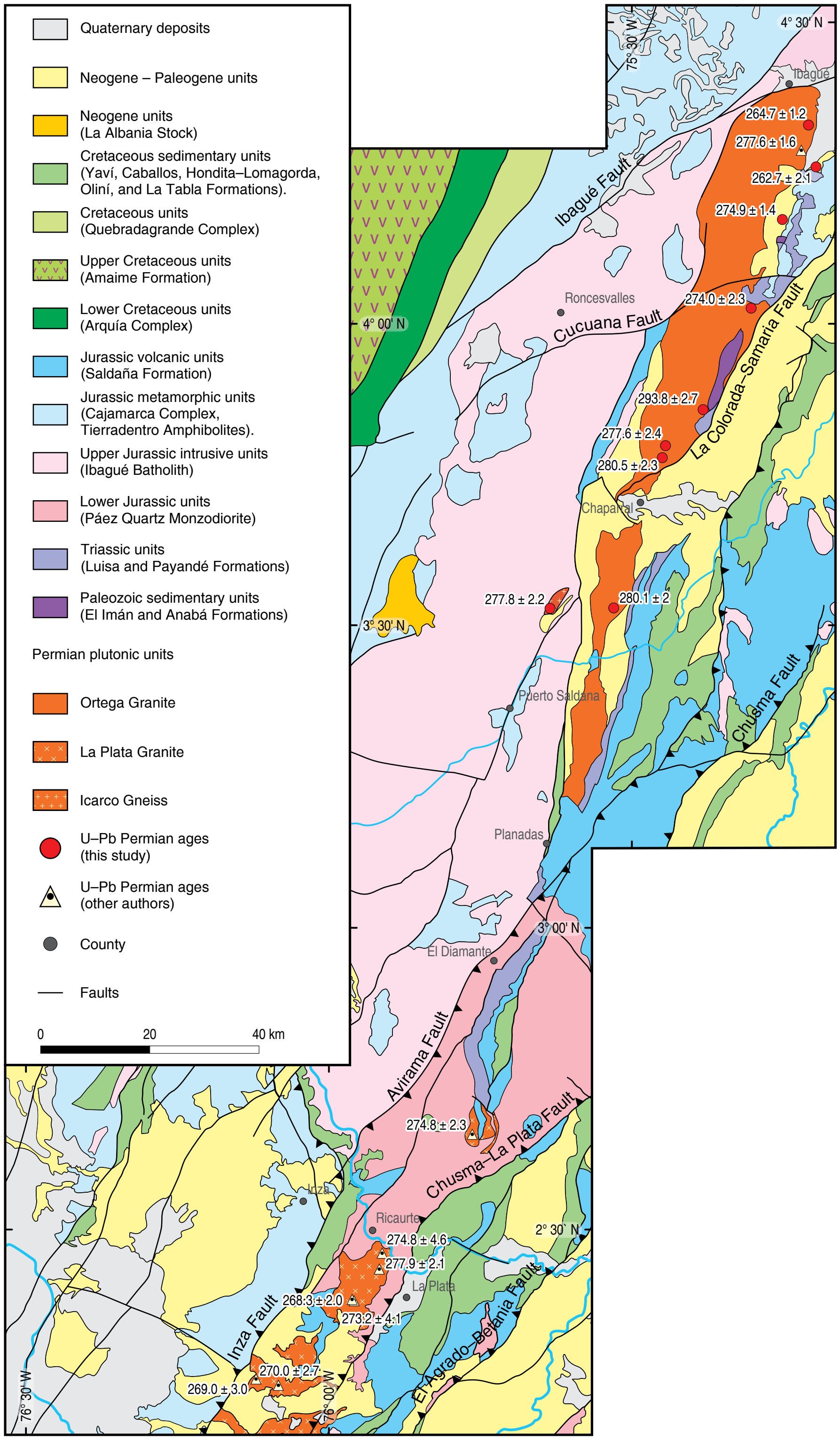

Figure 2. Geology and location of the Permian plutons in the Upper Magdalena Valley (UMV) and on the eastern slope of the Colombian Central Andes. Simplified from Gómez et al. (2015a). Data source: U–Pb zircon ages from Cochrane et al. (2014), Gómez et al. (2015b), Leal–Mejía (2011), Rodríguez et al. (2017), Villagómez (2010), and this study.

(Rodríguez et al., 2014). According to Restrepo et al. (2011), the unit has a Permian crystallization age and a Triassic metamorphic age.

The entire assemblage is covered by Lower Jurassic volcano–sedimentary successions grouped as the Noreán Formation (Clavijo, 1995; Royero, 1996), Mesozoic sedimentary and vol-

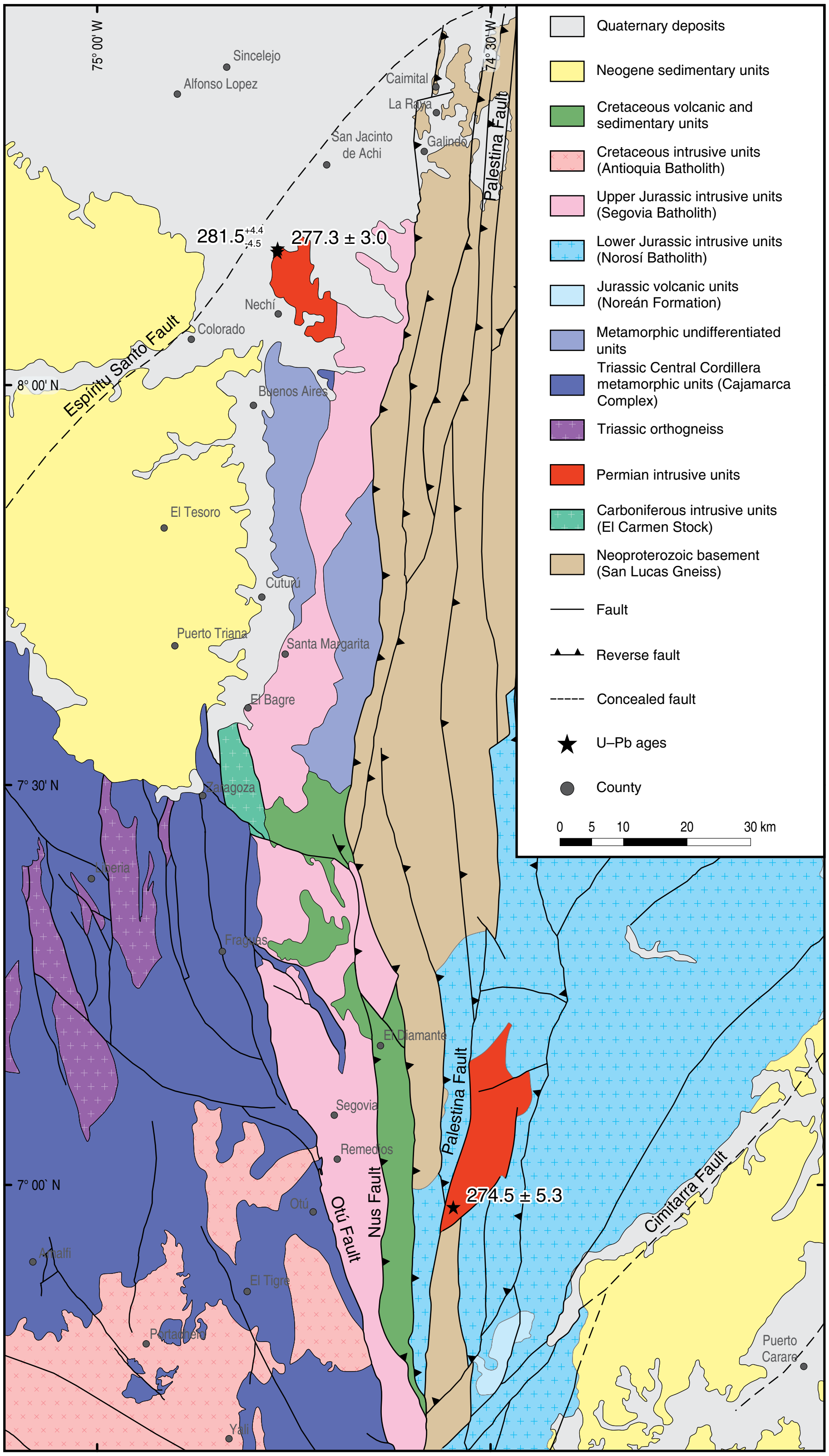

Figure 3. Geology and location of Permian plutons in the serranía de San Lucas and distribution of the U–Pb ages. Taken from Gómez et al. (2015a).

Table 2. Modal composition of rocks from the Nechí Pluton.

Sample	Latitude N	Longitude W	Qtz	Pl	Kfs	Hbl	Bt	Op	Ap	Zrn	Ttn	Ep	Petrographic classification
900563	8° 10’ 12.46”	74° 46’ 33.67”	26.7	34.2	0	22.6	11	0.6	Tr		2	2.9	Pl, Qtz, Hbl, Bt with Ttn gneiss
900584	8° 07’ 34.19”	74° 45’ 45.61”	23.8	49	13.2	4.6	6			Tr	1	2.4	Pl, Qtz, Kfs with Bt and Hbl gneiss
900585	8° 07’ 50.83”	74° 46’ 02.66”	17.2	36.6	4.8	13.8	14.5	Tr	Tr		3	10.1	Pl, Qtz, Bt, Hbl, and Ep gneiss
900586	8° 07’ 50.83”	74° 46’ 02.66”	18.8	44.4	0.7	0.7	20.8	Tr	Tr	Tr	1.4	13.2	Pl, Bt, Qtz, Ep gneiss
900588	8° 07’ 35.52”	74° 45’ 51.49”	39	28.1	3.1	20.1	7.9	Tr	Tr	Tr	1	0.8	Pl, Qtz, Hbl, Bt with Kfs gneiss
900589	8° 10’ 01.21”	74° 46’ 25.39”	12.1	56.4	0	5	7.1	0.7			4	14.7	Pl, Qtz, Hbl, Ep, Bt gneiss
900590	8° 10’ 01.21”	74° 46’ 25.39”	19.4	46.9	3.3	16.7	3.7	0.8			1	8.2	Pl, Qtz, Ep, Bt, Hbl with Ttn gneiss
SCC–21*	8° 07’ 02.88”	74° 45’ 48.27”	20	40	0	20	20					Tr	Quartz diorite
SMC–8*	8° 06’ 49.43”	74° 45’ 51.19”	10	20	15	30	20					4	Qtz, Pl with Bt gneiss
SMC–17*	8° 06’ 55.62”	74° 45’ 49.66”	25	20	10	10	25					5	Qtz, Pl with Hbl and Bt gneiss
JC011–G*	8° 07’ 34.90”	74° 45’ 51.46”	38	25	20		15					Tr	Qtz, Pl with Bt gneiss
JC011–X*	8° 07’ 34.90”	74° 45’ 51.46”	20	10		65	5				Tr	Tr	Hornblende gneiss
MI–4*	8° 08’ 42.72”	74° 45’ 56.28”	25	45	15		10					2	Granodiorite
JC021*	8° 07’ 02.88”	74° 45’ 48.27”	20	53		10	15					2	Tonalite
NPM–1*	8° 07’ 26.96”	74° 45’ 48.54”	10	50		40						Tr	Quartz diorite
NSE–1*	8° 09’ 57.74”	74° 46’ 57.72”	30		40		20					10	Migmatite granulite
NSE–2*	8° 08’ 41.35”	74° 46’ 01.60”	15	10	25	25	25				Tr	Tr	Quartz–feldspar gneiss

Source: Data from Rodríguez et al. (2014).
*Data from Montoya & Ordóñez–Carmona (2010).
Tr: Traces of accessory mineral.

cano–sedimentary successions and Cenozoic alluvial deposits near the edges of the block (Figure 3).

2.3. Sierra Nevada de Santa Marta (SNSM)

The Sierra Nevada de Santa Marta is a triangular block in northern Colombia, delimited by the Santa Marta–Bucaramanga Fault to the southwest, the Oca Fault to the north, and Cesar Ranchería Basin to the northeast (Figures 1, 5).

Its metamorphic basement comprises the Neoproterozoic Los Mangos Granulite and Buritaca Gneiss consisting of gneisses, anorthositic gneisses, amphibolites, anatectic granitoids, and migmatites in granulite to amphibolite facies (Ibañez–Mejia et al., 2011; Ordóñez–Carmona et al., 2002; Piraquive, 2017; Tschanz et al., 1969, 1974). These are discordantly covered by Paleozoic sedimentary units (Tschanz et al., 1969).

To the northwest, the basement is in faulted contact with the Muchachitos Gneiss and San Lorenzo Schists (Tschanz et al., 1969, 1974) of Late Jurassic age (Piraquive, 2017) (Figure 5). In addition, gabbro bodies (Tschanz et al., 1969) and Permian mylonitic granitoids, such as El Encanto Orthogneiss (Cardona et al., 2010b; Piraquive, 2017) (Table 1), are deformed and associated with the aforementioned Upper Jurassic metamorphic rocks.

The mylonitic granitoids of Valencia Creek in the Sierra Nevada de Santa Marta were described by Cardona et al. (2010b) as a body of mylonites and protomylonites that formed from quartz–feldspar rocks. Piraquive (2017) described a new unit termed El Encanto Orthogneiss (Figure 5) that includes the mylonites identified by Cardona et al. (2010b). El Encanto Orthogneiss consists of coarse–grained phaneritic rocks with amphibole bands, plagioclase, and ductilely deformed quartz veins. The unit includes mylonites and protomylonites with K–feldspar porphyroclasts (5–40 %), plagioclase (10–40 %), and biotite (<5%) surrounded by a matrix that formed during deformation and crystallization, consisting

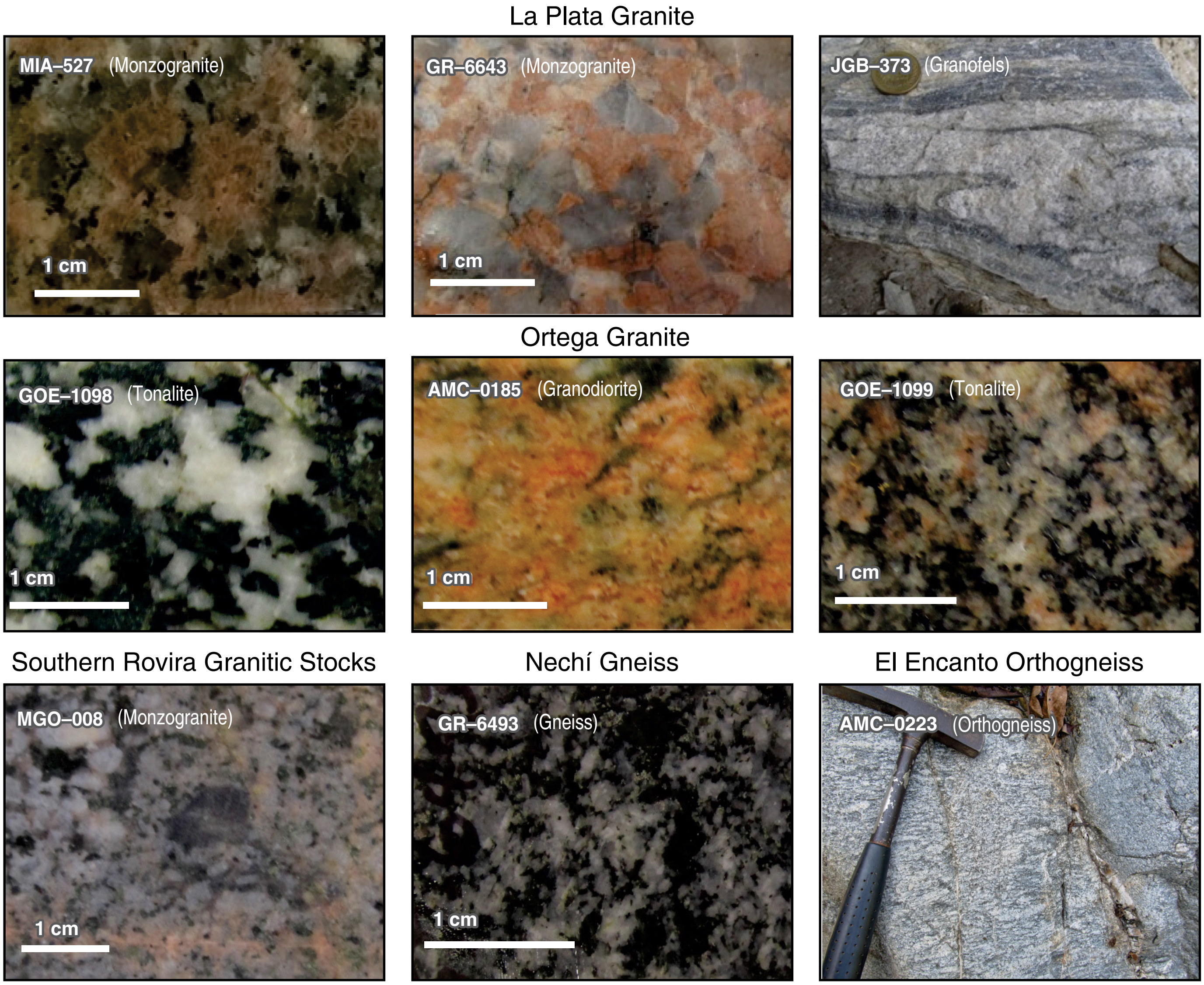

Figure 4. Macroscopic view of Permian bodies: La Plata Granite, Ortega Granite, southern Rovira Granitic Stocks, Nechí Gneiss, and El Encanto Orthogneiss.

of muscovite (5–25 %), biotite (10–30 %), quartz (20–40 %), epidote (3–20 %), chlorite, and titanite. The primary accessory minerals are zircon, titanite, apatite, and opaque minerals (Cardona et al., 2010b).

Jurassic batholiths of monzodioritic to monzogranitic composition and smaller bodies of dacitic and rhyolitic porphyries intrude the Precambrian and Paleozoic units. These are overlain by Lower to Middle Jurassic volcanic and pyroclastic rocks (Tschanz et al., 1969).

West of the Jurassic metamorphic rocks, the SNSM is formed by Upper Cretaceous to Paleogene metamorphic belts (Bustamante et al., 2009; Mora et al., 2017; Tschanz et al., 1969, 1974; Zuluaga & Stowell, 2012). Both metamorphic belts are separated by the Eocene Santa Marta Batholith (Duque–Trujillo, 2009; Tschanz et al., 1974).

2.4. Methods and Analytical Procedures

Regional cartographic studies and published articles were compiled to analyze the Permian magmatism of the UMV, SSL, and SNSM. Field control, rock sampling, petrographic, geochemical, and geochronological analyses were performed on samples collected along the eastern slope of the Central Cordillera and the UMV between Ibagué and Planadas (Figure 2). Finally, the analyses and interpretation of the results were completed including information from all tectonic blocks.

3. Petrography

All of the thin sections were analyzed using a Leitz petrographic microscope under polarized light. Mineralogical counting

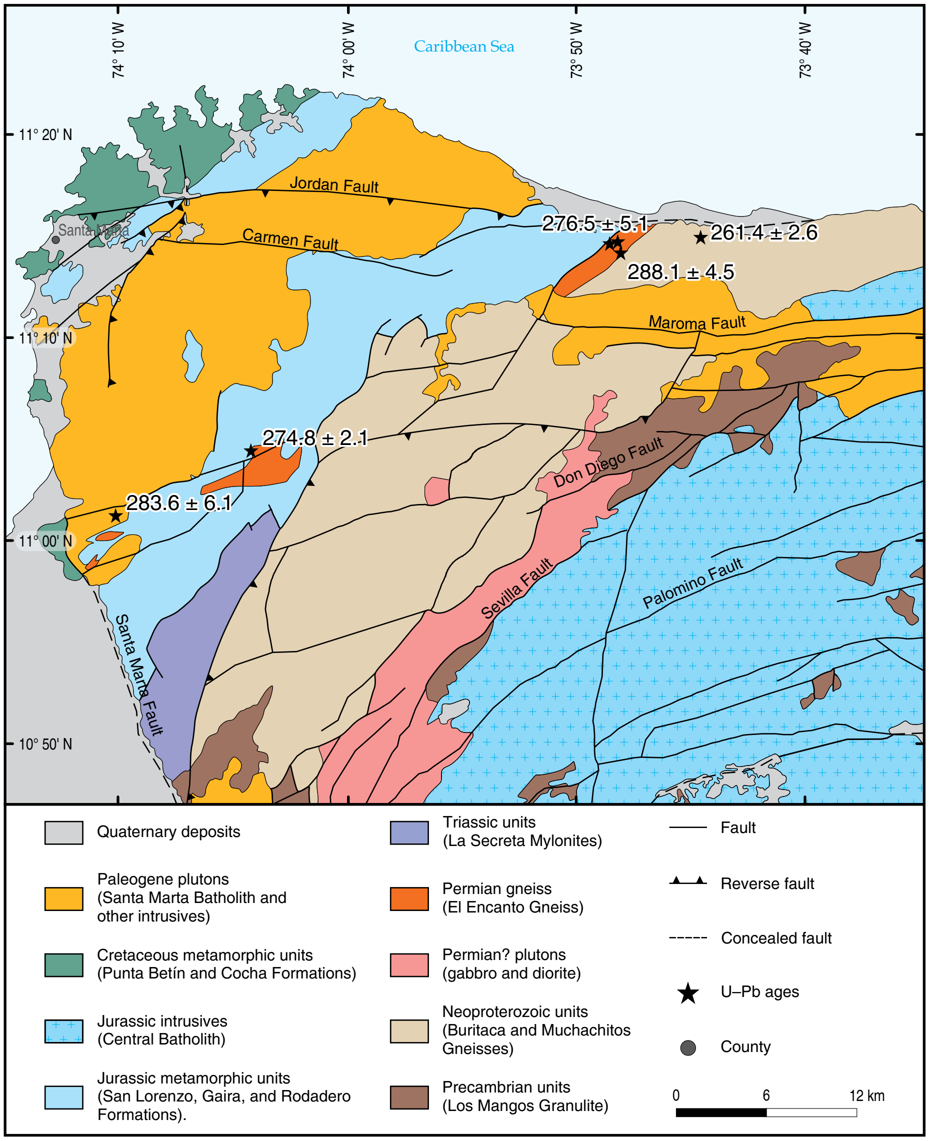

Figure 5. Geology and location of Permian plutons in the Sierra Nevada de Santa Marta and distribution of the U–Pb ages. Taken from Piraquive (2017).

was completed at 300 points per sample, identifying the primary and secondary minerals. Rocks were classified following Streckeisen (1974, 1979) considering the recommendations from Le Maitre (2002).

4. Lithogeochemistry

Whole rock geochemical analyses were performed at the laboratory of the SGC in Bogotá. Major oxides were determined using X–ray fluorescence in an analytical AXIOS Mineral spectrometer, including trace elements such as V, Mo, Nb, Ta, W, Zr, and Hf. MRC–GSR–2 and MRC–BHVO–2 were used as standards. Some elemental concentrations, such as those for Hf and Ta, were less than the detection limit of the device and are therefore not reported in the tables. Major oxides were quantified in a sample fused with lithium metaborate and tetraborate, and minor elements were quantified in a pressed sample. To interpret the major oxides, the values were recalculated considering the loss on ignition (LOI).

Trace elements were measured with inductively coupled plasma mass spectrometry (ICP–MS) using a Perkin Elmer NEXION mass spectrometer and the AGV–2 standard. The samples were gradually dissolved in strong inorganic acids (HF, HNO_3, $HClO_4$, and HCl). The process was conducted in an open system using various temperature ramps and heating times.

5. U–Pb Zircon Geochronology

U–Pb zircon dating of most samples was performed at the Laser Ablation Laboratory of the SGC. One sample (AMC–

0159A) was analyzed at the Isotopic Studies Laboratory at the Geosciences Center of the Universidad Nacional Autónoma de México (UNAM).

The concentration of zircons was obtained by panning and using a Frantz magnetic separator. Cathodoluminescence (CL) images of the crystals were acquired before isotopic analysis in the Laser Ablation Laboratory of the SGC. Some samples were photographed at the Lithological Characterization Laboratory of the Universidad Nacional de Colombia using a CITL CL8200 MK–5 adapted to a Leica DM 2500P petrographic microscope. Secondary and backscattered scanning electron microscopy – cathodoluminescence images of other samples were acquired using a JEOL scanning electron microscope, model JSM IT–300LV, equipped with secondary (SED) and backscattered (BED) electron and energy dispersive X–ray spectroscopy (EDS, OXFORD 51–XMX 1181) and cathodoluminescence (CL, Gatan miniCL EGA 0028) detectors.

Isotopic analysis was performed at the Laser Ablation Laboratory of the SGC using an inductively coupled plasma mass spectrometer ELEMENT 2™ coupled to a laser ablation system photon machines with a 193–nm excitation laser. Integration times of 0–38 s were used for the baseline, whereas integration times of 32.5–8 s were used for the samples and reference standards. The ablation points were 30 µm in diameter, and Plešovice (337.13 ± 0.37 Ma; Sláma et al., 2008), 91500 (1065 Ma; Wiedenbeck et al., 1995) and M. Dromedary (99.12 ± 0.14 Ma; Schoene et al., 2006) were used as reference standards. Data reduction was performed using the software Iolite Igor Pro, and the results were corrected for common lead according to the model of Stacey & Kramers (1975). Discordance was evaluated based on the differential between the $^{206}Pb/^{238}U$ and the $^{207}Pb/^{235}U$ ages. The sample ages were calculated using the weighted mean values of the $^{206}Pb/^{238}U$ ages for crystals <800 Ma and $^{207}Pb/^{206}Pb$ ages for crystals >800 Ma. Final results are presented discriminating to two standard deviations and plotted in Isoplot (Ludwig, 2012).

At the UNAM laboratory, zircon cathodoluminescence images were acquired using an ELM–3R luminoscope (Marshall, 1988). U–Pb isotopic analyses of zircons were performed using the laser ablation method (LA–ICP–MS) with a "Resonetics" laser, model Resolution M50, consisting of a 193 nm wavelength excimer laser LPX 220 coupled to a quadruple mass spectrometer (ICP–MS) "Thermo X–Series." The diameter of the laser beam was 23 µm. The zircon concentrations of Th, Si, P, Ti, Y, Zr, Nb, Hf, and rare earth elements (REEs) were measured during the analyses. A glass standard (NIST 610) and two natural zircon standards, a primary (91500; Wiedenbeck et al., 1995) and a secondary (Plešovice; Sláma et al., 2008), were intercalated in the analytical sequences for quality control. Methodological details are described in Solari et al. (2010).

6. Results

The Permian units described in the following phrase are geographically organized from south to north: La Plata Granite, Ortega Granite (new unit), southern Rovira Granitic Stocks (Upper Magdalena Valley and eastern slope of the Central Cordillera), Nechí Gneiss (serranía de San Lucas), and mylonitic granitoids–El Encanto Orthogneiss (Sierra Nevada de Santa Marta).

6.1. Macroscopic and Microscopic Characteristics

Forty–three igneous plutonic rocks (24 of the Ortega Granite and 19 of the southern Rovira Granitic Stocks) were studied. Table 3 presents the mineral counting of all samples analyzed. Figure 4 includes the macroscopic characteristics of the rocks present in the Permian units and Figure 6 their classification in the diagram by Streckeisen (1979).

6.1.1. Upper Magdalena Valley (UMV)

The Icarco Complex consists of amphibolites, amphibolic gneisses, feldspar–quartz gneisses, and migmatitic rocks with igneous protoliths that are considered Precambrian based on their lithological similarities to the Garzón Massif (Murillo et al., 1982). However, within this unit, Permian granitoids were identified during the present study. These occurrences were associated in the geological mapping to the Ibagué Batholith, but based on our recent findings, they are related to the Ortega Granite.

The Ortega Granite is proposed as a new unit based on its compositional and geochronological differences compared to the Upper Jurassic Ibagué Batholith (Carvajal et al., 1993; Esquivel et al., 1991; Gómez et al., 1999; Mosquera et al., 1982; Nelson, 1957; Núñez & Murillo, 1982; Núñez et al., 1984a, 1984b; Vesga & Barrero, 1978). The body is on the eastern slope of the Central Cordillera and Upper Magdalena Valley, from south of Chaparral to the Ibagué Fault to the north, between La Colorada–Samaria Fault to the east and the Avirama Fault (Figure 2) (also termed La Soledad Fault farther north) to the west.

The Ortega Granite is a heterogeneous intrusive body that consists of quartz monzodiorites, monzonites, tonalites, granodiorites, monzogranites, and rare syenogranites that are macroscopically either pink with black and white spots or white with black spots, with a predominantly granular texture and medium grain size (Figures 4, 6). It consists of quartz, plagioclase, alkali feldspar, biotite, and hornblende in addition to opaque minerals, apatite, zircon, and epidote as accessory minerals (Table 3). It locally shows microdioritic enclaves, and is intruded by andesitic, dacitic, rhyolitic, and granitic dikes; epidote veins

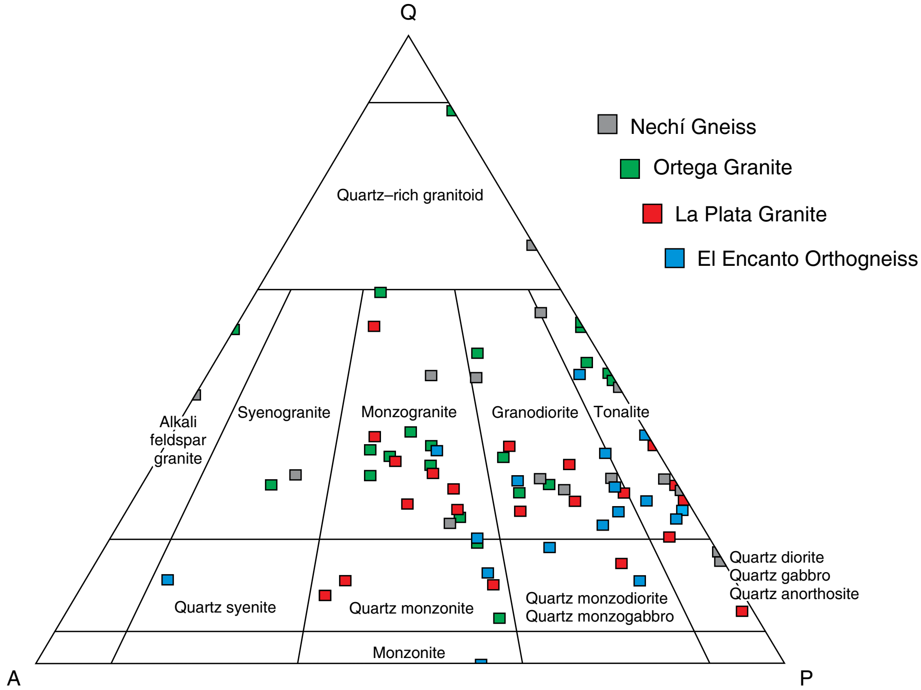

Figure 6. Modal composition of Permian granitoids in the Streckeisen triangle (1974), specified for La Plata Granite (red), Ortega Granite (green), Nechí Gneiss (gray), and El Encanto Orthogneiss (blue). Sources: Montoya & Ordóñez–Carmona (2010), Piraquive (2017), Rodríguez (1995a), Rodríguez et al. (2014, 2017).

with associated pink potassium alterations; calcite veinlets; and granitic–pegmatitic dikes.

Northeast of the Ortega Granite, Núñez et al. (1984a) defined the southern Rovira Granitic Stocks that correspond to a long intrusive body, consisting of quartz monzodiorites, quartz monzonites, monzonites, granodiorites, tonalites, and rare alkali feldspar syenites (Figure 4; Table 3). The rocks are pink or pink with black and white spots, holocrystalline, have a granular texture (Figure 4), and consist of quartz, plagioclase, alkali feldspar, biotite, and occasionally hornblende in addition to opaque, apatite, zircon, and epidote as accessory minerals (Table 3). The plutons, considered of Permian age based on their stratigraphic relations, intrude El Imán Formation (Middle Devonian) and are discordantly overlain by the Luisa (Permian – Triassic?), Payandé (Upper Triassic), and Saldaña (Lower Jurassic) Formations (Núñez et al., 1984a). These stocks are included in the Ortega Granite unit.

6.2. Geochemistry

Thirty–seven samples from La Plata Granite (red; Rodríguez et al., 2017), Ortega Granite (green), Nechí Gneiss (gray; Rodríguez et al., 2014), and mylonitic intrusions of El Encanto Orthogneiss (blue; Cardona et al., 2010b, Piraquive, 2017) were analyzed and reinterpreted (Figure 7; Table 4).

In the diagram by Middlemost (1994) (Figure 7a), the samples correspond to granites, quartz monzonites, gabbrodiorites, monzonites, and diorites similar to their petrographic classifications. The analyzed rocks have LOI values <3% that suggest low alteration, as is corroborated by the petrography, except for samples 901724 and 901725 (3.61 wt % and 4.50 wt %).

The samples from the Ortega Granite show a SiO_2 content ranging from 56.77 to 72.41 wt %, Al_2O_3 content from 14.04 to 18.80 wt %, and MgO content from 0.81 to 4.01 wt %. The Mg# (100 × MgO/(MgO + Fe_2O_3)) ranges from 26.64 to 38.42. The LOI values range from 0.64 to 4.5 wt %. The SiO_2 content of the samples from La Plata Granite ranges from 58.92 to 77.39 wt %, Al_2O_3 content from 12.14 to 16.74 wt %, and MgO content from 0.10 to 3.10 wt %. The Mg# ranges from 12.20 to 31.57. The LOI values range from 0.25 to 1.06 wt % (Table 4).

In the samples from the Nechí Gneiss, the SiO_2 content ranges from 57.58 to 64.26 wt %, Al_2O_3 content from 14.98 to 16.52 wt %, and MgO content from 2.48 to 3.60 wt %. The #MgO ranges from 31.72 to 33.88. The LOI values range from 0.72 to 1.38 wt %. The samples from El Encanto Orthogneiss show a SiO_2 content ranging from 58.87 to 76.26 wt %, Al_2O_3 content from 11.83 to 17.60 wt %, and MgO content from 0.31 to 3.03 wt %. The Mg# ranges from 11.30 to 32.00 wt %. The LOI values range from 0.9 to 3.7 wt % (Table 5).

The AFM diagram (Figure 7b) shows that most samples plot within the field of the calc–alkaline series, except for sample A12, which is a granitic mylonite of El Encanto Orthogneiss. Figure 7c shows that regardless of the rock type and tectonic block location of the sample, the rocks show characteristics ranging

Table 3. Modal composition of Permian bodies in the Upper Magdalena Valley (UMV) and on the eastern slope of the Central Andes.

IGM	Sample	Latitude N	Longitude W	Qtz	Pl	Kfs	Hbl	Bt	Op	Ap	Zrn	Ttn	Ep	Others	Petrographic classification
							Ortega Granite								
901723	GR–6869	4° 02’ 39.12”	75° 18’ 04.65”	7.2	78.7	1.3		12.2	0.6	Tr	Tr				Quartz diorite
157749	AN–1354	3° 37’ 13.80”	75° 33’ 22.39”	12.6	55.9	10.8	9	10.8	0.9	Tr	Tr	Tr			Quartz monzodiorite
901714	GOE–1102	3° 44’ 20.31”	75° 31’ 40.72”	9	28.1	47.2		5.6					9	1.1	Quartz monzonite
157773	GTJ–145	3° 39’ 26.23”	75° 33’ 37.51”	8.5	38	22.5	5	12	2.5	2	1	6.5	2		Quartz monzonite
20782	PM–3872	4° 03’ 11.10”	75° 16’ 46.65”	10.8	29.4	43.2	8.8	6.8	Tr	Tr	Tr				Quartz monzonite
901052	AMC–0157A	4° 03’ 23.83”	75° 21’ 16.01”	27	36	15	6	16	Tr	Tr	Tr				Granodiorite
901699	AMC–0185	3° 53’ 02.51”	75° 22’ 34.16”	31	55	12.5		1.5			Tr				Granodiorite
901709	GOE–1096	4° 02’ 59.10”	75° 18’ 08.18”	17.7	40.5	10.1		19	3.8		5.1	2.5		1.3	Granodiorite
20761	DMT–3585	4° 13’ 50.59”	75° 15’ 56.87”	21	46	20	3	10	Tr	Tr					Granodiorite
901712	GOE–1100	3° 32’ 13.34”	75° 39’ 00.41”	14.8	37.5		19.3	20.5	4.5	1			2.3		Meta–Tonalite
157753	AN–1391	3° 33’ 36.61”	75° 34’ 31.04”	22.9	29	24	3.43	6.87	2.67	5.72	1.14	3.05		1.14	Monzogranite
901062	GOE–1008	4° 17’ 43.16”	75° 15’ 49.19”	18.9	18.48	20.6	22.2	6.72	4.42	5.04	1.68				Monzogranite
901727	GR–6874	3° 32’ 55.33”	75° 39’ 46.92”	22.1	40.7	28.5	5.2	2.9	0.6	Tr	Tr				Monzogranite
77164	HC–840	3° 32’ 24.05”	75° 37’ 39.43”	25.9	19.8	26.5	14.1	6.7	2.35	2	0.33	1.34	0.67		Monzogranite
77165	HC–841	3° 32’ 42.38”	75° 39’ 52.25”	41.4	14.2	21.3	8.36	7.9	2.09	1.67	0.4	1.67	0.83		Monzogranite
20757	PM–3612	4° 13’ 50.66”	75° 16’ 57.66”	23	35	25	9	8	Tz						Monzogranite
20787	PM–3555	4° 12’ 32.98”	75° 13’ 52.75”		49	33		8.2	3.8	3.6	2.2	1	Tr		Monzonite
901104	MIG–083	4° 11’ 56.98”	75° 19’ 34.20”	17.3	82.7			Tr					Tr		Plagiogranite?
157756	DF–86	3° 31’ 09.08”	75° 35’ 32.66”	16.6	24.1	24.5	4.1	18.3	2.5	6.25	1.6				Syenogranite
901710	GOE–1098	3° 48’ 40.05”	75° 26’ 28.00”	14.3	40.3		13	18.2		2.6		7.8	3.9		Tonalite
901711	GOE–1099	3° 33’ 27.23”	75° 30’ 52.48”	20.5	47.7			20.5	4.5	1.1	5.7				Tonalite
901724	GR–6871	3° 47’ 13.25”	75° 27’26.51”	23.5	56.6	6.7	0.6	12.6	Tr	Tr	Tr				Tonalite
901725	GR–6872A	3° 50’ 03.73”	75° 26’ 05.77”	15	55.6	3.9	7.2	17	0.7	Tr	Tr	0.6			Tonalite
20753	PM–3546	4° 12’ 28.26”	75° 17’ 32.71”	31	59			10	Tr				Tr		Tonalite
							Southern Rovira Granitic Stocks								
20736	AC–549	4° 06’ 29.29”	75°15’15.69”	25	43	18		11	Tr	Tr	Tr	4			Granodiorite
23553	Pm–4398	4° 07’ 30.63”	75° 15’ 25.35”	10.1	57.8	9.8	13.8	3.7	0.9	Tr	Tr	Tr		3.7	Quartz monzodiorite
23552	Pm–4374	4° 08’ 05.83”	75° 14’ 55.74”	16.5	53.5	19.7	7.1	1.6	0.8	Tr	Tr	0.8			Quartz monzodiorite
23544	AC–1041–A	4° 06’ 44.48”	75° 14’ 39.09”	13.8	50	30		6.2	Tr		1				Quartz monzonite
23566	DBL–3020A	4° 06’ 15.39”	75° 15’ 59.60”	10.9	41.8	25.1		7.94		2.09			12.1		Quartz monzonite
20763	DMT–3605	4° 11’ 53.90”	75° 14’ 08.58”	17	43	27		9	4				Tr		Quartz monzonite
901055	AMC–0159A	4° 11’ 35.20”	75° 13’ 58.21”	20	53.5	4	6	15	1	0.5	Tr				Dacite
23554	PM–4423	4° 07’ 41.40”	75° 15’ 07.37”	21.1	47.8	6.31	3.15		6.31	1.57	0.52	2.1	1.05		Granodiorite
20781	PM–3846	4° 04’ 52.02”	75° 16’ 35.78”	22	60	9			4	1	1				Granodiorite
23540	AC–971	4° 07’ 23.17”	75° 15’ 10.26”	17	50	10	6	8							Monzodiorite
901096	MGOQ–008	4° 17’ 26.69”	75° 11’ 28.03”	25	27	22	13	11	2		Tr		Tr		Monzogranite
20787	PM–3555	4° 12’ 32.98”	75° 13’ 52.75”		49	33		8.2	3.8	3.6	2.2	1	Tr		Monzonite
20768	PM–3636	4° 10’ 20.56”	75° 15’ 08.25”	4.94	4.18	28.1		16	7.99	0.19	0.38		0.9		Hypersthene syenite
23557	Pm–4469	4° 06’ 40.19”	75° 15’ 16.20”	18	55	1		18	1.4	2	2	0.5			Tonalite
23558	PM–4476	4° 06’ 48.02”	75° 15’ 09.08”	14.2	45.4	1.53	20	5.5	4	2.5	1.5	2.2			Tonalite
23550	PM–4345	4° 07’ 56.36”	75° 15’ 13.39”	22.4	51.7			10.3	4.3	4	1.72		2.89		Tonalite
23551	Pm–4361	4° 08’ 00.28”	75° 15’ 06.91”	37.2	40.1	3.22	4.3	2.5	5.01	2.15	0.71		1.07		Tonalite
20772	PM–3669	4° 08’ 56.63”	75° 14’ 40.25”	19.1	34	4		3	4.2	Tr	Tr	2.6	17.8	14.9	Tonalite
20722	AC–469	4° 05’ 36.65”	75° 16’ 06.51”	30	52			17	1				Tr		Tonalite

Tr: Traces of accessory mineral.

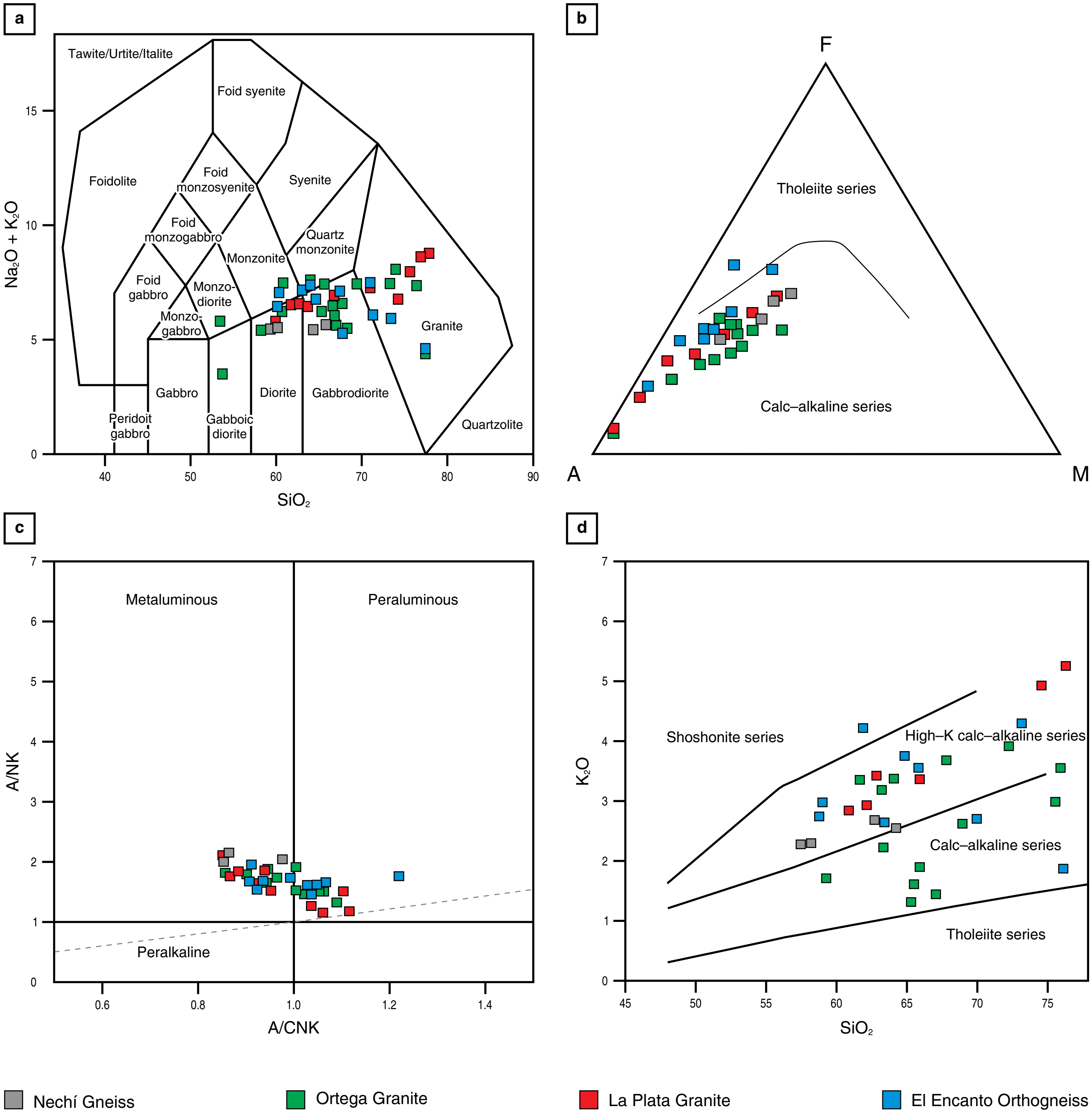

Figure 7. Classification and discrimination diagrams for Permian granitoids: **(a)** Total Alkali versus Silica (TAS) diagram by Middlemost (1994), **(b)** AFM (A (Al_2O_3 – $3K_2O$), F (FeO – TiO_2 – Fe_2O_3), and M (MgO)) diagram (Irvine & Baragar, 1971), **(c)** Alumina saturation index diagram by Shand (1943), and **(d)** Alkalinity index diagram by Peccerillo & Taylor (1976) for La Plata Granite (red), Ortega Granite (green), Nechí Gneiss (gray), and El Encanto Orthogneiss (blue). Data sources: Cardona et al. (2010b), Piraquive (2017), Rodríguez et al. (2014, 2017), and this study.

from metaluminous ($Al_2O_3 > CaO + Na_2O + K_2O$) to peraluminous ($Al_2O_3 > CaO + Na_2O + K_2O$), except for the rocks from the Nechí block that clearly show a metaluminous character.

The Peccerillo & Taylor (1976) diagram (Figure 7d) shows that the samples belong to the calc–alkaline and high–K calc–alkaline series.

The N–MORB–normalized (Sun & McDonough, 1989) samples from La Plata Granite, Ortega Granite, Nechí Gneiss, and El Encanto Orthogneiss show similar patterns of enrichment in large–ion lithophile elements (LILEs) more so than high field strength elements (HFSEs) and rare earth elements (REEs). An exception is El Encanto Orthogneiss in which

Table 4. Major and trace elements of samples from La Plata Granite (retrieved from Rodríguez et al., 2017) and Ortega Granite (this study).

Sample	900724	900729	900806	900802	900807	900732	900723	900739	900770	900800	901049	901050	901054	901055	901062	901077	901087	901096	901709	901710	901711	901712	901714	901723	901724	901725	901727
wt %	La Plata Granite										Ortega Granite																
SiO_2	77.39	76.56	74.76	62.18	66.05	62.88	73.34	58.92	69.80	60.85	72.41	63.43	67.99	61.88	67.14	69.03	63.32	64.16	60.43	56.96	64.34	60.95	65.97	58.89	61.99	56.77	67.00
Al_2O_3	12.14	13.18	13.26	16.11	15.45	16.03	13.13	16.74	14.72	16.50	14.04	15.71	14.94	16.06	15.93	15.47	15.71	16.03	18.56	18.18	17.72	16.22	14.81	18.80	15.94	15.58	14.73
Fe_2O_3	0.68	0.72	1.58	5.59	4.24	5.61	2.43	6.72	3.21	5.98	2.23	4.46	3.20	5.34	3.19	2.80	4.85	4.87	5.18	5.98	4.02	6.34	3.94	5.83	4.95	7.89	4.02
MgO	0.10	0.10	0.30	2.38	1.69	2.51	0.43	3.10	1.11	2.46	0.81	2.50	1.78	2.17	1.99	1.33	1.92	1.90	1.50	3.03	0.99	2.84	1.65	1.60	2.46	4.01	2.04
CaO	0.32	0.14	1.08	4.87	3.84	4.44	2.67	6.20	1.86	5.00	1.27	3.88	2.33	2.50	4.04	2.21	2.74	2.84	2.94	5.83	3.06	5.46	3.22	3.12	3.74	4.27	3.92
Na_2O	1.83	3.54	3.31	3.89	3.69	3.21	2.50	3.21	3.31	3.82	3.82	4.09	3.84	4.30	4.17	4.64	4.16	4.30	5.29	4.27	4.67	3.74	4.04	5.75	3.95	3.68	3.25
K_2O	7.21	5.27	4.90	2.90	3.37	3.40	4.33	2.73	4.09	2.82	3.90	2.23	3.69	3.35	1.46	2.62	3.17	3.35	2.84	2.10	3.24	1.73	3.21	2.13	2.22	1.64	3.54
TiO_2	0.11	0.15	0.20	0.83	0.61	0.73	0.13	0.85	0.47	0.82	0.33	0.67	0.52	0.80	0.45	0.38	0.72	0.72	0.73	0.86	0.56	0.76	0.60	0.70	0.67	1.07	0.58
P_2O_5	0.02	0.02	0.05	0.34	0.21	0.20	0.06	0.26	0.16	0.34	0.08	0.16	0.15	0.31	0.14	0.11	0.28	0.28	0.27	0.28	0.18	0.21	0.17	0.27	0.18	0.33	0.14
LOI	0.25	0.44	0.44	0.57	0.58	0.73	0.80	0.90	1.00	1.06	0.98	2.62	1.41	3.02	1.37	1.15	2.81	1.24	1.84	2.25	0.82	1.45	2.22	2.53	3.61	4.50	0.64
ppm																											
Ba	253.81	217.16	748.40	1165.91	1047.58	754.58	683.79	917.29	816.96	1205.15	868.88	648.91	828.01	872.47	432.33	1579.59	1044.35	1186.88									
Cs	5.29	2.23	4.17	2.62	3.22	5.05	3.21	3.26	5.49	3.32	0.89	0.95	1.98	2.76	0.63	1.35	1.53	1.68									
Co	7.75	8.77	9.91	20.96	16.16	20.83	18.51	21.84	16.05	20.84	14.47	17.54	16.09	19.31	19.76	19.00	18.03	19.50									
Sc	0.34	2.43	3.70	16.14	12.49	16.53	4.97	20.75	9.04	17.19	8.88	19.49	13.87	14.36	11.55	9.93	13.02	13.90									
Ga	11.84	14.78	14.95	23.02	22.26	19.44	13.92	21.66	22.99	24.45																	
Nb	5.20	15.90	9.00	9.30	10.90	10.00	3.10	7.10	10.60	9.10	9.50	9.20	8.60	10.30	5.20	11.20	8.40	9.40									
Rb	190.53	181.49	217.68	93.71	142.39	136.23	142.78	106.86	166.24	106.14	133.70	75.92	146.35	114.21	29.34	74.27	82.31	104.12									
Sr	250.79	48.98	157.12	724.88	592.08	509.07	390.44	685.75	413.08	780.90	219.07	388.14	384.00	553.70	722.21	788.48	712.58	810.03									
Th	31.63	30.30	25.33	13.79	21.26	18.96	9.69	11.58	38.77	11.05																	
U	5.20	2.66	7.60	4.00	5.47	4.36	4.81	1.57	8.46	3.00	4.01	1.95	2.96	1.70	1.59	0.93	1.80	1.73									
Cr	1.18	1.58	10.45	21.84	22.67	13.30	19.84	17.19	21.87	20.86																	
Zr	< 130	< 130	115.40	155.40	173.90	162.87	244.30	177.67	142.40	190.40																	
Y	6.56	83.18	19.98	18.88	22.63	19.68	7.44	15.50	19.29	21.19	21.69	23.94	21.03	17.98	12.69	13.12	18.81	20.60									
La	29.83	36.84	34.30	35.66	44.65	30.37	8.17	25.95	41.36	36.26	30.78	25.24	30.09	31.98	18.08	23.00	32.55	34.55									
Ce	50.34	80.29	65.42	70.67	82.93	61.62	16.72	50.93	76.33	70.54	52.21	44.72	51.32	62.46	32.78	39.65	58.93	62.29									
Pr	5.05	7.86	7.08	8.57	9.91	7.57	1.97	6.22	8.98	9.04	6.17	5.94	6.55	8.55	4.17	4.75	7.86	7.84									
Nd	14.79	27.32	21.99	32.51	36.67	29.18	7.11	24.92	28.20	32.78	23.74	22.74	24.63	32.82	15.65	18.98	31.26	33.72									
Sm	1.91	4.35	4.37	6.46	6.84	5.24	1.37	4.72	6.02	7.02	4.23	4.50	4.88	5.72	2.82	3.28	5.28	5.69									
Eu	0.47	0.44	1.02	2.35	2.03	1.69	0.72	1.88	1.49	2.43	0.91	1.07	1.13	1.29	0.76	1.35	1.50	1.58									
Gd	1.99	4.06	4.23	5.88	6.25	4.91	1.30	4.36	5.40	6.36	4.03	4.40	4.62	5.08	2.70	3.10	4.93	5.21									
Tb	0.19	0.49	0.62	0.78	0.90	0.73	0.19	0.63	0.76	0.89	0.64	0.69	0.69	0.70	0.38	0.42	0.71	0.74									
Dy	0.83	2.08	3.41	3.99	4.50	3.63	1.00	2.95	3.94	4.58	3.31	3.70	3.53	3.28	1.95	2.16	3.46	3.69									
Ho	0.17	0.39	0.71	0.79	0.88	0.70	0.21	0.58	0.80	0.90	0.69	0.74	0.70	0.65	0.38	0.42	0.67	0.69									
Er	0.61	1.22	2.28	2.44	2.76	2.13	0.67	1.70	2.52	2.75	2.12	2.25	2.10	2.01	1.16	1.30	2.02	2.22									
Tm	0.09	0.17	0.34	0.33	0.39	0.29	0.10	0.22	0.36	0.37	0.31	0.32	0.29	0.27	0.16	0.18	0.28	0.29									
Yb	0.65	1.27	2.42	2.30	2.60	1.92	0.73	1.41	2.57	2.50	2.02	2.08	1.88	1.74	1.08	1.24	1.80	1.94									
Lu	0.11	0.20	0.39	0.36	0.41	0.28	0.12	0.22	0.39	0.38	0.33	0.33	0.29	0.27	0.17	0.20	0.28	0.30									
(La/Yb)n	30.59	19.34	9.45	10.34	11.45	10.55	7.46	12.27	10.73	9.67	10.18	8.09	10.70	12.22	11.14	12.41	12.04	11.84									
(Eu/Yb)n	2.07	0.99	1.20	2.92	2.23	2.51	2.82	3.81	1.66	2.78	1.28	1.47	1.72	2.12	2.00	3.11	2.37	2.33									
Nb/La	0.36	0.53	0.93	0.50	0.61	0.34	1.30	0.42	0.64	0.47	0.31	0.36	0.29	0.32	0.29	0.49	0.26	0.27									
#MgO	12.82	12.20	15.96	29.86	28.50	30.91	15.03	31.57	25.69	29.15	26.64	35.92	35.74	28.89	38.42	32.20	28.36	28.06									

LOI: loss on ignition; n—normalized to chondrite values of Nakamura (1974).

Table 5. Major and trace elements of samples from the Nechí Gneiss (retrieved from Rodríguez et al., 2017) and El Encanto Orthogneiss (retrieved from Cardona et al., 2010b).

Sample	900584	900588	900586	900585	A44	A13	A15	A12	A11	A21	A16	A26	24
wt %	Nechí Gneiss				Sierra Nevada de Santa Marta–El Encanto Orthogneiss								
SiO_2	64.26	58.23	62.75	57.58	70.01	76.26	65.82	58.87	59.05	63.38	61.85	65.87	65.05
Al_2O_3	14.98	15.83	15.47	16.52	16.16	11.83	15.91	17.60	16.84	16.71	16.09	15.83	14.68
Fe_2O_3	4.84	7.09	5.92	7.04	1.87	2.90	4.09	7.69	6.44	4.13	5.60	4.21	7.25
MgO	2.48	3.58	2.75	3.60	0.31	0.95	1.16	0.98	3.03	1.35	1.73	1.06	2.09
CaO	4.56	5.72	4.44	6.15	2.52	1.58	3.71	5.48	4.27	4.41	3.68	2.88	1.14
Na_2O	3.27	3.35	2.91	3.27	4.87	2.90	4.09	3.80	4.19	4.48	2.94	3.64	1.41
K_2O	2.54	2.29	2.67	2.28	2.73	1.88	3.37	2.77	3.00	2.65	4.22	3.58	3.76
TiO_2	0.59	0.85	0.69	0.83	0.19	0.39	0.54	0.79	0.88	0.55	1.11	0.52	0.73
P_2O_5	0.15	0.25	0.20	0.24	0.06	0.05	0.19	0.32	0.29	0.23	0.66	0.19	0.18
LOI	0.72	0.83	1.00	1.38	0.90	0.90	1.00	1.50	1.60	1.70	1.70	1.80	3.70
ppm													
Ba	1300.00	1130.00	769.00	996.00	1052.70	1029.00	1052.30	790.60	746.10	841.40	1321.90	1205.40	639.20
Cs	1.30	6.60	5.50	2.30	0.40	2.40	1.70	2.70	2.20	2.50	1.60	1.50	2.20
Co	21.00	27.00	25.00	29.00	1.30	5.80	6.90	6.50	14.60	5.90	9.10	6.40	12.90
Sc	16.00	20.00	16.00	21.00	2.00	6.00	6.00	8.00	16.00	6.00	9.00	6.00	14.00
Ga	17.00	20.00	19.00	20.00									
Nb	6.50	8.60	5.40	8.50	7.70	8.30	25.20	20.10	15.70	24.00	18.30	23.90	16.00
Rb	62.00	84.00	118.00	84.00	43.00	67.60	90.80	92.50	107.70	97.40	128.40	105.30	109.20
Sr	516.00	668.00	524.00	676.00	674.10	285.80	694.10	763.50	560.00	757.90	362.10	575.70	123.90
Th	11.00	8.00	11.00	7.90									
U	1.60	5.20	1.00	1.60	1.70	1.90	5.90	5.50	3.50	3.80	1.00	4.30	4.00
Cr	40.00	54.00	49.00	49.00									
Zr	178.00	163.00	148.00	141.00	82.70	197.80	199.40	219.60	176.00	200.00	281.70	178.60	183.60
Y	19.00	20.00	12.00	19.00	9.20	9.10	23.10	29.10	30.90	24.00	24.60	22.70	33.20
La	48.00	35.00	42.00	33.00	7.80	33.70	36.10	30.60	30.40	38.80	59.60	28.30	35.10
Ce	92.00	73.00	85.00	69.00	16.60	73.20	74.30	70.50	79.80	78.40	149.00	64.00	78.30
Pr	8.40	7.40	7.90	7.10	1.98	8.13	7.85	8.48	10.18	8.48	19.46	7.29	9.16
Nd	25.00	27.00	24.00	25.00	8.40	28.60	27.90	33.30	40.40	31.40	80.60	27.70	34.60
Sm	5.80	6.00	4.80	5.60	1.63	4.62	5.10	6.69	7.42	5.81	14.13	5.08	6.62
Eu	1.90	1.90	1.30	1.80	0.59	0.98	1.37	1.85	1.54	1.48	2.04	1.25	1.46
Gd	5.20	5.40	4.40	5.10	1.47	2.93	3.91	5.17	5.75	4.51	9.82	4.31	5.73
Tb	0.71	0.75	0.51	0.73	0.27	0.45	0.66	0.89	0.95	0.76	1.22	0.72	1.07
Dy	3.80	4.00	2.50	3.90	1.33	1.78	3.31	4.37	5.05	3.83	5.17	3.74	5.13
Ho	0.73	0.80	0.48	0.76	0.25	0.31	0.65	0.87	0.94	0.73	0.77	0.70	0.97
Er	2.30	2.50	1.40	2.30	0.78	0.75	2.04	2.63	2.72	2.30	2.02	2.16	2.95
Tm	0.30	0.31	0.17	0.31	0.14	0.12	0.33	0.39	0.43	0.32	0.22	0.32	0.41
Yb	2.00	2.10	1.10	2.10	0.96	0.76	2.21	2.81	2.63	2.28	1.32	2.15	2.94
Lu	0.30	0.32	0.18	0.31	0.16	0.14	0.35	0.44	0.36	0.35	0.18	0.35	0.43
(La/Yb)n	16.00	11.11	25.45	10.48	5.42	29.56	10.89	7.26	7.71	11.35	30.10	8.78	7.96
(Eu/Yb)n	2.71	2.59	3.38	2.45	1.76	3.68	1.77	1.88	1.67	1.85	4.42	1.66	1.42
Nb/La	0.33	0.33	0.50	0.41	0.00	0.00	0.00	0.00	0.00	0.00	0.00	0.00	0.00
#MgO	33.88	33.55	31.72	33.83	14.22	24.68	22.10	11.30	32.00	24.64	23.60	20.11	22.38

LOI: loss on ignition

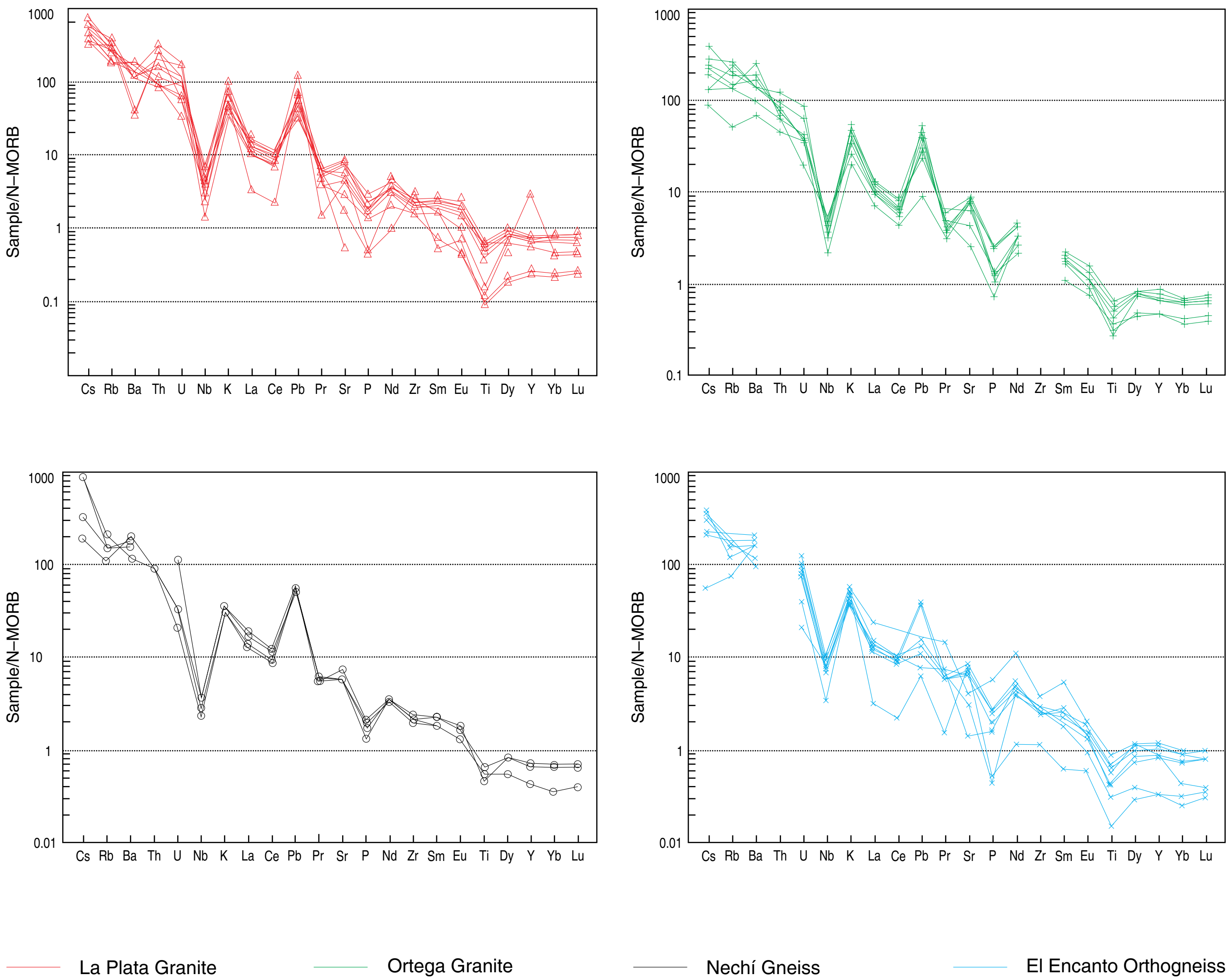

Figure 8. Normal Mid–Ocean Ridge Basalt (N–MORB) normalized trace element diagrams (Sun & McDonough, 1989) for La Plata Granite (red), Ortega Granite (green), Nechí Gneiss (black), and El Encanto Orthogneiss (blue). Data sources: Cardona et al. (2010b), Piraquive (2017), Rodríguez et al. (2014, 2017), and this study.

some samples present more dispersed patterns (Cardona et al., 2010b). The bodies show negative Nb, P, and Ti anomalies and enrichment in Cs, Ba, and K (Figure 8) that are typical of a continental arc environment formed in a subduction tectonic regime.

Chondrite–normalized (Nakamura, 1974) REEs show enrichment in light over heavy rare earth elements with a negative slope (Figure 9). These patterns are similar to those of rocks generated above subducting plates.

The Ortega Granite shows values of (La/Yb)n = 8.09–12.41, and La Plata Granite values range from 7.46 to 12.27 with two high values (19.34–30.59) corresponding to samples 900724 and 900729. The samples from the Nechí Gneiss show (La/Yb)n values ranging from 10.48 to 25.45. El Encanto Orthogneiss shows (La/Yb)n ratios = 5.42–11.35, and samples A13 and A16 have high (La/Yb)n values ranging from 19.2 to 30 (related to SiO_2 values higher than 75 wt %).

The Eu/Eu* anomaly is negative in most cases, with values ranging from 0.69 to 0.95, suggesting Eu fractionation by plagioclase crystallization. Most samples from the Ortega Granite show negative Eu anomalies, with values of Eu/Eu* = 0.68–0.89, and one sample has a value of Eu/Eu* = 1.30. The samples from La Plata Granite show negative (Eu/Eu* = 0.32–0.95) and positive (Eu/Eu* = 1.02–1.117) Eu anomalies (samples 900732, 900800, 900802, 900739) that could indicate plagioclase accumulation. The Nechí Gneiss shows positive Eu anomalies with values of Eu/Eu* = 1.03–1.06 except for sample 900586 (Eu/Eu* = 0.87). El Encanto Orthogneiss shows values

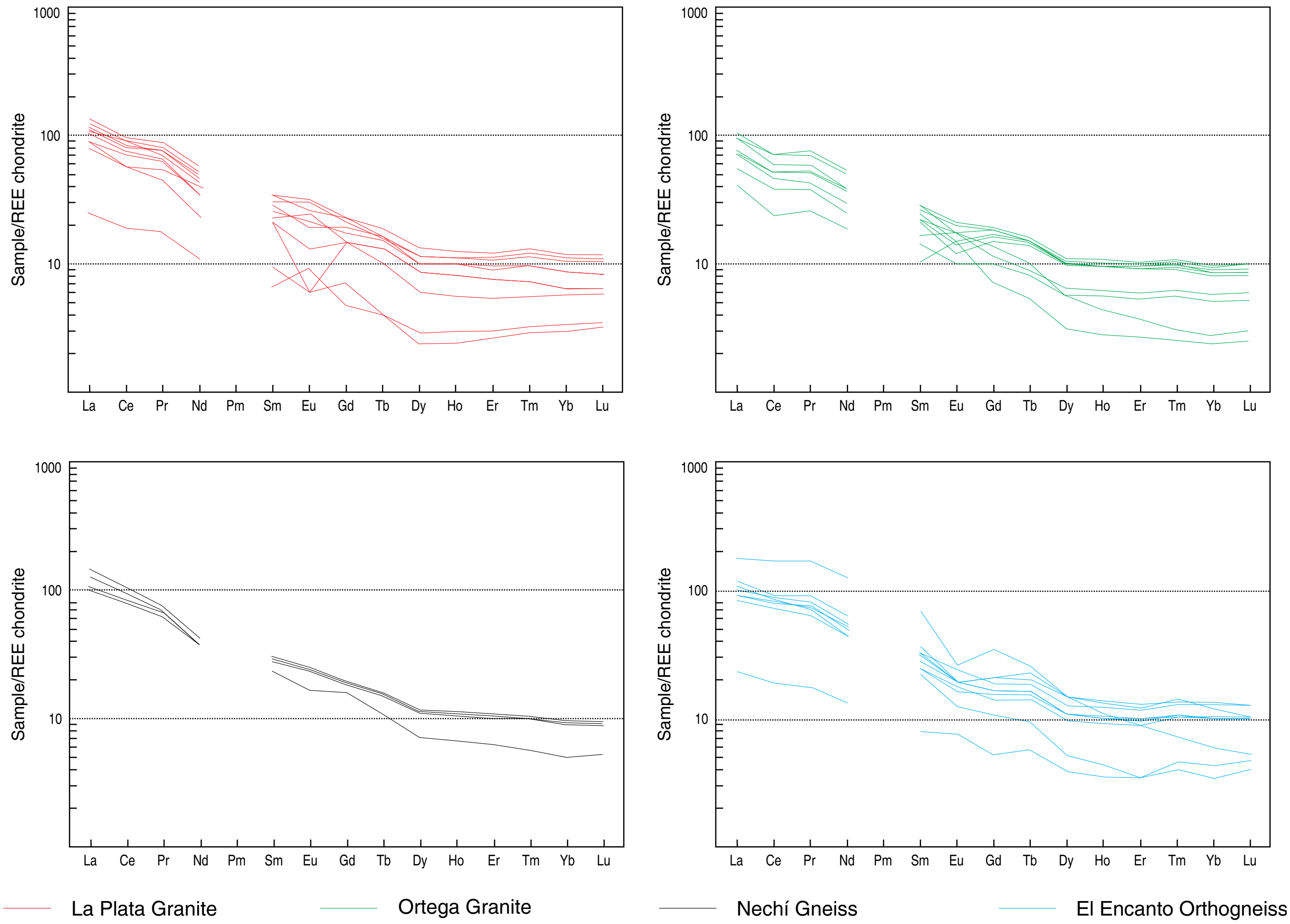

Figure 9. Chondrite–normalized rare earth element (REE) diagrams (normalizing values after Nakamura, 1974) for La Plata Granite (red), Ortega Granite (green), Nechí Gneiss (black), and El Encanto Orthogneiss (blue). Data sources: Cardona et al. (2010b), Piraquive (2017), Rodríguez et al. (2014, 2017), and this study.

of Eu/Eu* = 0.72–0.94 and a positive Eu anomaly of Eu/Eu* = 1.17 (sample A44).

The analyzed granitoids have high ratios of (La/Yb)n versus Sr/Y that place them within the continental arcs (Figure 10a) because of the garnet retention of heavy rare earth elements and Y, reflecting deep melting in a convergent margin (Condie & Kröner, 2013). In the Chappell & White (1974) discrimination diagram, most samples fall within the type–I granite field (Figure 10b).

6.3. Geochronology

A total of nine samples were dated in this study using the U–Pb zircon LA–ICP–MS method: one sample (GOE–1100) from the Icarco Complex, six samples (GOE–1099, GOE–1098, GR–6872B, AMC–0185, GOE–1096, and JPZ–010A) from the Ortega Granite, and two samples (AMC–0159A and MGOQ–008) from the southern Rovira Granitic Stocks. The locations of the samples are shown in Figure 2, and the resulting ages are outlined in Table 6. The nomenclature used for the inherited zircons followed the definitions of Miller et al. (2007) and Siégel et al. (2018).

The zircons of sample GOE–1100 are prismatic subhedral to short prismatic, ranging in size from 50 × 90 μm to 100 × 200 μm. Under CL, two different textures showed: low–luminescence homogeneous zones with intermediate–luminescent edges, and zones with different and irregular luminescence (Figure 11). Crystals with concentric zoning patterns are scarce. Any analysis with a discordance higher than 10% was disregarded during interpretation. Four inherited ages were obtained (Table 6): two that were Neoproterozoic, one Late Ordovician, and one Late Pennsylvanian. The principal group of ages ranges from 298 to 260 Ma, and the weighted mean average of the concordant data is 277.8 ± 2.2 (MSWD = 2.4) (Figure 12), which is interpreted as the age of the igneous crystallization. Forty–nine crystals show a Th/U ratio higher than 0.31, with a mode of 0.79, which is associated with the values of igneous zircons

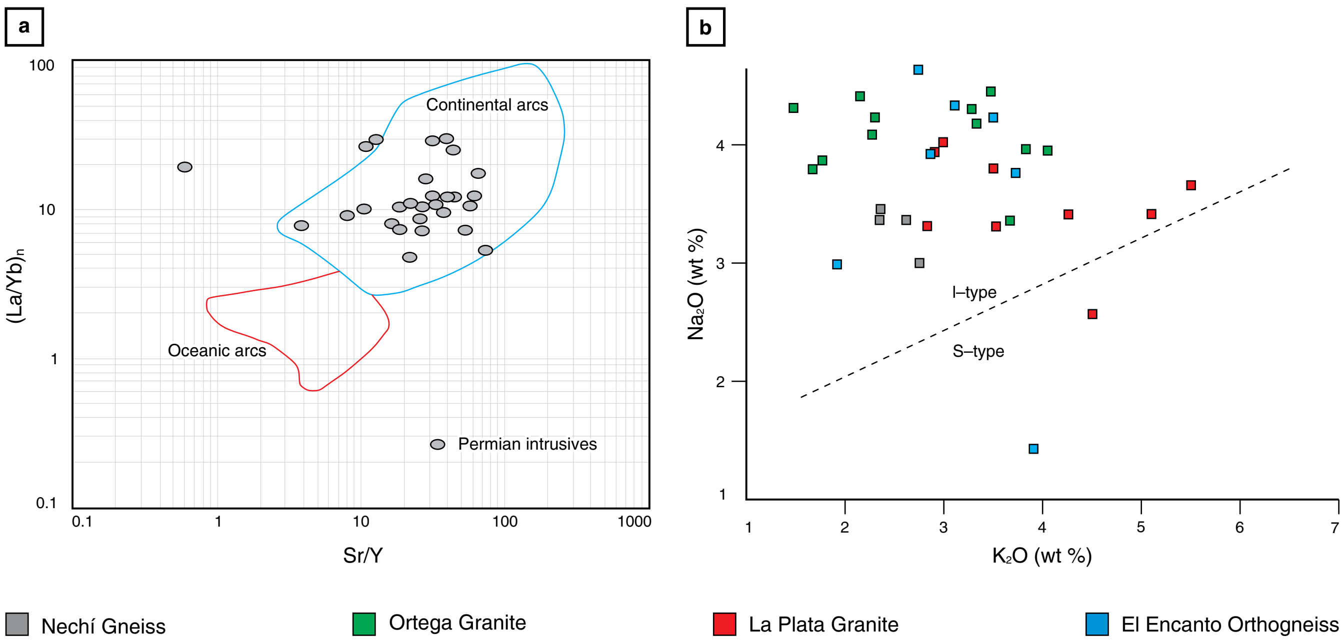

Figure 10. Tectonic environment discrimination diagrams for Permian units. **(a)** Condie & Kröner (2013) diagram. **(b)** Chappell & White (1974) diagram.

Table 6. Geochronological results of this study.

Sample	Lithology	Latitude N	Longitude W	$^{238}U/^{206}Pb$ age (Ma) ± 2σ	MSWD	Inheritance ages (Ma)
			Upper Magdalena Valley			
			Icarco Complex			
GOE–1100	Metatonalite	3° 32' 13.34"	75° 39' 00.41"	277.8 ± 2.2	2.4	990 ± 46; 911 ± 32; 457 ± 16; 304 ± 11
			Ortega Granite			
GOE–1099	Tonalite	3° 33' 27.23"	75° 30' 52.48"	280.1 ± 2.0	1.9	300.1 ± 7.5 – 292.1 ± 9.3, n = 5
GOE–1098	Tonalite	3° 48' 40.05"	75° 26' 28.00"	280.5 ± 2.3	2.2	322.8 ± 8.0; 319.8 ± 8.0; 322.8 ± 8.0; ca. 305 ± 8.0, n = 2; ca. 304 ± 8.0, n = 2; 299.4 ± 8.7
GR–6872B	Dyke of tonalite	3° 50' 03.73"	75° 26' 05.77"	277.6 ± 2.4	2.2	304.3 ± 11.8
AMC–0185	Granodiorite	3° 53' 02.51"	75° 22' 34.16"	293.8 ± 2.7	2.1	363 ± 16 – 362 ± 14, n = 2; 332.7 ± 9.3 – 309.7 ± 9.9, n = 22
GOE–1096		4° 02' 59.10"	75° 18' 08.18"	274.0 ± 2.3	1.04	954 ± 39; 326 ± 11.8; 312 ± 7.5; 311 ± 5.9; 306 ± 11 – 287 ± 8, n = 34; 285 ± 9 – 279 ± 9, n = 15
JPZ–010A	Granodiorite	4° 22' 09.12"	75° 13' 39.12"	264.7 ± 1.2	1.8	312 ± 8; 307.7 ± 7.5; 286–281 (mean = 282.9 ± 2.8; n = 7)
			Southern Rovira Granitic Stocks			
AMC–0159A	Dacite	4° 11' 35.20"	75° 13' 58.21"	274.9 ± 1.4	0.96	
MGOQ–008	Monzogranite	4° 17' 26.69"	75° 11' 28.03"	262.7 ± 2.1	1.6	1104 ± 80; 924 ± 54; 345 ± 11; 307.8 ± 9.3; 281 ± 7 – 275 ± 4, n = 4

Data for GOE–1100, GOE–1099, GOE–1098, GR–6872B, AMC–0185, GOE–1096, JPZ–010A, AMC–0159A, and MGOQ–008 is included in the Tables 1–7 of the Supplementary Information.
n: number of results in the ages range.

(Rubatto, 2002). Notably, the zircon textural characteristics observed under CL and the wide age range suggest a process of zircon recrystallization or modification after initial crystallization; however, the time limit between both processes could not be defined based on available data. Three concordant younger age results (ca. 245 Ma, ca. 242 Ma, and ca. 223 Ma with a Th/U of 0.76, 0.14, and 0.22, respectively) were excluded from the calculation of the mean age.

In sample GOE–1099, the zircons are prismatic, euhedral, some having bipyramidal terminations, and reaching up to 150 μm

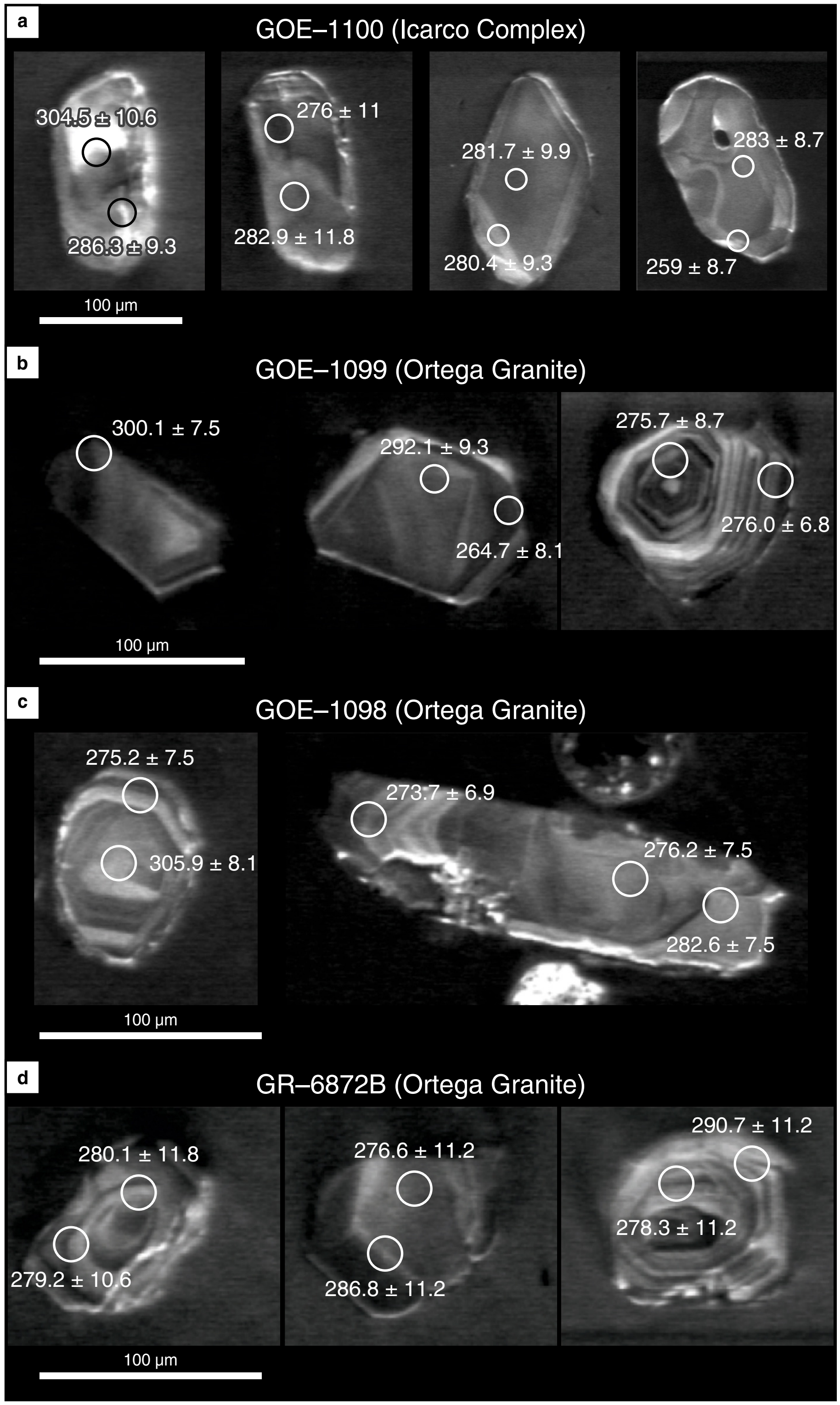

Figure 11. Cathodoluminescence images of representative zircons from samples: **(a)** GOE–1100, **(b)** GOE–1099, **(c)** GOE–1098, and **(d)** GR–6872B.

along their largest dimension. Under CL, nearly all crystals show concentric zoning patterns and have a few inherited cores (Figure 11). Four analyses showed discordances higher than 10%, and these were discarded during interpretation. Textural and temporal differences are observed between the zircon cores

⟶

Figure 12. Tera–Wasserburg concordia diagrams and medians and/or means of Permian samples of plutons from the Icarco Complex and the Ortega Granite. Gray ellipses: discarded results; blue ellipses: analysis of inherited zircons and anticrystals; green ellipses: Permian igneous ages; light yellow ellipses: Triassic results with no known geological meaning thus far.

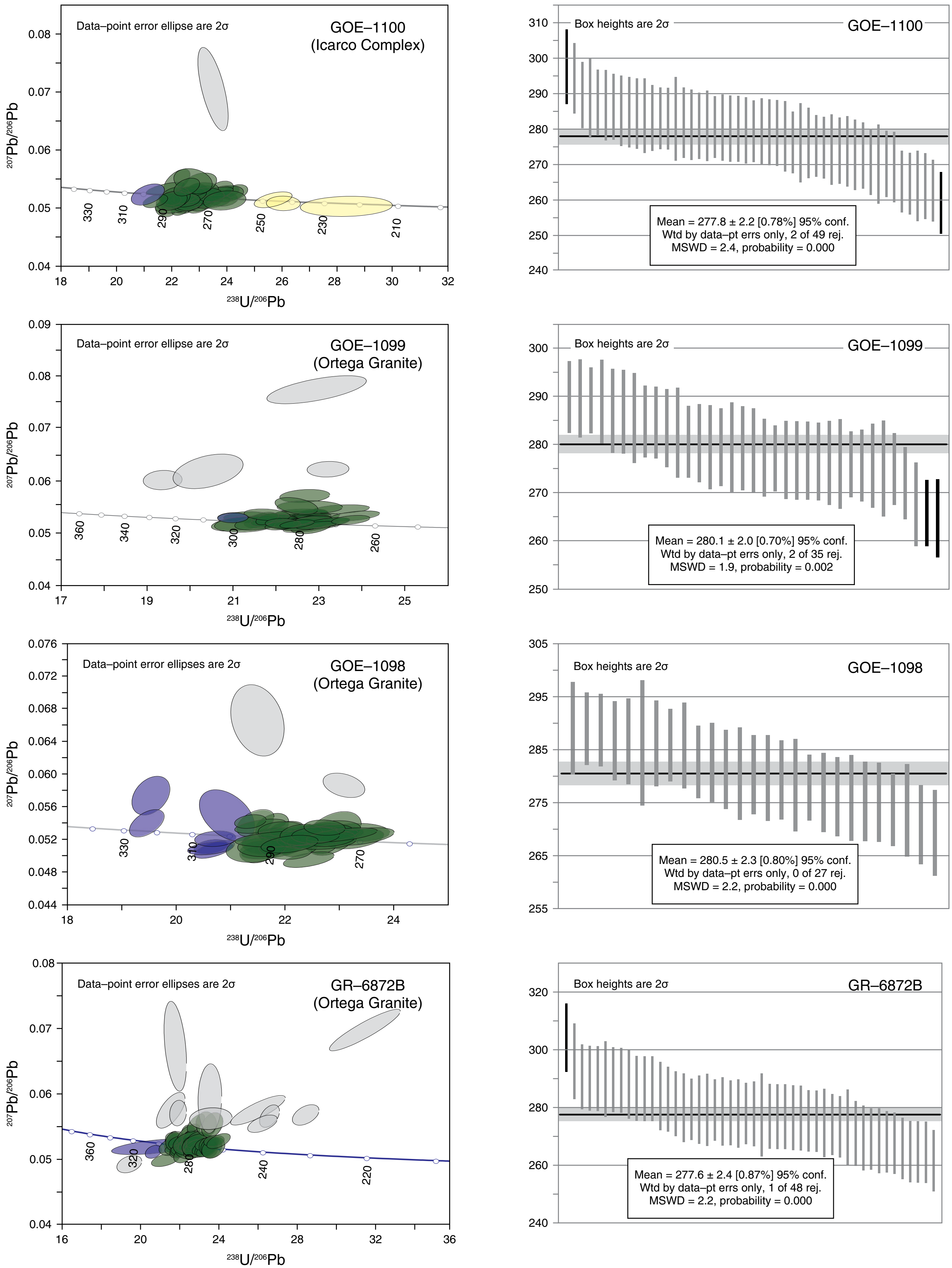
Data–point error ellipse are 2σ
GOE–1100
(Icarco Complex)
$^{207}Pb/^{206}Pb$
$^{238}U/^{206}Pb$
Box heights are 2σ
GOE–1100
Mean = 277.8 ± 2.2 [0.78%] 95% conf.
Wtd by data–pt errs only, 2 of 49 rej.
MSWD = 2.4, probability = 0.000
Data–point error ellipse are 2σ
GOE–1099
(Ortega Granite)
$^{207}Pb/^{206}Pb$
$^{238}U/^{206}Pb$
Box heights are 2σ
GOE–1099
Mean = 280.1 ± 2.0 [0.70%] 95% conf.
Wtd by data–pt errs only, 2 of 35 rej.
MSWD = 1.9, probability = 0.002
Data–point error ellipses are 2σ
GOE–1098
(Ortega Granite)
$^{207}Pb/^{206}Pb$
$^{238}U/^{206}Pb$
Box heights are 2σ
GOE–1098
Mean = 280.5 ± 2.3 [0.80%] 95% conf.
Wtd by data–pt errs only, 0 of 27 rej.
MSWD = 2.2, probability = 0.000
Data–point error ellipses are 2σ
GR–6872B
(Ortega Granite)
$^{207}Pb/^{206}Pb$
$^{238}U/^{206}Pb$
Box heights are 2σ
GR–6872B
Mean = 277.6 ± 2.4 [0.87%] 95% conf.
Wtd by data–pt errs only, 1 of 48 rej.
MSWD = 2.2, probability = 0.000

and edges, suggesting the occurrence of inherited antecrysts with ages from 300.1 ± 7.5 Ma to 292.1 ± 9.3 Ma. The ages of the principal group of zircons range from ca. 290 to 265 Ma, yielding a mean age of 280.1 ± 2.0 Ma (Figure 12) and a MSWD of 1.9, likely indicating the crystallization age of the rock. Spots with ages between 298 and 265 Ma show Th/U ratios ranging from 0.28 to 0.75, corroborating the igneous origin of the zircons.

Sample GOE–1098 presents stubby, prismatic, short–prismatic, and sub–spherical zircons. Under CL, most crystals show concentric zoning patterns, and a few inherited cores are truncated by external zoning or inherited cores of homogeneous texture (Figure 11). Of the 48 analyses, 2 were disregarded from the interpretation because these showed discordances higher than 10%. Seven inherited Carboniferous xenocrysts were identified (Table 6), presenting Th/U ratios ranging from 0.36 to 0.96. Three crystals with ages between 293–292 Ma and a Th/U ratio of 0.58–0.72 likely represent antecrysts. The remaining 27 ages vary between 289 and 269 Ma, with a Th/U ratio ranging from 0.39 to 1.04. These data yield a mean age of 280.5 ± 2.3 Ma and an MSWD of 2.2 (Figure 12), which is interpreted as the rock crystallization age.

In GR–6872B, the zircons are stubby and sub–spherical, with a maximum dimension of 100 μm. Under CL, crystals show homogeneous and irregular textures and few concentric zoning patterns (Figure 11). Results with discordances higher than 8%, inverse discordances lower than –5%, and $^{206}Pb/^{238}U$ ratio errors higher than 9% were disregarded during interpretation. One zircon, despite meeting the aforementioned criteria, yielded an age of ca. 140 Ma. This age was discarded because its geological meaning is unknown. A mean age of 277.6 ± 2.4 Ma with a MSWD of 2.2 and Th/U ratios ranging from 0.14 to 1.06 was obtained from 47 crystals (Figure 12). One crystal yielded a Carboniferous age (Table 6), likely corresponding to an inherited zircon.

Sample AMC–0185 shows short, prismatic zircon crystals of up to 80 × 120 μm. Under CL, two populations are differentiated: one consists of zoned crystals with homogenous cores and concentrically zoned rims, and the second encompasses crystals with zoned, inherited cores that are equivalent to the first population described, with overgrowths, which may be zoned or homogeneous (Figure 13). Nine of the 62 analyses were disregarded during interpretation because of discordances or uncertainties higher than 5%. Population 1, defined by 24 crystals with ages ranging from 363 to 309 Ma (Th/U ranging from 0.36 to 1.02), is interpreted as inheritance from Devonian – Carboniferous boundary and early – late Carboniferous rocks. Population 2 comprises zircons with ages ranging from 305.5 Ma to 262.5 Ma (n = 29 with Th/U ratio between 0.23 and 0.93). These zircons yielded a mean age of 293.8 ± 2.7 with a MSWD of 2.1 and are interpreted as the rock crystallization age.

Sample GOE–1096 contains prismatic zircons, most of which have large homogeneous cores and thin zoned mantles. Few crystals show truncation between cores and mantles or thick areas with concentric zoning (Figure 13). Results with discordances and uncertainties higher than 10% were disregarded. Sixty–one analyses with Th/U ratios ranging from 0.31 to 1.10 yielded ages between 303 and 262 Ma. Using the function "unmix ages" of Isoplot (Ludwig, 2012), three populations were determined as follows: (i) between ca. 306–287 Ma, yielding a mean age of 294.52 ± 1.6 Ma; (ii) between ca. 285–279 Ma, yielding a mean age of 284.3 ± 3.0 Ma; and (iii) between ca. 277–261 Ma, yielding a mean age of 274.0 ± 2.3 Ma and a MSWD of 1.04 likely corresponding to the crystallization age (Figure 14). An inherited Neoproterozoic crystal and four Carboniferous crystals were also obtained (Table 6).

Sample JPZ–010A shows prismatic zircons with bipyramidal terminations that under CL show concentric zoning with rare inherited cores (Figure 13). Results with discordances higher than 7% were disregarded during interpretation. Two datasets of inherited ages are identified as follows: the first consists of ages ranging from 312 to 307 Ma, and the second of ages from 286 to 281 Ma. Fifty–seven results with Th/U ratios ranging from 0.31 to 1.09 and ages ranging from 275 to 256 Ma yielded a mean age of 264.7 ± 1.2 Ma with a MSWD of 1.8 (Figure 14), which is interpreted as the rock crystallization age.

Sample AMC–0159A contains prismatic zircons with maximal dimensions ranging from 100 to 300 μm. Concentric zoning is identified in some cases (Figure 13). In total, 35 analyses were performed and the results with a discordance higher than 10% were disregarded. The Th/U ratios range from 0.54 to 1.24, typical of igneous zircons, and the ages range from 286 to 268 Ma. The group of 31 data yielded a mean of 274.9 ± 1.4 Ma with a MSWD of 0.96 (Figure 15), which is interpreted as the igneous rock crystallization age.

Sample MGOQ–008 shows prismatic euhedral zircons with bipyramidal terminations of up to 150 μm, many of which contain inclusions. Most zircons show concentric zoning under CL (Figure 13). Ten of the 40 analyses were disregarded because they had discordances higher than 10%. Four results correspond to inherited zircons: two of Proterozoic and two of Carboniferous age. Four ages between ca. 281–275 Ma could correspond to antecrysts. The other results ranged from 272 to 252 Ma, yielding a mean age of 262.7 ± 2.1 Ma and an MSWD of 1.6 (Figure 15). These data show Th/U ratios ranging from 0.44 to 1.55, typical of igneous zircons. The mean age corresponds to the rock crystallization age.

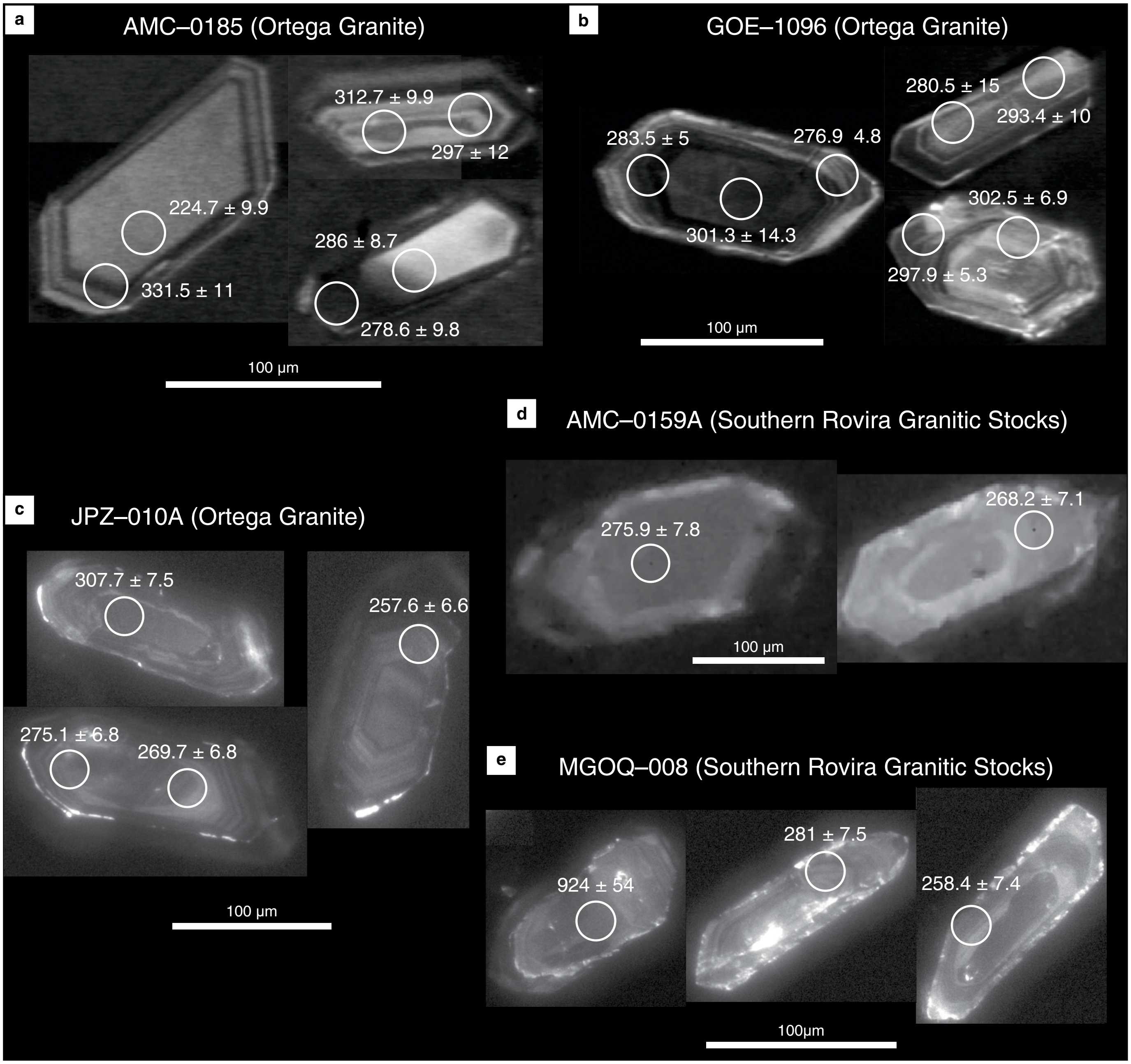

Figure 13. Cathodoluminescence images of representative zircons from samples: **(a)** AMC–0185, **(b)** GOE–1096, **(c)** JPZ–010A, **(d)** AMC–0159A, and **(e)** MGOQ–008.

7. Discussion and Conclusions

7.1. Characteristics of Permian Magmatism in Colombia

The composition of the Permian plutonic bodies in Colombia corresponds to quartz diorites, quartz monzonites, tonalites, granodiorites, monzogranites, and syenogranites (except for sample AMC–0159 of dacitic composition), including the rocks with migmatitic structures of La Plata Granite (Rodríguez et al., 2017) and granitoids within the Icarco Complex. In addition, some units show superimposed dynamic deformation, such as the Nechí Gneiss (Restrepo et al., 2011; Rodríguez et al., 2014) and El Encanto Orthogneiss (Cardona et al., 2010b; Piraquive, 2017), forming mylonites.

The geochemical data show that the Permian granitoids and gneisses are of calc–alkaline to high–K calc–alkaline character, varying from metaluminous to peraluminous, with negative Nb and Ti anomalies, and enrichment in Th and Nb. This suggests the input of recycled material from the crust during subduction processes (Pearce, 2008). The values of the (La/Yb)n versus Sr/Y ratios place these magmas in the field of continental arc magmas.

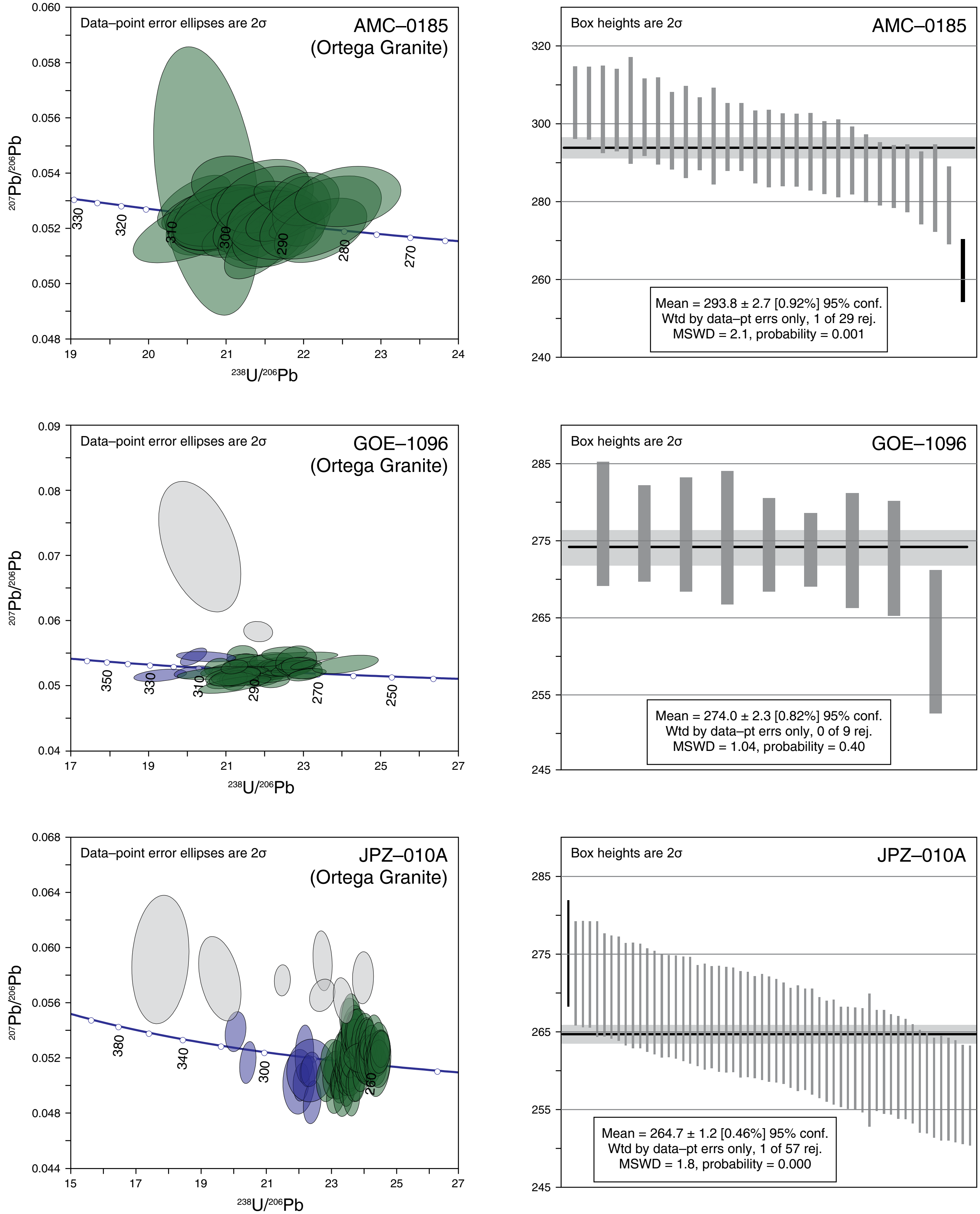

Figure 14. Tera–Wasserburg concordia diagrams and medians and/or means of Permian samples from the Ortega Granite. Gray ellipses: discarded results; blue ellipses: analysis in inherited zircons and anticrystals; green ellipses: Permian igneous ages.

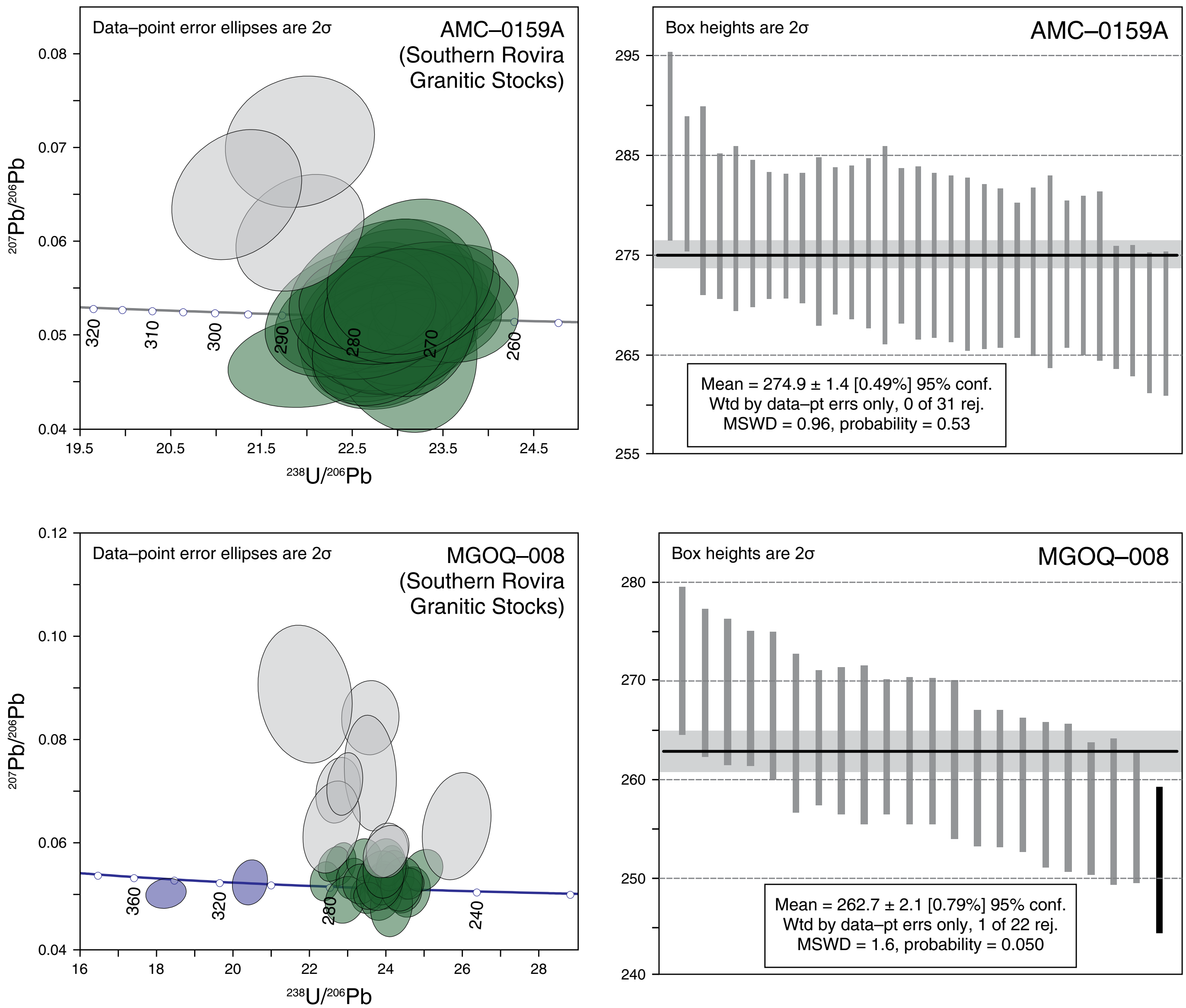

Figure 15. Tera–Wasserburg concordia diagrams and medians and/or means of samples from the southern Rovira Granitic Stocks. Gray ellipses: discarded results; blue ellipses: analysis of inherited zircons; green ellipses: Permian igneous ages.

The U–Pb Permian ages obtained in the granitoids are interpreted as pluton crystallization ages ranging from ca. 294 to 260 Ma. Figure 16 shows that during this period, several magmatic pulses occurred. In the Ortega Granite, ages range between ca. 294–290 Ma and ca. 283–263 Ma, presenting a major peak between 279–275 Ma. In El Encanto Orthogneiss, ages range from ca. 288 to 264 Ma. In an area near the serranía de San Lucas, ages range from ca. 281 to 263 Ma. In the southern Rovira Granitic Stocks ages range from ca. 275 to 263 Ma, and in La Plata Granite, ages range from ca. 278 to 268 Ma.

The inherited zircons yield Carboniferous and, to a lesser extent, Proterozoic, Cambrian, Ordovician, and Devonian ages (Figure 17a; Table 6). The few Proterozoic and Paleozoic inheritances (Figure 17b, xenocrysts) may suggest that the Permian arc locally assimilated the Neoproterozoic – Paleozoic basement. The Carboniferous inheritances are shown in Figure 17c.

Only two reports of magmatism during the Carboniferous have been published in Colombia. Leal–Mejía (2011) yielded igneous crystallization ages ranging from 333 to 310 Ma in diorites and tonalites of El Carmen Stock (west of the serranía de San Lucas on the northeastern slope of the Central Cordillera), and Silva–Arias et al. (2016) yielded an igneous crystallization age of 300 ± 1.3 Ma in a pyroxene gabbro in the Lower Magdalena Valley (Sitio Nuevo–1 well). Figure 17d shows that the Carboniferous inherited ages of the Permian units match the ages of the Carboniferous igneous occurrences known in Colombia.

The abundant Carboniferous inheritances (Th/U 0.34 to 1.02) in addition to the previous reports of Carboniferous units

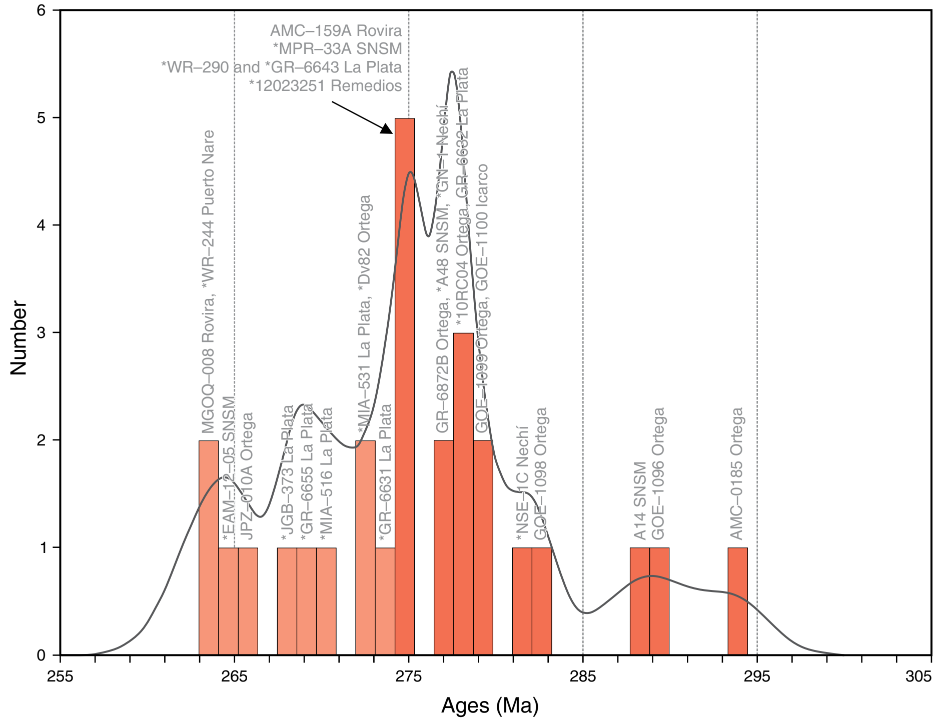

Figure 16. Probability density function of Permian igneous ages. Samples from other authors are preceded by an asterisk (*) (see Table 1 for references).

in Colombia (Figure 17c, 17d) suggest the existence of a larger arc that remains unidentified upon which the Permian arc was built, or that the magmatic activity began at the end of the Mississippian or the beginning of the Pennsylvanian (Figure 17c). This magmatism would have continued into the Permian, forming various plutonic bodies that crystallized during different pulses, similar to the Permian – Carboniferous arc of southwestern México (Ortega–Obregón et al., 2014).

7.2. Implications of the Metamorphism in Permian Rocks

The presence of metamorphic and plutonic rocks inside some units that comprise the Permian arc is difficult to explain and may be interpreted in several manners.

Although the structures and microtextures of La Plata Granite display metamorphic characteristics (see JGB–373A in Figure 18), all zircons yielded similar crystallization ages. These crystals are prismatic with concentric structures and Th/U ratios of approximately 1.0, without metamorphic overgrowths (Rodríguez et al., 2017). In addition, whole rock trace element and zircon geochemistry data indicate a geotectonic formation environment in a continental margin arc (Rodríguez et al., 2017). This suggests a tectonic environment in which the simultaneous formation of igneous and metamorphic rocks occurred.

Similarly, the granitoids of the Icarco Complex (Figures 2, 18) (Murillo et al., 1982) also exhibit metamorphic features. The analysis of a rock collected along the Río Blanco–Gaitán route (GOE–1100; crystallization age of 277.8 ± 2.1 Ma) presents slight mineral orientation, development of internal structures, and recrystallization resulting from thermal metamorphism (see GOE–1100 in Figure 18) likely caused by the intrusion of the Ibagué Batholith. Two Triassic concordant ages (ca. 245 Ma and ca. 223 Ma) obtained in the zircon cores of this sample show Th/U values of 0.76 and 0.22, suggesting an igneous origin for these crystals, and an additional age of ca. 242 Ma and a Th/U value of 0.14, which may reflect a metamorphic event. However, more data are required to validate this hypothesis.

We propose that La Plata Granite and the Icarco Complex blocks are part of the roots of the Permian arc.

The Nechí Gneiss, in contrast to the Permian bodies of the UMV, presents metamorphism following igneous crystallization. This unit outcrops west of the Neoproterozoic San Lucas Gneiss, and it is unknown if it is part of this basement or that of the Triassic metamorphic basement of the Central Cordillera (Restrepo et al., 2011) (Figure 3). According to Restrepo et al. (2011), U–Pb zircon ages of ca. 236 Ma suggest a Triassic metamorphic event that could be correlated with the metamorphism of the Tahamí Terrane. If so, these rocks would not be part of a Permian arc intruding the Neoproterozoic basement. On the other hand, we propose the possibility that the

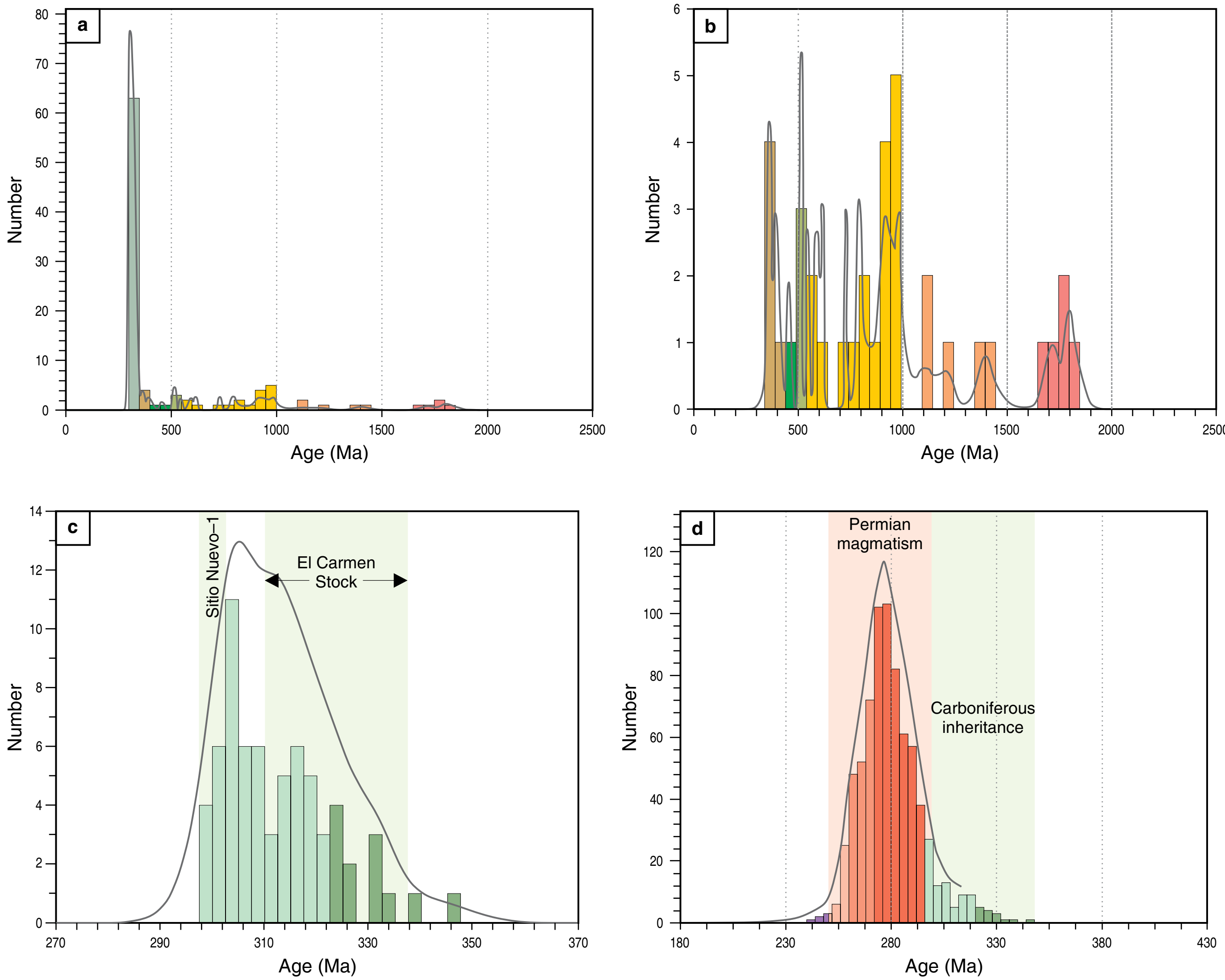

Figure 17. Relative probability diagrams with inheritances in the zircons from Permian rocks. **(a)** All inheritances from the Paleoproterozoic through the Carboniferous. **(b)** Detail of the inheritances between the Paleoproterozoic and the Devonian. **(c)** Probability diagram of the Carboniferous inheritances in Permian igneous rocks; the igneous age ranges of plutonic rocks from El Carmen Stock (Leal–Mejía, 2011) and the Sitio Nuevo–1 well (Silva–Arias et al., 2016) are indicated in fields highlighted in very light green. **(d)** Probability diagram of inherited and igneous ages of Permian rocks. Data sources: Cardona et al. (2010b), Rodríguez et al. (2017), Villagómez (2010), and this study.

ductile deformation characterizing this unit could be a result of the collision between the Neoproterozoic and Triassic basements during the Jurassic (Blanco–Quintero et al., 2014). In this case, the current position of the Nechí Gneiss would be tectonic in a Jurassic metamorphic block (hitherto inferred) and the age of metamorphism would be Late Jurassic. However, we still do not have an explanation for the Triassic metamorphic event.

The quartz–feldspar rocks of the Sierra Nevada de Santa Marta are mylonites and protomylonites (Cardona et al., 2010b; Piraquive, 2017) with Permian igneous crystallization ages and Neoproterozoic and Paleozoic inheritances, suggesting that these were emplaced in the Neoproterozoic basement (Cardona et al., 2010b). These bodies are tectonically along the western edge of the Neoproterozoic basement and inside Upper Jurassic metamorphic rocks. The ductile deformation and the development of metamorphic minerals are likely associated with collision between the Neoproterozoic (the Chibcha Terrane) and Triassic basements (the Tahamí Terrane) during the Late Jurassic.

7.3. Tectonic Implications and Correlations

Our results indicate that the Permian arc, previously reported in the SNSM (Cardona et al., 2010b) and the Central Cordillera (Cochrane et al., 2014; Leal–Mejía, 2011; Rodríguez et al., 2017; Villagómez, 2010), is more extensive and voluminous and includes parts of the SSL and UMV. This Permian magmatism may have peaked at the end of the Cisuralian, assimilating most rocks that originated during the previous stages of the arc

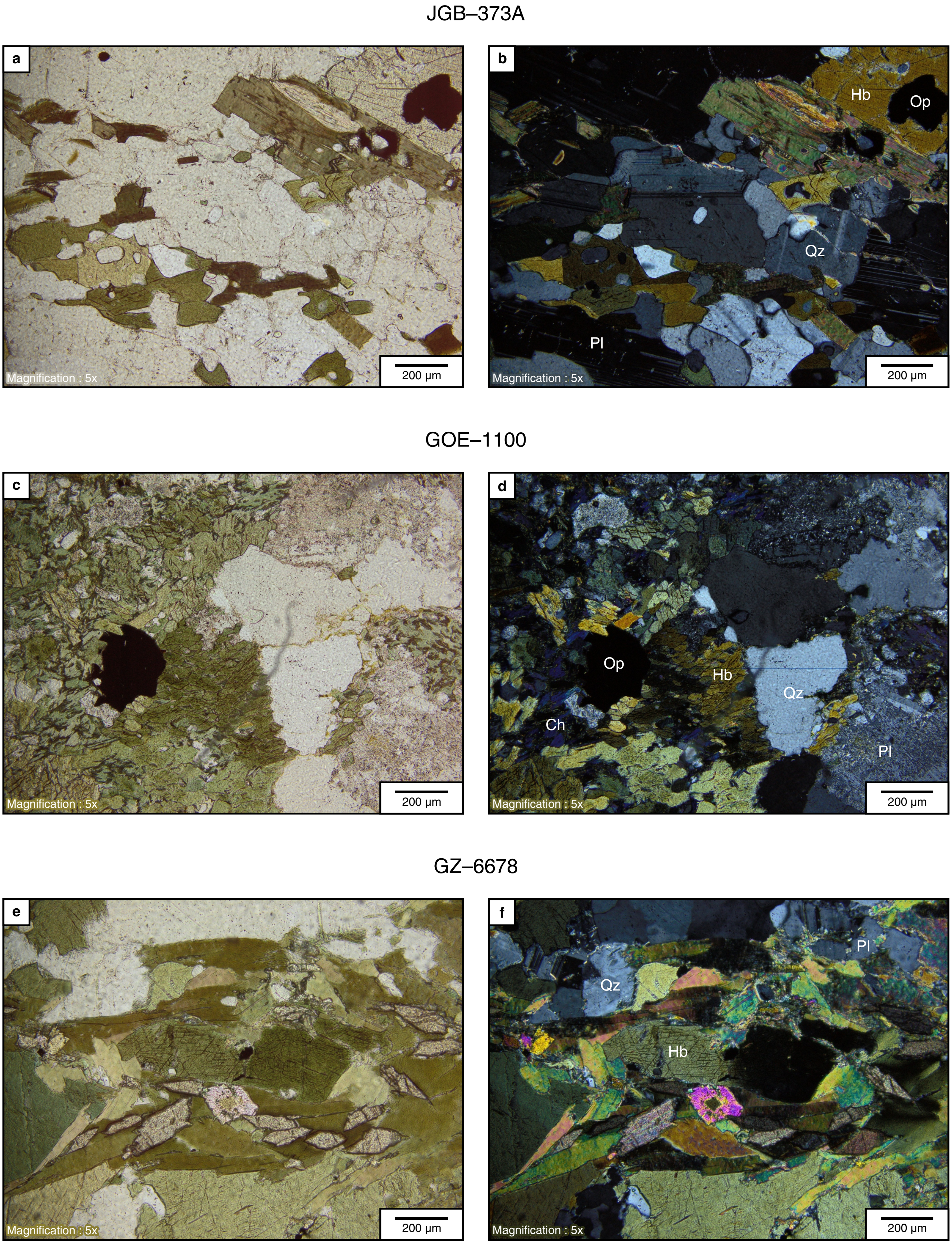
JGB–373A
a
Magnification : 5x
200 µm
b
Hb
Op
Qz
Pl
Magnification : 5x
200 µm
GOE–1100
c
Magnification : 5x
200 µm
d
Op
Hb
Qz
Ch
Pl
Magnification : 5x
200 µm
GZ–6678
e
Magnification : 5x
200 µm
f
Pl
Qz
Hb
Magnification : 5x
200 µm

←

Figure 18. Microscopic aspect of metamorphic rocks of Permian age. **(a)** and **(b)** La Plata Granite (JGB–373A—granofels) granoblastic and granonematoblastic textures. **(c)** and **(d)** Icarco Complex (GOE–1100—meta–quartz diorite) recrystallization texture forming subgrains. **(e)** and **(f)** Nechí Gneiss (GZ–6678—gneisses) hornblende porphyroclasts and plagioclase and lepidoblastic metamorphic bands.

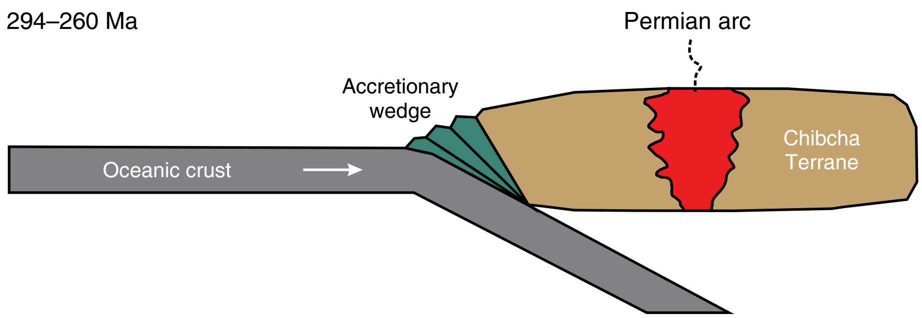

Figure 19. Tectonic model of a Permian arc on the western boundary of the Chibcha Terrane.

during the Carboniferous and the early Permian, intruding the Neoproterozoic basement of the Colombian Andes (Chibcha Terrane; Figure 19). Later, the arc was faulted in tectonic blocks together with the Early to Middle Jurassic arc.

The Permian arc rocks in Colombia are coeval with multiple plutonic units in Venezuela (serranía de Perijá sensu Dasch, 1982; El Baúl Massif sensu Viscarret et al., 2007, and Paraguaná Peninsula sensu van der Lelij et al., 2016); Ecuador (Paul et al., 2018); the Eastern Cordillera of Perú (Mišković et al., 2009); México (granitoids in the Chiapas and Mixtec Massifs sensu Weber & Köhler, 1999; Weber et al., 2005, 2007; and the Oaxaca and Acatlán Complexes sensu Ortega–Obregón et al., 2014).

In addition, their mineralogical and geochemical composition is consistent with rocks originating in a continental arc margin, as proposed by Cardona et al. (2010b). Vinasco et al. (2006) and Piraquive (2017), however, associate the genesis of the granitoids with the Ouachita–Alleghanian orogeny, caused by the Laurentia–Gondwana collision as a consequence of the closure of the Rheic Ocean during the Permian. Piraquive (2017) interprets the ages between 300–280 Ma as the result of collisional magmatism, while the ca. 278 Ma granitoids are post–collisional anatectic melts.

We suggest that the Permian arc originated in a subduction zone formed between the proto–Pacific Plate and the western margin of Pangea, coeval with the closure of the Rheic Ocean (Keppie et al., 2008; Nance et al., 2012). This arc was likely continuous from Perú to México and, as proposed by other authors, may have extended to the southern part of North America (Ortega–Obregón et al., 2014).

Acknowledgments

The authors express their gratitude to the Servicio Geológico Colombiano for their support in conducting the research project “Magmatismo Jurásico en Colombia” and to geologists Tomas CORREA, Lina María CETINA, Milton OBANDO, María Isabel GIRALDO, and Gilberto ZAPATA who aided in the sampling efforts. We would like to thank Diego RAMÍREZ for editing the text. Special thanks go to the staff of the Laser Ablation Geochronology Laboratory, Servicio Geológico Colombiano, including Jimmy Alejandro MUÑOZ, Cindy Lizeth URUEÑA, and Lorena del Pilar RAYO, for performing the U–Pb zircon dating and for acquiring luminescence images of the samples reported in this study.

References

Arango, M.I., Rodríguez, G., Zapata, G. & Bermúdez, J.G. 2015. Catálogo de unidades litoestratigráficas de Colombia: Monzogranito de Mocoa, cordillera Oriental, departamentos de Putumayo, Huila, Cauca y Nariño. Servicio Geológico Colombiano, 41 p. Bogotá.

Blanco–Quintero, I.F., García–Casco, A., Toro, L.M., Moreno–Sánchez, M., Ruiz, E.C., Vinasco, C.J., Cardona, A., Lázaro, C. & Morata, D. 2014. Late Jurassic terrane collision in the northwestern margin of Gondwana (Cajamarca Complex, eastern flank of the Central Cordillera, Colombia). International Geology Review, 56(15): 1852–1872. https://doi.org/10.1080/00206814.2014.963710

Bogotá, J. & Aluja, J. 1981. Geología de la serranía de San Lucas. Geología Norandina, (4): 49–55.

Botero, G. 1940. Geología sobre el Ordoviciano de Antioquia. Revista Minería, 17(99): 8249–8256.

Bustamante, C., Cardona, A., Saldarriaga, M., García–Casco, A., Valencia, V. & Weber, M. 2009. Metamorfismo de los esquistos verdes y anfibolitas pertenecientes a los Esquistos de Santa Marta, Sierra Nevada de Santa Marta (Colombia): ¿Registro de la colisión entre el arco del Caribe y la margen suramericana? Boletín de Ciencias de la Tierra, (25): 7–26.

Cárdenas, J., Fuquen, J. & Núñez, A. 1998. Geología de la plancha 388 Pitalito. Scale 1:100 000. Ingeominas. Bogotá.

Cardona, A., Chew, D., Valencia, V.A., Bayona, G., Mišković, A. & Ibañez–Mejia, M. 2010a. Grenvillian remnants in the northern Andes: Rodinian and Phanerozoic paleogeographic perspectives. Journal of South American Earth Sciences, 29(1): 92–104. https://doi.org/10.1016/j.jsames.2009.07.011

Cardona, A., Valencia, V., Garzón, A., Montes, C., Ojeda, G., Ruiz, J. & Weber, M. 2010b. Permian to Triassic I to S–type magmatic switch in the northeast Sierra Nevada de Santa Marta and adjacent regions, Colombian Caribbean: Tectonic setting and implications within Pangea paleogeography. Journal of South American Earth Sciences, 29(4): 772–783. https://doi.org/10.1016/j.jsames.2009.12.005

Carvajal, C., Fúquen, J.A. & Gómez, L.A. 1993. Geología de la plancha 282 Chaparral. Scale 1:100 000. Ingeominas. Ibagué.

Cediel, F., Mojica, J. & Macía, C. 1980. Definición estratigráfica del Triásico en Colombia, Suramérica. Formaciones Luisa, Payandé y Saldaña. Newsletters on Stratigraphy, 9(2): 73–104.

Chappell, B.W. & White, A.J.R. 1974. Two contrasting granite types. Pacific Geology, 8: 173–174.

Clavijo, J. 1995. Memoria explicativa: Mapa geológico de la plancha 75 Aguachica. Scale 1:100 000. Ingeominas, 48 p. Bucaramanga.

Cochrane, R.S. 2013. U–Pb thermochronology, geochronology and geochemistry of NW South America: Rift to drift transition, active margin dynamics and implications for the volume balance of continents. Doctorade thesis, University of Geneva, 118 p. Geneva. https://doi.org/10.13097/archive-ouverte/unige:30029

Cochrane, R., Spikings, R., Gerdes, A., Winkler, W., Ulianov, A., Mora, A. & Chiaradia, M. 2014. Distinguishing between in–situ and accretionary growth of continents along active margins. Lithos, 202–203: 382–394. https://doi.org/10.1016/j.lithos.2014.05.031

Condie, K.C. & Kröner, A. 2013. The building blocks of continental crust: Evidence for a major change in the tectonic setting of continental growth at the end of the Archean. Gondwana Research, 23(2): 394–402. https://doi.org/10.1016/j.gr.2011.09.011

Cuadros, F.A. 2012. Caracterização geoquímica e geocronológica do embasamento mesoproterozóico da parte norte da serranía de San Lucas (Colômbia). Master thesis, Universidade de Brasilia, 113 p. Brasilia.

Cuadros, F.A., Botelho, N.F., Ordóñez–Carmona, O. & Matteini, M. 2014. Mesoproterozoic crust in the San Lucas Range (Colombia): An insight into the crustal evolution of the northern Andes. Precambrian Research, 245: 186–206. https://doi.org/10.1016/j.precamres.2014.02.010

Dasch, L.E. 1982. U–Pb geochronology of the Sierra de Perijá, Venezuela. Master thesis, Case Western Reserve University, 183 p. Cleveland, USA.

Duque–Trujillo, J.F. 2009. Geocronología (U/Pb y $^{40}Ar/^{39}Ar$) y geoquímica de los intrusivos paleógenos de la Sierra Nevada de Santa Marta y sus relaciones con la tectónica del Caribe y el arco magmático circun–caribeño. Master thesis, Universidad Nacional Autónoma de México, 189 p. Queretaro, México.

Esquivel, J., Flores, D. & Núñez, A. 1991. Mapa geológico de la plancha 301 Planadas. Scale 1:100 000. Ingeominas. Ibagué.

Feininger, T., Barrero, D. & Castro, N. 1972. Geología de parte de los departamentos de Antioquia y Caldas (sub–zona II–B). Boletín Geológico, 20(2): 1–173.

Geyer, O.F. 1973. Das präkretazische Mesozoikum von Kolumbien. Geologisches Jahrbuch, 5: 1–155.

Gómez, J., Morales, C.J., Marquínez, G. & Velandia, F. 1999. Geología de la plancha 322 Santa María. Scale 1:100 000. Ingeominas. Bogotá.

Gómez, J., Montes, N.E., Nivia, Á. & Diederix, H., compilers. 2015. Geological Map of Colombia 2015. Scale 1:1 000 000. Servicio Geológico Colombiano, 2 sheets. Bogotá. https://doi.org/10.32685/10.143.2015.936.

Gómez, J., Montes, N.E., Alcárcel, F.A. & Ceballos, J.A. 2015b. Catálogo de dataciones radiométricas de Colombia en ArcGIS y Google Earth. In: Gómez, J. & Almanza, M.F. (editors), Compilando la geología de Colombia: Una visión a 2015. Servicio Geológico Colombiano, Publicaciones Geológicas Especiales 33, p. 63–419. Bogotá.

González, H. 2001. Memoria explicativa: Mapa geológico del departamento de Antioquia. Scale 1:400 000. Ingeominas, 240 p. Medellín.

Grosse, E. 1931. Acerca de la geología del sur de Colombia: Informe rendido al Ministerio de Industrias sobre un viaje al Huila y alto Caquetá. Boletín de Minas y Petróleo, IV, (23–24): 413–476.

Hubach, E. & Alvarado, B. 1932. Estudio geológico en la ruta Popayán–Bogotá. Servicio Geológico Nacional, Internal report 213, 133 p. Bogotá.

Ibañez–Mejia, M., Ruiz, J., Valencia, V.A., Cardona, A., Gehrels, G.E. & Mora, A. 2011. The Putumayo Orogen of Amazonia and its implications for Rodinia reconstructions: New U–Pb geochronological insights into the Proterozoic tectonic evolution of northwestern South America. Precambrian Research, 191(1–2): 58–77. https://doi.org/10.1016/j.precamres.2011.09.005

Ibañez–Mejia, M., Pullen, A., Arenstein, J., Gehrels, G., Valley, J., Ducea, M., Mora, A., Pecha, M. & Ruiz, J. 2015. Unraveling crustal growth and reworking processes in complex zircons from orogenic lower–crust: The Proterozoic Putumayo Orogen of Amazonia. Precambrian Research, 267: 285–310. https://doi.org/10.1016/j.precamres.2015.06.014

Irvine, T.N. & Baragar, W.R.A. 1971. A guide to the chemical classification of the common volcanic rocks. Canadian Journal of Earth Sciences, 8(5): 523–548. https://doi.org/10.1139/e71-055

Jiménez–Mejía, D.M., Juliani, C. & Cordani, U.G. 2006. P–T–t conditions of high–grade metamorphic rocks of the Garzón Massif, Andean basement, SE Colombia. Journal of South American Earth Sciences, 21(4): 322–336. https://doi.org/10.1016/j.jsames.2006.07.001

Keppie, J.D., Dostal, J., Murphy, J.B. & Nance, R.D. 2008. Synthesis and tectonic interpretation of the westernmost Paleozoic Variscan orogen in southern Mexico: From rifted Rheic margin to active Pacific margin. Tectonophysics, 461(1–4): 277–290. https://doi.org/10.1016/j.tecto.2008.01.012

Kroonenberg, S. & Diederix, H. 1992. Geology of the uppermost Magdalena Valley, 21th Field Conference. In: Geotec Ltda. (editor), Geological field–trips: Colombia 1980–1989. Asociación Colombiana de Geólogos y Geofísicos del Petróleo, p. 73–89. Bogotá.

Leal–Mejía, H. 2011. Phanerozoic gold metallogeny in the Colombian Andes: A tectono–magmatic approach. Doctorade thesis, Universitat de Barcelona, 989 p. Barcelona.

Le Maitre, R.W., editor. 2002. Igneous rocks. A classification and glossary of terms. 2nd edition. Recommendations of the International Union of Geological Sciences Subcommission on the systematics of igneous rocks. Cambridge University Press, 236 p. New York, USA. https://doi.org/10.1017/CBO9780511535581

Ludwig, K.R. 2012. User's manual for Isoplot 3.75. A geochronological toolkit for Microsoft Excel. Berkeley Geochronology Center, Special Publication 5, 75 p. Berkeley, California.

Marshall, D.J. 1988. Cathodoluminescence of geological materials. Unwin Hyman, 146 p. London.

Martens, U., Restrepo, J.J., Ordoñez–Carmona, O. & Correa–Martínez, A.M. 2014. The Tahamí and Anacona Terranes of the Colombian Andes: Missing links between South American and Mexican Gondwana margins. The Journal of Geology, 122(5): 507–530. https://doi.org/10.1086/677177

Middlemost, E.A.K., 1994. Naming materials in the magma/igneous rock system. Earth–Science Reviews, 37(3–4): 215–224. https://doi.org/10.1016/0012-8252(94)90029-9

Miller, J.S., Matzel, J.E., Miller, C.F., Burgess, S.D. & Miller, R.B. 2007. Zircon growth and recycling during the assembly of large, composite arc plutons. Journal of Volcanology and Geothermal Research, 167(1–4): 282–299. https://doi.org/10.1016/j.jvolgeores.2007.04.019

Mišković, A., Spikings, R.A., Chew, D.M., Košler, J., Ulianov, A. & Schaltegger, U. 2009. Tectonomagmatic evolution of western Amazonia: Geochemical characterization and zircon U–Pb geochronologic constraints from the Peruvian eastern cordilleran granitoids. Geological Society of America Bulletin, 121(9–10): 1298–1324. https://doi.org/10.1130/B26488.1

Mojica, J. 1980. Observaciones acerca del estado actual del conocimiento de la Formación Payandé (Triásico Superior), valle superior del río Magdalena, Colombia. Geología Colombiana, (11): 67–88.

Mojica, J., Villarroel, C., Cuerda, A. & Alfaro, M.A. 1988. La fauna de graptolites de la Formación El Hígado (Llanvirniano?–Llandeiliano), serranía de Las Minas, Valle Superior del Magdalena, Colombia. V Congreso Geológico Chileno. Memoirs, II, p. 189–202. Santiago.

Montoya, J.C. & Ordóñez–Carmona, O. 2010. Cartografía geológica y caracterización petrográfica de las unidades litológicas asociadas a los cuerpos vetiformes de oro en el distrito minero Bagre–Nechí. Informe técnico, Grupo de Investigación en Georecursos, Minería y Medio Ambiente (GEMMA). Universidad Nacional de Colombia, 140 p. Medellín.

Mora, A., Ibañez–Mejia, M., Oncken, O., De Freitas, M., Vélez, V., Mesa, A. & Serna, L. 2017. Structure and age of the Lower Magdalena Valley Basin basement, northern Colombia: New reflection–seismic and U–Pb–Hf insights into the termination of the central Andes against the Caribbean Basin. Journal of South American Earth Sciences, 74: 1–26. https://doi.org/10.1016/j.jsames.2017.01.001

Mosquera, D., Núñez, A. & Vesga, C.J. 1982. Mapa geológico preliminar de la plancha 244 Ibagué. Scale 1:100 000. Ingeominas, 27 p. Bogotá.

Murillo, A., Esquivel, C. & Flores, D. 1982. Mapa geológico preliminar de la plancha 281 Rioblanco. Scale: 1:100 000. Ingeominas. Ibagué.

Nakamura, N. 1974. Determination of REE, Ba, Fe, Mg, Na and K in carbonaceous and ordinary chondrites. Geochimica et Cosmochimica Acta, 38(5): 757–775. https://doi.org/10.1016/0016-7037(74)90149-5

Nance, R.D., Gutiérrez–Alonso, G., Keppie, J.D., Linnemann, U., Murphy, J.B., Quesada, C., Strachan, R.A. & Woodcock, N.H. 2012. A brief history of the Rheic Ocean. Geoscience Frontiers, 3(2): 125–135. https://doi.org/10.1016/j.gsf.2011.11.008

Nelson, H.W. 1957. Contribution to the geology of the Central and Western Cordillera of Colombia in the sector between Ibagué and Cali. Leidse Geologische Mededelingen, 22: 1–75.

Núñez, A. & Murillo, A. 1982. Memoria explicativa: Geología y prospección geoquímica de las planchas 244 Ibagué y 263 Ortega. Ingeominas, Informe 1879, 388 p. Ibagué.

Núñez, A., Mosquera, D. & Vesga, C.J. 1984a. Geología de la plancha 263 Ortega. Scale 1:100 000. Ingeominas, 1 sheet. Bogotá.

Núñez, A., Mosquera, D. & Vesga, C.J. 1984b. Memoria explicativa: Mapa geológico preliminar de la plancha 263 Ortega. Scale 1:100 000. Ingeominas, 21 p. Bogotá.

Ordóñez–Carmona, O., Pimentel, M.M. & De Moraes, R. 2002. Granulitas de Los Mangos: Un fragmento grenvilliano en la parte oriental de la Sierra Nevada de Santa Marta. Revista de la Academia Colombiana de Ciencias Exactas, Físicas y Naturales, 26(99): 169–179.

Ordóñez–Carmona, O., Frantz, J.C., Chemale, F. & Londoño, C. 2009. Serranía de San Lucas: Mineralizaciones auríferas, intrusiones de 1500 Ma, metamorfismo Grenville y magmatismo Jurásico. XII Congreso Colombiano de Geología. Memoirs in CD ROM, T003–R117, 1 p. Paipa, Boyacá.

Ortega–Obregón, C., Solari, L., Gómez–Tuena, A., Elías–Herrera, M., Ortega–Gutiérrez, F. & Macías–Romo, C. 2014. Permian

– Carboniferous arc magmatism in southern Mexico: U–Pb dating, trace element and Hf isotopic evidence on zircons of earliest subduction beneath the western margin of Gondwana. International Journal of Earth Sciences, 103(5): 1287–1300. https://doi.org/10.1007/s00531-013-0933-1

Paul, A., Spikings, R., Ulianov, A. & Ovtcharova, M. 2018. High temperature (>350 °C) thermal histories of the long lived (>500 Ma) active margin of Ecuador and Colombia: Apatite, titanite and rutile U–Pb thermochronology. Geochimica et Cosmochimica Acta, 228: 275–300. https://doi.org/10.1016/j.gca.2018.02.033

Pearce, J.A. 2008. Geochemical fingerprinting of oceanic basalts with applications to ophiolite classification and the search for Archean oceanic crust. Lithos, 100(1–4): 14–48. https://doi.org/10.1016/j.lithos.2007.06.016

Peccerillo, A. & Taylor, S.R. 1976. Geochemistry of Eocene calc–alkaline volcanic rocks from the Kastamonu area, northern Turkey. Contributions to Mineralogy and Petrology, 58(1): 63–81. https://doi.org/10.1007/BF00384745

Piraquive, A. 2017. Structural framework, deformation and exhumation of the Santa Marta Schists: Accretion and deformational history of a Caribbean Terrane at the north of the Sierra Nevada de Santa Marta. Doctorade thesis, Université Grenoble Alpes and Universidad Nacional de Colombia, 393 p. Grenoble–Bogotá.

Restrepo, J.J. & Toussaint, J.F. 1989. Terrenos alóctonos en los Andes colombianos: Explicación de algunas paradojas geológicas. V Congreso Colombiano de Geología. Memoirs, I, p. 92–107. Bucaramanga.

Restrepo, J.J., Ordóñez–Carmona, O., Martens, U. & Correa–Martínez, A.M. 2009. Terrenos, complejos y provincias en la cordillera Central de Colombia. Ingeniería, Investigación y Desarrollo, 9(2): 49–56.

Restrepo, J.J., Ordóñez–Carmona, O., Armstrong, R. & Pimentel, M.M. 2011. Triassic metamorphism in the northern part of the Tahamí Terrane of the Central Cordillera of Colombia. Journal of South American Earth Sciences, 32(4): 497–507. https://doi.org/10.1016/j.jsames.2011.04.009

Rodríguez, G. 1995a. Petrografía del Macizo de La Plata, departamento del Huila. Revista Ingeominas, (5): 5–16.

Rodríguez, G. 1995b. Petrografía y microtexturas del Grupo Garzón y el Granito de Anatexis de El Recreo, Macizo de Garzón, cordillera Oriental, Colombia. Revista Ingeominas, (5): 17–36.

Rodríguez, G., Ferreira, P., Velandia, F. & Núñez, A. 1998. Geología de la plancha 366 Garzón. Scale 1:100 000. Ingeominas. Ibagué.

Rodríguez, G., Zapata, G., Velásquez, M.E., Cossio, U. & Londoño, A.C. 2003. Memoria explicativa: Geología de las planchas 367 Gigante, 368 San Vicente del Caguán, 389 Timaná, 390 Puerto Rico, 391 Lusitania (parte noroccidental) y 414 El Doncello. Scale 1:100 000. Ingeominas, 166 p. Bogotá.

Rodríguez, G., Arango, M.I., Zapata, G. & Bermúdez, J.G. 2014. Petrografía y geoquímica del Neis de Nechí. Boletín de Geología, 36(1): 71–84.

Rodríguez, G., Zapata, G., Arango, M.I. & Bermúdez, J.G. 2015. Catálogo de unidades litoestratigraficas de Colombia: Monzogranito de Algeciras. Servicio Geológico Colombiano, 37 p. Medellín.

Rodríguez, G., Arango, M., Zapata, G. & Bermúdez, J. 2016. Catálogo de unidades litoestratigráficas de Colombia: Formación Saldaña. Servicio Geológico Colombiano, 91 p. Medellín.

Rodríguez, G., Zapata, G., Arango, M.I. & Bermúdez, J.G. 2017. Caracterización petrográfica, geoquímica y geocronología de rocas granitoides pérmicas al occidente de La Plata y Pacarní, Huila, Valle Superior del Magdalena, Colombia. Boletín de Geología, 39(1): 41–68. https://doi.org/10.18273/revbol.v39n1-2017002

Rodríguez, G., Arango, M.I., Zapata, G. & Bermúdez, J.G. 2018. Petrotectonic characteristics, geochemistry and U–Pb geochronology of Jurassic plutons in the Upper Magdalena Valley, Colombia: Implications on the evolution of magmatic arcs in the NW Andes. Journal of South American Earth Sciences, 81: 10–30. https://doi.org/10.1016/j.jsames.2017.10.012

Royero, J.M. 1996. Memoria explicativa: Geología de la plancha 65 Tamalameque (departamentos de Cesar y Bolívar). Ingeominas, 78 p. Bucaramanga.

Rubatto, D. 2002. Zircon trace element geochemistry: Partitioning with garnet and the link between U–Pb ages and metamorphism. Chemical Geology, 184(1–2): 123–138. https://doi.org/10.1016/S0009-2541(01)00355-2

Schoene, B., Crowley, J.L., Condon, D.J., Schmitz, M.D. & Bowring, S.A. 2006. Reassessing the uranium decay constants for geochronology using ID–TIMS U–Pb data. Geochimica et Cosmochimica Acta, 70(2): 426–445. https://doi.org/10.1016/j.gca.2005.09.007

Shand, S.J. 1943. Eruptive rocks. Their genesis, composition, classification, and their relation to ore deposits, with a chapter on meteorites. Geological Magazine, 64(7): 329–330. https://doi.org/10.1017/S0016756800103504

Siégel, C., Bryan, S.E., Allen, C.M. & Gust, D.A. 2018. Use and abuse of zircon–based thermometers: A critical review and a recommended approach to identify antecrystic zircons. Earth–Science Reviews, 176: 87–116. https://doi.org/10.1016/j.earscirev.2017.08.011

Silva–Arias, A., Páez–Acuña, L.A., Rincón–Martínez, D., Tamara–Guevara, J.A., Gómez–Gutiérrez, P.D., López–Ramos, E., Restrepo–Acevedo, S.M., Mantilla–Figueroa, L.C. & Valencia, V. 2016. Basement characteristics in the Lower Magdalena Valley and the Sinú and San Jacinto fold belts: Evidence of a Late Cretaceous magmatic arc at the south of the Colombian Caribbean. Ciencia, Tecnología y Futuro, 6(4): 5–36.

Sláma, J., Košler, J., Condon, D.J., Crowley, J.L., Gerdes, A., Hanchar, J.M., Horstwood, M.S.A., Morris, G.A., Nasdala, L., Norberg, N., Schaltegger, U., Schoene, B., Tubrett, M.N. & Whitehouse, M.J. 2008. Plešovice zircon–A new natural reference material for U–Pb and Hf isotopic microanalysis. Chemical Geology, 249(1–2): 1–35. https://doi.org/10.1016/j.chemgeo.2007.11.005

Solari, L., Gómez–Tuena, A., Bernal, J., Pérez–Arvizu, O. & Tanner, M. 2010. U–Pb zircon geochronology with an integrated LA–ICP–MS microanalytical workstation: Achievements in precision and accuracy. Geostandards and Geoanalytical Research, 34(1): 5–18. https://doi.org/10.1111/j.1751-908X.2009.00027.x

Spikings, R., Cochrane, R., Villagómez, D., van der Lelij, R., Vallejo, C., Winkler, W. & Beate, B. 2015. The geological history of northwestern South America: From Pangaea to the early collision of the Caribbean Large Igneous Province (290–75 Ma). Gondwana Research, 27(1): 95–139. https://doi.org/10.1016/j.gr.2014.06.004

Stacey, J.S. & Kramers, J.D. 1975. Approximation of terrestrial lead isotope evolution by a two–stage model. Earth and Planetary Science Letters, 26(2): 207–221. https://doi.org/10.1016/0012-821X(75)90088-6

Stibane, F. & Forero, A. 1969. Los afloramientos del Paleozoico en La Jagua (Huila) y río Nevado (Santander del sur). Geología Colombiana, (6): 31–66.

Streckeisen, A. 1974. Classification and nomenclature of plutonic rocks recommendations of the IUGS subcommission on the systematics of igneous rocks. Geologische Rundschau, 63(2): 773–786. https://doi.org/10.1007/BF01820841

Streckeisen, A. 1979. Classification and nomenclature of volcanic rocks, lamprophyres, carbonatites, and melilitic rocks: Recommendations and suggestions of the IUGS subcommission on the systematics of igneous rocks. Geology, 7(7): 331–335. https://doi.org/10.1130/0091-7613(1979)7<331:CANOVR>2.0.CO;2

Sun, S.S. & McDonough, W.F. 1989. Chemical and isotopic systematics of oceanic basalts: Implications for mantle composition and processes. In: Saunders, A.D. & Norry, M.J. (editors), Magmatism in the ocean basins. Geological Society of London, Special Publication 42, p. 313–345. https://doi.org/10.1144/GSL.SP.1989.042.01.19

Tschanz, C.M., Jimeno, A. & Cruz, J. 1969. Mapa geológico de reconocimiento de la Sierra Nevada de Santa Marta. Scale 1:200 000. Ingeominas. Bogotá.

Tschanz, C.M., Marvin, R.F., Cruz, J., Mehnert, H.H. & Cebula, G.T. 1974. Geologic evolution of the Sierra Nevada de Santa Marta, northeastern Colombia. Geological Society of America Bulletin, 85(2): 273–284. https://doi.org/10.1130/0016-7606(1974)85<273:GEOTSN>2.0.CO;2

van der Lelij, R., Spikings, R., Ulianov, A., Chiaradia, M. & Mora, A. 2016. Palaeozoic to Early Jurassic history of the northwestern corner of Gondwana, and implications for the evolution of the Iapetus, Rheic and Pacific Oceans. Gondwana Research, 31: 271–294. https://doi.org/10.1016/j.gr.2015.01.011

Velandia, F., Ferreira, P., Rodríguez, G. & Núñez, A. 1996. Levantamiento geológico de la plancha 366 Garzón, Huila. Ingeominas, Internal report 2321, 121 p. Ibagué.

Velandia, F., Morales, C.J, Caicedo, J.C. & Núñez, A. 1999. Geología de la plancha 345 Campoalegre. Scale 1:100 000. Ingeominas. Ibagué.

Velandia, F., Ferreira, P., Rodríguez, G. & Núñez, A. 2001a. Memoria explicativa: Levantamiento geológico de la plancha 366 Garzón. Ingeominas, 82 p. Bogotá.

Velandia, F., Nuñez, A. & Marquínez, G. 2001b. Memoria explicativa: Mapa geológico departamento del Huila. Scale 1:300 000. Ingeominas, 151 p. Bogotá.

Vesga, C.J. & Barrero, D. 1978. Edades K/Ar en rocas ígneas y metamórficas de la cordillera Central de Colombia y su implicación geológica. II Congreso Colombiano de Geología. Abstracts, p. 19. Bogotá.

Villagómez, D.R. 2010. Thermochronology, geochronology and geochemistry of the Western and Central Cordilleras and Sierra Nevada de Santa Marta, Colombia: The tectonic evolution of NW South America. Doctorade thesis, University of Geneva, 143 p. Geneva. https://doi.org/10.13097/archive-ouverte/unige:14270

Villarroel, C. & Mojica, J. 1988. El Paleozoico superior (Carbonífero–Pérmico) sedimentario de Colombia. Afloramientos conocidos y características generales. Geología Colombiana, (16): 81–87.

Vinasco, C.J., Cordani, U.G., González, H., Weber, M. & Peláez, C. 2006. Geochronological, isotopic, and geochemical data from Permo–Triassic granitic gneisses and granitoids of the Colombian central Andes. Journal of South American Earth Sciences, 21(4): 355–371. https://doi.org/10.1016/j.jsames.2006.07.007

Viscarret, P., Wright, J. & Urbani, F. 2007. Dataciones U/Pb SHRIMP en circón de rocas del Macizo El Baúl, estado Cojedes, Venezuela. IX Congreso Geológico Venezolano. Memoirs in CD ROM, p. 94–95. Caracas.

Weber, B. & Köhler, H. 1999. Sm–Nd, Rb–Sr and U–Pb geochronology of a Grenville Terrane in southern Mexico: Origin and geologic history of the Guichicovi Complex. Precambrian Research, 96(3–4): 245–262. https://doi.org/10.1016/S0301-9268(99)00012-1

Weber, B., Cameron, K.L., Osorio, M. & Schaaf, P. 2005. A late Permian tectonothermal event in Grenville crust of the southern Maya Terrane: U–Pb zircon ages from the Chiapas Massif, southeastern Mexico. International Geology Review, 47(5): 509–529. https://doi.org/10.2747/0020-6814.47.5.509

Weber, B., Iriondo, A., Premo, W.R., Hecht, L. & Schaaf, P. 2007. New insights into the history and origin of the southern Maya Block, SE México: U–Pb–SHRIMP zircon geochronology from metamorphic rocks of the Chiapas Massif. International Journal of Earth Sciences, 96(2): 253–269. https://doi.org/10.1007/s00531-006-0093-7

Wiedenbeck, M., Allé, P., Corfu, F., Griffin, W.L., Meier, M., Oberli, F., von Quadt, A., Roddick, J.C. & Spiegel, W. 1995. Three natural zircon standards for U–Th–Pb, Lu–Hf, trace element and REE analyses. Geostandards and Geoanalytical Research, 19(1): 1–23. https://doi.org/10.1111/j.1751-908X.1995.tb00147.x

Zapata, G., Rodríguez, G., Arango, M.I. & Bermúdez, J.G. 2015. Catálogo de unidades litoestratigráficas de Colombia: Cuarzomonzodiorita de Páez, cordillera Central, Cauca–Huila. Servicio Geológico Colombiano, 50 p. Bogotá.

Zuluaga, C.A. & Stowell, H. 2012. Late Cretaceous – Paleocene metamorphic evolution of the Sierra Nevada de Santa Marta: Implications for Caribbean geodynamic evolution. Journal of South American Earth Sciences, 34: (1–9). https://doi.org/10.1016/j.jsames.2011.10.001

Explanation of Acronyms, Abbreviations, and Symbols:

CL	Cathodoluminescence
EDS	Energy dispersive X–ray spectroscopy
HFSE	High field strength element
ICP–MS	Inductively coupled plasma mass spectrometry
LA–ICP–MS	Laser ablation inductively coupled plasma mass spectrometry
LILE	Large–ion lithophile element
LOI	Loss on ignition
REE	Rare earth element
SGC	Servicio Geológico Colombiano
SNSM	Sierra Nevada de Santa Marta
SGC	Servicio Geológico Colombiano
SSL	Serranía de San Lucas
UMV	Upper Magdalena Valley
UNAM	Universidad Nacional Autónoma de México

Authors' Biographical Notes

Gabriel RODRÍGUEZ–GARCÍA graduated in 1987 with a degree in geological engineering from the Universidad Nacional de Colombia, Sede Medellín. Subsequently, he completed specialization studies at the École Nationale Supérieure des Mines de Paris in 1995, specializing in technical evaluation–economics of mining projects. He has worked for 30 years at the Servicio Geológico Colombiano. He was the head of cartography of the regional headquarters of Ibagué, and acts as coordinator of projects and regional cartography and of work groups for the exploration and evaluation of deposits. He currently coordinates the Medellín headquarters and the Grupo de Estudios Geológicos Especiales of the Servicio Geológico Colombiano. He has previously been a professor of Colombian Geology, Field Geology I, and Physical Geology at Universidad EAFIT and the director of geology of Grupo Argos. He has authored over 100 publications, including geological maps, memoirs, and scientific articles in geology.

Ana María CORREA–MARTÍNEZ graduated in geological engineering from the Universidad Nacional de Colombia, Sede Medellín and has a PhD in geology from the Universidade de Brasília (Brasil), where she studied the petrogenesis of the Aburrá Ophiolite in the Colombian Central Cordillera. Between 2008 and 2013, she worked as a gold exploration geologist and chief of mineral exploration projects. She was lecturer at the Universidad Nacional de Colombia (Medellín) in the Departamento de Recursos Minerales. Since 2014, she has worked in the Servicio Geológico Colombiano on geochronology of metamorphic units from the northwestern slope of the Central Cordillera and on the project "Jurassic Magmatism in the Colombian Andes".

Juan Pablo ZAPATA–VILLADA is a geological engineer and MS in mineral resources of Universidad Nacional de Colombia Sede Medellín. He worked for the Cordilleran project of México (Tectonic Analysis), and has expertise in GIS, U–Pb analysis, and heavy minerals. He works for the Servicio Geológico Colombiano. His job includes GIS and the geochronology, and geochemistry of the Western Cordillera and Jurassic magmatism in Colombia. He has participated as a speaker at the Colombian Geological Congress, winning the Ricardo Lleras Codazzi in the XIV edition.

Gloria OBANDO–ERAZO has a BS in geology, Universidad Nacional de Colombia Sede Bogotá, an MS in environmental geology with an emphasis in geophysics, processing and interpretation of aerial gamma ray spectrometry and aerial magnetometry (Universidade de Brasília, 2001), and is a PhD candidate in aerial geophysics (Universidade de Brasilia, 2006). She has worked since 1995 on multiple projects in Colombia using potential fields at the Servicio Geológico Colombiano. Since 2014, she has been working in the Grupo de Estudios Geológicos Especiales of the Servicio Geológico Colombiano on the project "Jurassic Magmatism in the Colombian Andes".

Bogotá, Colombia
2020